(This page deliberately left blank)

(This page deliberately left blank)

Mechanics of Machines

A Computer-Oriented Course of Study in the Kinematics, Statics, Dynamics & Vibrations of Machines

Samuel Doughty, Ph.D.
Professor of Mechanical Engineering
Retired

Second Edition
Version 2.1

Preface

This book is the second edition of a book with the same title first published in 1988. Traditional methods for the study of kinematics and dynamics of machines emphasized the use of graphical methods of analysis. Anyone familiar with this approach is well aware that the accuracy of the result depends entirely on how sharp the pencil point is. Such a limitation cries out for a mathematical approach. The intention to utilize analytical methods implemented with digital computer methods for a rigorous approach to the material as intended in the first edition is preserved in this edition. In the three decades since the original book was produced, digital computing has become entirely common place and readily available. This means that very precise results are readily available to anyone willing to write a simple computer program, often far less effort than the construction of an accurate graphical solution.

The focus on analytical methods for computer implementation leads naturally to the use of energy methods in preference to vector methods. Vectors continue to be used where they offer the most clear understanding, but most problems eventually lead to an energy based formulation. This idea was dominant in the first edition, and remains so in the second.

The entirety of the original text has been carefully reviewed, and some content reductions have been made. Some types of cam and follower systems are eliminated with the recognition that those who want that material can still find it in the first edition which remains in print through the print-on-demand publisher Lulu.com. The material on development of tooth numbers for very close approximations to specified gear ratios (the Brocot Table and the Continued Fractions Approximation) are also removed but remain available in the first edition.

Two new aspects are introduced in this revision: (1) extensive use of SI units, and (2) an introduction to vibrations. Each requires some comment.

The traditional inch-pound-second system of units remains widely in use in the USA at the present time. For the past six decades, since the launch of the Russian Sputnik in October, 1957, the US has been poised on the verge of conversion to metric units. The definition of the SI units system in the early 1960s made this conversion appear inevitable, and most nations of the world have indeed made that conversion while the USA has held out. Metric units have been legal for commerce in the USA for more than a century, but they have not been made universal. There are indications that the final change to SI units in the USA is coming soon due to the globalization of commerce. This has led to an increased emphasis on SI units in American education in recent years. For the present, engineering students in America must be conversant in both US Customary (inch-pound-second) units and SI units. No one can say with certainty how long this situation will continue.

In times past, the theory of machines and vibrations were considered as separate subjects in the engineering curriculum. This was clearly reflected in the way the two courses were taught. In many linear vibration problems, there is only trivial kinematic complexity, and this is the reason they were taught separately. However, in any situation in which there is a mechanism involved, such as a four-bar linkage, a slider-crank, or other real machine system, the need for unification of these topics becomes immediately evident.

The writer's own industrial experience in the area torsional vibrations of internal combustion engine driven machine trains and reciprocating compressors has compelled him to see a close connection between the two. The slider-crank mechanism is universally used in internal combustion engines (except for the Wankel engine), and is a major source of torsional vibration excitation. This area can only be correctly addressed by bringing an analytical approach to kinematics and machine dynamics to bear on the torsional vibration problem. This is particularly done in the final chapter of this edition.

Many of the homework problems posed in this second edition are new, although there are a number carried over from the previous edition. There is a serious effort to present problems that clearly relate to actual machinery, as opposed to problems that are so idealized as to never be seen in practice. The hope is that these problems will motivate the student, recognizing that the purpose is to deal with reality, not idealized fantasy.

The author has received much assistance in the development of this work from many quarters over the years. Much of the text has been reviewed by Dr. Ettore Infante, Dr. Robert White, and Dr. Ronald Slovikoski, each of whom offered valuable comments. Much of the author's experience with cam systems is due to work with Mr. John Andrews, a manufacturer of automotive cams. Mr. James Hardy provided much helpful guidance regarding electric motors. The book was composed entirely in LaTeX by use of Scientific WorkPlace, with the final LaTeX formatting of the book developed by Dr. Thomas Price, a most valuable contribution.

The first edition of this work was well received around the world, and it is hoped that this second edition will gain even wider acceptance. To that end, the book is offered on the Internet without charge, and may be freely distributed to anyone. Proper attribution will be appreciated.

Samuel Doughty

Dubuque, IA

March, 2019

Dedication

This second edition is dedicated to God, the author of all truth, knowledge, wisdom, and understanding, and the grantor of salvation to all mankind through His Son, Jesus Christ, our Lord and Saviour.

Venite, exultemus Domino[1]

O Come, let us sing unto the Lord;
let us heartily rejoice in the strength of our salvation.

Let us come before his presence with thanksgiving;
and show ourselves glad in him with psalms.

For the Lord is a great God;
and a great King above all gods.

In his hand are all the corners of the earth;
and the strength of the hills is his also.

The sea is his and he made it;
and his hands prepared the dry land.

O come, let us worship and fall down,
and kneel before the Lord our Maker.

For he is the Lord our God;
and we are the people of his pasture,
and the sheep of his hand.

O worship the Lord in the beauty of holiness;
let the whole earth stand in awe of him.

For he cometh, for he cometh to judge the earth;
and with righteousness to judge the world,
and the peoples with his truth.

[1] An adaptation from Psalms 95 and 96.

Revision Record

Release 1 – 31 March 2019 Because of advancing age and concern that I may not be physically able to complete this second edition in every respect, it is my intention to release it in progressive revisions. The first will include a limited number of homework problems, even though the intent is that the final version will contain many such problems.

As is always the case, there are no doubt errors in the text. In addition to expanding the homework problem set, the author will be making corrections in future revisions. This includes both errors of fact (statements that are not correct) and problems that are thought to be impossible as stated due to lack of information or internal contradictions. Please identify fully any errors found so that they may be corrected in the next revision of the text. Anyone using the text who finds an error is encouraged to write to the author at this e-mail address:

`MechanicsOfMachinesBook@gmail.com`

Release 2 – All Souls Day 2019 This second release of the text is particularly significant in two aspects These are:

- Development and inclusion of a major example induction motor driven torsional vibration instability, placed at the end of Chapter 12. It is a fitting final example for many concepts discussed in this book. In particular, in a single example, it provides a final application of a variety of concepts discussed in this book, including
  - Utilize the improved induction motor torque-speed model developed by Gärtner, building on the earlier work of Kloss;
  - Demonstrate the effect of including a greater number of degrees of freedom to better approximate reality;
  - Demonstrate yet again the power of numerical solution techniques applied to ordinary differential equations;
  - Show the reduction of a gear coupled system to an equivalent single shaft system;
  - Show again the application of the eigensolutions and modal analysis;
  - Utilize Taylor series to linearize a nonlinear system;
  - Show the application of linear single degree of freedom modeling to explain a multidegree of freedom instability by raising and applying the concept of negative damping.
- The inclusion of an Index. While the Table of Contents (which was present in the first release) enables users to get an overall understanding of the scope of the book, the Index is extremely important to find discussion on specific items.

In addition to these two major improvements, there have been numerous small wording changes to improvement clarity and smoothness. As before, please identify fully any errors found so that they may be corrected in the next revision of the text. Anyone using the text who finds an error is encouraged to write to the author at this e-mail address:

MechanicsOfMachinesBook@gmail.com

Contents

Appendicies

Chapter 1

Introduction

1.1 Initial Comments and Definitions

The term *mechanics of machines* is here understood to include the kinematics, dynamics, and vibrations of mechanical systems of the type commonly found in machinery. Introductory courses in statics and dynamics usually provide little in these areas because of the kinematic complexity of real machines. In regard to dynamics and vibrations, the complications of varying effective inertia, multiple degrees of freedom, and geometric complexity again limit elementary courses. In this text, these problems are all addressed directly.

There are a number of words used in this study that need precise technical definitions, despite the fact that they all have common, everyday meanings. The word **machine** means a device that transmits or modifies force or motion to do useful work. Contrast this with the word **structure**, usually referring to a stationary support. A **mechanism** is an assembly of mechanical components to achieve a particular motion. Thus a washing machine (in the nontechnical sense of the word machine) involves both a structure or frame, and a mechanism that agitates the clothes. The words mechanism and machine are often used interchangeably, but the word *mechanism* tends to emphasize the motion while the word *machine* points more toward the work done. Thus an engine is usually called a machine while a clock is a mechanism.

The first topic of this book is Kinematics of Machines, beginning in Chapter 2. *Kinematics* is the study of motion without regard for the forces involved in the motion. After laying a foundation in kinematics, the study moves on to Dynamics of Machines. *Dynamics of Machines* is the study of motion and the associated forces in machines, as distinct in most cases from astronomy or particle physics. Although the same basic principles apply in both cases, the concrete nature of this study sets it apart from the more esoteric

topics. Finally, the last major topic is Vibrations of Machines. *Vibration of Machines* is the oscillatory motion of machine components, usually rapid and of small amplitude. Vibration is often of concern as a cause of noise and the rapid accumulation of fatigue cycles within the material comprising the machine components.

There are four major ideas that underlie all of the material in this book, and it is well to point them out here so that the reader may be alert for them as they appear repeatedly throughout the book. They are:

1. **Position Vector Loop Equations** – In typical machinery systems, the machine components form closed loops that change shape as the motion proceeds, but always remain closed. Each loop can be described as a vector sum equal to zero at all times. If enough information has been specified to determine the mechanism configuration uniquely, these vector equations or their scalar equivalents can be solved for the unknown position variables.

2. **Velocity Coefficients** and **Velocity Coefficient Derivatives** – The velocity coefficient is a position dependent function relating an output motion velocity to the input motion velocity. Velocity coefficient derivatives are simply the derivatives of the velocity coefficients with respect to position. They are used particularly in expressing accelerations.

3. **Principle of Virtual Work** – This is one of the oldest energy principles of classical dynamics and it provides the means to define system equilibrium in terms of a generalized force acting on the system.

4. **Energy Based Equations of Motion** – The development of equations of motion, based on energy considerations, is usually associated with the names of Lagrange and, to a lesser extent, with Eksergian. These methods provide an alternative to the application of Newton's Second Law, an alternative that is often much more easily applied than the vector methods of Newton.

Each of these concepts has a long history, and each can certainly be applied in hand calculations. The maximum benefit comes, however, when they are applied together in a computer implementation. The solution of the position vector loop equations often involves the numerical solution of systems of nonlinear transcendental equations. In such a case, closed form solutions are often impossible, but numerical solutions by iterative techniques are often required. The calculation of velocity coefficients involves the solution of a system of simultaneous linear equations. Although this is simple in concept, it is excessively laborious for more than two equations. When applying the principle of virtual work, it is often necessary to solve a system of nonlinear equations, and again, numerical iteration by means of the computer is the only feasible way to proceed. Finally, it is important to note that the equations of motion for most mechanisms are highly nonlinear differential equations. Irrespective of the methods used to obtain the equations of motion,

solution by analytical means is usually impossible; numerical integration is required and this is only practical when implemented in a computer code.

The whole process of writing a system of equations to describe the response of a physical system is often called **mathematical modeling.** This is to distinguish this process from that of physical modeling in which a physical scale model is constructed. Mathematical modeling from one point of view is simply a matter of applying the equations learned in elementary physics to the description of the machine components. However, when considered more carefully, it is more than that. Each of these descriptions recalled from elementary physics carries with it particular assumptions. In mathematical modeling of a particular system, it is important to examine these assumptions to assure that they are appropriate to the system under consideration.

A simple example may help at this point. In elementary physics, it is common to write the magnitude of the force developed in a spring as the product of stiffness with deformation, that is, the simple linear relationship $F = k \cdot \delta$. This is certainly true for many springs, but it is not true for all. There are types of springs where it may be necessary to write $F = c_1\delta + c_2 |\delta| \delta + c_3\delta^3 + \ldots$ When applying this relation in a mathematical model, it is important to examine whether it is true for the particular case.

One of the most common assumptions, made in most parts of this text but certainly not all, is that each machine component is rigid. *A* **rigid body** *is understood to remain undeformed, no matter what loads are imposed upon it.* This is often a very useful assumption, enabling an analysis to advance where it might otherwise be stymied. The whole idea of a rigid body is, however, in conflict with reality; in the physical world, there are no true rigid bodies. All real physical bodies are to a degree *flexible*. They are said to be *compliant*, meaning that they deform under load. While it is useful in many parts of this book to assume that the parts of the system are rigid bodies, it is important to remember that this is never absolutely true. The analyst must ask himself at every point to what extent this assumption is satisfied.

In the construction of machinery, it is common to use primarily two kinds of connections (other types are considered later):

1. **Pin** – If two parts are allowed to overlap so that a pin may be passed through both of them, this is referred to as a pin joint, a hinge, or other similar terminology. In the classic terminology of kinematics this is called a *revolute joint*, suggesting the idea that the two bodies may revolve independently about the axis of the pin.

2. **Slider** – If an extension of one body is only allowed to move in such a way that it is guided by a rail, a groove, or similar rigid boundary on the second body, this is called a slider because it slides along the guide. In the classical terminology, this joint is called a *prismatic joint*, suggesting the ability of two prisms to slide freely along their common generating lines while not penetrating either body.

More detailed discussion of joints is provided later where the need arises.

One of the common characteristics of all physical bodies is the scalar property known as **mass**. This is the property that resists acceleration when a body is acted upon by a non-zero net force, as indicated by Newton's Second Law of Motion written in vector form as

$$\sum \mathbf{F} = m\mathbf{a} \tag{1.1}$$

where

$\mathbf{F}$ is a force (vector) acting on the body,

m is the body mass,

$\mathbf{a}$ is the acceleration (vector) for the center of mass.

When rotational motion is involved, the comparable expression is usually written as in scalar form for rotation about a particular axis b as

$$\sum T_b = I_{bb}\alpha_b \tag{1.2}$$

where

T_b is a torque with respect to axis b acting on the body;

I_{bb} is known as the mass moment of inertia (MMOI) with respect to the axis b;

α_b is the angular acceleration of the body about the axis b.

The **mass moment of inertia** is the item of most common interest in this book, and it is defined by the following integral:

$$I_{MMOI} = \iint_{Body} r^2 \, dm \tag{1.3}$$

where the integration extends over the entire mass of the body. The quantity r is the distance from the axis of rotation to the integration element.

Written in this way, the mass moment of inertia appears as a scalar quantity. It is usually denoted as I, although the symbol J is also frequently used. From a more advanced perspective, the mass moment of inertia is a second order tensor, representable as a symmetric square matrix.

Finally, because it is often a source of confusion, there is also the *area moment of inertia*, also often denoted either as I or J. This quantity appears in many beam problems and

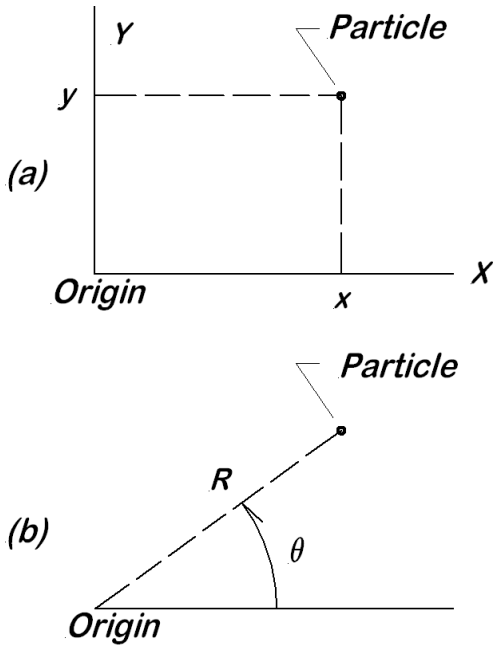

Figure 1.1: Particle in Two Dimensions

shaft torsion calculations. The polar area moment of inertia is defined as J_{area},

$$I_{area} = \iint_{SectionArea} r^2 \, dA \tag{1.4}$$

where the integration extends over the applicable cross sectional area.

1.2 Degrees of Freedom

The term **degrees of freedom** has long been used in classical dynamics to refer to the number of *independent* variables that are required to describe the position of a mechanical system. The concept is introduced at this point, and understanding of the term is expected to grow with progress through the following chapters.

Consider a particle free to move in two dimensions as shown in Figure 1.1. In the upper diagram, (a), the particle is shown with a superimposed rectangular Cartesian coordinate system, and it is evident that the location of the particle is specified by the ordered pair (x, y). The lower diagram, (b), shows exactly the same particle in the same position, but with a plane polar coordinate superimposed. From this diagram, it is evident that the position of the particle is given by the ordered pair (R, θ). The important point is that no matter which coordinate system is used, there are two data items required to specify

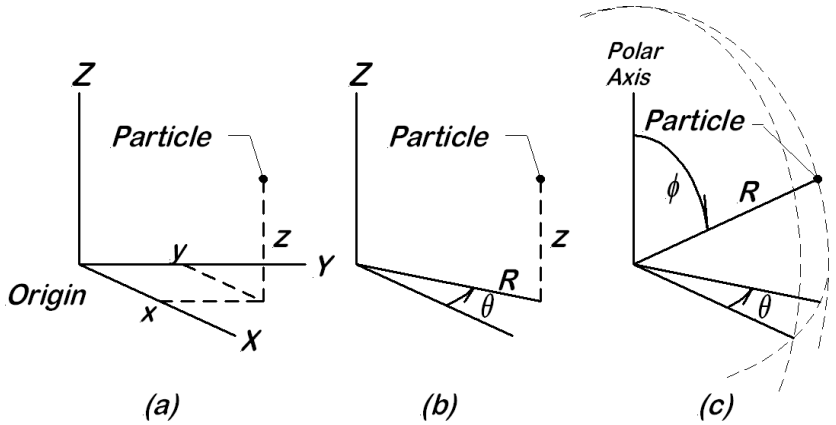

Figure 1.2: Single Particle in Three Dimensions

the location of the particle. The location cannot be specified with less than two data items, and there is no need for more than two. The particle is said to have two degrees of freedom, often abbreviated as 2DOF.

In a similar manner, consider a particle allowed to move in three dimensions, such as is shown in Figure 1.2. In the left most diagram, (a), the particle is shown with a rectangular Cartesian coordinate system. It is evident that the position of the particle is fully described provided the three numbers (x, y, z) are specified. In the center diagram, (b), the same particle is shown occupying the same location in space. This time, a cylindrical coordinate system is used, and the specification of the particle location is complete with the three values (R, θ, z). In the right most diagram, (c), the same particle is again shown, with a spherical coordinate system. It is clear that in this third case, the location of the particle is completely specified by three values (R, θ, ϕ). (Note that R is defined differently for the spherical coordinates as compared with the cylindrical coordinate system.) It is also evident that, for any case in three dimensions, three values must be specified and no smaller number will suffice.

In Figure 1.3 (a), two particles are shown, #1 and #2, and each is free to move in two dimensions. From the discussion above, it is evident that the system of two particles has four degrees of freedom. The four degrees of freedom can be fully specified by (x_1, y_1) and (x_2, y_2). It is important to keep in mind that the number of degrees of freedom is simply *the number of data items required* to fully specify the configuration of the system; it is not the coordinate system choices (rectangular Cartesian, polar, or something else), nor is it the coordinate values themselves.

The same two particles are shown in Figure 1.3 (b), but a massless rigid link joining the two particles has been added to the system. All that this link does is to hold constant the distance between the two particles; they are required to always be exactly d distance

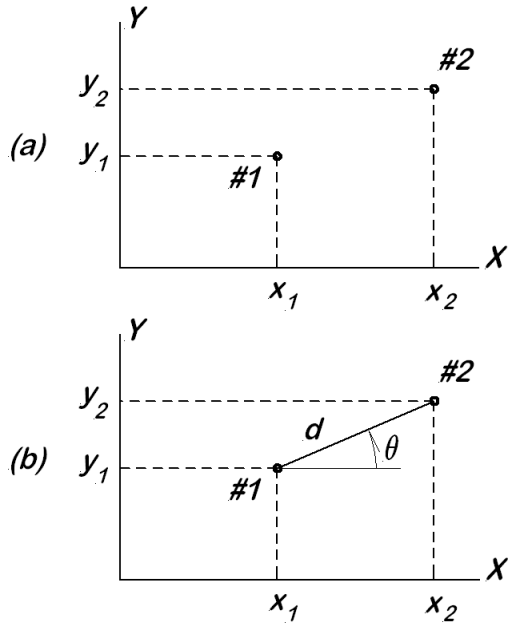

Figure 1.3: Two Particles in Two Dimensions

apart. It is evident then, by the Pythagorean Theorem, that

$$d^2 = (x_2 - x_1)^2 + (y_2 - y_1)^2 \tag{1.5}$$

This equation is called a constraint; it expresses a constraint or extra condition that the system must always satisfy.

Now, how many *independent variables* are required to specify the system configuration (recall that the number of degrees of freedom is the number of independent variables required)? Imagine a process in which (x_1, y_1) are assigned arbitrarily; they are clearly independent. Next, imagine that x_2 is assigned at will, subject only to $|x_2 - x_1| \leq d$. When this is done, the system configuration is fully specified; there is nothing left that can be arbitrarily specified. Thus there are three independent variables after the rigid link is added to the system. **The effect of the constraint is remove one degree of freedom.** The preceding statement is true in most cases, but not quite all. The whole subject is discussed in more detail in Chapter 2 under the heading Constraints. For now, the reader should accept this as a guiding principle, to be modified slightly later. Thus, extrapolation is possible, leading to the conclusion that *for a system of N particles in two dimensions and subject to M constraints, the number of degrees of freedom is $2N - M$.*

Finally, consider the effect of several particles with multiple constraints between them as shown in Figure 1.4. In the upper diagram, Figure 1.4(a), there are three particles with three rigid links between them, all constrained to move only in the $X - Y$ plane. By the

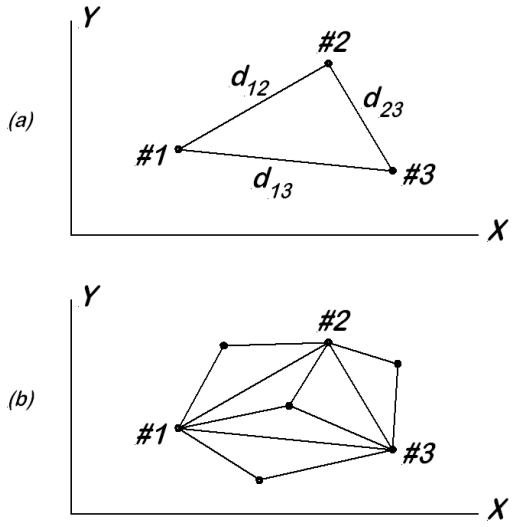

Figure 1.4: Several Particles Moving in Two Dimensions

reasoning of the previous paragraph, the number of degrees of freedom is expect to be

$$DOF = 2\,(3) - 3 = 3 \tag{1.6}$$

This is the familiar result from prior experience; a triangle forms the most elementary rigid body. The critical result is that **a rigid body has three degrees of freedom in planar motion.** The corresponding result in three dimensions (not demonstrated here) is that **a rigid body has six degrees of freedom in three dimensions**.

If one of the rigid links, say d_{23}, were removed, leaving only two constraints, then there would be four degrees of freedom. These four degrees of freedom might be associated with the coordinates as (x_1, y_1) to locate particle #1, then perhaps y_2 to locate the second particle and y_3 to locate the third particle. This is only one of the many ways that the coordinates can be associated with the degrees of freedom, but it demonstrates the idea that the removal of one constraint adds a degree of freedom.

Still considering Figure 1.4, but moving to the lower diagram, the result of adding more particles with rigid constraints is shown. It is clear that, every time an additional particle is added with two more constraints, the result remains simply a rigid body with three degrees of freedom. Note that it is also possible to over constrain the system, that it, to apply more constraints than necessary to make the system rigid. This is the case in Figure 1.4(b). Do you see the unnecessary constraint(s)? This supports the idea that **a typical rigid body,** composed of a vast number of particles, still **has only three degrees of freedom in planar motion and six degrees of freedom in three dimensional motion.**

1.3 Use of Mathematics

One of the questions that must be of interest to every student of engineering is, "Who is an engineer?" or similarly, "What defines an engineer?" The word *engineer* is used loosely around the world to mean many different positions, including the janitor who may be called a housekeeping engineer, the boiler operator or locomotive driver who is often called an operating engineer, the draftsman who spends all day working on CAD to produce drawings, the designer who actually makes decisions about how the machine will work, or the supervisor whose only concern is with project schedules and costs. But who is really an engineer?

In many jurisdictions around the world, the term *engineer* is legally defined as *a person qualified to design* equipment. The definitions often mention the ability to apply a knowledge of *physical science and mathematics*. The governmental bodies that make these definitions recognize that the economic and safe development of the products of modern life depend upon the ability to put to use the principles of physics, chemistry, and other sciences. Further, it is generally appreciated that the full application of these principles can only be done with skill in mathematics.

The sad truth is that far too many engineers do not utilize the mathematics to which they were exposed during their formal education. This limits the professional growth of the individual engineer just as surely as a mill stone placed around the neck of a child will limit his growth. It means that the engineer will not advance, and society will not have the benefit of that engineer's full capability.

The traditional approach to Kinematics and Dynamics has long been graphical. This has entailed large scale layouts of mechanisms with a very sharp pencil to draw solutions. The accuracy of such solutions is inherently limited by the accuracy of the drawing and the width of the pencil lines. In the mechanical watch industry where the author once worked, it was common to draw mechanisms forty times oversize $(40:1)$ in order to see part engagements and clearances.

With the microcomputer now available on every engineer's desk, scale drawings must be a thing of the past for several reasons. Most importantly, there is the matter of accuracy; the microcomputer can provide almost instant solutions accurate to eight or more digits with ease. Perhaps more importantly, the microcomputer makes it possible to solve mechanism problems for many positions, where a graphical solution requires a complete new drawing for each position.

One of the objectives of this book is to encourage readers to make full use of all the mathematics that they may know, and where necessary, to seek out additional knowledge. To this end, complete mathematical descriptions of actual physical systems are emphasized, while graphical solutions are ignored.

1.3.1 Calculus

Sir Isaac Newton is usually credited with the invention of calculus. Strangely, it was an outbreak of plague that contributed to this creation, an outbreak that interrupted his studies at Cambridge University during the years 1665 - 1667. When he was forced to leave the university and return to his rural home to escape the disease, the solitude of the countryside provided the opportunity for the development of many important discoveries, including the law of universal gravitation and differential and integral calculus [1][1]. The co-inventor of calculus, Gottfried Wilhelm Leibniz, began to publish some of his first work on calculus, beginning in 1684 [2].

Given the long time that calculus has been available for use, it is very sad that most graduate engineers today make little or no use of this powerful tool. The principal questions of kinematics, namely position, velocity, and acceleration, naturally call for the use of calculus for their proper description. The areas of dynamics and vibrations each resolve largely into the formulation and solution of ordinary differential equations. It is therefore entirely natural that students working in this area should expect to apply calculus freely; it is the natural language of the subject matter.

1.3.2 Matrix Notation

Many of the problems to be encountered in this book involve vector quantities. If written out in scalar form, there are at least two equations to be considered simultaneously, and often many more. In some cases, it is convenient to use vector notation to formulate such problems, but when it is time to compute numbers, vector notation does not lend it self to digital computation because the computer cannot deal with vectors as such. The computer can, however, readily deal with arrays of numbers, and any vector can be represented as a one dimensional array. If $\mathbf{a}$ is a vector in three dimensions with components a_x, a_y, and a_z, then these can be very neatly considered as a column vector $\{a\} = \mathrm{col}\,(a_x, a_y, a_z)$.

Throughout this book, matrix notation is used extensively. In particular, note that

- $\{a\}$ denotes a column vector $(n \times 1)$
- (a) denotes a row vector $(1 \times n)$
- $\{a\}^T$ denotes the transpose of $\{a\}$, $\quad \{a\}^T = (a)$
- $[b]$ denotes a rectangular array, usually square $(n \times n)$

[1] See References at the end of the chapter.

- $\lceil b \rfloor$ denotes a diagonal rectangular array $(n \times n)$[2]
- $\lceil I \rfloor$ is the diagonal matrix called the identity matrix = diag$(1, 1, 1, \ldots 1)$
- $[b]^T$ denotes the transpose of $[b]$, obtained by interchanging rows and columns
- $[b]^{-1}$ denotes the inverse of $[b]$, which if it exists, is such that $[b]\,[b]^{-1} = [b]^{-1}\,[b] = [I]$

Matrix notation is only a *notation*, but it has much to recommend it. By itself, it does nothing that could not be done in other ways, but it provides an orderly, systematic means to deal with the computational bookkeeping problem. It adapts readily to computer implementation in a way such that when a problem is formulated in matrix notation, the computer code required for the solution is usually quite easily written.

1.4 Computer-Aided Solutions

Engineering analysis always revolves around problem solving of one type or another, and the computer can be a great aid in many situations. It is a mistake, however, to ever think that the computer can do the entire job, an attitude that often leads to much lost time. This misunderstanding becomes obvious when the steps involved in problem solving are considered, so a quick review is provided here.

The typical steps involved in solving a mechanics of machines problem are these:

1. **Problem Definition.** This is the task of determining exactly what problem is to be solved and what information is available to begin the solution process. Failure to attend properly to this step often results in great loss of time!
2. **Conceptual Solution.** Based on the information gathered in step 1, an overall plan of attack must be formulated. This plan is established on the assumption that no unexpected difficulties arise. For this reason, the plan of attack may require later modification. Despite that possibility, there is no point at all in beginning without at least a tentative route to the solution in mind. If a computer solution is indicated, a rough flow chart should be drafted at this point.
3. **Detailed Analysis.** The conceptual solution usually presumes that the governing equations can all be written. This is the point where that step must be actually performed and the equations developed. It is time to establish all of the necessary equations and put them in the form required for later use. This step

[2]Brackets closed at one end only, such as $\lceil b \rfloor$, are intended to suggest the need only to capture the main diagonal of the array, whereas brackets closed at both ends, like $[b]$, suggests the need to contain all rows and columns.

often involves (a) the use of calculus, and (b) casting the resulting equations in matrix form. At the end of this step, all engineers should be prepared to turn to the computer for numerical solution.

4. **Computer Implementation.** This is the point where computer code is written, debugged, and finally executed to produce the final numerical results. The need to test the code, often in pieces before requiring everything to work together, is absolutely vital. If any part of the code fails to function, you can be assured it will not all function together! As an example, consider a kinematics problem that requires determining position, velocity and accelerations functions. It is wise to assure that the position solution is correct before attempting to program the velocity and acceleration solutions. Each depends on the part that proceeds it, and thus errors in the early stages simply propagate into the latter parts.

5. **Interpretation of Results.** This is the most essential part of any analysis. Engineering analysis is always done with a purpose – to answer a particular question. Typical acceptable results are, (a) "The maximum velocity is 187 m/s^2," or (b) "The maximum bearing force occurs when the crank position is $\theta = 205^o$," or (c) "The arm will fail due to excessive dynamic loading." It is **never sufficient** to submit a stack of computer output as an engineering report. Often, it is useful to submit the computer output as an appendix to your report, and to indicate in that output where the results appear. This indication may be done simply by circling the results with a red pen, or it may be something you program the computer to identify for you, such as with a row of asterisks and a label like `********* Max Velocity`.

1.5 Programming Languages

There are a great number of computer languages in use today for engineering work. The days are long gone when FORTRAN was the standard engineering computer language, and new languages are regularly coming into use. The primary claim for many of the newer languages is greater execution speed. Indeed, greater speed is significant for applications like real-time control and robotic systems. On the other hand, for typical engineering desk work, it matters very little whether the execution time is measured in microseconds or milliseconds. For this latter case, what is important is (1) ease of program development, (2) availability of features such as matrix operations, plotting, and other utilities. In recent years, there has been great interest in languages such as C, C++, and other similar programs. On the other side of the fence, there are many who prefer the use of packages such as MathCAD®, MATLAB®, Mathematica®, or Maple®. Each of these has its own particular merits, and personal familiarity is a major factor as well. In the hands of a skilled user, it is probable that any of these is adequate to the tasks at hand.

In developing an engineering textbook, it is often useful to include sample programs to illustrate various ideas in the text. For this purpose, a choice must be made that will serve all users. The choice made in this case is a language called True BASIC®, a version of the BASIC computer language re-worked by the original creators of BASIC, Prof. John Kemeny and Prof. Thomas Kurtz both of Dartmouth, after receiving much feedback. It is relatively fast, powerful, easy to use, and most importantly, the code is rather transparent. In saying that the code is transparent, what is intended is to convey the idea that the actions of the code are completely obvious to anyone with a computer background. Thus a user of another language can easily read a True BASIC program file and know what it does. He can quickly and rather easily make whatever changes may be required to cast the code into his preferred language.

With regard to True BASIC itself, the author has used this language for many years in personal research, in consulting work, in work for the US Navy, and as a teaching tool. It provides the user with excellent control and functionality. All of the common matrix operations are available as single line statements, so it is well adapted to mechanics of machines problems. The numerical results are usually correct to between 14 and 15 decimal digits, far more than is usually required for engineering work.

Because True BASIC was developed by mathematicians (Kemeny and Kurtz), the standard form for every replacement statement is "`LET x = ...`" where the `LET` is a reflection of the mathematician's mode of speech. Because this author does not like to use `LET` to begin every replacement, all the example programs begin with the statement `OPTION NOLET` which simply tells the code not to expect `LET`. True BASIC also allows array indices to begin with either 0 or 1. Beginning with 0 is usually a bad practice, so most of the example programs include the statement `OPTION BASE 1`. This has the effect to set all array counters initially to 1. Both of these statements, `OPTION NOLET` and `OPTION BASE 1`, simply become standard parts of every program.

1.6 Units

The question of what system of units to use is an continuing problem for engineering students, educators, and practicing engineers. The large majority of the countries of the world use the International System of Units (SI), although often not in its pure form. In many places, it is common practice to introduce non-SI units, such as the bar for pressure, even though it does not follow strict SI conventions. On the other side, the USA is a major factor in world trade, and it continues to use the US Customary System of Units (USC). This situation seems unlikely to change in the near future.

There are advantages to each system. The obvious advantage of the SI system is the incorporation of powers of 10, with prefixes that denote the required exponent. On the other side, the meter is far too large a unit to use for measuring the thickness of sheet

metal; inches are much more to the scale of most mechanical engineering matters. The Newton is a very small force unit, while the meter is relatively large. This makes the basic SI unit for either pressure or stress, the Pascal, extremely small. It is so small that 10^5 Pascal = 1 bar is just a little under one atmosphere or 14.7 pounds per square inch. The final answer appears to be that, there are advantages to both systems, and both units will continue in use for an extended time.

What this means for the student or the practicing engineer is simply this: It is necessary to be able to work in both systems of units, depending on the situation at hand. Each person will no doubt have their personal preference, usually for the system with which they are most acquainted, but it will be important to be fluent in the use of both systems.

If mathematical equations are written correctly, the entire matter of units should be transparent. All equations should be written such that they are **valid in any consistent system**. That is the key right there, the use of consistent units throughout every equation. Both the SI and US Customary systems are fully consistent within themselves, so every engineer should be able to use either. One of the essential requirements, however, is to use the correct units only. Thus, if working in SI, pressure or stress should always be expressed in Pascals (Pa), not in megapascals even if it may be convenient to convert the final result to megapascals or bars. Similarly, if working in USC, mass must always be expressed in proper mass units, namely a pound-second square per inch (lb-s^2/in), even through the unit appears clumsy and has no generally accepted name. In USC, weight or any other force is always in pounds; in SI, weight or any force must be in Newtons (N). The use of pressure or stress in units such as kilograms/cm^2 is entirely incorrect, and it will result in hopeless confusion.

As a general rule, problems should always be worked in the units in which the problem data appears. This minimizes the opportunity for errors introduced in converting units. If the given data is partly in one system and partly in another, then a choice must be made. It is usually best to convert as little of the data as possible, again, to minimize opportunities for error.

There is, however, one significant exception to the general rule given in the previous paragraph. If the work involves any sort of electrical or magnetic variables, the only reasonable choice is to use SI units. The USC units for electrical and magnetic quantities are absurdly difficult to use. It is always recommended model and solve electrical or electromechanical problems in SI units.

Table 1.1 Unit Conversions

Quantity	**USC Unit**		**SI Equivalent**	
Time	1 sec	=	1 sec	exact
Length	1 in	=	0.0254 m	exact
Force	1 lb	=	4.448222 N	
Mass	1 $\frac{\text{lb-s}^2}{\text{in}}$	=	175.12685 kg	
Mass Moment				
of Inertia	1 lb-s^2-in	=	0.1129848 kg-m^2	
Work	1 in-lb	=	0.1129848 J	[=]N-m
Power	1 $\frac{\text{in-lb}}{\text{s}}$	=	0.1129848 W	[=] $\frac{\text{N-m}}{\text{s}}$
Linear Spring Stiffness	1 $\frac{\text{lb}}{\text{in}}$	=	175.12685 $\frac{\text{N}}{\text{m}}$	
Torsion Spring Stiffness	1 $\frac{\text{in-lb}}{\text{rad}}$	=	0.1129848 $\frac{\text{N-m}}{\text{rad}}$	
Linear Damping Coeff	1 $\frac{\text{lb}}{\text{in/s}}$	=	175.12685 $\frac{\text{N}}{\text{m/s}}$	
Torsional Damping Coeff	1 $\frac{\text{in-lb}}{\text{rad/s}}$	=	0.1129848 $\frac{\text{N-m}}{\text{rad/s}}$	

1.7 Unit Conversions

There are times when it is necessary to convert between SI and USC units in order to get all of the problem data into a consistent system. In so far as possible, the most exact conversions possible should be used. It is useful to keep in mind that 25.4 mm = 1.0 inches is an exact conversion relation for length. One of the most important physical constants is the acceleration of gravity. While not entirely constant, it varies only slightly from one location to another. For the purposes of this book, the value is taken as $g = 9.807$ m/s^2, rounded from the exact value defined by the National Institute of Standards and Technology (NIST) as $g = 9.80665$ m/s^2 (exact value). For USC units, the exact standard gravity value converts to $g = 386.088583$ m/s^2, which for most purposes is rounded to $g = 386.088$ in/s^2. The following table will facilitate units conversions where required. One other constant that is useful is the atmospheric pressure. In USC units, $P_{atm} = 14.7$ lb/in^2, which is equivalent to the SI value $P_{atm} = 101325$ Pa.

1.8 Conclusion

The discussion about the use of calculus, matrix notation, computer problem solving, and the matter of computer languages indicate the nature of the material to follow in this book. It is certainly assumed that computer solutions are the ultimate goal in all that follows. The discussion regarding degrees of freedom and generalized variables is perhaps the most critical part of this chapter because there will be frequent mention of the number of degrees of freedom in a particular system throughout the remainder of the book. This is essential to understanding that which follows. The reader is encouraged to look for all of these ideas as they develop in the remainder of the book.

References

[1] Simmons, G.F., *Calculus Gems*, McGraw-Hill, 1992, p. 131.

[2] ibid., p. 154.

Problems

Determine the number of degrees of freedom for each of the following systems, using the approach described in this chapter. Fully document your reasoning for each case. In making the determination, make the following assumptions:

(a) All bodies are rigid, so there are no deformations;

(b) Belts do not slip or creep;

(c) All single-pin joints allow rotation;

(d) All bodies are free to move in two dimensions unless restraint is indicated.

In the event of an ambiguity, explain the possibilities and determine the number of degrees of freedom for each case.

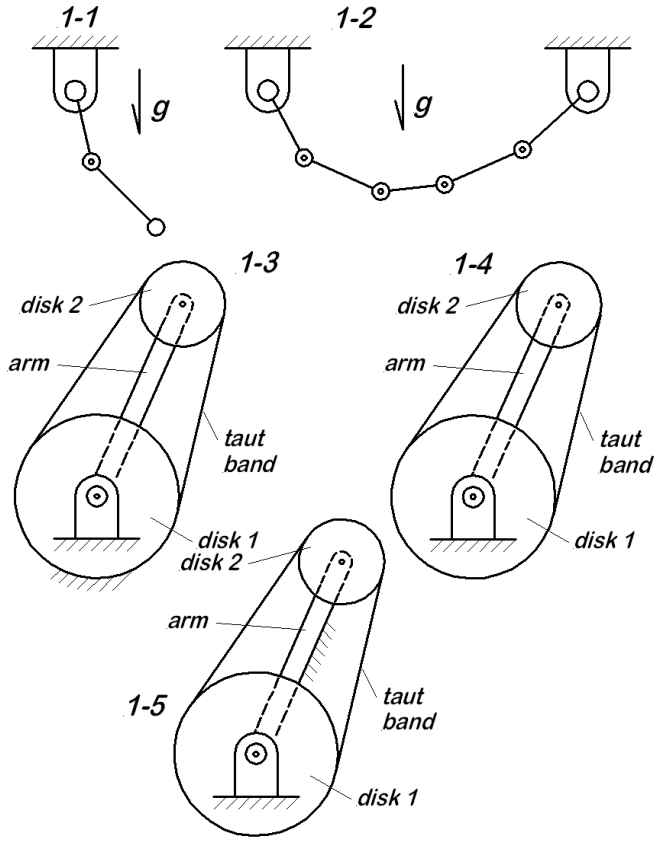

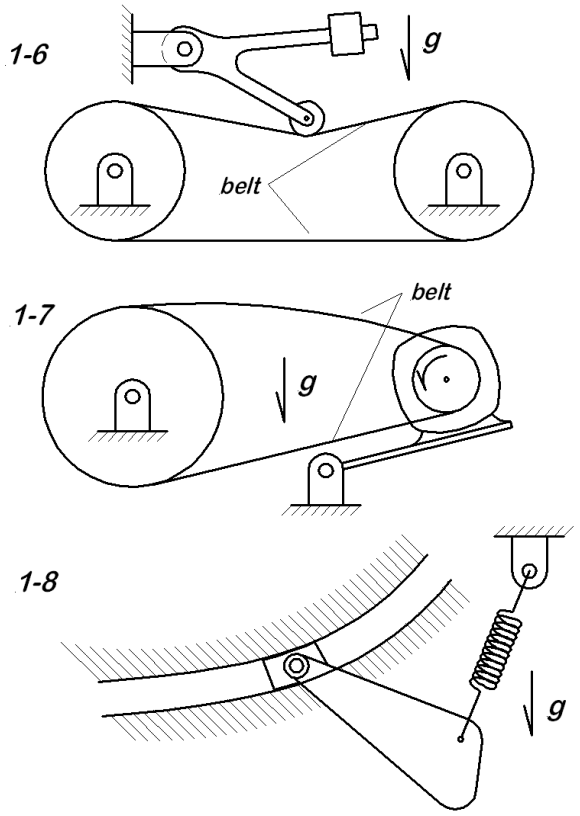

1-9

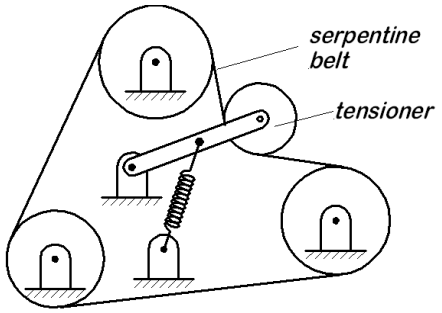

1-10

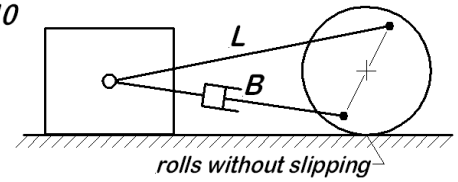

1-11

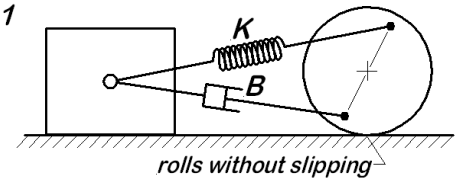

1-12

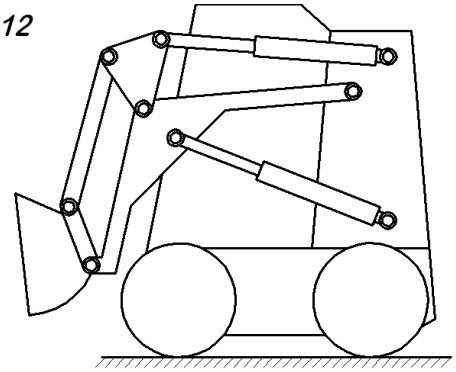

1-13

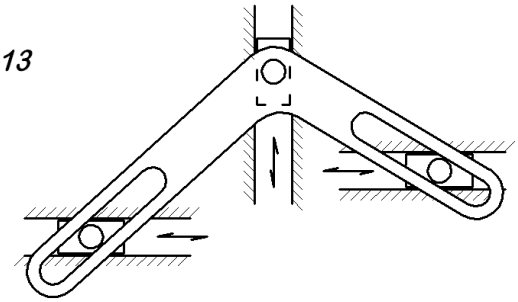

1-14

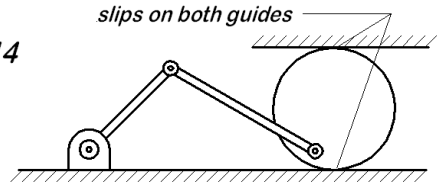

1-15

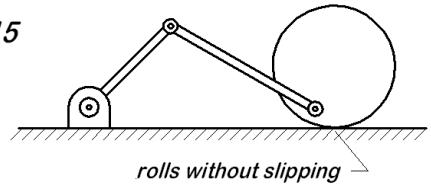

1-16

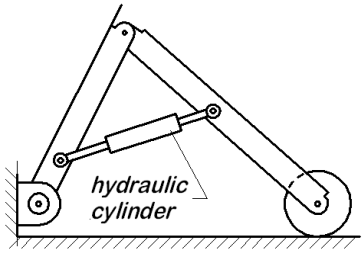

1-17

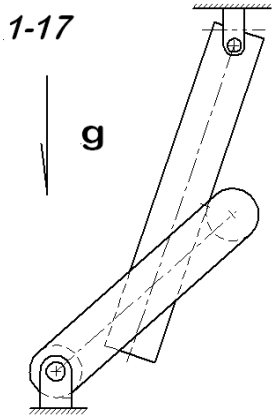

1-18

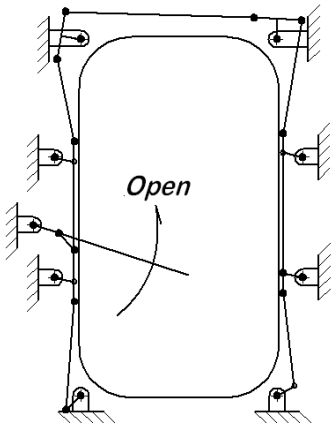

Exterior Door Locking
Linkage for Warship

Part I

Kinematics of Mechanisms

Chapter 2

SDOF Kinematics

2.1 An Overview of the Process

This chapter addresses the kinematic analysis of mechanisms having only one degree of freedom. Recall from Chapter 1.2, one degree of freedom means that only one primary variable is required to fully define the position of all parts of the mechanism. For a kinematic analysis, the one degree of freedom is associated with some suitable coordinate, the primary variable, and considered as an assigned value (an "input") for the problem. In some cases, the problem statement may ask for solutions throughout a specified range on the primary variable, such as over one crank revolution. Such a problem statement asks for a sequence of solutions, one for every position of the primary variable within the range. The value of using the computer for these many solutions is obvious.

The complete kinematic analysis of a mechanism is usually understood to mean development of equations describing the position, velocity, and acceleration of all points of interest in the mechanism for chosen values of the primary variable, its speed, and its acceleration. In many cases, the position, velocity coefficients, and velocity coefficient derivatives (the latter two concepts yet to be defined) are actually preferable, particularly if the kinematic solution is for use in a static or dynamic analysis.

Here the process is presented in some detail by means of a simple example. Later sections in this chapter present two important common cases, the slider-crank mechanism and the four-bar linkage. The introduction of constraints describing sliding and rolling is introduced in Chapter 2.7. The final section discusses single degree of freedom mechanisms with multiple loops.

2.2 Crank-Lever Mechanism Example

For an introductory example, consider the crank-lever mechanism shown pictorially in Figure 2.1. and in a kinematic skeleton in Figure 2.2. In Figure 2.1, the drawing looks like the actual machine parts while in Figure 2.2, the drawing preserves only the functional features of the mechanism, without keeping the actual shape of the parts.

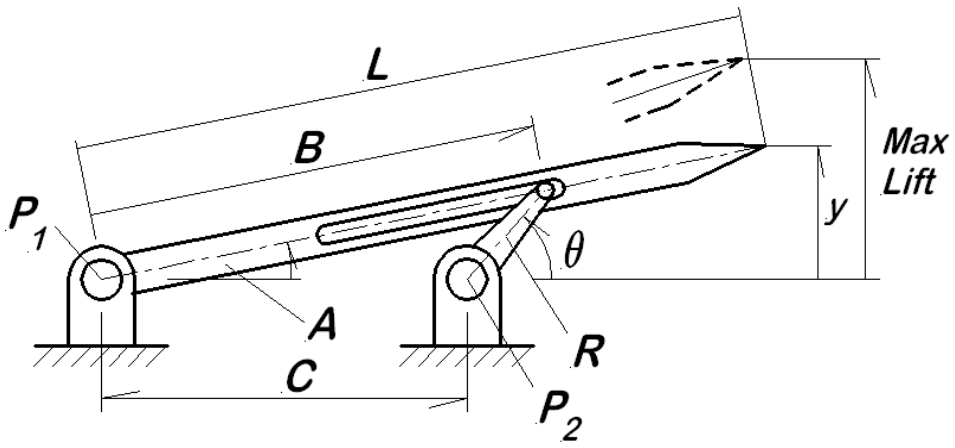

Figure 2.1: Pictorial Representation of Crank-Lever Mechanism

The lever is pivoted at point P_1 while the crank rotates through a full circle about point P_2. Figure 2.1 shows the crank tip engaging a slot in the lever while Figure 2.2 shows the lever as a rod passing through a block at the crank tip. Both constructions are possible, and they are kinematically equivalent; they produce exactly the same motion. This simple mechanism is found in various feeder devices and other machines.

The center-to-center distance C and the crank radius R are known dimensions. If a value is assigned to the crank angle θ, the mechanism configuration is fully specified, so this is evidently a single degree of freedom (SDOF) system. The position variables that remain to be determined are the angle A and the distance B.

2.2.1 Position Analysis

The first step is to establish the position vector loop equations. Consider the three position vectors $\mathbf{B}$, $\mathbf{C}$, and $\mathbf{R}$ shown in Figure 2.3. By vector arithmetic, it is evident that

$$\mathbf{B} - \mathbf{R} - \mathbf{C} = \mathbf{0} \tag{2.1}$$

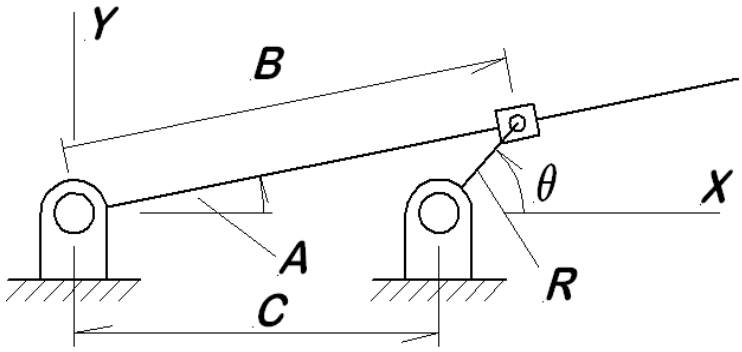

Figure 2.2: Kinematic Skeleton for Crank Lever Mechanism

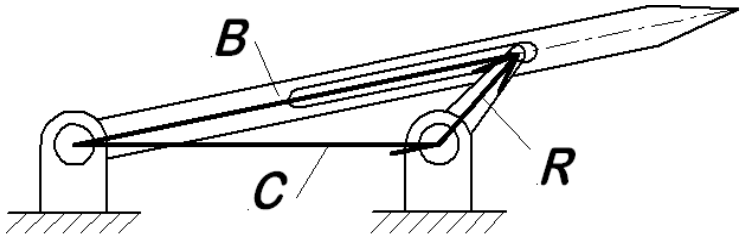

Figure 2.3: Position Vector Loop

or, in scalar form,

$$B\cos A - R\cos\theta - C = 0 \qquad \text{horizontal component} \tag{2.2}$$

$$B\sin A - R\sin q = 0 \qquad \text{vertical component} \tag{2.3}$$

These equations, equation (2.2) and (2.3), are the nonlinear position vector loop equations for this mechanism. The angle θ is assigned, and the dimensions C and R are known, but the secondary variables, A and B, remain unknown.

The next step is to solve these equations for A and B. In many cases, this step will require numerical solution, but for this example, that is not the case. The possibility of a closed form (algebraic) solution should always be considered, and developed if possible.

Eliminating B between equations (2.2) and (2.3) gives

$$\tan A = \frac{R\sin\theta}{C + R\cos\theta} \tag{2.4}$$

from which A can be determined using the principal value of the arctangent function. With A then known, B is determined by solving either of the equations:

$$B = \frac{C + R\cos\theta}{\cos A} \qquad \text{or} \qquad B = \frac{R\sin\theta}{\sin A} \tag{2.5}$$

There are definitely positions for which $\sin A$ is zero, and for some proportions of the linkage, $\cos A$ can also go to zero. Even if both of these events can occur, they do not happen simultaneously, so B can always be evaluated using one of these expressions. For computer implementation, an appropriate test (`if abs(cos(A))<0.1 then ...`) should be included to choose the appropriate expression for evaluating B.

If the calculations are to be done numerically (in a computer), this is quite far enough. Only if further analysis is to be done with these results should any consideration be given to algebraically eliminating A from the calculation of B. For computer work, this elimination is a definite waste of time.

2.2.2 Velocity Analysis

In performing the velocity analysis, it is assumed that the position analysis has been previously performed and that those results are available as well as the original known data. For this problem, this means that the known information now includes θ, R, C, A, B and $\dot{\theta}$ while the unknowns now sought are $\dot{A}$ and $\dot{B}$. The velocity loop equations are obtained by differentiating the position loop equations to give

$$\dot{B}\cos A - B\dot{A}\sin A + R\dot{\theta}\sin\theta = 0 \tag{2.6}$$

$$\dot{B}\sin A + B\dot{A}\cos A - R\dot{\theta}\cos\theta = 0 \tag{2.7}$$

In view of the information already known, these are actually a pair of linear simultaneous algebraic equations in the two unknowns $\dot{A}$ and $\dot{B}$. This is perhaps more clearly evident when they are cast in matrix form as

$$\begin{bmatrix} -B\sin A & \cos A \\ B\cos A & \sin A \end{bmatrix} \begin{Bmatrix} \dot{A} \\ \dot{B} \end{Bmatrix} = \dot{\theta}R \begin{Bmatrix} -\sin\theta \\ \cos\theta \end{Bmatrix} \tag{2.8}$$

To solve these equations in closed form, it is necessary to premultiply by the inverse of the coefficient matrix on the left[1]. The determinant of the coefficient matrix is simply $-B$. The solution for the velocities is

$$\begin{aligned} \begin{Bmatrix} \dot{A} \\ \dot{B} \end{Bmatrix} &= -\frac{\dot{\theta}R}{B} \begin{bmatrix} \sin A & -\cos A \\ -B\cos A & -B\sin A \end{bmatrix} \begin{Bmatrix} -\sin\theta \\ \cos\theta \end{Bmatrix} \\ &= \dot{\theta} \begin{Bmatrix} (R/B)\cos(A-\theta) \\ R\sin(A-\theta) \end{Bmatrix} \end{aligned} \tag{2.9}$$

[1] For the case of a (2×2) matrix, Appendix 1.5 provides the closed form inverse. Because this occurs often in simple problems, this is worth noting.

Note that this solution shows each of the unknown velocities, $\dot{A}$ and $\dot{B}$, as the product of the primary velocity, $\dot{\theta}$, multiplied by a position dependent factor. This suggests the definition of the *velocity coefficients* as

$$K_A(\theta) = \frac{\dot{A}}{\dot{\theta}} = (R/B)\cos(A-\theta) \tag{2.10}$$

$$K_B(\theta) = \frac{\dot{B}}{\dot{\theta}} = R\sin(A-\theta) \tag{2.11}$$

For any value of $\dot{\theta}$, the velocity analysis is readily accomplished by simply evaluating the velocity coefficient without the need to specify a value for $\dot{\theta}$.

2.2.3 Acceleration Analysis

In order to develop the acceleration analysis, it is assumed that all of the previous results are available. Thus the list of known data now includes C, R, θ, A, B, $\dot{\theta}$, $\dot{A}$, $\dot{B}$, and additionally, $\ddot{\theta}$. The unknowns to be determined are $\ddot{A}$ and $\ddot{B}$.

There are two approaches to the acceleration analysis; both are described here because each gives a different insight into the process. The first is time differentiation of the scalar velocity loop equations (2.6) and (2.7). This gives

$$\ddot{B}\cos A - 2\dot{A}\dot{B}\sin A - B\ddot{A}\sin A - B\dot{A}^2\cos A + R\ddot{\theta}\sin\theta + R\dot{\theta}^2\cos\theta = 0 \tag{2.12}$$

$$\ddot{B}\sin A + 2\dot{A}\dot{B}\cos A + B\ddot{A}\cos A - B\dot{A}^2\sin A - R\ddot{\theta}\cos\theta + R\dot{\theta}^2\sin\theta = 0 \tag{2.13}$$

Once again, the result is a pair of linear, simultaneous algebraic equations in the unknowns $\ddot{A}$ and $\ddot{B}$, because all of the nonlinear terms involve only quantities previously determined. As before, the linear relation is more apparent when these equations are cast in matrix form:

$$\begin{bmatrix} -B\sin A & \cos A \\ B\cos A & \sin A \end{bmatrix} \begin{Bmatrix} \ddot{A} \\ \ddot{B} \end{Bmatrix} = \begin{Bmatrix} 2\dot{A}\dot{B}\sin A + \dot{A}^2 B\cos A - R\ddot{\theta}\sin\theta - R\dot{\theta}^2\cos\theta \\ -2\dot{A}\dot{B}\cos A + \dot{A}^2 B\sin A + R\ddot{\theta}\cos\theta - R\dot{\theta}^2\sin\theta \end{Bmatrix} \tag{2.14}$$

When this system is solved for $\ddot{A}$ and $\ddot{B}$, and the $\dot{A}$ and $\dot{B}$ factors are replaced in terms

of the velocity coefficient expressions, the result is

$$\ddot{A} = \ddot{\theta}\frac{R}{B}\cos(A-\theta) + \frac{\dot{\theta}^2}{B}\left[-2K_A K_B + R\sin(A-\theta)\right] \tag{2.15}$$

$$\ddot{B} = \ddot{\theta}R\sin(A-\theta) + \dot{\theta}^2\left[K_A^2 B - R\cos(A-\theta)\right] \tag{2.16}$$

Equations (2.15) and (2.16) show that the accelerations, $\ddot{A}$ and $\ddot{B}$, each consists of two terms, one proportional to $\ddot{\theta}$ and a second proportional to $\dot{\theta}^2$. The fact that this is true, and the significance of the two factors, is more evident when the second approach to acceleration analysis is employed. For that purpose, return to the velocity coefficient relations written as

$$\dot{A} = \dot{\theta}\cdot K_A(\theta) \tag{2.17}$$

$$\dot{B} = \dot{\theta}\cdot K_B(\theta) \tag{2.18}$$

The accelerations are obtained directly by differentiating these expressions, where the chain-rule is required in the differentiation of the velocity coefficients.

$$\ddot{A} = \ddot{\theta}K_A(\theta) + \dot{\theta}^2\frac{dK_A(\theta)}{d\theta} \tag{2.19}$$

$$\ddot{B} = \ddot{\theta}K_B(\theta) + \dot{\theta}^2\frac{dK_B(\theta)}{d\theta} \tag{2.20}$$

With this approach to the acceleration analysis, it is evident that the two terms are:

(1) the velocity coefficient multiplying the primary acceleration,

(2) the velocity coefficient derivative multiplying the square of the primary velocity.

Looking back at the first approach, it can be seen that the coefficients are indeed just as described. This leads to the formal definition of two more functions called *velocity coefficient derivatives*, denoted $L_A(\theta)$ and $L_B(\theta)$

$$L_A(\theta) = \frac{d}{d\theta}K_A(\theta) = \frac{d^2}{d^2\theta}A(\theta) \tag{2.21}$$

$$L_B(\theta) = \frac{d}{d\theta}K_B(\theta) = \frac{d^2}{d^2\theta}B(\theta) \tag{2.22}$$

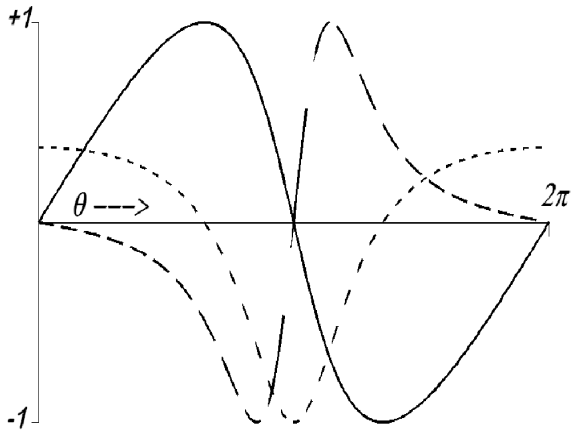

Figure 2.4: Normalized Plots of $A(\theta)$ (full line), $K_A(\theta)$ (short dash), and $L_A(\theta)$ (long dash) Versus θ

2.2.4 Numerical Values

For numerical evaluation of this example, specific data are required, so the following values are assigned:

$$C = 2.5 \text{ in.}$$
$$R = 0.75 \text{ in.}$$

The previous analysis is implemented numerically, and the results are plotted in normalized form[2] for one full crank revolution in Figures 2.4 and 2.5.

2.2.4.1 Summary of Observations

The simple Crank-Lever Mechanism analysis shows many features that are common to other single degree of freedom system analyses. Note particularly the following points:

1. The position loop equations are developed using the known dimensional data and understanding the primary variable to be assigned at will. These position loop equations are solvable for the secondary variables, either in closed form or by numerical means.

[2] To plot a function in normalized form means that the function is divided by its maxium value, so that the extreme points on the curve lie at either +1 or -1. This has the benefit of expanding each curve to the largest possible view for maximum detail. It does mean that values cannot be compared between curves. This type of plotting is used frequently in this book.

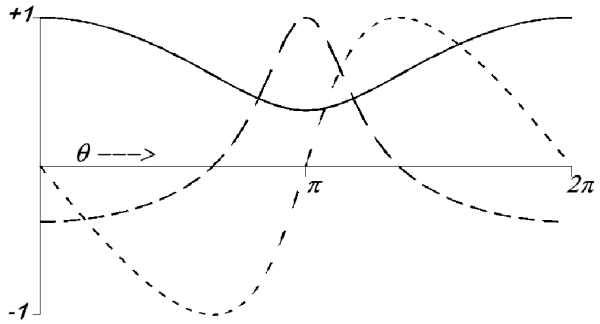

Figure 2.5: Normalized Plots for B (full line), $K_B(\theta)$ (short dash), and $L_B(\theta)$ (long dash) Versus θ

2. The velocity analysis begins with the differentiation of the position loop equations to obtain the velocity loop equations. This differentiation may be either with respect to time to obtain the secondary velocities, or with respect to the primary variable to obtain the velocity coefficients.

3. The acceleration analysis continues with the differentiation of the velocity equations to obtain the secondary accelerations. If time differentiations are employed, the actual secondary accelerations are obtained. If the differentiations are with respect to the primary variable, the velocity coefficient derivatives are obtained. Both approaches have value in different circumstances.

4. The extreme values of the $B(\theta)$ curve (Figure 2.5) set the limits on the minimum length for the slot, remembering that there must also be room for the pin that connects the two.

For the Crank-Lever Mechanism, the position loop equations are of the form

$$f_1(\theta, A, B) = 0 \tag{2.23}$$
$$f_2(\theta, A, B) = 0 \tag{2.24}$$

When these are differentiated to obtain the velocity equations and those are cast in matrix form, the coefficient matrix on the left side is of the form

$$\begin{bmatrix} \frac{\partial f_1}{\partial A} & \frac{\partial f_1}{\partial B} \\ \frac{\partial f_2}{\partial A} & \frac{\partial f_2}{\partial B} \end{bmatrix} = \begin{bmatrix} -B\sin A & \cos A \\ B\cos A & \sin A \end{bmatrix} \tag{2.25}$$

This is called the *Jacobian Matrix* for this system. The left side of equation (2.25) is the general form for a Jacobian while the right side is simply the form for this particular

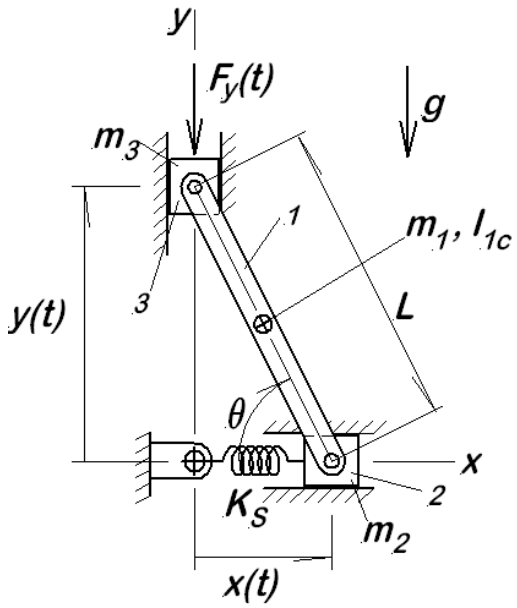

Figure 2.6: Spring-Loaded Trammel

example. This same Jacobian is also seen in the acceleration equation solution. When it is necessary to solve the position equations numerically, the Jacobian matrix figures prominently in the numerical solution process called the Newton-Raphson solution (see Appendix 2). The appearance of the Jacobian matrix in these three related instances is not accidental, and it is to be expected. Should it fail to appear, this is an indication that an error has likely been made.

Whenever the Jacobian matrix is to be evaluated numerically, the same block of code, in the form of a subroutine, should be used for each evaluation. The position solution, velocity solution, and acceleration solution will exist only when the determinant of the Jacobian matrix is non-zero. Positions for which the Jacobian is zero are called *singular points*; these positions require special treatment.

2.3 Example: Spring-Loaded Trammel

Figure 2.6 shows a mechanism called a trammel; the complete system is shown in considerable detail. The trammel consists of a single link, item 1, with two sliders that move in guides along the $x-$ and $y-$ axes, items 2 and 3, respectively. The data considered as known include L, the length of the link, m the mass of the link, I_c the mass moment of inertia for the link with respect to the link center of mass, m_x and m_y, the masses of the two sliders, and K, the spring constant. The link is symmetric from end to end, so the center of mass is at the middle of the link. For the present example, two things are

required:

1. Express all of the system geometric configuration in terms of a single primary variable;
2. Express the center of mass coordinates in terms of that same primary variable.

Before attacking the problem requirements, it is well to study the given figure in some detail. Notice in particular that:

- The direction of the acceleration of gravity is shown, indicating that the mechanism operates in the vertical plane;
- A spring is shown, acting on the horizontal slider;
- A force, $F_y(t)$, is shown acting on the vertical slider.

Remembering that this problem is a purely kinematics problem, do any of these three bits of information make any difference? The general answer is NO, they are all irrelevant, and this is typical of many real engineering problems. It is often necessary to sort out irrelevant information and not let it distract attention from what is actually important. That said, the presence of the spring does have some limited significance. It suggests that the range of motion of the horizontal slider will be limited; the spring can only be stretched up to its breaking point. Otherwise, the presence of all of these extraneous bits of information is simply a distraction, but they happen frequently in actual practice.

The first step in the kinematic analysis is the determination of the number of degrees of freedom and the choice of a primary variable. It is quickly evident that if any one of x, y, or θ are known, then entire system configuration is determined, and thus there is only one degree of freedom. Similarly, any one of these three variables is a satisfactory choice as the primary variable. For the present example, the variable θ is chosen as primary, and both x and y are then expressed in terms of θ. By inspection, the secondary variable positions are

$$x(\theta) = L\cos\theta \tag{2.26}$$
$$y(\theta) = L\sin\theta \tag{2.27}$$

Taking derivatives produces the velocity coefficients and the velocity coefficient derivatives

$$K_x(\theta) = -L\sin\theta \tag{2.28}$$
$$K_y(\theta) = L\cos\theta \tag{2.29}$$
$$L_x(\theta) = -L\cos\theta \tag{2.30}$$
$$L_y(\theta) = -L\sin\theta \tag{2.31}$$

The center of mass of the link is at the mid–point, so that $(x_c, y_c) = [x(\theta)/2, y(\theta)/2]$. The kinematics of this system are very simple indeed, and the center of mass values are simply half of these values above. This completes the kinematic analysis.

2.4 Kinematics of the Slider-Crank

One of the most important common mechanisms is the Slider-Crank Mechanism. It is the principal part of many air and steam engines, compressors, pumps, crushers, pumps, and injectors. It is central to the diesel and gasoline engines that are so much a part of modern life. It is shown in kinematic skeleton form in Figure 2.7. In most cases, the crank rotates continuously in the same direction, although there are applications where the crank motion may be oscillatory. The analysis presented here is sufficiently general to apply to any slider-crank device.

As shown in Figure 2.7, the crank rotates about a fixed pivot located at the origin of the $X-Y$ coordinate system. The $X-$axis passes through the pivot point, and runs parallel to the direction of the slider motion. Note, however, that the slider may be offset an amount ε as shown. The offset may be positive (as shown), zero, or negative. In many applications, $\varepsilon = 0$, but this is only a minor matter. The $Y-$axis is perpendicular to X at the origin. The crank is joined to the slider by means of the connecting rod, a link of fixed length, L. The crank radius, R, the connecting rod length, L, and the offset, ε, are all considered as known dimensional data. The crank angle, θ, the connecting rod obliquity angle, ϕ, and the slider position, x, are all variables.

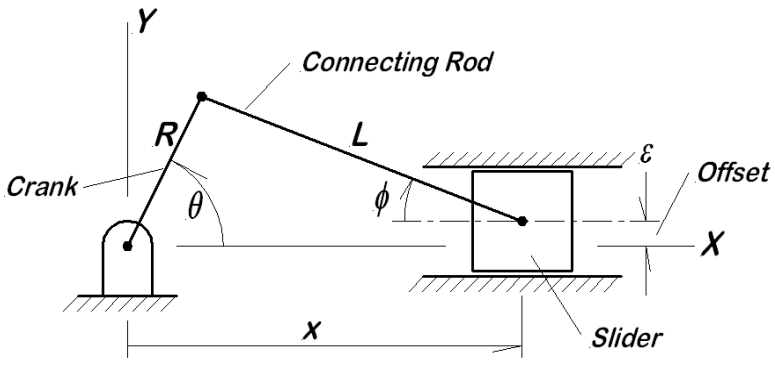

Figure 2.7: Kinematic Skeleton for Slider-Crank Mechanism

2.4.1 Number of Degrees of Freedom

Before beginning the kinematic analysis, it is necessary to determine the number of degrees of freedom associated with the mechanism. For this purpose, consider Figure 2.8. All dimensional data are known, and the process begins by assigning a value to the crank angle, θ. With this, the crank can be laid off, as in Figure 2.8 (a). Using the value of the offset, ε, the center line of the slider motion can be laid out, as in Figure 2.8 (b). The connecting rod is located by swinging an arc, centered on the crank tip and having the radius equal to the connecting rod length, L, as shown in Figure 2.8 (c). The intersection of that arc with the slider center line determines the second end of the connecting rod. It only remains to draw in the slider, as in Figure 2.8 (d), to complete the kinematic skeleton.

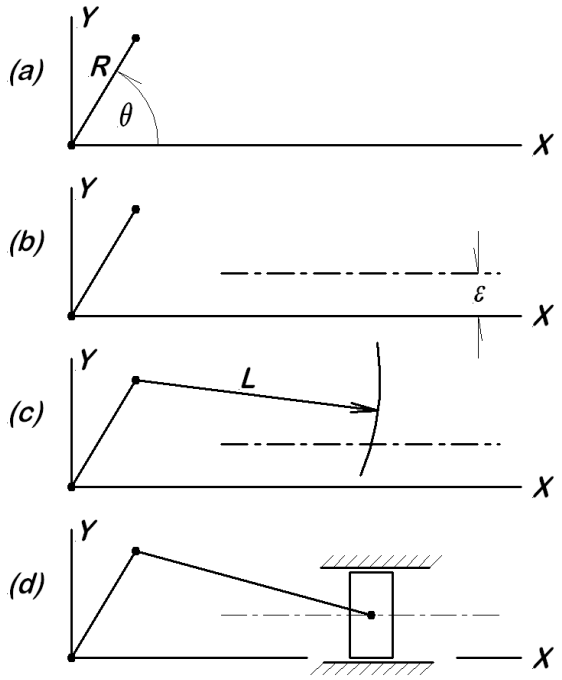

Figure 2.8: Construction to Demonstrate SDOF Nature of Slider-Crank

Now, look back at the process. With the dimensional data known, once the crank angle is assigned, all other positions are fully determined. This demonstrates that there is only a single degree of freedom in the slider-crank mechanism.

The graphical thought process just described has broad applicability; it can be adapted to determine the number of degrees of freedom for a wide variety of mechanisms. In every case, the central question is, "How many variables must be assigned (in addition to the dimensional data) to graphically construct the mechanism?" The word *construct*

means that known lengths or angles can be measured and laid out accordingly. Other points must be located and lines defined strictly in the sense of Euclidean geometric construction, performed using only a compass and straight edge. When this approach is applied to systems with multiple degrees of freedom, the need to specify additional variables becomes apparent as the construction proceeds. Except for very complicated systems, it is rarely necessary to actually draw the construction; for most engineers a mental construction is sufficient.

2.4.2 Position Analysis

As discussed in the previous section, the slider-crank mechanism position is fully determined by a single variable, here taken as the crank angle, θ. The secondary variables of interest are the connecting rod obliquity angle, ϕ, and the slider position, x (see Figure 2.7). It is convenient to think in terms of a single position vector loop, starting at the origin, moving out to the tip of the crank, down along the connecting rod to the slider, dropping down the amount of the offset, and then returning to the origin. Based on that loop, the following scalar loop equations are written:

$$R\cos\theta + L\cos\phi - x = 0 \tag{2.32}$$

$$R\sin\theta - L\sin\phi - \varepsilon = 0 \tag{2.33}$$

These equations are solved for ϕ and x to give

$$\phi = \arcsin\left(\frac{R\sin\theta - \varepsilon}{L}\right) \tag{2.34}$$

$$x = R\cos\theta + L\cos\phi \tag{2.35}$$

Because the angle ϕ can only lie in the first or fourth quadrants, the principal value of the arcsine is correct. These solutions are readily checked by substitution back into the position loop equations.

2.4.3 Velocity Coefficients

The object at this point is to obtain the position dependent velocity coefficients, $K_\phi(\theta)$ and $K_x(\theta)$. To this end, differentiate the position loop equations with respect to θ to obtain

$$-R\sin\theta - K_\phi L\sin\phi - K_x = 0 \tag{2.36}$$

$$R\cos\theta - K_\phi L\cos\phi = 0 \tag{2.37}$$

When these two equations are recast in matrix form, the result is

$$\begin{bmatrix} -L\sin\phi & -1 \\ -L\cos\phi & 0 \end{bmatrix} \begin{Bmatrix} K_\phi \\ K_x \end{Bmatrix} = R \begin{Bmatrix} \sin\theta \\ -\cos\theta \end{Bmatrix} \tag{2.38}$$

The (2×2) matrix on the left side of equation (2.38) is the Jacobian matrix for the slider-crank mechanism. In Appendix 1, the closed form solution for a system of two, simultaneous, linear equations is shown. For the present system of equations, the solution is

$$\begin{aligned} \begin{Bmatrix} K_\phi(\theta) \\ K_x(\theta) \end{Bmatrix} &= \frac{-R}{L\cos\phi} \begin{bmatrix} 0 & 1 \\ L\cos\phi & -L\sin\phi \end{bmatrix} \begin{Bmatrix} \sin\theta \\ -\cos\theta \end{Bmatrix} \\ &= \begin{Bmatrix} R\cos\theta/(L\cos\phi) \\ -R\sin\theta - R\cos\theta\tan\phi \end{Bmatrix} \end{aligned} \tag{2.39}$$

The expression for $K_x(\theta)$ is further simplified by using the second of the positions equations to replace $R\sin\theta$ with $L\sin\phi + \varepsilon$. After some algebra, the final result is

$$K_x(\theta) = -(\varepsilon + x\tan\phi) \tag{2.40}$$

2.4.4 Velocity Coefficient Derivatives

As mentioned earlier, there are two approaches to obtaining the accelerations. The indirect approach is used here, that based on separating the accelerations each into two terms, one dependent on the primary acceleration while the other depends on the square of the primary velocity. To that end then, the objective at this point is to obtain the velocity coefficient derivatives. This begins by differentiating equations (2.36) and (2.37) with respect to θ to obtain

$$-R\cos\theta - L_\phi L\sin\phi - K_\phi^2 L\cos\phi - L_x = 0 \tag{2.41}$$

$$-R\sin\theta - L_\phi L\cos\phi + K_\phi^2 L\sin\phi = 0 \tag{2.42}$$

These equations are then recast into matrix form to obtain

$$\begin{bmatrix} -L\sin\phi & -1 \\ -L\cos\phi & 0 \end{bmatrix} \begin{Bmatrix} L_\phi \\ L_x \end{Bmatrix} = \begin{Bmatrix} R\cos\theta + K_\phi^2 L\cos\phi \\ R\sin\theta - K_\phi^2 L\sin\phi \end{Bmatrix} \tag{2.43}$$

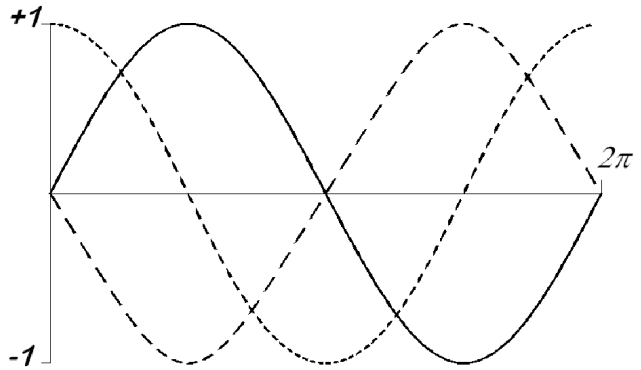

Figure 2.9: Normalized plots of $\phi(\theta)$ – solid line, $K_\phi(\theta)$ – dotted line, and $L_\phi(\theta)$ – broken line versus θ for a full crank revolution

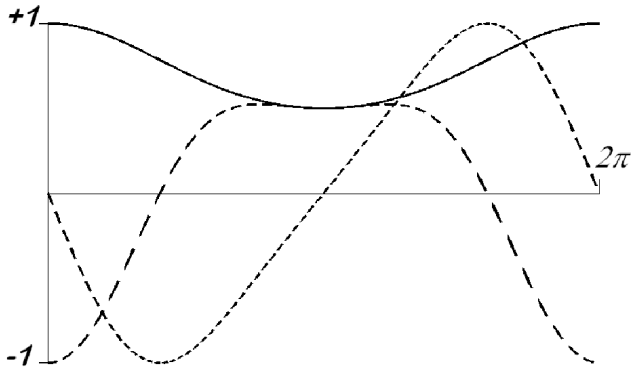

Figure 2.10: Normalized plots of $x(\theta)$ – solid line, $K_x(\theta)$ – dotted line, and $L_x(\theta)$ – broken line versus θ for one full crank revolution

for which the solution is

$$\left\{ \begin{array}{c} L_\phi(\theta) \\ L_x(\theta) \end{array} \right\} = \left\{ \begin{array}{c} -R\sin\theta / \left(L\cos\phi\right) + K_\phi^2 \tan\phi \\ -\left[LK_\phi^2 + R\cos\left(\theta+\phi\right)\right] / \cos\phi \end{array} \right\} \tag{2.44}$$

To illustrate the application of these equations, consider a slider-crank mechanism with the parameters: $R = 0.2850$ m, $L = 1.400$ m, and zero offset. The obliquity angle and the slider position plots are shown in Figures 2.9 and 2.10.

In Figure 2.9, the plots of ϕ, K_ϕ, and L_ϕ versus θ, the extreme values of the functions are: $\phi_{\max} = 0.205$ rad, $K_{\phi_{\max}} = 0.2036$ rad/rad, and $L_{\phi_{\max}} = 0.2080$ rad/rad. Similarly, in Figure 2.10, the extreme values are: $x_{\max} = 1.6845$ m, $K_{x_{\max}} = 0.2908$ m/rad, and $L_{x_{\max}} = 0.3430$ m/rad. Note the units attached to each function; these are the result of the units of the input data, in this case, SI units for the lengths.

2.4.5 Motion of Points of Interest

Up to this point, the kinematic analysis has only provided information about a few aspects of the motion, primarily the motion of the pin joints. It is common to require information about other points within each body. Such additional points are usually referred to as "points of interest." A typical example is the center of mass of a particular machine component. This type of requirement is addressed here in the context of the slider-crank mechanism, but the ideas presented are applicable to systems of all sorts.

2.4.5.1 Body Coordinate Systems

In order to deal with additional points in a mathematical description, it is necessary to first have a means to describe the location of such points within the body. In the development of the slider-crank kinematics to this point, the external coordinate system $O - XY$ has been used; this is usually called a *global* or *base coordinate system.* Later, when dealing with dynamics, the global coordinates are considered to be fixed (inertial) coordinates. What is needed to locate specific points within a moving part is a *body coordinate system*, that is, a coordinate system fixed to the body and moving with it.

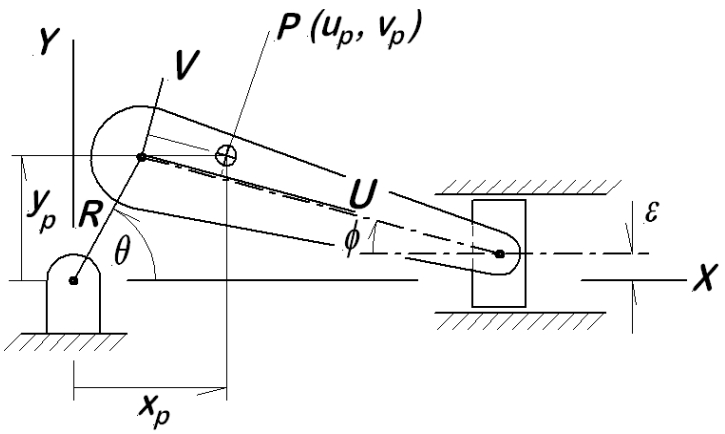

Figure 2.11: Slider-Crank Pictorial Showing Connecting Rod Body Coordinates

In Figure 2.11, the connecting rod is shown as an asymmetrical body, with the body coordinate system $U - V$ indicated. (The asymmetrical connecting rod form is not uncommon in diesel engines; it is done ease of removal from the engine.) The origin of the $U - V$ system is at the crank pin, and the $U-$axis is along the connecting rod center line. The $V-$axis is perpendicular to the $U-$axis at the origin. In every case, it is up to the user to define body coordinates as needed. They should always be located with respect to some clearly defined features of the body (in this case, the origin at one of the pin connections and the $U-$axis along the line between the two pin connections).

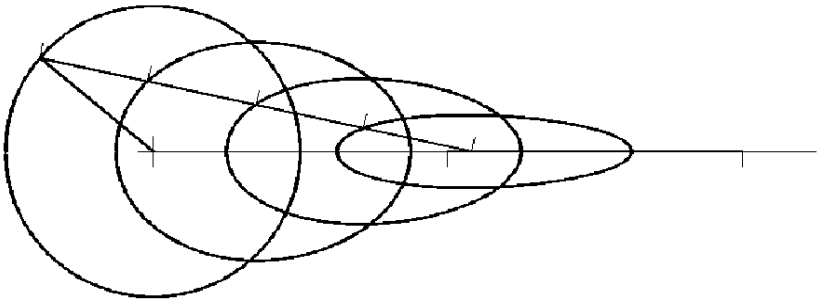

Figure 2.12: Slider-Crank Connecting Rod Point Loci

2.4.5.2 Position

A point P having body coordinates (u_p, v_p) is indicated. Any point in the body can be identified simply by giving the proper body coordinates for the point. The body coordinates move with the body, so the location of any point in the body is a constant in that coordinate system. For any particular point, (u_p, v_p), there are also global coordinates, (x_p, y_p) that vary with the crank angle, θ. From the geometry, it is evident that

$$x_p(\theta) = R\cos\theta + u_p\cos\phi + v_p\sin\phi \tag{2.45}$$
$$y_p(\theta) = R\sin\theta - u_p\sin\phi + v_p\cos\phi \tag{2.46}$$

Provided the initial kinematic analysis has already been completed for $\phi(\theta)$ and $x(\theta)$, it is a simple matter to evaluate the global coordinates for the point P.

Figure 2.12 shows the slider-crank mechanism in the position $\theta = 2.0$ and also the paths traced by five equally spaced points on the connecting rod. The point at the left end is connected to the crank, and thus travels with it in a circular path. Similarly, the point at the right end is connected to the slider and travels with it in a straight line. Short vertical marks denote the ends of the slider stroke. The three intermediate points on the connecting rod each trace ovals of a sort; note that short marks perpendicular to the connecting rod centerline denote the particular points.

2.4.5.3 Velocity

The velocity components for point P relative to the global coordinates are found by differentiation:

$$\dot{x}_p = \dot{\theta}\left[-R\sin\theta - K_\phi\left(u_p\sin\phi - v_p\cos\phi\right)\right] \tag{2.47}$$
$$\dot{y}_p = \dot{\theta}\left[R\cos\theta - K_\phi\left(u_p\cos\phi + v_p\sin\phi\right)\right] \tag{2.48}$$

From the form of these two equations, it is evident that there are two velocity coefficients for the point P,

$$K_{px}(\theta) = -R\sin\theta - K_\phi(u_p\sin\phi - v_p\cos\phi) \tag{2.49}$$
$$K_{py}(\theta) = R\cos\theta - K_\phi(u_p\cos\phi + v_p\sin\phi) \tag{2.50}$$

This is exactly analogous to the situation for the secondary variables, with the exception that there are two velocity coefficients because the point is moving in two dimensions.

2.4.5.4 Velocity Coefficient Derivatives

The velocity coefficient derivatives are readily determined by differentiation,

$$\begin{aligned} L_{px}(\theta) &= \frac{d}{d\theta}K_{px}(\theta) \\ &= -R\cos\theta - L_\phi(u_p\sin\phi - v_p\cos\phi) \\ &\quad -K_\phi^2(u_p\cos\phi + v_p\sin\phi) \end{aligned} \tag{2.51}$$

$$\begin{aligned} L_{py}(\theta) &= \frac{d}{d\theta}K_{py}(\theta) \\ &= -R\sin\theta - L_\phi(u_p\cos\phi + v_p\sin\phi) \\ &\quad -K_\phi^2(-u_p\sin\phi + v_p\cos\phi) \end{aligned} \tag{2.52}$$

so that, once again,

$$\ddot{x}_p = \ddot{\theta}\,K_{px}(\theta) + \dot{\theta}^2\,L_{px}(\theta) \tag{2.53}$$
$$\ddot{y}_p = \ddot{\theta}\,K_{py}(\theta) + \dot{\theta}^2\,L_{py}(\theta) \tag{2.54}$$

With these tools in hand, the position, velocity, and acceleration of any point in the connecting rod can be calculated with ease.

For design studies, it may be of interest to study the path (locus of positions) for several points as the crank sweeps out a full revolution. This is a simple matter in a computer code that, for each crank angle, (1) evaluates the secondary variables, their velocity coefficients, and velocity coefficient derivatives, and (2) calculates global coordinates, global velocity coefficients, and global velocity coefficient derivatives.

2.5 Kinematics of the Four-Bar Linkage

The four-bar linkage is one of the most versatile common mechanisms. It is found in a wide variety of machines, including clamps, oil field pump jacks, electric shavers, hidden

hinges, and centerless grinders, to name only a few. The variety of motions that can be generated with the four-bar linkage include approximate straight lines (Watt and Scott Russel linkages), closed curves, and even circles (Galloway mechanism). This wide range of adaptability has attracted the interest of designers of the years down to the present day.

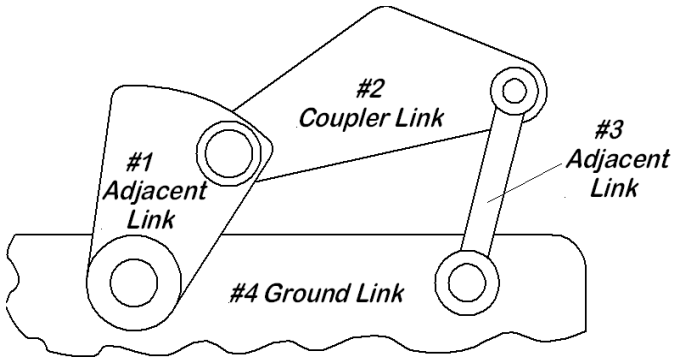

Figure 2.13: Pictorial Representation of Typical Four-Bar Linkage

The four-bar linkage consists of four bars or links of constant length, as the name implies. Figure 2.13 shows a pictorial view of a typical four-bar linkage. The four links are connected by four pin (revolute) joints. One of the links is usually stationary, in which case, it is called the *ground link,* item #4. It does not look like a link in the usual sense, but it functions exactly like the others in maintaining the distance between the two pivot points supporting the rest of the mechanism. There are two links, each adjacent to the ground link, #1 and #3, and opposite the ground link is the *coupler link,* #2. A link that is able to rotate in a full circle is called a *crank*; it is said to *revolve.* A link that does not able to revolve must oscillate and is called a *rocker.*

Four-bar linkages are usually used in one of two ways:

1. The mechanism is used to transmit motion from one link adjacent to the ground link (called the *input link*) to the other adjacent link (the *output link*);

2. A point on the coupler may be driven along a useful path by the input crank rotation. That path is often called a *coupler curve.*

It is also possible, but relatively uncommon, for the input to a force or torque applied to driving a specific point on the coupler.

2.5.1 Classification: Grashof's Criterion

For any collection of four links, there is the immediate question as to what sorts of motion they permit. Consider four links, where s denotes the length of the shortest link, p and q are the two intermediate lengths, and l is the length of the longest link. For the moment, assume that all of the lengths are distinct, that is, that no two are equal to each other, so that $s < p < q < l$.

First, it is evident that for assembly (that is, in order to be able to put the joint pins in place), it must be true that

$$l \leq s + p + q \tag{2.55}$$

If the equality holds, then the links will assemble, but they will be unable to move. That case is simply a structure and is of no further interest here; it is therefore assumed that the inequality is satisfied.

> Grashof's Theorem states that a necessary and sufficient condition that at least one link will be a crank (that is, capable of full rotation), provided that
>
> $$s + l < p + q \tag{2.56}$$
>
> If this condition is met, the linkage is said to be a Grashof mechanism. If the condition is not satisfied, then the linkage is said to be non-Grashof and no link will be a crank. Grashof's theorem was first stated in 1883, but not formally proven until 1979 [1].

For a Grashof mechanism, the location of the shortest link further assigns the mechanism to one of three categories, remembering that there is always at least one crank in a Grashof mechanism:

1. If the shortest link is adjacent to the ground, the mechanism is called a *crank-rocker*. The link opposite the shortest link will execute an oscillatory motion only.
2. If the shortest link is the ground link, then both adjacent links are cranks capable of full rotation. The mechanism is called a *double crank mechanism*.
3. If the shortest link is shortest, both of the links adjacent will be rockers, a *double rocker mechanism*. The coupler will, however, be fully able to revolve.

For a non-Grashof mechanism (where the inequality is reversed), there will be no links able to revolve, but all will be rockers only. Such a mechanism is called a *triple rocker mechanism*.

All of this is summarized in the following Table 2.1:

Table 2.1 Four Bar Linkage Types[3]

Case	$\frac{l+s}{p+q}$	Location of Shortest Link	Mechanism Type
—	—	————	————
A	< 1	Adjacent to Ground	Crank Rocker
B	< 1	Ground Link	Double Crank
C	< 1	Coupler Link	Double Rocker
D	$= 1$	Anywhere	Change Point
E	> 1	Anywhere	Triple Rocker

Note that, in the table above, Cases A, B, and C all satisfy the Grashof condition, while the last Case, E, describes a non-Grashof mechanism.

If, instead of the inequality there is an equality as indicated in Case D of the table above, the mechanism is said to be Grashof neutral, and is called a *change point mechanism*. This is most easily understood in the context of a specific example. Consider a four bar linkage of the change point type, at rest along the positive $x-$axis. The input link is pivoted at the origin, and it is colinear with the coupler, both extending to the right. From the extreme right, the output link extends back to the left where it connects to the ground link. If the input link is moves counter clockwise, the left end of the coupler must rise and move to the left. This can be accomplished by having the right end of the coupler

(1) move up and to the left, or

(2) move down and to the left.

Either of these will satisfy the demands of the input link motion, but neither is preferred. The situation is kinematically indeterminate. In an actual physical system, if it was already in motion, momentum would carry it through the change point, but for a purely kinematic system, or for a physical system at rest so that there is no momentum, the motion is completely indeterminate. The colinearity condition will occur twice per revolution of the input link, meaning that this indeterminate condition exists twice in every revolution of the input link.

[3] Adapted from [1].

It should be noted that all the discussion of classification is of very little value in terms of analysis. The value of classification is primarily in design, where it can serve as a guide to choosing a four-bar linkage suited to a particular purpose. Thus, for example, if an application requires that the output link be able to revolve in response to a revolution of the input link, then only Grashof linkages will be suitable, and of those, only choices where the ground link is shortest will do the job.

2.5.2 Position Loop Equations

The four-bar linkage is a single degree of freedom mechanism. This is readily seen by mentally applying the "graphical construction" test described earlier in this chapter to the crank-lever and slider-crank mechanisms. It is most often convenient to associate the one degree of freedom with the angular position of the input crank. It is on this basis that the position, velocity, and acceleration analyses are now developed for the four-bar linkage. The equations developed in the position analysis do admit of closed form solutions (see Crossley [2] and also Shigley and Uicker [3] for this solution), but the process is not very enlightening and a bit unwieldy. Instead, the opportunity is taken here to introduce a general numerical technique, the Newton-Raphson Method, for solving the position equations. This method is developed in Appendix 2 for those wanting more mathematical detail

For purposes of analysis, consider the four-bar linkage shown in Figure 2.14 where

C_1 = length of input link

C_2 = length of the coupler link

C_3 = length of the output link

C_4 = length of the ground link

θ = input crank angle

α = coupler angle

β = second crank angle

Note that there are other possible choices for the angle of the output link, all equally workable. The choice made here has the small advantage that all of the angles are acute and therefore the deduction of the proper terms for the position loop equations is easier. As usual, the input variable, θ is understood to be specified, along with all of the dimensional values, C_1, C_2, C_3, and C_4. The objective is to write equations for the

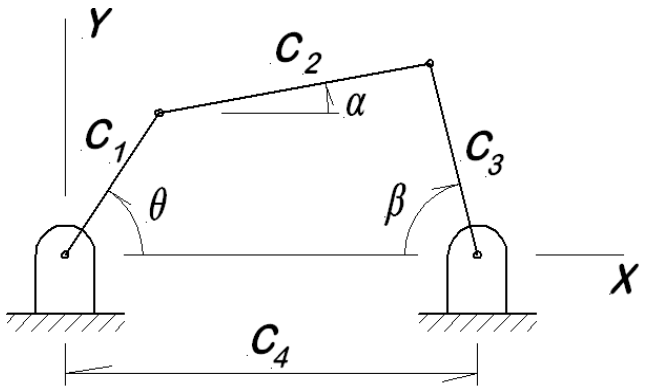

Figure 2.14: Kinematic Skeleton for Four-Bar Linkage

determination of α and β, the two secondary variables. The position loop equations are

$$f_1(\theta, \alpha, \beta) = C_1 \cos\theta + C_2 \cos\alpha + C_3 \cos\beta - C_4 = 0 \tag{2.57}$$

$$f_2(\theta, \alpha, \beta) = C_1 \sin\theta + C_2 \sin\alpha - C_3 \sin\beta = 0 \tag{2.58}$$

2.5.2.1 Newton-Raphson Solution

The solution of these equations is not self-evident. As mentioned earlier, a numerical procedure called the Newton-Raphson Method is to be used to solve these equations. The details of the Newton-Raphson solution are given in Appendix 2 and should be reviewed at this point if unfamiliar. In the notation of the development given in the Appendix, the vector of unknowns is called $\{S\}$ for secondary variables,

$$\{S\} = \begin{Bmatrix} \alpha \\ \beta \end{Bmatrix} \tag{2.59}$$

and the residual vector is $\{F\}$,

$$\{F\} = \begin{Bmatrix} f_1(\theta, \alpha, \beta) \\ f_2(\theta, \alpha, \beta) \end{Bmatrix} \tag{2.60}$$

The Jacobian matrix, $[J]$, for this system is determined by partial differentiation, with the result

$$[J] = \begin{bmatrix} \frac{\partial f_1}{\partial \alpha} & \frac{\partial f_1}{\partial \beta} \\ \frac{\partial f_2}{\partial \alpha} & \frac{\partial f_2}{\partial \beta} \end{bmatrix} = \begin{bmatrix} -C_2 \sin\alpha & -C_3 \sin\beta \\ C_2 \cos\alpha & -C_3 \cos\beta \end{bmatrix} \tag{2.61}$$

Using the residual vector $\{F\}$ and the Jacobian $[J]$ just defined, the position loop solution may be computed iteratively to any required degree of precision. This is demonstrated in an example problem that follows shortly.

One requirement for the application of the Newton-Raphson method is an initial estimate for the solution. This estimate may be obtained in many possible ways, including a rough calculation, scaling of a graphical solution, or simply a good guess; any reasonably close initial estimates will suffice because the process converges for a wide range of initial estimates. Conversely, the better the initial estimate, the more rapidly the process converges to an acceptable solution. If the initial estimates are too far afield, the solution may well converge to another solution, one that is not useful for present purposes.

2.5.2.2 Kinematic Singularity

There are situations where assigned values of the input angle lead to impossible geometries. Most often this happens when the system simply cannot be assembled in the position assigned. To see a specific example of this, consider the four-bar linkage shown in Figure 2.14 for which the link lengths are

$$C_1 = 1.4379 \quad C_3 = 1.6641$$
$$C_2 = 2.3365 \quad C_4 = 3.5000$$

where the units are irrelevant; only the ratios of the link lengths are relevant. First look at the Grashof criterion:

$$\frac{s+l}{p+q} = \frac{1.4379 + 3.5000}{1.6641 + 2.3365} = \frac{4.9379}{4.0006} > 1 \tag{2.62}$$

Since the ratio is greater than 1, it is evident that this is a non-Grashof linkage, and no link will revolve. If none revolve, then there will be definite limits to the motion, and the system is a triple rocker. How do the limits occur?

In this example, the limiting conditions are rather easy to visualize; they happen when the coupler link aligns with either the input or output link. This exact linkage is shown in a multi-position plot in Figure 2.15. Imagine the input link starting at the initial position, $\theta \approx -99.6500^o$. In that position, the coupler link is aligned with the output link, with $\alpha = -\beta \approx 20.75^o$. It is not possible for θ to become any more negative without stretching the coupler link – output link combination. This is a kinematic singularity.

Next, consider the input link to move in a counter clockwise sense, causing the coupler to move upward and to the right as shown in the early intermediate positions. At $\theta \approx 20.10^o$, the input link and the coupler become colinear. This results in another

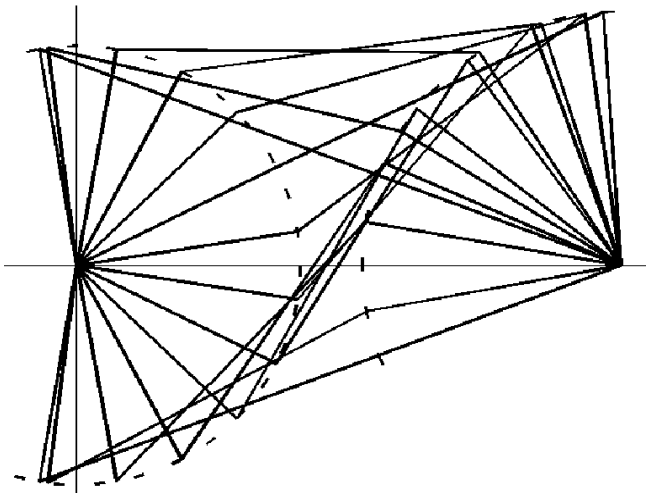

Figure 2.15: Motion of Four-Bar Linkage Showing Singular Configurations

kinematic singularity, with $\beta \approx 86.19^o$. There is no possibility of a greater value for β as this would necessitate stretching the input link and coupler combination.

Finally, as the input crank continues to move counter clockwise, at $\theta \approx +99.6500^o$, the motion is again stopped, another kinematic singularity. This is simply the mirror image of the starting position, so the angles are just the negatives of those at the beginning. Note that, as demonstrated, no link is able to fully revolve, and the mechanism is truly a triple rocker.

One of the important characteristics of a kinematic singularity is the vanishing of the Jacobian determinant. Thus, at the singular positions, the value of the Jacobian goes to zero and the Jacobian matrix cannot be inverted. This means that the position loop equations, as written in equations (2.57) and (2.58), cannot be solved by Newton-Raphson. Kinematic singularities require special handling. If a conventional position loop solution is attempted by Newton-Raphson but the Jacobian is found to be zero (or any extremely small value), a singular condition should be suspected.

Program FourBar.Tru, Newton-Raphson Solution for the Four-BarLinkage

```
100 ! FourBar.Tru
101 OPTION NOLET
102 OPTION BASE 1
103 DIM x(2),f(2),d(2),jac(2,2),jaci(2,2)
```



```
104 img$="   theta = +###.### deg  alpha = +###.### deg  beta = +###.### deg"
105 CLEAR
106 c1=1.4370
107 c2=2.3365
108 c3=1.6641
109 c4=3.5000
110 th1=-99.65*pi/180                ! extreme angle
111 alpha1=20.7527*pi/180            ! known from separate
112 beta1=-20.7527*pi/180            ! solution
113 th=th1
114 x(1)=0.5                         ! starting solution estimates
115 x(2)=-0.18
116 ! Print initial extreme position
117 PRINT using img$: th1*180/pi,alpha1*180/pi,beta1*180/pi
118 ! Begin Newton-Raphson for intermediate positions
119 jmx=11                           ! number of interior positions
120 itmx=30                          ! max number of iterations allowed
121 FOR j=1 to jmx
122     th=-1.7+(j-1)*3.4/(jmx-1)
123     FOR i=1 to itmx
124         alpha=x(1)               ! extract current estimates
125         beta=x(2)
126         f(1)=c1*cos(th)+c2*cos(alpha)+c3*cos(beta)-c4
127         f(2)=c1*sin(th)+c2*sin(alpha)-c3*sin(beta)
128         fsq=f(1)^2+f(2)^2        ! f-squared
129         IF fsq<1e-12 then EXIT FOR     ! normal exit
130         jac(1,1)=-c2*sin(alpha)  ! evaluate Jacobian
131         jac(1,2)=-c3*sin(beta)
132         jac(2,1)=c2*cos(alpha)
133         jac(2,2)=-c3*cos(beta)
134         MAT jaci=inv(jac)
135         MAT d=jaci*f             ! calculate adjustment
136         dsq=d(1)^2+d(2)^2        ! d-square
137         MAT x=x-d                ! revised solution estimates
138         IF dsq<1e-14 then
139            PRINT "  i = ";i
140            PRINT "  f-square = ";fsq
141            PRINT "  d-square = ";dsq
142            PRINT "  d-square too small, solution stalled"
143            STOP
144         END IF
145         IF i=itmx then
146            PRINT "   fsq = ";fsq
147            PRINT "   exceeds iteration limits, no solution"
```



```
148            STOP
149         END IF
150     NEXT i
151     alpha=x(1)                    ! extract converged values
152     beta=x(2)
153     PRINT using img$: th*180/pi,alpha*180/pi,beta*180/pi
154 NEXT j
155 ! Print solution for final extreme position
156 PRINT using img$: -th1*180/pi,-alpha1*180/pi,-beta1*180/pi
157 END
```

The computer listing shown above illustrates the application of the Newton-Raphson solution technique for the intermediate positions; the extreme positions are understood to have been previously determined by a different program. There are a number of comments to be made regarding this program.

1. The program is written in True BASIC, and is entirely executable exactly as printed here.
2. The line numbers are entirely unnecessary; they are provided only for ease in discussing the code. They can be removed completely without affecting the program at all.
3. The first line, #100, is a comment, giving the name of the program. It is not executable.
4. The next line, #101, eliminates the requirement for `LET` at the beginning of each replacement statement.
5. Line #102 declares the starting index for all arrays to 1 (the option 0 is also allowed).
6. Line #103 declares the several arrays that will be used.
7. Line #104 defines the format for the output list that will be the final result of the calculation.
8. Line #105 simply clears the screen.
9. Lines #106 – #109 declare the problem data, the link lengths.
10. Lines #110 – #112 state the extreme position solution found by means of another program; this is taken as input data for this program to be included in the final listing for completeness.
11. Line # 113 sets the initial value of `th=th1`, the starting value for $\theta = \theta_1$.

12. Lines #114 and #115 assign the starting estimates for α and β equal to the values for the extreme position.

13. Line #117 prints the first output, the solution for the initial extreme position.

14. Line #119 specifies the number of interior positions.

15. Line #120 specifies the maximum number of iterations allowed for any single solution.

16. Line #121 begins the sweep through the interior solutions in 11 steps.

17. Line #122 assigns the value of θ for each solution, varying θ in steps of 0.34 radians. It is written in this form because in program development, it was convenient to vary the number of steps, and this form simply specifies the prescribed number of equal increments.

18. Line #123 begins the inner loop to execute the Newton-Raphson iterative solution.

19. Lines #124 and #125 extract the values of α and β from the vector of unknowns, `x()`, so that they may be used to express the functions f_1 and f_2 in the customary notation.

20. Lines #126 and #127 evaluate the functions f_1 and f_2 defined by the loop equations.

21. Line #128 calculates $|f|^2$ to be used in the termination test of line #129.

22. Lines #130 – #133 evaluate the Jacobian matrix to be inverted in line #134.

23. Line #135 calculates the adjustment vector $\{d\}$, and line #136 evaluates $|d|^2$.

24. Line #137 calculates the latest revision of the solution estimates.

25. Lines #138 – #144 test for termination based on a small adjustment and print warnings before stopping execution.

26. Lines #145 – #149 end the process when the number of iterations exceeds the allowed limit, along with printing a warning.

27. Line #150 sends the Newton-Raphson process back to the beginning.

28. If the solution process gets to line #151, the solution is understood to be fully converged and the values are extracted for output at line #153.

29. Line #154 send the angle sweep back to the beginning, line #121, to be executed for the next angle. *Note that, in so doing, the last solution found becomes the initial estimate for the next position.* This works extremely well provided the positions are fairly close to each other.

30. Line #156 prints the final extreme position solution to complete the table.

31. The results from the computer code are presented as a table such as that shown below. Please note that, for output only, the angles are expressed in degrees, but for all computations, the angles are in radian measure.

Table 2.2 Output from FourBar.Tru

theta =	- 99.650 deg	alpha =	+ 20.753 deg	beta =	- 20.753 deg
theta =	- 97.403 deg	alpha =	+ 28.745 deg	beta =	- 10.434 deg
theta =	- 77.922 deg	alpha =	+ 47.858 deg	beta =	+ 11.342 deg
theta =	- 58.442 deg	alpha =	+ 57.389 deg	beta =	+ 26.544 deg
theta =	- 38.961 deg	alpha =	+ 60.306 deg	beta =	+ 42.587 deg
theta =	- 19.481 deg	alpha =	+ 55.515 deg	beta =	+ 60.384 deg
theta =	+ .000 deg	alpha =	+ 43.904 deg	beta =	+ 76.816 deg
theta =	+ 19.481 deg	alpha =	+ 30.331 deg	beta =	+ 85.569 deg
theta =	+ 38.962 deg	alpha =	+ 18.769 deg	beta =	+ 84.124 deg
theta =	+ 58.442 deg	alpha =	+ 9.353 deg	beta =	+ 74.580 deg
theta =	+ 77.922 deg	alpha =	+ .434 deg	beta =	+ 58.766 deg
theta =	+ 97.403 deg	alpha =	- 13.537 deg	beta =	+ 31.849 deg
theta =	+ 99.650 deg	alpha =	- 20.753 deg	beta =	+20.753 deg

2.5.3 Velocity Coefficients

The velocity coefficients are determined in the conventional manner by differentiating the position loop equations (2.57) and (2.58) with respect to the input angle θ, to give

$$[J] \begin{Bmatrix} K_\alpha(\theta) \\ K_\beta(\theta) \end{Bmatrix} = C_1 \begin{Bmatrix} \sin\theta \\ -\cos\theta \end{Bmatrix} \tag{2.63}$$

where $[J]$ is the Jacobian matrix, expressed in equation (2.61), $K_\alpha(\theta)$ and $K_\beta(\theta)$ are the velocity coefficients for the two angles. Providing the mechanism is not in a kinematically singular position, there is no difficult in solving this system of equations. As the mechanism approaches a singular position, the velocity coefficients should be expected to become unbounded.

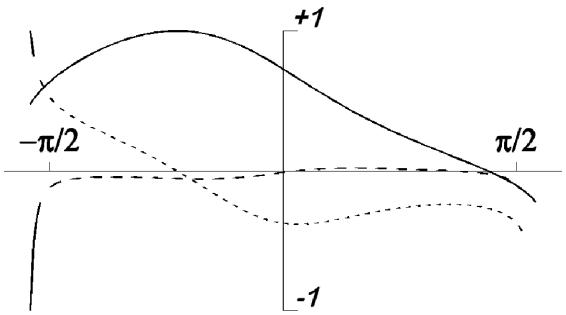

Figure 2.16: $\alpha(\theta)$ – solid line, $K_\alpha(\theta)$ – short broken line, and $L_\alpha(\theta)$ – longer broken line Versus θ for the Linkage of Figure 2.14

2.5.4 Velocity Coefficient Derivatives

Another differentiation of the position loop equations provides the system of equations solvable for the velocity coefficient derivatives:

$$[J]\begin{Bmatrix} L_\alpha(\theta) \\ L_\beta(\theta) \end{Bmatrix} = C_1\begin{Bmatrix} \cos\theta \\ \sin\theta \end{Bmatrix} + C_2K_\alpha^2(\theta)\begin{Bmatrix} \cos\alpha \\ \sin\alpha \end{Bmatrix} + C_3K_\beta^2(\theta)\begin{Bmatrix} \cos\beta \\ -\sin\beta \end{Bmatrix} \tag{2.64}$$

where again $[J]$ is the Jacobian matrix, $L_\alpha(\theta)$ and $L_\beta(\theta)$ are the unknown velocity coefficient derivatives, and all of the right side terms are known from previous evaluations.

$$f_1(\theta,\alpha,\beta) = C_1\cos\theta + C_2\cos\alpha + C_3\cos\beta - C_4 = 0 \tag{2.65}$$
$$f_2(\theta,\alpha,\beta) = C_1\sin\theta + C_2\sin\alpha - C_3\sin\beta = 0 \tag{2.66}$$

The usual sets of three curves for the secondary variables are shown for the linkage of Figure 2.14 with the link lengths as stated in the singularity discussion above.

An examination of the Jacobian determinant shows that it is positive at all locations between $\theta \approx -99.6500^o$ and $\theta \approx +99.6500^o$, but gets extremely close to zero at each end. This is exactly as expected.

2.6 Coupler Point Motions

Much of the interest in four-bar linkages arises from the vast assortment of possible motions generated by points on the coupler link. In order to discuss this, consider the

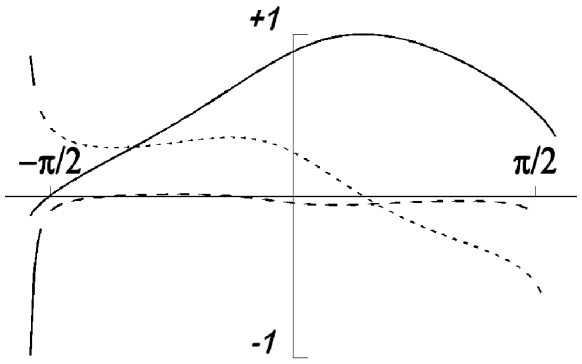

Figure 2.17: $\beta(\theta)$ – solid line, $K_\beta(\theta)$ – short broken line, and $L_\beta(\theta)$ – longer broken line Versus θ for the Linkage of Figure 2.14

specific four-bar linkage shown in Figure 2.18, a crank-rocker mechanism. This figure is a hybrid form, partly kinematic skeleton but partly pictorial in that it shows the outline for the coupler link, an extended body encompassing far more than simply the line between the two connecting pins.

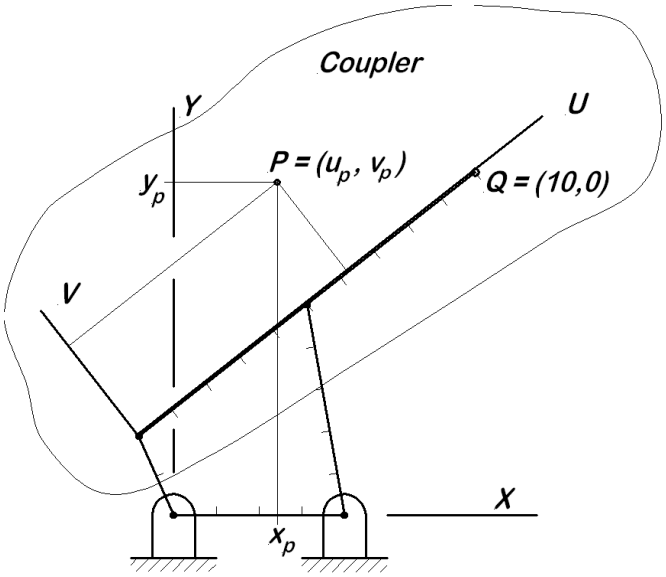

Figure 2.18: Four-Bar Linkage With Body Coordinates and Coupler Points

In order to describe the location of coupler points, a body coordinate system is the preferred approach; such a body coordinate system is shown in Figure 2.18. Note that the origin of the body coordinates is at the tip of the input link, with the $U-$axis extending through the tip of the output link. The $V-$axis is then perpendicular at the origin. Any point on the extended coupler is clearly located by the body coordinate pair (u_p, v_p) as indicated on the figure. Remember that, by definition, a body coordinate system moves

with the body, so that a point fixed in the coupler has constant body coordinates, even though the coupler link itself moves.

The first concern for the body point P is to establish the global (or base) coordinates for the point by a process similar to that used in Section 2.3.5 for the slider-crank mechanism. It is assumed that the initial analysis is complete, giving values for $\alpha(\theta)$, $\beta(\theta)$, $K_\alpha(\theta)$, $K_\beta(\theta)$, $L_\alpha(\theta)$, and $L_\beta(\theta)$ for any input angle θ of interest. The, by a process exactly like that used previously for the slider-crank, the global coordinates for point P are written:

$$x_p(\theta) = C_1 \cos\theta + u_p \cos\alpha(\theta) - v_p \sin\alpha(\theta) \tag{2.67}$$

$$y_p(\theta) = C_1 \sin\theta + u_p \sin\alpha(\theta) + v_p \cos\alpha(\theta) \tag{2.68}$$

The velocity coefficient equations are obtained by differentiation of equations (2.67) and (2.68) to give

$$K_{px}(\theta) = -C_1 \sin\theta - K_\alpha(\theta)\left[u_p \sin\alpha(\theta) + v_p \cos\alpha(\theta)\right] \tag{2.69}$$

$$K_{py}(\theta) = C_1 \cos\theta + K_\alpha(\theta)\left[u_p \cos\alpha(\theta) - v_p \sin\alpha(\theta)\right] \tag{2.70}$$

Yet another differentiation gives the velocity coefficient derivative expressions:

$$\begin{aligned} L_{px}(\theta) = {} & -C_1 \cos\theta - L_\alpha(\theta)\left[u_p \sin\alpha(\theta) + v_p \cos\alpha(\theta)\right] \\ & -K_\alpha^2\left[u_p \cos\alpha(\theta) - v_p \sin\alpha(\theta)\right] \end{aligned} \tag{2.71}$$

$$\begin{aligned} L_{py}(\theta) = {} & -C_1 \sin\theta + L_\alpha(\theta)\left[u_p \cos\alpha(\theta) - v_p \sin\alpha(\theta)\right] \\ & -K_\alpha^2(\theta)\left[u_p \sin\alpha(\theta) + v_p \cos\alpha(\theta)\right] \end{aligned} \tag{2.72}$$

Figure 2.19 illustrates two coupler point curves for the linkage of Figure 2.18 where the data are

$C_1 = 2.0 \qquad C_2 = 5.0$

$C_3 = 5.0 \qquad C_4 = 4.0$

The two coupler points considered have body coordinates: $P = (6.2, 2.4)$ and $Q = (10.0, 0.0)$.

The two closed curves are traced out by the two points as the input crank goes through a full revolution. The lengths of the dashes is proportional to the coupler point speed at each location, with a longer dash representing more rapid motion. The point P was chosen at random, and there is nothing of particular interest about its coupler curve. The point Q is another matter. For Q, note that

- The lower side of the loop is almost (but not quite) exactly straight;

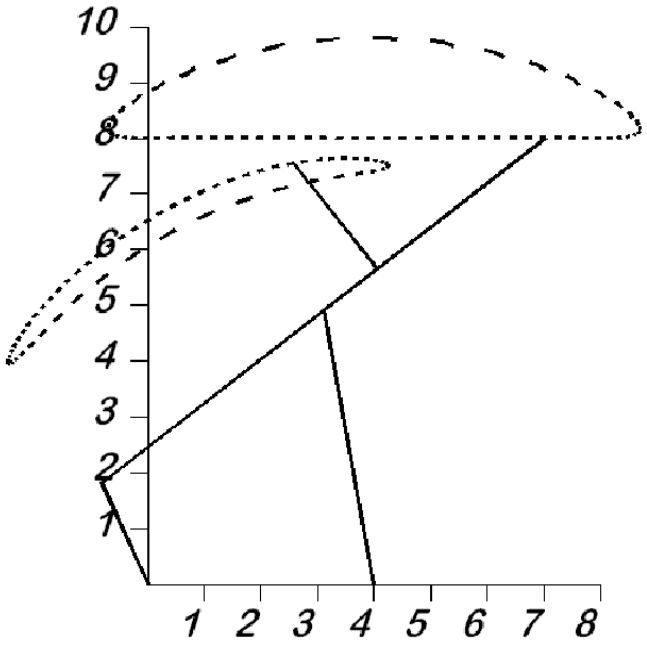

Figure 2.19: Two Coupler Point Curves for the Linkage of Figure 2.18

- The lower side is traced at nearly constant speed,
- The upper side of the loop is essentially a quick return motion.

The (nearly) straight line motion of the $Q-$ curve is a matter of considerable interest as straight line motion is often required in manufacturing automation operations. The (nearly) straight line motion of the $Q-$ curve, coupled with the nearly constant speed and the quick return action suggest that this might be a suitable candidate for moving a paint sprayer that needs to repeatedly make passes over a flat surface.

2.7 Constraints

When the word *constraint* is used in reference to the motion of a mechanical system, it is an acknowledgement that there are forces acting in the system that cannot be known until the motion is fully known. These forces act to *constrain*, that is, to limit, the motion in some way. Consequently, the resulting limitation itself must enter the motion description, in place of the unknown, and unknowable, forces. If the system motion is to be described by the application of Newton's Second Law with the appropriate kinematical relations, the discussion of a constraint indicates that there are unknown forces that cannot be included in the force sums. Instead of including the forces, it is necessary to *include*

the effects that they produce. Usually this takes the form of one or more additional equations that describe the result of the unknown forces. An example helps to establish the concept.

Consider a wheel in a vertical plane rolling in a straight line on a horizontal plane surface. Initially, it might be suggested that this system has two degrees of freedom, one associated with the location of the wheel center (x), and the second with the wheel angular position (ϕ). If there is no friction between the wheel and the supporting surface, the wheel motion can be any combination of rolling and sliding. For that case, it is correct that there are two degrees of freedom.

If on the other hand the plane surface is *perfectly rough*, no sliding is allowed. The term perfectly rough means that there exist whatever forces may be required to prevent sliding, even though the magnitude of that friction force cannot be determined until the motion is known. For the perfectly rough plane, the effect of the friction force is to create a direct relation between the displacement (x) and the wheel rotation (ϕ). No sliding implies that the relative velocity between the contact point on the wheel and the contact point on the wheel is zero:

$$R\,\frac{d\phi}{dt} - \frac{dx}{dt} = 0 \tag{2.73}$$

or, after integrating,

$$R\,\phi - x + \text{constant} = 0 \tag{2.74}$$

Either equation (2.73) or (2.74) may be called the *equation of constraint*. In this example, the equation of constraint reduces the number of degrees of freedom from two to one. Such a reduction is often the case, but not always; read on.

All constraints are classified into one of two categories. They are:

- Holonomic Constraints, which always reduce the number of degrees of freedom;
- Nonholonomic Constraints, which by definition do not reduce the number of degrees of freedom.

They are also classified according to forms, thus:

1. Finite equality constraints (such as equation (2.74)) which are always holonomic and thus reduce the number of degrees of freedom;
2. Inequality constraints which are always nonholonomic but often present little difficulty as shown below by example;

3. Differential constraints which may be either holonomic or nonholonomic, depending upon their exact form.

Here the second and third types are briefly discussed before returning to the first type in more detail.

As an example of the second type, the inequality constraint, consider the motion of a projectile toward a spherical target centered on the origin of coordinates. The equations of motion formulated for this problem apply only while the projectile is outside the target. When the projectile penetrates the target, different equations of motion are required to describe the penetration process. Thus, if the projectile position in three dimensions is (x, y, z), the equations of motion for the free flight apply only while

$$x^2 + y^2 + z^2 > R^2 \tag{2.75}$$

where R is the radius of the spherical target. In solving the motion problem, the solution proceeds with no attention to the inequality constraint other than checking whether it is satisfied or not. It does not enter into the solution of the differential equations, except to specify a point where the solution ceases to be valid. This is the typical handling of inequality constraints.

For the third type, the differential constraint, the condition may be, or may not be, holonomic. Suppose the differential constraint is of the form

$$c_x\, dx + c_y\, dy + c_z\, dz = 0 \tag{2.76}$$

If this form, equation (2.76), is the exact differential of some function, $f(x, y, z)$, then equation (2.76) must be equivalent to

$$df = \frac{\partial f}{\partial x}dx + \frac{\partial f}{\partial y}dy + \frac{\partial f}{\partial z}dz \tag{2.77}$$

which means that equation (2.76) could (in principle) be integrated to find $f(x, y, z)$. That last, being a finite form, reduces the number of degrees of freedom, so that equation (2.76) is discovered to have been a holonomic constraint. The conditions under which a differential form can be integrated are described in textbooks on differential equations [4]. In the event that it is not possible to integrate the differential form, then no function $f(x, y, z)$ exists satisfying equation (2.76) and that differential form must represent a nonholonomic constraint.

In mechanical systems, nonholonomic constraints are most often associated with rolling contacts. There are three classic problems commonly used to illustrate nonholonomic constraint, although they are not the only possibilities. They are (1) a sphere rolling on

a rough plane, (2) a coin rolling on a rough plane, and (3) a pair of wheels on a common axle where both wheels roll on a rough plane. As a variation on the third problem, consider two skates moving on ice while rigidly joined by a stiff rod perpendicular to both of them.

2.7.1 Example: Sphere Rolling on Rough Plane

> Consider a solid sphere of radius R rolling without slipping on a rough level plane. For any rigid body moving freely in three dimensions, there are six degrees of freedom requiring six generalized coordinates. It is common to associate three of these coordinates with the location of the center of the sphere, while the other three are associated with the angular orientation of the body. For the sphere on the plane, the constraint of continued contact with the plane imposes one equality constraint ($z = R$), reducing the number of degrees of freedom to five. The condition of rolling without slipping provides one more constraint, so how many degrees of freedom does the system have?

Define a stationary rectangular Cartesian coordinate system with $x - y$ parallel to the plane and the origin at the level of the center of the sphere while the $z-$axis points upward, away from the plane. Let $\mathbf{i}$, $\mathbf{j}$, and $\mathbf{k}$ denote the usual unit vectors associated with the x, y, and z axes. Then the angular velocity of the sphere must be expressible as

$$\boldsymbol{\omega} = \omega_x \mathbf{i} + \omega_y \mathbf{j} + \omega_z \mathbf{k} \tag{2.78}$$

where ω_x, ω_y, and ω_z are functions of the three angular coordinate rates $\dot{\theta}$, $\dot{\phi}$, and $\dot{\psi}$. The vector to the point of contact between the sphere and the plane is $\boldsymbol{\rho}$, and the velocity of the contact point is $\dot{\boldsymbol{\rho}}$**:**

$$\dot{\boldsymbol{\rho}} = \dot{x}\mathbf{i} + \dot{y}\mathbf{j} + \boldsymbol{\omega} \times (-R\mathbf{k}) \tag{2.79}$$

The sphere must remain in contact with the plane, so the $z-$ component of $\dot{\boldsymbol{\rho}}$ must be zero. Further, since the sphere rolls without slipping, the other two components of $\dot{\boldsymbol{\rho}}$ must also be zero. This gives two more equations of the form

$$f_1\left(\dot{x}, \dot{y}, \dot{\theta}, \dot{\phi}, \dot{\psi}\right) = 0 \tag{2.80}$$

$$f_2\left(\dot{x}, \dot{y}, \dot{\theta}, \dot{\phi}, \dot{\psi}\right) = 0 \tag{2.81}$$

These two equations of constraint are nonintegrable and therefore nonholonomic. Thus the answer to the question is that the system requires five generalized coordinates but it has only three degrees of freedom. This is the typical situation; nonholonomic systems usually require more generalized coordinates than the number of degrees of freedom.

This presentation of the rolling sphere problem has, of necessity, been somewhat sketchy to avoid the need for Euler angles and other advanced concepts. For those who wish to pursue the matter further, these three classical examples are discussed in a number of other texts [5, 6, 7, 8].

2.7.2 Two Dimensional Rolling Constraint

One of the common constraints encountered in the mechanics of machines is the two dimensional rolling constraint. This refers to the two dimensional problem of one body rolling along a fixed line on the other, such as the rolling along the ground or one gear rolling around another. The problem of the wheel rolling along the ground was briefly discussed at the beginning of the discussion on constraints. In that case, the equation of constraint was first written in differential form, and then the equivalent finite form was written. For two dimensional rolling problems such as this, the equation of constraint can always be written in finite form, and thus the two dimensional rolling constraint is always holonomic. This means that the constraint equation can always be used to eliminate one of the coordinates as well as a degree of freedom, keeping the number of degrees of freedom and the number of generalized coordinates equal.

In the earlier discussion, to assure rolling motion, the surfaces in contact were described as perfectly rough. This implies that there is sufficient shear force available at the surface to prevent sliding under all conditions. In reality, there are no perfectly rough plane surfaces. Problems in elementary mechanics are often solved first by assuming that there is no slip, and then after the resulting motion is determined, the required friction force is determined. If it exceeds the available friction force, then the problem must be solved again with the assumption that slip is occurring.

The primary device used in machinery to assure that slip does not occur, and thus to approximate a perfectly rough surface, is to cut mating teeth into the two bodies over the contact zone. If the two bodies are disks, the result is a pair of gears. IF one body is straight while the other is a disk, the result is a rack and pinion. For properly formed teeth, the teeth do not affect the motion at all other than to assure that no slip occurs. The matter of proper tooth forms for gears and racks is considered in Chapter 5. For the present, it is sufficient to consider a gear as a perfectly rough wheel. The effective radius of a gear is known in gear terminology as the *pitch radius.*

The introduction of a rolling constraint slightly modifies the established procedure for kinematic analysis. With constraints involved, the combined set of position loop equations and constraint equations must be solved simultaneously for the secondary variables. For the velocity coefficients and velocity coefficient derivatives, the constraint equations are differentiated along with the position loop equations and again included in the solutions. This process is illustrated in the example problem that follows. For this example,

the initial assembly position plays a significant role as is often the case.

2.7.3 Example: Rolling Constraint

Consider a system comprised of a disk rolling without slipping along a rail such as shown in Figure 2.20. The disk is moved by pulling the connecting link that passes through the eye-block and is pinned to the wheel. The radii R and r are known values. Figure 2.20 (a) shows the system as originally assembled (subscripts o), where the length S_o is known. In the original position, the connecting link pin is directly above the contact between the disk and the rail. In the original assembly position, the connecting link extends to exactly the eye-block pivot. As the connecting link is drawn through the eye-block, the disk rolls to the left to a position such as that shown in Figure 2.20 (b). Set up all equations required to determine the secondary kinematic variables.

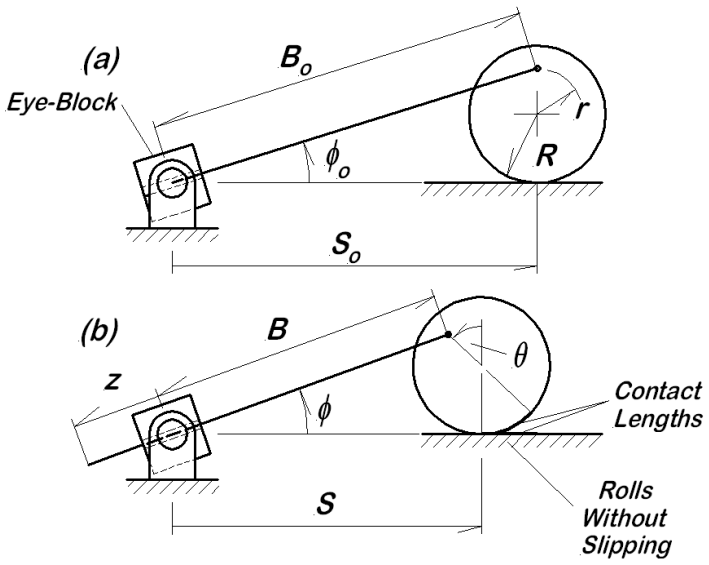

Figure 2.20: System With Rolling Constraint: (a) Initial Position, (b) Displaced Position

Consider first the original assembly position. Sufficient information is provided to determine B_o and the angle ϕ_o as follows:

$$B_o = \left[S_o^2 + (R+r)^2\right]^{1/2} \tag{2.82}$$

$$\phi_o = \arctan\left[(R+r)/S_o\right] \tag{2.83}$$

There is no disk rotation in the original assembly position.

Next, turn to the displaced position as shown in Figure 2.20 (b). There is one degree of freedom, here associated with the length z, the amount of the connecting rod drawn through the eye-block. There is one position loop, from which the loop equations are

$$(B_o - z)\cos\phi + r\sin\theta - S = 0 \tag{2.84}$$
$$(B_o - z)\sin\phi - r\cos\theta - R = 0 \tag{2.85}$$

The secondary unknowns appearing in the two position loop equations are ϕ, θ, and S. The necessary third is equation is the constraint expressing rolling without slipping. Along the rail, the point of contact moves a distance $S_o - S$; on the curved edge of the disk, the point of contact moves a length $R\theta$. These two distance must be the same for rolling without slipping, so

$$S_o - S - R\theta = 0 \tag{2.86}$$

After B_o and ϕ_o have been evaluated using equations (2.82) and (2.83), the system of equations to be solved simultaneously for ϕ, θ, and S are equations (2.84), (2.85) and (2.86). A closed-form solution for these three equations may be sought, or a numerical solution by Newton-Raphson solution may be used.

The determination of velocity coefficients and velocity coefficient derivatives proceeds in the usual fashion, with the constraint equation differentiated at each step along with the loop equations.

2.8 Multiloop Mechanisms

All of the mechanisms considered to this point are described in terms of a single position vector loop (two scalar equations) and have only one degree of freedom. This might suggest that one degree of freedom necessarily implies a single position vector loop, but that is not correct. In this section, multiloop, single degree of freedom mechanisms are addressed by means of an example. For multiple loops, the procedure for kinematic analysis is much the same as for the single loop case, except that more equations are required.

In writing the position loop equations, note that the loops used must be independent. In the example following, a kinematic analysis is developed for a single degree of freedom mechanism involving two independent position vector loops. Additional loops can be identified, but they are not independent. *For independence, each loop must include some segment not a part of any other loop.*

2.8.1 Four-Bar/Toggle Linkage

Figure 2.21 shows the kinematic skeleton for a mechanism sometimes used for a punch press. For this purpose, the input crank pivoted at the upper left is driven by a prime mover, usually with a large flywheel, while the punch tool is attached to the slider at the bottom of the diagram. For each revolution of the input crank, the tool executes one punch cycle. The link lengths R, C_1, C_2, C_3, and C_5 are known, as is the input crank pivot location, (x_1, y_1). The single degree of freedom is associated with the input crank rotation angle, θ. Set up the equations governing the secondary variable positions and velocity coefficients.

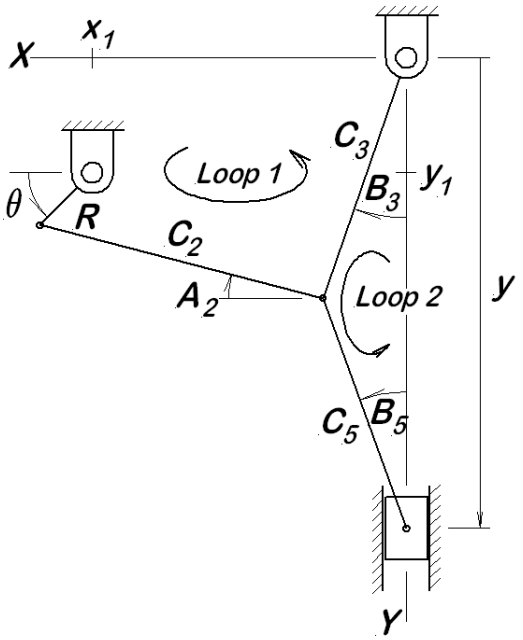

Figure 2.21: Four-Bar / Toggle Linkage

2.8.1.1 Position Analysis

The two loops to be used for this analysis are identified in Figure 2.21. There is a third loop, obtained by tracing around the outside of the mechanism, but the equations describing the third loop are merely linear combinations of the equations determined for the first two loops; they contain no new information and are, therefore, dependent equations. As usual,the position loop equations are determined by summing displacements around each of the two independent loops. Each sum begins at the origin of coordinates (upper

right corner of the figure), but that is just for convenience and is certainly not required. With two vector loops, four scalar position loop equations are obtained, as shown here:

$$f_1 = x_1 + R\cos\theta - C_2\cos A_2 - C_3\sin B_3 = 0 \tag{2.87}$$
$$f_2 = y_1 + R\sin\theta + C_2\sin A_2 - C_3\cos B_3 = 0 \tag{2.88}$$
$$f_3 = C_3\sin B_3 - C_5\sin B_5 = 0 \tag{2.89}$$
$$f_4 = C_3\cos B_3 + C_5\cos B_5 - y = 0 \tag{2.90}$$

This is a set of four simultaneous, nonlinear equations in the four unknowns A_2, B_3, B_5 and y, numerically solvable for any assigned value of θ. For a Newton-Raphson solution for this system of equations, the vector of secondary kinematic unknowns is

$$\{S\} = \mathrm{col}(A_2, B_3, B_5, y) \tag{2.91}$$

and the Jacobian matrix is

$$[J] = \left[\begin{array}{cc|cc} C_2\sin A_2 & -C_3\cos B_3 & 0 & 0 \\ C_3\cos A_2 & C_3\sin B_3 & 0 & 0 \\ \hline 0 & C_3\cos B_3 & -C_5\cos B_5 & 0 \\ 0 & -C_3\sin B_3 & -C_5\sin B_5 & -1 \end{array}\right] \tag{2.92}$$

As discussed previously, the Newton-Raphson solution is achieved by an iterative refinement of the initial solution estimate.

Before leaving the position solution, there is one other noteworthy point. Look again at Figure 2.21. The upper loop is recognized as a four-bar linkage that is determined completely when θ is specified. The second loop is a slider-crank mechanism for which B_5 and y are determined once B_3 is known. (Because the slider-crank in this situation only works through much less than a full crank revolution, this is sometimes called a *toggle linkage*, and the whole assembly is termed a four-bar/toggle linkage mechanism.) This suggests that it should be possible first to solve the four-bar linkage loop equations without considering the rest of the mechanism; then, with that solution known, to solve the slider-crank equations. Because this is indeed possible, this mechanism is said to be *weakly coupled*. If this type of separation were not possible, the system would be strongly coupled. Look at the Jacobian matrix just presented, and notice the null partition in the upper right corner; *the null partition indicates the weak coupling*. Weak coupling is somewhat dependent on the manner in which the equations are written. If a closed-form solution is sought, then certainly advantage should be taken of weak coupling whenever it exists. If a numerical solution by the Newton-Raphson method is to be employed, then weak coupling is usually not significant.

2.8.1.2 Velocity Coefficient Analysis

When the position equations are differentiated with respect to θ, the velocity coefficient loop equations are obtained. In matrix form, these equations are

$$\left[\frac{\partial f}{\partial s}\right]\{K_S\} = -\left\{\frac{\partial f}{\partial \theta}\right\} \tag{2.93}$$

Because the coefficient matrix on the left is the Jacobian matrix that was presented above, all that remains to be specified is the vector on the right side:

$$\left\{\frac{\partial f}{\partial \theta}\right\} = R\begin{Bmatrix} -\sin\theta \\ \cos\theta \\ 0 \\ 0 \end{Bmatrix} \tag{2.94}$$

These equations may be solved readily for the secondary variable velocities or for the velocity coefficients. The preceding position and velocity coefficient solutions are demonstrated with the following numerical values.

2.8.1.3 Numerical Values

Consider a four-bar/toggle linkage with the following link lengths and crank pivot location:

$C_2 = 355$ mm $\quad R = 127$ mm

$C_3 = 685$ mm $\quad X_1 = 345$ mm

$C_5 = 1120$ mm $\quad Y_1 = 457$ mm

For this system, the secondary kinematic variable values and the velocity coefficients are determined when the input crank position is $\theta = 1.0$ radian. The analysis described is implemented in a computer program 4BarTogl, listed below. The program consists of these major parts:

1. The usual title lines, Option Nolet and Option Base 1 statements, and the Dimension statement;
2. Seven lines of problem data, including $\theta = 1.0$. This code could readily be adapted to other positions by simply changing this line and the Starting Estimates.

3. Starting Estimates for each of the unknowns in order to begin the Newton-Raphson;

4. Control values for the maximum allowable residual (`fmx`) and the maximum number of iterations allowed (`itmx`);

5. The iterative solution loop;

- (**a**) Extraction of the variables by name for use in the function evaluations;
- (**b**) Residual function evaluations and calculation of $|f|^2$;
- (**c**) Test to exit if the solution is fully converged;
- (**d**) Evaluation of the Jacobian and Jacobian inverse;
- (**e**) Evaluation of the adjustment and calculation of $|d|^2$;
- (**f**) Test for a stalled solution, with warning output if required;
- (**g**) Test for failure to converge, with warning output if necessary;
- (**h**) End of the loop, return to the beginning;

6. Extraction of the final converged results for output.

The program output for $\theta = 1.0$ follows:

```
Solution after 22 iterations"
fsq = 9.7570123e-11
A2 = .33478272
B3 = .1145972
B5 = 6.9992296e-2
YY = 1797.7648
```

The program listing that produced this output follows below:

```
! 4BarTogl.Tru
! Four-Bar/Toggle Linkage Kinematics
OPTION NOLET
OPTION BASE 1
DIM x(4),f(4),d(4),jac(4,4),jaci(4,4)
R=127                              ! system data
C2=355
C3=685
C5=1120
X1=345
```



```
Y1=457
th=1.0                          ! crank angle, theta
! Starting Estimates
x(1)=0.1
x(2)=0.3
x(3)=x(2)
x(4)=C3+C5
fmx=1e-5                        ! max allowable function value
itmx=30                         ! max allowable number of iterations
FOR i=1 to itmx                 ! iterative solution loop
    A2=x(1)                     ! extract variables for functions
    B3=x(2)
    B5=x(3)
    YY=x(4)
    f(1)=X1+R*cos(th)-C2*cos(A2)-C3*sin(B3)
    f(2)=Y1+R*sin(th)+C2*sin(A2)-C3*cos(B3)
    f(3)=C3*sin(B3)-C5*sin(B5)
    f(4)=C3*cos(B3)+C5*cos(B5)-YY
    fsq=f(1)^2+f(2)^2+f(3)^2+f(4)^2    ! f-square
    IF fsq<fmx^2 then EXIT FOR    ! test for fully converged solution
    MAT jac=zer
    jac(1,1)=C2*sin(A2)
    jac(1,2)=-C3*cos(B3)
    jac(2,1)=C3*cos(A2)
    jac(2,2)=C3*sin(B3)
    jac(3,2)=C3*cos(B3)
    jac(3,3)=-C5*cos(B5)
    jac(4,2)=-C3*sin(B3)
    jac(4,3)=-C5*sin(B5)
    jac(4,4)=-1
    MAT jaci=inv(jac)
    MAT d=jaci*f                ! calculate adjustment
    dsq=d(1)^2+d(2)^2+d(3)^2+d(4)^2    ! d-square
    MAT x=x-d                   ! revise solution estimate
    IF dsq<1e-14 then           ! test for stalled solution
       PRINT "   i = ";i
       PRINT "   f-square = ";fsq
       PRINT "   d-square = ";dsq
       PRINT "   d-square too small, solution stalled"
       STOP
    END IF
    IF i=itmx then              ! test for failure to converge
       PRINT "   i = itmx"
       PRINT "   fsq = ";fsq
```



```
      PRINT "   exceeds iteration limit, no solution"
      STOP
    END IF
NEXT i
A2=x(1)                          ! extract solutions for output
B3=x(2)
B5=x(3)
YY=x(4)
PRINT "   Solution after ";i;" iterations"
PRINT "   fsq = ";fsq
PRINT "   A2 = ";A2
PRINT "   B3 = ";B3
PRINT "   B5 = ";B5
PRINT "   YY = ";YY
END
```

As illustrated here, the existence of multiple independent loops increases the number of equations required in each of the position, velocity, and acceleration solutions. Otherwise, it is exactly like any other single degree of freedom system analysis.

2.9 A Computer Algebra Approach

For simple mechanisms, the methods of analysis demonstrated in the previous sections are easily carried out. However, when there are many secondary variables, the number of loop equations and constraint equations becomes large and the differentiation required can be laborious. The purpose for this section is to present an approach that may be of use to those with access to a computer algebra program such as Maple™, Mathematica™, or other similar program. These programs are often called **c**omputer **a**lgebra **s**ystems (CAS). The point here is to exploit the symbolic differentiation capability of such a program to facilitate the kinematic study of single degree of freedom mechanisms. The distinction between total and partial differentiation is critical to what follows here.

Consider a system for which there are N loop equations and constraints, each of the homogeneous form

$$f_i = f_i\left(s_1, s_2, s_3, \ldots, q\right) = 0 \qquad i = 1, 2, \ldots N \tag{2.95}$$

where $s_1, s_2, \ldots$ are the secondary variables and q is the primary variable. These are the equations that must be solved numerically by Newton-Raphson to obtain the secondary positions. That solution requires the use of the Jacobian matrix, but it occurs naturally

in the development of the velocity coefficients below. The whole set of equations may be arranged in a column vector as $\{f\} = \mathrm{col}\,(f_1, f_2, \ldots f_N) = \{0\}$.

Now form the total derivative of this vector with respect to q thus:

$$\begin{aligned}\frac{d\{f\}}{dq} &= \frac{\partial\{f\}}{\partial s_1}\frac{ds_1}{dq} + \frac{\partial\{f\}}{\partial s_2}\frac{ds_2}{dq} + \cdots + \frac{\partial\{f\}}{\partial s_N}\frac{ds_N}{dq} + \frac{\partial\{f\}}{\partial q} \\ &= \frac{\partial\{f\}}{\partial s_1}K_{s1} + \frac{\partial\{f\}}{\partial s_2}K_{s2} + \cdots + \frac{\partial\{f\}}{\partial s_N}K_{sN} + \frac{\partial\{f\}}{\partial q} \qquad (2.96) \\ &= [J]\{K\} + \frac{\partial\{f\}}{\partial q} \qquad (2.97)\end{aligned}$$

where the last result follows from the definition of the Jacobian matrix. The computer algebra program can be coded to develop the expression in equation (2.96) and thus develop all of the components of equation (2.97). Recalling that $d\{f\}/dq = \{0\}$, it is evident that the velocity coefficients can be determined directly by numerical solution of equation (2.97) set to zero.

Now consider a second total derivative of $\{f\}$ with respect to q. This will be of the form

$$\begin{aligned}\frac{d^2\{f\}}{d^2q} &= \frac{\partial^2\{f\}}{\partial^2 s_1}\left(\frac{ds_1}{dq}\right)^2 + \frac{\partial\{f\}}{\partial s_1}\left(\frac{d^2s_1}{d^2q}\right) \\ &\quad + \frac{\partial^2\{f\}}{\partial^2 s_2}\left(\frac{ds_2}{dq}\right)^2 + \frac{\partial\{f\}}{\partial s_2}\left(\frac{d^2s_2}{d^2q}\right) \\ &\quad + \cdots + \frac{\partial^2\{f\}}{\partial^2 q} \\ &= \frac{\partial^2\{f\}}{\partial^2 s_1}K_{s1}^2 + \frac{\partial\{f\}}{\partial s_1}(L_{s1}) \\ &\quad + \frac{\partial^2\{f\}}{\partial^2 s_2}K_{s2}^2 + \frac{\partial\{f\}}{\partial s_2}(L_{s2}) \\ &\quad + \cdots + \frac{\partial^2\{f\}}{\partial^2 q} \\ &= [J]\{L\} + \frac{\partial^2\{f\}}{\partial^2 s_1}K_{s1}^2 + \frac{\partial^2\{f\}}{\partial^2 s_2}K_{s2}^2 + \cdots + \frac{\partial^2\{f\}}{\partial^2 q} \qquad (2.98)\end{aligned}$$

There are two important points to remember in forming the second derivative expression:

- Since $\{f\} = \{0\}$, all its derivatives are zero as well;
- From equation (2.97), it is evident that the second derivative contains the term $[J]\{L\}$ and various other terms involving the primary and secondary variables and the several velocity coefficients.

From the second point, it is evident that the second derivative can be written as

$$\frac{d^2\{f\}}{d^2q} = [J]\{L\} - \{V_2\} \tag{2.99}$$

where $\{V_2\}$ contains all of the other terms. The expression for $\{V_2\}$ is evaluated symbolically (in the computer algebra system) as

$$\{V_2\} = [J]\{L\} - \frac{d^2\{f\}}{d^2q} \tag{2.100}$$

This only requires a bit of symbolic matrix arithmetic since both $d^2\{f\}/d^2q$ and $[J]$ are previously determined within the computer algebra program. Then, the equation to be solved numerically for the velocity coefficient derivatives is

$$[J]\{L\} = \{V_2\} = \left([J]\{L\} - \frac{d^2\{f\}}{d^2q}\right) \tag{2.101}$$

where the right side is evaluated numerically after being formed symbolically.

In simple cases, it may be useful to carry out in closed form the full solution for the velocity coefficients and the velocity coefficient derivatives. However, this tends to result in very complicated expressions for each of the functions, expressions that are meaningless for interpretation and difficult to code correctly for the computer. More often, the real utility of this approach is in expressing the forms for $\{V_1\}$ and $\{V_2\}$ to then be programmed for numerical solution within the computer.

This approach is particularly useful for systems involving more than two loop equations, such as the case of a multiloop mechanism or the imposition of additional constraints. The detailed implementation of this approach depends upon (a) the particular problem and (b) the computer algebra program available. While the exact details of the implementation depend upon these matters, the following outline is recommended for the implementation of this approach.

1. Write the governing equations (position loops and/or constraints, if any), as a homogeneous vector function, $\{f(s_1, s_2, s_3, \ldots, q)\} = \{0\}$;
2. Differentiate the result of the first step to form the complete differential, $\{df\}$. In so doing, introduce the notation K_{s_i} for the derivative of s_i with respect to q;
3. Differentiate the result of the second step to form the second differential, $\{d^2f\}$. In this operation, further introduce the notation L_{s_i} for the derivative of K_{s_i} with respect to q;

4. Extract the Jacobian matrix as the coefficients of the various K_{s_i} in $\{df\}$;

5. Form the right side vector for the velocity coefficient calculation, $\{V_1\}$;

6. Form the right side vector for the velocity coefficient derivative calculation, equation (2.100), $\{V_2\}$;

7. Numerically solve the system of linear equations for the velocity coefficients, equation (2.99);

8. Numerically solve the system of linear equations for the velocity coefficient derivatives, equation (2.101).

Considerable care in coding and checking is required to implement this approach, but it is a powerful tool for use on more complicated mechanisms.

2.10 Conclusion

The basic approach to the kinematic analysis of single degree of freedom mechanisms has been presented in this chapter. The process begins with the selection of a primary coordinate to be associated with the degree of freedom. The mechanism position is described by position equations that are the scalar components of the closed position vector loops and are written in terms of the primary coordinate and such secondary coordinates as may be required. The user needs to assign these variables as required in order to write the position loops. These equations can be solved to provide values for the secondary variables when a value is assigned to the primary variable.

The velocities and accelerations of the secondary variables may be determined from the differentiated position loop equations.

- The velocity of any secondary variable is directly proportional to the velocity of the primary variable, and this makes possible use of a position dependent velocity coefficient to express the secondary velocity in terms of the primary velocity. The velocity coefficient is available directly by differentiating the secondary variable with respect to the primary variable.

- The acceleration of any secondary variable can be expressed as the sum of two terms—the first, the product of the velocity coefficient with the acceleration of the primary variable, and the second, the product of the velocity coefficient derivative with the square of the primary velocity. The required velocity coefficient derivative is the derivative of the velocity coefficient with respect to the primary variable.

For any point on a moving body, base coordinates are readily expressed from the geometry in terms of the primary variable, the secondary variables, and the body coordinates for that point of interest. When these relations are differentiated with respect to time, the base coordinate velocity and acceleration are obtained. For any such point in two-dimensional motion, there are two velocity coefficients and two velocity coefficient derivatives—one associated with each direction.

Writing the position loop equations is a process unique to each mechanism. After that, the solutions for the position loop equations, velocity coefficient equations, and equations for velocity coefficient derivatives may or may not be possible in closed form, although numerical solutions are generally available.

If the ideas summarized here have been mastered, there should be little difficulty in the kinematic analysis of any single degree of freedom mechanism. These ideas play a major role in the later static and dynamic analysis of such mechanisms, so kinematic analysis is only the beginning of their application.

References

[1] Chang, W-T, Lin, C-C, and Wu, L-I, "A Note on Grashof's Theorem," *J. of Marine Science and Technology*, Vol. 13, No. 4, 2005, pp. 239-248.

[2] Crossley, F.R.E., *Dynamics in Machines*, Ronald Press, 1954, pp. 73-74.

[3] Shigley, J.J. and Uicker, J.J. Jr., *Theory of Machines and Mechanisms*, 2nd. ed., McGraw-Hill, 1995.

[4] Ince, E.L, *Ordinary Differential Equations*, Dover, 1944, pp. 52 - 55.

[5] Goldstein, H.S., *Classical Mechanics*, Addison-Wesley, 1959, p. 13

[6] Greenwood, D.T., *Principles of Dynamics*, Prentice-Hall, 1965, pp. 234-235.

[7] Kilmister, C.W. and Reeve, J.E., *Rational Mechanics*, Elsevier, 1966, p. 200.

[8] Synge, J.L., "Classical Dynamics" in *Encyclopedia of Physics*, S. Flugge, ed., Vol. III/1, Springer, 1960, pp. 40-41.

Problems

2-1 The device shown was used in early, mechanical analog computation. The dimensions A and B are known constants, and the input x is assigned.

(a) Express the output displacement, R,in terms of A, B, and x;

(b) Determine the velocity coefficient $K_R = dR/dx$;

(c) Determine the velocity coefficient derivative, $L_R = dK_R/dx$;

(d) Given that $A = 50$ mm and $B = 17$ mm, evaluate R, K_R, and L_R for $x = 35$ mm;

(e) Using the results from (d), evaluate $\dot{R}$ and $\ddot{R}$ for $\dot{x} = -25$ mm/s, $\ddot{x} = 12$ mm/s^2.

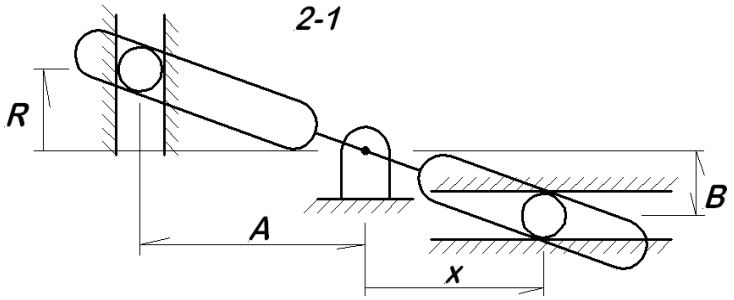

2-2 The mechanism show is called a *quick return mechanism* and it is used in the machine tool called a *shaper*. The flywheel is driven by a motor (not shown), causing the lever to oscillate to the left and right. In the shaper application, a cutting tool is mounted on the horizontal slider and makes a cut during the slow motion part of the stroke before returning rapidly in preparation for the next cut. The dimensions C, D, and R are all known constants.

(a) Determine the displacement, x, as a function of θ, in closed form;

(b) Determine the velocity coefficient, $K_X = dx/d\theta$ as a function of θ, again in closed form;

(c) Determine the velocity coefficient derivative, $L_x = dK_x/d\theta$ as a function of θ, also in closed form;

(d) Given the dimensions below, evaluate $x, \dot{x}$, and $\ddot{x}$ for $\theta = \pi/6$ rad, $\dot{\theta} = 22.5$ rad/s, and $\ddot{\theta} = 147$ rad/s^2.

$C = 0.4$ m $\quad D = 0.75$ m $\quad R = 0.085$ m

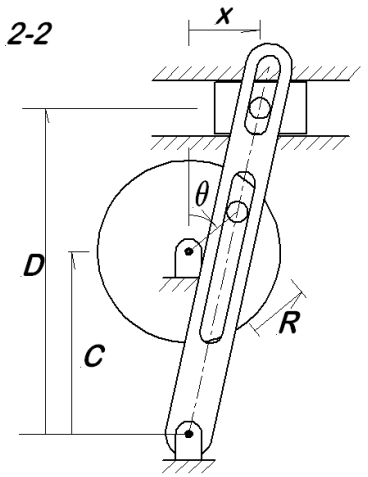

2-3 The Geneva mechanism (also called a Geneva wheel) is a device to provide intermittent angular motion based on a continuous input rotation. The derive pin on the input disk (right side) engages a slot in the output wheel, causing it to rotate until the drive pin eventually exits the slot. At the point of initial engagement, and again as the drive pin exits the slot, the pin must move along a radius of the Geneva wheel in order to avoid operating problems and noise. For the five slot Geneva shown, the input rotation is described by θ while the output motion is A; the dimensions R_1, R_2, and D are all known and the drive pin is assumed to have zero diameter for this problem (the finite diameter drive pin is considered in the next problem).

(a) Determine in closed form the output rotation, $A(\theta)$, as applicable while the pin is engaged with a slot;

(b) Determine the maximum and minimum values of θ for pin-slot engagement;

(c) Determine the velocity coefficient, $K_A(\theta)$, and the velocity coefficient derivative, $L_A(\theta)$, for that same interval;

(d) Given the dimensional data below, determine A, $\dot{A}$, and $\ddot{A}$ for $\theta = 0.15$ rad, $\dot{\theta} = 12.4$ rad/s, and $\ddot{\theta} = -29.0$ rad/s^2.

$R_1 = 110$ mm $\quad R_2 = 152$ mm $\quad D = 187$ mm

2-4 To avoid impact as the drive pin engages the slot in the Geneva wheel, the pin velocity must be along the centerline of the slot at the entrance, as pointed out in the previous problem. View 2-4(a) shows a driving pin of (nearly) zero radius located at the radius R_1 on the driving disk; it is engaging with a Geneva wheel of N slots.

(a) Determine an expression for the appropriate value of R_2 in terms of R_1 and N;

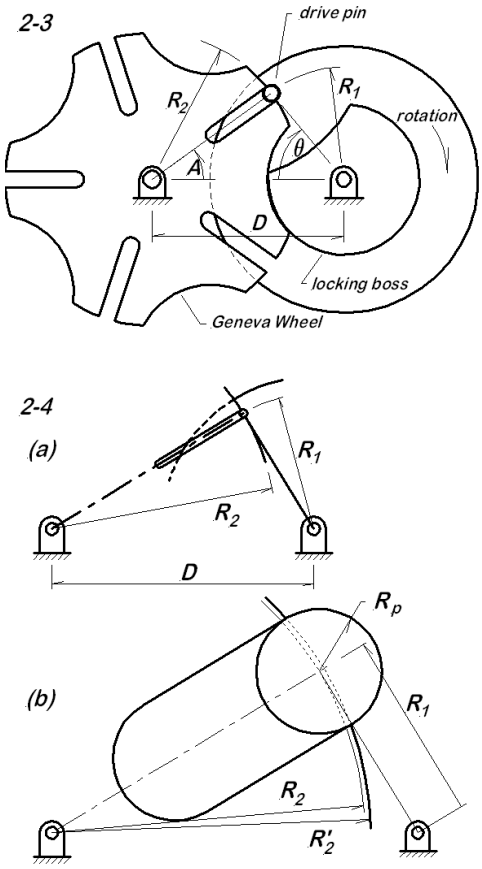

(b) Determine an expression for the center-to-center distance D.

The value determine in part (a), based on a zero radius drive pin, cannot be the actual case. Proper support at the entrance (and exit) condition requires the use of the slightly larger radius R_2' as shown in 2-4(b).

(c) If the drive pin radius is denoted as R_p, develop an expression for the appropriate value of R_2';

(d) If a drive pin diameter of 14.3 mm is to be used with a five-slot Geneva wheel with the dimensions given in problem 2-3(d), evaluate R_2'.

2-5 The figure shows a double acting gas compression cylinder. The crank is turned by a prime mover (not shown) causing the cross head, piston rod, and piston to reciprocate. The piston rod, piston, and cylinder cavity are all right circular cylinders, and the dimensions R, L_1, L_2, X_1, X_2, D_p, D, and T_p are all known data (L_2 extends from the center of the cross head pivot to the left side of the piston).

(a) Determine expressions for the chamber volumes V_1 and V_2 in terms of the known data

and the crank angle θ (be sure to allow for the volume of the piston rod and the piston thickness);

(b) Develop expressions for the derivatives $dV_1/d\theta$ and $dV_2/d\theta$.

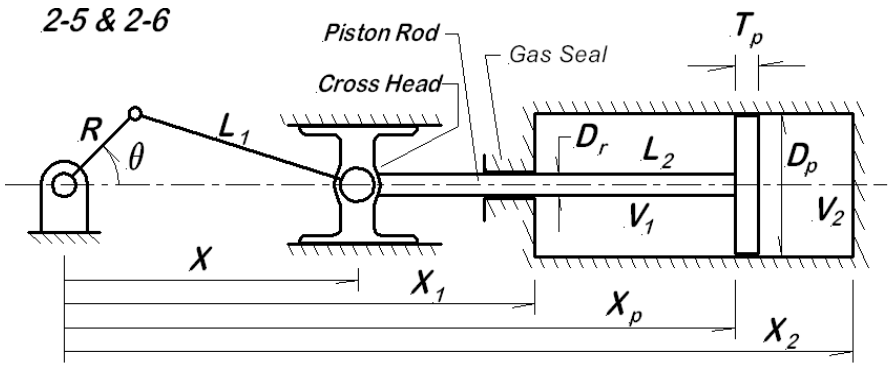

2-6 For the double acting compression cylinder of problem 2-5, assume the data given below.

(a) Make plots of $V_1(\theta)$ and $dV_1/d\theta$ versus θ;

(b) Make plots of $V_2(\theta)$ and $dV_2/d\theta$ versus θ.

$R = 200$ mm $\quad L_1 = 560$ mm $\quad L_2 = 510$ mm $\quad T_p = 50$ mm

$X_1 = 890$ mm $\quad X_2 = 1245$ mm $\quad D_p = 200$ mm $\quad D_r = 57$ mm

2-7 It is proposed to use a hydraulic cylinder to drive a crank connected to a load; the system is shown in schematic form below. The outboard end of the hydraulic cylinder is pivoted on a fixed support at an angle A above the horizontal. The dimensions A, d, L, and R are assumed known.

(a) Develop expressions for s and ϕ as functions of the crank angle θ and the known data;

(b) Develop expressions for the derivatives $ds/d\theta$ and $d\phi/d\theta$ as functions of θ.

2-8 The system shown in the accompanying figure has been proposed as a perpetual motion machine. All three legs are identical. Assume that gravity acts downward, and that each $a \times a$ rectangle has mass M_a, with center of mass at the geometric center of the rectangle. Each leg of length b has mass M_b, with center of mass at the center of the arm. Each upright of length h has mass M_h, with center of mass at the center of the arm. Each leg with length L has mass M_L, with center of mass at the middle of the leg. What is the path of the system center of mass as the assembly rotates?

2-9 The figure depicts a type of aircraft landing gear used to fold the wheel into a well

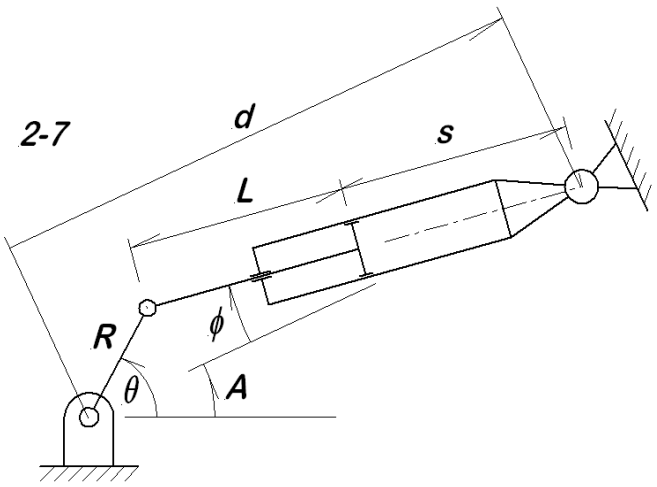

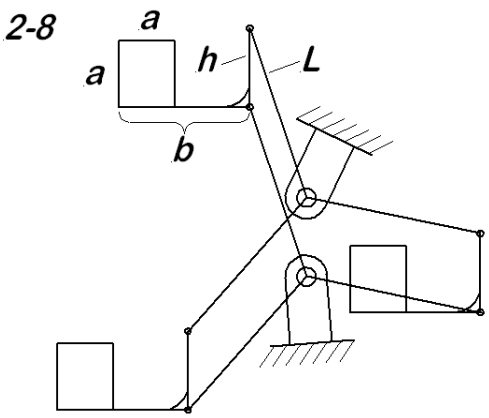

in the lower surface of the wing in order to reduce drag during flight. In the mechanism shown, the wheel strut is pivoted about an axis through point A that is perpendicular to the page. As shown, the gear is partially deployed. Full deployment for use requires that the strut be extended to a vertical position. The stowed position has the strut and wheel in a horizontal position. Deployment and retraction are driven by the hydraulic cylinder shown.

The system has one degree of freedom associated with the overall length of the hydraulic actuation cylinder, q. The secondary variables are identified on the drawing: θ, λ, ϕ, and ψ. The geometry of the bell crank is fully defined by the lengths of the three sides. For problem parts (a), (b), and (c), treat the angle β as known.

(a) Write all of the position loop equations and the Jacobian matrix;

(b) Obtain the equations for the several velocity coefficients in matrix form;

(c) Obtain the equations for the several velocity coefficient derivatives, again in matrix

form;

(d) Using the dimensional data given below and trigonometry, determine the angle β;

(e) Continuing with the dimensional data below and the value of β found in (d), determine

- The value of q for $\phi = 0$ (full retraction);
- The value of q for $\phi = \pi/2$ rad (or 90^o) (full deployment);

(f) For q from $q_{\min}$ to $q_{\max}$, plot the angles, velocity coefficients, and velocity coefficient derivatives as functions of q for each of the secondary variables (make computer generated plots with a minimum of 100 points on each curve).

Link Lengths (mm)

$AB = 441.0$ $\quad DE = 501.0$

$BC = 861.0$ $\quad CE = 462.0$

$CD = 330.0$

Fixed Pivot Locations (mm)

Point A : $\quad x_A = 0.0 \quad y_A = 0.0$

Point E : $\quad x_E = 1107.0 \quad y_E = -222.0$

Point F : $\quad x_F = 2412.0 \quad y_F = 0.0$

2-10 The figure shows a *pump jack*, a common sight in a producing oil field. Power from the drive motor (far right) is transferred through the gear box to turn the crank (1-2) that carries massive cast steel counter weights. Motion of the crank is passed through the coupler (2-3) to the rocking beam (3-4). On the end of the rocking beam, a flexible band is wrapped around a circular head and connected to the sucker rod that drives the pump mechanism far down the well bore.

The primary mechanism is a four bar linkage, with fixed pivots at 1 and 4. When referred to the coordinate system shown, the fixed pivot locations are

$x_1 = 3369$ mm $\quad y_1 = 1816$ mm

$x_4 = 1650$ mm $\quad y_4 = 4068$ mm

The link lengths are

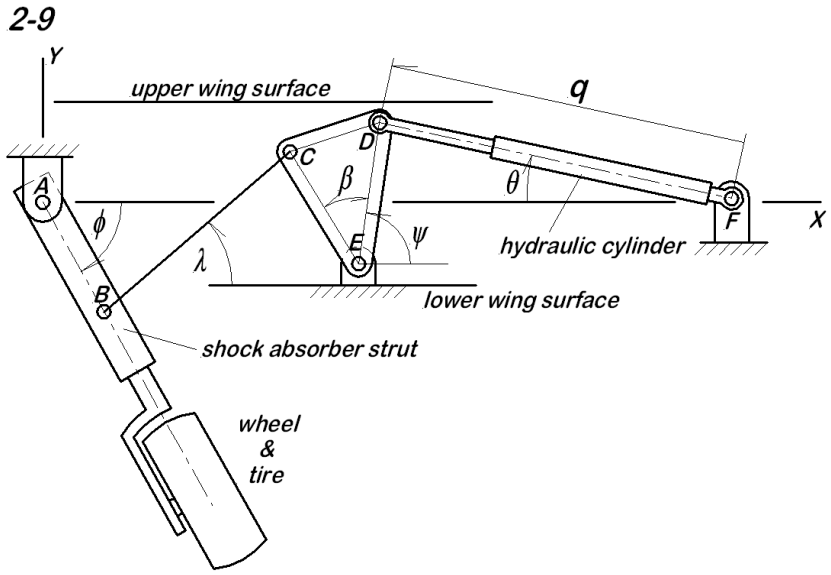

$R_{12} = 854$ mm	crank
$c_{23} = 2200$ mm	coupler
$c_{34} = 1648$ mm	pivot to pivot along the beam

Assuming the crank speed is steady at 47 rpm, determine

(a) the length of the sucker rod stroke (minimum to maximum coupling elevations);

(b) maximum and minimum sucker rod velocity values;

(c) maximum absolute acceleration of the sucker rod;

A computer search for the extreme values is required; use 1 degree increments on θ for the search.

2-11 The mechanism shown is another type of retractable landing gear for aircraft. It draws the wheel and shock absorbing strut up into the fuselage of the aircraft with a motion entirely in the fore and aft vertical plane. The solid lines show the gear partially deployed while the broken lines show both the fully deployed (vertical) and fully retracted (horizontal) positions. The motion is driven by a hydraulic cylinder between points A and B, where B moves in a guide slot. The necessary dimensional data is given in a table below.

The system has one degree of freedom easily associated with the length of the hydraulic cylinder assembly, A-$B = q$. With the wheel fully down, $q = q_o$, while with the wheel fully

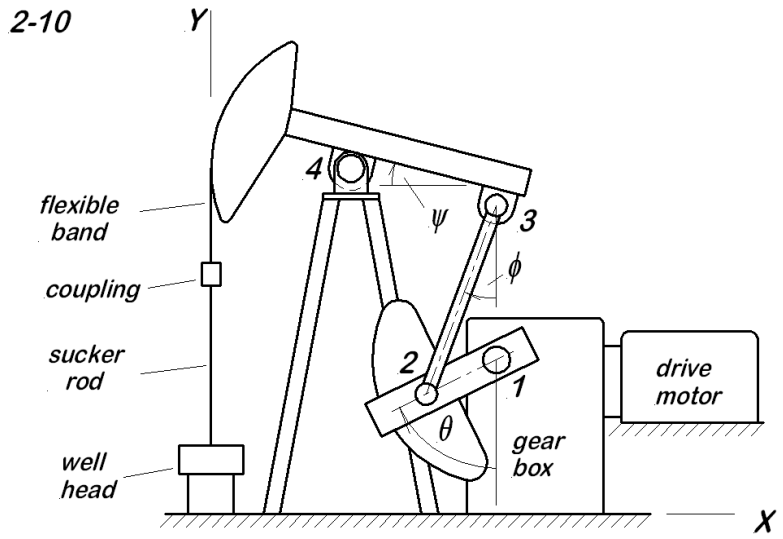

up, $q = q_f$. Note the $x - y$ coordinate system shown. With respect to that coordinate system, the strut is pivoted at the origin of coordinates, while one end of the hydraulic cylinder is fixed in the aircraft structure at (x_A, y_A), coordinates tabulated below. The following angle definitions are useful for the analysis:

$\alpha = 32^o$ = slot inclination angle;

β = inclination angle for the hydraulic cylinder axis with respect to the horizontal;

γ = inclination of the link BC with respect to the horizontal;

θ = angle of the wheel strut with respect to the vertical.

It will likely be necessary to introduce an additional variable in order to formulate the kinematic equations; call that variable s. When the landing gear is fully deployed ($\theta = 0^o$), the point B is on the $x-$axis at a point designated as x_{B1}. In this position, the link BC is exactly aligned with the guide slot.

System Data

$BC = 1404$ mm

$x_A = -846$ mm $\qquad y_A = 463$ mm

(a) Determine the required numerical values for the necessary geometric parameters not given, specifically CD, x_{B1}, q_o, q_f. and the cylinder stroke $stroke = q_o - q_f$;

(b) Write all of the position loop equations, identify the unknowns in a list, and write the Jacobian matrix. Put the list of unknowns in alphabetical order, Latin letters first,

followed by Greek letters;

(c) Obtain an expression that can be solved numerically for the velocity coefficients (do not solve; the method of Sect. 2.9 is recommended);

(d) Obtain an expression that can be solved numerically for the velocity coefficient derivatives (do not solve; the formulation of Sect. 2.9 is recommended);

(e) Develop and execute computer code to numerically solve for all positions, velocity coefficients, and velocity coefficient derivatives over the full stroke of the mechanism. Plot the results in normalized form.

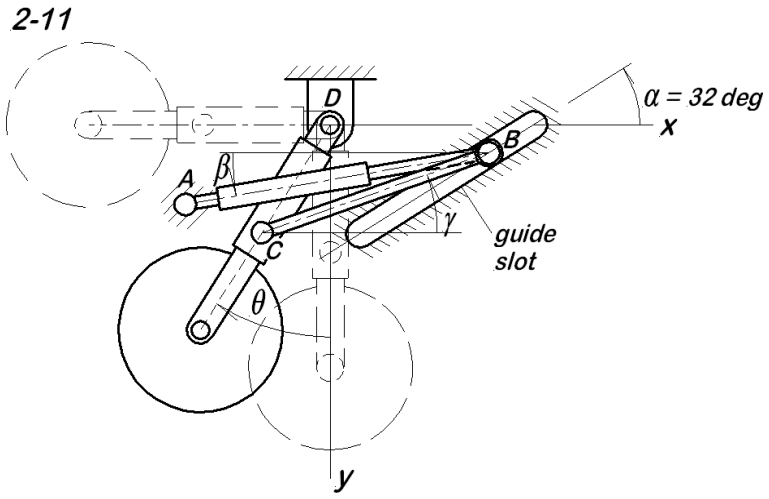

2-12 The figure shows an application of a four bar linkage as a rock crusher. The position of the crusher plate is described by the angle θ, while the rotation of the driving motor is ϕ. All dimensions shown are in millimeters.

(a) Write the position loop equations for the four bar linkage, the Jacobian, and the matrix equations solvable for the velocity coefficients, and velocity coefficient derivatives (do not solve);

(b) Develop an expression for the spring length, S as a function of both θ and ϕ, and also the expression for the velocity coefficient $\partial S/\partial\theta$.

2-13 The figure shows a light duty air compressor of novel design. The spherical piston, wrist pin, and connecting rod functions are all combined in a single molded plastic part; the cylinder is also a molded plastic part. Notice that the crank is actually just an eccentric circle. When the crank angle is $\theta = 0$, the piston is 1 mm from the top of the cylinder. With the data below, express the cylinder volume, $V(\theta)$ as a function of the crank angle.

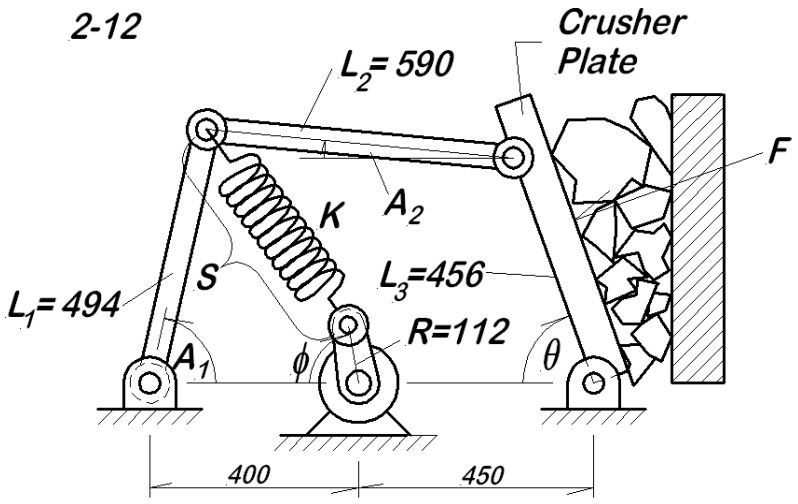

$R_1 = 11$ mm $\quad R_2 = 22$ mm $\quad R_3 = 30$ mm $\quad D = 82$ mm

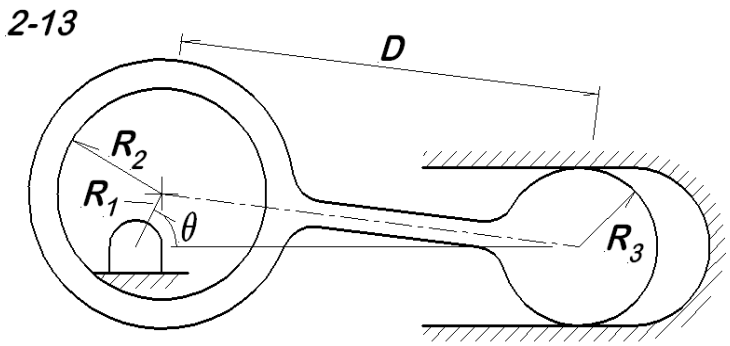

2-14 The mechanism shown is a *disappearing platform*, used to support a typewriter, computer, sewing machine, or other equipment that is only required on the work surface part of the time. In the fully raised position, the platform is level and the variable s is negative. When s is increased, the platform tilts to the right and down, lowering the unnecessary equipment so that a flat cover can be dropped in place. The system is shown in solid lines in the partly lowered position. Assume that the system data C_1, C_2, C_3, X_o, and Y_o is all given.

(a) Determine the system of equations to be solved for B_1, B_2, and B_3 for any assigned value of s (do not solve);

(b) Set-up the equations for the velocity coefficients K_{B1}, K_{B2}, and K_{B3} (do not solve).

2-15 The garage door mechanism shown is a four bar linkage, with the door itself comprising one of the four bars (*C-E-B*). The figure shows the door partially opened in solid line, and also in broken line in the fully closed (down) position. All of the basic geometric

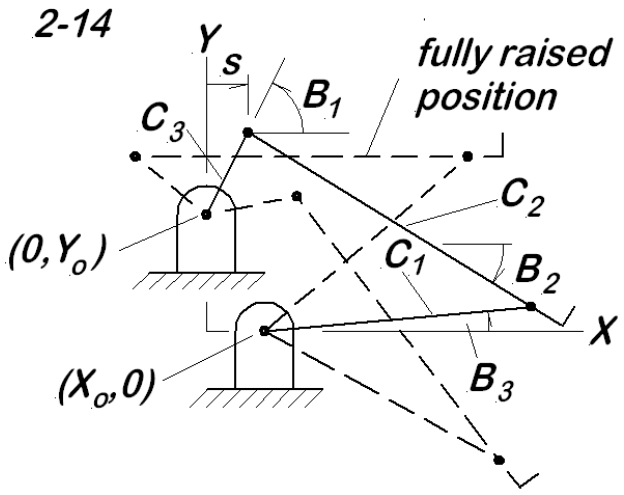

data is specified, including all fixed point locations and all dimensions (see problem 2-16 for notations).

(a) Considering the angle θ as primary, analyze the mechanism for all secondary variables (do not solve);

(b) Express all of the velocity coefficients;

(c) Express the spring length, S;

(d) Express the derivative $dS/d\theta$.

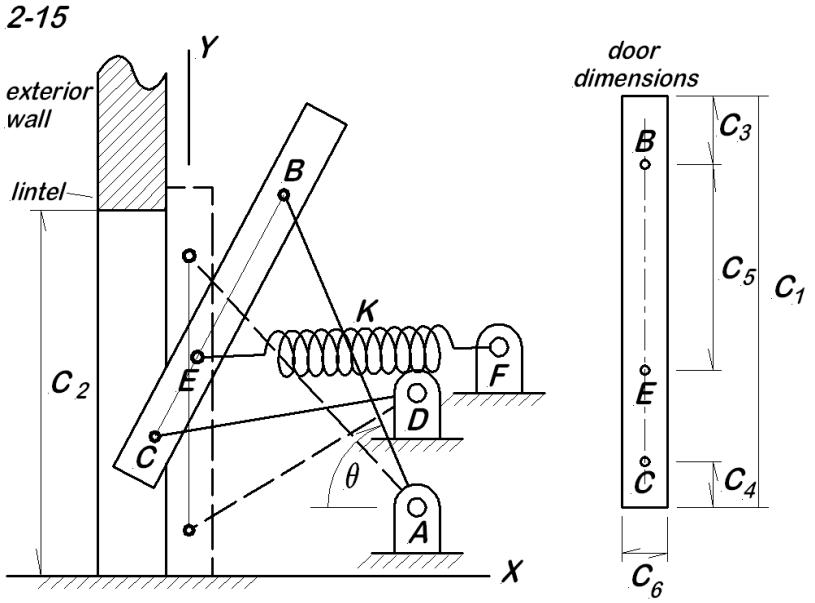

2-16 For the garage door mechanism of problem **2-15**, the numeric data below apply.

(a) What is the minimum value of θ?

(b) Will the lower edge of the door clear the lintel?

(c) If the maximum value of θ is $\theta_{\max} = 1.92$ rad, plot the function $S(\theta)$ over the full range of θ values;

(d) Plot the function $dS/d\theta$ over the full range of θ values.

$C_1 = 2134$ mm	$C_2 = 2079$ mm	$C_3 = 274$ mm
$C_4 = 274$ mm	$C_5 = 213$ mm	$C_6 = 90$ mm
$x_A = 1402$ mm	$y_A = 183$ mm	lower pivot location
$x_D = 1402$ mm	$y_D = 975$ mm	upper pivot location
$x_F = 2286$ mm	$y_F = 1066$ mm	spring anchor location

2-17 The wheel shown rolls without slipping while under the control of the crank and connecting rod. The mechanism is originally assembled with the crank and connecting rod aligned, and with the wheel center a distance S_o to the right of the crank pivot, as shown in broken line. The dimensional values C_1, C_2, r, R, and S_o are all known. The crank angle θ is considered the primary variable.

(a) Set up the equations required to determine the secondary variables (do not solve);

(b) Set up the equations for the velocity coefficients;

(c) Set up the equations for the velocity coefficient derivatives.

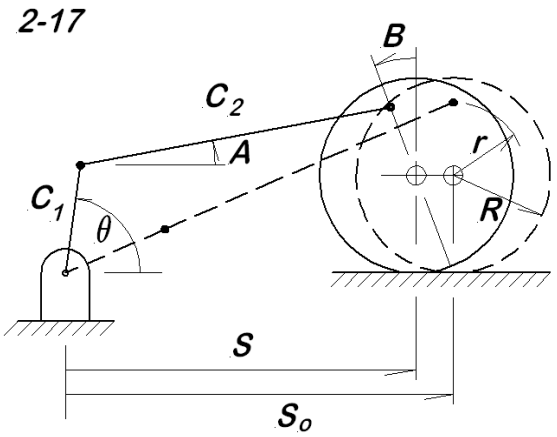

2-18 The circular disk rolls without slipping up and over the semicircular support as the

slider moves to the left. The mechanism is assembled as shown in the broken line with $A = 0$ and $s = 0$. The dimensions C_1, C_2, R_1, R_2, and r are all known. The focus is on the relation between A and s, with s considered as the primary variable. It will likely be necessary to define other constants and variables in order to solve the problem.

(a) Set up the equation(s) solvable for A as a function of s;

(b) Set up the equation(s) solvable for $K_A = dA/ds$;

(c) Set up the equation(s) solvable for $L_A = d^2A/d^2s$.

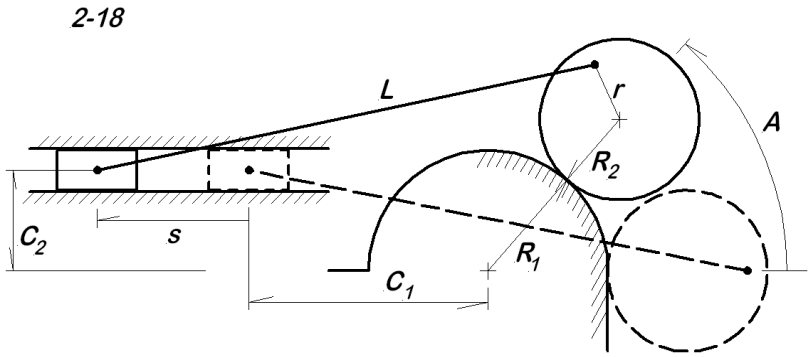

2-19 The wheel rolls without slipping in the circular guide (think of this as a ring gear with a pinion rolling inside it) while the slotted lever is pivoted at the center of the guide arc. A pin on the wheel engages the slotted lever. The system is initially assembled with $\theta = 0$ as shown in the broken lines. Consider θ as the primary variable.

(a) Set up the system of equations solvable for all secondary variables (do not solve);

(b) Set up the system of equations solvable for all secondary velocity coefficients (do not solve);

(c) Set up the system of equations solvable for all secondary velocity coefficient derivatives (do not solve).

2-20 The figure shows the mechanism of a pneumatically powered press. It is designed to take ordinary shop air (6 bar) and develop a very high force[4]. Be aware that the drawing is not to scale, either with respect to lengths or angles; it simply shows what elements connect to each other and what their *relative* positions are. The angles of the main link are not given because the calculation seems to be rather sensitive to their exact values. Thus it is preferable that the angles be determined internally to the computer code by use of the law of cosines.

[4]Based on a design problem described by R.T. Hinkle, *Design of Machines*, Prentice-Hall, 1957, pp. 119-124.

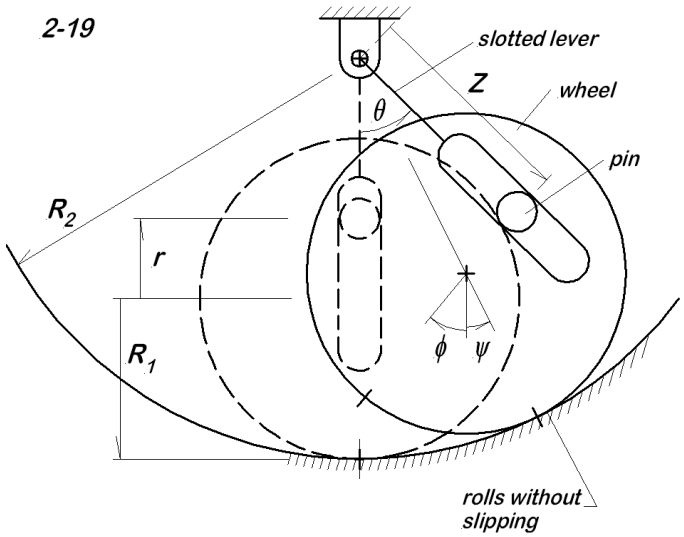

(a) Formulate the equations for the determination of the main link angles E_1, E_2, E_3, and E_4 but do not evaluate numerically;

(b) Formulate the full system of equations required to describe the kinematics of this system using the piston displacement q as the primary variable;

(c) Formulate the equations solvable for all of the velocity coefficients;

(d) Formulate the equations solvable for the velocity coefficient derivatives;

Press System Data

$B_1 = 27.94$	$B_2 = 137.84$	$B_3 = 193.04$	$B_4 = 334.34$	mm
$C_1 = 25.4$	$C_2 = 330.20$	$C_3 = 469.90$	$C_4 = 355.60$	mm
$C_5 = 1016.00$	$C_6 = 152.40$			mm
$L_1 = 180.34$	$L_2 = 230.87$	$L_3 = 330.22$	$L_4 = 571.66$	mm

$ac = 165.10$	mm	Main Link Diagonal (see Detail for corner notations)
$diam = 208.79$	mm	Air Cylinder Piston Diameter
$stroke = 300$	mm	Air Cylinder Piston Stroke Length
$P = 6.0$	bar	Air Cylinder Pressure

2-21 This problem is the further computer implementation of the analysis of the system considered in problem **2-20**. All data given there is understood to apply here as well.

(a) In a computer code, use B_1, B_2, B_3, B_4, and ac to determine E_1, E_2, E_3, and E_4 by

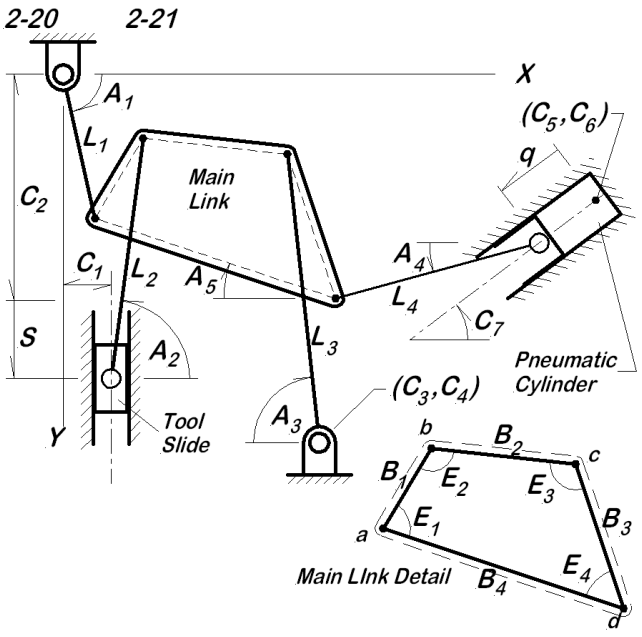

use of the law of cosines; be sure to store and use the full internal computer accuracy without rounding;

(b) Compute solutions for the full range of piston displacements in order to build a table of values at 25 mm increments from 0 to 300 mm (note: it will probably be useful to generate solutions on 1 mm increments, but only send every 25^{th} value to the output list);

(c) Use the solution values generated in the previous step to develop a computer animation of this mechanism during the forward stroke;

(d) Use the computer to generate a plot of tool position, $S\,(q)$, over the full stroke;

(e) Make a computer generated plot of $K_S\,(q)$ over the full stroke.

Chapter 3

MDOF Mechanisms

3.1 Introduction

Linkages and other mechanisms with multiple degrees of freedom (MDOF) require more than a single generalized coordinate, a number equal to the number of degrees of freedom. The linkage configuration is not fully specified until all of the generalized coordinates are specified. For kinematic analysis, this is equivalent to saying that there are multiple assigned primary variables. This has relatively little effect on the position solution, but it significantly complicates the velocity and acceleration analyses. As a result, multidegree of freedom kinematic analysis is often best handled on a case-by-case basis, rather than seeking a general approach comparable to that developed in the previous chapter.

In Chapter 2, in the context of single degree of freedom mechanisms, most of the concepts and tools required for this chapter were introduced. These include the idea of primary and secondary variables, position loop equations, the Newton-Raphson numerical solution technique, the Jacobian matrix, velocity and acceleration equations, and body coordinates. With mostly minor modifications, all of these appear again in this chapter in the context of multiple degree of freedom systems. Since there are few new theoretical tools to be introduced, most of the presentation is done by means of examples.

3.2 Closed-Form Kinematic Analysis

As demonstrated in the previous chapter, the kinematic analysis for some mechanisms can be completed in closed form, without resort to numerical methods. Although this is applicable for only a limited class of mechanisms, it is useful to consider this case for the insight it gives to the analysis process; sometimes the logic of the analysis is clouded by

the numerical solutions.

In the following two degree of freedom example, the positions, velocities, and accelerations for the secondary variables are determined in closed form. The modifications required to accommodate multiple degrees of freedom soon become evident. The motion of a particular point of interest is also developed.

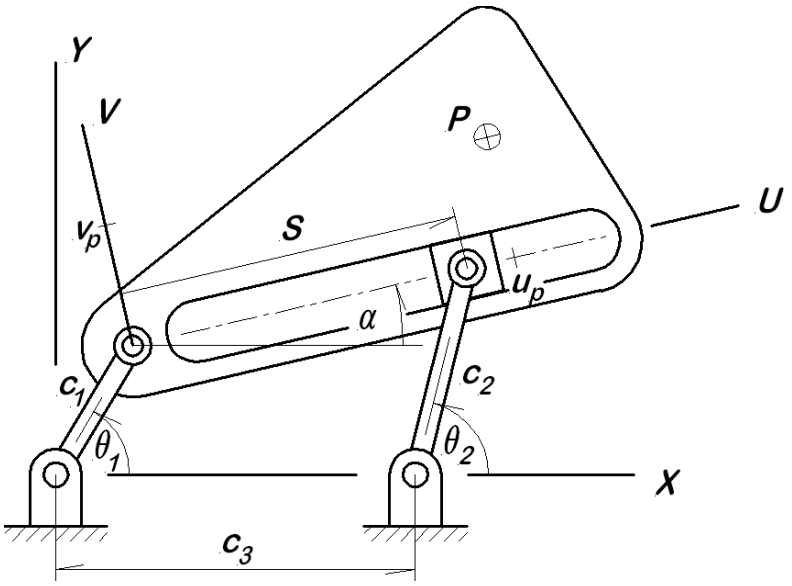

Figure 3.1: Sliding Four-Bar Linkage

3.2.1 Sliding Four-bar Example

A sliding four-bar mechanism is shown in Figure 3.1 (the name is something of a misnomer since the fourth bar, the coupler, is not of fixed length). It differs from the conventional four-bar mechanism in that the pivot connecting the second crank to the coupler is mounted on a slider embedded in the coupler, rather than being firmly attached at a fixed point. This has the effect of making the coupler length variable. The system has two degrees of freedom, here associated with the crank angles θ_1 and θ_2. The secondary coordinates are the coupler angle, α, and the slider position, s, that is the effective length of the coupler. A generic coupler point P with body coordinates (u_p, v_p) is also shown. Determine the position, velocity, and acceleration for the secondary variables and the point P.

3.2.1.1 Position Analysis

The mechanism involves a single position vector loop from which there are two scalar position loop equations:

$$c_1 \cos\theta_1 + s\cos\alpha - c_2\cos\theta_2 - c_3 = 0 \tag{3.1}$$
$$c_1 \sin\theta_1 + s\sin\alpha - c_2\sin\theta_2 = 0 \tag{3.2}$$

These equations are to be solved for the two secondary variables α and s. Although numerical methods are certainly applicable here, they are not required since there is a closed form solution available, first for α:

$$\tan\alpha = \frac{c_2\sin\theta_2 - c_1\sin\theta_1}{c_3 + c_2\cos\theta_2 - c_1\cos\theta_1} \tag{3.3}$$

For the linkage proportions indicated in the figure, $-\pi/2 < \alpha < \pi/2$. Consequently, this equation can be solved for α with the principal value of the arctangent function. That value is then available for use in the solution for s:

$$s = \frac{c_3 + c_2\cos\theta_2 - c_1\cos\theta_1}{\cos\alpha} \tag{3.4}$$

This completes the closed form solution for the secondary positions.

3.2.1.2 Velocity Analysis

When the position loop equations are differentiated with respect to time, the velocity loop equations are the result:

$$-c_1\dot{\theta}_1\sin\theta_1 + \dot{s}\cos\alpha - s\dot{\alpha}\sin\alpha + c_2\dot{\theta}_2\sin\theta_2 = 0 \tag{3.5}$$
$$c_1\dot{\theta}_1\cos\theta_1 + \dot{s}\sin\alpha + s\dot{\alpha}\cos\alpha - c_2\dot{\theta}_2\cos\theta_2 = 0 \tag{3.6}$$

Since the values of θ_1, θ_2, $\dot{\theta}_1$ and $\dot{\theta}_2$ are all assigned values, and the values of α and s have been determined, what remains is simply a pair of linear simultaneous equations in $\dot{\alpha}$ and $\dot{s}$. When these equations are cast in matrix form, the coefficient matrix on the left side is recognized as the familiar Jacobian matrix.

$$\begin{bmatrix} -s\sin\alpha & \cos\alpha \\ s\cos\alpha & \sin\alpha \end{bmatrix} \begin{Bmatrix} \dot{a} \\ \dot{s} \end{Bmatrix} = \begin{bmatrix} c_1\sin\theta_1 & -c_2\sin\theta_2 \\ -c_1\cos\theta_1 & c_2\cos\theta_2 \end{bmatrix} \begin{Bmatrix} \dot{\theta}_1 \\ \dot{\theta}_2 \end{Bmatrix} \tag{3.7}$$

When these equations are solved for the velocities, the result is

$$\begin{Bmatrix} \dot{a} \\ \dot{s} \end{Bmatrix} = \begin{bmatrix} -(c_1/s)\cos(\alpha-\theta_1) & (c_2/s)\cos(\alpha-\theta_2) \\ -c_1\sin(\alpha-\theta_1) & c_2\sin(\alpha-\theta_2) \end{bmatrix} \begin{Bmatrix} \dot{\theta}_1 \\ \dot{\theta}_2 \end{Bmatrix} \tag{3.8}$$

This shows that the two secondary velocities, $\dot{\alpha}$ and $\dot{s}$, can be written as a linear combination of the two primary velocities, $\dot{\theta}_1$ and $\dot{\theta}_2$. On the one hand, this is exactly the result that would be expected, but notice that the secondary velocities are proportional to a **combination** of primary velocities, rather than being proportional to a single primary velocity. The velocity coefficients are no longer a simple column vector as in Chapter 2, but now appear as a (2×2) matrix.

In general, for the multidegree of freedom situation, the velocity coefficient matrix is a rectangular matrix, with the number of columns equal to the number of primary variables and the number of rows equal to the number of secondary variables. It is simply a coincidence that in this example problem those two numbers are equal, resulting in a square velocity coefficient matrix.

3.2.1.3 Acceleration Analysis

The accelerations are obtained in the usual manner by differentiation of the velocity equations, starting with the velocity coefficient form. The alternative is to differentiate the velocity loop equations, requiring that the system be solved for the secondary accelerations. Following the route indicated, the process is

$$\begin{Bmatrix} \ddot{\alpha} \\ \ddot{s} \end{Bmatrix} = [K] \begin{Bmatrix} \ddot{\theta}_1 \\ \ddot{\theta}_2 \end{Bmatrix} + \dot{\theta}_1 \frac{\partial}{\partial\theta_1}([K]) \begin{Bmatrix} \dot{\theta}_1 \\ \dot{\theta}_2 \end{Bmatrix} + \dot{\theta}_2 \frac{\partial}{\partial\theta_2}([K]) \begin{Bmatrix} \dot{\theta}_1 \\ \dot{\theta}_2 \end{Bmatrix} \tag{3.9}$$

$$= [K] \begin{Bmatrix} \ddot{\theta}_1 \\ \ddot{\theta}_2 \end{Bmatrix} + \dot{\theta}_1 [L_1] \begin{Bmatrix} \dot{\theta}_1 \\ \dot{\theta}_2 \end{Bmatrix} + \dot{\theta}_2 [L_2] \begin{Bmatrix} \dot{\theta}_1 \\ \dot{\theta}_2 \end{Bmatrix} \tag{3.10}$$

where the $[L_j]$ are velocity coefficient *partial* derivatives. In computing each of these partial derivatives, one of the primary variables is varied, along with the secondary variables

as they depend upon that particular primary variable.

$$[K] = \begin{bmatrix} -(c_1/s)\cos(\alpha-\theta_1) & (c_2/s)\cos(\alpha-\theta_2) \\ -c_1\sin(\alpha-\theta_1) & c_2\sin(\alpha-\theta_2) \end{bmatrix} \tag{3.11}$$

Thus consider the calculation of the $(1,1)$ element for the $[L]_1$ matrix, the partial derivative with respect to θ_1:

$$\begin{aligned} L_1(1,1) &= \frac{\partial}{\partial\theta_1}(K_{11}) + \frac{\partial}{\partial\alpha}(K_{11})\frac{\partial\alpha}{\partial\theta_1} + \frac{\partial}{\partial s}(K_{11})\frac{\partial s}{\partial\theta_1} \\ &= \frac{\partial}{\partial\theta_1}(K_{11}) + K_{11}\frac{\partial}{\partial\alpha}(K_{11}) + K_{21}\frac{\partial}{\partial s}(K_{11}) \\ &= (c_1/s)(K_{\alpha 1}-1)\sin(\alpha-\theta_1) + \left(c_1/s^2\right)K_{s1}\cos(\alpha-\theta_1) \end{aligned} \tag{3.12}$$

The others are done in a similar manner to give the results

$$[L_1] = \frac{\partial[K]}{\partial\theta_1} = \begin{bmatrix} (c_1/s)(K_{11}-1)\sin(\alpha-\theta_1) & -(c_2/s)K_{11}\sin(\alpha-\theta_2) \\ +(c_1/s^2)K_{21}\cos(\alpha-\theta_1) & -(c_2/s^2)K_{21}\cos(\alpha-\theta_2) \\ \\ c_1(1-K_{11})(\alpha-\theta_1) & c_2K_{11}\cos(\alpha-\theta_2) \end{bmatrix} \tag{3.13}$$

$$[L_2] = \frac{\partial[K]}{\partial\theta_2} = \begin{bmatrix} (c_1/s)K_{12}\sin(\alpha-\theta_1) & (c_2/s)(1-K_{12})\sin(\alpha-\theta_2) \\ +(c_1/s^2)K_{22}\cos(\alpha-\theta_1) & -(c_2/s^2)K_{22}\cos(\alpha-\theta_2) \\ \\ -c_1K_{12}\cos(\alpha-\theta_1) & -c_2(1-K_{12})\cos(\alpha-\theta_2) \end{bmatrix} \tag{3.14}$$

3.2.1.4 Position, Velocity, and Acceleration for Point P

The base coordinates of P are readily expressed after the secondary variables have been determined:

$$x_p = c_1 \cos\theta_1 + u_p \cos\alpha - v_p \sin\alpha \tag{3.15}$$
$$y_p = c1 \sin\theta_1 + u_p \sin\alpha + v_p \cos\alpha \tag{3.16}$$

With one time differentiation, the velocity components are

$$\begin{Bmatrix} \dot{x}_p \\ \dot{y}_p \end{Bmatrix} = \begin{bmatrix} -c_1 \sin\theta_1 & 0 \\ c_1 \cos\theta_1 & 0 \end{bmatrix} \begin{Bmatrix} \dot{\theta}_1 \\ \dot{\theta}_2 \end{Bmatrix} + \begin{bmatrix} -u_p \sin\alpha - v_p \cos\alpha & 0 \\ u_p \cos\alpha - v_p \sin\alpha & 0 \end{bmatrix} \begin{Bmatrix} \dot{\alpha} \\ \dot{s} \end{Bmatrix}$$
$$= \begin{bmatrix} -c_1 \sin\theta_1 - K_{11}\left(u_p \sin\alpha + v_p \cos\alpha\right) & -K_{12}\left(u_p \sin\alpha + v_p \cos\alpha\right) \\ c_1 \cos\theta_1 + K_{11}\left(u_p \cos\alpha - v_p \sin\alpha\right) & K_{12}\left(u_p \cos\alpha - v_p \sin\alpha\right) \end{bmatrix} \begin{Bmatrix} \dot{\theta}_1 \\ \dot{\theta}_2 \end{Bmatrix} \tag{3.17}$$

The coefficient matrix on the right is the velocity coefficient matrix for point P, denoted as $[K_p]$. Note that again, a 2×2 matrix is obtained, rather than just a column vector.

With $\ddot{\alpha}$ and $\ddot{s}$ already determined, perhaps the quickest way to obtain $\ddot{x}_p$ and $\ddot{y}_p$ is to simply differentiate the first form given above for the velocity components, leaving $\ddot{\alpha}$ and $\ddot{s}$ in the final result. The results of those differentiations are

$$\ddot{x}_p = -c_1\ddot{\theta}_1 \sin\theta_1 - c_1\dot{\theta}_1^2 \cos\theta_1 - \ddot{\alpha}\left(\sin\alpha + v_p \cos\alpha\right) - \dot{\alpha}^2\left(u_p \cos\alpha - v_p \sin\alpha\right) \tag{3.18}$$
$$\ddot{y}_p = c_1\ddot{\theta}_1 \cos\theta_1 - c_1\dot{\theta}_1^2 \sin\theta_1 + \ddot{\alpha}\left(u_p \cos\alpha - v_p \sin\alpha\right) - \dot{\alpha}^2\left(u_p \sin\alpha + v_p \cos\alpha\right) \tag{3.19}$$

3.2.1.5 Numerical Values

The particular system for which these numerical values are calculated is defined by the following parameters:

$c_1 = +0.150$ m $\qquad u_p = +0.620$ m

$c_2 = +0.220$ m $\qquad v_p = +0.350$ m

$c_3 = +0.350$ m

The calculations are made for an instant when the primary variable motions are these:

$$\begin{array}{llll} \theta_1 = +0.85000 & \text{rad} & \theta_2 = +0.25000 & \text{rad} \\ \dot{\theta}_1 = -2.6000 & \text{rad/s} & \dot{\theta}_2 = +3.50000 & \text{rad/s} \\ \ddot{\theta}_1 = +0.42000 & \text{rad/s}^2 & \ddot{\theta}_2 = +0.68000 & \text{rad/s}^2 \end{array}$$

Substituting these results into the previous analysis gives

$$\begin{array}{llll} \alpha = -0.12487 & \text{rad} & s = +0.46781 & \text{m} \\ \dot{\alpha} = +1.99960 & \text{rad/s} & \dot{s} = -0.60471 & \text{m/s} \\ \ddot{\alpha} = +5.07616 & \text{rad/s}^2 & \ddot{s} = -1.64646 & \text{m/s}^2 \end{array}$$

The velocity coefficient and velocity coefficient partial derivatives may be of interest:

$$[K] = \begin{bmatrix} -0.17997 & +0.43762 \\ +0.12414 & -0.08055 \end{bmatrix}$$

$$[L_1] = \begin{bmatrix} +0.36090 & -0.43762 \\ +0.09934 & -0.03684 \end{bmatrix}$$

$$[L_2] = \begin{bmatrix} -0.14712 & -0.02148 \\ -0.03684 & -0.11513 \end{bmatrix}$$

For the point P specified above, the global coordinates, velocity, and accelerations are

$$\begin{array}{llll} x_p = +0.75779 & \text{m} & y_p = +0.38275 & \text{m} \\ \dot{x}_p = +0.09817 & \text{m/s} & \dot{y}_p = +1.05987 & \text{m/s} \\ \ddot{x}_p = -4.72141 & \text{m/s}^2 & \ddot{y}_p = +1.54397 & \text{m/s}^2 \end{array}$$

The velocity coefficients for this point are

$$[K_p] = \begin{bmatrix} -0.06409 & -0.11818 \\ -0.01956 & +0.28829 \end{bmatrix} \text{ m}$$

This completes the numerical example for the sliding four bar linkage.

3.3 Numerical Kinematic Analysis

Multidegree of freedom mechanisms that lend themselves to complete closed-form solutions, such as in the preceding section, are relatively rare. Mechanisms that require numerical solutions for the kinematic equations are far more common.

3.3.1 Position and Velocity Analysis

The position solution proceeds exactly as before, beginning with the development of the position loop equations. The solution is obtained with the Newton-Raphson method; this is exactly as was done for single degree of freedom systems. The Newton-Raphson process requires the Jacobian matrix, and this may be obtained directly or as a part of the velocity analysis. For the latter, the position loop equations are differentiated with respect to time to obtain the velocity equations, a system of linear simultaneous equations. In preparation for determination of the unknown secondary velocities, the velocity loop equations can be re-arranged to the matrix form

$$\underbrace{[J]}_{n_2 \times n_2} \quad \underbrace{\left\{\dot{S}\right\}}_{n_2 \times 1} = \underbrace{[B]}_{n_2 \times n_1} \quad \underbrace{\{\dot{q}\}}_{n_1 \times 1} \tag{3.20}$$

where

$[J]$ is the $(n_2 \times n_2)$ Jacobian matrix,

$[B]$ is a $(n_2 \times n_1)$ rectangular coefficient matrix,

$\left\{\dot{S}\right\}$ is the $(n_2 \times 1)$ column vector of unknown secondary velocities,

$\{\dot{q}\}$ is the $(n_1 \times 1)$ column vector of assigned primary velocities.

There are several items to note at this point:

- For n_1 degrees of freedom, there are n_1 primary coordinates (provided that the system is holonomic);
- The number of secondary variables may well be different from the number of primary variables, so it is denoted as n_2;
- The secondary variables are collected into the single vector $\{S\}$ simply to represent all of them together;

- The primary velocities are designated as $\{\dot{q}\}$. This is because the classical notation for the primary variables (often called generalized variables) is q_i.

The velocity coefficient matrix is defined in the usual way as

$$\left\{\dot{S}\right\} = [K]\{\dot{q}\} \tag{3.21}$$

so it is evident that

$$[K] = [J]^{-1}[B] \tag{3.22}$$

Depending upon the software available for the evaluation of $[K]$, in many cases it is more advantageous to solve the system of linear equations $[J][K] = [B]$, but this depends on the tools available for the calculation.

3.3.2 Acceleration Analysis

The analysis of secondary accelerations proceeds exactly as was demonstrated in the closed-form solution, beginning by differentiating equation (3.21) with respect to time to obtain

$$\begin{aligned}\left\{\ddot{S}\right\} &= \dot{q}_1\frac{\partial[K]}{\partial q_1}\{\dot{q}\} + \dot{q}_2\frac{\partial[K]}{\partial q_2}\{\dot{q}\} + \cdots + [K]\{\ddot{q}\} \\ &= \dot{q}_1[L_1]\{\dot{q}\} + \dot{q}_2[L_2]\{\dot{q}\} + \cdots + [K]\{\ddot{q}\}\end{aligned} \tag{3.23}$$

where the notation $[L_i]$ represents $\partial[K]/\partial q_i$. As introduced in the earlier section, the $[L_i]$ are velocity coefficient partial derivative matrices, analogous to the velocity coefficient derivative vectors found for single degree of freedom systems. The next question is how to obtain these matrices by numerical means.

As mentioned above, the velocity coefficient matrix is defined by the relation

$$[J][K] = [B] \tag{3.24}$$

where the elements of $[J]$ and $[B]$ are known explicitly. This expression can be differentiated as a product to give

$$\frac{\partial [J]}{\partial q_i}[K] + [J]\frac{\partial [K]}{\partial q_i} = \frac{\partial [B]}{\partial q_i} \tag{3.25}$$

The required velocity coefficient partial derivative matrix is obtained as the solution of a system of simultaneous equations,

$$[L_i] = \frac{\partial [K]}{\partial q_i} = [J]^{-1}\left(\frac{\partial [B]}{\partial q_i} - \frac{\partial [J]}{\partial q_i}[K]\right) \tag{3.26}$$

Following this numerical evaluation, the secondary positions, velocities, and accelerations are readily determined by numerical means.

3.3.3 Numerical Example

Consider the four-bar linkage with one crank on a translating pivot as shown in Figure 3.2. For this mechanism, the system parameters are:

$c_1 = 2.24$ m $\quad x_4 = 4.00$ m

$c_2 = 2.26$ m $\quad y_4 = 0.50$ m

$c_3 = 1.77$ m

At the moment of interest, the system configuration is described by

$s = +1.040$ m $\qquad \theta = 1.107$ rad

$\dot{s} = -0.520$ m/s $\quad \dot{\theta} = -0.270$ rad/s

$\ddot{s} = +0.390$ m/s^2 $\quad \ddot{\theta} = 1.350$ rad/s^2

The problem is to determine α, $\dot{\alpha}$, $\ddot{\alpha}, \beta$, $\dot{\beta}$, and $\ddot{\beta}$ by the numerical process described in the preceding section.

The position loop equations are these:

$$f_1 = s + c_1\cos\theta + c_2\cos\alpha - c_3\cos\beta - x_4 = 0 \tag{3.27}$$

$$f_2 = c_1\sin\theta + c_2\sin\alpha - c_3\sin\beta - y_4 = 0 \tag{3.28}$$

The standard Newton-Raphson technique provides a solution for the given configuration,

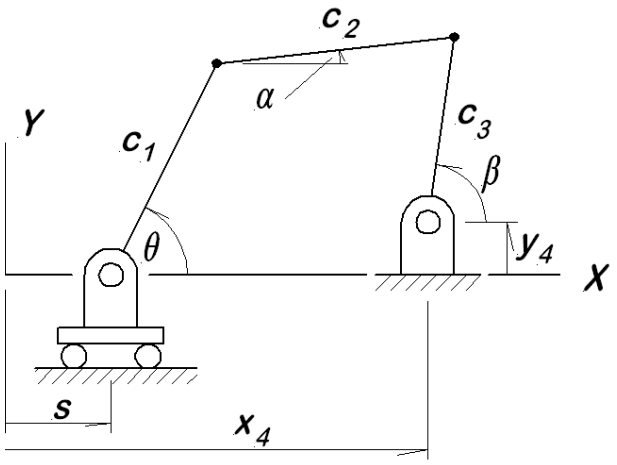

Figure 3.2: Kinematic Skeleton for Four-Bar Linkage with Translating Crank Pivot

$\alpha = 0.10768$ rad and $\beta = 1.40680$ rad. There is nothing at all novel about this part of the problem.

The Jacobian matrix is required, both for the Newton-Raphson and for the velocity analysis. It is evaluated as

$$\begin{aligned}[J] &= \begin{bmatrix} -c_2 \sin\alpha & c_3 \sin\beta \\ c_2 \cos\alpha & -c_3 \cos\beta \end{bmatrix} \\ &= \begin{bmatrix} -0.24288 & 1.74625 \\ 2.24691 & -0.28897 \end{bmatrix} \end{aligned} \tag{3.29}$$

The matrix $[B]$ for the right side of the velocity equation is also required; it is

$$\begin{aligned}[B] &= \begin{bmatrix} -1 & c_1 \sin\theta \\ 0 & -c_1 \cos\theta \end{bmatrix} \\ &= \begin{bmatrix} -1.0 & 2.00337 \\ 0.0 & -1.00206 \end{bmatrix} \end{aligned} \tag{3.30}$$

Together, these produce the velocity coefficient matrix, $[K]$,

$$\begin{aligned}[K] &= [J]^{-1}[B] \\ &= \begin{bmatrix} -0.07499 & -0.30386 \\ -0.58308 & +1.10497 \end{bmatrix}\end{aligned} \tag{3.31}$$

Applying this result for the velocity coefficients give the secondary velocities,

$$\dot{\alpha} = 0.12104 \text{ rad/s} \tag{3.32}$$

$$\dot{\beta} = 0.00486 \text{ rad/s} \tag{3.33}$$

The accelerations are calculated by equation (3.26), for which there are several parts:

$$\frac{\partial [B]}{\partial s} = \begin{bmatrix} 0 & 0 \\ 0 & 0 \end{bmatrix} \tag{3.34}$$

$$\frac{\partial [B]}{\partial \theta} = \begin{bmatrix} 0 & c_1 \cos\theta \\ 0 & c_1 \sin\theta \end{bmatrix} \tag{3.35}$$

$$\frac{\partial [J]}{\partial s} = \begin{bmatrix} -K_{11} c_2 \cos\alpha & K_{21} c_3 \cos\beta \\ -K_{11} c_2 \sin\alpha & K_{21} c_3 \sin\beta \end{bmatrix} \tag{3.36}$$

$$\frac{\partial [J]}{\partial \theta} = \begin{bmatrix} -K_{12} c_2 \cos\alpha & K_{22} c_3 \cos\beta \\ -K_{12} c_2 \sin\alpha & K_{22} c_3 \sin\beta \end{bmatrix} \tag{3.37}$$

When all of the numerical values are entered and the arithmetic performed, the velocity coefficient partial derivatives are

$$[L_1] = \begin{bmatrix} -0.27485 & +0.53016 \\ -0.08725 & +0.20968 \end{bmatrix} \tag{3.38}$$

$$[L_2] = \begin{bmatrix} +0.53016 & +0.01606 \\ +0.20968 & +0.49283 \end{bmatrix} \tag{3.39}$$

Finally, the secondary acceleration are obtained from equation (3.26), with the results

$$\ddot{\alpha} = -0.36374 \text{ rad/s}^2 \tag{3.40}$$
$$\ddot{\beta} = 1.33552 \text{ rad/s}^2 \tag{3.41}$$

This completes the evaluation of the secondary variables, their velocities, and their accelerations. It should be clear that the process is complicated, even for this relatively simple system. A highly systematic approach is the key to accurate results.

3.4 Other Systems

It is apparent that velocity and acceleration in multidegree of freedom system are more complicated than single degree of freedom systems, and further that the degree of complexity grows rapidly with the number of degrees of freedom. This is particularly true when there are more position loops involved.

In the first edition of this book, there is an example of motion analysis for the boom, digger stick, and bucket of a crawler excavator that illustrates the above statement well. For that system, there are three hydraulic cylinders involved, which indicates that there are three degrees of freedom. The linkage is such that there are four loops, so in a two dimensional analysis, there are eight equations in eight unknown secondary variables. Despite the greater system complexity, the position solutions are rather straight forward; the velocity and acceleration solutions are awkward at best. For any who are interested, the details can be found at [1]. At the other extreme, there are a number of fairly simple multidegree of freedom linkages that are fairly easy to analyze. Some of these find application in computing mechanisms [2].

An interesting exception occurs in the torsional vibration of the multicylinder internal combustion engine. The usual representation of this system is to assign one degree of freedom to each crank angle or other rotating element, so the number of degrees of freedom is equal to the number of cylinder plus any other rotating components. Such a system may involve a rather large number of degrees of freedom. But, with regard specifically to the slider-crank mechanisms of the engine, it is actually a collection of single degree of freedom mechanism that are elastically connected through the rotating shaft. In this situation, it is common to treat all of the slider-crank mechanisms as independent, single degree of freedom mechanism. This is all explored in some detail in Chapter 12.

3.5 Robotics Problem

In the typical kinematics problems considered to this point, the motion of the primary variables is specified and the motion of some particular point, usually denoted as P, is determined. This is sometimes described as the *forward kinematics problem.* In contrast, consider that the motion of point P is specified, and the question is to determine the primary motions required to cause that motion at P. This latter is called an *inverse kinematics problem.* In the terminology of robotics, the point P is selected as the location of the *end effector*, that is the tool that performs some useful work.

For example, in a robotic welder assembling an automobile, the electrode tip is the end effector, and the requirement is that electrode tip follow a specific path in executing a weld. The computer driving the robot does not control the electrode tip directly, but rather commands the necessary joint movements in the robot to create the required electrode motion. Usually there are servo motors, hydraulic or pneumatic cylinders, or other similar actuators under the direct control of the computer, and by the proper motion of these actuators, the required motion of the end effector is generated.

As an example of an inverse kinematics problem, consider the 2D robotic arm shown in Figure 3.3 tracing the stylized letter A in figure shown. A tool at the outer end of the arm is perhaps cutting the A into a panel, or maybe it is simply spraying paint to show the letter. In any event, the tool location is required to follow the centerline of the A. It is understood that the coordinates for the defining corners of the A are all known: (x_1, y_1), (x_2, y_2), (x_3, y_3), (x_4, y_4) and (x_5, y_5); this is simply the definition of the product. The values used for this example are:

$$x_1 = 10 \qquad y_1 = 2$$

$$x_2 = 20 \qquad y_2 = 25$$

$$x_3 = 18 \qquad y_3 = 2$$

$$x_4 = 14 \qquad y_2 = 11.2$$

$$x_5 = 21 \qquad y_5 = 11.2$$

The parameters that describe the robot itself are the pitch radius (R_p) for the drive gear and the centerline offset (C). For this example, the values used are $R_p = 1.8$, and $C = 2.6$. The units for the robot dimensions and for the (x_i, y_i) pairs may be considered to be either in inches or in centimeters; the choice has no effect on the analysis, provided the same units are used consistently throughout.

For the system shown, the primary variables, those directly driven, are the angle θ and ϕ. The arm is held in a housing that allows it to slide, thus varying the distance D. The change in D is driven directly by the pinion rotation ϕ, causing the rack to slide through

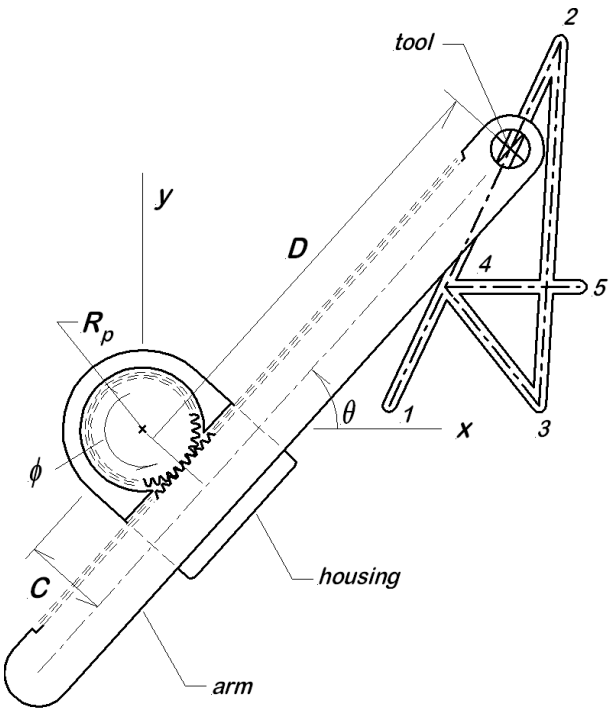

Figure 3.3: 2D Robotic Arm for Inverse Kinematics Problem

the guide groove in the housing. Angular motion of the arm is accomplished by rotating the housing through the angle described by θ. It is all conceptually pretty simple, but there is a complication. If ϕ is held fixed while θ is varied, this also varies D; the length D depends upon both θ and ϕ.

The reader may be concerned about θ and ϕ are driven. It is necessary to assume a pair of coaxial shafts, located behind the plane of the paper, and each shaft driving one variable. The inner shaft is coupled directly to the pinion, so it drives ϕ. The outer shaft is coupled to the underside of the housing, and thus drives θ. The necessary bearings, gearing, etc. are all understood to be exist behind the plane of the page.

3.5.1 Starting Point

In Figure 3.3, the zero position for θ is clearly identified as the $x-$axis, but there is some ambiguity about where ϕ is zero. The constraint relation between the rack and the pinion is

$$D = R_p\,(\phi - \theta) + D_o \tag{3.42}$$

where D_o is a constant. It is convenient to take $\phi = \theta$ so that $D = D_o$ when the tool is at position 1 of the work piece. If the coordinates of position 1 are (x_1, y_1) then

$$f_1 = C\sin\theta + D_o\cos\theta - x_1 = 0 \tag{3.43}$$
$$f_2 = -C\cos\theta + D_o\sin\theta - y_1 = 0 \tag{3.44}$$

where x_1, y_1 and C are all known, and $\theta = \phi$ and D_o are the unknowns to be determined by the Newton-Raphson method. If the unknowns here are considered as a vector $X = \mathrm{col}\,(D_o, \theta)$, and the functions to be solved are a vector $\{f\}$, the Jacobian matrix for this system is

$$[J] = \begin{bmatrix} \cos\theta & C\cos\theta - D_o\sin\theta \\ \sin\theta & C\sin\theta + D_o\cos\theta \end{bmatrix} \tag{3.45}$$

With the parameters given for the robot and the coordinates assigned for point #1, the numerical solutions are $D_o = 9.8610344$ and $\phi_o = \theta_o = 0.45519256$ rad for the starting position.

3.5.2 Tracing the Letter

The next matter to consider is how to trace out the letter, in this case, the stylized A, now that the starting point, (x_1, y_1) and starting values $(D_o, \phi_o = \theta_o)$ are known.

Consider first the leg from point 1 to point 2, having length L_{12}. To locate N_{12} evenly spaced points along this leg, including the end points, denote the distance from the first point by s_i, where

$$s_i = \frac{(i-1)}{N_{12}-1} L_{12} \tag{3.46}$$

where $i = 1, 2, \ldots, N_{12}$. The rectangular coordinates for a point s_i away from the first point are (x_i, y_i):

$$x_i = x_1 + \frac{s_i}{L_{12}}(x_2 - x_1) \tag{3.47}$$
$$y_i = y_1 + \frac{s_i}{L_{12}}(y_2 - y_1) \tag{3.48}$$

The similar equations are also used for all later legs of the A, with modifications as required, to describe points on the other lines. For each point, the position loop equations are

$$f_1 = C\sin\theta_i + D_i\cos\theta_i - x_i = 0 \tag{3.49}$$
$$f_2 = -C\cos\theta_i + D_i\sin\theta_i - y_i = 0 \tag{3.50}$$

which are solved for the values (D_i, θ_i) as before. As before, ϕ_i is then determined from the constraint equation,

$$\phi_i = \theta_i + (D_i - D_o)/R_p \tag{3.51}$$

This completes the process for the first leg of the A; the entire process must be repeated for each of the four legs in order to obtain the complete letter.

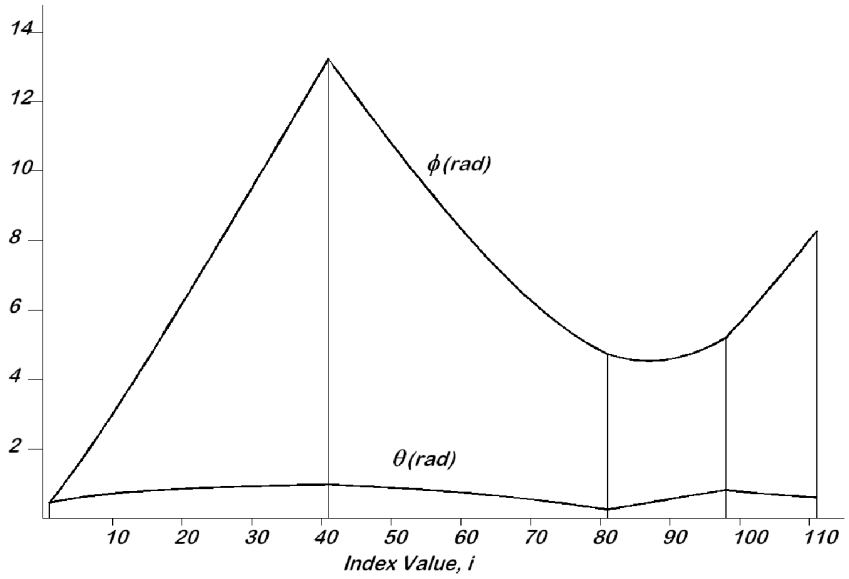

Figure 3.4: Input Angles Required to Trace the Letter A

Figure 3.4 shows plots of ϕ_i and θ_i against the index, i. The portions related to each leg of the A are clearly marked off by vertical lines. All together, there are 111 points used to describe the letter. It is evident that most of the input motion happens at the gear that drives the arm in and out; the input gear rotation begins at $\phi_o = 0.45519$ radians, and goes as high as $\phi_{\max} = 13.22671$ radians. The rotation of the housing, which rotates the arm as well, is a much smaller range of motion, $0.25472 \leq \theta \leq 0.97736$ radians.

It is evident that the inverse kinematics problem is fundamentally no different from the forward problem; it is simply a matter of different variables assigned and those to be determined.

3.6 Conclusion

It is evident that, with regard to positions only, there is little difference between single and multiple degree of freedom mechanism kinematics. In both cases, the position loop equations are solvable by the Newton-Raphson method. When velocities are considered, there is a significant increase in complexity for multiple degree of freedom systems. Finally, that increase is greatly compounded when accelerations are required. All of this is such that general solution formulations are not very practical, although many specific problems are workable on a case-by-case basis.

The matter of robot kinematics and the inverse problem is only considered slightly here, the details going well beyond the scope of the present book. It should be noted that for the particular example considered here, there is a unique solution. This is not always the case robot kinematics, particularly with more degrees of freedom. For those who are interested, there is a growing body of literature on the subject.

References

[1] Doughty, S., *Mechanics of Machines*, Wiley, 1988, pp.95-102.

[2] Svoboda, A., *Computing Mechanisms and Linkages,* Dover, 1969.

Problems

3-1 The figure shows a tape wound on a reel; the tape remains taut at all times. The free end is initially at the point (R, R) so that the initially unsupported length is $B_o = R$; in this state, the angle $\phi = 0$. The free end of the tape is then moved to (x, y), increasing the unsupported length to B.

(a) Set up equations solvable for B and ϕ for assigned values of x and y; do not solve;

(b) Set up the equations solvable for $\dot{B}$ and $\dot{\phi}$ in terms of $x, y, \dot{x}$, and $\dot{y}$.

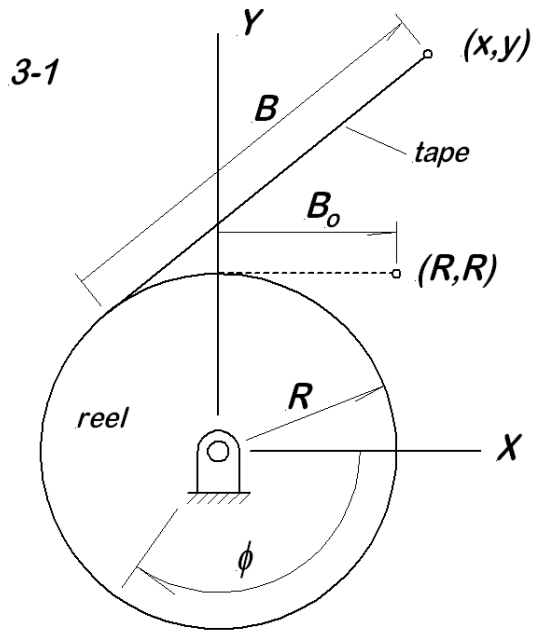

3-2 The mechanism shown may be considered as a "floating slider-crank" because the crank pivot is not stationary. The dimensions R, L, and C are known.

(a) Set up the position loop equations and solve in closed form for the secondary variables x and ϕ in terms of the primary variables s and θ; solve these in closed form;

(b) Obtain a closed form solution for the velocity coefficient matrix;

(c) Using the dimensions given below, evaluate x and ϕ for $s = 0.095$ m and $\theta = 0.35$ rad;

(d) Using the solution from (c) and the dimensions below, evaluate $\dot{x}$ and $\dot{\phi}$ for $\dot{s} = 2.45$ m/s and $\dot{\phi} = 1.35$ rad/s.

$R = 145$ mm $\quad L = 278$ mm $\quad C = 0.008$ mm

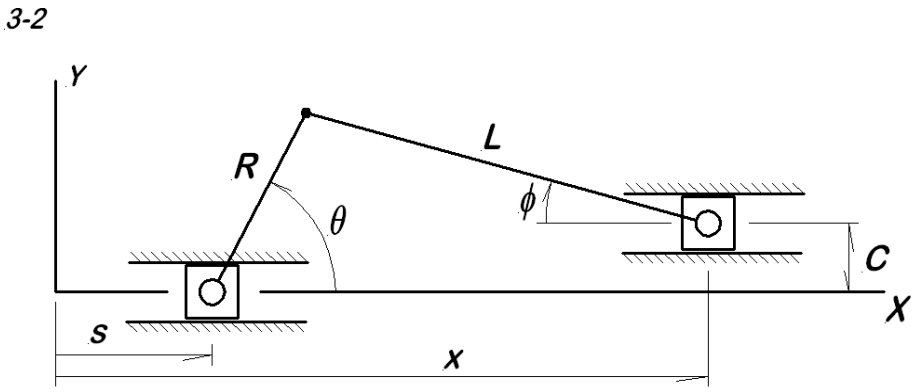

3-3 The figure shows a fork lift carrying a crate. There are three degrees of freedom associated with (1) the forward motion of the vehicle, (2) the hydraulic cylinder controlling the angle of the lift, and (3) the elevation of the forks. The dimensions D_1, D_2, D_3, u_c, and v_c are all known.

(a) Set up equations solvable for the secondary variables (do not solve);

(b) Set up equations solvable for the velocity coefficients (do not solve);

(c) Determine global coordinates for the center of mass of the crate;

(d) Determine the (2×3) velocity coefficient matrix for the center of mass.

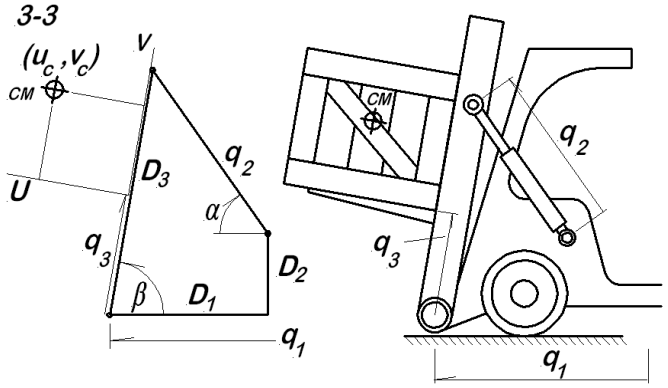

3-4 The figure shows what could be called a "floating four bar" linkage, floating in the sense that both of the crank pivots are moveable (and clearly there is no fourth bar). The dimensions C_1, C_2, C_3, C_4, and C_5 are all known values.

(a) Write the position loop equations, taking x, y, and θ as primary variables (do not solve);

(b) Set up the matrix equations solvable for the (2×3) velocity coefficient matrix (do

not solve).

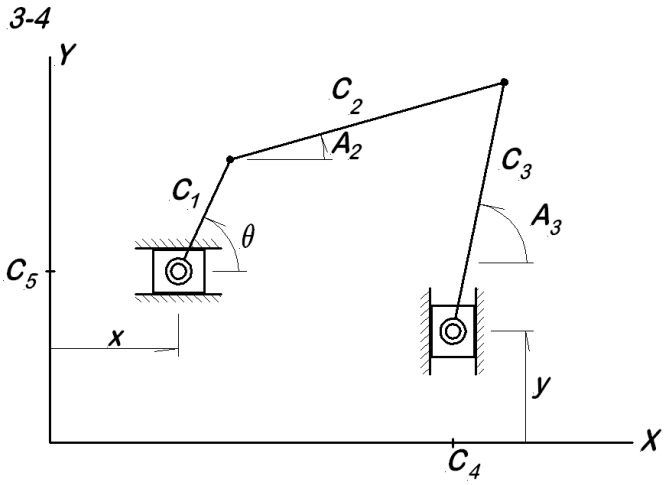

3-5 The figure shows a solid roller inside a hollow cylinder. At each interface there is rolling without slipping. The radii, r_i, r_o, and r_r are all known values. Take x and ϕ as primary variables.

(a) Write the position equations, including any constraints (do not solve);

(b) Write equations solvable for the secondary variable velocity coefficients (do not solve).

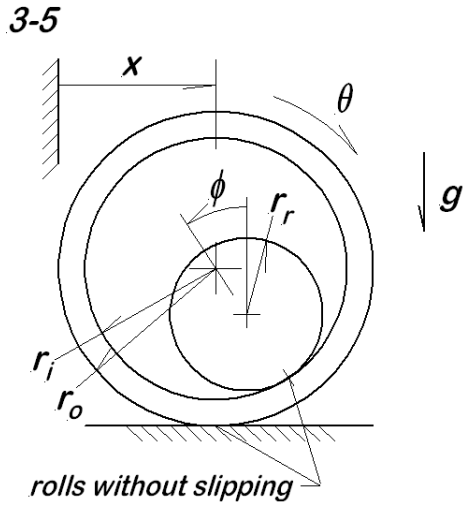

3-6 The figure shows a system of rollers, arranged as a planetary friction drive (this could equally well be a planetary gear train). On the left, the system is shown in an edge view with the planet carrier rotated into the picture plane. On the right the whole assembly is shown in an axial view, the planet carrier is rotated with respect to the vertical. The input rotations are θ_1 and θ_2, while the output is θ_o, all rotations about axes fixed in space. The ring rotation, θ_r, is about the same axis as the sun rotation, θ_2. Note that all

rotations are taken positive in the same sense. The points of fiction contact are identified as: C_1- drive gear 1 bearing against the ring; C_2- planet gear bearing against the ring; C_3- sun gear bearing against the planet gear. These are the only places where friction contact occurs, although C_2 and C_3 each occur twice. All contacts roll without slip. The sun, the planets, and the #1 drive roller all have radius r_p. The inner radius of the ring gear is therefore $r_r = 3r_p$.

(a) Determine an expression for the output rotation, θ_o, in terms of the input rotations θ_1 and θ_2 and the various radii;

(b) If the sun gear is fixed, determine the train ratio θ_o/θ_1;

(c) If the input θ_1 is held fixed, determine the train ratio θ_o/θ_2.

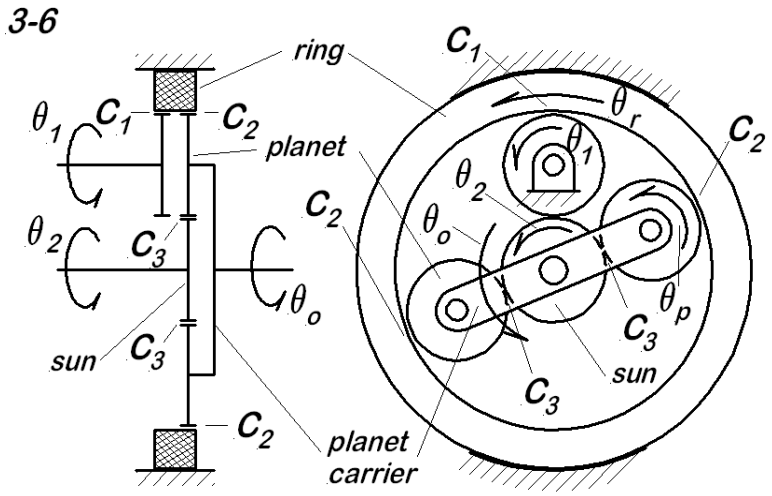

Chapter 4

Cams

4.1 Introduction

A *cam* is a solid body shaped such that its motion imparts a prescribed motion to a second body called the *follower* that is maintained in contact with the cam. The shape of the cam and the physical relation between the cam and the follower defines a particular functional relation between the cam position and the follower position over a range of cam motions. Cams provide one of the simplest ways to generate complex motions with high repeatability, reliability, and with reasonable costs. For these reasons, cams continue to be used in many types of modern machinery.

There are many types of cam and follower combinations, some of which are illustrated in Figures 4.1 and 4.2, but this is by no means an exhaustive compilation. All of the cams in Figure 4.1 shows what are called *disk cams* or *plate cams*, a reference to their generally plate-like form. Disk cams are commonly found in internal combustion engines, timer mechanisms, machine tools, and a host of other applications. In Figure 4.2, two other cam and follower types are shown, including a *wedge cam* and a *barrel* or *cylinder cam*. The wedge type is used in some vending machines and in such heavy industry applications as automated forming of nuts for use with bolts. The barrel cam is often used in automated assembly processes. Note the fact that the barrel cam is essentially a wedge cam wrapped around a cylinder.

The discussion of this chapter is limited to disk cams only; similar ideas apply for other cam-follower types. Even within the limitation of disk cams only, there is still considerable possible variation. From Figure 4.1, it is evident that the flat follower types shown in (a) and (b) involve sliding contact with the cam. While this is satisfactory for very low speeds and light loads, modern design practice strongly favors the use of roller followers such as those shown in (c) and (d). Roller followers produce quieter operation, reduced

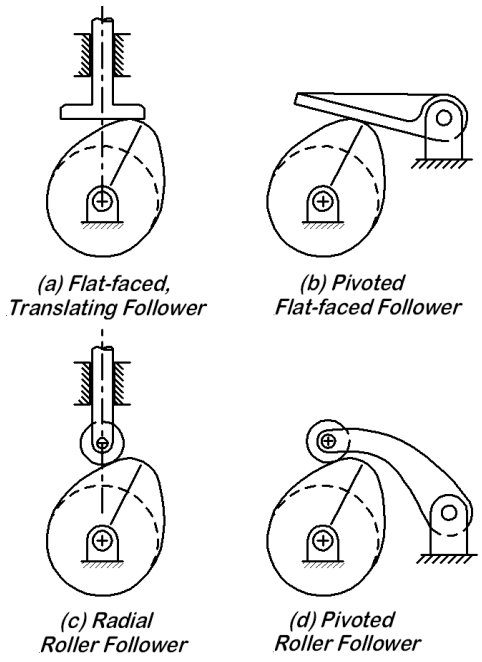

Figure 4.1: Disk or Plate Cams With Various Follower Types

friction and wear, and overall better performance than that available with sliding contact followers. Roller followers do, however, cost more. Flat-faced followers have the virtue of simplicity, ruggedness, and low cost. It should be noted in passing that curved-faced solid followers are used at times to approximate the shape of a roller follower in places where the environment is not suitable for a roller follower, but they still involve sliding contact.

The type of follower to be used is determined largely by the type of output motion required. In Figure 4.1 (c), a rotational input motion produces a translating output motion. In Figure 4.1 (d), a similar rotational input results in a rotational output motion. The choice between the several types shown in Figure 4.1 is dictated entirely by the type of output motion needed, performance demands, and costs.

In almost every application, the motion of the follower in a cam driven system is periodic; it repeats over and over again. This is obviously true when the input motion is a continuing rotation, but it is also true when the input motion is a reciprocating motion, such as that indicated for the wedge cam in Figure 4.2 (a).

For a cam and follower system with periodic motion, the total cycle of operation is typically similar to that shown in Figure 4.3. The system begins with the follower in a reference position, designated as zero displacement for the follower. As the input motion advances, the follower is forced to displace up to some maximum value; this initial action is called a *rise*. The full amount of the rise is usually called the *lift*, denoted as h. If the

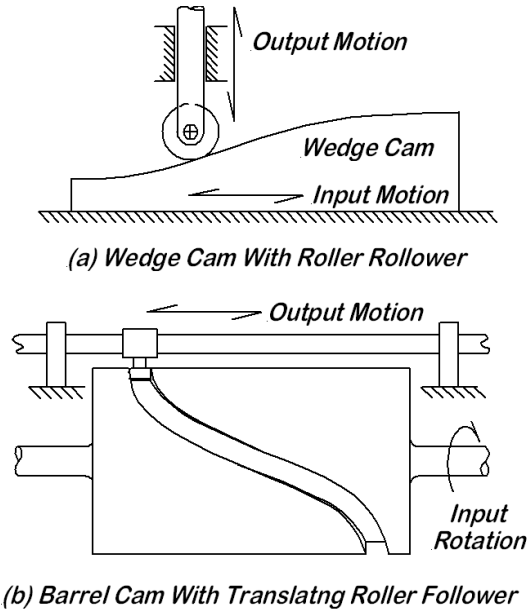

Figure 4.2: Other Cam and Follower System Types

follower displacement is denoted as $s(\theta)$, it is common practice to write this in terms of the product of the lift with a *nondimensional displacement function*, $f(\theta)$, so that $s(\theta) = h \cdot f(\theta)$. Note that $0 \leq f(\theta) \leq 1$. If the follower is held in a fixed position over some interval, this is called a *dwell*, and a dwell at maximum displacement is called a *high dwell*. With the input continuing to advance, the follower moves back down to the reference position; this motion is called a *return*. Following the return, the follower may dwell at the reference position through an interval called a *low dwell*. Each of these motions is called an *event*, and the amount of input motion associated with the interval is the *event length*, usually denoted as β.

To understand the significance of each phase, consider an IC engine valve train driven by a cam geared from the crankshaft. From a thermodynamic perspective, low dwell is extremely important; this it the interval when the valves are closed, combustion is occurring, and power is generated. Further, at high dwell the valves are open, and either a fresh charge is introduced or combustion products are expelled. The thermodynamicist would like the two dwells to be as long as possible, and the rise and return to occur instantaneously. From a dynamics perspective, the dwells are relatively uninteresting events; there is no motion in the system at all during a dwell. It is the rise and return that are significant in terms of dynamics, and particularly the facts that (1) rise and return cannot be instantaneous and (2) the associated forces involved must be limited. Thus the question as to which intervals are most significant depends entirely on the perspective of the questioner. Note also that, in particular applications, either or both of the dwells may be reduced to zero length. If both are zero, then the follower is continuously in motion as the input moves. Since the present discussion is primarily in

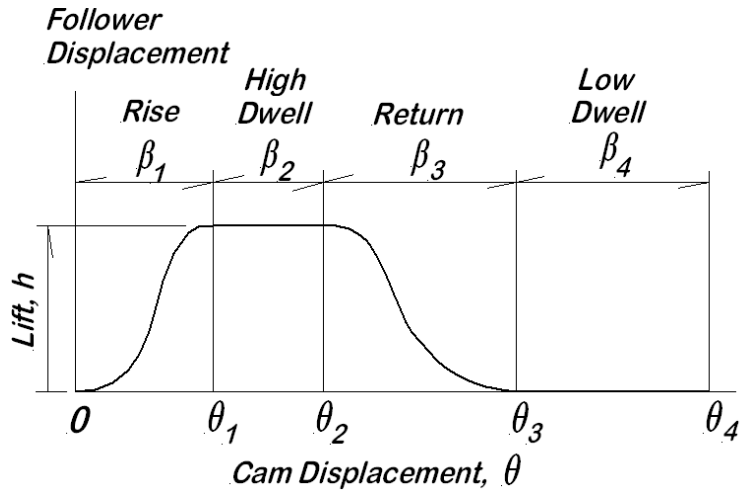

Figure 4.3: Typical Cam Displacement Diagram

regard to the system kinematics and dynamics, the discussion focus is on the rise and return phases and the associated end point transitions from one phase to the next.

It was mentioned at the very beginning that the follower is maintained in contact with the cam. This is essential if the cam is to control the position of the follower, but how is this continuous contact accomplished? What is there to prevent them from separating? In all the disk cam variations shown in Figure 4.1, there is nothing indicated to keep them together. There are two approaches to this problem. *Force closure* involves applying an external force to maintain the contact. This might be nothing more than a gravitational force, although much more often it involves a pre-loaded spring. It may reasonably be assumed that there is a spring applied to maintain closure in all the variations shown in Figure 4.1. *Form closure* means that there is a kinematic constraint that maintains the closure. This is illustrated in Figure 4.2 (b) where the follower is confined between the two walls of a groove on the cam cylinder. In actual operation, the barrel cam-follower system shown there must allow a small clearance between the follower and the groove walls; the roller cannot simultaneously roll on both sides of the groove. Thus, at least in this example, form closure is imperfect because a clearance is required. Difficulty of this sort is not uncommon in form closed cam-follower systems. Form closure is also used in disk-cam systems as well. The interested reader may wish to research further on (1) constant breadth cams and (2) desmodromic valve systems.

Figure 4.3 presents a *displacement diagram*, but what does it describe? The displacement diagram shows the functional relation between the cam input motion and the follower output motion. For any cam and follower system, the follower response motion is defined as the motion of a specific point in the follower system called the *trace point*. Here there is a major shift in view point for the cam discussion as compared with that in the two previous chapters. In Chapters 2 and 3, the focus is on the kinematic analysis of a given

system. In the present chapter regarding cams, the focus shifts from dealing with a given system to that of (1) defining a system that will satisfy certain operating criteria, and (2) analyzing the characteristics of a proposed solution. This is the shift from analysis to an engineering design focus.

In any situation for which a cam-follower system is proposed as a solution, there is some motion that must be accomplished. It usually involves moving some part from an initial position to another position, and in most cases, back to the initial position. In most cases, the extreme positions are specified, the time intervals available for each motion are stated, but the exact details of the motion are frequently not specified. The cam designer must choose a motion that satisfies all of the given specifications, that is physically realizable at reasonable costs, and that will function well throughout the expected life of the overall system. Referring back to Figure 4.3, this means that the upper and lower displacement limits are given and the event lengths are specified, but exact shape for the rise and return events must be specified by the designer. This is the design challenge.

The remainder of the chapter deals with the following topics:

- Detailed discussion of various types of displacement functions (the function described by the displacement diagram) and their relative advantages and disadvantages;
- Presentation of operational concerns such as pressure angles and associated side thrust on the follower, and profile radius of curvature which impacts contact concerns.

4.2 Displacement Functions

Over the years, many different displacement functions have been tried for various purposes. The discussion here focuses on rise curves, with the understanding that the displacement function, $f(\theta)$ can be manipulated in a variety of ways in order to apply it in various situations. It is useful at this point to discuss those manipulations briefly.

1. Although often written as simply $f(\theta)$, the engineer must remember that the angle θ always appears in a cam displacement function as a ratio with the event length, that is, in the form θ/β. Thus the *domain* of f is always the closed interval $[0, 1]$ and the *range* is also $[0, 1]$. This means that, when it is required to *stretch the function* to span a different cam rotation angle, all that is required is a new value for the event length, β.
2. The displacement function can be *translated*, so that it operates over a different portion of the cam cycle, by simply subtracting the new beginning point in the

argument. Thus, for $f(\theta/B)$ that would naturally as start to rise when $\theta = 0$, the beginning of the rise can be translated to the position Θ by simply writing $f[(\theta - \Theta)/\beta]$. Notice that the argument is zero at the beginning point ($\theta = \Theta$), and it is one for $\theta = \Theta + \beta$.

3. To create a return curve, the rise function $f(\theta)$ can *turned upside down* by simply subtracting it from one after being suitably translated, so that the return function is $1 - f(\theta/\beta)$.

4. Another way to create a return curve is to *flip the rise function from left-to-right.* Suppose that the return event is to occur between Θ_1 and Θ_2, two specific locations separated by the event length β. Then starting with the displacement function $f(\theta/\beta)$, the left-to-right flip is made by replacing the argument θ/β with the new argument $(\Theta_2 - \theta)/\beta$. Thus, when $\theta = \Theta_1$, the beginning of the event, the argument becomes $(\Theta_2 - \Theta_1)/\beta = 1$. At the other end of the event, when $\theta = \Theta_2$, the argument is $(\Theta_2 - \Theta_2)/\beta = 0$.

The reader might want to consider this question: What is the difference between #3 and #4, since each develops a return curve based on the original function $f(\theta/\beta)$?

Let the input motion be considered as a rotation through the angle θ, and the follower motion (either linear or angular) is denoted as $y(\theta) = h \cdot f(\theta)$. The displacement function $f(\theta)$ then completely describes $y(\theta)$, except for the scale factor h, whether the output is a linear motion or an angular motion and irrespective of the follower type. Then applying the chain rule for differentiation, it is evident that the derivatives of this motion are obtained as follows:

$$\begin{aligned}
&y(\theta) = h \cdot f(\theta) && \text{displacement function} \\
&\tfrac{dy}{dt} = h \tfrac{f(\theta)}{d\theta} \tfrac{d\theta}{dt} && \text{velocity function} \\
&\tfrac{d^2y}{d^2t} = h \left[\tfrac{f(\theta)}{d\theta} \tfrac{d^2\theta}{d^2t} + \tfrac{f^2(\theta)}{d^2\theta} \left(\tfrac{d\theta}{dt}\right)^2 \right] && \text{acceleration function} \\
&\tfrac{d^3y}{d^3t} = h \left[\tfrac{df}{d\theta} \tfrac{d^3\theta}{d^3t} + 3\tfrac{d^2f}{d^2\theta} \tfrac{d\theta}{dt} \tfrac{d^2\theta}{d^2t} + \tfrac{d^3f}{d^3\theta} \left(\tfrac{d\theta}{dt}\right)^3 \right] && \text{jerk function}
\end{aligned} \tag{4.1}$$

Because many cam applications operate at (approximately) constant input speed ($\dot{\theta} =$ constant), it is common practice in cam discussions to refer to $df/d\theta$, $d^2f/d^2\theta$, and $d^3f/d^3\theta$ as the velocity, acceleration and jerk, but this must be done with great caution because it is almost never entirely true. The operation of the cam usually implies a force exerted to move the follower, and the action of that force causes the mechanism to accelerate. The jerk function, which is the time derivative of the acceleration, may be unfamiliar to many readers. It is most often used in the context of cam operations and acoustics.

Although all of the displacement functions tried in the past superficially appear to be reasonable, it is quickly evident that some are much better than others for particular applications. In order to fully appreciate the sort of difficulties that make for a bad cam design (and are thus to be avoided), the discussion that follows begins with a bad choice that might seem a good choice to the uninformed.

4.2.1 Simple Harmonic Motion - A Bad Choice

Consider a displacement function to generate a simple harmonic lift over an event length β. This is accomplished by the function $f_{shm}(\theta)$

$$f_{shm}(\theta) = \frac{1}{2}\left[1 - \cos\left(\pi\theta/\beta\right)\right] \tag{4.2}$$

where the subscript shm denotes simple harmonic motion. Note that this function is 0.0 for $\theta = 0$, it is 1.0 for $\theta = \beta$, and it is smooth and differentiable everywhere. What could make it a bad choice?

Consider the derivatives of the proposed displacement function:

$$f'_{shm}(\theta) = \frac{\pi}{2\beta}\sin\left(\frac{\pi\theta}{\beta}\right) \tag{4.3}$$

$$f''_{shm}(\theta) = \frac{\pi^2}{2\beta^2}\cos\left(\frac{\pi\theta}{\beta}\right) \tag{4.4}$$

$$f'''_{shm}(\theta) = -\frac{\pi^3}{2\beta^3}\sin\left(\frac{\pi\theta}{\beta}\right) \tag{4.5}$$

While it is certainly true that the derivatives are smooth everywhere in the interior of the interval $0 < \theta < \beta$, it is important to examine their values at the ends of the interval to evaluate the transition to the next event. It is clear that the end point values are

$$\begin{aligned} f_{shm}(0) &= 0 & f_{shm}(\beta) &= 1 \\ f'_{shm}(0) &= 0 & f'_{shm}(\beta) &= 0 \\ f''_{shm}(0) &= \tfrac{\pi^2}{2\beta^2} & f''_{shm}(\beta) &= -\tfrac{\pi^2}{2\beta^2} \\ f'''_{shm}(0) &= 0 & f'''_{shm}(\beta) &= 0 \end{aligned} \tag{4.6}$$

If the adjoining event, either before or after the current event, is a dwell, then there will be a discontinuity in the second derivative, $f''(\theta)$, at the transition. The adjoining dwell has $f'' = 0$ at the transition point, while the sinusoid has a nonzero value for f'' at each end. This requires that there be a discontinuous change in the acceleration (assuming $\dot{\theta}$ = constant), and such a discontinuity requires the sudden application of a force (or torque), an impact event. Since impact is always to be avoided in such a system, the sinusoidal function is not a satisfactory displacement curve. Continuity in the displacement function and its derivatives through the entire operating cycle is the key smooth operation in cam systems, and discontinuities simply must be avoided.

Other simple functions have been considered in the past, such as parabolic and cubic displacement functions. In most cases, they are unsatisfactory in one respect or another. Several useful displacement functions are discussed next.

4.2.2 Commercially Useful Displacements

There are many cam applications in manufacturing, applications in which the cycle times are on the order of 100 cycles/minute or less. This includes various spot welding operations, pick-and-place operations, package sealing, and other similar applications. A wide variety of cam displacement curves have been developed over the years for such applications, and the three presented below are simply a sample.

4.2.2.1 Cycloidal Displacement Curve

Despite the fact that simple harmonic motion is not an acceptable choice in most cases, one of the attractive aspects of that choice is the fact that a single smooth function describes the entire process. This leads the cam designer to consider other similar curves while seeking to avoid the difficulties associated with the simple sinusoid. One such curve that has found wide application is the *cycloidal displacement curve*, identified by the subscript *cy* for cycloidal and described by the following equations:

$$f_{cy}(\theta) = \frac{\theta}{\beta} - \frac{1}{2\pi}\sin\left(\frac{2\pi\theta}{\beta}\right) \tag{4.7}$$

$$f'_{cy}(\theta) = \frac{1}{\beta}\left[1 - \cos\left(\frac{2\pi\theta}{\beta}\right)\right] \tag{4.8}$$

$$f''_{cy}(\theta) = \frac{2\pi}{\beta^2}\sin\left(\frac{2\pi\theta}{\beta}\right) \tag{4.9}$$

$$f'''_{cy}(\theta) = \frac{4\pi^2}{\beta^3}\cos\left(\frac{2\pi\theta}{\beta}\right) \tag{4.10}$$

Thus the first two derivatives are zero for $\theta = 0$ and at $\theta = \beta$, while the third derivative has a finite positive value at both ends. This makes it acceptable for many applications in terms of a transition to a dwell at each end. The negative aspects of this function are primarily:

- Relatively high velocity at the middle of the event, requiring more kinetic energy in the entire cam driven mechanism train;
- Relatively steep slopes at the quarter points of the event, resulting in larger contact forces in the cam system.

4.2.2.2 Modified Sine Curve

The cycloidal curve of the previous discussion utilized a single functional form for the full duration of the event, but this is not a requirement. The modified sine curve separates the complete event into three parts, using a different definition for $f(\theta)$ in each part. In order to accomplish this, continuity in the function and its derivatives at the junctions is an absolute necessity. The modified sine, subscript ms, is defined as shown in the equations below:

$$f_{ms}(\theta) = \begin{cases} \frac{1}{\pi+4}\left[\frac{\pi\theta}{\beta} - \frac{1}{4}\sin\left(\frac{4\pi\theta}{\beta}\right)\right] & \theta \le \frac{1}{8}\beta \\ \frac{1}{\pi+4}\left[2 + \frac{\pi\theta}{\beta} - \frac{9}{4}\sin\left(\frac{4\pi\theta}{3\beta} + \frac{\pi}{3}\right)\right] & \frac{1}{8}\beta \le \theta \le \frac{7}{8}\beta \\ \frac{1}{\pi+4}\left[4 + \frac{\pi\theta}{\beta} - \frac{1}{4}\sin\left(\frac{4\pi\theta}{\beta}\right)\right] & \theta \ge \frac{7}{8}\beta \end{cases} \tag{4.11}$$

$$f'_{ms}(\theta) = \begin{cases} \frac{\pi}{(\pi+4)\beta}\left[1 - \cos\left(\frac{4\pi\theta}{\beta}\right)\right] & \theta \le \frac{1}{8}\beta \\ \frac{\pi}{(\pi+4)\beta}\left[1 - 3\cos\left(\frac{4\pi\theta}{3\beta} + \frac{\pi}{3}\right)\right] & \frac{1}{8}\beta \le \theta \le \frac{7}{8}\beta \\ \frac{\pi}{(\pi+4)\beta}\left[1 - \cos\left(\frac{4\pi\theta}{\beta}\right)\right] & \theta \ge \frac{7}{8}\beta \end{cases} \tag{4.12}$$

$$f''_{ms}(\theta) = \begin{cases} \frac{4\pi^2}{(\pi+4)\beta^2}\sin\left(\frac{4\pi\theta}{\beta}\right) & \theta \le \frac{1}{8}\beta \\ \frac{4\pi^2}{(\pi+4)\beta^2}\sin\left(\frac{4\pi\theta}{3\beta} + \frac{\pi}{3}\right) & \frac{1}{8}\beta \le \theta \le \frac{7}{8}\beta \\ \frac{4\pi^2}{(\pi+4)\beta^2}\sin\left(\frac{4\pi\theta}{\beta}\right) & \theta \ge \frac{7}{8}\beta \end{cases} \tag{4.13}$$

$$f'''_{ms}(\theta) = \begin{cases} \frac{16\pi^3}{(\pi+4)\beta^3}\cos\left(\frac{4\pi\theta}{\beta}\right) & \theta \le \frac{1}{8}\beta \\ \frac{16\pi^3}{3(\pi+4)\beta^3}\cos\left(\frac{4\pi\theta}{3\beta} + \frac{\pi}{3}\right) & \frac{1}{8}\beta \le \theta \le \frac{7}{8}\beta \\ \frac{16\pi^3}{(\pi+4)\beta^3}\sin\left(\frac{4\pi\theta}{\beta}\right) & \theta \ge \frac{7}{8}\beta \end{cases} \tag{4.14}$$

As with the cycloidal curve, the modified sine has zero first and second derivatives at both ends of the event, making it suitable for transition to a dwell at either end in many situations. It accomplishes this with slightly lower values of peak velocity and peak acceleration than were found with the cycloidal curve.

- The principal negative aspect of the modified sine is the relatively large value of the third derivative at each end. This is a greater third derivative discontinuity than that presented by the cycloid.

4.2.2.3 Modified Trapezoidal Curve

The use of a multi-segment definition for the displacement function is further exploited with the modified trapezoidal motion curve. Consider first three definitions:

$$f_1(\theta) = \frac{1}{\pi+2}\left[\frac{2\theta}{\beta} - \frac{1}{2\pi}\sin\left(\frac{4\pi\theta}{\beta}\right)\right] \tag{4.15}$$

$$f_2(\theta) = \frac{1}{\pi+2}\left[\frac{1}{4} - \frac{1}{2\pi} + \frac{2}{\beta}\left(\theta - \frac{\beta}{8}\right) + \frac{4\pi}{\beta^2}\left(\theta - \frac{\beta}{8}\right)^2\right] \tag{4.16}$$

$$f_3(\theta) = \frac{1}{\pi+2}\left[\frac{-\pi}{2} + 2(\pi+1)\frac{\theta}{\beta} + \frac{1}{2\pi}\sin\left(4\pi\frac{\theta-\beta/2}{\beta}\right)\right] \tag{4.17}$$

Rothbart [1] uses these three functions to define the first half of the modified trapezoidal curve as

$$f(\theta) = \begin{cases} f_1(\theta) & 0 \le \theta < \beta/8 \\ f_2(\theta) & \beta/8 \le \theta < 3\beta/8 \\ f_3(\theta) & 3\beta/8 \le \theta < \beta/2 \end{cases} \tag{4.18}$$

But notice that this only gives a definition over the first half of the event! How is the remainder of the event to be defined? This provides an opportunity to demonstrate how these functions can be manipulated to apply to different parts of the overall displacement function. The whole process begins with a major observation: *The second half is to be an inverted mirror image of the first half of the event.* This means that the same three functions form the basis for the second half, but with two modifications:

1. If the functions f_1, f_2, and f_3 in the first half of the event are considered as measuring displacement up from $s = 0$, then those same functions will be used to measure displacement downward from $s = 1$, so the forms of interest are $1 - f_j$;

2. In the first half of the event, the angle θ measures distance from the beginning of the event. For the second half of the event, the angle used must measure distance from end of the event, that is, $\beta - \theta$.

This leads to the definition of three more functions for the second half of the event:

$$f_4(\theta) = 1 - f_3(\beta - \theta) = \frac{-\beta\pi^2 + 4\pi\theta(1+\pi) + \sin\left[\frac{2\pi(2\theta-\beta)}{\beta}\right]}{2\pi\beta(\pi+2)} \tag{4.19}$$

$$\begin{aligned} f_5(\theta) &= 1 - f_2(\beta - \theta) \\ &= \frac{-\left(33\pi^2\beta^2 - 8\beta^2 - 32\pi\beta\theta - 112\pi^2\beta\theta + 64\pi^2\theta^2\right)}{16\pi\beta^2(\pi+2)} \end{aligned} \tag{4.20}$$

$$f_6(\theta) = 1 - f_1(\beta - \theta) = \frac{2\pi^2\beta + 4\pi\theta + \sin\left[\frac{4\pi}{\beta}(\theta - \beta)\right]}{2\pi\beta(\pi+2)} \tag{4.21}$$

With these three additional functions defined, the definition for the modified trapezoidal curve, subscript mt, is

$$f_{mt}(\theta) = \begin{cases} f_1(\theta) & 0 \le \theta < \beta/8 \\ f_2(\theta) & \beta/8 \le \theta < 3\beta/8 \\ f_3(\theta) & 3\beta/8 \le \theta < \beta/2 \\ f_4(\theta) & \beta/2 \le \theta < 5\beta/8 \\ f_5(\theta) & 5\beta/8 \le \theta < 7\beta/8 \\ f_6(\theta) & 7\beta/8 \le \theta \le \beta \end{cases} \tag{4.22}$$

4.2.2.4 Comparisons

In Figure 4.4, there is a graphical comparison of the three displacement functions discuss just above. There are several points to be made regarding these graphs and the accompanying Table 4.1.

1. All the curves in each row are plotted to the same vertical scale, and all plots have the same horizontal scale, $0 \le \theta \le \beta$ where for convenience in plotting, the value $\beta = 1$ is assigned. This means that the peak values for each function (or

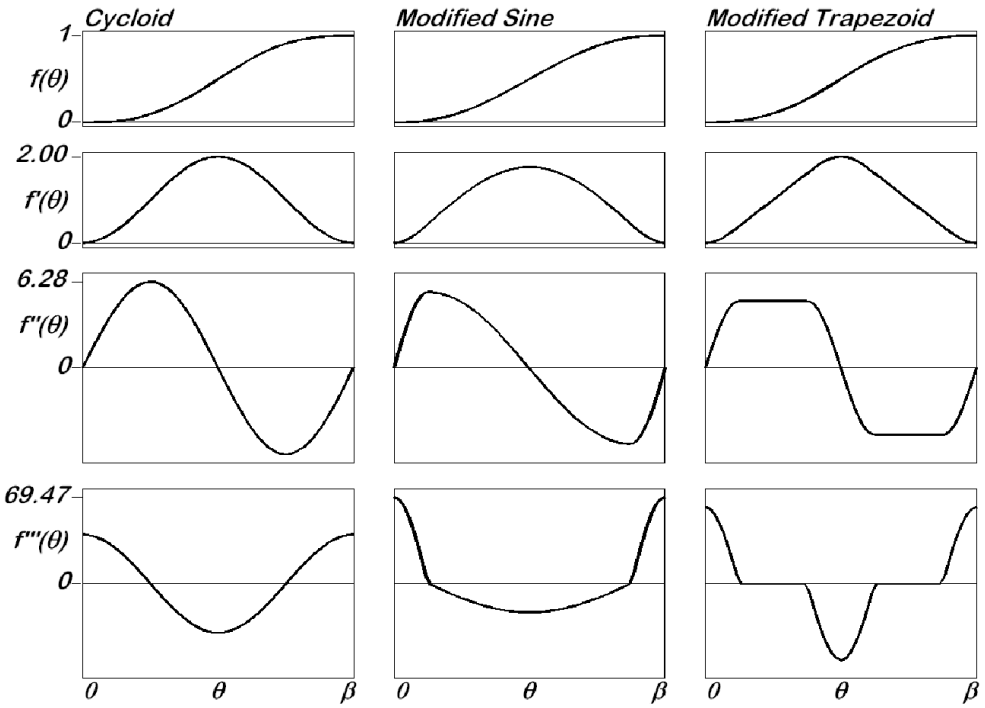

Figure 4.4: Sine, and Modified Trapezoidal Displacement Functions and Their Derivatives

function derivative) can be visually compared. For example, in the first row, all of the $f(\theta)$ values are in the range $[0, 1]$ (as expected), while in the second row, both the cycloidal and modified trapezoidal motions have peak value 2.0, while the modified sine peak is somewhat less.

2. On each row, at the left margin, the maximum value of the function (or the derivative) is plotted. These values are rounded to two decimal places to conserve space on the plot. More precise values of the extreme values for each function are given in Table 4.1.

3. Looking at the top row, the $f(\theta)$ curves for each displacement function, it is clear that they all appear identical to the eye. It is only in the derivatives that the differences become apparent. This shows the critical fact that extremely small variations in the cam profile can have a large impact on cam-follower operation.

4. In the second row, there are only small differences evident in the plots of $f'(\theta)$, although the almost straight sides on the modified trapezoidal motion curve tend to stand out. The somewhat reduced peak value associated with the modified sine is attractive in that it indicates less kinetic energy in the cam-follower system.

5. In the third row, there are clear differences between the three displacement functions in the second derivatives. Even so, they also remain somewhat similar, being positive over the first half of the event and negative over the second half. The lower

peak values associated with the modified trapezoid indicate reduced contact forces between the cam and follower because of less acceleration required.

6. In the last row, all three functions show finite end point discontinuities in $f'''(\theta)$. These are least severe with the cycloid and worst with the modified trapezoid.

Table 4.1 Extreme Values for Displacement Functions

	Cycloidal Motion	Modified Sine Motion	Modified Trapezoidal Motion
$f(\theta) =$	1.00000	1.000000	1.000000
$f'(\theta) =$	$2.00000/\beta$	$1.759603/\beta$	$2.000000/\beta$
$f''(\theta) =$	$6.283185/\beta^2$	$5.524590/\beta^2$	$4.888124/\beta^2$
$f'''(\theta) =$	$39.478418/\beta^3$	$69.466357/\beta^3$	$61.425975/\beta^3$

These are well known displacement functions, discussed by numerous authors including Moon [2], Rothbart [3], and Norton [4] .

4.2.3 Polynomial Displacement Functions

For high speed applications, the displacement functions of the previous sections do not perform adequately. This is particularly true for internal combustion engines, where the operating speed for the cam is often several thousand cycles per minute. In these situations, displacement functions expressed as polynomial power series are often preferred.

For the polynomial displacement functions, a polynomial rise function is written in the form

$$f(\theta) = c_o + c_1(\theta/\beta) + c_2(\theta/\beta)^2 + \cdots + c_n(\theta/\beta)^n \tag{4.23}$$

where, as before, β is the event length. The complete definition of the function requires (1) choosing the degree n for the polynomial, and (2) determination of the coefficients, c_o, c_1, ..., c_n to satisfy the necessary transition conditions at the ends of the event. The differentiation of such a form is trivial and need not be written out here.

4.2.3.1 3-4-5 Polynomial Displacement

The name *3-4-5 Polynomial* is a description of the nonzero terms in the final polynomial, along with the subscript *345*. For the *3-4-5* polynomial, the degree of the polynomial is chosen as 5, so that there are six coefficients to be determined. The end of event transition conditions that can be imposed are:

$$\begin{aligned} f(0) = 0 \;\; f'(0) = 0 \;\; f''(0) = 0 \\ f(\beta) = 1 \;\; f'(\beta) = 0 \;\; f''(\beta) = 0 \end{aligned} \tag{4.24}$$

When the polynomial and its derivative are evaluated at the ends, the result is six equations in the six unknown coefficients. When these equations are solved, the final form for the polynomial is

$$\begin{aligned} f_{345}(\theta) &= 10(\theta/\beta)^3 - 15(\theta/\beta)^4 + 6(\theta/\beta)^5 && (4.25) \\ &= (\theta/\beta)^3 \{10 - (\theta/\beta)[15 - 6(\theta/\beta)]\} && (4.26) \end{aligned}$$

It is a simple matter to differentiate this function to verify that it does indeed satisfy the six conditions specified. But note also that no condition is imposed upon the third derivative at the transition points, and it has a finite positive value at each end.

4.2.3.2 4-5-6-7 Polynomial Displacement

From the result of the previous section, it is evident that, if zero jerk is required at both transitions, a polynomial of higher degree is required. Thus choose $n = 7$ and impose the following transition conditions:

$$\begin{aligned} f(0) = 0 \;\; f'(0) = 0 \;\; f''(0) = 0 \;\; f'''(0) = 0 \\ f(\beta) = 1 \;\; f'(\beta) = 0 \;\; f''(\beta) = 0 \;\; f'''(0) = 0 \end{aligned} \tag{4.27}$$

The solution of the resulting equations for the polynomial coefficients produces the form

$$\begin{aligned} f_{4567}(\theta) &= 35(\theta/\beta)^4 - 84(\theta/\beta)^5 + 70(\theta/\beta)^6 - 20(\theta/\beta)^7 && (4.28) \\ &= (\theta/\beta)^4 (35 + (\theta/\beta)\{-84 + (\theta/\beta)[70 - 20(\theta/\beta)]\}) && (4.29) \end{aligned}$$

Again, it is a simple matter to verify that this function does indeed satisfy all of the eight transition conditions shown. In a manner similar to the previous case, the name *4-5-6-7 Polynomial* is a description of the nonzero terms in the final form and identified with the subscript *4567*.

There are many other options available using the power series polynomial form. These include the assignment of more transition constraints and the assignment of specific values at points interior to the event. As with any application of higher order power series, there is also the risk of inducing unwanted motion features, so this approach must be employed with some discretion.

4.2.3.3 Polynomial Evaluation - Horner's Method

The general problem of evaluation of polynomials and their derivatives has received considerable attention in applied mathematics, both in regard to potential for rounding errors and computing speed. When the signs alternate, as they do in the cam displacement applications, there is the possibility of serious loss of accuracy due to subtraction of nearly equal quantities. A paper by Burrus, et al. [5] suggests some ideas, based on what is usually called Horner's method, that can be adapted to the evaluation of the polynomial forms found in cam displacement functions. In particular, consider again the *3-4-5* polynomial cam displacement in its factored form, equation (4.26), here re-written as

$$\begin{aligned} f_{345}(\theta) &= a_3(\theta/\beta)^3 + a_4(\theta/\beta)^4 + a_5(\theta/\beta)^5 \\ &= (\theta/\beta)^3\{(\theta/\beta)[(\theta/\beta)a_5 + a_4] + a_3\} \end{aligned} \tag{4.30}$$

where

$$a_3 = 10 \quad a_4 = -15 \quad a_5 = 6$$

Horner's method uses a loop structure to numerically evaluate the sequence of parentheses, beginning with the inner most parenthesis pair and working outward. A fragment of computer code implementing this approach is shown below. The fragment includes (a) a portion of the main program where the parameters are set and a loop is established to cycle through many values of θ such that $0 \leq \theta \leq \beta$, and (b) a subroutine `Cam345` that evaluates the polynomial and its first three derivatives at each point. The central operation is executed in the `For-Next` loop of the subroutine in which f_{345}, f'_{345}, f''_{345} and f'''_{345} are evaluated, starting with `ip=5` and stepping backwards to `ip=3`; this is the sequential evaluation of each parenthesis pair.


```
    (Main Program)

beta=...
imx=...
FOR ix=1 to imx
    theta=(ix-1)*beta/(imx-1)
    CALL Cam345
NEXT ix

SUB Cam345
    DIM a(5)
    a(1)=1      ! this assignment of a(1) and a(2) is req'd
    a(2)=1
    a(3)=10
    a(4)=-15
    a(5)=6
    z=theta/beta
    f=0
    fp=0
    fpp=0
    fppp=0
    FOR ip=5 to 3 step -1
        f=f*z+a(ip)
        fp=z*fp+ip*a(ip)
        fpp=z*fpp+ip*(ip-1)*a(ip)
        fppp=z*fppp+ip*(ip-1)*(ip-2)*a(ip)
    NEXT ip
    f=f*z^3                        ! f(theta)
    fp=fp*z^2/beta                 ! f'(theta)
    fpp=fpp*z/beta^2               ! f''(theta)
    fppp=fppp/beta^3               ! f'''(theta)
END SUB
```

4.2.4 Example Problem

As an example of the application of the several displacement functions presented above, and particularly their manipulation to serve in different places, consider the cam timing diagram shown in Figure 4.5. The objective here is to develop the complete displacement description, and to evaluate the maximum velocity and acceleration when the cam rotation rate is constant at $\dot{\theta} = 200$ rad/s.

Note particularly the use of the capital Greek theta (Θ) to represent the typical rota-

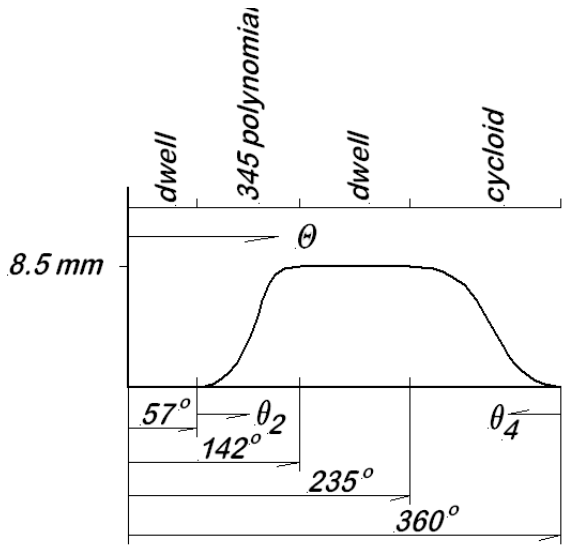

Figure 4.5: Timing Diagram for Example Problem

tion of the cam. This is done to distinguish it from the lower case letter, θ, used to represent angular position within the event. Mind the distinction; it is critical to correct understanding!

There are four events in the cam cycle[1], defined by the transition locations $\Theta_1 = 57^o$, $\Theta_2 = 142^o$, $\Theta_3 = 235^o$, and $\Theta_4 = 360^o$. Evaluation for each event is discussed separately here:

1. Low Dwell – The length of the first event is $\beta_1 = \Theta_1 = 0.99484$ rad. The displacement during this event is trivial,

$$y(\Theta) = \dot{y}(\Theta) = \ddot{y}(\Theta) = 0 \tag{4.31}$$

2. *3-4-5* **Polynomial Rise** – The length of the second event is $\beta_2 = \Theta_2 - \Theta_1 = 85^o = 1.4835$ rad. The relative rotation angle is $\theta_2 = \Theta - \beta_1$. This is employed in the evaluation of the motion, either by means of equation (4.25) or by equation (4.30) implemented in the subroutine Cam345 previously shown.

3. High Dwell – The length of the high dwell is $\beta_3 = \Theta_3 - \Theta_2 = 93^o = 1.6232$ rad. The displacement during this event is again trivial,

[1]For the purposes of this book, the reference angular position of the cam is as shown in Figure 4.3, with $\theta = 0$ at the end of the low dwell and the beginning of the rise curve. However, for this one example, the displacement diagram in Figure 4.5 is shifted to begin with a low dwell. This is done purposely to illustrate how the diagram can be mathematically shifted along the rotation axis as well as how rise curves can be reversed to serve as return curves.

$$y(\Theta) = 0.0085 \text{ m} \tag{4.32}$$
$$\dot{y}(\Theta) = \ddot{y}(\Theta) = 0 \tag{4.33}$$

4. Cycloidal Return – The length of the final event is $\beta_4 = \Theta_4 - \Theta_3 = 2.1817$ rad. For this event, the cycloidal motion equations are required, equations (4.7), (4.8), (4.9) and (4.10). The relevant angular argument for those equations, θ, is that shown in Figure 4.5 as $\theta_4 = \Theta_4 - \Theta$, with the event length $\beta = \beta_4$. Note particularly what happens in the derivative calculation for this event. The process described in the previous paragraph says that, within this event,

$$y(\Theta) = h \cdot f_{cy}(\Theta_4 - \Theta) \tag{4.34}$$

so that the velocity is

$$y = \frac{dy}{d\theta}\frac{d\theta}{d\Theta}\frac{d\Theta}{dt} = h\frac{df_{cy}}{d\theta}(-1)\omega = -h\omega f'_{cy}(\theta) \tag{4.35}$$

Because of the substitution used, $\theta_4 = \Theta_4 - \Theta$, a negative sign is introduced in the differentiation. When the second derivative is calculated, another negative sign is introduced, effectively canceling the first. The result is that the algebraic signs of the first and third derivatives must reversed as a result of this substitution.

A computer code implementing the entire process above is listed below. Note that it assumes the existence of four subroutines:

`sub LowDwell` – sets f and all derivatives to zero;

`sub Cam345` – evaluates the function f_{345} and derivatives during the rise event;

`sub HighDwell` – sets $f = 1$ with all derivatives equal to zero;

`sub Cycloid` – evaluates the function f_{cy} and derivatives for the return.

None of these four subroutines is listed here, but `Cam345` is listed previously. When the computer code is executed, the extreme values are found to be:

Max Position	$\|y\|_{Max}$	=	0.0085	m
Max Velocity	$\left\|\frac{dy}{dt}\right\|_{Max}$	=	2.147997	m/s
Max Acceleration	$\left\|\frac{d^2y}{d^2t}\right\|_{Max}$	=	891.91649	m/s^2
Max Jerk	$\left\|\frac{d^3y}{d^3t}\right\|_{Max}$	=	1249601	m/s^3

Not surprisingly, the very high jerk value is at the transitions before and after the second event, the *3-4-5* polynomial cam. This is not likely to be considered an acceptable cam design. The computer code fragment is listed below:

Computer Code Fragment for Example Problem

```
! Problem Data
h=0.0085
omega=200
capTH1=57*pi/180
capTH2=142*pi/180
capTH3=235*pi/180
capTH4=360*pi/180

beta1=capTH1
beta2=capTH2-capTH1
beta3=capTH3-capTH2
beta4=capTH4-capTH3

thmx=...                            ! number of angular positions
FOR ith=1 to thmx
    capTH=(ith-1)*2*pi/(thmx-1)
    ths(ith)=capTH                  ! save this value
    IF capTH<capTH1 then            ! event 1
       CALL LowDwell
    ELSE IF capTH1<=capTH and capTH<capTH2 then  ! event 2
       beta=beta2                   ! set event length
       th=capTH-capTH1              ! lower case theta2
       CALL Cam345
    ELSE IF capTH2<=capTH and capTH<capTH3 then  ! event 3
       CALL HighDwell
    ELSE IF capTH3<capTH then       ! event 4
       beta=beta4                   ! set event length
       th=capTH4-capTH              ! lower case theta4
       CALL Cycloid
```



```
      fp=-fp                    ! th4 increases backwards!
      fppp=-fppp                ! th4 increases backwards!
   END IF
   yy(ith)=h*f                  ! position
   yd(ith)=h*omega*fp           ! velocity
   ydd(ith)=h*omega^2*fpp       ! acceleration
   yddd(ith)=h*omega^3*fppp     ! jerk
   ymx=max(ymx,yy(ith))
   ydmx=max(ydmx,abs(yd(ith)))
   yddmx=max(yddmx,abs(ydd(ith)))
   ydddmx=max(ydddmx,abs(yddd(ith)))
NEXT ith
PRINT "     ymx = ";ymx;" m"
PRINT "    ydmx = ";ydmx;" m/s"
PRINT "   yddmx = ";yddmx;" m/s^2"
PRINT "  ydddmx = ";ydddmx;" m/s^3"

SUB Plotter
...
END SUB

SUB LowDwell
...
END SUB

SUB Cam345
...
END SUB

SUB HighDwell
...
END SUB

SUB Cycloid
...
END SUB
```

4.3 Practical Cam System Design

The foregoing discussion regarding displacement functions makes it clear that cam design analysis is rather computationally intensive. The sections that follow further demonstrate this fact. The wide availability of digital computation makes possible today far more

detailed analysis than would ever have been possible in earlier days. For this reason, it is assumed that anyone undertaking cam design analysis today has full access to digital computation, including the ability to develop computer code as required.

The design requirements for cam systems often include limitations on extreme values for velocity, acceleration, jerk, and radius of curvature. Excluding points of discontinuity, these functions are most easily studied by simply tabulating and graphing them over the appropriate domain. For rotating cams, most of these can be very well described by simply evaluating the functions at one degree intervals. While this may not show the mathematically true extreme values (which rarely occur at integer degree locations), in most cases it provides an adequate engineering approximation to the extreme value. Thus, with a cam-follower system operating at constant speed, computer generated plots of $y(\theta), \dot{y}(\theta), \ddot{y}(\theta)$ based on one degree tabulations of the functions provide the necessary visual understanding and the computer can also track the extreme tabulated value, all as illustrated in the computer code above. This also provides for easy and rapid design iteration with alternate parameter values. It is strongly recommended that this approach be adopted in practice, and certainly in working classroom problems.

4.4 Kinematic Theorem for Rigid Bodies

Consider a rigid body rotating about the fixed point O, as shown in Figure 4.6. The points denoted as O, 1, and 2 are fixed in the body and move with it. The rotation of the body is described by the angle θ measured from a stationary horizontal line to the line $O-1$. There is a second line inscribed on the body from point 1 to point 2 and beyond, designated $A-B$. Let $\mathbf{i}$, $\mathbf{j}$, and $\mathbf{k}$ be the base vectors for the fixed coordinate system, while $\mathbf{e}_{12}$ is a unit vector along $A-B$.

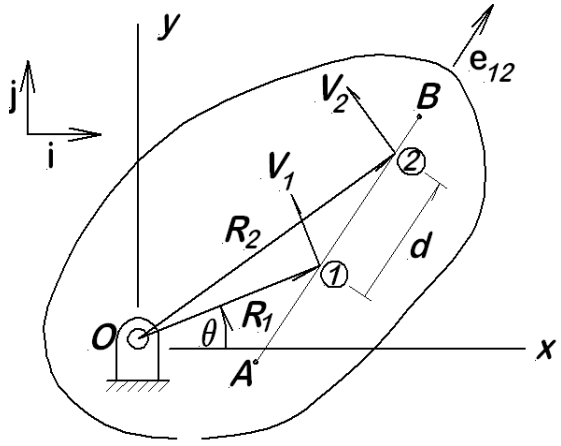

Figure 4.6: Velocities at Points Along the Line A-B on a Rigid Body

The position of point 2 is expressed in terms of the position of point 1 as

$$\mathbf{R}_2 = \mathbf{R}_1 + d\,\mathbf{e}_{12} \tag{4.36}$$

where d = distance from point 1 to point 2. The velocity of point 2 is then obtained by differentiation, using the rule for differentiation of a rotating vector of fixed length,

$$\mathbf{V}_2 = \dot{\mathbf{R}}_2 = \mathbf{V}_1 + \dot{\theta}\,\mathbf{k} \times d\,\mathbf{e}_{12} \tag{4.37}$$

The component of $\mathbf{V}_2$ along the line $A - B$ is

$$\begin{aligned} \mathbf{e}_{12} \cdot \mathbf{V}_2 &= \mathbf{e}_{12} \cdot \Big(\mathbf{V}_1 + \dot{\theta}\, d\,\mathbf{k} \times \mathbf{e}_{12} \Big) \\ &= \mathbf{e}_{12} \cdot \mathbf{V}_1 \end{aligned} \tag{4.38}$$

The last term is zero because $\mathbf{k} \times \mathbf{e}_{12}$ is perpendicular to $\mathbf{e}_{12}$. The last result shows that the component of velocity for point 2 along $A - B$ is the same as that for point 1 *along the same line*, no matter what value the distance d may have. This is summarized in the following theorem:

> *All points along a line inscribed on a rotating body have the same component of velocity along that line.*

If the axis is not stationary, an additional velocity component is imposed upon the entire body. In that case, the theorem remains true, although the development is slightly more complicated.

The theorem becomes completely obvious when considered on physical grounds in view of the definition of a rigid body. Recall that the definition includes the fact that the separations between all particles must remain constant. Consider any line through a particular particle. For all particles along that line, the components of their velocities along the line must be the same in order to avoid changing the separations between particles along the line. This theorem is used repeatedly in the discussion of cam systems and gears.

4.5 Cam–Follower Systems

As mentioned in the Introduction, there is a wide variety of cam and follower system in use today, but for present purposes, only disk cams are considered. Even with that limitation, there are still four types commonly found; two of these are discussed in detail below, while the other two are only sketched.

In the previous portion of this chapter, much attention has been given to the description of follower motion in terms of displacement functions. For this section, it is assumed that a displacement function is selected, and what remains is to define the specific cam that can impart the required motion to the follower.

In times past, cam design was done entirely by graphical methods, with a draftsman laying out the shape of the cam, often with the aid of a French curve. As demonstrated in the earlier study of displacement functions, tiny differences in the displacement, which are the natural result of tiny variations in the cam shape, can have a very large impact on the operating characteristics of the cam and follower system. Just as digital computation makes possible the very precise description of the displacement function, in the same manner, it also makes possible the accurate description of the shape of the cam disk itself. This process is called *analytical design*, meaning to mathematically describe all of the details of the cam shape. This is the approach followed below; much of this is based on the work of Raven [6] .

4.5.1 Translating Flat-faced Follower Systems

Figure 4.7 shows a disk cam with a flat-faced, translating follower. The term *flat-faced* refers to the fact a flat surface on the follower bears against the cam disk. The term *translating* means that the motion of the follower is rectilinear translation without rotation. Notice that the cam is shown rotating counter clockwise (CCW).

In order to describe the rotation of the cam, both a stationary reference line and a line fixed on the cam are required. The self-evident choice for the stationary reference is the line shown, a line through the cam axis of rotation and parallel to the follower motion. The more difficult question is what to use for the rotating line on the cam. This is difficult because of the lack of identifiable features on the cam itself; it has no holes, sharp corners, or other well defined features, so this presents some difficulty, both in theory and in manufacturing practice. There are three items to note at this point:

1. For instructional purposes, it is most convenient to chose the line $\widehat{OM}$ on the cam (as shown in Figure 4.7) as the rotating mark, where M is the transition from the base circle onto the rise event. This choice is consistent with Figure 4.3

and the discussion given there regarding the displacement curve, where $\theta = 0$ is the beginning of the rise event, following the preceding dwell. With this understanding, the system as shown in Figure 4.7 is in the rise event. This choice is used in the development below.

2. For manufacturing and applications, the line $\widehat{OT}$, where T is the highest point on the cam, is often the preferred rotating reference, with the cam understood to be rotating in the clockwise sense. This is particularly true in the automotive industry where point of maximum follower displacement is the most easily identifiable location in the cam cycle [7]. Most of the cams used in internal combustion engines have no high dwell; they employ simply rise-return-dwell displacement functions. With this understanding, the system as shown in Figure 4.7 is in the return event in view of the indicated direction of cam rotation.

3. It is simply a matter of mathematically translating the displacement curve by the angle $\angle MOT$ to move from one description to the other. This angle may have any value; it should not be assumed to be a right angle.

The reference line $\widehat{OM}$ may be thought to be inscribed on the cam and rotating with it, so that the angular position of the cam is described by the angle θ as has been done previously. (The line $\widehat{OM}$ exists without regard to whether there is any physical manifestation of it; it is fully defined by the two points O and M. Inscribing it upon the cam surface would only serve to make it visible.) The *trace point* is any point in the flat lower surface of the follower; all such points have the motion described by the displacement function. The *base radius,* R_b, defines a circle representing the closest that the trace point can approach the cam axis of rotation. For this system, the motion of the trace point is written as

$$y(\theta) = R_b + h \cdot f(\theta) \tag{4.39}$$

where

R_b = base radius

h = full lift value

$f(\theta)$ = displacement function

The choice of a base radius value determines the overall size of the cam disk. It is a design decision, as are h and the function for $f(\theta)$; it is here assumed that the choice has been made, although more is said about the base radius choice below.

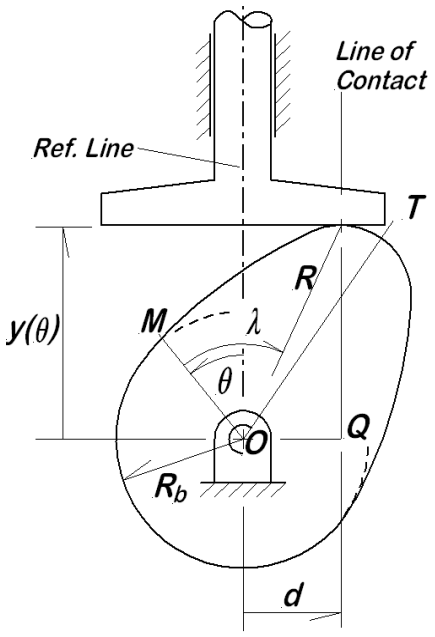

Figure 4.7: Cam With Flat-faced Translating Follower

4.5.1.1 Contact Location

The line of contact is a line parallel to the follower motion and passing through the point of contact between the follower and the cam; it is located at the variable distance d to the right as shown. For continuous contact between the follower and the cam (a necessary condition for the cam to control the follower motion), the velocity of the contact point in the follower must always be exactly the same as the vertical velocity of the contact point in the cam disk. By the theorem of the previous section, the last is the same as the vertical velocity of every other point along the line of contact in the cam, in particular, the same as that of point Q where the velocity is easily expressed. Thus for the contact point in the cam, the vertical velocity, taken positive upward, is

$$V_c = \dot{\theta} \cdot \widehat{OQ} = \dot{\theta} \cdot d \tag{4.40}$$

while in the follower, the vertical velocity is

$$V_f = \frac{dy}{dt} = \frac{d}{dt}\left[R_b + h \cdot f\left(\theta\right)\right] = \dot{\theta}\, h\, f'\left(\theta\right) \tag{4.41}$$

To satisfy the continuous contact requirement, these two expressions must be equal so that

$$d = h \cdot f'(\theta) \tag{4.42}$$

Thus the contact is located a distance d to the right of the cam axis of rotation, and the extreme values are

$$d_{\min} = h\, f'_{\min} \tag{4.43}$$
$$d_{\max} = h\, f'_{\max} \tag{4.44}$$

4.5.1.2 Cam Profile

The term cam profile refers to the actual shape of the cam disk (which is not the same as the displacement function), and it is described relative to the reference line $\widehat{OM}$ by the polar coordinates (R, λ). Consider the two loop equations

$$R\sin(\lambda - \theta) = d = h \cdot f'(\theta) \tag{4.45}$$
$$R\cos(\lambda - \theta) = y(\theta) = R_b + h \cdot f(\theta) \tag{4.46}$$

The polar coordinates of the contact point are easily determined as

$$\lambda = \theta + \arctan\left[\frac{h \cdot f'(\theta)}{R_b + h \cdot f(\theta)}\right] \tag{4.47}$$
$$R = \left\{[h \cdot f'(\theta)]^2 + [R_b + h \cdot f(\theta)]^2\right\}^{1/2} \tag{4.48}$$

This result describes the shape of the actual cam surface, the polar coordinates (R, λ), in terms of the parameter θ. To generate the entire shape, it is only required to let θ sweep through the full range $[0, 2\pi]$.

4.5.1.3 Contact Stresses

When two bodies are pressed together, as in the case of the cam and follower, there is local deformation around the point of contact and the contact force is distributed over a finite area around that point. The resulting stresses near the point of contact can lead to surface

fatigue damage, such as cracking and spalling, with accelerated wear. Stresses arising from one body bearing directly on another are called *Hertz contact stresses* after Heinrich Hertz who developed their mathematical description in the 19^{th} century. Although the actual situation is always three dimensional, contact stresses are usually evaluated using two dimensional elastic theory, either *plane stress* or *plane strain*. It is important to be clear which approximation is appropriate for each particular case.

> **Plane Stress.** Consider a thin plate in the X-Y plane subject to in-plane loads only. The upper and lower surfaces are stress free. The stresses σ_{zz}, σ_{xz}, and σ_{yz} are thus zero on both boundaries and may reasonably be assumed small through the thickness. The only remaining non-zero stresses are the two dimensional system σ_{xx}, σ_{xy}, and σ_{yy}. This condition is called *plane stress*.
>
> **Plane Strain.** Consider a cylinder extending along the Z-axis with loading perpendicular to the cylindrical surface at various points along the length. Particles in the interior of the body are constrained against axial motion by the presence of the adjacent material on either side. Thus the strains ε_{zz}, ε_{xz}, and ε_{yz} must be zero, leaving only the two dimensional strain system composed of ε_{xx}, ε_{xy}, and ε_{yy}. This is the condition called *plane strain*.

In many applications, a disk cam is relatively thin and the plane stress approximation is valid. This may be less true for something like an automotive cam shaft, where the cam is a part of an extended shaft and only slightly larger than the shaft itself; in that case, the plane strain approximation may be more appropriate.

Hertz' results are given in many places on the Internet, but they are particularly well done in the long ago work of Spotts [8]. The principal result is this; for two curved bodies in plane stress contact, the maximum normal stress is given by

$$\sigma_{\max} = \sqrt{\frac{F}{\pi t}\frac{(\rho_1 + \rho_2)}{\rho_1 \rho_2}\frac{E_1 E_2}{(E_1 + E_2)}} \tag{4.49}$$

where

F = total contact force

t = axial length of the contact, typically the cam thickness

E_1, E_2 = Young's modulus values for each of the two materials

ρ_1, ρ_2 = local surface radii of contact for the two bodies

In the event that one of the bodies is flat at the point of contact, the associated radius of curvature is infinite, and the previous equation reduces to

$$\sigma_{\max} = \sqrt{\frac{F}{\pi t}\frac{1}{\rho}\frac{E_1 E_2}{(E_1 + E_2)}} \tag{4.50}$$

where ρ is the local radius of curvature of the body that is not flat.

Similar results are available for the plane strain case, as may be found in the literature. It should be mentioned that this information is applicable to cams of all sorts, not only those employing flat-faced translating followers.

4.5.1.4 Radius of Curvature

The stress analysis results of the previous section points to a need to determine the cam profile radius of curvature. There are also operational and manufacturing concerns that require this same information. For proper operation, the cam profile must be smooth and have a continuously turning tangent line. If this is not true, then the cam has a *cusp* or "corner" and it is obvious that there are stress and wear problems at such a corner.

For a typical cam profile, the radius of curvature varies from point to point along the cam surface. Thus for finite rotations, this variable radius of curvature must be taken into account. However, for infinitesimal rotations, the cam surface may properly be locally approximated as a circular arc with an associated *center of curvature*. As long as attention is focused only on the *local description*, the shape of the remainder of the profile is irrelevant (remember that only infinitesimal rotations are considered!). In Figure 4.8, the contact zone is replaced by a circular arc while the remainder of the cam is replaced by an irregular curve to emphasize that it plays no role in this description. The local center of curvature is the point C^*, and the radius of curvatures is denoted as ρ. The center of curvature has the polar coordinates (R_c, C), both unknown at the beginning.

Consider the pair of position equations

$$d(\theta) = h\, f'(\theta) = R_c \sin(C - \theta) \tag{4.51}$$

$$y(\theta) = R_b + h \cdot f(\theta) = R_c \cos(C - \theta) + \rho \tag{4.52}$$

Differentiating the first of these with respect to the rotation angle gives

$$h \cdot f''(\theta) = -R_c \cos(C - \theta) \tag{4.53}$$

When this last is added to the second position equation, both R_c and C are eliminated, and the result is readily solved for the radius of curvature, ρ:

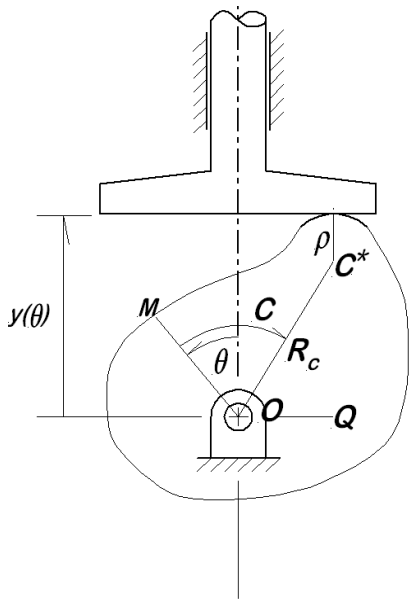

Figure 4.8: Radius of Curvature Determination

$$\rho = R_b + h \cdot [f(\theta) + f''(\theta)] \tag{4.54}$$

This provides a means to determine the local radius of curvature for every point on the cam profile simply by assigning values for θ over the range $[0, 2\pi]$.

As drawn, the center of curvature, C^*, is shown below the follower, the usual location. It is important to note, however, that the center of curvature can fall above the follower. In that event, the radius of curvature is negative. This is a completely unacceptable design because it means that there cannot be continuous contact with the flat-faced follower throughout the cam cycle. A roller follower could overcome that objection, provided that the radius of the roller was smaller than the magnitude of the radius of curvature. Even in that case, there are manufacturing objections related to the radii of milling cutters and grinding wheels. Thus hollow profiles (profiles having negative radius of curvature) are used only in rare circumstances and then only with considerable care regarding the several associated difficulties.

4.5.1.5 Base Radius Determination

To this point, the base radius value has been assumed to be simply assigned, but nothing has been said about how that assignment is made. In view of the comments just made above and the expression developed for the radius of curvature, guidance for this choice is now at hand. In most cases, it is desirable to minimize the base radius in order to

minimize material costs, weight, and size. To this end, the last result above is solved for the minimum acceptable base radius, with the result:

$$R_{b_{\min}} = \{\rho - h \cdot [f(\theta) + f''(\theta)]\}_{\min} \tag{4.55}$$

The minimum acceptable radius of curvature may be assigned by manufacturing considerations or based on contact stress considerations. If the contact force is constant, as with a gravity loaded follower on a slowly moving system, the minimum acceptable radius of curvature is easily determined based on the allowable stress. For systems with significant acceleration involved and a spring loaded contact, the process becomes more involved, requiring an iterative approach. For whatever approach is used, note that it is the minimum of the sum on the right that is required, not the sum of the individual minima.

4.5.1.6 Milling Cutter Coordinates

In the manufacture of cams, numerically controlled milling machines are most commonly used today. The milling cutter is a rotating, cylindrical tool with cutting edges evenly spaced around the circumference. To manufacture a particular cam, it is necessary to determine the path of the milling cutter axis of rotation around the cam profile. This information may be required in either global coordinates, (x_m, y_m) or in cam body coordinates (u_m, v_m), depending on the particular system employed.

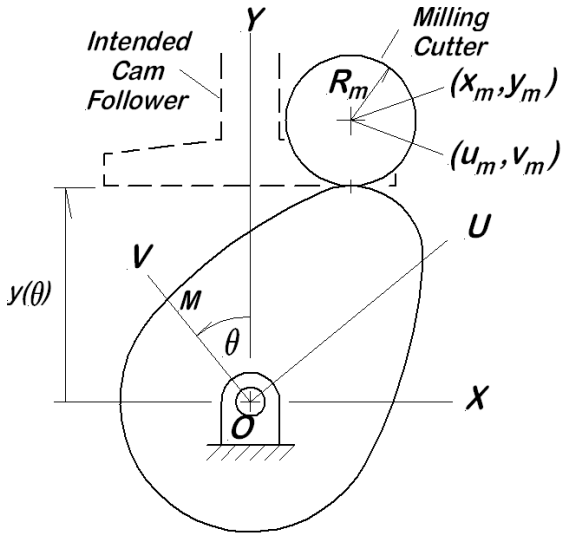

Figure 4.9: Milling Cutter Coordinate Determination for Cam With Flat-Faced Translating Follower

Figure 4.9 shows the cam being cut by a cutter of radius R_m, located at the global coordinates (x_m, y_m). The "shadow" of the intended flat-faced translating follower is also shown in broken line to show the relation between the cutter and the planned follower. It is apparent that the milling cutter coordinates for this position, expressed in the global coordinate system, are simply

$$x_m = d = h \cdot f'(\theta) \tag{4.56}$$
$$y_m = y(\theta) + R_m = R_b + h \cdot f(\theta) + R_m \tag{4.57}$$

The body coordinate system is defined by the axis of rotation and the point M where the lift begins; this line is the $V-$axis. The $U-$axis is perpendicular to V, as shown. Expressing the milling cutter coordinates in the body coordinates is accomplished by a rotation,

$$u_m = x_m \cos\theta + y_m \sin\theta \tag{4.58}$$
$$v_m = -x_m \sin\theta + y_m \cos\theta \tag{4.59}$$

4.5.2 Translating Radial Roller Follower Systems

In order to have a translational output motion (as in the previous section) with reduced friction and wear, a follower equipped with a roller tip is employed; such a system is shown in Figure 4.10. As shown there, the follower is radial, meaning that the line of follower motion passes through the cam axis of rotation. In some situations, the follower is offset laterally, but only radial roller followers are considered here. As in the previous case, the cam axis of rotation is designated as O, and the rotation angle is θ. The natural choice of reference lines, the radial line along the follower axis and the line to the beginning of the rise, are chosen for use here. All of the comments made in the previous section regarding the choice of reference lines should be understood to apply here as well.

For a follower of this type, *the trace point*, that is, the point that executes the motion specified by the follower displacement curve, *is the axis of the roller follower*, as shown in Figure 4.10. Three new terms must also be defined for this follower type: *prime circle, pitch curve,* and *pressure angle.*

Prime Circle: The radius of the roller follower is a design decision, similar to the base circle. In most cases, it is governed by the commercial availability of suitable rollers; in any event, it is assumed to be assigned. With R_f chosen, the *prime circle* is a geometric (not physical) circle, concentric with the base circle and one follower radius outside the

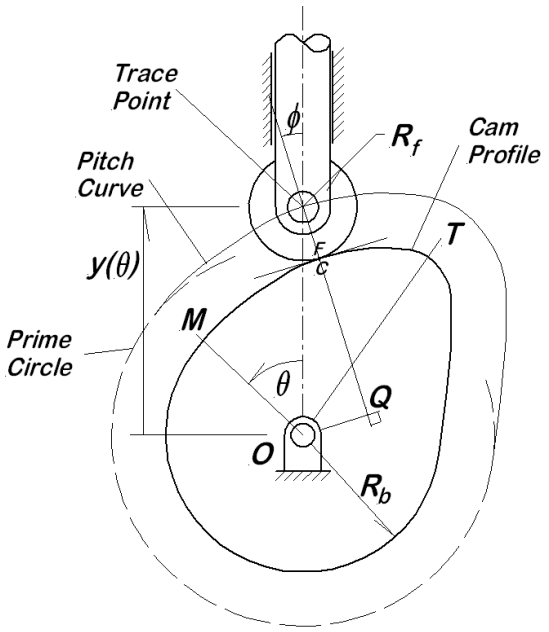

Figure 4.10: Cam With Radial Roller Follower

base circle. It is clear than the trace point cannot come closer to the cam axis of rotation than the prime circle. Thus the prime circle plays a role for the roller follower system similar to that of the base circle for a flat-face follower system.

Pitch Curve: The pitch curve is the path of the trace point around the cam body. It is exactly one follower radius outside the cam profile at all points. A part of the pitch curve includes the prime circle, but over the active portion of the follower motion, the pitch curve is outside the prime circle.

Pressure Angle: There is a natural reference line along the line of motion for the radial roller follower. As seen in Figure 4.10, the line of contact between the cam profile and the roller follower is usually at an angle to the first reference line. This angle is called the *pressure angle*, denoted as ϕ. When the point of contact is on the base circle, the pressure angle is zero (true only for *radial* roller followers). At other contact positions, the pressure angle may be positive (as shown) or negative, but in either case, it results in lack of parallelism between the contact force and the motion of the follower.

4.5.2.1 Pressure Angle Determination

With these definitions in hand, it is evident that the position of the trace point is given by

$$y(\theta) = R_b + R_f + h \cdot f(\theta) \tag{4.60}$$

where the sum of the first two terms give the radius of the prime circle while the third term is the displacement arising from the cam profile. The next step is to determine the pressure angle, ϕ.

At the point of contact between the cam profile and the roller follower, there is shown (a) a line representing the tangent plane at that point, (b) a point F in the follower at the contact location, and (c) a point C in the cam also at the contact location. It is clear than that F and C must be touching, even though they belong to separate components. In order for the cam to control the motion of the follower, there must be continuous contact between the cam profile and the follower surface. If they separate, the cam no longer controls the follower motion; if one penetrates the other, a physical impossibility occurs. Consequently, they must both remain exactly at the same location, even though both points are moving. This condition is satisfied if, and only if, the velocities of both points, along the line of contact, are the same. Note that it is not necessary that their total velocities match; the only requirement is regarding the velocity components along the line of contact.

By the rigid body theorem of Section 4.3, in the cam, all points along the line of contact have the velocity component $\dot{\theta}\,\widehat{OQ}$ along the line of contact, but $\widehat{OQ}$ is related to the pressure angle and the follower displacement, so that

$$V_{C_\parallel} = \dot{\theta} \cdot y(\theta) \sin\phi \tag{4.61}$$

In the follower, the complete velocity of point F consists of the vertical velocity of the follower ($\dot{y}$) plus a tangential component due to the rotation of the roller. The component of velocity at F in the direction of the line of contact is therefore

$$V_{F_\parallel} = \dot{y}\cos\phi = \dot{\theta} \cdot h f'(\theta) \cos\phi \tag{4.62}$$

Thus the requirement for continuous contact between the cam profile and the roller follower provides an expression for the pressure angle when these two velocity expressions are equated:

$$\phi = \arctan\left[\frac{h f'(\theta)}{R_b + R_f + f(\theta)}\right] \tag{4.63}$$

The pressure angle is a measure of the lateral component of the follower contact force, a force that tends to bind the follower shaft in its guide, resulting in increased friction and

wear. Experience indicates that for satisfactory cam performance the maximum pressure angle should not exceed $30^o = \pi/6$ radians. From the preceding equation, it is evident that increasing either component of the prime circle radius decreases the pressure angle, so that these design choices becomes a means to control the pressure angle.

4.5.2.2 Cam Profile

Using the pressure angle determined in the previous section, the cam profile polar coordinates, (R, λ), with respect to the body coordinates are determined here. Referring to Figure 4.11, it is evident that

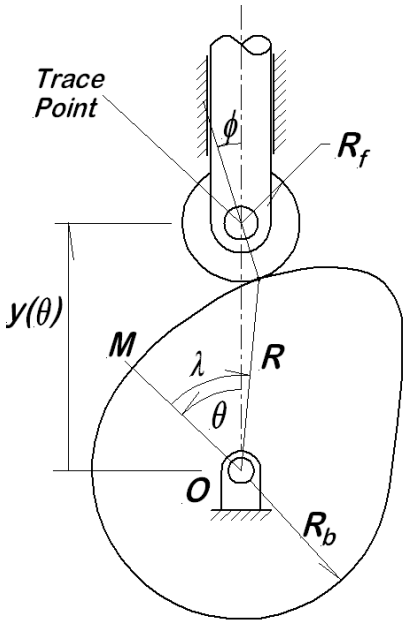

Figure 4.11: Cam Profile Determination for Radial Roller Follower

$$R\sin(\lambda-\theta) - R_f\sin\phi = 0 \tag{4.64}$$
$$R\cos(\lambda-\theta) + R_f\cos\phi - y(\theta) = 0 \tag{4.65}$$

from which the profile coordinates are

$$R = \left[y^2(\theta) + R_f^2 - 2R_f\, y(\theta)\cos\phi\right]^{1/2} \tag{4.66}$$
$$\lambda = \theta + \arctan\left[\frac{R_f\sin\phi}{y(\theta) - R_f\cos\phi}\right] \tag{4.67}$$

As in the case of the flat-faced translating follower, the cam profile coordinates are expressed in terms of the cam rotation angle, θ, as a parameter.

4.5.2.3 Radius of Curvature

For a radial roller follower cam system, the cam radius of curvature determination is very similar to that given previously for the cam with a flat-faced translating follower. As before, the cam profile is locally replaced with a circular arc, and the center of that arc is the center of curvature, designated C^*, at a distance R_c from the cam axis of rotation. The distance from the center of curvature to the cam profile is then the cam radius of curvature at the contact point, denoted as ρ.

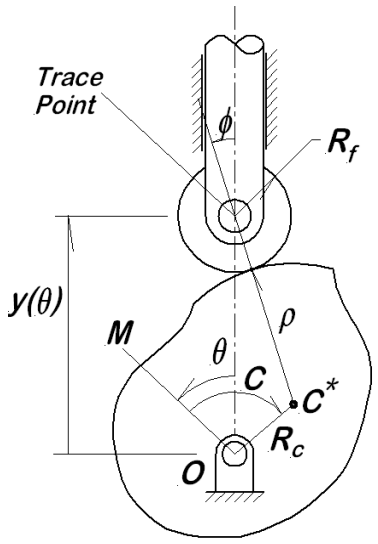

Figure 4.12: Radius of Curvature Determination With Radial Roller Follower

The following two loop equations apply:

$$R_c \sin(C-\theta) - (\rho + R_f)\sin\phi = 0 \tag{4.68}$$

$$R_c \cos(C-\theta) + (\rho + R_f)\cos\phi = y(\theta) \tag{4.69}$$

Differentiating the first equation with respect to θ gives

$$-R_c \cos(C-\theta) - (\rho + R_f)\,\phi' \cos\phi = 0 \tag{4.70}$$

When this is added to the second equation, the result is solvable for the radius of curvature,

$$\rho(\theta) = \frac{y(\theta)}{[1 - \phi'(\theta)]\cos\phi(\theta)} - R_f \tag{4.71}$$

where

$$\phi'(\theta) = \frac{h\left[y(\theta) \cdot f''(\theta) - f'^2(\theta)\right]}{y^2(\theta) + [h \cdot f'(\theta)]^2} \tag{4.72}$$

If the R_f term is moved to the left side, the sum on the left is the radius of curvature of the pitch curve. With this expression for the radius of curvature, the stress analysis can be carried out as described previously in the context of the flat-faced translating follower system.

4.5.3 Hollow Profiles and Undercutting

It might appear that the radius of curvature is a continuous function of the several design parameters, and for must purposes this is true, but it is not quite entirely so. In reviewing a proposed design, the engineer must be alert to sign changes in the radius of curvature; when the sign changes, there is trouble with the design. There are three ways that the sign of the radius of curvature can change:

1. It can pass continuously from positive values, down to zero. This indicates a cusp on the cam profile, a location where the radius of curvature is zero, resulting in a corner.

2. It can pass continuously from positive values, down through zero, and on into a region of negative values. This also indicates a cusp, but worse than that, it describes a condition called *undercutting*. When the profile is undercut, a portion of the surface required to support the follower axis along some part of the pitch curve is removed and no longer available to provide the required support. This is described in more detail below.

3. The radius of curvature can become large without limit, indicating a flat surface on the cam profile. If this trend continues, *the center of curvature jumps discontinuously to the opposite side of the profile curve*, so that the radius of curvature is then a very large negative value. The effect of this on the cam profile is to indicate a concave or "hollow" portion of the profile. This is completely unacceptable for a flat-faced follower, and often presents manufacturing difficulties where a roller follower is used.

Note that, in all three cases, the sign of the radius of curvature changes. In the first two cases, the change is continuous while in the third case the change is discontinuous.

4.5.4 Design Choices

One of the earliest design decisions that must be made is to assign the prime circle radius, $R_b + R_f$. It is clear that this in turn involves two individual design choices.

4.5.4.1 Base Circle Radius

The base circle radius controls the overall size of the cam. It is evident that it is desirable to make the base radius small to conserve material, weight, and space for the cam. On the other hand, if the base circle radius is too small, there are two possible adverse effects:

1. The pressure angle may become too large;
2. The state of stress in the cam may become unacceptably large.

Increasing the base radius mitigates both of these problems at the expense of greater cam size.

4.5.4.2 Roller Radius

In addition to commercial availability considerations, the roller radius is constrained by two considerations:

1. The effect on stresses in both the cam and the roller;
2. The kinematic response at a point of minimum cam profile radius of curvature.

The first of these is obvious, and has been previously discussed at some length. The second is more subtle and relates to a kinematically impossible situation known as *undercutting*, discussed more below.

4.5.4.3 More About Undercutting

After the base radius and the roller radius have been chosen, the complete pitch curve follows with the addition of the displacement curve contributions. This means that the path of the trace point, the rotation axis of the roller follower, is fully defined. The question remains, "Will the cam surface correctly support the follower at every location?"

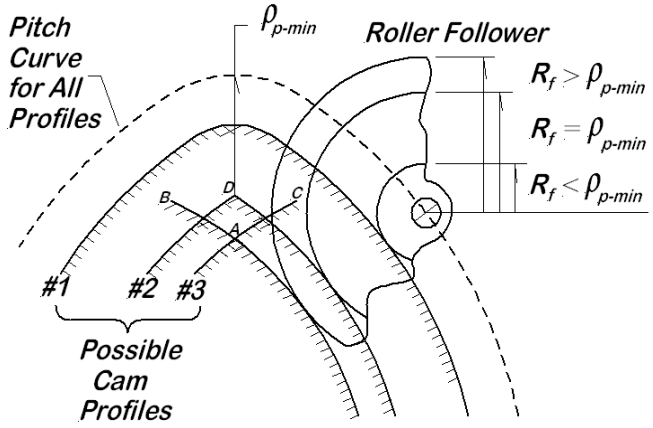

Figure 4.13: Undercutting Related to Pitch Curve Minimum Radius of Curvature and Roller Follower Radius

Figure 4.13 addresses this question for a particular pitch curve where the minimum radius of curvature for the pitch curve, $\rho_{p-\min}$, is identified. Three potential roller followers are shown for this pitch curve. For the smallest roller radius, $R_f < \rho_{p-\min}$, the follower smoothly travels the pitch curve across the top of the figure on cam profile #1. For the intermediate follower size, $R_f < \rho_{p-\min}$, the follower is operating on cam profile #2 that comes to a point at the top, point D. It is evident that this is not acceptable and will result in very high stresses and rapid wear at that point. The situation is even worse for the largest follower, $R_f > \rho_{p-\min}$. If the follower is thought of as approaching the tip from the right side, it functions normally until it reaches point A where the cam profile is pointed. If the cam is to follow the prescribed pitch curve, it must continue on up to point B, but there is no profile surface to support the follower between A and B; it is cut away in the undercutting process. For this impossible motion to continue, the support point must jump from B to C, again a motion with no supporting surface, and then finally the follower must continue on, unsupported from C to A where it again begins to be supported by the cam surface. The fanciful motion just described cannot actually happen; the follower does not go where there is no supporting surface. This problem is the result of removing part of the supporting surface that is later required to support the follower through part of its motion. This is called *undercutting*.

Undercutting can also occur in disk cams with flat-faced translating followers. It happens anywhere the cam profile radius of curvature becomes negative by passing continuously

through zero, resulting in a cusp on the cam profile.

4.5.5 Pivoted Flat-Faced Follower Systems

Referring back to the four different cam-follower system types shown in Figure 4.1, the type there identified as (b) involving a pivoted flat-faced follower is briefly considered here. In Figure 4.14 (a), the cam is shown in its initial position, that is, $\theta = 0$ with the follower in contact with the cam profile at the end of the base circle arc and the beginning of the rise curve. The initial angular position of the follower arm, ψ_o, and the initial contact location, d_o, are determined by loop equations written for this position. Notice that the cam angular reference line, the line where $\theta = 0$, is inclined at the angle ψ_o with respect to the Y-axis.

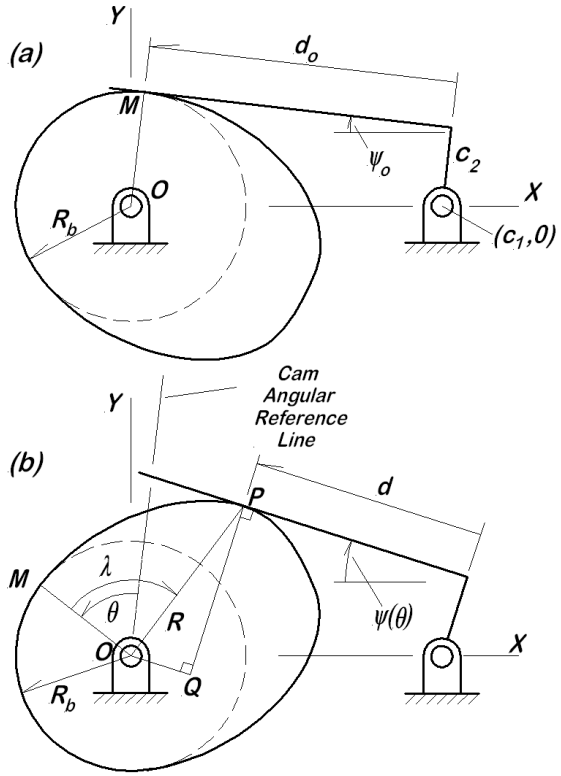

Figure 4.14: Cam With Pivoted Flat-Faced Follower

In Figure 4.14 (b), the cam is shown rotated counter clockwise through the angle θ. This causes the follower motion $\psi(\theta)$ according to whatever displacement function is specified for the cam, so that

$$\psi(\theta) = \psi_o + h \cdot f(\theta) \tag{4.73}$$

The contact location, point P, is defined by the polar coordinates (R, λ) as done for the previous cases, and the entire analysis proceeds along similar lines. It is not developed in any further detail here.

4.5.6 Pivoted Roller Follower Systems

Again, referring back to Figure 4.1, the final cam follower type shown there is (d), the disk cam with a pivoted roller follower that is briefly described here. The system is shown in Figure 4.15 (a) in the initial position, such that $\theta = 0$ and the roller follower contacts the cam profile at the transition between the base circle and the rise curve. In this position, the angular position of the follower is ψ_o and the trace point (the roller follower axis) is along the line OM extended. Loop equations written for this position enable the determination of ψ_o and η, the orientation the cam angular reference line.

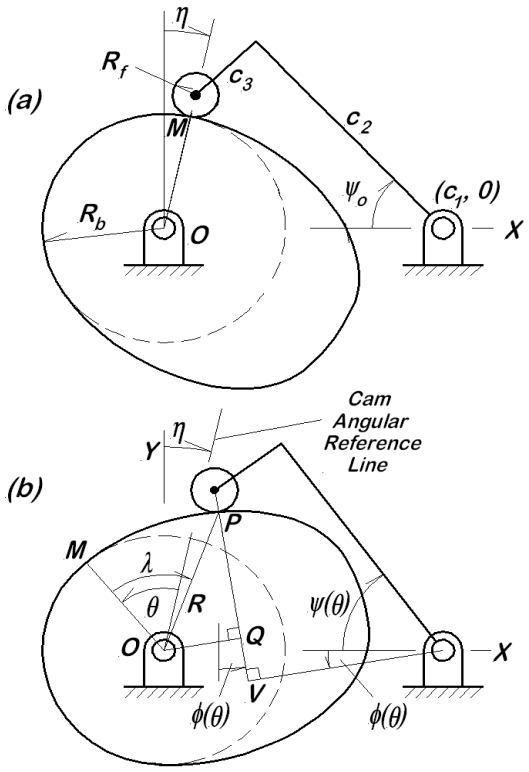

Figure 4.15: Cam With Pivoted Roller Follower

In Figure 4.15 (b), the cam is rotated through the positive angle θ, and the roller contacts the profile at point P with polar coordinates (R, λ). The response angle is $\psi(\theta)$, again given by equation (4.73). The angle ϕ describes the orientation of the line of contact, and as such, it plays a role similar to that of the pressure angle for a cam with a translating

follower. The angle ϕ is shown in two different locations in the figure, both significant. The details for this case are similar to those presented previously, but are not developed here.

4.6 Conclusions

The subject of cam system kinematics is a very large topic, extending to many areas of application. The range of operating speeds involved is immense, ranging from very low speed timing cam that operates a switch in a washing machine to the high speed cam in a race car engine operating at many thousands of revolutions per minute, and every thing in between. Some cams operate at very light loads, such that stresses are not of concern at all while others operate at very high loads with the corresponding concerns about stresses and wear.

In some machine types, there is a tendency to move away from cams to use electronic devices such as solenoid actuators in their place. The main advantage claimed for this substitution is the ability to change the function easily through electronic control. While this is no doubt important in some situations, it is very difficult to improve on the reliability, repeatability, and economy of a well designed cam system. The evidence for this is the continued popularity of cam systems in a wide variety of applications, and the vast literature associated with cams and cam systems design.

References

[1] Rothbart, H.A., *Cam Design Handbook*, Ch. 4, H.A. Rothbart, ed., McGraw-Hill, 2004, pp. 61-67.

[2] Moon, C.H., *A Manual for Engineers and Draftsmen*, Commercial Cam Division, Emerson Electric Co., 1962.

[3] Rothbart, H.A., *Cams - Design, Dynamics, and Accuracy*, Wiley, 1956.

[4] Norton, R.L, *Cam Design and Manufacturing Handbook*, Industrial Press, 2002.

[5] Burrus, C.S., Fox, J.W., Sitton, G.A., and Treitel, S., "Horner's Method for Evaluating and Deflating Polynomials," published on-line by *Connexions*, Open Educational Resources, 2003.

[6] Raven, F.H., "Analytical Design of Disk Cams and Three-Dimensional Cams by Independent Position Equations," *J. Applied Mechanics, Trans. ASME*, March, 1959, pp.

18 - 24.

[7] Andrews, J., Andrews Products Corp., Private Communication, June, 2018.

[8] Spotts, M.F., *Mechanical Design Analysis*, Prentice-Hall, 1964, pp. 166-171.

Problems

4-1 A cam-follower system is to be designed to have a maximum displacement of 12 mm occurring over a rise of 122^o. The rise curve is to be of the modified trapezoidal form. (Table 4.1 is useful here.)

(a) What is the maximum velocity of the follower?

(b) What is the maximum acceleration of the follower?

(c) What is the maximum jerk of the follower?

4-2 A cam-follower system uses the modified sine displacement form to accomplish a return of 8.7 mm over an event of 110^o. (Table 4.1 is useful here.)

(a) What is the extreme velocity of the follower? Is it positive or negative?

(b) What is the extreme acceleration of the follower? Is it positive or negative?

(c) What is the extreme jerk of the follower? Is it positive or negative?

4-3 A cam follower system uses a cycloidal rise over an event length of 67^o and a modified trapezoidal return curve over a return event of 52^o. The total lift is 15 mm. (Figure 4.4 and Table 4.1 may be useful here.)

(a) What is the maximum absolute velocity of the follower? Is this in the rise or the return?

(b) What is the maximum absolute acceleration of the follower? Is this in the rise or the return?

(c) What is the maximum absolute jerk of the follower? Is this in the rise or the return?

4-4 Using the computer code examples of Section 4.2 as models, write computer code to calculate displacement, velocity, acceleration, and jerk over a full cam revolution involving rise, dwell, return, and low dwell. Provide for entering the maximum lift and the four event lengths. Allow provisions to specify either cycloidal or 3-4-5 polynomial curves for either the rise or the return curves.

4-5 Extend the computer code developed in problem **4-4** to include modified sine displacement curves.

4-6 Extend the computer code developed in problem **4-4** to include modified trapezoidal displacement curves.

4-7 Extend the computer code developed in problem **4-4** to include 4-5-6-7 polynomial displacement curves.

4-8 Extend the computer code of problem **4-4** to allow for a flat-faced translating follower employed with the cam. As a test case, consider a cam that has a rise of 10 mm occurring over an initial rise of 132^o and a return over 122^o beginning at $\theta = 210^o$. The rise is according to the 3-4-5 polynomial, while the return is cycloidal.

(a) Have the computer code calculate the minimum acceptable face length;

(b) Have the computer code calculate and plot the actual cam profile;

(c) Have the computer code calculate the profile radius of curvature at all points and identify the minimum and maximum values;

(d) Calculate and plot all of the functions for the test case cam system. (Make normalized plots such that the extreme value on each curve is 1.0.)

(e) Iterate to find the smallest base radius for which the radius of curvature is always greater than 60 mm.

4-9 Extend the computer code of problem **4-4** to allow for a radial roller follower operating with the cam. Consider a follower radius of 9 mm, and the same motion specification as the test case of problem **4-8**.

(a) Have the computer code calculate the pressure angle for all positions;

(b) Have the computer code plot the cam profile;

(c) Have the computer code calculate the profile radius of curvature at all points and identify the minimum and maximum values;

(d) Calculate and plot all of the functions for the test case cam system. (Make normalized plots such that the extreme value on each curve is 1.0.)

(e) Iterate to find the smallest base radius for which the radius of curvature is always greater than 60 mm.

Chapter 5

Gears

5.1 Introduction

The transmission of power from one rotating shaft to another, often with a change in the speed of rotation, is frequently accomplished with gears. Gears are found in a wide variety of everyday items such as alarm clocks, kitchen mixers, automobiles, office copiers, and electric drills. Gears are also used in agricultural and industrial equipment such as lathes, winches, tractors, harvesters, and printing presses. Certainly gears are among the most commonly used machine elements.

If two circular disks are pressed together in edge-to-edge contact, it is possible to transmit rotation from the first disk to the second. Friction between the two contacts acts to transmit torque from one disk to the other; such disks are called *friction wheels*, and are actually used in a few applications. As long as the disks roll without slipping, a definite angular position relation is maintained between the two disks. If the torque required exceeds the friction capacity of the contact, the disks slip. When slip happens, the positional relation between the two disks is changed, and the required torque is not met. To prevent slipping, the contact force can be increased, resulting in an increase in the friction capacity of the contact. This is done, however, at the expense of increased bearing loads, bearing friction, stresses and deflection in the shafting, and stresses within the disks.

A better way to prevent slippage is to increase the coefficient of friction with a more rough surface on the disk edges. A rougher surface involves larger surface irregularities that resist shear when they are in contact; this more effectively prevents slipping. The extreme extension of this idea is the use of teeth cut on the edges of the two disks, in which case the disks are called *gears*.

Teeth cut straight across the edge of the disk, in a direction parallel to the axis of rotation, are called *spur gears*. Alternatively, the teeth may be cut along a helix generated around the axis of rotation to produce what is called a *helical gear*. Because of their helical form, helical gears tend to exert an axial force upon the shaft carrying the gear when operated under load. This requires the use of a thrust bearing on the shaft, or perhaps the use of what is called a *double helical gear,* that is, a gear tooth formed with two helices of opposite senses. This is equivalent to two single helical gears of opposite sense, mounted back to back, and the axial force on the shaft is cancelled.

There are many other variations on the idea of a gear, such as *bevel gears* that transmit power between two shafts that are not parallel. In the case of bevel gears, the teeth are cut on the surface of a cone, and the gear pair act like two cones in rolling contact. Various other gear types include skew gears, hypoid gears, and worm gears. For the purposes of this chapter, the discussion is limited to simple spur gears. For information on other types, the reader may wish to consider the references at the end of the chapter or the many articles and videos available on the Internet.

5.2 Velocity Ratio

Gear never function alone; they are always found in pairs. (The one exception to this is the case of a rack and pinion, but the rack is simply a gear with an infinite radius.) The ratio of the angular velocity of one gear to that of the second is called the *velocity ratio*. This is a parameter of fundamental importance. For satisfactory operation, it is essential that this ratio be absolutely constant, not only on the average but at every instant. In order to better appreciate this, consider a situation in which the average ratio is constant but the instantaneous value is variable.

5.2.1 Nonconstant Velocity Ratio Example

Figure 5.1 shows a medieval lantern and spoke gear set consisting of M_1 radial spokes on the spoked gear and M_2 pins parallel to the axis of rotation for the lantern gear. Gearing of this sort appeared in medieval Europe in grain mills, water pumping machinery, and various other early machines. They were usually made entirely of wood and did not require any sophisticated machining in their construction.

Referring to Figure 5.2, the loop equations are

$$R_1 \cos\theta + (R_2 + w)\sin\psi + s\cos\psi - C = 0 \tag{5.1}$$

$$R_1 \sin\theta + (R_2 + w)\cos\psi - s\sin\psi = 0 \tag{5.2}$$

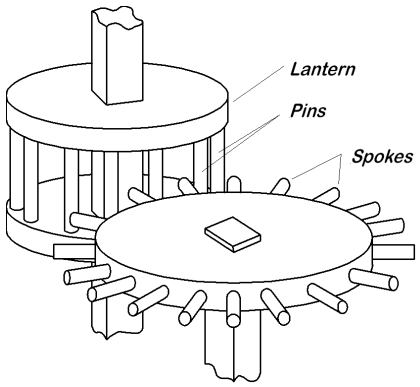

Figure 5.1: Medieval Lantern and Spoked Gear in Mesh

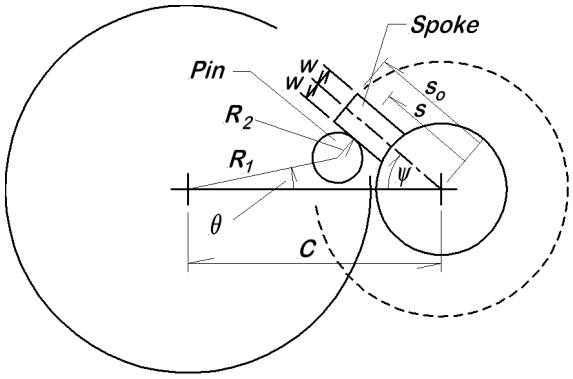

Figure 5.2: Schematic Diagram for Lantern and Spoke Gear Pair

These relations apply over a particular angular interval, $\theta_1 \leq \theta \leq \theta$ during the engagement of a single pin and spoke pair with a corresponding range $\psi_1 \leq \psi \leq \psi_2$. The dimensions R_1, R_2, w, s_o, and C are presumed known, and the loop equations are solvable for ψ (Greek letter *psi*) and s as functions of θ. The velocity coefficient relations result from differentiating the position loop equations with respect to θ in the usual fashion. Both the position solution $\psi(\theta)$ and the velocity coefficient $K_\psi(\theta)$ are shown in Figure 5.3. It is evident from the figure that the velocity coefficient is not constant at all, but rather varies through the duration of the engagement. These curves apply for a single tooth pair until such time as another pair begin to engage, causing the first pair to disengage.

The key point here is the variability of the velocity coefficient, and with it, the ratio of angular velocities, $\dot{\psi}/\dot{\theta}$. If the input speed, $\dot{\theta}$ is constant, the average value of $\dot{\psi}$ taken over a full revolution is constant, but the instantaneous value is not constant at all. The reader may well ask, "What difference does it make if the velocity ratio varies?" Suppose that the input speed is held exactly constant, perhaps through the use of a very large flywheel. The output gear is connected though a shaft of finite stiffness to a driven

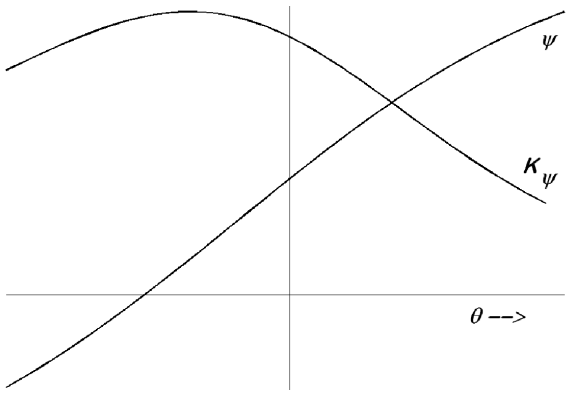

Figure 5.3: Position and Velocity Coefficient Curves for Lantern and Spoke Gear Pair

machine with substantial mass moment of inertia. As the angular velocity of the output gear varies, the shaft will be alternately twisted and relaxed in a cyclic manner as the shaft attempts to cause the driven machine to follow the speed variations of the output gear. The alternating torque in the shaft excites torsional vibrations in the entire system, and causes fatigue damage to the shaft. The result is noisy operation, vibrations in the structure, and increased wear on the gears and the bearings. For crude, low-speed, low-torque machinery this may be tolerable, but for modern high speed, high power machines it is totally unacceptable.

5.2.2 Condition for Constant Velocity Ratio

It is necessary to establish the condition for a constant velocity ratio in a gear pair since it is evidently of great importance. In Figure 5.4, two cams are shown, representing teeth on two gears. The two cams rotate about fixed pivots, C_1 and C_2, separated by the center distance C. Gear #1 is the driver, and gear #2 is driven.

It is important to focus on the point of contact between the two cams; no other part of the cam geometry matters at this instant. The point of contact is designated as H. The line $N_1 - N_2$ is normal to the two cam surfaces at the point of contact, and the line $T_1 - T_2$ is tangent at that same point. The instantaneous angular velocities of the two cams are $\dot{\theta}$ and $\dot{\psi}$, the velocities are perpendicular to the radii from their respective fixed pivots; these velocities are shown as $\mathbf{V}_1$ and $\mathbf{V}_2$ in the figure.

The normal line, $N_1 - N_2, s$ is often called the *line of action* or the *line of contact*. As discussed previously with regard to cams, the contacting surfaces must never be allowed to separate or to overlap. For this condition to be satisfied, it is necessary that the *velocity components along the line of contact* be exactly the same for both bodies. This requires that the velocity component $V_{1\|} = V_{2\|}$, where *parallel* is understood to mean

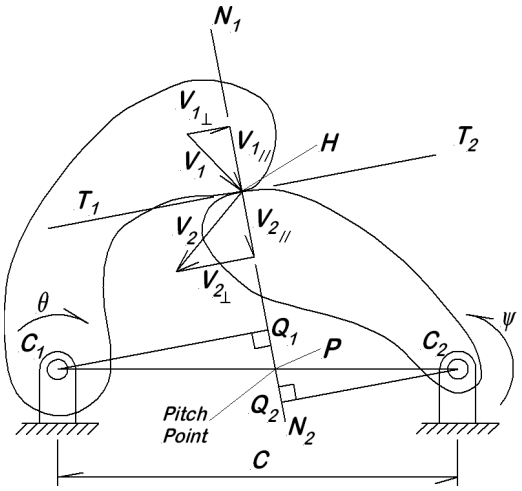

Figure 5.4: Two Cams Representing the Teeth of Two Gears

parallel to the line of action. According to the theorem developed in Section 4.3, the components of $\mathbf{V}_1$ and $\mathbf{V}_2$ along the line of action are

$$V_{1\|} = \dot{\theta}\,\widehat{C_1Q_1} \tag{5.3}$$

$$V_{2\|} = \dot{\psi}\,\widehat{C_2Q_2} \tag{5.4}$$

Since proper operation requires that these two be equal, the velocity ratio is then

$$\dot{\psi}/\dot{\theta} = \frac{\widehat{C_1Q_1}}{\widehat{C_2Q_2}} \tag{5.5}$$

The intersection of the line of contact with the line of centers defines a point P, called the *pitch point* (this is a very important definition!). The two triangles C_1Q_1P and C_2Q_2P are geometrically similar. Recall a theorem from plane geometry to the effect that corresponding parts of similar triangles are proportional to each other. Consequently, the velocity ratio is

$$\dot{\psi}/\dot{\theta} = \frac{\widehat{C_1P}}{\widehat{C_2P}} \tag{5.6}$$

If the velocity ratio is to remain constant, the ratio $\widehat{C_1P}/\widehat{C_2P}$ must be constant, so that the pitch point remains fixed. This is often stated as the *Fundamental Law of Gearing:*

For a constant angular velocity ratio, the pitch point must remain stationary.

5.2.3 Sliding Velocity at the Point of Contact

Figure 5.4 also provides information regarding the sliding velocity at the point of contact. The sliding velocity is significant in terms of friction and wear on gear teeth. For each cam in Figure 5.4, the magnitude of the velocity at the point of contact is easily written in terms of the radius to the contact location and the angular velocity of the cam. With that, and the Pythagorean theorem, the magnitude of the velocity components normal to the line of action can be written:

$$\begin{aligned} V_{1\perp}^2 &= |V_1|^2 - V_{1\parallel}^2 = \left(\widehat{C_1H_1}^2 - \widehat{C_1Q_1}^2\right)\dot{\theta}^2 = \widehat{Q_1H_1}^2\dot{\theta}^2 \\ V_{1\perp} &= \widehat{Q_1H_1}\dot{\theta} \end{aligned} \tag{5.7}$$

and similarly

$$V_{2\perp} = \widehat{Q_2H_2}\dot{\psi} \tag{5.8}$$

The velocity components normal to the line of action are in opposite directions, so the total sliding velocity is their sum. Taking all lengths as positive and adding the velocity components leads to the final result for the sliding velocity after some algebra,

$$V_s = V_{1\perp} + V_{2\perp} = \widehat{PH}\left(\dot{\theta} + \dot{\psi}\right) \tag{5.9}$$

The result is that *the sliding velocity is proportional to the sum of the gear speeds and the distance from the pitch point to the contact.*

5.3 Conjugate Profiles

In the previous section, the Fundamental Law of Gearing was established which states that a constant angular velocity ratio requires that the pitch point be stationary. In order for the pitch point to be stationary, the line of action (the line tangent to both base circles) must intersect the line of centers continuously at the same location while the point of contact moves through the tooth engagement. If the tooth profiles are such that the pitch point remains stationary, the two profiles are said to be *conjugate* to each other. Thus conjugate gear tooth profiles satisfy the Fundamental Law of Gearing, and gears with conjugate tooth profiles have a constant velocity ratio. In the lantern and spoke gear example of Section 5.2,the tooth forms are not conjugate, the pitch point is not stationary, and the velocity ratio for the pair is not constant.

Notice that the property of being conjugate (or non-conjugate) is a property of a pair of tooth forms, and not a property of either tooth form individually. For any given tooth

form, it is possible, in principle, to determine a second tooth form conjugate to the first. A procedure for this is given by Beggs [1] . In practice, the required conjugate form for the second gear often cannot be realized physically because it requires material bodies to pass through each other.

It is established that (1) conjugate tooth profiles are desirable, and (2) that a conjugate form can, in principle, be developed for any given tooth form. This would seem to suggest that there would be a great variety of tooth forms in use, but in fact this is not the case. The vast majority of gears in use today employ the *involute tooth profile*, although there are a few other forms such as cycloidal teeth (which are conjugate) and Novikov (which are non-conjugate) that are used in special circumstances. Only involute tooth forms are considered further in this discussion. Before discussing the involute gear tooth, it is necessary to develop the properties of the involute.

5.4 Properties of the Involute

The *involute of a circle* is the path traced by the tip of a taut string unwinding from the circle. In Figure 5.5, the string is initially wound on a circle called the *base circle*, with the free end at the intersection of the base circle and the vertical axis. The radius of the base circle is denoted as R_b and called the *base radius*. The string is inextensible and must remain taut, so the initial motion is radially outward from the base circle. The situation shown in Figure 5.5 is when the string has been unwound through approximately 40^o around the base circle. The broken line at the top shows the further development that occurs when more of the string is unwound. The length of the straight segment of the string is denoted as P and is the instantaneous radius of curvature for the involute at that point.

The polar coordinates for the free end of the string are (R, β) , the radius and the polar angle to the current location on the involute curve. The polar angle to the point where the string is tangent to the base circle is the sum of two angles $\beta + \alpha$, where the second angle, α, is called the *flank angle*. Note that the flank angle is identified a second time in Figure 5.5 as the angle between the tangent to the involute and the radial line to the point on the involute; it is the same angle in both cases.

The radius of curvature, P, is expressible in two forms, once in terms of the unwound arc length, and again in terms of the trigonometry of a right triangle:

$$P = R_b \left(\alpha + B\right) = R_b \tan \alpha \tag{5.10}$$

This is solvable for the angle β thus:

$$\beta = \tan \alpha - \alpha = inv \left(\alpha\right) \tag{5.11}$$

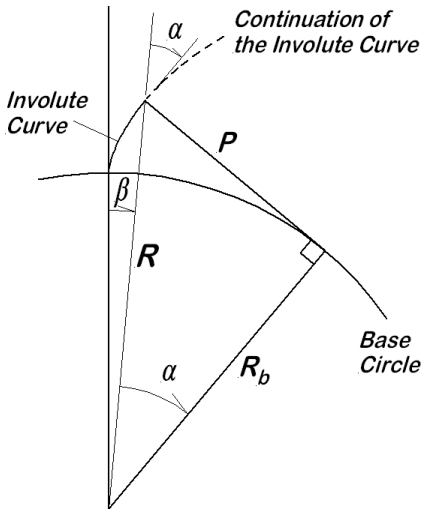

Figure 5.5: Geometry of the Involute Curve

where $inv\,(\alpha)$ denotes the *involute function*, defined as $inv\,(\alpha) = \tan\alpha - \alpha$. The radius to the current point on the involute is expressible in terms of α through a simple right triangle relation,

$$R = R_b/\cos\alpha \tag{5.12}$$

Thus the polar coordinates for every point on the involute, (R, β) are readily written in terms of the flank angle parameter α.

If a point on the involute is specified, either by giving R or β, the other can be determined. If the value of R is specified, then the flank angle is readily determined from Equation (5.12) and from there, the polar angle β is determined from Equation (5.11). If the value of β is given, the solution is more involved. Equation (5.11) must be solved numerically for α based on the given value for β. With α determined numerically, the radius is quickly evaluated from equation (5.12). The necessary numerical solution is easily accomplished with Newton's Method (the Newton-Raphson with only one unknown). Typically solutions with a residual of magnitude less that 10^{-6} are obtained in no more than six iterations.

When the involute is used as a gear tooth form, it is common practice to use two involutes facing in opposite directions in order to create a tooth form that will function correctly in either direction. Figure 5.6 shows two involute profiles thus arranged, resulting in a pointed tooth form. The length *along a circular arc* from one involute to the other is called the *circular thickness*, and it obviously depends upon the radius where it is measured, $T\,(R)$, as shown. The figure includes a notation *Pitch Circle*, a circular thickness designated as T_p, and a radius R_p. All of these last are related to the pitch point, but it is premature to get into those details here; this will all make complete sense after reading the next section. For the present, consider R_p as simply a particular radius, and T_p is

the circular thickness associated with R_p.

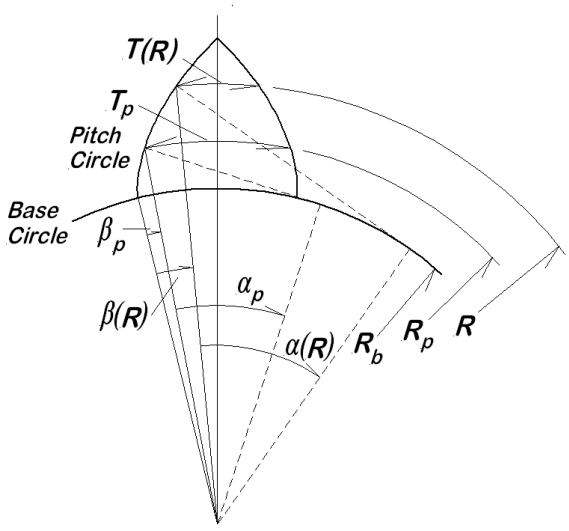

Figure 5.6: Determination of Gear Tooth Circular Thickness

It is often necessary to determine the circular thickness at a specified radius, $T(R)$, given R_b, R_p, T_p. and R. The first three are the primary parameters of the gear tooth form, and the last is the radius where the circular thickness is required. The flank angle at R is $\alpha(R)$ and is determined from the right triangle relation

$$\alpha(R) = \cos^{-1}(R_b/R) \tag{5.13}$$

With $\alpha(R)$ known, the polar angle $\beta(R)$ is determined by evaluating the involute function

$$\beta(R) = inv[\alpha(R)] = \tan[\alpha(R)] - \alpha(R) \tag{5.14}$$

This same process is also applied at the pitch circle, to give

$$\alpha_p = \cos^{-1}(R_b/R_p) \tag{5.15}$$

$$\beta_p = \tan(\alpha_p) - \alpha_p \tag{5.16}$$

Now looking at the arc length difference between $\frac{1}{2}T(R)$ and $\frac{1}{2}T_p$, the following relation is evident:

$$\frac{T_p}{2R_p} - \frac{T(R)}{2R} = \beta(R) - \beta_p \tag{5.17}$$

This last can be solved for the required circular thickness, $T(R)$

$$\begin{aligned} T(R) &= 2R\left[\frac{T_p}{2R_p} + \beta_p - \beta(R)\right] \\ &= 2R\left[\frac{T_p}{2R_p} + inv(\alpha_p) - inv[\alpha(R)]\right] \end{aligned} \tag{5.18}$$

Conversely, if a particular value is specified for $T(R)$, equation (5.18) can be solved numerically for R by Newton's method.

5.5 Involute As A Gear Tooth

To understand the functioning of involute gear teeth, it is useful to consider the process of winding a thin, flexible but inextensible string or tape from one disk or drum to another. The two disks are mounted on fixed pivots with center distance C as shown in Figure 5.7 (a). The radii of the two disks are R_{b1} and R_{b2}, respectively. The string or tape is wound partially around each disk, with the unsupported portion of the string lying along the line of action as shown; the points of tangency are T_1 and T_2, points that are fixed in space. A particular point on the string is marked s, and initially this point coincides with T_1 as shown in Figure 5.7 (a). As the disk on the left rotates clockwise, point s moves down and to the right along the line of action as shown in Figure 5.7 (b); note that the original location on the left disk is marked s'. As s lifts off the left disk, it traces an involute as described in Section 5.4. At the same time that s is leaving the left disk, it is also approaching the surface of the right disk, following an involute generated from the right disk. The point that started at s' moves to s on the line of action while approaching the location s'' on the second disk, as shown in Figure 5.7 (c). The short section of broken line indicates the continuation of each involute curve past the location of s. Before the point s reached T_1, and again after it passes T_2, it travels on a circular path around one of the two disks. In the process just described, the two disks function as base circles, hence their radii are denoted as R_{b1} and R_{b2}.

Now suppose that the two involute curves are replaced with cams of those shapes, while at the same time, the string is eliminated. Is the relative motion of the two disks changed in any way? It should be evident that it is not. The two cams enforce exactly the same angular relationship between the disks as that imposed by the taut string. For the process as just described, there are two important observations to be made: (1) the two cams must be tangent to each other at the point s because s is simultaneously on both involutes, and (2) as noted in the beginning, the point s travels down the line of action and where this line crosses the line of centers, there is the pitch point P. The pitch point is stationary, and therefore the velocity ratio is constant.

But notice that, if there are physical cams controlling the rotation, then there is no need for the base circles in physical form. The base circles always exist as geometrical concepts, the basis for the involute curves, but only rarely is there a physical feature identifiable as a base circle. This is an important observation, because many are inclined to want to see the base circles; in almost all cases, there is nothing at all to see.

All contact between the gear teeth occurs along the line of action. Recall that, in Figure 5.7, the line of action is the path followed by the point s in transit from one base circle

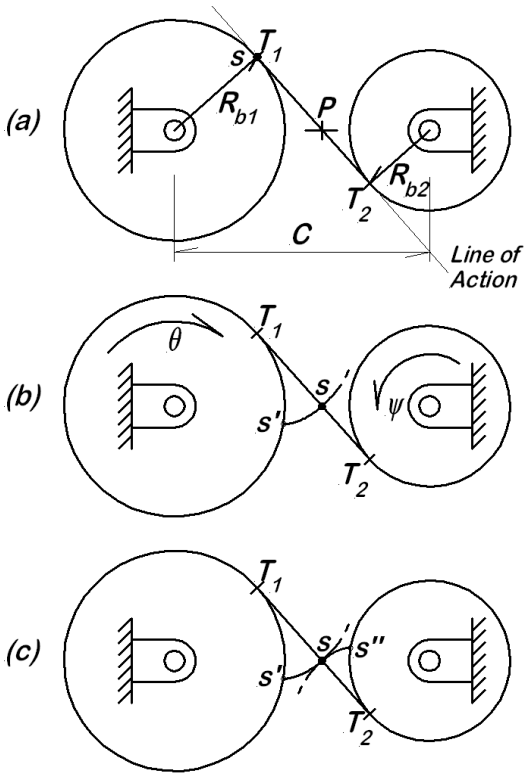

Figure 5.7: Involute Tooth Action: Winding a Tape from One Base Circle to Another

to the other, and the gears are always mutually tangent at that point. In the absence of friction, the contact force is directed along the line of action, a line that has a fixed orientation. This orientation is described in Figure 5.8 by the angle ϕ, called the *actual pressure angle*. Note that ϕ is measured between the line of action and the normal to the line of centers. For a pair of involute teeth *in mesh at the pitch point*, the flank angle at the contact is equal to the pressure angle; this is also illustrated in Figure 5.8.

As shown in both Figures 5.7 and 5.8, if the gear on the left rotates through an angle θ, the contact point moves along the line of action a distance $\theta \cdot R_{b1}$. At the same time, the contact point moves toward the gear on the right a distance $\psi \cdot R_{b2}$, and these two distances must be exactly the same provided contact is maintained. From this, it is evident that

$$\psi/\theta = \dot{\psi}/\dot{\theta} = R_{b1}/R_{b2} \tag{5.19}$$

The *pitch radius* is defined as the distance from a base circle center to the pitch point, and the pitch radii are identified in Figure 5.8 as R_{p1} and R_{p2}. The pitch radius is related to the base radius by

$$R_b = R_p \cos\phi \tag{5.20}$$

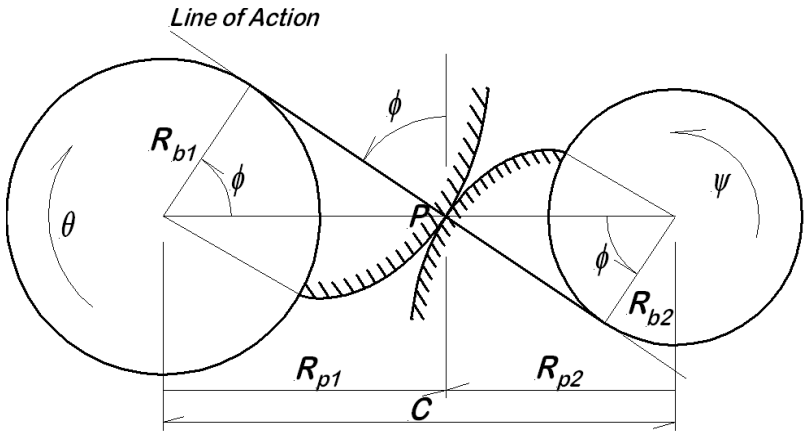

Figure 5.8: Definition of Actual Pressure Angle and Actual Pitch Radii

Since the pitch radii are proportional to the base radii, the ratio of rotations and the velocity ratio can be easily written in terms of the pitch radii,

$$\psi/\theta = \dot{\psi}/\dot{\theta} = R_{p1}/R_{p2} \tag{5.21}$$

All of this suggests that the motion of a pair of involute gears is kinematically exactly equivalent to that of two friction wheels of radii R_{p1} and R_{p2}. This is an important observation primarily because it simplifies thinking the engagement of an involute pair to simply dealing with a pair of friction disks. This is particularly significant when considering a train consisting of several gears in sequence.

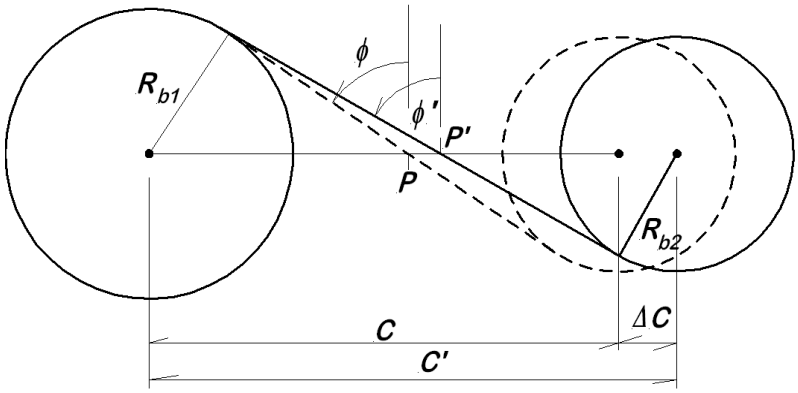

Figure 5.9: Effect of Changing Center Distance

A base circle and the associated base radius are a properties of single gear. Other properties discussed above are *properties of a gear pair*, specifically:

- Center distance

- Line of action
- Pitch point (actual)
- Pressure angle (actual)
- Pitch radii (actual)

Figure 5.9 illustrates this point by showing the effect of different center distances on what are otherwise the same gear pair. In that figure, the base circle at left is held fixed while the right base circle is shifted an amount ΔC. In this process, (1) the center distance goes from C to C', (2) the line of action is shifted from the broken line to the solid, (3) the pitch point moves from P to P', (4) the pressure angle is increased from ϕ to ϕ', and the pitch radii are each increased because of the shifted pitch point.

Despite the change in the pitch radii, the velocity ratio for the gear pair remains constant. This illustrates an extremely important property of the involute gear tooth. It means that there is some flexibility in setting the center distances, and that there is no need for extreme accuracy in locating the gear centers. This last is very important in terms of ease of manufacturing and costs.

5.6 Internal Gearing

Everything said about the use of the involute as a gear tooth form to this point has been in terms of external gear teeth, that is, teeth formed on the outer rim of a gear disk. But what of teeth formed on the inside of a hollow cylinder? Such teeth are an essential part of what is called *planetary gearing*, or more technically, *epicyclic gearing*. In the discussion above, it is demonstrated that involute gear teeth offer major advantages, particularly constant velocity ratio with a degree of flexibility in the mounting center distance. But how does this work for the planetary case?

Figure 5.10 shows two base circles (the larger one is only partially shown) in solid lines. In all of the discussion prior to this point, the base circles have been non-intersecting, but here they overlap. *For one of the gears to be an internal gear, it is essential that the base circles intersect;* this is a major distinction between internal and external gear pairs. As in the earlier discussion, the line tangent to both base circles is the line of action. Again as before, the intersection of the line of action with the line of centers is the pitch point, P, at the far right.

The pressure angle is defined exactly as in the previous case, namely the angle between the normal to the line of centers and the line of action. As before, it is also shown in two

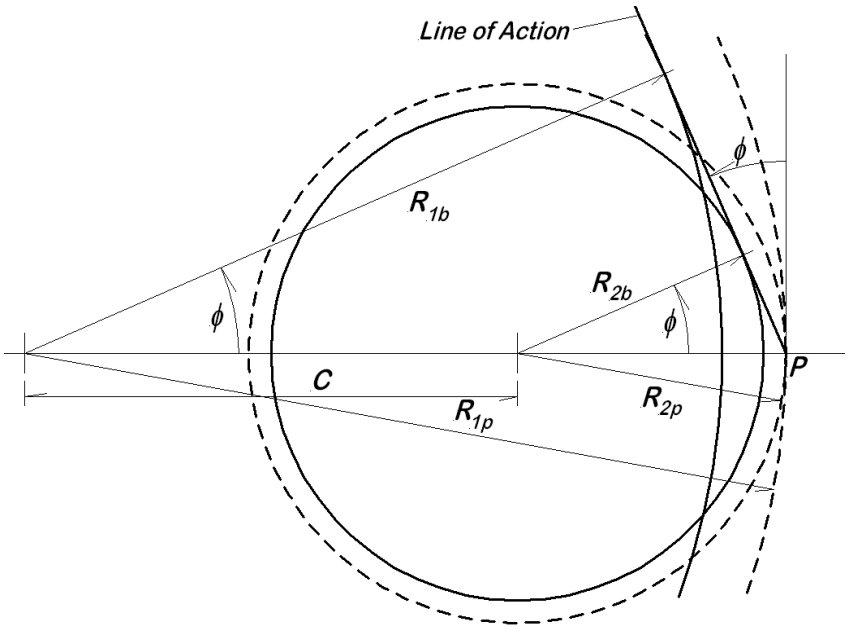

Figure 5.10: Internal Gear Mesh Geometry

other locations. The pressure angle is computed by

$$\phi = \cos^{-1}\left(\frac{R_{b1} - R_{b2}}{C}\right) \tag{5.22}$$

The pitch radii are defined as before, the distances from the respective centers to the pitch point. But notice that, in the case of internal gearing, the sum of the pitch radii is greater than the center distance, quite different from the situation of external gearing. The pitch radii are computed using equation (5.20), exactly as before.

The construction of the involute curves is not shown, but it is done in exactly the same manner as before, beginning at a point on the base circle and proceeding outward as the string or tape is unwound from the base circle. The result is that while the external gear requires a solid surface under, or some might say, inside, the involute, the internal gear leaves material above, or outside, the involute. The result is that both the internal and external gear teeth are involutes (defined on different base circles), but the external tooth presents a convex surface while the internal gear has a concave surface.

5.7 Gear Terminology

Assuming that an involute tooth form is to be used, there is still quite a large vocabulary required to describe the features of each gear. Note too that, in talking about a single

gear, it is customary to speak in terms of the *nominal properties*, which may differ somewhat from the *actual properties*, as finally mounted. An example of this is the term *nominal pitch radius*. As described above, the *actual pitch radius* is not defined until the gear pair is engaged and mounted, such that (1) the center distance is fixed, (2), the line of action defined, (3) an actual pitch point exists, thus dividing the center distance into actual pitch radii. Despite these essential requirements, it is still possible to define an intended or *nominal pitch radius* for a gear, that is the pitch radius at which the individual gear is designed to operate. Whether the gear is actually mounted and used at the intended center distance is another matter, but there is some particular pitch radius for which the gear is designed.

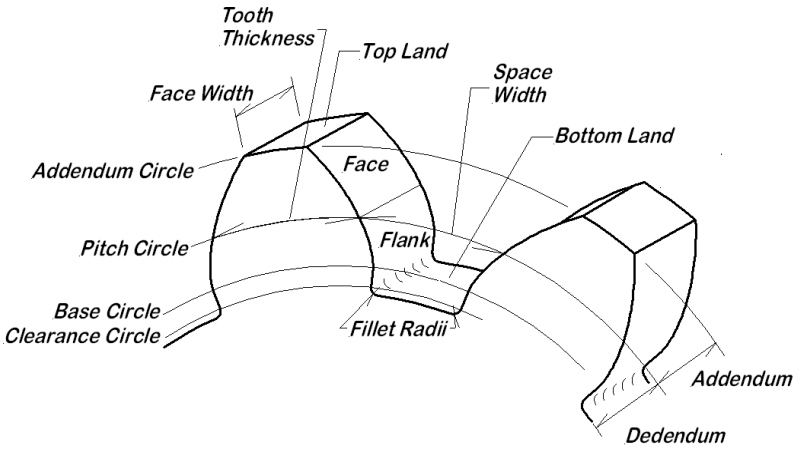

Figure 5.11: Gear Terminology

A list of common gear terms follows below, and many of them are illustrated in Figure 5.11.

- *Pitch Circle:* A circle with the nominal pitch radius; this circle rolls without slipping on the pitch circle of the mating gear when the two are in mesh.
- *Addendum:* The radial distance from the nominal pitch circle to the outer tip of the tooth, the top land.
- *Dedendum:* The radial distance from the nominal pitch circle to the floor of the space between the teeth, the bottom land.
- *Addendum Circle:* A circle passing through the tip of the teeth.
- *Dedendum Circle* (also called the *Root Circle*): A circle passing through the bottom land.
- *Whole Depth:* The sum of the addendum and dedendum dimensions.
- *Working Depth:* The sum of the addendum dimensions for a pair of gears in mesh.

- *Clearance:* The amount by which the dedendum of the gear exceeds the addendum of the other gear in the mesh.
- *Circular Thickness:* The arc length between the two sides of a gear tooth, measured along the pitch circle unless otherwise specified.
- *Backlash:* The amount that the space width exceeds the circular thickness of the engaging gear as measured along the pitch circle.
- *Circular Pitch:* The arc length along the pitch circle between corresponding points on adjacent teeth; the spatial period of the gear teeth as measured along the pitch circle equal to the sum of the tooth thickness and the space width.
- *Base Pitch:* The arc length along the base circle between corresponding points on adjacent teeth; the spatial period as measured along the base circle. This is also the distance along the line of action from one tooth to the next on the same gear.
- *Spur Gear:* A gear with teeth cut straight across the outside of a central disk.
- *Internal Gear:* A gear with teeth cut on the inside of a hollow circular part; this is also called a *Ring Gear*.
- *Pinion:* The smaller of two gears in a mesh. The larger is simply called the *gear*.
- *Diametral Pitch:* The number of teeth per inch of pitch diameter, *used with US Customary units only*. The diametral pitch has units of *teeth per inch*.
- *Module:* The pitch circle diameter per tooth, *used with SI units only*. The module has units of *millimeters* (actually millimeters per tooth, but the last is not expressed).

5.8 Standard Tooth Proportions

Gear tooth proportions are typically stated in terms of two parameters, the nominal pressure angle and a second parameter to indicate the size of the individual tooth.

Gear application is a continuously evolving art, and as such, standard practice continues to change over time. Every gear is designed to function at, or near, a specified nominal pressure angle (recall that the center distance for involute gears can be varied to a degree, and when this is done, the actual pressure angle deviates from the nominal value). When the pressure angle is very low, the component of force along the line of action is nearly normal to the line of centers. This produces relatively low bearing forces, but it requires long, slender gear teeth that are susceptible to bending fatigue failure. Increasing the pressure angle causes an increase in bearing loads for the same transmitted power, but

it gives a thicker tooth form less prone to fatigue failure. The choice is the classic design trade-off problem.

In the early 20^{th} century, the standard nominal pressure angle was $14\frac{1}{2}^o$. This choice is largely abandoned today, with most gears employing $\phi_{nom} = 20^o$, although there are some applications going up as far as 25^o. For the purposes of this book, $\phi_{nom} = 20^o$ is assumed unless stated otherwise. In American terminology, the parameter describing the size of the gear is the *diametral pitch*, usually denoted as P and defined as the total number of teeth on the gear divided by the nominal pitch circle diameter. In SI usage, the size parameter is the *module*, denoted as m, and defined as the pitch circle diameter, expressed in millimeters, divided by the number of teeth on the gear.

From the definition of the module, that it is conceptually the inverse of the diametral pitch. On one level, it may be said that this is the only difference, but on a different level, there are significant differences. The differences are particularly apparent when *preferred values* are considered (preferred values are those commonly specified choices for which standard manufacturing tooling is readily available). In the US Customary system, the preferred diametral pitch values for coarse pitch gears are: $P = 1$, 2, 4, 6, 8, 10, 12, 14, 16, and 18 teeth per inch of (nominal) pitch diameter. Typical preferred modules are $m = 0.8$, 1, 1.25, 1.5, 2, 2.5, 3, 4, 5, 6, 8, 10, 12, 15, 20, ... mm. For a specified number of teeth, when either the diametral pitch (P) or the module (m) is chosen, the nominal pitch diameter of the gear is defined. For example, a 19 tooth gear with a diametral pitch $P = 6$, the nominal pitch diameter is $D_p = 19/6 = 3.1667$ inches; similarly, for a 27 tooth gear with a module $m = 4$ mm, the nominal pitch diameter is $D_p = 27 \cdot 4 = 108.0$ mm. These nominal values are used for design calculations particularly to define the base radius, but the actual values of pitch radius and pressure angle are determined only when a pair of gears are mounted on fixed centers. Typical standard dimensions for spur gear teeth are given in Table 5.1.

In some situations, the dedendum circle is outside the base circle. When this happens, the tooth profile is an involute curve all the way to the fillet, at which point the fillet blends it into the dedendum surface. The other case is that the dedendum circle is inside the base circle, in which case there is a portion of the flank that cannot be an involute curve because the involute is not defined inside the base circle. The exact form taken by this non-involute surface is largely determined by the particular method used to cut the teeth, but it is common practice to draw this part as simply a radial line from the top of the fillet up to the base circle. As long as there is no contact inside the base circle, the main concern is with regard to the strength of the tooth and the stresses in that area. This is more discussion about this topic in the next section.

Table 5.1 Standard Spur Gear Teeth

Item	US Customary	SI
	$P < 20$	
Pressure Angle	$\phi = 20^o$	$\phi = 20^o$
Number of Teeth	N	N
Pitch Radius (Nominal)	$R_p = N/(2P)$	$R_p = m \cdot N/2$
Base Radius	$R_b = R_p \cos\phi$	$R_b = R_p \cos\phi$
Addendum	$1/P$	$1 \cdot m$
Dedendum	$1.25/P$	$1.25 \cdot m$
Clearance	$0.25/P$	$0.25 \cdot m$
Working Depth	$2/P$	$2 \cdot m$
Whole Depth	$2.25 \cdot P$	$2.25\cdot$,
Circular Thickness	$\pi/(2P)$	$1.5708 \cdot m$

5.9 Contact Ratio

Consider a gear and pinion engaged as shown in Figure 5.12. All contact between gear teeth must occur in the space between the two addendum circles and at a point on the line of action. Thus first contact happens when the pinion tooth cuts the line of action at the point designated as a. Contact continues down the line of action, through the pitch point, and on to the point b where the gear tooth cuts the line of action. The distance from point a to point b is called the *length of action*, L_{ab}. The angle turned while contact moves from a to the pitch point is called the *arc of approach*; the angle turned from the pitch point until contact is broken is called the *arc of recess*. During the approach, the tooth engagement is progressively deeper; the depth of engagement reduces through recess to the point where engagement is broken at b.

For smooth operation, it is vital that a second pair of teeth engage before the first pair lose contact. This requires that in many positions, there are two or more pairs of teeth in contact while in some positions there will be fewer pairs carrying the load. The ratio of the length of action to the distance between adjacent tooth contact points is the average number of teeth engaged; this ratio is called the *contact ratio*. The contact ratio is an important measure of the quality of a gear mesh design; a higher contact ratio indicates a better design. In all cases, the contact ratio must be greater than 1.0, with minimum values in the range 1.2 to 1.4.

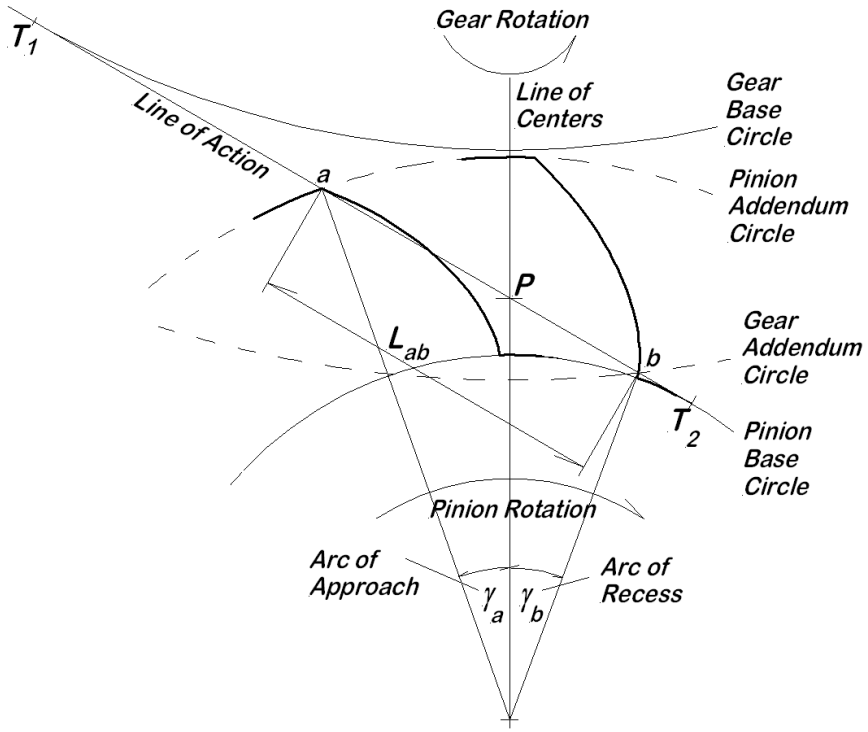

Figure 5.12: Contact Ratio and Interference Considerations

As shown in Figure 5.12, the line of action is defined as tangent to the two base circles at T_1 and T_2. Where the line of action intersects the line of centers defines the pitch point, P. The following notations apply:

C = center distance

R_{ap} = addendum radius of the pinion

R_{bp} = base radius of the pinion

R_{ag} = addendum radius of the gear

R_{bg} = base radius of the gear

ϕ = actual pressure angle

With these notations, the length of action is

$$\begin{aligned} L_{ab} &= \widehat{aT_2} + \widehat{T_1 b} - \widehat{T_1 T} \\ &= \sqrt{R_{ap}^2 - R_{bp}^2} + \sqrt{R_{ag}^2 - R_{bg}^2} - C \sin\phi \end{aligned} \tag{5.23}$$

where

$$\phi = \sin^{-1}\left(\frac{R_{bp} + R_{bg}}{C}\right) \tag{5.24}$$

Now consider the situation where two pinion teeth are simultaneously in contact with two gear teeth. Both points of contact are at locations on the line of action. The separation of the contact points is equal to the base pitch, the arc length along the base circle between consecutive tooth involutes and denoted as P_b. It is evident that the essential feature required for two pinion teeth to be in simultaneous contact with two gear teeth is that the base pitch must be the same for both the gear and the pinion; if this is not true, the teeth will not be properly spaced to achieve simultaneous meshing. For a gear (or pinion) with N teeth and base radius R_b, the base pitch is

$$P_b = 2\pi R_b/N \tag{5.25}$$

The contact ratio, M_c, is then

$$M_c = L_{ab}/P_b \tag{5.26}$$

5.10 Interference & Undercutting

For the gear pair in Figure 5.12, consider increasing the addendum radius of the gear while holding all other parameters fixed. As R_{ag} increases, it is evident that point b will soon reach the base circle of the pinion at T_2; any further increase creates the potential for non-involute contact inside the pinion base circle. Contact on a non-involute surface is called *interference*. In the same way, if the pinion addendum were increased, there is the possibility of interference at the base circle of the gear as a approaches T_1. To avoid interference, the addendum radii must be less than their critical values:

$$R_{ag-Crit} = \sqrt{R_{bg}^2 + C^2 \sin^2\phi} \tag{5.27}$$

$$R_{ap-Crit} = \sqrt{R_{bp}^2 + C^2 \sin^2\phi} \tag{5.28}$$

In the manufacturing of gears, some methods employ a cutter shaped like a pinion that moves parallel to the gear axis of rotation. If there is interference between the gear being cut and the cutter, the cutter simply removes the interfering material from the flank of the gear. This is called *undercutting*, and it can seriously weakening the gear tooth. It is obvious that undercutting must be avoided in good gear pair design.

5.11 Simple and Compound Gear Trains

The remainder of this chapter addresses combinations of gears running together to accomplish useful motions. Such combinations are called *gear trains*. The essential requirement for a pair gears to run together is that they have the same circular pitch, or equivalently, that their base pitch values be the same. Recall that the circular pitch is the arc length, measured at the pitch radius, from one tooth profile to the next. If two gears have the same circular pitch, then the teeth on each will arrive at the point of engagement at the same time. It is not difficult to show that this equivalent to requiring that they have the same diametral pitch or the same module, depending on whether USC or SI units are being used.

Consider several gears running together and supported on bearings in such a way that they are all in the same plane. This is called a *simple gear train*, and an example is shown in Figure 5.13. All of the gears in a simple train must have the same diametral pitch or the same module.

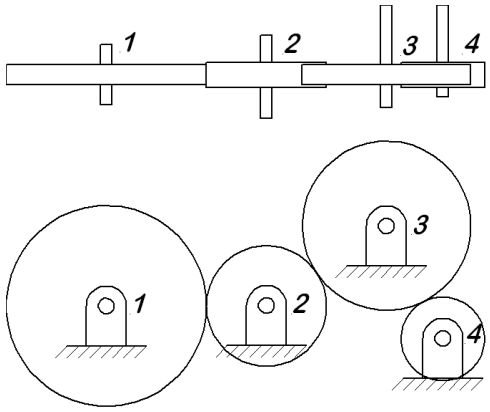

Figure 5.13: Simple Gear Train

As shown in Figure 5.13, the gear are represented by their pitch circles, drawn tangent to each other at the pitch point on each line of centers. Conjugate action assures that the pitch circles roll on each other without slipping, thus allowing each actual gear to be conceptually replaced by a friction wheel. Denote the pitch radii as R_{1p}, R_{2p}, R_{3p}, and R_{4p}, respectively, while the rotations are θ_1, θ_2, θ_3, and θ_4, taken positive in alternating senses. Thus the rolling equations are

$$\theta_2 R_{2p} = \theta_1 R_{1p} \qquad \text{at the } 1-2 \text{ mesh} \tag{5.29}$$

$$\theta_3 R_{3p} = \theta_2 R_{2p} \qquad \text{at the } 2-3 \text{ mesh} \tag{5.30}$$

$$\theta_4 R_{4p} = \theta_3 R_{3p} \qquad \text{at the } 3-4 \text{ mesh} \tag{5.31}$$

If θ_1 is understood as an "input" and θ_4 as an "output," then the ratio of output to input

is called the *train ratio*, θ_4/θ_1,

$$\begin{aligned} \theta_4 &= (R_{3p}/R_{4p})\,\theta_3 \\ &= (R_{3p}/R_{4p})\,(R_{2p}/R_{3p})\,\theta_2 \\ &= (R_{3p}/R_{4p})\,(R_{2p}/R_{3p})\,(R_{1p}/R_{2p})\,\theta_1 \\ \theta_4/\theta_1 &= R_{1p}/R_{4p} = N_1/N_4 \end{aligned} \tag{5.32}$$

where N_1 is the number of teeth on the input gear, and N_4 is the number of teeth on the output gear. Recall that the pitch radii are proportional to the number of teeth on the gear. This shows that only the input and output gears affect the train ratio. The other gears have no effect on the train ratio; they are called *idlers* for this reason. Idlers simply fill the space between the input and output gears, and in some cases they serve to reverse the sense of rotation. If there is also driven machinery attached to the shafts of gears 2 and 3, then they become "output gears" and there is a train ratio for each of them:

$$\theta_2/\theta_1 = R_{1p}/R_{2p} = N_1/N_2 \tag{5.33}$$

$$\theta_3/\theta_1 = R_{1p}/R_{3p} = N_1/N_3 \tag{5.34}$$

Where very large train ratios are required, simple gear trains are not practical because of the very large size required for one or more of the gears. A system called a compound gear train is usually much more compact. A typical compound train is shown in Figure 5.14.

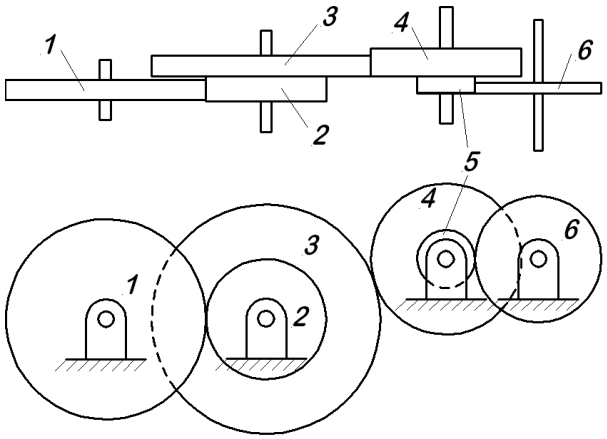

Figure 5.14: Compound Gear Train

The thing that makes this a *compound train* are the use of *compound gears* 2-3 and 4-5. Looking at the top view, it is evident that each of these is actually two gears on a common shaft, locked together so that they have the same rotation. While bearing in mind that any of the shafts may be considered either an "input" or an "output," for the purposes

of illustration, consider gear 1 as the input and gear 6 as the output. It is required to find the train ratio, θ_6/θ_1, where all rotations are taken positive as they naturally occur in the train. The rolling constraints are

$$\theta_1 R_{1p} = \theta_{23} R_{2p} \qquad \text{at the } 1-2 \text{ mesh} \tag{5.35}$$

$$\theta_{23} R_3 = \theta_{45} R_{4p} \qquad \text{at the } 3-4 \text{ mesh} \tag{5.36}$$

$$\theta_{45} R_{5p} = \theta_6 R_{6p} \qquad \text{at the } 5-6 \text{ mesh} \tag{5.37}$$

After eliminating all the intermediate rotations, the final result in terms of the tooth numbers is

$$\begin{aligned} \theta_6/\theta_1 &= (R_{5p}/R_{6p})\,(R_{3p}/R_{4p})\,(R_{1p}/R_{2p}) \\ &= \frac{N_5}{N_6} \cdot \frac{N_3}{N_4} \cdot \frac{N_1}{N_2} \end{aligned} \tag{5.38}$$

The replacement of the pitch radius ratios with the tooth number ratio is correct because in each case, the particular gears in each ratio must have the same diametral pitch or the same module.

In certain circumstances, it may be required that the input and output shafts be colinear (aligned); such a train is called a *reverted compound train*. For a two stage reverted train, that is one involving four gears, the center distances must therefore be exactly the same for both meshes, as shown in Figure 5.15. If the ratio is the same in each mesh, there is no difficulty; if different ratios are required in the two meshes, it may not be possible to accomplish the design with standard gears. Allowing the center distance to increase provides a degree of design flexibility, at the expense of increased pressure angle and decreased contact ratio.

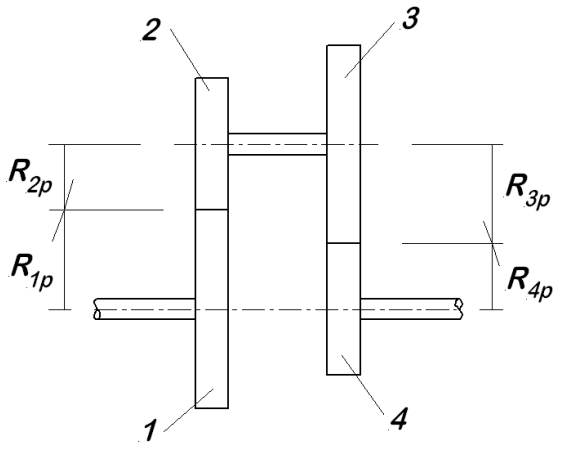

Figure 5.15: Reverted Compound Train

5.12 Tooth Numbers

The role of tooth numbers in determining a train ratio is evident in the developments above. It is useful therefore to say a little about how they are chosen, beginning with a simple example. Consider a single pair of spur gears with tooth numbers $N_1 = 30$ and $N_2 = 60$, for which the train ratio is $2 : \dot{1}$. Suppose that a particular tooth on the first gear has a flaw, an irregularity that will increase wear and noise. Such a flaw might be a material defect, a manufacturing error, or damage sustained in operation. This tooth comes into repeated contact with exactly the same two teeth on the second gear, no matter how many revolutions the gears make. The defect works repeatedly to damage these same two teeth. Clearly, it would be advantageous if the damage from that flawed tooth could be spread to all the teeth of the second gear, rather than being concentrated on just two.

To extend this discussion, two definitions are required:

- A *prime number* is an integer divisible only by itself and one. This means that it has no other factors. Examples of prime numbers include 1, 2, 3, 5, 7, 11, 13, 17, 19, ...
- Two integers are said to be *relatively prime* if they have no common factors. For example, $27 = 3^3$ and $32 = 2^5$ are relatively prime, even though neither of them is a prime number. Further, 27 and $33 = 3 \cdot 11$ are not relatively prime because of the common factor 3.

The problem with the initial example involving two gears with $N_1 = 30$ and $N_2 = 60$ is called a *common factor error*, a design error to be avoided if at all possible. The problem is avoided provided the tooth numbers in each gear mesh are *relatively prime*. Note that this does not require that either of them be a prime number, but only that they be relatively prime. It is true, however, that a prime number is relatively prime to all integers other than itself.

The development of equations (5.32) and (5.38) show that in each case, the train ratio can be written as

$$\begin{matrix}\text{Train} \\ \text{Ratio}\end{matrix} = \frac{\text{Product of driving gear tooth numbers}}{\text{Product of driven gear tooth numbers}} \tag{5.39}$$

In equation (5.38), the tooth numbers are grouped by meshes, so that each fraction represents a particular mesh. Equation (5.39) indicates that the same train ratio can

be achieved in other ways, by rearranging the factors in either the numerator or the denominator, with the provision that at every mesh, the same diametral pitch or same module is used for both gears.

In order to avoid interference and undercutting, no gear may have too few teeth. For coarse pitch gears with a diametral pitch less than 20, no pinion should have fewer than 18 teeth. In the rearrangement suggested in the previous paragraph, it is possible that a particular gear may be left with too few teeth. In this case, it is possible to introduce a common factor in both the numerator and the denominator to increase that tooth number. To do this and still avoid the common factor error, the common factor must be placed a different meshes.

In the design of a gear train, one of the questions to be asked is whether the train ratio is required to be exactly a particular value, or only near that stated value. In many machinery applications, it makes no difference whether the output shaft is exactly 1435 rpm, or it could equally well be only 1432 rpm. There are other more exacting applications, such as clockwork, where the ratio between the second hand to the minute hand must be exactly 60 : 1. If a loose approximation to a specified train ratio is satisfactory, then a few moments creative thought will usually enable the designer to come up with a workable approximation. If an exact train ratio is required, the problem is substantially more difficult. The development of very close approximations to specified train ratios is a well developed art in the field of horology (clock and timing mechanisms). This was developed at some length in the first edition of this book, and the interested reader is referred there for further information.

5.13 Planetary Gear Trains

All of the gear trains discussed in the preceding involve gear shaft centerlines that are stationary in space. There is a second type of train called a *planetary* (or *epicyclic*) *gear train* for which some of the gear centerlines are not stationary. Typical simple and compound planetary trains are shown in Figures 5.16 and 5.17. The name *planetary* arises from the rather obvious analogy with the solar system. The central gear is usually called the *sun* gear, and the gears that circle around the sun are called *planets*. However, there is no astronomical analog for the *ring gear*, and internal gear that engages outside of the planets. The planet shafts are all supported on what is called the *planet carrier*, also called the *spider* or *arm*. The alternative name for the entire assembly, *epicyclic train*, comes from the fact that the planet gear teeth trace epicycloidal curves.

On the left side of both Figures 5.16 and 5.17, there is a pictorial view of the assembly, seen looking in the axial direction. The right side of each figure shows a schematic section diagram for the same system in each case. In the schematic, the planets are always rotated into the picture plane. Even when there are three or more planets, the schematic view

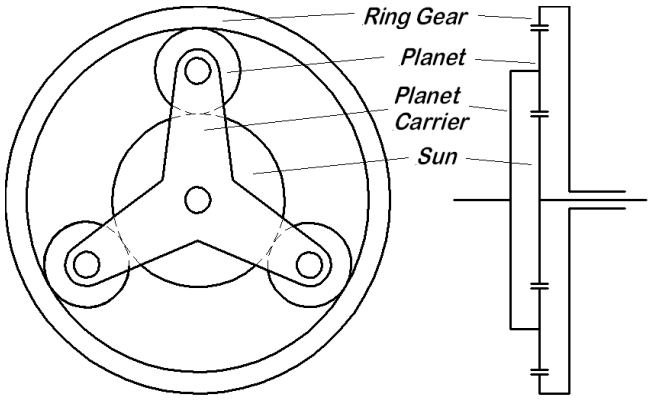

Figure 5.16: Simple Planetary Train

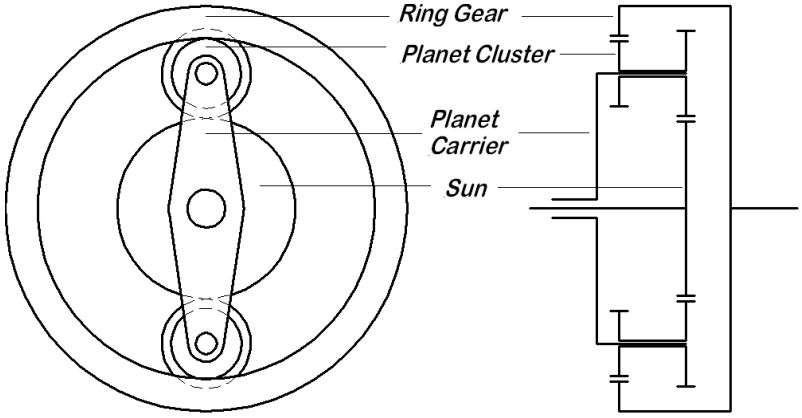

Figure 5.17: Compound Planetary Train

never shows more than two in the picture plane. The gear shafts appear simply as lines in the schematic, often representing concentric tubular shafts. The schematic is always symmetric about the horizontal centerline, so it is common practice to show only the top half.

Notice that there are three shafts coming out of the planetary train, one for each of the sun gear, the planet carrier, and the ring gear. In some cases, one of the shafts is attached to the frame, so that only two shafts need to be actually brought out (it is easy to see how the ring gear could be attached to the frame). If all three are allowed to rotate, then at least two of the shafts must be coaxial. If the planet carrier is fixed to the frame, then the assembly is no different from the trains considered in previous sections because this means that all the centerlines are fixed in space. The planets are not directly driven from the outside.

With three connecting shafts, it is evident that the planetary train must have two assigned

rotations in order to determine the third; *this is a two degree of freedom mechanism.* If any of the shafts is fixed and cannot rotate, that reduces the number of degrees of freedom by one, and the result is then a single degree of freedom mechanism.

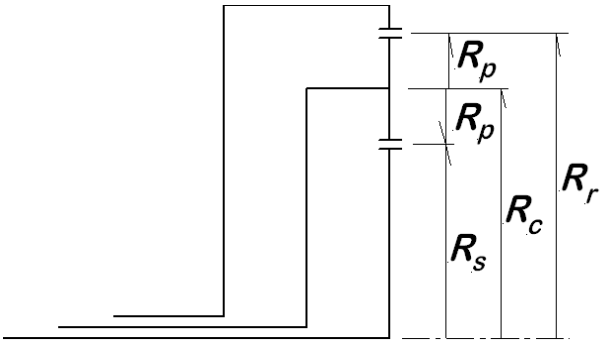

Figure 5.18: Schematic Half Section of a Simple Planetary Train

Consider the simple planetary train shown in Figure 5.18 where the three concentric shafts are connected to the sun, the planet carrier, and the ring gear. Pitch radii for all the gears are indicated, along with the planet carrier radius. Let θ_s, θ_c, θ_p, and θ_r denote the rotations of the sun, the planet carrier, the planets, and the ring gear, *all measured positive in the same direction relative to a stationary reference frame.* To be specific, assume that a positive rotation of any component moves the upper edge out of the picture plane and toward the viewer. There are two rolling constraint equations to be written, one for each gear mesh in the schematic.

$$R_s\theta_s = R_c\theta_c - R_p\theta_p \qquad \text{Sun-Planet} \tag{5.40}$$

$$R_r\theta_r = R_c\theta_c + R_p\theta_p \qquad \text{Planet-Ring} \tag{5.41}$$

When the two constraint equations are added, the planet carrier rotation is eliminated with the result

$$R_s\theta_s + R_r\theta_r = 2R_c\theta_c \tag{5.42}$$

If any two of the rotations are specified, this expression is readily solved to give the third.

In many cases, the pitch radii are not known, but the tooth numbers are specified. Notice that the planet carrier radius must be equal to the simple average of the sun and ring pitch radii. Because the schematic in Figure 5.18 is a simple train, all of the gears must use the same diametral pitch or the same module. In such a case, the pitch radii are all proportional to the tooth numbers, so the proportionalities are substituted and the common factors removed to give

$$N_s\theta_s + N_r\theta_r = (N_s + N_r)\,\theta_c \tag{5.43}$$

where the Ns are the tooth numbers. If any component is fixed, the rotation for that component is zero and that term drops from the equation. This equation can be differentiated with respect to time to relate the angular velocities and accelerations.

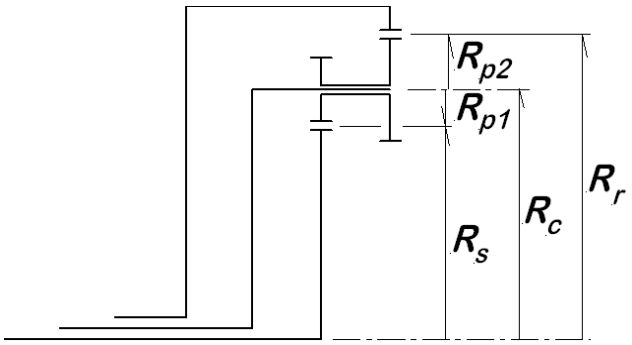

Figure 5.19: Schematic Half Section of a Compound Planetary Train

For the compound planetary train shown in Figure 5.19, the analysis is only slightly more involved. The rolling constraint equations are almost identical to those written for the previous case:

$$R_s\theta_s = R_c\theta_c - R_{p1}\theta_p \qquad \text{Sun-Planet} \tag{5.44}$$

$$R_r\theta_r = R_c\theta_c + R_{p2}\theta_p \qquad \text{Planet-Ring} \tag{5.45}$$

Elimination of the planet rotation is more complicated because the two planets have different pitch radii. When the algebra is carried out, the result is

$$R_{p2}R_s\theta_s + R_{p1}R_r\theta_r = R_c\left(R_{p1} + R_{p2}\right)\theta_c \tag{5.46}$$

As before, it is usually preferable to express this relation in terms of tooth numbers. To that end, the pitch radii of the gears and the planet carrier radius are expressed in terms of the module (alternatively, the diametral pitch could be used). The required expressions are

$$\begin{aligned} R_s &= m_s \cdot N_s/2 & R_r &= m_r \cdot N_r/2 \\ R_{p1} &= m_s \cdot N_{p1}/2 & R_{p2} &= m_r \cdot N_{p2}/2 \\ R_c &= R_s + R_{p1} & R_c &= R_r - R_{p2} \\ &= \tfrac{1}{2}m_s\left(N_s + N_{p1}\right) & &= \tfrac{1}{2}m_r\left(N_r - N_{p2}\right) \end{aligned} \tag{5.47}$$

When the substitutions are all completed (both substitutions for R_c are required), the final result is

$$N_sN_{p2}\theta_s + N_rN_{p1}\theta_r = \left(N_rN_{p1} + N_sN_{p2}\right)\theta_c \tag{5.48}$$

If this equation is solved for any of the rotations, the resulting tooth number ratios involve only ratios of gears having a common diametral pitch or module. The whole procedure is demonstrated in the following example.

5.13.1 Compound Planetary Train Example

Consider the planetary train shown in Figure 5.20 where there is no ring gear, but two sun gears are used with a planet cluster. Both pitch radii and tooth numbers are indicated in the figure, but only the tooth numbers are known. The input is the rotation θ_1 applied to the first sun gear. (1) What is the relation comparable to equation (5.48) for this system? (2) If the second sun gear is considered fixed and the output is the the planet carrier rotation. What is the train ratio under the second situation? Note that there is no requirement that the two planets be of the same diametral pitch or module, and in most cases, they are not the same.

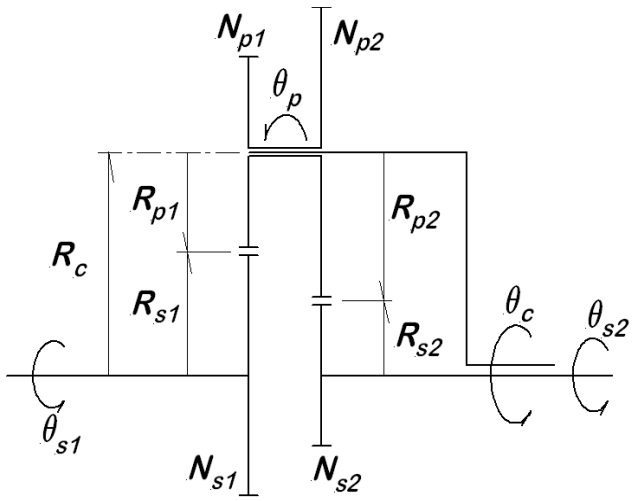

Figure 5.20: Compound Planetary Train for Example

As before, the first step is to express the rolling constraint for each gear mesh.

$$R_{s1}\theta_{s1} = -R_{p1}\theta_p + R_c\theta_c \tag{5.49}$$

$$R_{s2}\theta_{s2} = -R_{p2}\theta_p + R_c\theta_c \tag{5.50}$$

Eliminating the planet rotation, θ_p, gives a single relation between the two sun rotations and that of the planet carrier:

$$R_{s1}R_{p2}\theta_{s1} - R_{s2}R_{p1}\theta_{s2} = R_c\left(R_{p2} - R_{p1}\right)\theta_c \tag{5.51}$$

Let m_1 denote the (unknown) module for the first sun gear and its planet, while m_2 is the (unknown) module for the second sun gear and its planet. To eliminate the gear pitch radii in favor of the tooth numbers, the following substitutions are useful:

$$\begin{aligned} R_{s1} &= m_1 \cdot N_{s1}/2 & R_{s2} &= m_2 \cdot N_{s2}/2 \\ R_{p1} &= m_1 \cdot N_{p1}/2 & R_{p2} &= m_2 \cdot N_{p2}/2 \\ R_c &= R_{s1} + R_{p1} & R_c &= R_{s2} + R_{p2} \\ &= \tfrac{1}{2} m_1 \left(N_{s1} + N_{p1}\right) & &= \tfrac{1}{2} m_2 \left(N_{s2} + N_{p2}\right) \end{aligned} \tag{5.52}$$

When the substitutions are all made (making use of both substitutions for R_c), the final result is

$$N_{s1} N_{p2} \theta_{s1} - N_{s2} N_{p1} \theta_{s2} = \left(N_{s1} N_{p2} - N_{s2} N_{p1}\right) \theta_c \tag{5.53}$$

Thus equation (5.53) is the equation comparable to equation (5.48) in answer to the first question.

If sun gear number 2 is fixed, then $\theta_{s2} = 0$ and equation (5.53) reduces to

$$N_{s1} N_{p2} \theta_{s1} = \left(N_{s1} N_{p2} - N_{s2} N_{p1}\right) \theta_c \tag{5.54}$$

Taking the planet carrier rotation as the output, the train ratio is

$$\theta_c / \theta_{s1} = \frac{N_{s1} N_{p2}}{N_{s1} N_{p2} - N_{s2} N_{p1}} \tag{5.55}$$

Assume the tooth numbers are

$$\begin{aligned} N_{s1} &= 42 & N_{p1} &= 53 \\ N_{s2} &= 22 & N_{p2} &= 67 \end{aligned}$$

Thus the train ratio is

$$\theta_c / \theta_{s1} = \frac{(42)(67)}{(42)(67) - (22)(53)} = 1.7075 \tag{5.56}$$

This answers the second question asked.

5.14 Conclusion

Familiarity with gearing is an essential skill for mechanical engineers. Gears have been, and continue to be, one of the most important elements in mechanical power transmission. There can be no doubt that this will continue to be true far into the future. They provide highly efficient, precise, positive power transmission at relatively low cost when produced in large volume.

The discussion of this chapter has been limited to spur gearing only, but many other types of gearing are in common use as well. The basic knowledge regarding the involute curve is the key to understanding most types of gearing. The concepts of contact ratio, interference, and undercutting carry over to other types of gearing as well. There are countless sources of information on gearing available on the Internet and in various reference books such as the well known work of Dudley [2] . Not all of it is of equal value, and the user must evaluate it with care. The reader will do well to master the concepts presented here as a first step toward dealing with other types of gearing.

References

[1] Beggs, J.S., *Mechanism*, McGraw-Hill, New York, 1955, pp. 68 - 72.

[2] Dudley, D.W. *Gear Handbook*, McGraw-Hill, 1962.

Problems

Note: In the problems that follow, all tooth forms are assumed to be involutes unless otherwise specified.

5-1 Consider a gear tooth for which the circular thickness is 13 mm at a radius of 95 mm. The pressure angle for contact at this point is 21^o. This tooth is to be extended until it is pointed.

(a) What is the tip radius?

(b) What is the pressure angle for contact at the tip?

(c) What is the flank angle at the tip?

5-2 Draw a base circle arc of radius $R_b = 52$ mm, and then construct an involute on this arc. This may be done either manually (compass, straight edge, etc.), or by means of a computer calculation;

5-3 An external gear with 37 teeth is designed for a nominal pressure angle of 20^o with a module $m = 4$ mm. This gear runs with a pinion of 18 teeth.

(a) What is the nominal center distance for this pair?

(b) What is the addendum radius for each gear?

(c) What is the base radius of each gear?

(d) If the center distance is increased by 1.6%, what is the modified center distance?

(e) With the modification of part (d), what is the modified pressure angle?

5-4 Consider the gear pair of problem **5-3**.

(a) What is the contact ratio when running on the nominal center distance?

(b) What is the contact ratio after the modification of problem **5-3** (d)?

(c) Is there a problem of interference? Why?

5-5 An internal gear with 111 teeth is designed for a nominal pressure angle of 20^o and a module $m = 2.5$ mm. This mates with a pinion of 23 teeth.

(a) How far is the pitch point from the center of the internal gear?

(b) What is the base radius of the internal gear?

(c) What is the nominal center distance for this pair?

(d) If the center distance is decreased by 0.5%, what is the actual pressure angle?

5-6 Consider the gear pair of problem **5-3**.

(a) What is the diametral pitch for the gear?

(b) What is the diametral pitch for the pinion?

5-7 Consider a simple gear train consisting of three gears such that #1 and #2 engage and #2 and #3 engage. The rotation of #1 is the input and the rotation of #3 is the output. For tooth numbers $N_1 = 19$, $N_2 = 31$, and $N_3 = 29$, what is the train ratio?

5-8 Consider the compound gear train shown in Figure 5.14, but assume that all the gear axes lie along the same horizontal line. The tooth numbers are: $N_1 = 83$, $N_2 = 27$, $N_3 = 117$, $N_4 = 49$, $N_5 = 19$, and $N_6 = 31$.

(a) What is the train ratio?

(b) If all gears are specified to use the same module, and it is required that the overall length of the train (left end to right end) be less than 950 mm, what is the largest integer module that can be used for these gears?

5-9 A symmetric reverted train is to be designed, similar to Figure 5.5. The overall train ratio is to be a close approximation to 9.5, while the parallel shaft offset is to be no more than 115 mm. The minimum number of teeth allowed on the pinion to avoid undercutting is 18 teeth with a maximum allowed is 120 teeth. What is the largest integer or integer plus one half module (i.e., 0.5, 1, 1.5, 2, 2.5, ...) that can be used for these gears, assuming that the same module is to be used for all four gears? Iteration is likely to be required.

5-10 Consider a compound planetary train such as that shown in Figure 5.19. The sun gear engages planet #1 which is on the same shaft as planet #2. Planet #2 engages the ring gear. The tooth numbers are: $N_s = 31$, $N_{p1} = 23$, $N_{p2} = 29$, and $N_r = 91$.

(a) Is it possible that all the gears are made to the same module?

(b) If the sun gear is held fixed, the planet carrier is taken as the input, and the ring gear rotation is the output, what is the train ratio?

(c) If the ring gear is held fixed, the planet carrier is the input, and the sun gear is the output, what is the train ratio?

Part II

Dynamics of Machines

Chapter 6

Statics and Virtual Work

6.1 Introductory Comments

The subject of statics is the familiar science of equilibrium. In an introductory mechanics sequence, this is usually one of the first topics discussed, and almost invariably presented in terms of Newton's First Law for a particle and its various extensions to translation and rotation of rigid bodies. Thus, the conditions for equilibrium are usually associated with the vanishing of certain force and moment sums. Although these methods are relatively simple and work well for simple problems, another approach is available that is often superior in the context of machinery problems.

This alternative approach is called the *Principle of Virtual Work*. In a related form called the Principle of Virtual Velocities, this principle can be traced back to the third century B.C. In western Europe, the Principle of Virtual Work is associated with such famous names of science as Leonardo da Vinci, Descartes, Lagrange, Gauss, Navier, Clapeyron, and Kirchoff. It is also the oldest of what are termed the *Energy Principles of Mechanics*, and has been suggested to be the fundamental axiom of mechanics. Consequently, the Principle of Virtual Work has played a major role in the theoretical development of mechanics. However, it is often omitted or only lightly included in current engineering curricula. Because it is especially useful in applications to machines, this chapter attempts to remedy that slight.

Statics problems can be classified in two types, depending on whether the geometry is constant or non-constant. For the first type, many situations exist in which there is no gross motion as the loads are applied, so that the loaded equilibrium geometry is very nearly the same as the unloaded geometry, that is, the geometry is essentially constant. Most civil structures, such as bridges, towers, and dams, are examples of this type. The second type includes those cases in which gross motion may occur as the loads are

applied, and the equilibrium position is often not a known part of the problem. For these cases, the geometry is not constant. The second type includes most devices designed to move, particularly machines. Examples include a pair of pliers compressing a spring, the pendulum scale mechanism, and the slider-crank mechanism used in automotive engines. Situations of the second type are often difficult to address by means of Newton's First Law (Equilibrium). The Principle of Virtual Work applies to both types of problems, but it is especially suited to the second type, where application of force and moment sums often leads to difficulty.

Most mechanisms transform mechanical power of one sort to another, such as a gear box that transforms high-speed rotary power to low-speed rotary power. If it is necessary to determine the relation between input force (torque) and output force (torque) by application of the First Law, a sequence of free-body diagrams, including internal forces and reactions, is required with an associated large number of equations. When this problem is approached from the Principle of Virtual Work, *the reactions and internal forces are not involved in the formulation*, and the number of equations is greatly reduced.

The following sections of this chapter present the Principle of Virtual Work, a presentation initially based on Newton's First Law, and then show applications of this principle to several machine problems. In the applications, it is useful to consider also the First Law formulation to gain an insight into the difficulties to be expected there and to see the types of problems best suited to each approach.

6.2 Principal of Virtual Work

The Principle of Virtual Work is a statement of the conditions for equilibrium in terms of work, a scalar quantity, significantly different from the vectorial force and moment sums derived from Newton's First Law as extended to rigid bodies. The concept of work is assumed to be familiar, but the modifier *virtual* requires some explanation. It is necessary to define a virtual displacement before the virtual work can be defined. Following these definitions, the Principle of Virtual Work is stated and justified.

Consider a particle located by the position vector $\mathbf{r}$. A virtual displacement of that particle, denoted $\delta\mathbf{r}$, is a postulated, arbitrary differential displacement of the particle, performed in zero-elapsed time, and consistent with any applicable constraints. Note the features of the virtual displacement:

1. It is a differential quantity, an infinitesimal;

2. It is postulated, or proposed for discussion, rather than a displacement associated with an actual motion;

3. It occurs in zero elapsed time, which means that time is constant during a virtual displacement;

4. It is arbitrary, insofar as that is possible consistent with the applicable constraints.

The first three characteristics are reasonably clear in themselves, but the fourth may require an illustration. For a single particle moving without any constraints, the virtual displacement is completely arbitrary in both infinitesimal magnitude and direction. If the particle is then constrained to remain a constant distance from a fixed point, then the particle must move on the surface of a sphere. The virtual displacement is then arbitrary in magnitude and in direction *on the surface of the sphere*. A virtual displacement normal to the surface of the sphere would not be consistent with an applicable constraint. If the particle is part of a rigid body, then the virtual displacement of the particle must be consistent with the virtual displacement of the rigid body as a whole.

The delta notation, using the lowercase Greek delta, δ, denotes an operator similar to the more common differential operator, d. The four characteristics just noted are actually the properties of the delta operator. For comparison, consider the two operators are applied to a function $f(x, y, z, t)$

$$df = \frac{\partial f}{\partial x}dx + \frac{\partial f}{\partial y}dy + \frac{\partial f}{\partial z}dz + \frac{\partial f}{\partial t}dt \tag{6.1}$$

$$\delta f = \frac{\partial f}{\partial x}\delta x + \frac{\partial f}{\partial y}\delta y + \frac{\partial f}{\partial z}\delta z \tag{6.2}$$

Notice that δf involves the delta operator applied to each of the coordinates, x, y, and z. Because of the third characteristic item in the initial list, the delta operator applied to the time variable is zero.

As just used, applying the delta operator to the position vector $\mathbf{r}$ produces $\delta\mathbf{r}$, called a *virtual displacement*. In other circumstances, the result of applying the delta operator to the function f is called the *variation of* f. This is a carryover from the *calculus of variations*, an advanced mathematical topic in which the delta operator is widely used. However, the calculus of variations is not required for any work in this book. It is well to be aware that the terms "virtual something" and "variation of something" are, in fact, the same operations, and both denote the application of the delta operator.

If a force $\mathbf{F}$ is applied to a particle undergoing a virtual displacement $\delta\mathbf{r}$, then the force does virtual work δW, a scalar expressed in terms of a dot product:

$$\delta W = \mathbf{F} \cdot \delta\mathbf{r} \tag{6.3}$$

Thus, virtual work is the work associated with a finite force applied through a virtual displacement. The four characteristics, associated with the use of the delta operator, apply to virtual work.

6.2.1 Principle of Virtual Work for a Particle

For a single particle, the Principle of Virtual Work says that the particle is in equilibrium if the virtual work of all forces acting on the particle is zero. Because the determination of equilibrium conditions based on Newton's First Law is a familiar approach, the first objective is to show that the Principle of Virtual Work is fully equivalent to Newton's First Law. This requires two steps: (1) to show that the Principle of Virtual Work is a necessary consequence of the First Law (necessity); and (2) to show that the First Law is a consequence of the Principle of Virtual Work (sufficiency). These are both given in detail for the present situation. For later cases, only necessity shown; the sufficiency arguments are similar but more involved than the one given here.

To show that the Principle of Virtual Work *is a necessary* consequence of Newton's First Law for the case of a single particle, consider the conditions for equilibrium according to the First Law:

$$\sum_i \mathbf{F}_i = \mathbf{0} \tag{6.4}$$

The particle is located by the position vector $\mathbf{r}$, and if given a virtual displacement $\delta\mathbf{r}$, the virtual work is

$$\delta W = \left(\sum_i \mathbf{F}_i \right) \cdot \delta\mathbf{r} \tag{6.5}$$

Because one factor in the dot product is zero, the product is zero. Thus, if the First Law is satisfied, the virtual work is necessarily zero.

To show that the Principle of Virtual Work *is sufficient for equilibrium*, the argument begins with the vanishing of the virtual work and show that the First Law conditions are a consequence. The Principle of Virtual Work says that equilibrium exist provided the virtual work is zero. That is,

$$\delta W = \left(\sum_i \mathbf{F}_i \right) \cdot \delta\mathbf{r} = 0$$

This demonstration is by contradiction, so assume that

$$\sum_i \mathbf{F}_i = |\mathbf{F}|\, \mathbf{e}_F \qquad |\mathbf{F}| \neq 0 \tag{6.6}$$

that is, assume that the sum of forces is non-zero. The quantity $\mathbf{e}_F$ is a unit vector in the direction of the resultant force, whereas $|\mathbf{F}|$ is the magnitude of the resultant. Now because $\delta\mathbf{r}$ is completely arbitrary, it could be that

$$\delta\mathbf{r} = |\delta\mathbf{r}|\, \mathbf{e}_F \qquad |\delta\mathbf{r}| \neq 0 \tag{6.7}$$

in which case the virtual work is positive,

$$\delta W = |\mathbf{F}|\,\mathbf{e}_F \cdot |\delta\mathbf{r}|\,\mathbf{e}_F = |\mathbf{F}|\,|\delta\mathbf{r}| \tag{6.8}$$

There is no way that this can be zero for arbitrary $|\delta\mathbf{r}|$, except to violate the assumption that $|\mathbf{F}|$ is non-zero. Thus, it must be concluded that the vanishing of the virtual work implies the vanishing of the resultant force on the particle, the condition for equilibrium. This completes the sufficiency argument for the single particle case.

6.2.2 Principle of Virtual Work for a Rigid Body

Next consider the extension of the Principle of Virtual Work to a rigid body. Figure 6.1 shows a rigid body typified by three particles, labeled (1), (2), and (3). For each of the particles there is a position vector, $\mathbf{r}_1$, $\mathbf{r}_2$, and $\mathbf{r}_3$. On particle (1) there are three forces shown: $\mathbf{F}_1$ is an external force applied to the body at the location of this particle, whereas $\mathbf{f}_{12}$ and $\mathbf{f}_{13}$ are internal forces required to enforce the rigid body condition. Similar forces act on the other particles. If the body is in equilibrium, then each particle is in equilibrium and the First Law requires that

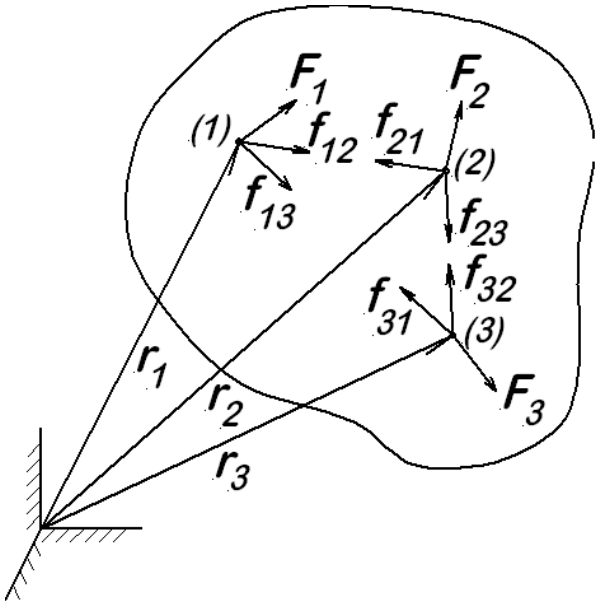

Figure 6.1: Single Rigid Body Represented by Three Typical Particles

$$\mathbf{F}_1 + \mathbf{f}_{12} + \mathbf{f}_{13} = \mathbf{0} \tag{6.9}$$
$$\mathbf{F}_2 + \mathbf{f}_{21} + \mathbf{f}_{23} = \mathbf{0} \tag{6.10}$$
$$\mathbf{F}_3 + \mathbf{f}_{31} + \mathbf{f}_{32} = \mathbf{0} \tag{6.11}$$

Because each force sum is zero, the sum of the virtual work of these force sums is also zero:

$$\delta\mathbf{r}_1 \cdot (\mathbf{F}_1 + \mathbf{f}_{12} + \mathbf{f}_{13}) + \delta\mathbf{r}_2 \cdot (\mathbf{F}_2 + \mathbf{f}_{21} + \mathbf{f}_{23}) + \delta\mathbf{r}_3 \cdot (\mathbf{F}_3 + \mathbf{f}_{31} + \mathbf{f}_{32}) = 0 \tag{6.12}$$

Now look at a pair of terms in this summation, and recall that the internal forces must be equal and opposite to each other, $\mathbf{f}_{ij} = -\mathbf{f}_{ji}$

$$\begin{aligned} \delta\mathbf{r}_1 \cdot \mathbf{f}_{12} + \delta\mathbf{r}_2 \cdot \mathbf{f}_{21} &= \delta\mathbf{r}_1 \cdot \mathbf{f}_{12} - \delta\mathbf{r}_2 \cdot \mathbf{f}_{12} \\ &= (\delta\mathbf{r}_1 - \delta\mathbf{r}_2) \cdot \mathbf{f}_{12} \end{aligned} \tag{6.13}$$

Let $\mathbf{e}_{12}$ denote a unit vector directed from particle 1 toward particle 2, and use $\mathbf{e}_{12}$ to express the force $\mathbf{f}_{12}$:

$$\mathbf{e}_{12} = \frac{\mathbf{r}_2 - \mathbf{r}_1}{|\mathbf{r}_2 - \mathbf{r}_1|} \tag{6.14}$$

$$\mathbf{f}_{12} = |\mathbf{f}_{12}|\,\mathbf{e}_{12} \tag{6.15}$$

Then, the difference in virtual displacements appearing in the virtual work of the internal forces is

$$\begin{aligned} \delta\mathbf{r}_1 - \delta\mathbf{r}_2 &= \delta(\mathbf{r}_2 - \mathbf{r}_1) = \delta(|\mathbf{r}_2 - \mathbf{r}_1|\,\mathbf{e}_{12}) \\ &= \mathbf{e}_{12}\delta|\mathbf{r}_2 - \mathbf{r}_1| + |\mathbf{r}_2 - \mathbf{r}_1|\,\delta\mathbf{e}_{12} \end{aligned}$$

Because the body is rigid, $|\mathbf{r}_2 - \mathbf{r}_1|$ is constant and $\delta|\mathbf{r}_2 - \mathbf{r}_1|$ must be zero; this eliminates the first term on the right side. Any change in the unit vector $\mathbf{e}_{12}$ must be normal to $\mathbf{e}_{12}$, so that $\mathbf{e}_{12} \cdot \delta\mathbf{e}_{12}$ must also be zero. The two terms from the virtual work considered at the beginning of this argument then vanish from the following:

$$\delta\mathbf{r}_1 \cdot \mathbf{f}_{12} + \delta\mathbf{r}_2 \cdot \mathbf{f}_{21} = |\mathbf{r}_2 - \mathbf{r}_1|\,\delta\mathbf{e}_{12} \cdot |\mathbf{f}_{12}|\,\mathbf{e}_{12} = 0 \tag{6.16}$$

In a similar manner, the virtual work of each of the other internal force pairs can be shown to be zero. This reduces the original virtual work sum to

$$\delta\mathbf{r}_1 \cdot \mathbf{F}_1 + \delta\mathbf{r}_1 \cdot \mathbf{F}_2 + \delta\mathbf{r}_1 \cdot \mathbf{F}_3 = 0 \tag{6.17}$$

The conclusion is that equilibrium of the rigid body requires that the virtual work of the external forces be zero. This, then, is the Principle of Virtual Work for a Rigid Body. Note that in forming the sum, the virtual displacements are subject to the constraint that the particles must move as parts of a rigid body.

6.2.3 Principle of Virtual Work for a System of Rigid Bodies

Before attempting to extend the Principle of Virtual Work to multiple rigid bodies, it is necessary to point out one of the key features in the preceding discussion for a single rigid body. The rigid body assumption prevents the absorption of any work by the system, either by elastic deformation or by friction with eventual conversion to heat. This avoidance of energy absorption by the system is a key assumption in dealing with systems of rigid bodies. This does not, however, prevent the inclusion of friction forces external to the system, but it does preclude friction at the contact points between the bodies. A system of rigid bodies for which there is no energy absorption at the points interconnection is called an *ideal system*.

An ideal system of two pin-jointed rigid bodies is shown in Figure 6.2(a); free-body diagrams for the two bodies are shown in Figure 6.2(b).

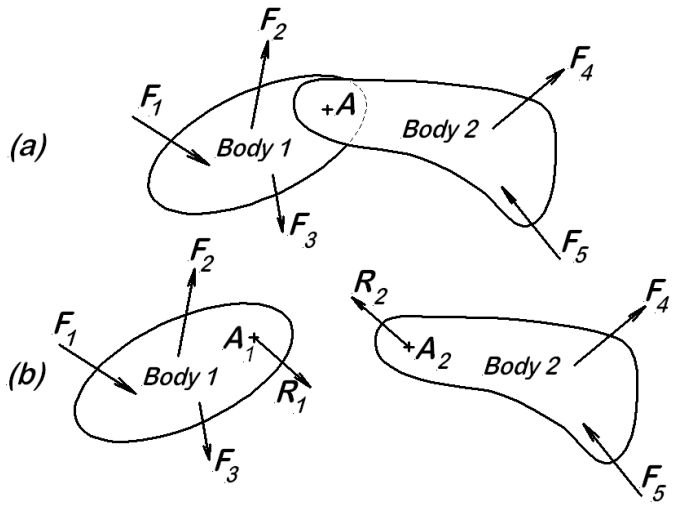

Figure 6.2: (a) An Ideal System of Rigid Bodies; (b) Free-Body Diagrams for the Two Rigid Bodies

Note that the reactions forces, $\mathbf{R}_1$ and $\mathbf{R}_2$, are unknown in both direction and magnitude. However, it is known that they are equal and opposite, $\mathbf{R}_1 = -\mathbf{R}_2$ by Newton's Third Law. The equilibrium condition in terms of virtual work for each rigid body, taken individually, has already been established. It is as follows:

$$\text{Body 1 :} \qquad \delta\mathbf{r}_1 \cdot \mathbf{F}_1 + \delta\mathbf{r}_2 \cdot \mathbf{F}_2 + \delta\mathbf{r}_3 \cdot \mathbf{F}_3 + \delta\mathbf{r}_{A1} \cdot \mathbf{R}_1 = 0 \tag{6.18}$$

$$\text{Body 2 :} \qquad \delta\mathbf{r}_4 \cdot \mathbf{F}_4 + \delta\mathbf{r}_5 \cdot \mathbf{F}_5 + \delta\mathbf{r}_{A2} \cdot \mathbf{R}_2 = 0 \tag{6.19}$$

The two bodies are to remain connected at A, so there is a constraint on the virtual

displacements

$$\delta \mathbf{r}_{A1} = \delta \mathbf{r}_{A2} = \delta \mathbf{r}_A \tag{6.20}$$

Adding the two virtual work expressions together and eliminating the internal force terms because of the Third Law relation between $\mathbf{R}_1$ and $\mathbf{R}_2$ and that between $\delta \mathbf{r}_{A1}$ and $\delta \mathbf{r}_{A1}$ results in

$$\delta \mathbf{r}_1 \cdot \mathbf{F}_1 + \delta \mathbf{r}_2 \cdot \mathbf{F}_2 + \delta \mathbf{r}_3 \cdot \mathbf{F}_3 + \delta \mathbf{r}_4 \cdot \mathbf{F}_4 + \delta \mathbf{r}_5 \cdot \mathbf{F}_5 = 0 \tag{6.21}$$

The Principle of Virtual Work for an Ideal System of Rigid Bodies says that the system will be in equilibrium provided the virtual work of the forces external to the system is zero. Note that the forces $\mathbf{R}_1$ and $\mathbf{R}_2$ are internal to the system and, therefore, are not included in the statement of the Principle of Virtual Work. Similarly, reactions at stationary supports are external forces, but they do no virtual work and, thus, are not required in the application of the Principle of Virtual Work. The fact that these two types of terms are not required is one of the major advantages of the Principle of Virtual Work. This development shows why the statement is limited to ideal systems; if non-zero work could be done at the point of interconnection during a virtual displacement, then other terms would need to be included in the virtual work expression. A simple example will help to clarify the ideas presented above and to demonstrate their application.

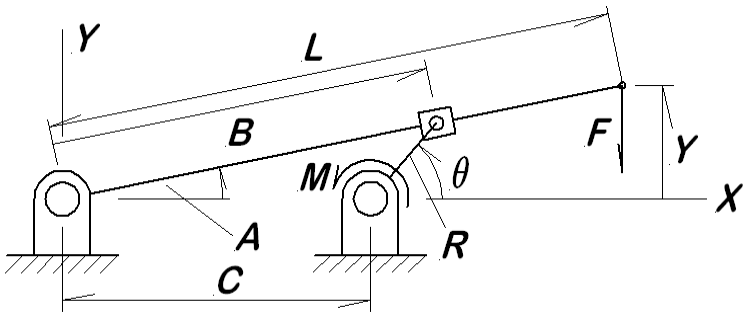

Figure 6.3: Crank-Lever Mechanism

6.2.3.1 Crank-Lever Mechanism

Consider the crank-lever mechanism shown in Figure 6.3. The external loads applied to the system that can do virtual work include the vertical force F and the moment M acting on the crank. The system is in equilibrium under these loads. Determine the relation between F, M, and the angle θ in the equilibrium condition.

According to the Principle of Virtual Work, the equilibrium relation is described by

$$\delta W = M\,\delta\theta - F\,\delta Y = 0 \tag{6.22}$$

Notice that the work of the moment is positive because M and θ are in the same sense. Similarly, the work of the force F has a negative sign because F and the coordinate Y are in opposite senses. This is a single degree of freedom mechanism, and it is convenient to associate that degree of freedom with the angle θ. There must then be a kinematic relation expressing Y in terms of θ. From the analysis done in Chapter 2, the angle A is expressed by

$$\tan A = \frac{R \sin \theta}{C + Rc \cos \theta} \tag{2.4}$$

The coordinate Y is then related to A (and thus indirectly to θ) by

$$Y = L \sin A \tag{6.23}$$

A virtual change in Y is required for the virtual work expression, and this necessitates an expression for the virtual change in A expressed in terms of $\delta\theta$. These are obtained by differentiation:

$$\delta A = \frac{dA}{d\theta}\delta\theta = K_A(\theta)\ \delta\theta = \frac{R}{B}\cos(A-\theta)\ \delta\theta \tag{6.24}$$

from equation (2.10) and

$$\delta Y = \frac{dY}{d\theta}\,\delta\theta = K_Y(\theta)\ \delta\theta = \frac{RL}{B}\cos A\cos(A-\theta)\ \delta\theta \tag{6.25}$$

Using this expression for the virtual displacement δY, the virtual work expression is

$$\delta W = M\,\delta\theta - F\,\frac{RL}{B}\cos A\cos(A-\theta)\ \delta\theta \tag{6.26}$$

Due to the fact that this expression must be zero for equilibrium, and because $\delta\theta$ is arbitrary and not necessarily zero, the coefficient of $\delta\theta$ must be zero, with the following result:

$$M - F\,\frac{RL}{B(\theta)}\cos A(\theta)\cos[A(\theta)-\theta] = 0 \tag{6.27}$$

This last equation involves the variables M, F, A, B, and q; earlier work (Chapter 2) relates both A and B to θ.

One way to present the relation between M, F, and θ in graphical form is to rearrange the equation to a nondimensional form, reading

$$\frac{M}{FL} = \frac{R}{B(\theta)}\cos A(\theta)\cos[A(\theta)-\theta] = f(\theta) \tag{6.28}$$

and then plot the ratio $M/(FL)$ versus θ. A plot of this sort is presented in Figure 6.4 for the parameters $C = 11$ in. and $R = 5$ in. This plot shows that when the crank and the lever are colinear, $\theta = 0$, the maximum moment is required. When the crank angle is $\theta = \pm 2.0426$ radians, the required moment is zero. This occurs because the crank is then normal to the lever. With the positive sign, the load F is supported by compression in the crank with no moment required; this position is not stable, but it is an equilibrium configuration. If the negative sign is taken, the load F is supported by tension in the crank, and the result is a stable equilibrium position.

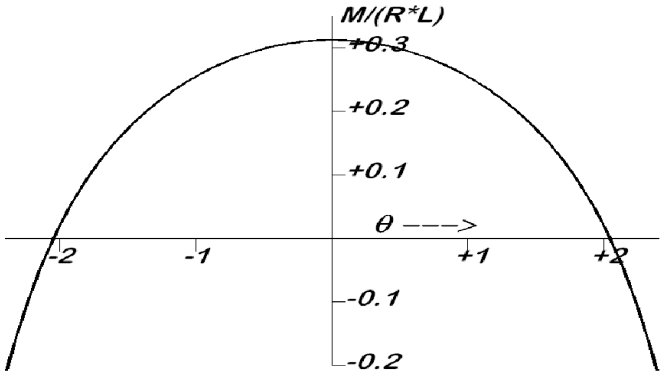

Figure 6.4: Moment to Load Ratio for Crank-Lever Mechanism

6.2.4 Principle of Virtual Work with Multiple Degrees of Freedom

In the preceding example, the virtual angular displacement, $\delta\theta$, was eventually displayed as one factor of a product that must be zero. The argument made was that $\delta\theta$ is arbitrary, and that there could be no assurance that it is zero. On this basis, it was then concluded that the coefficient of $\delta\theta$ must be zero because the relation was to hold for any $\delta\theta$. This simple reasoning was possible because of the fact that the system had only one degree of freedom. However, note that even this argument could not be made until δA and δY were expressed in terms of a virtual change in the single generalized coordinate, θ. In the event that the system has multiple degrees of freedom, a more involved argument is required.

Consider next a system with N_1 degrees of freedom associated with the generalized coordinates q_1, q_2, ..., q_{N_1}. The position vectors for the load application points can be

expressed as

$$\begin{aligned} \mathbf{r}_1 &= \mathbf{r}_1\left(q_1, q_2, \ldots q_{N_1}\right) \\ \mathbf{r}_2 &= \mathbf{r}_2\left(q_1, q_2, \ldots q_{N_1}\right) \\ &\vdots \end{aligned} \tag{6.29}$$

For this system, the virtual work of the external loads is

$$\begin{aligned} \delta W &= \mathbf{F}_1 \cdot \delta\mathbf{r}_1 + \mathbf{F}_2 \cdot \delta\mathbf{r}_2 + \cdots \\ &= \mathbf{F}_1 \cdot \left(\frac{\partial \mathbf{r}_1}{\partial q_1}\delta q_1 + \frac{\partial \mathbf{r}_1}{\partial q_2}\delta q_2 + \cdots \frac{\partial \mathbf{r}_1}{\partial q_{N_1}}\delta q_{N_1}\right) \\ &\quad + \mathbf{F}_2 \cdot \left(\frac{\partial \mathbf{r}_2}{\partial q_1}\delta q_1 + \frac{\partial \mathbf{r}_2}{\partial q_2}\delta q_2 + \cdots \frac{\partial \mathbf{r}_2}{\partial q_{N_1}}\delta q_{N_1}\right) \\ &\quad \vdots \\ &\quad + \mathbf{F}_{N_1} \cdot \left(\frac{\partial \mathbf{r}_{N_1}}{\partial q_1}\delta q_1 + \frac{\partial \mathbf{r}_{N_1}}{\partial q_2}\delta q_2 + \cdots \frac{\partial \mathbf{r}_{N_1}}{\partial q_{N_1}}\delta q_{N_1}\right) \\ &= \delta q_1 \left(\mathbf{F}_1 \cdot \frac{\partial \mathbf{r}_1}{\partial q_1} + \mathbf{F}_2 \cdot \frac{\partial \mathbf{r}_2}{\partial q_1} + \cdots + \mathbf{F}_{N_1} \cdot \frac{\partial \mathbf{r}_{N_1}}{\partial q_1}\right) \\ &\quad + \delta q_2 \left(\mathbf{F}_1 \cdot \frac{\partial \mathbf{r}_1}{\partial q_2} + \mathbf{F}_2 \cdot \frac{\partial \mathbf{r}_2}{\partial q_2} + \cdots + \mathbf{F}_{N_1} \cdot \frac{\partial \mathbf{r}_{N_1}}{\partial q_2}\right) \\ &\quad \vdots \\ &\quad + \delta q_{N_1} \left(\mathbf{F}_1 \cdot \frac{\partial \mathbf{r}_1}{\partial q_{N_1}} + \mathbf{F}_2 \cdot \frac{\partial \mathbf{r}_2}{\partial q_{N_1}} + \cdots + \mathbf{F}_{N_1} \cdot \frac{\partial \mathbf{r}_{N_1}}{\partial q_{N_1}}\right) \end{aligned} \tag{6.30}$$

The Principle of Virtual Work states that the virtual work expression shown will be zero if the system of forces is in equilibrium, but this is only a single, scalar equation. Where will the necessary N_1 simultaneous equations come from? The answer to this question comes from the definition of a generalized coordinate as discussed in Section 1.2. One of the characteristics of a generalized coordinate discussed there was that generalized coordinates are independent. Each generalized coordinate can be varied independently, having no effect on the others. In the current situation, this means that each of the δq_i is independent of all the others. The last form for the virtual work above shows that it is as a sum of terms, each involving the virtual change in a generalized coordinate multiplied by a coefficient. Assume first that these coefficients are not all zero. The Principle of Virtual Work states that this sum is zero for arbitrary δq_i. This means that the virtual work sum is zero, *no matter how the δq_i are chosen*. A non-zero δq_1, multiplied by a non-zero coefficient, makes a non-zero contribution to the sum. Without much difficulty, it should be possible to choose δq_2 such that the second term will also make a non-zero contribution of the same sign as that of the first term, and so on. The eventual consequence of this reasoning is that the virtual work sum can be made non-zero by some choices of the variations. The only way to assure that the sum must be zero,

no matter what choices are made for the δq_i, is for each of the coefficients to be zero. There are N_i coefficients, so this provides the required N_i equilibrium equations. In the abstract, this appears quite awkward, but in practice it is quite simple to apply. An example will demonstrate the application.

6.2.4.1 Summing Linkage

One very simple multidegree of freedom mechanism is the summing linkage. Figure 6.5 shows the summing linkage in equilibrium under the applied loads P_1, P_2, and F. Determine the values of P_1 and P_2 in terms of F.

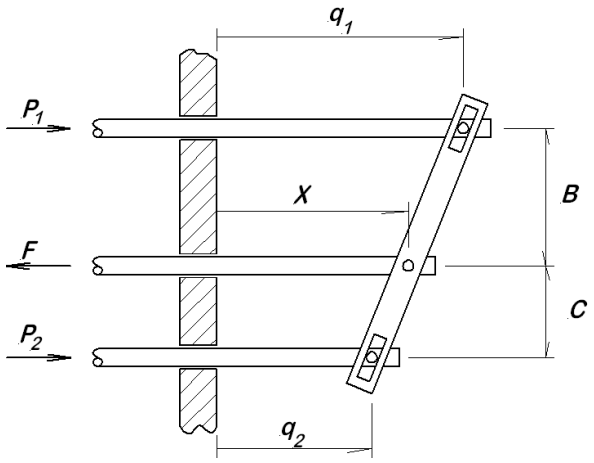

Figure 6.5: Summing Link in Equilibrium Under Forces P_1, P_2, and F

For this mechanism, there are two degrees of freedom, most easily associated with the coordinates q_1 and q_2. A very simple kinematic analysis shows that the output motion, X, is expressed as

$$X = \frac{Cq_1 + Bq_2}{B + C} \tag{6.31}$$

Applied to this situation, the Principle of Virtual Work states

$$\delta W = P_1\,\delta q_1 + P_2\,\delta q_2 - F\,\delta X = 0 \tag{6.32}$$

and the virtual displacement δX is

$$\delta X = \frac{C}{B + C}\delta q_1 + \frac{B}{B + C}\delta q_2 \tag{6.33}$$

The virtual work of the external forces, expressed in terms of virtual displacements in the generalized coordinates, is

$$\delta W = \left(P_1 - F\frac{C}{B+C} \right) \delta q_1 + \left(P_2 - F\frac{B}{B+C} \right) \delta q_2 = 0 \tag{6.34}$$

According to the preceding argument, the coefficients of δq_1 and δq_2 must each be zero. From this the forces P_1 and P_2 are

$$P_1 = F\frac{C}{B+C} \tag{6.35}$$

$$P_2 = F\frac{B}{B+C} \tag{6.36}$$

These results are readily verified by using moments about the top and bottom pin joints. As is observed in that verification, using moment sums for this simple problem is probably a quicker way to the result. The purpose here, however, is to demonstrate the method – a method of great power in more complicated problems.

6.2.5 Potential Energy Representation of Conservative Forces

In extending the Principle of Virtual Work to systems of rigid bodies, care was taken to exclude systems that could absorb energy in a virtual displacement. It is now useful to relax that restriction, allowing the inclusion of interconnections in which there is fully recoverable energy storage. Therefore, conservative energy storage will now be included, but nonconservative energy absorption remains excluded. Two obvious examples of effects to be included are springs (both linear and nonlinear) and gravitational forces.

Consider a system of several rigid bodies subject to external loads F_i (which are inherently nonconservative) and to conservative, working internal loads f_j. Any internal loads that do not move during the virtual displacement are called *nonworking internal loads*. An example of such a nonworking load is the reaction at a fixed support; it cannot move and, thus, does no work. When the virtual work of the forces acting on each body are summed, the virtual work of this force system is

$$\delta W = \mathbf{F}_1 \cdot \delta\mathbf{r}_1 + \mathbf{F}_2 \cdot \delta\mathbf{r}_2 + \cdots + \mathbf{f}_1 \cdot \delta\mathbf{R}_1 + \mathbf{f}_2 \cdot \delta\mathbf{R}_2 + \cdots \tag{6.37}$$

where $\mathbf{r}_i$ are the position vectors for the points of application of the external loads and $\mathbf{R}_j$ are the position vectors for the points of application of the working, conservative internal forces. For every conservative force there exists a potential function, V, such that

$$\mathbf{f}_j = -\boldsymbol{\nabla} V_j \tag{6.38}$$

where the del operator (∇), denoted by the inverted capital Greek delta, indicates the following operation *in rectangular Cartesian coordinates*:

$$\boldsymbol{\nabla} = \mathbf{i}\frac{\partial}{\partial x} + \mathbf{j}\frac{\partial}{\partial y} + \mathbf{k}\frac{\partial}{\partial z} \tag{6.39}$$

Note that this is just an operator; it requires an operand on which to operate. Note also that the form given for the del operator here is specifically for rectangular Cartesian coordinates; in other coordinate systems the del operator takes different forms. In terms of the potential function, the virtual work of one of the conservative, working internal forces is

$$\begin{aligned} \delta W_j &= (-\boldsymbol{\nabla} V_j) \cdot \delta \mathbf{R}_j \\ &= -\left(\mathbf{i}\frac{\partial V_j}{\partial x} + \mathbf{j}\frac{\partial V_j}{\partial y} + \mathbf{k}\frac{\partial V_j}{\partial z}\right) \cdot (\mathbf{i}\,\delta x + \mathbf{j}\,\delta y + \mathbf{k}\,\delta z) \\ &= -\delta V_j \end{aligned} \tag{6.40}$$

When the virtual work sum is rewritten, there are two types of terms to be included

$$\delta W = \sum_i \mathbf{F}_i \cdot \delta \mathbf{r}_i - \sum_j \delta V_j \tag{6.41}$$

where the first sum is the virtual work of the external loads and the second sum is the contribution from the potential energy changes. The Principle of Virtual Work, modified to allow for the inclusion of some forces in terms of potential functions, requires that the preceding expression vanish for equilibrium. The potential functions just described are nothing other than the familiar potential energy functions. Thus, if a gravitational force is to be represented, with z positive along the upward vertical, the potential function is

$$V = Mgz \tag{6.42}$$

where M is the mass of the body and g is the gravitational constant. The variation of this potential is

$$\delta V = Mg\,\delta Z \tag{6.43}$$

The case of a spring is slightly more complicated. Consider an unstretched spring oriented along the X-axis with free length S_o. The spring constant is denoted K. In the equilibrium configuration, the ends of the spring are at X_1 and x_X, respectively, and there is a tensile force F in the spring:

$$F = K(X_2 - X_1 - S_o) \tag{6.44}$$

Now consider small displacements of both ends from their equilibrium positions, δX_1 and δX_2, stretching the spring in the process. Because these displacements are small, the force in the spring is approximately constant during the displacements. The **work done on the rigid bodies** during these displacements consists of the sum of the work done at the ends:

$$\begin{aligned} \delta W &= -F\,\delta X_2 + F\delta X_1 \\ &= -K(X_2 - X_1 - S_o)\,(\delta X_2 - \delta X_1) \\ &= -\delta\left[\frac{1}{2}K(X_2 - X_1 - S_o)^2\right] \\ &= -\delta\left[\frac{1}{2}K\,(\text{deformation})^2\right] \end{aligned} \tag{6.45}$$

It is evident that the negative variation of the potential energy function for the spring provides the correct terms for the virtual work done on the rigid bodies. These ideas are illustrated in the following example problem.

6.2.5.1 Spring Supported Lever

The spring supported lever shown in Figure 6.6 supports the weight $W = 15$ lb. The spring is anchored at a distance$3C = 42$ in. above the pivot point, and the spring is attached to the lever at a distance $3C$. The spring rate is $K = 50$ lb/in., and the free length of the spring is $3C$. The full length of the lever is $4C = 56$ in., and the lever is weightless. There is an external moment $M = 35$ in-lb acting to help support W. What is the equilibrium value for the angle ϕ? What is the tension in the spring at equilibrium?

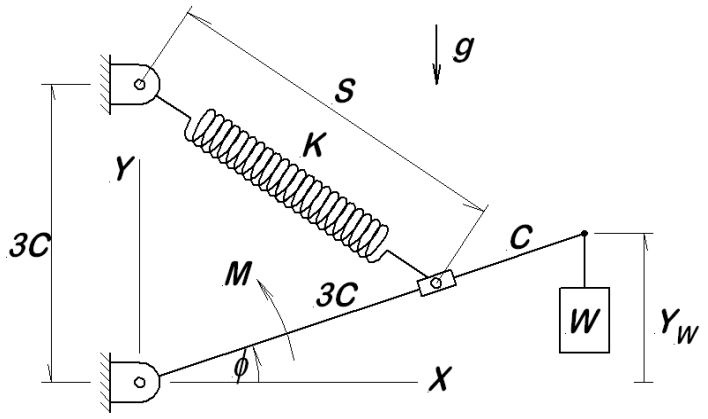

Figure 6.6: Spring Supported Lever Holding Weight W

First consider the kinematic aspects of the problem. Let Y_W denote the elevation of the end of the rod:

$$Y_W = 4C\sin\phi \tag{6.46}$$
$$\delta Y_W = \delta\phi\, 4C\cos\phi \tag{6.47}$$

The length of the spring is S, while the free length is denoted S_o.

$$\begin{aligned} S^2 &= (3C - 3C\sin\phi)^2 + (3C\cos\phi)^2 \\ &= 2\,(3C)^2\,(1-\sin\phi) \end{aligned} \tag{6.48}$$
$$\delta S = -\frac{9C^2\cos\phi}{S}\delta\phi \tag{6.49}$$

With these geometric relations established, the potential energy terms are

$$\begin{aligned} V_W &= W\cdot Y_W \\ \delta V_W &= W\,\delta Y_W = 4CW\cos\phi\,\delta\phi \end{aligned} \tag{6.50}$$

$$\begin{aligned} V_S &= \frac{1}{2}K\,(S-S_o)^2 \\ \delta V_S &= K\,(S-S_o)\;\delta S \\ &= -K\frac{(S-S_o)}{S}9C^2\cos\phi\,\delta\phi \end{aligned} \tag{6.51}$$

The condition for equilibrium, expressed in terms of virtual work is

$$\delta W = M\,\delta\phi - \delta V_W - \delta V_S = 0 \tag{6.52}$$

After substitutions and minor rearrangement of terms, the equilibrium equation to be solved for ϕ is

$$M - 4CW\cos\phi + 9C^2K\cos\phi\left[1 - \frac{1}{(2-2\sin\phi)^{1/2}}\right] = 0 \tag{6.53}$$

Using the parameter values just given, an iterative solution gives $\phi = 0.51302$ radians. With this known, it is relatively straightforward to determine the equilibrium length of the spring, S, and then the spring tension, $T_s = K(S - So) = 19.2178$ lb. Note that both gravitational and spring potential energy are demonstrated in this problem. Further examples of the use of potential energy terms are shown in the next section.

6.3 Applications of Virtual Work

In this section, two more applications of the Principle of Virtual Work are given. For each case, it is well to consider the alternative approach, specifically the application of force and moment sums to the same problems. The power of the Principle of Virtual Work becomes more evident with the increasing complexity of the application.

6.3.1 Phase-Shifting Device

The mechanism shown in Figure 6.7 is a chain or timing belt system with provisions for adjusting the phase relation between the driving motion, q_1 and the output motion, A. The phase adjustment is controlled by the second primary variable, q_2. For this example, consider the system to be in equilibrium under the the effects of the external force P_2 (holding the control block stationary), the driving moment M_1, and the load moment M_A. The problem is to determine the relations between M_1, M_A, and P_2. Note that the chain or belt may be moving or not, but in either case the system speed is considered constant.

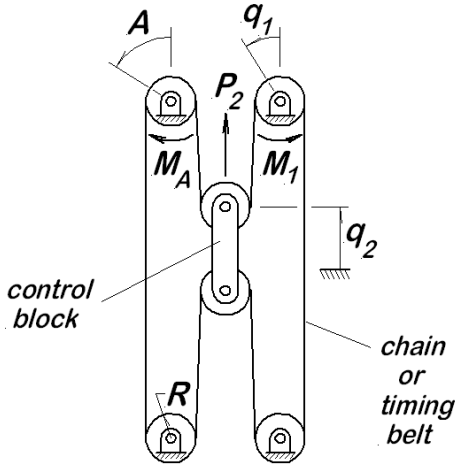

Figure 6.7: Phase Shifting Device in Equilibrium

The kinematic relation between q_1, q_2, and A is

$$A = q_1 + (2/R)\, q_2 \tag{6.54}$$

which gives the following relation among the system virtual displacements

$$\delta A = \delta q_1 + \frac{2}{R}\delta q_2 \tag{6.55}$$

where R is the radius of each of the four corner sprockets with fixed centers. The condition for equilibrium is that the virtual work vanish:

$$\begin{aligned}\delta W &= M_1\,\delta q_1 + P_2\,\delta q_2 - M_A\,\delta A \\ &= M_1\,\delta q_1 + P_2\,\delta q_2 - M_A\left(\delta q_1 + \frac{2}{R}\delta q_2\right) \\ &= \delta q_1\,(M_1 - M_A) + \delta q_2\left(P_2 - \frac{2}{R}M_A\right) \\ &= 0 \end{aligned} \tag{6.56}$$

By virtue of the fact that q_1 and q_2 are generalized coordinates, and thus are mutually independent, the coefficients for each virtual displacement must be zero to assure the vanishing of the virtual work for all possible virtual displacements. From those two statements come the final relations:

$$M_1 = M_A \tag{6.57}$$

$$P_2 = \frac{2}{R}M_A \tag{6.58}$$

This shows that, without any losses, the required driving moment is exactly equal to the load moment, exactly as expected.

6.3.2 L-shaped Bracket

> Consider a weightless L-shaped bracket with leg lengths B and C as shown in Figure 6.8(a). This bracket is constrained to roll without slipping on a stationary cylinder of radius R under the influence of a spring and an external force F (Figure 6.8(b)). When the legs of the bracket are parallel to the $X-$ and $Y-$axes (shown in broken line), the bracket extends a distance a below the $X-$axis, and the spring force is zero. The lower end of the spring is anchored at the point (X_o, Y_o), the spring rate is K, and the free length is S_o. As the horizontal force F is increased, the point of contact between the bracket and the stationary cylinder moves through the angle θ. Determine the equilibrium value for angle θ and the corresponding tension in the spring.

This problem involves a single degree of freedom that is readily associated with the angle θ. It is useful to define body coordinates U and V along the legs of the bracket. Any point on the bracket can then be located in terms of the body coordinates for that point, (u_p, v_p). From Figure 6.8(b), it is evident that the base coordinates for such a point are given by

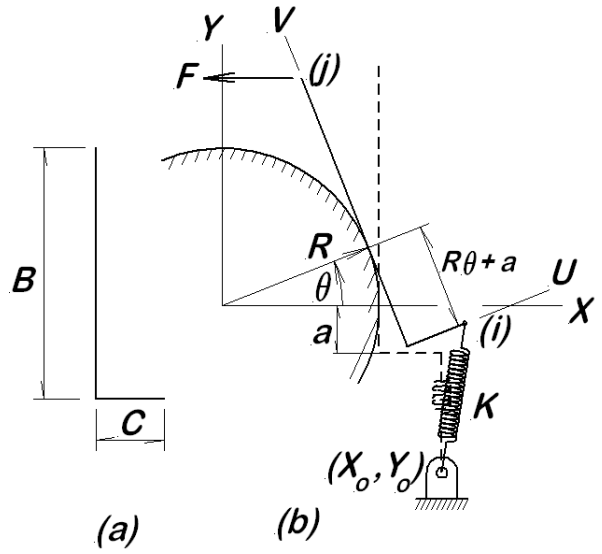

Figure 6.8: L-shaped Bracket in Equilibrium Under the External Force F and the Spring Action

$$\left\{ \begin{array}{c} X_p \\ Y_p \end{array} \right\} = \left[\begin{array}{cc} \cos\theta & -\sin\theta \\ \sin\theta & \cos\theta \end{array} \right] \left\{ \begin{array}{c} R + u_p \\ v_p - a - R\theta \end{array} \right\} \tag{6.59}$$

$$\begin{aligned} \left\{ \begin{array}{c} \delta X_p \\ \delta Y_p \end{array} \right\} &= \delta\theta \left\{ \begin{array}{c} dX_p/d\theta \\ dY_p/d\theta \end{array} \right\} \\ &= \delta\theta \left\{ \begin{array}{c} K_{px}(\theta) \\ K_{py}(\theta) \end{array} \right\} \\ &= \delta\theta \left\{ \begin{array}{c} -u_p \sin\theta + (a + R\theta - v_p)\cos\theta \\ u_p \cos\theta + (a + R\theta - v_p)\sin\theta \end{array} \right\} \end{aligned} \tag{6.60}$$

Note that the derivatives are, in fact, the velocity coefficients for the particular point with respect to the generalized coordinate θ. Let (i) and (j) denote the points of spring attachment and load application, respectively, as shown in the figure. The virtual work of the applied force will be simply $-F\,\delta X_j = -F K_{X_j} \delta\theta$, so no further analysis is required for this term. For the potential energy of the spring, it is necessary to first express the length of the spring as a function of θ

$$S^2 = (X_i - X_o)^2 + (Y_i - Y_o)^2 \tag{6.61}$$

$$\delta S = \frac{(X_i - X_o)\,K_{X_i} + (Y_i - Y_o)\,K_{Y_i}}{S} \delta\theta \tag{6.62}$$

(Note that is often easier to write S^2 than S; this is because the usual approach is via the Pythagorean Theorem. This leads to the form shown for the derivative, a result that is simple to compute.)

The spring free length value, S_o, was given as part of the problem statement. This implies that $S_o + a = -Y_o$ for the initial geometry. The spring potential energy is V_S

$$\begin{aligned} V_S &= \frac{1}{2} K \left(S - S_o\right)^2 \\ \delta V_S &= K \frac{(S - S_o)}{S} \left[\left(X_i - X_o\right) K_{X_i} + \left(Y_i - Y_o\right) K_{Y_i}\right] \delta\theta \end{aligned} \tag{6.63}$$

The virtual work expression, including the modification to allow for representation of conservative forces through the use of the potential energy, is

$$\begin{aligned} \delta W &= -F\,\delta X_j - \delta V_S \\ &= \left\{ -F K_{X_j} - K \frac{(S - S_o)}{S} \left[\left(X_i - X_o\right) K_{X_i} + \left(Y_i - Y_o\right) K_{Y_i}\right] \right\} \delta\theta \end{aligned} \tag{6.64}$$

Because the virtual displacement $\delta\theta$ is arbitrary, the coefficient must be zero and the equilibrium equation is

$$F K_{X_j} + K \frac{(S - S_o)}{S} \left[\left(X_i - X_o\right) K_{X_i} + \left(Y_i - Y_o\right) K_{Y_i}\right] = 0$$

This equation, along with the expressions for S, X_i,Y_i, K_{X_1}, K_{Y_1}, and K_{X_j} must be solved for the equilibrium value of θ. Because of the complexity of the equations involved, an iterative solution is indicated.

6.3.2.1 Numerical Values

It should be noted that some of the data are interrelated. Specifically, the following relations must be true:

$$R + C = X_o \tag{6.65}$$

$$S_o + a = -Y_o \tag{6.66}$$

For numerical work, take the following values for the system parameters:

$B = 0.3048$ m $\quad C = 0.0762$ m

$R = 0.1270$ m $\quad a = 0.0508$ m

$X_o = 0.2032$ m $\quad Y_o = -0.2032$ m

$S_o = 0.1524$ m

$F = 44.4822$ N $\quad K = 2627.9$ N/m

An iterative solution, based on these parameter values, gives the equilibrium position

$$\theta = 0.3385 \text{ radian} \tag{6.67}$$

With the angular position known, it is a simple matter to evaluate the spring length and from that to determine the spring tension T_S:

$$\Delta S = 0.030865 \text{ m} \tag{6.68}$$

$$T_S = 81.080 \text{ N} \tag{6.69}$$

6.3.3 Spring-Loaded Trammel

The spring loaded trammel was previously introduced in Section 2.3 and the kinematic analysis is developed there. The same system is shown at rest in Figure 6.9. The question of interest here is to find the equilibrium position of the mechanism. Note that the system operates in the vertical plane, so the rest position requires the force developed in the spring to support the weight of the link and the vertical slider.

The trammel consists of a single link with two sliders that move in guides along the $x-$ and $y-$axes, respectively. The system operates in the vertical plane, so that gravity forces are operative, and there is also a spring acting on the horizontal slider. In the initial state, the weight of the system is supported on the deformation of the spring.

The kinematic analysis in Chapter 2 established the following expressions:

$$\begin{aligned} x &= L\cos\theta \\ y &= L\sin\theta \\ K_x &= -L\sin\theta \\ K_y &= L\cos\theta \\ L_x &= -L\cos\theta \\ L_y &= -L\sin\theta \end{aligned} \tag{2.26-2.31}$$

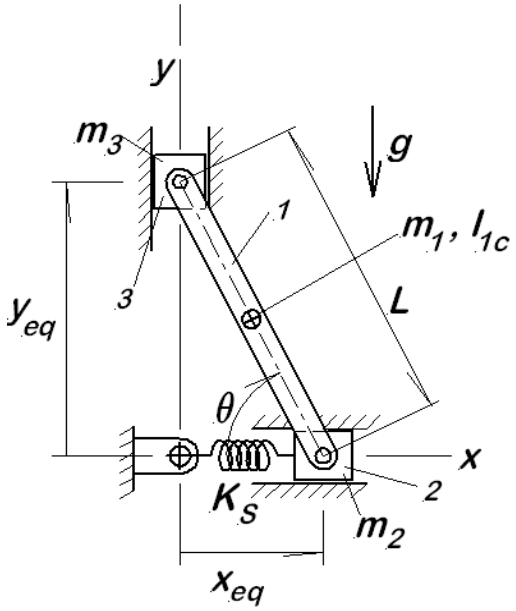

Figure 6.9: Spring Loaded Trammel at Equilibrium Rest

The center of mass of the link is at the middle, so that the center of mass values are simply half of the values shown above.

6.3.3.1 Relations for the Spring

The spring is understood to be a simple, linear spring, such that the force through the spring is proportional to the elongation of the spring. Let $x = x_o$ describe the state of the assembly when the spring is strain free, that is when there is no force in the spring. The free length is a design parameter and thus is assumed to be known. Then the force in the spring is given by

$$F_S = K_S (x - x_o) = K (L \cos\theta - x_o) \tag{6.70}$$

The task at hand is to find the rest value of x_{eq}, that is, the position in which the assembly sits at rest equilibrium. This must be a number different from x_o because there must be some force in the spring in order to support the weight of the assembly at rest.

The external forces acting on the mechanism are (1) gravity and (2) the spring force. Both of these are conservative forces and thus can be represented entirely by the use of potential energy. Application of the Principle of Virtual Work thus begins by writing the

system potential energy function for a typical position:

$$\begin{aligned} V &= m_1 g y_c + m_3 g y + \frac{1}{2} K_S \left(x - x_o\right)^2 \\ &= \left(m_3 + \frac{1}{2} m_1\right) g L \sin\theta + \frac{1}{2} K_S \left(L\cos\theta - x_o\right)^2 \end{aligned} \tag{6.71}$$

where

y_c is the elevation of the link center of mass

y is the elevation of the vertical slider

The virtual work expression is simply the negative of the partial derivative of the potential energy with respect to θ, so that

$$\begin{aligned} \delta W &= -\frac{\partial V}{\partial \theta}\delta\theta \\ &= -\left[\left(m_3 + \frac{1}{2} m_1\right) g L\cos\theta - K_S \left(L\cos\theta - x_o\right)\left(-L\sin\theta\right)\right]\delta\theta \end{aligned} \tag{6.72}$$

Setting the virtual work to zero shows gives the expression for the equilibrium condition, thus

$$\left(m_3 + \frac{1}{2} m_1\right) g L\cos\theta_{eq} - K_S L\sin\theta_{eq}\left(L\cos\theta_{eq} - x_o\right) = 0 \tag{6.73}$$

6.3.3.2 Numerical Values

Consider the specific case where the coupling link, body 1, is a steel bar, with $L = 30$ in., $w_1 = 48.287$ lb, $I_{1c} = 9.3800$ lb–s^2–in. For the $x-$axis slider, $w_2 = 17$ lb, and for the $y-$axis slider, $w_3 = 25$ lb, the spring stiffness is $K_S = 60$ lb/in, and the free length of the spring is $x_o = 12$ inches. Note that the weights of the components are given rather than the masses. Since the masses only appear in the equation in combination with the acceleration of gravity, this requires only that an mg product be replaced with the relevant weight.

The equation above is most easily solved numerically (a closed form solution is unknown). In the range $0 \leq \theta \leq \pi/2$, there are two solutions for the equilibrium equation.

1. **Equilibrium Position #1 – Unstable** – The first solution gives a very small value of $\theta_{eq} \approx 0.04555 = 2.6098^o$. In this position, the link is almost level and the spring is greatly stretched. The spring is stretched almost 18 inches, and the load

in the spring is over 1000 lb. It should be intuitively evident that this is an unstable equilibrium position. For most purposes, unstable equilibrium positions are of no further interest, and this one is disregarded for all that follows.

2. **Equilibrium Position #2 – Stable** – The second equilibrium solution is stable at $\theta_{eq} = 1.1458$ rad[1] $= 65.647^o$. For this position, the horizontal slider position is $x_{eq} = 12.371$ in., and the spring force is $F_{S-eq} = 22.244$ lb. In this position, the spring is stretched only a little less that 0.4 in., and the spring force is quite moderate.

6.4 Static Stability

In the previous section, the word *stable* has been used, relying on the general background of the reader for its understanding. Stability is an important concept, and it merits further discussion here.

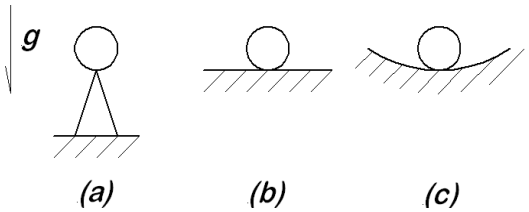

Figure 6.10: Concept of Static Stability

Figure 6.10 shows three common examples used to illustrate the concept of static stability, each case involving a ball at rest. In the first case, (a), the ball is balanced on the point of a pencil. In the second case, (b), the ball is at rest on a flat, level surface, while in the third case, (c), the ball rests in a shallow dish. In each case, the weight of the ball is supported, so the ball is in vertical equilibrium.

All readers will know intuitively that the ball on the pencil point will not remain there, but rather it will fall off. It is *unstable*, because even the tiniest disturbance, such as a breath of air, causes it to depart grossly from its initial position. Considering the other extreme, Figure 6.10 (c), everyone will agree that the ball will remain in the shallow dish indefinitely. While it is certainly true that the ball can be removed from the dish by the applications of sufficient force, it is certainly true that small disturbances will not cause it to significantly depart from its initial position. If slightly disturbed, it will move a short distance, but then it will return to its initial position. The ball in the dish is *stable.*

[1]Where it is important to show that the Principle of Virtual Work is satisfied numerically, it may prove necessary to use the more exact value $\theta_{eq} = 1.145755765$ radians.

Finally, look at the center figure, Figure 6.10 (b), where the ball rests on the flat, level surface. If it is slightly disturbed, it moves a short distance and then stops. But it does not return to its initial location. The ball on the level surface is said to be *neutrally stable.*

The key question in considering static stability is this: How does the system respond to a small displacement from the initial configuration?

- If the system returns to its initial configuration, it is stable.
- If the system diverges from its initial configuration, it is unstable.
- If the system moves to a nearby equilibrium configuration, it is neutrally stable.

6.5 Another Look at Virtual Work

Earlier in this chapter, vector notation involving dot products was used extensively, even though the resulting virtual work expressions are always scalars. It is useful to reexamine the principle of virtual work using matrix notation, as it offers a different perspective on that principle and on the meaning of the generalized force. Consider a force $\mathbf{F}_i$ acting at the point $\mathbf{r}_i$ on a rigid body, where $\mathbf{r}_i$ is a function of the generalized coordinates. The virtual work of this force is then

$$\begin{aligned} \delta W &= \mathbf{F}_i \cdot \delta \mathbf{r}_i \\ &= (\mathbf{i}F_{ix} + \mathbf{j}F_{iy}) \cdot (\mathbf{i}\delta X_i + \mathbf{j}\delta Y_i) \\ &= F_{ix}\delta X_i + F_{iy}\delta Y_i \end{aligned} \tag{6.74}$$

The components of the virtual displacement are

$$\delta X_i = \sum_j \frac{\partial X_i}{\partial q_j}\delta q_j \tag{6.75}$$

$$\delta Y_i = \sum_j \frac{\partial Y_i}{\partial q_j}\delta q_j \tag{6.76}$$

These sums are readily indicated by the matrix products

$$\begin{Bmatrix} \delta X_i \\ \delta Y_i \end{Bmatrix} = \begin{bmatrix} K_{iX1} & K_{iX2} & K_{iX3} & \cdots \\ K_{iY1} & K_{iY2} & K_{iY3} & \cdots \end{bmatrix} \begin{Bmatrix} \delta q_1 \\ \delta q_2 \\ \vdots \end{Bmatrix} \tag{6.77}$$

where the Ks are the velocity coefficients for the particular point. For several forces applied at several different points, the notation is readily expanded:

$$\begin{Bmatrix} \delta X_1 \\ \delta Y_1 \\ \delta X_2 \\ \delta Y_2 \\ \vdots \end{Bmatrix} = \begin{bmatrix} K_{1X1} & K_{1X2} & K_{1X3} & \cdots \\ K_{1Y1} & K_{1Y2} & K_{1Y3} & \cdots \\ K_{2X1} & K_{2X2} & K_{2X3} & \cdots \\ K_{2Y1} & K_{2Y2} & K_{2Y3} & \cdots \\ \vdots & \vdots & \vdots & \ddots \end{bmatrix} \begin{Bmatrix} \delta q_1 \\ \delta q_2 \\ \delta q_3 \\ \vdots \end{Bmatrix} \tag{6.78}$$

For the virtual work of these several forces, matrix notation is again useful to represent the necessary summations:

$$\begin{aligned} \delta W &= (F_{1X}, F_{1Y}, F_{2X}, \cdots) \begin{Bmatrix} \delta X_1 \\ \delta Y_1 \\ \delta X_2 \\ \vdots \end{Bmatrix} \\ &= (F_{1X}, F_{1Y}, F_{2X}, \cdots) \begin{bmatrix} K_{1X1} & K_{1X2} & K_{1X3} & \cdots \\ K_{1Y1} & K_{1Y2} & K_{1Y3} & \cdots \\ K_{2X1} & K_{2X2} & K_{2X3} & \cdots \\ K_{2Y1} & K_{2Y2} & K_{2Y3} & \cdots \\ \vdots & \vdots & \vdots & \ddots \end{bmatrix} \begin{Bmatrix} \delta q_1 \\ \delta q_2 \\ \delta q_3 \\ \vdots \end{Bmatrix} \\ &= (Q_1, Q_2, Q_3, \ldots) \begin{Bmatrix} \delta q_1 \\ \delta q_2 \\ \delta q_3 \\ \vdots \end{Bmatrix} \end{aligned} \tag{6.79}$$

where

$$\begin{Bmatrix} Q_1 \\ Q_2 \\ Q_3 \\ \vdots \end{Bmatrix} = \begin{bmatrix} K_{1X1} & K_{1X2} & K_{1X3} & \cdots \\ K_{1Y1} & K_{1Y2} & K_{1Y3} & \cdots \\ K_{2X1} & K_{2X2} & K_{2X3} & \cdots \\ K_{2Y1} & K_{2Y2} & K_{2Y3} & \cdots \\ \vdots & \vdots & \vdots & \ddots \end{bmatrix}^T \begin{Bmatrix} F_{1X} \\ F_{1Y} \\ F_{2X} \\ \vdots \end{Bmatrix} \tag{6.80}$$

This last product defines the generalized forces associated with each of the generalized coordinates. The usual terminology is to speak of the generalized force *conjugate* to a particular generalized coordinate, because neither the generalized force nor the generalized coordinate has a direction in the vectorial sense. With this definition, the virtual work is written as $\{Q\}^T \{\delta q\}$. Because the generalized coordinates are independent and their variations are completely arbitrary, the vanishing of the virtual work requires the vanishing of each of the generalized forces. This is directly parallel to Newton's First Law, but it is a more general statement. It does, however, help to focus attention on the generalized forces as the cause of equilibrium or, in the dynamic situation, as the cause of nonequilibrium.

Velocity coefficients play a very important role in the definition of the generalized force. For a large, complicated problem, it may be very useful to evaluate the generalized forces using the matrix product as indicated, while for less complex problems, a less formal approach may be useful. In either event, the expression for the generalized force should be a sum of terms, with each term the product of a velocity coefficient with an actual force or moment.

6.6 Conclusion

The Principle of Virtual Work is a very powerful tool that has been frequently slighted in recent years. This approach makes possible omitting all internal forces and nonworking external constraint forces in the problem formulation, which is a great advantage in the area of machinery statics. The generalized coordinate and velocity coefficient concepts are employed again in this chapter, as they will be in Chapters 7 and 8. The velocity coefficient concept facilitates the application of the Principle of Virtual Work, because it neatly connects the virtual displacement at the point of application of a force to the virtual changes in the generalized coordinates. The idea of generalized force follows naturally from the expression of virtual work in terms of virtual changes in the generalized coordinates.

References

[1] Beer, F. P. and Johnston, E. R., *Vector Mechanics for Engineers, Statics and Dynamics*, 4th ed. New York, McGraw-Hill, 1984, Ch. 10.

[2] Meriam, J. L., *Engineering Mechanics—Statics and Dynamics*, SI Version. New York, John Wiley, 1980, Ch. 7.

[3] Timoshenko, S., and Young, D. H., *Engineering Mechanics*, 4th ed. New York, McGraw-Hill, 1956, Ch. 5.

Problems

6-1 The figure shows a pulley and cable system supporting two blocks of equal weight. The system is assumed to be without friction at any point. All the dimensions, weights, mass moments of inertia, are known. The cable has mass per unit length m (kg/m). It should be obvious that the system is in equilibrium in the configuration shown. Consider a small downward displacement of the block on the right.

(a) Is the system stable?

(b) What is the critical parameter?

(c) What common assumption would change the system stability if it could be implemented?

(d) With that assumption, what is the system stability?

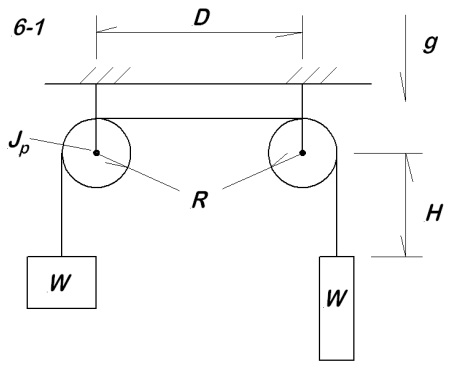

Figure 6.11: System in Equilibrium

6-2 The figure shows a top view of a mechanism called *Raphson's Slide*. It is most often used to control the rudder on large, ocean-going ships. In such vessels, the rudder post is a very large shaft passing vertically down through the ship and supporting the rudder on the lower end. The ship is steered by turning the rudder which requires that the rudder post be rotated. The action of the water, and possible collisions with floating objects, can produce large, sudden torques on the rudder post, making it difficult to maintain the rudder position[2]. Raphson's slide is a mechanism for implementing hydraulic control of the rudder angle. The hydraulic cylinder is double acting which means that it can exert force in either direction, a requirement that may change quite rapidly with each passing wave. When the piston is centered, $q = 0$, the rudder angle $\theta = 0$. The distance C is

[2]Raphson's slide has a structural advantage that is not entirely obvious. Because the hydraulic cylinder is stationary, it can be supported over a relatively large area. Large ships are built somewhat like boxes, and while very strong when a load is distributed over the whole structure, they are not designed to take large point loads, such as would be the result of a pivoted hydraulic cylinder.

known, as are the effective piston areas A_1 and A_2 and the cylinder pressures P_1 and P_2. The torque T_r is externally applied to the rudder. Take the piston position, q, as the primary variable. Determine the equilibrium value of T_r in terms of the q, C, A_1, A_2, P_1, and P_2.

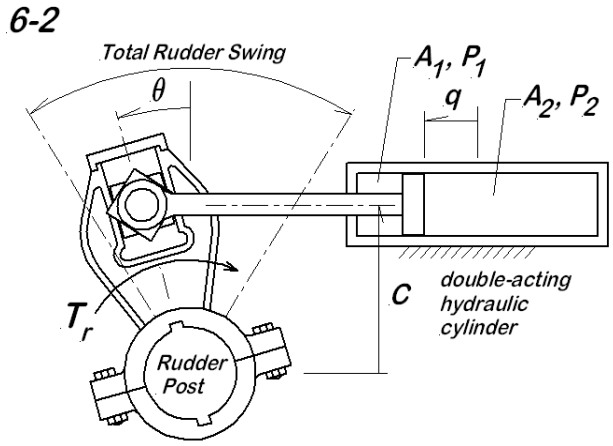

6-3 The mechanism shown is an air-actuated press that moves upward for the working stroke. The crank is defined by the three side lengths s_1, s_2, and s_3. Air is supplied to the cylinder at a constant pressure P_o and the effective piston area is A_o,.The working force reaction on the ram is F. The support location values x_o and y_o are known.

(a) Set up the equations for a complete position analysis (do not solve);

(b) Assuming that the position solutions have been determined, develop the matrix equations required to determine the velocity coefficients (do not solve);

(c) With the positions and velocity coefficients all assumed to be known, express the static working force F in terms of P_o, A_o, q and the various dimensions.

6-4 For the system of problem **6-3**, the piston stroke is such that 350 mm$\leq q \leq$ 475 mm. Use the data below as needed to make calculations and a plot at 101 positions over the length of the piston stroke:

(a) Numerically solve the position loop equations at each position;

(b) Compute the velocity coefficients at each position;

(c) Plot the equilibrium value of the working force F versus q.

$s_1 = 280$ mm $\quad s_2 = 450$ mm $\quad s_3 = 620$ mm

$x_o = 750$ mm $\quad y_o = 508$ mm $\quad L = 800$ mm

$P_o = 4 \cdot 10^5$ Pa $\quad A_o = 0.0025$ m^2

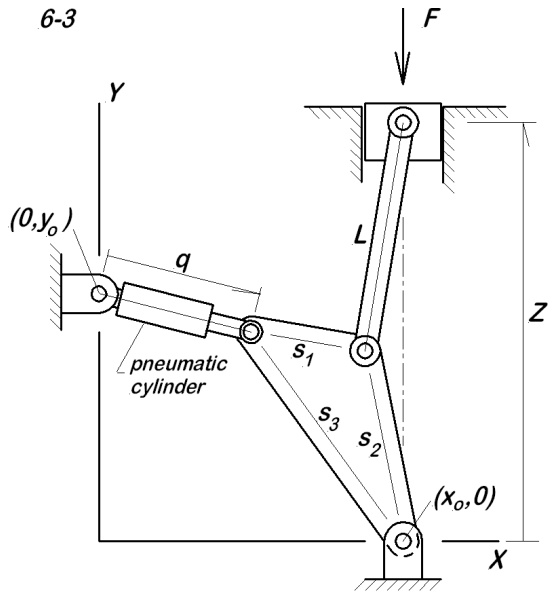

6-5 The figure shows a mobile rocket launch system. In the upper view (a), the rocket is horizontal. In that position, the weight of the rocket and the launch platform are supported by the fixed support post at the left and the pin connection at the right. In the lower view (b), the rocket is shown in an elevated position, ready to launch. It should be evident from the figures that the elevation is accomplished by extending the single acting hydraulic cylinder shown. The angles A and B are to be determined. Let q denote the length of the single acting hydraulic cylinder assembly (pin-to-pin). The known data includes all of the dimensions in the table below, where M is the combined mass of the rocket and support platform. The hydraulic piston diameter is $d_p = 60$ mm.

$c_1 = 1455$ mm $\quad c_2 = 257$ mm $\quad c_3 = 2052$ mm

$c_4 = 955$ mm $\quad c_5 = 3112$ mm $\quad M = 1537$ kg

(a) What is the value of A when the rocket is in the horizontal (down) position?

(b) What is the value of q when the rocket is in the horizontal (down) position?

(c) What value of q is required to make the launch angle, B, equal to 45^o?

(d) What is the minimum pressure required to lift the launch assembly off the forward support?

(e) What is the pressure required in the hydraulic cylinder to raise the rocket and launcher to $B = 45^o$?

(f) Make a plot of launch angle B as a function of the cylinder pressure, P.

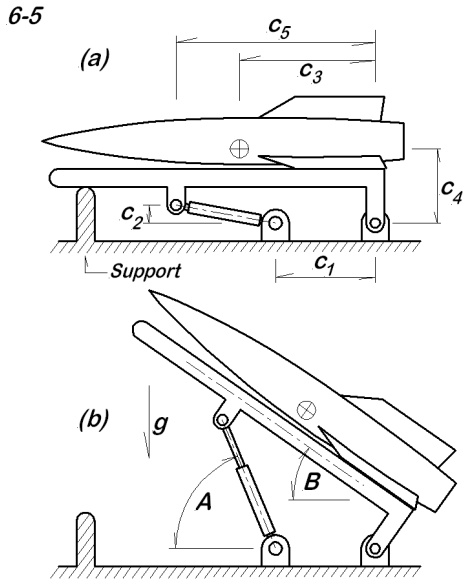

6-6 The two slabs shown are separated by rollers that do not slip at any location. In the upper view, the springs of the system are fully relaxed; in the lower view, the system is under the two applied loads F_1 and F_2. The free length values S_{1o} and S_{2o} are known. The larger rollers (between the two slabs) have radius R, while the smaller rollers (below the lower platform) have radius r.

(a) For given values of F_1 and F_2, determine equilibrium equations solvable for q_1 and q_2 (do not solve);

(b) Using the data below, evaluate q_1 and q_2 numerically for the case $F_1 = 75$ N and $F_2 = 50$ N.

$K_1 = 3500$ N/m $\quad S_{1o} = 100$ mm $\quad R = 188$ mm

$K_2 = 1400$ N/m $\quad S_{2o} = 150$ mm $\quad r = 9$ mm

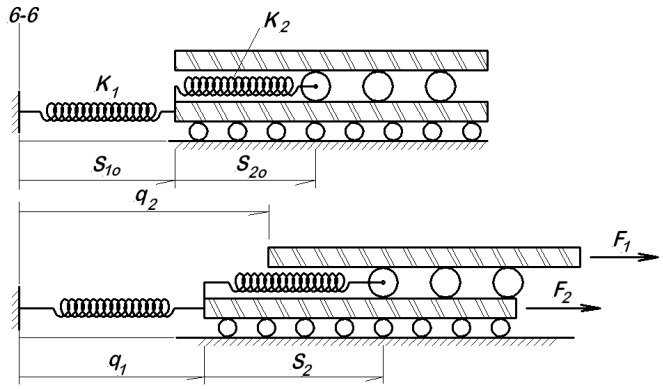

6-7 The system shown here is exactly the same as that in Problem **6-6**, except that the support is now inclined by the angle $\beta = 17^o$. Much of the system data is given in the previous problem and applies here as well. In addition, note that $M_1 = 12$ kg and $M_2 = 9.7$ kg, and finally, there are three large rollers, and the mass of each is $M_R = 0.385$ kg, while the masses of the small rollers can be neglected.

(a) For given values of F_1 and F_2, determine equilibrium equations solvable for q_1 and q_2 (do not solve);

(b) Using the data below, evaluate q_1 and q_2 numerically for the case $F_1 = 75$ N and $F_2 = 50$ N.

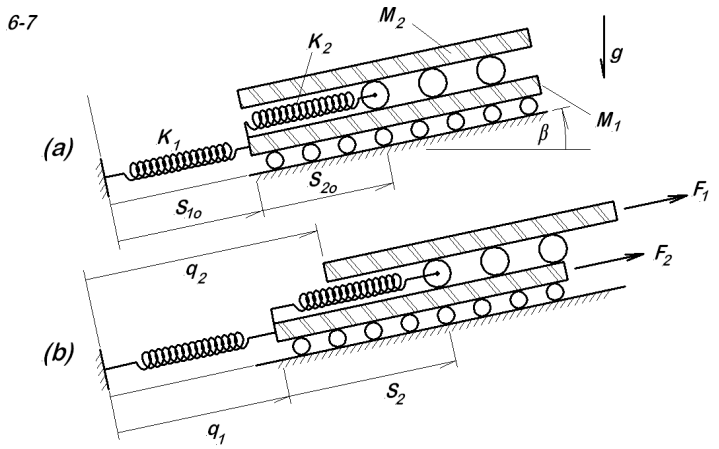

6-8 In the figure, the actual system of interest is the upper structure, (a). As shown in (a), the system is a structure, not a machine or mechanism; it has zero degrees of freedom. Notice that two of the components involve fixed right-angle elements. For an applied load $F = 100$ N, the concern is to calculate the reaction at the wall, R. Because the structure cannot move, it is often difficult to see how the method of virtual work can be applied to calculate R.

It is often useful to relax one of the constraints, thus allowing the system the possibility of motion; this is done in (b). That system has one degree of freedom, and thus the piston at the lower right can move in response to the applied load F. It is then only necessary to fix the value of x at its proper initial value to be fully equivalent to the structure in (a). Use this approach to employ the method of virtual work to calculate the reaction force, R. Take θ as the primary variable to be associated with the one degree of freedom resulting from the relaxed constraint.

$a = 1.00$ m $\quad b = 4.00$ m $\quad c = 3.00$ m

$d = 2.23$ m $\quad e = 1.00$ m

6-9 The system shown is in equilibrium under the applied horizontal force, F as resisted

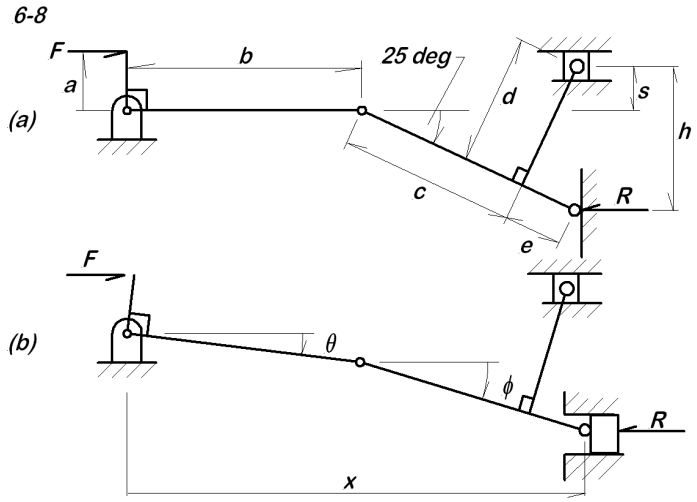

by the torsion spring; there is no gravity to be considered. The spring rate is K, and the spring is relaxed when the angle between the legs (A) is zero.

(a) Establish the equilibrium equation(s) and the kinematic position equations that must be solved to determine the equilibrium configuration ;

(b) Using the data below, determine the equilibrium values for X and θ when $F = 380$ N.

$L_1 = 2425$ mm $\quad L_2 = 1775$ mm

$C = 235$ mm $\quad K_t = 655$ N-m/rad

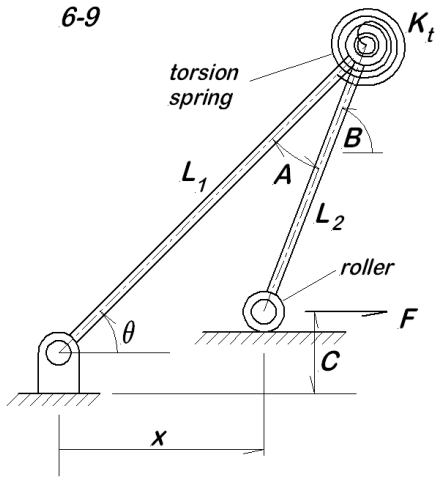

6-10 The system shown has two degrees of freedom described by the generalized coordinates q_1 and q_2. The system is in equilibrium under the loads F_1, F_2, F_x, and F_y. The lengths L_1 and L_2 are known, as are the angle C and the loads F_x and F_y.

(a) Develop any necessary kinematic analysis in symbolic form;

(b) Develop a system of equations solvable for A and B (do not solve);

(c) Develop expressions for any variations that are required for the application of the principle of virtual work;

(d) Using the data values given below, solve numerically for the equilibrium values of A, B, F_1 and F_2.

$q_1 = 3100$ mm $\quad q_2 = 2200$ mm $\quad F_x = 100$ N $\quad F_y = 50$ N

$L_1 = 3100$ mm $\quad L_2 = 3200$ mm $\quad C = 53^o$

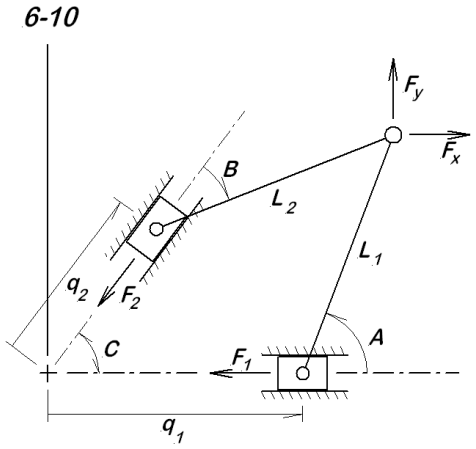

6-11 The system shown is in equilibrium under the force F and the applied torque T. The spring rate is K, and the free length of the spring is such that it is relaxed when $y = \theta = 0$. All of the dimensional values (A, C, D, E, R) are known.

(a) Set up all of the equations required for a complete position analysis for assigned values of y and θ;

(b) Develop expressions for all variations required for the application of the principle of virtual work;

(c) Use the principle of virtual work to write equations solvable for the position variables for assigned values of F and T (do not solve).

6-12 The spring-lever system is in equilibrium under the action of the force F; there is no gravity to consider in this problem. The dimensions A, B, C and D, and the spring rate K are all known. The free length of the spring is L_o.

(a) Use loop equations to determine the no-load value for θ;

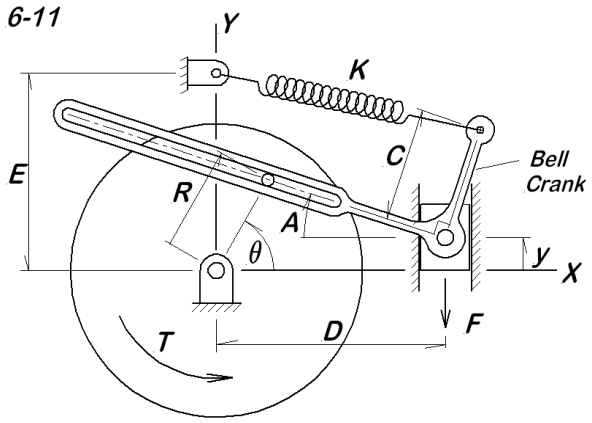

(b) Consider the load to slowly increase from zero to $5 \cdot 10^6$ N. As the load increases, the angle θ will slowly increase from the no-load value. What value does the angle θ approach asymptotically?

(c) Plot the angle θ as a function of the load F over the range $0 \leq F \leq 5 \cdot 10^6$ N.

(d) As F and θ increases beyond $F = 2 \cdot 10^6$ N,

(1) What is happening to the load in the spring?

(2) What is happening to the load in the lever?

$A = 151$ mm $\quad C = 250$ mm $\quad D = 50$ mm

$K = 14000 \cdot 10^3$ N/m $\quad L_o = 286$ mm $\quad R = 459$ mm

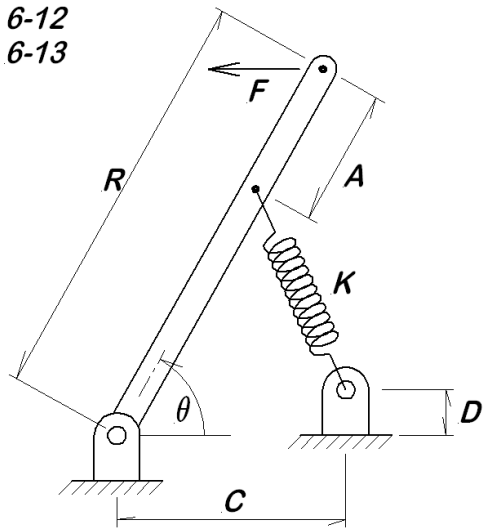

6-13 Return to the geometry of Problem **6-12** and consider particularly the effect of reducing the height of the spring anchor, the distance D.

(a) Make plots of the equilibrium angle θ as a function of the applied force F over the same range used previously for $D = 30$, 10, 1 and 0 mm.

(b) For all cases, the curves appear to cross each other near $F = 1 \cdot 10^6$ N. Describe in words the significance of this apparent crossing.

(c) As D is reduced, the curves move toward a "shoulder," that eventually becomes a sharp corner when $D = 0$. Describe in words what happens to the internal loads at that corner and beyond.

6-14 Consider again the air powered press of problems **2-20** and **2-21**. All system data given previously and previously developed analysis apply to this problem as well. It should be recognized that this system only moves very slowly and is thus always approximately in equilibrium.

(a) Use the method of virtual work to calculate the equilibrium value of the tool force at each position;

(b) Plot the equilibrium value of the tool force as a function of the piston position, $F = F(q)$;

(c) Plot the equilibrium value of the tool force as a function of the tool position, $F = F(S)$.

6-15 Return again to the geometry of Problem **6-12,** this time with a small modification. Now, instead of the fixed length for the lever (R), the lever length is variable since the lower end is slotted, rather than pinned at the support point. The extension of the lever is restrained by a spring with stiffness $K_2 \gg K_1$; this spring can operate in either tension and compression. The effective length of K_2 is $L_2 = R - A$. Note also that the dimension A is redefined, as compared to Problem **6-12**. The effect of the slotted lever is to add another degree of freedom to the problem, so that the preferred generalized variables are R and θ.

(a) Formulate all the necessary kinematic relations for this problem with R and θ as the generalized variables and F as an input value;

(b) Formulate the virtual work relations that describe the static equilibrium position;

(c) Using the data below, solve the equilibrium relations for value of F in the range $0 \leq F \leq 5 \cdot 10^6$ N;

(d) Keeping in mind the idea that $K_2 \gg K_1$, describe in words how this problem a

generalization of the problem previously considered in Problem **6-12**?

(e) What do you notice about the internal loads in the two springs? What happens when the applied load exceeds $2 \cdot 10^6$ N?

$A = 151$ mm	$C = 250$ mm	$D = 50$ mm	
$K_1 = 1.4 \cdot 10^7$ N/m	$L_{1o} = 286$ mm	$K_2 = K_1 \cdot 10^4$ N/m	$L_{2o} = 308$ mm

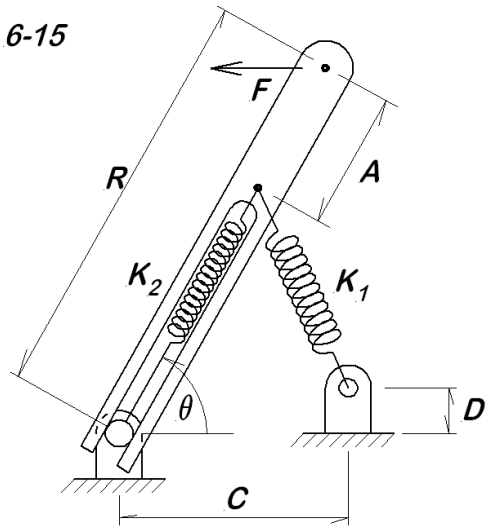

Chapter 7

SDOF Machine Dynamics

7.1 Introduction

Dynamics is the science of physical systems in motion, consisting of kinematics and kinetics. The term *kinetics* refers to the study of motion taking into account the forces causing the motion. This chapter focuses on the kinetics of systems having only a single degree of freedom. Although this is a somewhat special class, the large number of useful single degree of freedom mechanisms justify separate consideration. The kinetics of multiple degree of freedom systems is considered in Chapter 8. The significance of kinematics in the study of dynamics cannot be overestimated; the material of Chapters 2 and 3 is essential to the study of Chapters 7 and 8.

7.2 Kinetic Energy of Rigid Bodies

In all cases, the kinetic energy of a single rigid body can be separated into two terms, one that depends on the velocity of the center of mass and the other that depends on the angular velocity of the body. For a review of this development, see Appendix 6. Mechanism problems typically involve multiple rigid body components, for which the total kinetic energy is simply the sum of the kinetic energies of the individual components. Thus, for such a system the kinetic energy may be written as

$$\begin{aligned} T \;=\; & \frac{1}{2} M_1 \left(V_{1c}\right) \left\{V_{1c}\right\} + \frac{1}{2} \left(\omega_1\right) \left[J_{1c}\right] \left\{\omega_1\right\} \\ & + \frac{1}{2} M_2 \left(V_{2c}\right) \left\{V_{2c}\right\} + \frac{1}{2} \left(\omega_2\right) \left[J_{2c}\right] \left\{\omega_2\right\} + \cdots \end{aligned} \tag{7.1}$$

where $\{V_{1c}\}$, $\{V_{2c}\}$, ... $\{\omega_1\}$, $\{\omega_2\}$, ... and so forth are translational and angular velocity

components measured in an inertial coordinate system. Now, let all of the center of mass velocity components for the various mechanism elements be assembled into a column vector. Similarly, assemble all of the angular velocity components for the several parts as a second column vector. The results are

$$\{V_c\} = \mathrm{col}\,(V_{1x}, V_{1y}, V_{1z}, V_{2x}, V_{2y}, V_{2z} + \cdots) \tag{7.2}$$

$$\{\omega\} = \mathrm{col}\,(\omega_{1x}, \omega_{1y}, \omega_{1z}, \omega_{2x}, \omega_{2y}, \omega_{2z}, \cdots) \tag{7.3}$$

Then, with the appropriate definitions for the mass matrix $[M]$ and the center of mass moment of inertia matrix $[J_c]$, the system total kinetic energy is written as

$$T = \frac{1}{2}\{V_c\}^T [M] \{V_c\} + \frac{1}{2}\{\omega\}^T [J_c] \{\omega\} \tag{7.4}$$

For most single degree of freedom system, the vectors $\{V_c\}$ and $\{\omega\}$ can be written in terms of the generalized velocity, $\dot{\theta}$, and a vector of the appropriate velocity coefficients:

$$\{V_c\} = \dot{\theta}\{K_V(\theta)\} \tag{7.5}$$

$$\{\omega\} = \dot{\theta}\{K_\omega(\theta)\} \tag{7.6}$$

With these definitions, the entire kinetic energy can be written in terms of θ and $\dot{\theta}$:

$$T = \frac{1}{2}\dot{\theta}^2 \left(\{K_V(\theta)\}^T [M] \{K_V(\theta)\} + \{K_\omega(\theta)\}^T [J_c] \{K_\omega(\theta)\}\right) \tag{7.7}$$

By analogy with the expression for the kinetic energy of a single particle, the coefficient of $\frac{1}{2}\dot{\theta}^2$ is called the *generalized inertia*, a scalar quantity. Because the velocity coefficients are usually functions of the generalized coordinate, θ, the generalized inertia is also expected to be a function of θ. There is no universal notation for the generalized inertia; the notation $\mathbb{I}(\theta)$ or simply, $\mathbb{I}$, is used here.

A word of caution is required at this point. There are single degree of freedom systems with base displacement excitations, say an $X_o(t)$, for which the velocity required to express the kinetic energy is of the form $\left(\dot{X}_o + \dot{\theta}K_V\right)$. **In this case, the definition of the generalized inertia described above is not useful and the following discussion is not valid**. The problem develops because, in that circumstance, the term $\dot{\theta}K_V$ describes a *relative velocity*, rather than a velocity measured with respect to an inertial coordinate system. All such systems are here excluded from the discussions of this chapter; they are handled by the methods of Chapter 8.

To illustrate the idea of generalized inertia, consider the slider-crank mechanism shown in Figure 7.1 (for which the kinematics were studied in Section 2.4). Let M_2 and M_3 denote the masses of the connecting rod and the slider, respectively, while I_{1c} and I_{2c}

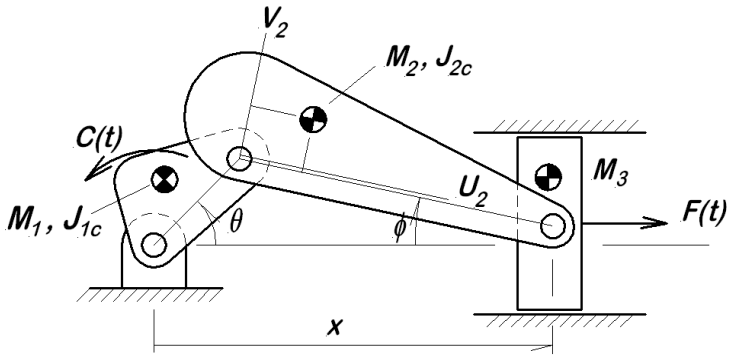

Figure 7.1: Slider-Crank Mechanism

are the mass moments of inertia for the crank and the connecting rod, each with respect to the component center of mass. The connecting rod center of mass is located by the body coordinates (u_{2c}, v_{2c}) from which the base coordinates (x_{2c}, y_{2c}) are determined. Similarly, consider a body coordinate system (U_1, V_1) on the crank having its origin at the crank pivot. In this body coordinate system, the crank center of mass is located at (u_{1c}, v_{1c}). The kinetic energy of the assembly is

$$\begin{aligned}
T &= T_{Crank} + T_{ConRod} + T_{Slider} \\
&= \frac{1}{2}M_1 V_{1c}^2 + \frac{1}{2}J_{1c}\theta^2 && \text{Crank} \\
&\quad + \frac{1}{2}M_2\left(\dot{x}_{2c}^2 + \dot{y}_{2c}^2\right) + \frac{1}{2}J_{2c}\dot{\phi}^2 && \text{Con Rod} \\
&\quad + \frac{1}{2}M_3\dot{x}_{3c}^2 && \text{Slider} \\
&= \frac{1}{2}\dot{\theta}^2 M_1\left(K_{1x}^2 + K_{1y}^2\right) + \frac{1}{2}\dot{\theta}^2 J_{1c} \\
&\quad + \frac{1}{2}\dot{\theta}^2 M_2\left(K_{cx}^2 + K_{2y}^2\right) + \frac{1}{2}\dot{\theta}^2 J_{2c}K_\phi^2 \\
&\quad + \frac{1}{2}\dot{\theta}^2 M_3 K_x^2 \\
&= \frac{1}{2}\dot{\theta}^2[M_1\left(K_{1x}^2 + K_{1y}^2\right) + J_{1c} \\
&\quad + M_2\left(K_{cx}^2 + K_{2y}^2\right) + J_{2c}K_\phi^2 + M_3 K_x^2] \\
&= \frac{1}{2}\dot{\theta}^2\left[J_{1o} + M_2\left(K_{cx}^2 + K_{2y}^2\right) + J_{2c}K_\phi^2 + M_3 K_x^2\right] \qquad (7.8)
\end{aligned}$$

In the last step above, the parallel axis theorem is employed to combine the two terms $M_1\left(K_{1x}^2 + K_{1y}^2\right) + I_{1c}$ into the single term J_{1o}, the mass moment of inertia of the crank with respect to the axis of rotation. This is to be expected for a body rotating about a fixed center. No similar simplification is possible for the connecting rod terms; the connecting rod does not rotate about a fixed center. As described above, the generalized

inertia for the slider-crank mechanism is the coefficient of $\frac{1}{2}\theta^2$. The generalized inertia is clearly dependent on θ and, in fact, oscillates about a non-zero mean value with two maxima and two minima for each crank revolution.

$$\mathbb{I}(\theta) = J_{1o} + M_2\left(K_{cx}^2 + K_{2y}^2\right) + J_{2c}K_{\phi}^2 + M_3K_x^2 \tag{7.9}$$

7.3 Generalized Forces

All of the forces and couples that work on the system influence its dynamic response. In Section 6.2, the generalized forces associated with both single and multiple degrees of freedom were developed; the single degree of freedom case is reviewed briefly here. The objective of this section is to determine a single generalized force that, when acting through a virtual coordinate change $\delta\theta$, will do virtual work $\delta W = Q\,\delta\theta$ equal to the sum of the virtual work of the actual forces and moments moving through their associated virtual displacements. Consider external forces $\mathbf{F}_i$ applied at locations defined by the position vectors $\mathbf{r}_i$, and similarly, couples $\mathbf{C}_j$ acting on angles A_j The virtual work of this force system is

$$\delta W = \sum_i \mathbf{F}_i \cdot \boldsymbol{\delta} r_i + \sum_j \mathbf{C}_j \cdot \delta\mathbf{A}_j \tag{7.10}$$

All the positions are functions of the single generalized coordinate, θ, so the virtual displacements can be written in terms of the virtual change in θ:

$$\delta\mathbf{r}_i = \frac{\partial\mathbf{r}_i}{\partial\theta}\delta\theta \tag{7.11}$$

$$\delta\mathbf{A}_j = \frac{\partial\mathbf{A}_j}{\partial\theta}\delta\theta \tag{7.12}$$

When these expressions are applied in the virtual work expression, the result is

$$\delta W = \delta\theta\left(\sum_i \mathbf{F}_i \cdot \frac{\partial\mathbf{r}_i}{\partial\theta} + \sum_j \frac{\partial\mathbf{A}_j}{\partial\theta} \cdot \delta\mathbf{A}_j\right) \tag{7.13}$$

The coefficient of $\delta\theta$ is the generalized force,

$$Q = \sum_i \mathbf{F}_i \cdot \frac{\partial\mathbf{r}_i}{\partial\theta} + \sum_j \frac{\partial\mathbf{A}_j}{\partial\theta} \cdot \delta\mathbf{A}_j \tag{7.14}$$

Although this looks formidable, the actual determination of the generalized force is usually quite simple. To continue with the illustration involving the slider-crank mechanism,

Figure 7.1 shows a couple $C(t)$ acting on the crank and a force $F(t)$ acting on the slider. These are the only two external forces that do work on the system. Other external forces, such as the bearing reactions or the transverse reaction on the slider, do no work and need not be included. The virtual work of this force system is

$$\begin{aligned} \delta W &= C(t)\ \delta\theta + F(t)\ \delta x \\ &= \delta\theta\left[C(t) + F(t)\, K_x\right] \end{aligned} \tag{7.15}$$

with the result that the generalized force is

$$Q = C(t) + F(t)\, K_x \tag{7.16}$$

Notice the role of the velocity coefficient, K_x. Why is there no velocity coefficient factor written with $C(t)$?

7.4 Eksergian's Equation of Motion

One of the theorems regularly established in introductory dynamics courses states that *the work done on a mechanical system is equal to the change in kinetic energy of the system.* For application here, that statement is considered in differentiated form:

$$\text{Power(into the system)} = \frac{d}{dt}\left(\text{Kinetic Energy}\right) \tag{7.17}$$

For a single degree of freedom system, the power into the system is

$$\begin{aligned} \text{Power} &= \sum_i \left(F_{ix}\dot{x}_i + F_{iy}\dot{y} + M_i\dot{A}_i\right) \\ &= \dot{\theta}\sum_i \left(F_{ix}K_{ix} + F_{iy}K_{iy} + M_iK_{A_i}\right) \\ &= Q\cdot\dot{\theta} \end{aligned} \tag{7.18}$$

while the kinetic energy is

$$T = \frac{1}{2}\mathbb{I}(\theta)\,\dot{\theta}^2 \tag{7.19}$$

Differentiating the kinetic energy with respect to time and equating this result to the power expression gives

$$\frac{dT}{dt} = \frac{1}{2}\frac{d\mathbb{I}(\theta)}{d\theta}\frac{d\theta}{dt}\dot{\theta}^2 + \mathbb{I}(\theta)\ \dot{\theta}\,\ddot{\theta} = Q\,\dot{\theta} \tag{7.20}$$

Eliminating the common factor $\dot{\theta}$ gives Eksergian's form for the equation of motion of a single degree of freedom system:

$$\mathbb{I}(\theta)\ \ddot{\theta} + \frac{1}{2}\frac{d\mathbb{I}(\theta)}{d\theta}\dot{\theta}^2 = Q \tag{7.21}$$

This, then, is the generalized equation of motion applicable to all single degree of freedom systems of the type considered in this chapter. This form for the equation of motion, and also the ideas of velocity coefficients and velocity coefficient derivatives, were used repeatedly by Eksergian in a series of papers on machinery dynamics [1][1]. If the generalized inertia is constant, the equation of motion reduces to the familiar Newton's Second Law statement: force = inertia × acceleration. For varying generalized inertia, the second term, known as the centripetal term, must also be included. The coefficient in the centripetal term, $\frac{1}{2}d\mathbb{I}/d\theta$, is given the symbol $\mathbb{C}(\theta)$ and called the *centripetal coefficient*. With this notation, Eksergian's form for the equation of motion is

$$\mathbb{I}(\theta)\ \ddot{\theta} + \mathbb{C}(\theta)\ \dot{\theta}^2 = Q \tag{7.22}$$

To apply Eksergian's equation of motion to the slider-crank mechanism considered earlier, it is necessary to determine the generalized inertia, $\mathbb{I}(\theta)$. From above, the generalized inertia is

$$\mathbb{I}(\theta) = J_{1o} + M_2\left(K_{2cx}^2 + K_{2cy}^2\right) + J_{2c}K_\phi^2 + M_3K_x^2 \tag{7.23}$$

Differentiation with respect to θ gives the centripetal coefficient, $\mathbb{C}(\theta)$:

$$\mathbb{C}(\theta) = M_2\left(K_{2cx}L_{2cx} + K_{2cy}L_{2cy}\right) + J_{2c}K_\phi L_\phi + M_3K_xL_x \tag{7.24}$$

Using these expressions in Eksergian's equation of motion, along with the generalized force previously identified, gives the equation of motion for the slider-crank mechanism:

$$\begin{aligned} & J_{1o} + M_2\left(K_{2cx}^2 + K_{2cy}^2\right) + J_{2c}K_\phi^2 + M_3K_x^2 \\ & + \left[M_2\left(K_{2cx}L_{2cx} + K_{2cy}L2_{cy}\right) + J_{2c}K_\phi L_\phi + M_3K_xL_x\right]\dot{\theta}^2 \\ = \ & C(t) + F(t)\,K_x \end{aligned} \tag{7.25}$$

This is an extremely complex nonlinear differential equation with variable coefficients, so there is little prospect of an analytical solution. There is, however, every reason to expect that a numerical solution can be obtained, and that matter is taken up later in this chapter.

[1] Eksergian seems to have been the first to present this equation of motion in an English-language publication, but it had appeared previously in the German literature. His work was far ahead of his time, and is only now practical because of the general availability of digital computers.

7.5 Potential Energy

There is an alternative to including conservative forces in the generalized force. A potential energy term can be included in Eksergian's equation of motion to account for them, while the nonconservative forces continue to be included in the generalized force. This modification is developed here; a parallel development was given for statics in Section 6.2.

Let the force acting on the system at point $\mathbf{r}_i$ consist of two parts, one part conservative and the other nonconservative. The conservative force can be written as the negative gradient of its associated potential function. Thus, any force can be written as

$$\begin{aligned} \mathbf{F}_i &= \mathbf{F}_i^c + \mathbf{F}_i^{nc} \\ &= -\boldsymbol{\nabla} V_i + \mathbf{F}_i^{nc} \end{aligned} \tag{7.26}$$

If this form is used to determine the generalized force, that result also consists of two terms:

$$\begin{aligned} Q &= \sum_i \mathbf{F}_i \cdot \frac{d\mathbf{r}_i}{d\theta} \\ &= \sum_i \left(-\boldsymbol{\nabla} V_i + \mathbf{F}_i^{nc}\right) \cdot \frac{d\mathbf{r}_i}{d\theta} \\ &= -\sum \frac{dV_i}{d\theta} + \sum_i \mathbf{F}_i^{nc} \cdot \frac{d\mathbf{r}_i}{d\theta} \\ &= -\frac{dV}{d\theta} + Q^{nc} \end{aligned} \tag{7.27}$$

Note that V with no subscript is used for the total potential energy of the system, while Q^{nc} is the total nonconservative generalized force. With this result applied to Eksergian's equation, and the potential energy term shifted to the left side, the modified form is

$$\mathbb{I}(\theta)\,\ddot{\theta} + \mathbb{C}(\theta)\,\dot{\theta}^2 + \frac{dV}{d\theta} = Q^{nc} \tag{7.28}$$

This modified form is particularly useful in cases that involve springs that of change direction as well as length as the mechanism moves. For such situations, expressing the potential energy of the spring in a typical position, and then including its effect through the indicated potential energy term is relatively simple. Direct inclusion in the generalized force term is also possible, although often more difficult.

Continuing with the slider-crank example used previously, let the force on the slider be replaced by a spring and dashpot arrangement as shown in Figure 7.2. The free length

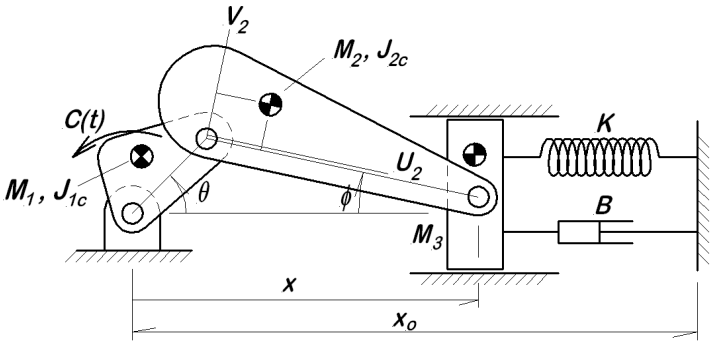

Figure 7.2: Slider-Crank Mechanism With Spring-Dashpot Assembly Added

of the spring is s_o. The potential energy of the spring is then

$$V = \frac{1}{2} K \left(x_o - x - s_o\right)^2 \tag{7.29}$$

with the derivative

$$\frac{dV}{d\theta} = -K \left(x_o - x - s_o\right) K_x \tag{7.30}$$

To include the dashpot and the time-dependent couple, the nonconservative virtual work is determined as follows:

$$\begin{aligned} \delta W^{nc} &= -B\,\dot{x}\,\delta x + C\left(t\right)\,\delta\theta \\ &= -B\left(\theta K_x\right)\left(K_x\,\delta\theta\right) + C\left(t\right)\,\delta\theta \\ &= \left[-B\,K_x^2 + C\left(t\right)\right]\,\delta\theta \\ Q^{nc} &= -B\,K_x^2 + C\left(t\right) \end{aligned} \tag{7.31}$$

Note that time-dependent external forces are necessarily nonconservative, and therefore must always enter through Q^{nc}. With these modifications, the equation of motion for the system is

$$\mathbb{I}\left(\theta\right)\,\ddot{\theta} + \mathbb{C}\left(\theta\right)\,\dot{\theta}^2 - K\,K_x\left(x_o - x - s_o\right) = -B\,K_x^2\,\dot{\theta} + C\left(t\right) \tag{7.32}$$

where the expressions for $\mathbb{I}\left(\theta\right)$ and $\mathbb{C}\left(\theta\right)$ remain as previously determined.

7.6 Mechanism Simulation

The differential equation that describes the motion of a single degree of freedom mechanism is often quite formidable because in most cases it is nonlinear with variable coefficients. Such equations are generally not solvable in closed form, but they are usually

amenable to numerical solution. The Runge-Kutta method is one numerical solution technique that usually gives good results for mechanism problems. It is presented in Appendix 3, with the particular form applicable to a single, second-order differential equation given in Appendix A3.1. That Appendix should be reviewed for details of the Runge-Kutta method; the present section addresses its implementation in a computer program. The resulting program is often referred to as a *simulation*, because the calculations performed in the program simulate, or behave like, the physical system from which the differential equation was derived.

The essential parts of any simulation program are

1. Initialization

2. Iterative advancement of the solution

    a. Evaluation of derivatives

    b. Determination of new solution values

    c. Recording of new solution values

    d. Testing for termination

In the initialization phase, all initial values are either set internally or entered from the keyboard. The time is usually initialized to zero internally, although this is not mandatory (any desired starting time can be used). The initial conditions, $\theta(0)$ and $\dot{\theta}(0)$, are entered from the keyboard if they are to be changed from one execution to the next; if not, they are often set internally as well. The constant parameters of the problem such as lengths, masses, and moments of inertia are also set in this phase.

Some type of termination criterion must be established and any parameters associated with that criterion (such as a maximum time) should be set during the initialization. As a final step, column headings should be printed and the initial conditions recorded as the first entries in the tabulated solution. Standard practice is to program the evaluation of the second derivative as a subroutine, often using other subroutines for the kinematics and other repeated calculations. This is then called with the appropriate argument sets for each of the four derivative evaluations required by the Runge-Kutta algorithm.

To be specific, consider a simulation program for the system described by the differential equation

$$\ddot{\theta} = f\left(t, \theta, \dot{\theta}\right) \tag{7.33}$$

When the second derivative subroutine is written, the variables used could be named `t`, `th`, and `dth` for t, θ, and $\dot{\theta}$. Then, in the main program, the variable names might be `ts`,

`ths`, and `dths`, where the final `s` denotes saved values of t, θ, and $\dot{\theta}$. Before calling the subroutine to evaluate the derivative, the appropriate values must be assigned for `t`, th, and `dth`. For the first evaluation, this is simply

```
t = ts

th = ths

dth = dths
```

For the second evaluation, the appropriate values are

```
t = ts + h/2

th = ths + h*dths/2 + h*kl/8

dth =dths + kl/2
```

where `kl` is determined from the first evaluation of the derivative. This is further illustrated in the examples in Section 7.6. After four evaluations of the derivative, each with different values assigned for t, θ, and $\dot{\theta}$, new values of the solution are calculated or, as it is sometimes phrased, the solution is "updated." In addition to updating the values for `ths` and `dths`, it is also necessary to update the time, `ts`. For the simplest type of simulation, the results are printed at every time step. Thus, after every update, the new results are printed. If very small time steps are required for solution accuracy, it may be desirable to print less frequently, perhaps every 10 steps. If this is required, the process of advancing the solution will involve two nested loops or a print cycle counter. The printed results usually include the values for t, θ, and θ, but any desired additional quantities such as forces, stresses, relative displacements, or relative velocities can also be evaluated and printed at each output time.

It is always necessary to provide some means to end the simulation program. This can be done in several ways, one of the most common being to end after a fixed time interval has been simulated. Other termination criteria may be based on the occurrence of some specified event, such as when the solution is greater than a prescribed value. For any such criterion, a test is needed to terminate the execution, usually in the form of an `IF`-statement test following each output sequence. Failure to include an achievable termination criterion causes the simulation to run until the operator intervenes; that is a wasteful approach. The term *achievable termination criterion* refers to an event that actually occurs at some time in the solution, as opposed to a criterion defined by an event that never occurs and hence, would allow the solution to run indefinitely. If the termination criterion is not met, control is transferred to the beginning of the loop to move forward another time step.

These steps are illustrated in the example problems given in the next section. The

reader should locate each of these steps in the computer program and trace the sequence of calculations.

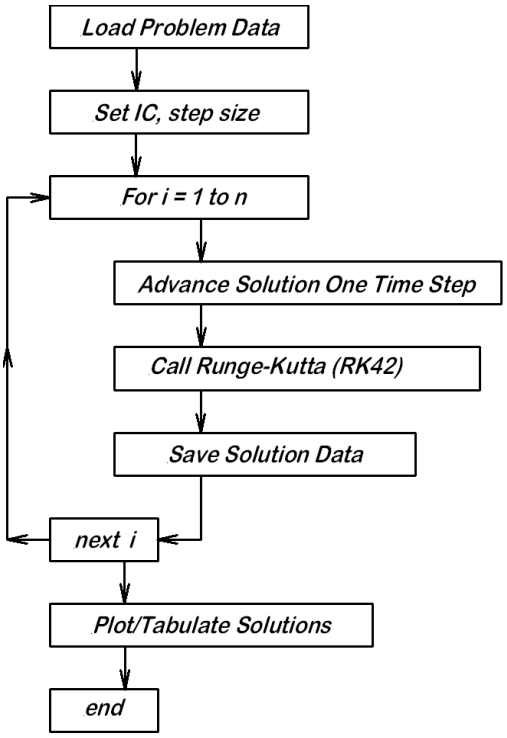

Figure 7.3: Runge-Kutta Flow Chart

7.7 Mechanism Simulation Examples

This section presents three examples of mechanism simulation using the Runge-Kutta integration algorithm and other ideas discussed in the preceding sections. Each example begins with a problem statement and formulation, followed by computer program results.

7.7.1 Rocker Response

This problem involves the dynamic response of the curved rocker as shown in Figure 7.4 to an impulsive force $F(t)$ applied at point (A); this problem is, in some respects, similar to the statics example problem involving an L-shaped bracket given in Section 6.3. For the current problem, the rocker is constrained to roll without slipping on the circular support, under the influence of the impulsive applied load, $F(t)$, and a spring and dashpot assembly

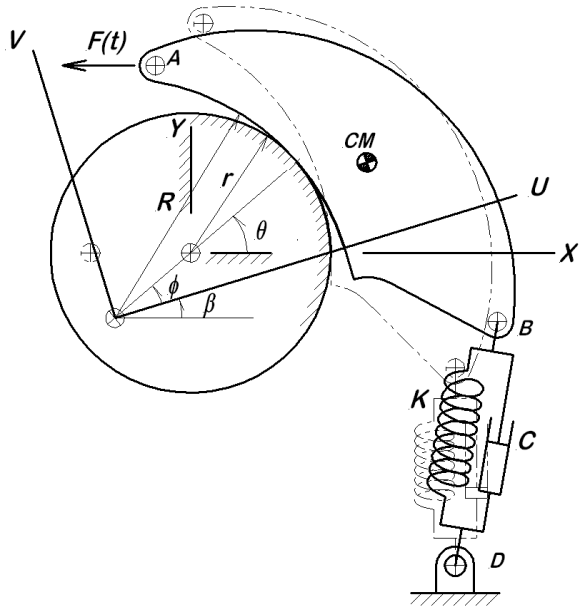

Figure 7.4: Rocker System Diagram

attached at point (B). The spring and dashpot assembly is anchored at point (D). Point (D) is 50 mm directly below point (B) when $\theta = 0$, and the spring-damper assembly is fully relaxed in that position.

The rocker support has a radius $R = 44.50$ mm. The rocker material is steel plate, thickness $t = 21$ mm, with a density $\rho = 7800.6$ kg/m^3. For the restraining spring, the spring rate is $K = 3500$ N/m and the dashpot coefficient is $C = 100$ N-s/m. The applied force is a single rectangular pulse acting horizontally to the left; its magnitude is 200 N lasting for a duration of 0.005 second. The system is initially at rest in an upright position, with the $U-$axis aligned with the $X-$axis, the $V-$axis parallel to the $Y-$axis, and supported by a stop (not shown) when the impulsive load is first applied.

The two primary objectives for this simulation are:

1. Determining the maximum excursion of the rocker;
2. Determining the rocker final velocity as it returns to the stop.

7.7.1.1 Mass Properties

The rocker geometry is shown in Figure 7.5 on a 10 mm grid, and the rocker thickness is 21 mm. Note that the origin of the body coordinate system is the center of the inside radius at the level of the beginning of the arc (below that point, the profile is straight). This coordinate system choice is made because of the circular form of the body boundary, most easily expressed with this choice. Using the **Planar Area Program.Tru** of Appendix 4, the following properties are determined for the rocker; this is carried out in detail in

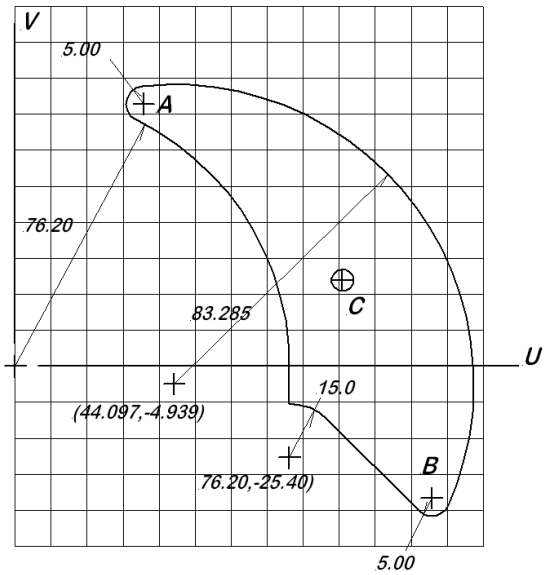

Figure 7.5: Rocker Geometry on a 10 mm Grid (all dimensions in millimeters)

Appendix 4 as a demonstration of the application of that program.

The essential results are summarized here:

$$\begin{aligned} M &= 0.82637 && \text{kg} \\ u_c &= 0.09188 && \text{m} \\ v_c &= 0.02331 && \text{m} \\ J_c &= 1.10864 \cdot 10^{-3} && \text{kg-m}^2 \end{aligned}$$

The other important data required is the location of the several attachment points. These are

$$\begin{aligned} u_A &= +0.035795 \text{ m} & v_A &= +0.072885 \text{ m} \\ u_B &= +0.115676 \text{ m} & v_B &= -0.036593 \text{ m} \\ x_D &= +0.083976 \text{ m} & y_D &= -0.086593 \text{ m} \end{aligned}$$

This completes all of the required geometrical and inertial data for this example.

7.7.1.2 Kinematics

For the formulation of any problem of this sort, the place to begin is always with the kinematics. Since this problem has not been considered previously, the necessary kinematic relations are developed here. The essential fact that must be grasped first is that the center of the rocker contact arc (the origin of the body coordinate system) moves in a circle of radius $R - r$ about the center of the fixed support. This means that both centers, that of the rocker contact arc and that of the fixed support, must lie on the common normal to the tangent line at the point of contact. Referring to Figure 7.4, it is then evident that the rolling constraint relation is simply

$$R\phi = r\theta \tag{7.34}$$

This is simply a statement that the contact arc on the rocker is equal to the contact arc on the fixed support.

The simulation is to be formulated in terms of the rocker contact angle, θ, but note that ϕ is not the rotation of the rocker. The rotation of the rocker is the angle β, and from simple geometry it is evident that

$$\theta = \phi + \beta \tag{7.35}$$

Putting this altogether, it is a simple matter to express β in terms of θ

$$\beta = \theta\,(1 - r/R) \tag{7.36}$$

Then the velocity coefficient and velocity coefficient derivative for β are

$$K_\beta = 1 - r/R \tag{7.37}$$
$$L_\beta = 0 \tag{7.38}$$

Next, consider any point P in the rocker with body coordinates (u_p, v_p); it will be necessary to eventually consider points A, B, and the center of mass, but one general formulation is sufficient for all. The global (base) coordinates for such a point are

$$x_p = u_p \cos\left[(1 - r/R)\theta\right] - v_p \sin\left[(1 - r/R)\theta\right] - (R - r)\cos\theta \tag{7.39}$$
$$v_p = u_p \sin\left[(1 - r/R)\theta\right] + v_p \cos\left[(1 - r/R)\theta\right] - (R - r)\sin\theta \tag{7.40}$$

Then taking derivatives with respect to θ produces the velocity coefficients and velocity coefficient derivatives

$$\begin{aligned} K_{px} = {} & -u_p\,(1 - r/R)\sin\left[(1 - r/R)\theta\right] \\ & -v_p\,(1 - r/R)\cos\left[(1 - r/R)\theta\right] + (R - r)\sin\theta \end{aligned} \tag{7.41}$$
$$\begin{aligned} K_{py} = {} & u_p\,(1 - r/R)\cos\left[(1 - r/R)\theta\right] \\ & -v_p\,(1 - r/R)\sin\left[(1 - r/R)\theta\right] - (R - r)\cos\theta \end{aligned} \tag{7.42}$$

$$\begin{aligned} L_{px} &= -u_p \left(1 - r/R\right)^2 \cos\left[(1 - r/R)\theta\right] \\ &\quad + v_p \left(1 - r/R\right)^2 \sin\left[(1 - r/R)\theta\right] + (R - r)\cos\theta \qquad (7.43) \\ L_{py} &= -u_p \left(1 - r/R\right)^2 \sin\left[(1 - r/R)\theta\right] \\ &\quad - v_p \left(1 - r/R\right)^2 \cos\left[(1 - r/R)\theta\right] + (R - r)\sin\theta \qquad (7.44) \end{aligned}$$

As noted above, these results are sufficient to describe the motions for points A, B, and the center of mass.

The effects of the spring and dashpot assembly are dependent on the length of that assembly, denoted as S, and the time derivative, $\dot{S}$. The length is

$$S\left(\theta\right) = \sqrt{\left(x_B - x_D\right)^2 + \left(y_B - y_D\right)^2} \qquad (7.45)$$

With the usual differentiation, the velocity coefficient K_S is determined:

$$K_S = \frac{\left(x_B - x_D\right)}{S\left(\theta\right)} K_{Bx} + \frac{\left(y_B - y_D\right)}{S\left(\theta\right)} K_{By} \qquad (7.46)$$

7.7.1.3 Equation of Motion

To apply Eksergian's form of the equation of motion, the kinetic energy is required. This can be expressed as the sum of terms dependent on translational and rotational velocities:

$$\begin{aligned} T &= \frac{1}{2} M \left(\dot{x}_c^2 + \dot{y}_c^2\right) + \frac{1}{2} J_c \dot{\beta}^2 \\ &= \frac{1}{2} \dot{\theta}^2 \left[M \left(K_{cx}^2 + K_{cy}^2\right) + J_c K_\beta^2\right] \qquad (7.47) \end{aligned}$$

From the kinetic energy, the generalized inertia is readily identified as the coefficient of $\frac{1}{2}\dot{\theta}^2$:

$$\mathbb{I}\left(\theta\right) = \left[M \left(K_{cx}^2 + K_{cy}^2\right) + J_c K_\beta^2\right] \qquad (7.48)$$

Because the generalized inertia is not constant, there is a non-zero centripetal coefficient:

$$\mathbb{C}\left(\theta\right) = M \left(K_{cx} L_{cx} + K_{cy} L_{cy}\right) \qquad (7.49)$$

The term $J_c K_\beta L_\beta$ is dropped because $L_\beta = 0$.

For this example, the effect of the spring is included through a potential energy term. The potential energy of the stretched spring is

$$V = \frac{1}{2} K \left[S(\theta) - S_o \right]^2 \tag{7.50}$$

with the derivative

$$\frac{dV}{d\theta} = K \left[S(\theta) - S_o \right] K_S \tag{7.51}$$

The final step in preparation for writing the equation of motion is to determine the nonconservative generalized force. The nonconservative virtual work is

$$\begin{aligned} \delta W^{nc} &= -F(t)\, \delta x_A - C\, \dot{S}\, \delta S \\ &= -\left[F(t)\, K_{Ax} + \dot{\theta} C K_S^2 \right] \delta\theta \end{aligned} \tag{7.52}$$

from which the nonconservative generalized force is

$$Q^{nc} = -\left[F(t)\, K_{Ax} + \dot{\theta} C K_S^2 \right] \tag{7.53}$$

The equation of motion is then obtained by applying Eksergian's form for the equation of motion:

$$\mathbb{I}(\theta)\, \ddot{\theta} + \mathbb{C}(\theta)\, \dot{\theta}^2 + \frac{dV}{d\theta} = Q^{nc} \tag{7.54}$$

where expressions have been obtained previously for $\mathbb{I}(\theta)$, $\mathbb{C}(\theta)$, V, and Q^{nc} for this problem. For use in the numerical solution, it is necessary to solve the equation of motion for the second derivative:

$$\ddot{\theta} = \frac{1}{\mathbb{I}(\theta)} \left[Q^{nc} - \mathbb{C}(\theta)\, \dot{\theta}^2 - \frac{dV}{d\theta} \right] \tag{7.55}$$

The foregoing analysis is the basis for the computer program that follows below. The first part of the program contains the initialization phase, the Runge-Kutta loop, and provisions for plotting and printing the results.

7.7.1.4 Program Listing for RckrDyn3.Tru

The program listing for the rocker simulation follows below. The reader should remember that the *line numbers are entirely optional* and may be dropped without affecting the operation of the program in anyway. They are included simply for easy reference to specific parts of the program.


```
101 !     RckrDyn3.Tru
102 ! Rocker Dynamics Calcs
103 ! This code is the actual simulation.
104 OPTION NOLET
105 OPTION BASE 1
106 LIBRARY "c:\tb305\true \tblibs \graphlib.tru"
107 DIM tsav(1500),thsav(1500),dthsav(1500),fsav(1500)
108 CLEAR
109 ! System Data
110 rho=7800.6                          ! mat'l density, kg/m^3
111 t=0.021                             ! thickness, m
112 capR=0.07620                        ! rocker rolling radius
113 rr=0.04450                          ! support radius
114 ua=35.795*10^(-3)                   ! force application point
115 va=72.885*10^(-3)
116 ub=115.676*10^(-3)                  ! spring/damper attachment location
117 vb=-36.593*10^(-3)
118 xd=ub-(capR-rr)                     ! spring/damper anchor location
119 yd=vb-0.050
120 area=5044.5897*10^(-6)              ! area, m^2
121 uc=91.878694*10^(-3)                ! uc, m
122 vc=23.306225*10^(-3)                ! vc, m
123 Iuu=7.4286318*10^6*10^(-12)         ! Iuu, m^4
124 Ivv=4.4664111*10^7*10^(-12)         ! Ivv, m^4
125 Iuuc=Iuu-area*vc^2                  ! centroidal values
126 Ivvc=Ivv-area*uc^2
127 M=rho*t*area                        ! mass, kg
128 Juuc=Iuuc*rho*t                     ! cm MMOI, kg-m^2
129 Jvvc=Ivvc*rho*t                     ! cm MMOI, kg-m^2
130 Jc=Juuc+Jvvc                        ! cm polar MMOI
131 CLEAR
132 PRINT
133 PRINT "    Program c:\mom \RckrDyn3.Tru"
134 PRINT "    "&time$&" on "&date$
135 PRINT
136 PRINT "    Inertial Data"
137 PRINT "    M    = ";M;"kg"
138 PRINT "    uc   = ";uc;"m"
139 PRINT "    vc   = ";vc;"m"
140 PRINT "    Juuc = ";Juuc;"kg-m^2"
141 PRINT "    Jvvc = ";Jvvc;"kg-m^2"
142 PRINT "    Jc   = ";Jc;"kg-m^2"
143 Kspring=3500                        ! spring rate, N/m
144 So=abs(vb-yd)                       ! free length of spring
```



```
145 Cdamp=100                          ! damper rate, N-s/m
146 FFmx=200                           ! ampl of force pulse, N
147 tfmx=0.005                         ! force pulse duration, s
148 GET KEY xxx
149 ! Initial values ...
150 t=0                                ! initial time
151 th=0                               ! initial theta
152 dth=0                              ! initial velocity
153 h=0.0001                           ! time step
154 CLEAR
155 ihmx=1135
156 FOR ih=1 to ihmx
157     ! Inputs are t=rk42t, y=rk42y, dy=rk42dy, h=rkr2h
158     CALL RK42(t,th,dth,h)          ! start Runge-Kutta
159     tsav(ih)=t                     ! save the results
160     thsav(ih)=th
161     dthsav(ih)=dth
162     thmx=max(thmx,th)              ! search for max values
163     dthmx=max(dthmx,abs(dth))
164     IF t<=tfmx then FF=FFmx        ! force pulse
165     IF t>tfmx then FF=0
166     fsav(ih)=FF
167 NEXT ih
168 CLEAR
169 SET WINDOW -.8*tsav(ihmx),1.9*tsav(ihmx),-1.4,2.1
170 PLOT TEXT, AT 0.6*tsav(ihmx),0.5: "Program RckrDyn3.Tru"
171 PLOT TEXT, AT 0.6*tsav(ihmx),0.4: date$
172 PLOT TEXT, AT 0.6*tsav(ihmx),0.3: time$
173 PLOT 0,0;                          ! horizontal axis
174 PLOT tsav(ihmx),0
175 PLOT 0,-.3;                        ! vertical axis
176 PLOT 0,1.1
177 FOR ix=1 to 11                     ! horizontal axis ticks
178     PLOT 0.01*ix,0;
179     PLOT 0.01*ix,.04
180     ix$=str$(.01*ix)
181     PLOT TEXT, AT 0.01*ix-.003,-.06: ix$
182 NEXT ix
183 FOR iz=1 to ihmx
184     PLOT tsav(iz),thsav(iz)/thmx;      ! normalized plot
185 NEXT iz
186 PLOT
187 PLOT TEXT, AT .4*tsav(ihmx),.90: "Theta max = "&str$(thmx)&" rad"
188 PLOT TEXT, AT .4*tsav(ihmx),.83: "          = "&str$(thmx*180/pi)&" deg"
```



```
189 FOR iz=1 to ihmx
190     PLOT tsav(iz),dthsav(iz)/dthmx;    ! normalized plot
191 NEXT iz
192 PLOT
193 PLOT TEXT, AT .4*tsav(ihmx),.76: "dth max   = "&str$(dthmx)&" rad/s"
194 FOR iz=1 to ihmx
195     PLOT tsav(iz),fsav(iz)/(FFmx);     ! normalized plot
196 NEXT iz
197 PLOT
198 PLOT TEXT, AT .4*tsav(ihmx),.69: "F max     = "&str$(FFmx)&" N"
199 GET KEY xxx
200 PRINT "    Do you want a listed output?"
201 PRINT "     y/n"
202 INPUT lo$
203 IF lo$="y" then
204    lc=0
205    CLEAR
206    blk$="     "
207    uug$="  t=#.#####  theta=#.#####  thdot=###.#####  F=###.##"
208    FOR iz=10 to ihmx step 10
209        PRINT using uug$: tsav(iz),thsav(iz),dthsav(iz),Fsav(iz)
210        IF thsav(iz)<=0 and dthsav(iz)<0 then EXIT FOR
211    NEXT iz
212    iz2=iz                          ! search for more precise impact event values
213    iz1=iz-9
214    FOR iz=iz1 to iz2
215        IF thsav(iz)>0 and thsav(iz+1)<0 then
216           izz=iz
217           PRINT blk$&"Best estimate for impact event"
218           PRINT blk$&"t = ";tsav(izz);"th = ";thsav(izz);"dth =";dthsav(izz)
219           EXIT FOR
220        END IF
221    NEXT iz
222    PRINT blk$&"step size, h = ";h;" sec"
223    PRINT blk$&"Program RckrDyn3.Tru  at "&time$&" on "&date$
224 END IF
225 SUB Deriv(tt,tth,dtth,ddtth)
226     theta=tth
227     CALL Kinem                     ! get current kinematic solutions
228     II=M*(Kcx^2+Kcy^2)+Jc*Kbeta^2      ! gen'l inertia
229     CC=M*(Kcx*Lcx+Kcy*Lcy)         ! centripetal coeff
230     dVdth=Kspring*(S-So)*Ks        ! dV/dth
231     FF=0                           ! force pulse
232     IF tt<=tfmx then FF=FFmx       ! force pulse
```



```
233     Qnc=-(FF*Kax+dtth*Cdamp*Ks^2)      ! gen'l nonconservative force
234     ddtth=(Qnc-CC*dtth^2-dVdth)/II     ! acceleration
235 END SUB
236 SUB Kinem
237     ! input is theta
238     beta=theta*(1-rr/capR)
239     Kbeta=1-rr/capR
240     Lbeta=0
241     ! Point A kinematic functions
242     up=ua
243     vp=va
244     CALL PointP
245     xa=xp                          ! save point A results
246     ya=yp
247     Kax=Kpx
248     Kay=Kpy
249     Lax=Lpx
250     Lay=Lpy
251     ! Point B kinematic functions
252     up=ub
253     vp=vb
254     CALL PointP
255     xb=xp                          ! save point B results
256     yb=yp
257     Kbx=Kpx
258     Kby=Kpy
259     Lbx=Lpy
260     Lby=Lpy
261     ! Center of mass kinematic functions
262     up=uc
263     vp=vc
264     CALL PointP
265     xc=xp                          ! save CM results
266     yc=yp
267     Kcx=Kpx
268     Kcy=Kpy
269     Lcx=Lpx
270     Lcy=Lpy
271     ! Spring/damper length
272     S=sqr((xb-xd)^2+(yb-yd)^2)     ! spring/damper length
273     Ks=((xb-xd)*Kbx+(yb-yd)*Kby)/S
274 END SUB
275 SUB PointP
276     ! inputs are theta,up,vp, outputs are xp,yp,kpx,kpy,Lpx,Lpy
```



```
277     fctr=(1-rr/capR)
278     arg=fctr*theta
279     xp=up*cos(arg)-vp*sin(arg)-(capR-rr)*cos(theta)
280     yp=up*sin(arg)+vp*cos(arg)-(capR-rr)*sin(theta)
281     Kpx=-up*fctr*sin(arg)-vp*fctr*cos(arg)+(capR-rr)*sin(theta)
282     Kpy=up*fctr*cos(arg)-vp*fctr*sin(arg)-(capR-rr)*cos(theta)
283     Lpx=-up*fctr^2*cos(arg)+vp*fctr^2*sin(arg)+(capR-rr)*cos(theta)
284     Lpy=-up*fctr^2*sin(arg)-vp*fctr^2*cos(arg)+(capR-rr)*sin(theta)
285 END SUB
286 SUB RK42(rk42t,rk42y,rk42dy,rk42h)
      (This part is Subroutine RK42, exactly as listed in App. 3)
322 END
```

The plotted results from the program are shown in Figure 7.6. The plot shows, in normalized form, curves for $\theta(t)$, $\dot{\theta}(t)$, and $F(t)$. (Note that $F(t)$ is just the short, rectangular pulse at the beginning.) It is immediately evident that the whole event is completed in slightly more than 0.1 seconds.

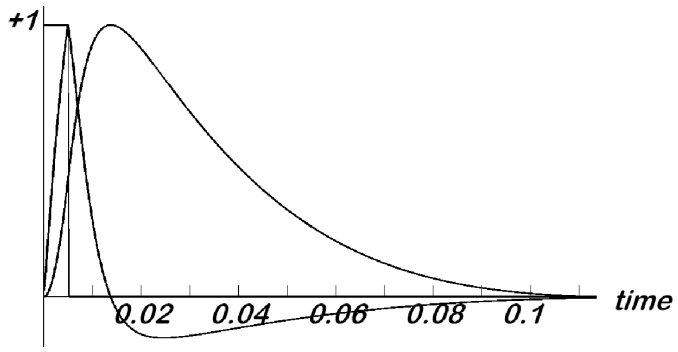

Figure 7.6: Normalized Rocker Response Curves for $F(t)$, $\theta(t)$, and $\dot{\theta}(t)$ versus time t

The last few lines of the tabulated results from the code above are as follows:

```
t= .11100  theta= .00044  thdot=-  .33079  F=    .00
t= .11200  theta= .00013  thdot=-  .30353  F=    .00
t= .11300  theta=-.00016  thdot=-  .27771  F=    .00
   Best estimate for impact event
   t =  .1124 th = 6.9892723e-6 dth =-.29303114
   step size, h =  .0001  sec
   Program RckrDyn3.Tru  at  15:54:06 on 20170831
```

Most of the results from the previous analysis can be found in subroutine `Deriv` that begins at line 225, subroutine `Kinem` beginning at line 236, and subroutine `PointP` be-

ginning at line 275. Note that in the subroutines, the values of time and θ are denoted by `tt` and `theta`; in the main program, these same variables are denoted by `t`, and `th`.

The answers to the two principal questions are read directly from the output. From the graph, the maximum excursion is $\theta_{Max} = 0.4927$ rad $= 28.232$ degrees. The output list operation includes the results of a search for the impact event (the computed solution closest to the impact), with the result that (approximately) $t_{impact} = 0.1124$ sec, $\dot{\theta}_{impact} = -0.29303$ rad/s. At this time, the position is still very slightly positive, $\theta_{impact} = 6.989 \cdot 10^{-6}$ rad, which for most purposes can be taken to be zero.

The simulation is ultimately terminated by simply running out the FOR-NEXT loop (lines 156-167) in steps of $h = 0.0001$ seconds. While this is rather crude, it is simple and effective; the number of steps to allow is determined by experimentation. The printed output is listed in steps of $10h$ as long as $\theta > 0$, stopping after the first negative value (lines 200-223). This initiates a search through the previously computed solution to locate a better estimate for the impact event (lines 212-221).

The program follows the basic flow chart given in Figure 7.3, particularly in that all of the results are generated before there is any output at all. Only after the simulation has ended (line 167) does the output begin, first with a plot of the results and later with the option for a list of values. The major parts of the program are these:

1. **Program Preliminariess** (lines 101-108) – This is just the usual headers, option statements, dimension statements, etc. found in most True BASIC programs.

2. **Data Input** (lines 109-148) – This is the problem data, the given information and that developed in Appendix 4. Note that the original planar area data, lines 120-126, is used to express the mass and moment of inertia, lines 127-130.

3. **Initialization** (lines 149-155) – This is the establishment of the initial values and the step size. The step size is developed by trial and error until a satisfactory value is determined.

4. **Runge-Kutta Step** (RK42, lines 286-321) – This is exactly as it is presented in Appendix 3.

5. **Subroutine Deriv** (lines 225-235) – This routine assembles the equation of motion, solved for $\ddot{\theta}$, based on values computed in other routines.

6. **Subroutine Kinem** (lines 236-274) - This begins with the rolling constraint relation, and then repeatedly calls PointP to make position, velocity coefficient, and velocity coefficient derivative calculations for the force application point (A), the spring-damper attachment point (B), and the center of mass (C). It also calculates the length and velocity coefficient for the spring-damper length, S.

7. **Subroutine PointP** (lines 275-285) – This routine implements the position, velocity coefficient, and velocity coefficient derivative calculations for any point (u_p, v_p). The use of a separate subroutine for this purpose is to avoid the rather tedious repeated programming of these equations.

8. **Graphical Output** (lines 168-199) – These are simply the commands to draw the axes for plotting, and then plot the several curves. Several lines of text are also added to the graph to provide maximum values.

9. **Tabular Output** (lines 200-224) – There is the option to list the results in steps of $10h$ (simply to avoid an overly long table). This tabulation continues as long as $\theta > 0$, and stopping after the first negative angle. When this occurs, a search through the previously generated results is undertaken to establish a more precise estimate of the time of impact and the approach velocity just before impact.

7.7.2 Trammel with Pulse Loading

Consider again the trammel system previously considered in Chapters 2 and 6, now dynamically displaced from the rest equilibrium position by the application of blow (a brief force pulse) applied to the vertical slider as shown in Figure 7.7. The problem at hand is to find the motion resulting from the vertical blow.

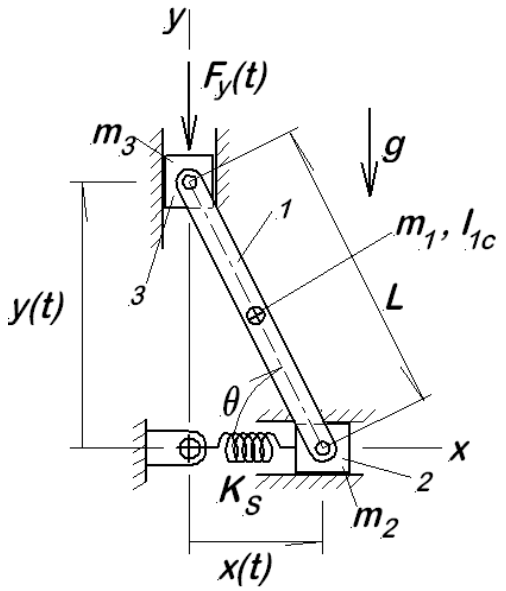

Figure 7.7: Trammel Dynamic System

The external vertical force $F_y(t)$ is only briefly nonzero, and is assumed to take the form

$$\begin{aligned} F_y(t) &= F_o \sin\left(\frac{\pi t}{\tau}\right) \qquad 0 \le t \le \tau = 0.45 \\ &= 0 \qquad\qquad\qquad\qquad t > \tau \end{aligned} \tag{7.56}$$

This functional form, known as a *half-sine pulse*, is a plausible approximation to the form for a force due to an impact from a hammer or similar object.

7.7.2.1 System Equation of Motion

For computing the dynamic response, it is necessary to formulate the equation of motion employing Eksergian's equation of motion. Begin by writing the system kinetic energy, making use of the kinematic results from Chapter 2:

$$\begin{aligned} T &= \frac{1}{2}m_1\left(\dot{x}_c^2 + \dot{y}_c^2\right) + \frac{1}{2}I_{1c}\dot{\theta}^2 + \frac{1}{2}m_2\dot{x}^2 + \frac{1}{2}m_3\dot{y}^2 \\ &= \frac{1}{2}\dot{\theta}^2\left[m_1\frac{L^2}{4}\left(\cos^2\theta + \sin^2\theta\right) + I_{1c} + m_2\left(-L\sin\theta\right)^2 + m_3\left(-L\cos\theta\right)^2\right] \\ &= \frac{1}{2}\dot{\theta}^2\left[\frac{1}{4}m_1L^2 + I_{1c} + m_2L^2\sin^2\theta + m_3L^2\cos^2\theta\right] \end{aligned} \tag{7.57}$$

From this the generalized inertia and centripetal coefficient are extracted

$$\mathbb{I} = \frac{1}{4}m_1L^2 + I_{1c} + m_2L^2\sin^2\theta + m_3L^2\cos^2\theta \tag{7.58}$$

$$\mathbb{C} = \frac{1}{2}\frac{d\mathbb{I}}{d\theta} = \left(m_2 - m_3\right)L^2\sin\theta\cos\theta \tag{7.59}$$

The external forces, other than the blow to the top, are all conservative, and are most easily included by use of a potential energy function, $V(\theta)$, as was done in Chapter 6:

$$V(\theta) = \left(\frac{w_1}{2} + w_3\right)L\sin\theta + \frac{1}{2}K_S\left(L\cos\theta - x_o\right)^2 \tag{7.60}$$

$$\frac{dV}{d\theta} = \left(\frac{w_1}{2} + w_3\right)L\cos\theta - K_S\left(L\cos\theta - x_o\right)L\sin\theta \tag{7.61}$$

In order to include the external blow on the vertical slider, a nonconservative virtual work expression is used to determine the nonconservative generalized force, Q^{nc}:

$$\delta W^{nc} = -F_y(t)\,\delta y = -F_yK_y\,\delta\theta \tag{7.62}$$

$$Q^{nc} = -F_y(t)\,K_y = -F_y(t)\,L\cos\theta \tag{7.63}$$

Then the equation of motion is

$$\begin{aligned} Q^{nc} &= \ddot{\theta}\mathbb{I} + \dot{\theta}^2\mathbb{C} + \frac{dV}{d\theta} \\ &\qquad [-F_y(t) L\cos\theta - \dot{\theta}^2 (m_2 - m_3) L^2 \sin\theta\cos\theta \\ \ddot{\theta} &= \frac{-\left(\frac{1}{2}m_1 + m_3\right) gL\cos\theta + K_S L\sin\theta (L\cos\theta - x_o)]}{\frac{1}{4}L^2 m_1 + I_{1c} + m_2 L^2 \sin^2\theta + m_3 L^2\cos^2\theta} \end{aligned} \tag{7.64}$$

The form of this equation of motion is such as to indicate that a closed form solution is not to be found, and therefore a numerical solution is required. At this point, it is necessary to appeal to the Runge-Kutta process described in Appendix 3.

7.7.2.2 Numerical Example

The physical data for the system remains as previously: $L = 30$ in., $w_1 = 48.287$ lb, $I_{1c} = 9.3800$ lb–s^2–in. For the $x-$axis slider, $w_2 = 17$ lb, and for the $y-$axis slider, $w_3 = 25$ lb, the spring stiffness is $K_S = 60$ lb/in, and the free length of the spring is $x_o = 12$ inches. The vertical blow applied to the top slider is described by

$$\begin{aligned} F_y(t) &= 450\sin\left(\frac{\pi t}{\tau}\right) \qquad 0 \le t \le \tau = 0.45 \text{ sec} \\ &= 0 \qquad\qquad\qquad\qquad \tau < t \end{aligned}$$

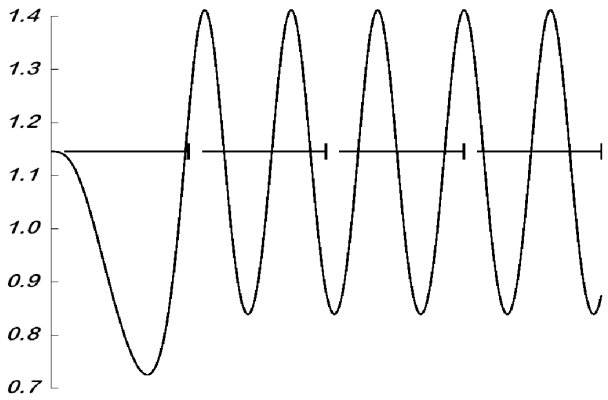

Figure 7.8: Trammel Dynamic Response, $\theta(t)$

There is no known closed form solution for the equation of motion, equation (7.64), but it is not difficult to solve using the Runge-Kutta numerical method described in Appendix 3. The result is plotted in Figure 7.8, along with a horizontal line at the level of the equilibrium value for the angle θ. The horizontal line at the equilibrium level is marked

off in multiples of τ, the duration of the blow that initiates the motion. The vertical axis scale shows the value of $\theta(t)$ in radians. There are several things to observe about the numerical solution:

1. The solution starts with $\theta(0) = \theta_{eq}$, the equilibrium value determined in Chapter 6.
2. The initial motion shows θ diminishing from the blow $F_y(t)$ to a minimum value.
3. The angle is actually above the equilibrium value before the end of the blow.
4. After $F_y(t)$ goes to zero, the system simply oscillates in free vibration.
5. The free vibration phase shows constant amplitude, indicating that there is no energy loss. This is consistent with the fact that no damping was included in the model. In a real system, there would certainly be damping due to the lubricated joints and other friction sources, and this would cause the free vibratory motion to gradually decay in amplitude.
6. The period of the steady oscillation following the end of the blow is $\tau \approx 0.2822$ sec, corresponding to a frequency $f = 3.544$ Hz. This value is determined by taking the time difference between passages through the equilibrium position with positive slope.

7.7.3 Four-Bar Mechanism

The mechanism shown in Figure 7.9 is used in a cardboard box manufacturing operation to spread a viscous glue on the cardboard before the boxes are assembled. This mechanism is a scaled version of the (approximate) straight-line mechanism previously shown in Figure 2.19. A brush-type applicator at point G spreads the glue during the straight line portion of the cycle, and a solenoid on the arm lifts the brush during the return portion of the cycle. While the brush is applying the glue, there is a viscous drag force that opposes the motion with viscous coefficient B; there is no drag force opposing the return motion. The glue application begins at $\theta = \theta_1$ and ends when $\theta = \theta_2$ (see table below for values). In addition to the viscous drag of the glue brush, miscellaneous bearing friction and windage contribute an effective drag $B_{Bearing}$ acting at the input crank.

The entire mechanism is powered by a NEMA Type B induction motor rated at 750 W at 1440 rpm (see Appendix 5.1.3 for the motor torque-speed curve). The motor speed is geared down to the crank speed using three stages of gearing. All of the gears are identical, with $N_g = 68$ teeth, and all of the pinions are identical with $N_p = 19$ teeth. The gearing mass moments of

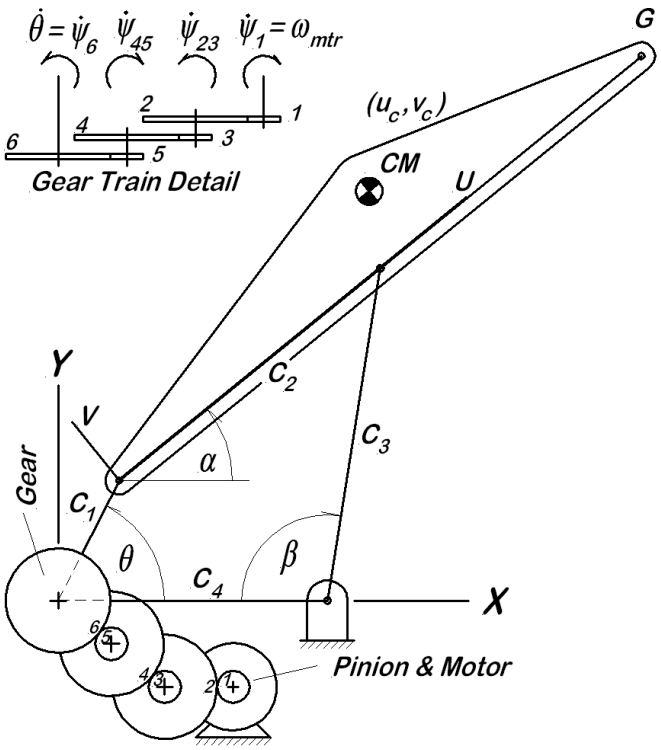

Figure 7.9: Motor Driven Four Bar Linkage for Glue Application Machine

inertia are J_p for each pinion, and J_g for each gear. Numerical values are given in Tables 7.1, 7.2, and 7.3.

The questions of primary interest are:

1. How long does it take for this motor to bring the whole mechanism up to steady speed? This implies that the torque-speed curve for the full speed range is required.

2. What is the cycle time for steady state?

Table 7.1 Dimensional Data	
$C_1 = 0.200$ m	Input Crank Length
$C_2 = 0.500$ m	Coupler Length
$C_3 = 0.500$ m	Second Crank Length
$C_4 = 0.400$ m	Stationary Link Length
$\theta_1 = 84^o$	Crank Angle Where Glue Application Begins
$\theta_2 = 276^o$	Crank Angle Where Glue Application Ends

Table 7.2 Inertial Data		
$J_{1o} =$	24.962 kg-m^2	Input Crank MMOI wrt Fixed Pivot
$J_{Mtr} =$	$4.6803 \cdot 10^{-7}$ kg-m^2	Motor Rotor MMOI
$J_p =$	$6.3315 \cdot 10^{-5}$ kg-m^2	Pinion MMOI
$J_g =$	$1.0388 \cdot 10^{-2}$ kg-m^2	Gear MMOI
$J_{2c} =$	39.003 kg-m^2	Coupler MMOI wrt CM
$M_2 =$	18.721 kg	Mass of Extended Coupler Link
$J_{3o} =$	390.098 kg-m^2	Second Crank MMOI wrt Fixed Pivot

Table 7.3 Additional Parameters	
$u_{2c} = 0.500$ m	Body Coordinate for Coupler Link CM
$v_{2c} = 0.100$ m	Body Coordinate for Coupler Link CM
$u_G = 1.000$ m	Body Coordinate for Glue Brush
$v_G = 0.000$ m	Body Coordinate for Glue Brush
$B_{Glue} = 200$ N-s/m	Glue Brush Viscous Drag Coefficient
217 N-s/m	Bearing Friction Viscous Coefficient

7.7.3.1 Mathematical Formulation

The input crank angle θ is chosen as the generalized coordinate, and the equations of motion must be determined. As indicated in Figure 7.9, the secondary variables are α and β, measured in the same manner as the four-bar mechanism considered in Section 2.5. Most of the necessary kinematic analysis was done in Chapter 2, and can simply be brought forward from there, with the exception of the gear train.

Gear Train From the problem statement, $N_p = 19\ T$ and $N_g = 68\ T$ for each train element pair. The gear train equations of constraint are

$$\psi_{45} = \frac{N_{g6}}{N_{p5}}\theta = \frac{N_g}{N_p}\theta \tag{7.65}$$

$$\psi_{23} = \frac{N_{g4}}{N_{p3}}\psi_{45} = \left(\frac{N_g}{N_p}\right)^2 \theta \tag{7.66}$$

$$\psi_1 = \frac{N_{g2}}{N_{p2}}\psi_{23} = \left(\frac{N_g}{N_p}\right)^3 \theta \tag{7.67}$$

where ψ_1 is the actual motor rotor rotation, $\dot{\psi}_1 = \omega_{mtr}$.

Kinetic Energy and Generalized Inertia As a next step, the kinetic energy of the system is

$$\begin{aligned} T &= \frac{1}{2}[(J_{1o}+J_g)\,\dot{\theta}^2 + (J_p+J_g)\,\dot{\psi}_{45}^2 + (J_p+J_g)\,\dot{\psi}_{23}^2 + (J_p+J_{Mtr})\,\dot{\psi}_1^2 \\ &\quad + J_{2c}\dot{\alpha}^2 + M_2\left(\dot{x}_{c2}^2 + \dot{y}_{c2}^2\right) + J_{3o}\dot{\beta}^2] \\ &= \frac{1}{2}\dot{\theta}^2[J_{1o} + J_g + (J_p+J_g)\left(\frac{N_g}{N_p}\right)^2 + (J_p+J_g)\left(\frac{N_g}{N_p}\right)^4 \\ &\quad + (J_p+J_{Mtr})\left(\frac{N_g}{N_p}\right)^6 + J_{2c}K_\alpha^2 + M_2\left(K_{2cx}^2 + K_{2cy}^2\right) + J_{3o}K_\beta^2] \end{aligned} \tag{7.68}$$

From the kinetic energy, the generalized inertia is identified as

$$\begin{aligned} \mathbb{I}(\theta) &= J_{1o} + J_g + (J_p+J_g)\left(\frac{N_g}{N_p}\right)^2 + (J_p+J_g)\left(\frac{N_g}{N_p}\right)^4 \\ &\quad + (J_p+J_{Mtr})\left(\frac{N_g}{N_p}\right)^6 + J_{3o}K_\beta^2 + J_{2c}K_\alpha^2 + M_2\left(K_{2cx}^2 + K_{2cy}^2\right) \end{aligned} \tag{7.69}$$

and the centripetal coefficient is

$$\mathbb{C}(\theta) = J_{2c}K_\alpha L_\alpha + J_{3o}K_\beta L_\beta + M_2\left(K_{2cx}L_{2cx} + K_{2cy}L_{2cy}\right) \tag{7.70}$$

Notice the role of the tooth number ratio (N_g/N_p) in magnifying the inertia of the motor rotor and gear train components as reflected at the input crank. Thus, even though the motor rotor has a relatively small mass moment of inertia about its own axis, at the input crank of the four bar linkage, it appears like a much larger inertia.

Nonconservative Virtual Work Point G is the point where the glue applicator is located. It traces an approximately straight line, but it is not exactly so. To have an exact expression for the work done by the glue brush, consider first the velocity of the brush, referred to global coordinates with the associated unit vectors $\mathbf{i}$ and $\mathbf{j}$,

$$\begin{aligned} \mathbf{v}_G &= \dot{x}_G\mathbf{i} + \dot{y}_G\mathbf{j} \\ &= \dot{\theta}\left(\mathbf{i}K_{Gx} + \mathbf{j}K_{Gy}\right) \end{aligned} \tag{7.71}$$

The virtual displacement of the contact point is $\delta\mathbf{r}_G$

$$\delta\mathbf{r}_G = \left(\mathbf{i}K_{Gx} + \mathbf{j}K_{Gy}\right)\,\delta\theta \tag{7.72}$$

The *virtual work done on the linkage* by the brush force is then

$$\begin{aligned} \delta W_{Brush} &= -B_{Glue}\, f(\theta)\, \mathbf{v}_G \cdot \delta \mathbf{r}_G \\ &= -B_{Glue}\, \dot{\theta}\, f(\theta)\, \left(K_{Gx}^2 + K_{Gy}^2\right)\, \delta\theta \end{aligned} \tag{7.73}$$

where the lifting of the glue brush (which ends the associated drag force) is described by $f(\theta) = +1$ for $\theta_1 < \theta < \theta_2$, and zero otherwise.

The *virtual work done on the linkage* by the motor torque is

$$\begin{aligned} \delta W_{Mtr} &= T_{Mtr}\left(\dot{\psi}_1\right)\, \delta\psi_1 \\ &= T_{Mtr}\left(\omega_{mtr}\right) \left(\frac{N_g}{N_p}\right)^3 \delta\theta \end{aligned} \tag{7.74}$$

so that the net external virtual work done on the linkage is

$$\delta W = \left[T_{Mtr}\left(\omega_{mtr}\right) \left(\frac{N_g}{N_p}\right)^3 - B_{Bearing}\dot{\theta} - B_{Glue}\, \dot{\theta}\, f(\theta) \left(K_{Gx}^2 + K_{Gy}^2\right) \right] \delta\theta \tag{7.75}$$

The generalized force is identified from the virtual work expression as

$$Q^{NC} = T_{Mtr}\left(\omega_{mtr}\right) \left(\frac{N_g}{N_p}\right)^3 - B_{Bearing}\dot{\theta} - B_{Glue}\, \dot{\theta}\, f(\theta) \left(K_{Gx}^2 + K_{Gy}^2\right) \tag{7.76}$$

From the terms just described, the equation of motion can be assembled to evaluate the second derivative, as will be required for the numerical integration. A review of the terms shows that the required kinematic solutions are $\alpha(\theta)$, $\beta(\theta)$, $K_\alpha(\theta)$, $K_\beta(\theta)$, $L_\alpha(\theta)$, and $L_\beta(\theta)$. All of the other required information, such as the base coordinates and velocity coefficients for point (G), the velocity coefficients, and velocity coefficient derivatives for the center of mass, and so on, can be determined directly from these six functions. The necessary function values can then be determined using the example program in Section 2.3.

Returning to the mainstream of the problem, the equation of motion is given by Eksergian's form as

$$\mathbb{I}(\theta)\, \ddot{\theta} + \mathbb{C}(\theta)\, \dot{\theta}^2 = Q^{NC} \tag{7.77}$$

with the initial conditions

$$\theta(0) = 0.0 \qquad\qquad \dot{\theta}(0) = 0.0 \tag{7.78}$$

All of the required coefficients are expressed above. Solving this for the second derivative, as required for the Runge-Kutta solution, gives:

$$\ddot{\theta} = \frac{1}{\mathbb{I}(\theta)} \left[Q^{NC} - \mathbb{C}(\theta)\, \dot{\theta}^2 \right] \tag{7.79}$$

7.7.3.2 Simulation Results

The equation of motion has been solved numerically using the RK42 algorithm presented in Appendix 3. The results of the simulation, plotted as normalized functions of time, are shown first in Figure 7.10. The maximum crank angle is approximately 5.3 revolutions, while the maximum crank speed is approximately 3.3 rad/s. The curve that starts at zero but soon begins to look almost like two straight lines is the input crank angle. Note that, for about 12 seconds, the motor labors, with the crank speed and correspondingly the motor speed, remaining very low. After that time, the rate of increase of the angle becomes much more rapid, again almost appearing as a straight line. The variations in crank speed are much more evident in the second curve which is a succession of peaks and valleys.

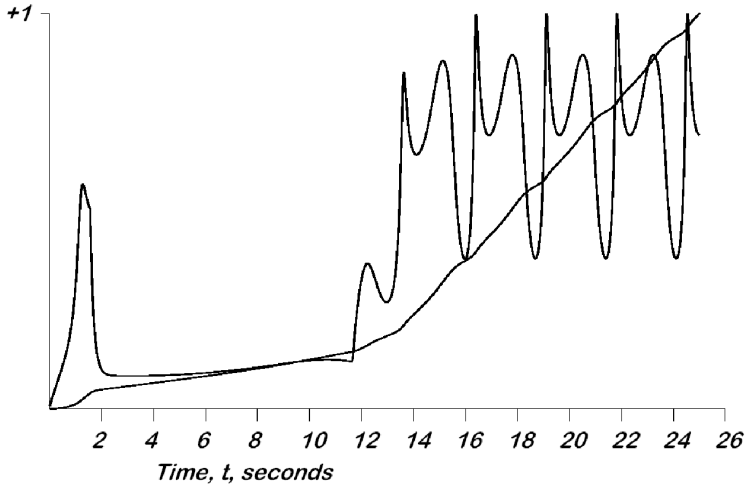

Figure 7.10: Input Crank Angle (smooth curve) and Crank Speed (jagged curve) Versus Time

The appearance of the curves in Figure 7.10 for the later time values suggests that a repeating speed variation is developing, and this is seen much more clearly in Figure 7.11. The two vertical lines are located at θ_1 and θ_2, the beginning and end of the glue application cycle.

In Figure 7.11, the input crank speed is shown as a function of crank angle over each revolution. The speed starts at zero and initially climbs rapidly until the load due to

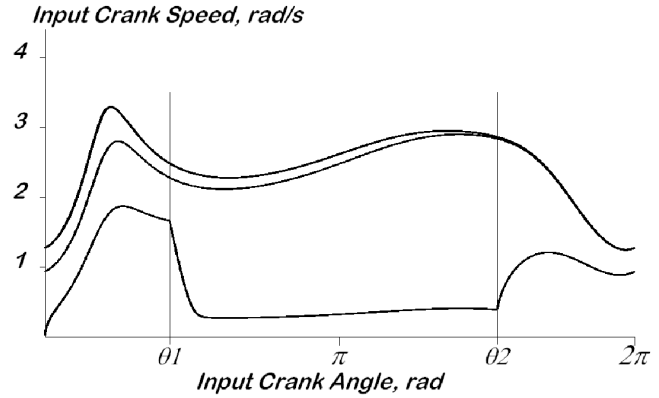

Figure 7.11: Input Crank Speed as a Function of Crank Angle

activation of the glue applicator slows it down. During that first revolution, the speed remains quite low until the glue applicator lifts and the drag is reduced. The end of the first (lowest) curve is continued as the next curve up on the left end. It is evident that, during the second cycle at just about θ_2, the system falls into the steady state. The steady state is described by the top curve which repeats over and over.

The cyclic nature of the speed variation is the defining characteristic for steady operation. It is evident that the crank angle, θ, does not repeat but rather increases endlessly. The crank speed, however, does show a periodic response and this has to be what has to be meant by steady state. **Note that steady state does not mean constant speed;** it only means a cyclic once per revolution variation in the speed.

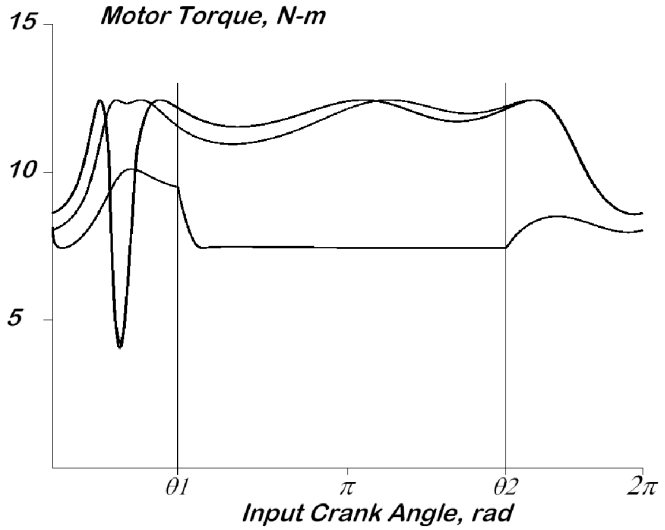

Figure 7.12: Motor Torque as a Function of Input Crank Angle

With the motor speed varying as shown in the two preceding figures, it is certainly to

be expected that the motor torque will likewise vary. Figure 7.12 shows the variation of motor torque for the first, second, and all later revolutions of the input crank. The effect of the glue applicator in loading the system during start-up is clearly evident in the flat line across the middle of the first cycle (lowest curve). On the second cycle, the motor torque is fairly constant through the entire revolution, but then when the steady state develops, it is seen that there is a sharp dip in the motor torque shortly before $\theta = \theta_1$. When this happens, the stored kinetic energy of the mechanism is providing most of the energy required to drive the system, but this condition lasts only briefly. The torque again rises to approximately 12 N-m until the end of the revolution where it drops to about 8 N-m. This cyclic variation continues indefinitely, as long as the system remains unchanged due to wear, loss of power, increased friction, or some other upset.

Returning at last to the two questions raised at the beginning, the results are these:

1. From Figure 7.10, the approximate beginning of steady state operation is about 14 seconds after electrical power is applied to the motor. This is nearing the end of the second revolution of the input crank.

2. From the plotting program, the times for each revolution can be fairly well estimated (when the program jumps back to start a new cycle curve). This gives an estimated cycle time of 2.708 seconds.

7.8 Conclusion

Eksergian's equation provides a simple, direct way to obtain the equation of motion for single degree of freedom mechanisms. The alternative approach, based on the application of Newton's Second Law to a group of free bodies, is much longer and more prone to errors for systems of even modest complexity. Furthermore, the alternative approach produces a large system of equations, from which the force terms must be eliminated to obtain the equation of motion. With application of Eksergian's equation, the equation of motion follows in just a few steps after the system kinetic energy is written.

The generalized inertia shows the role of each mass within the system as it affects the complete system inertia. The velocity coefficients tie this all together because they relate the individual component velocities to the generalized velocity. However, perhaps the most useful aspect of Eksergian's equation is the manner in which the effect of varying generalized inertia is taken into account through the centripetal coefficient. The use of velocity coefficient derivatives to express the centripetal coefficient shows the varying effect of each individual mass on the system as a whole. The generalized force, previously introduced in Chapter 6 as a term that must vanish for equilibrium, is here seen to drive the motion. In some cases, it is useful to split the generalized force into a nonconservative

term and a conservative term, the latter expressed as the gradient of a potential function. The velocity coefficients are again useful in expressing these terms.

For systems of any significant degree of complexity, the resulting differential equations are almost always unsolvable in closed form. They do, however, lend themselves readily to numerical solution by means of the Runge-Kutta algorithm. Thus there is really no need to consider the equations of motion as excessively difficult; the means for numerical solution is readily at hand!

References

[1] R. Eksergian, "Dynamical Analysis of Machines" in 15 parts, *J. of the Franklin Institute*, Vols. 209, 210, 211, 1930-1931.

[2] Myklebust, A., "Dynamic Response of an Electric Motor-Linkage System During Startup," *J. Mechanical Design, Trans. ASME*, Vol. 104, Jan. 1982.

[3] Myklebust, A., Fernandez, E.F., and Choy, T.S., "Dynamic Response of Slider Crank Machines During Startup," *J. Mechanisms, Transmissions, and Automation in Design, Trans. ASME*, Vol. 106, Dec. 1984.

[4] Paul, B., "Analytical Dynamics of Mechanisms A Computer Oriented Overview," *Mechanism and Machine Theory*, Vol. 10, 1975.

[5] Paul, B. *Kinematics and Dynamics of Planar Machinery*, Englewood Cliffs, N.J.: Prentice-Hall, 1979.

Problems

For all of the problems in this set, the objective is to formulate the equation of motion and the appropriate initial conditions. For that purpose, the following five parts are required for each problem:

a. Kinematic analysis as required;

b. Determination of kinetic energy, generalized inertia, and centripetal coefficient;

c. Determination of the complete generalized force, or the nonconservative generalized force and the appropriate potential function;

d. Determination of the equation of motion;

e. Determination of the appropriate initial conditions.

With regard to item **a**, in those cases where an analytical position solution appears practical, the solution should be done. In cases where no analytical position solution is evident, set up the position equations and note that a numerical solution is required. Then, develop the velocity coefficients, velocity coefficient derivatives, base coordinates, and so forth as will be required for the later parts of the problem. For the later parts, do not substitute the expressions for secondary variables, velocity coefficients, and velocity coefficient derivatives, but simply refer to them by the standard notations. Be careful to use consistent subscripting throughout. Many of the data items are indicated on the figures, such as M_1 or J_{4c}. These are understood to be known values, with the subscripts identifying the body with which they are associated. A subscript c on a mass moment of inertia is understood to indicate the center of mass as the reference point for that value. Similarly, a subscript o indicates that the reference point is a fixed pivot. Do not consider gravitational effects except when the gravity vector is shown in the figure. In most cases, the initial values can be determined in closed form, but there may be some cases where a numerical process is required. If so, set up the equations to be solved and identify the numerical procedure to be used, but do not attempt to complete the solution. In those cases where a generalized coordinate has been denoted by q or θ, the equation of motion should be written in terms of that variable. If no generalized coordinate is indicated, then a suitable choice must be made.

7-1 The two sliders with masses M_1 and M_2 are separated by a constant distance L. The center of mass for the connecting link is located by the body polar coordinates (R_c, A_c). Forces F_X and F_Y act at the point located by the body polar coordinates (R_F, A_F). Note the dashpot acting on the vertical slider, developing a force equal to the dashpot coefficient B multiplied by the velocity of the slider. The slider M_1 is initially moving to the right with speed V_{xo} and the horizontal slider pivot is at position X_o.

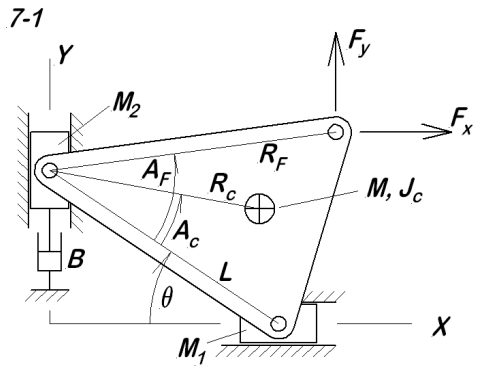

7-2 The four-bar linkage hangs as a pendulum, swinging in planar motion under the influence of gravity. The link lengths are C_1, C_2, C_3, and C_4, and the primary variable is the angle of the first crank, θ. For each link, the center of mass is at the center of the link. Do not make any small angle assumptions.

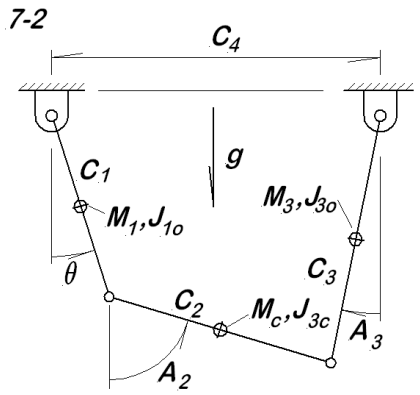

7-3 The roller rolls without slipping on the horizontal surface, while the lever rotates and slides along the stationary pin in the slot. Gravity acts vertically downward. The dimensions C, H,and R are all known. The system is initially at $\theta = 0$ with the roller moving to the right at the speed V_{xo}.

7-4 A slider of mass M_S and centroidal mass moment of inertia J_{SC} moves along the pendulum shaft under the control of gravity and an inextensible tape. The other end of the tape is wrapped around a stationary circular drum of radius C. When the pendulum is vertical, the slider position is $R = R_o$, a given value. There is also a spring with stiffness K acting between the pendulum and a fixed point to the left. The pendulum center of mass is at radius A and the pendulum has mass M_P and mass moment of inertia J_{PC}. The system is released from rest with $\theta = 35^o$, and at that position, the spring is relaxed.

7-5 The mass M_3 (with mass moment of inertia J_{3c}) slides without friction on both the ramp and the pendulum shaft. When the pendulum shaft is vertical, the slider center

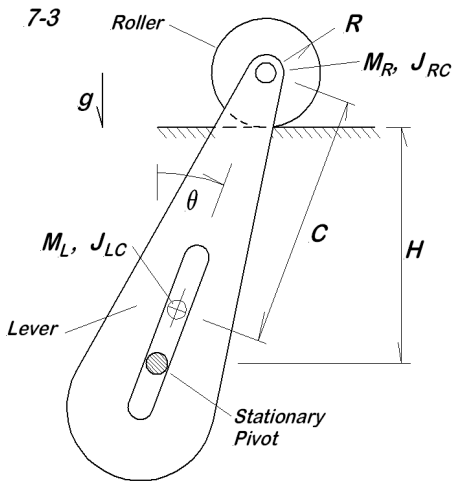

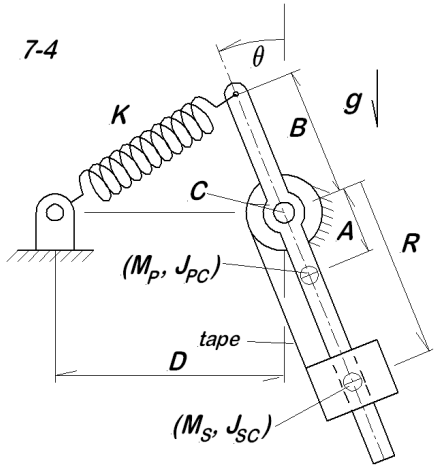

of mass is a distance B directly below the pivot. The pendulum shaft is of length L and mass M_1, while the bob is a thin, uniform disk of mass M_2 and diameter D. The associated mass moments of inertia for the bob should be determined. The system is released with $\theta = 0$, and the slider is moving with speed V_{3o} down the ramp, measured parallel to the ramp.

7-6 The trammel crank drive involves a drive disk with mass moment of inertia J_c, two slider, each with mass M_s and centroidal mass moment of inertia J_{sc}, a third slider with mass M_x, and a uniform connecting rod with mass distribution m = mass/length. Viscous friction, described by the coefficient B, acts at three places as indicated. The system is driven by the couple T_o as indicated. Initially, the slider M_x is at the midpoint of its stroke and its speed is V_{xo} to the right.

7-7 The figure shows one crank throw of an *integral engine-compressor*, a type of machine commonly used in the gas pipeline industry. The double-acting compressor cylinder is

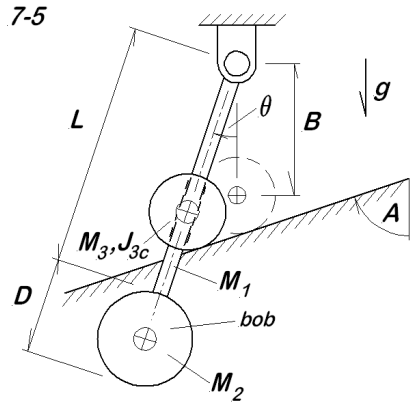

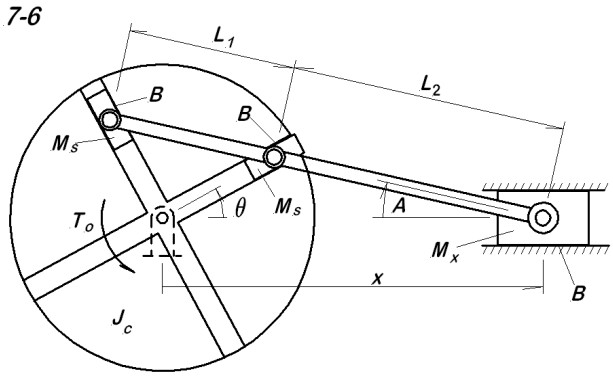

horizontal, while the power cylinder is inclined to the horizontal by the angle ϕ. An articulated connecting rod mechanism is used, with the master rod attached to the compressor crosshead. The slave rod goes to the power piston from the master rod. Consider the cylinder pressures to be the following known functions:

$P_h = P_h\left(X_1, \dot{X}_1\right)$ compressor head-end pressure, acting on area A_h

$P_c = P_c\left(\dot{X}, \dot{X}_1\right)$ compressor crank-side pressure, acting on area A_c

$P_p = P_p\left(X_2, \dot{X}_2\right)$ power cylinder pressure, acting on area A_p

The crank, with radius R, has mass moment of inertia J_o with respect to the fixed pivot. The master rod has length L_1, mass M_1, and mass moment of inertia J_{1c}; the master rod center of mass is located by body coordinates (u_c, v_c). The slave rod attaches to the master rod at the point (u_p, v_p) and the slave rod has mass M_2 and mass moment of inertia J_{2c}. The crosshead, piston rod, and piston assembly has mass M_3. The slave rod center of mass is a distance u_2 upward from the point of connection with the master rod, and the total length of the slave rod is L_2. At $t = 0$, the power piston is at top dead center, and the crosshead is moving to the left with speed V_{xo}.

7-8 Each link has uniform mass distribution, with m =mass/length, and the slider mass

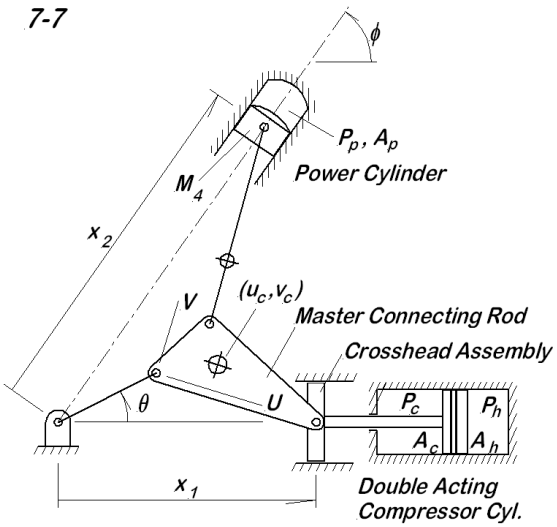

is M_s. The system is subject to the applied force F and the viscous force on the lower face of the slider. At $t = 0$, the system is at rest with the length L_2 perpendicular to L_3.

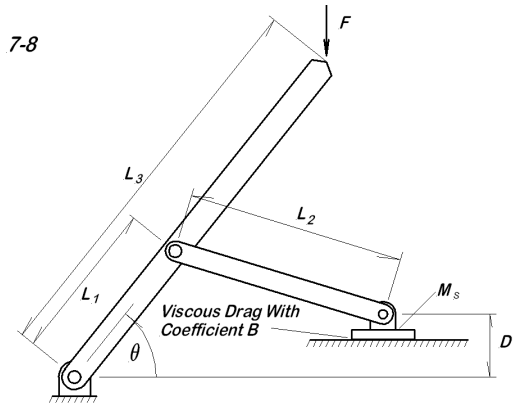

7-9 The figure shows a four-bar linkage with a massive coupler link; the other links are massless. The center of mass of the coupler link is located at (u_c, v_c), as indicated. The system is driven by applied forces F_x and F_y, and subject to a retarding force developed in the dashpot. The dashpot connection location (u_B, v_B) and the point of force application, (u_F, v_F), are all known. When the motion begins, the link C_1 is along the $Y-$axis, and the coupler center of mass has horizontal velocity V_{xo}.

7-10 The *quick return mechanism* consists of two sliders of mass M_1 and M_2, respectively, and uniform bars for the connecting link and the crank. The mass per unit length for the connecting link is m. The length of the connecting link is L and the crank radius is R. The slider where the crank drives the connecting link is considered massless. The mass moment of inertia of the crank with respect to the fixed pivot is J_R. The system is driven by the moment T acting on the crank and force F on the horizontal slider.

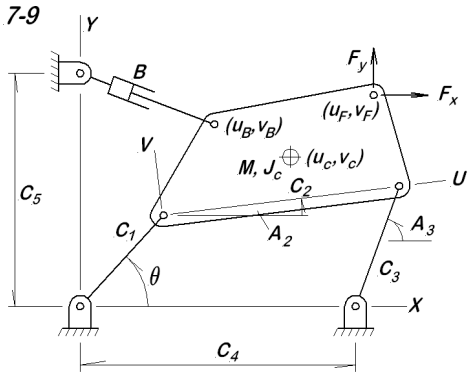

Viscous friction, described by coefficients B_1 and B_2, acts on the two sliders. At $t = 0$, the crank is perpendicular to the connecting link, and rotating clockwise at 20 rad/sec.

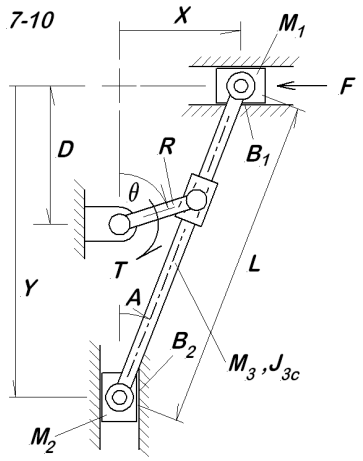

7-11 The figure shows another variation on the *quick return mechanism*. The lever has mass moment of inertia J_o with respect to the fixed point. The system is driven by the moment T and the force F acting on the horizontal slider. Viscous friction, described by B_s acts on the slider. Viscous friction, described by B_p, also acts on each pin sliding in the lever slots. The system is initially at $\theta = 0$ with the slider moving to the right with speed V_{xo}.

7-12 The mechanism shown is an air-actuated press that is used in a manufacturing operation; the alert reader will recall this system from problems **6-3** and **6-4**. The geometric data provided in problem **6-4** may be assumed for use here. The air cylinder is supplied air at gauge pressure P_a acting on an effective piston area A_a. The motion is resisted by the force $F(z)$. The significant masses in the system are the press ram and the crank; the other parts may be considered massless. The mass of the ram is M_R, and the crank has mass moment of inertia J_o with respect to the fixed point. The pivot locations on the crank are defined by the three distances S_1, S_2, and S_3. The system is initially at rest with $q = q_{\text{Min}}$, the minimum length of the air cylinder assembly.

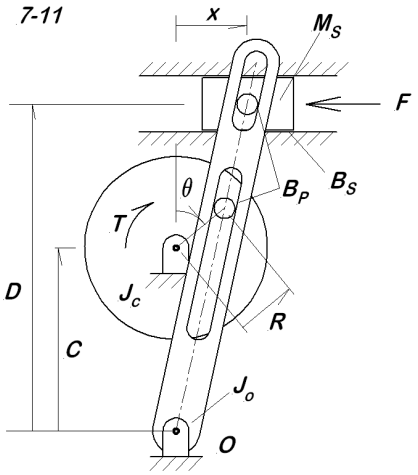

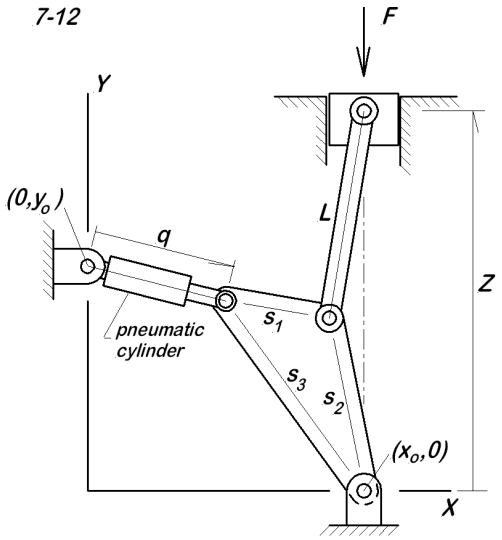

7-13 The mechanism shown is a double slider-crank device, proposed for use in cutting polymeric materials. The cutting action is the force F at a tool mounted on the slider at the upper right corner of the figure. Primary interest is in the steady state operation of the machine, The input crank at the origin of coordinates is driven by a torque, T_m, from an induction motor (see Appendix 5.1.4.1 for the linear model applicable near steady state). The actual cutting force is assumed to be a brief rectangular pulse lasting only through a short portion of the cycle. There is also a viscous damping action throughout the entire cycle that is proportional to the velocity of the cutting tool. The masses for each link, each slider, and the motor mass moment of inertia are all known. It is assumed that the center of mass for each link is at the center of mass for the link. Associate the single degree of freedom with the motor rotation angle, ϕ. The mechanism arises in a research paper published a few years ago from Serbia[2].

[2]Cveticanin, L, Maretic, R. and Zukovic,M, "Dynamics of Polymer Sheets Cutting Mechanism,"

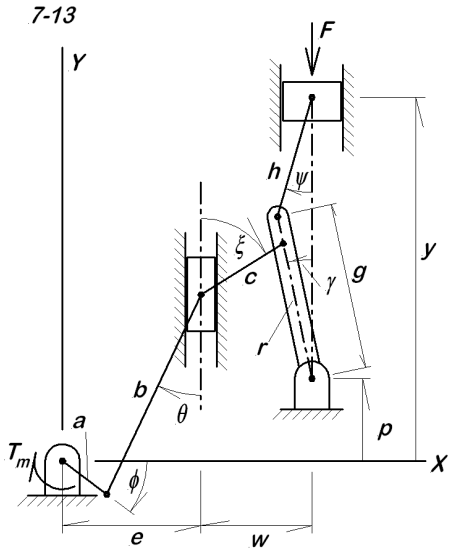

Strojniski Vestnik - Journal of Mechanical Engineering, Vol. 58, No. 5, 2012, pp. 354-361.

Chapter 8

MDOF Machine Dynamics

8.1 Introduction

In the previous Chapter 7, the dynamics of single degree of freedom systems were described by means of Eksergian's equation, an energy based approach to obtaining the system equations of motion for single degree of freedom systems. As demonstrated there, the energy approach is a very powerful way to deal with complicated systems involving machine components that are both rotating and translating. This chapter complements the previous chapter by introducing the Lagrange form for the equations of motion, an energy based approach to the equations of motion applicable to multidegree of freedom systems. As in the previous case, the kinetic energy plays a central role, and the use of potential energy is again optional. The Lagrange form can also be applied to single degree of freedom systems, but it is slightly less convenient than Eksergian's form. Where both are applicable, the final equation of motion is identical in both cases.

In Chapter 3, where the kinematics of multidegree of freedom mechanisms are considered, it was observed that (a) the process for position analysis is virtually identical to that for single degree of freedom mechanisms, but (b) the analysis of velocities and accelerations is considerably more complex. As indicated there, systems with multiple degrees of freedom are often best considered on a case-by-case basis, making use of the advantageous features of each specific problem, coupled with the insight of the analyst. To a large extent, these same comment applies to the dynamics of such systems as well as the kinematics, and this is the approach used through most of this chapter.

Even so, the lack of an entirely general approach has long posed a challenge for those who seek a single method for dealing with all problems. At the end of the current chapter, such a general approach is sketched as a starting point for those who wish to pursue the topic further.

8.2 Notation

In formulating theory for multidegree of freedom systems, it is convenient to utilize the classical notation for generalized coordinates, that is, $\{q\} = \text{col}\,(q_1,\ q_2,\ q_3,\ \ldots,\ q_n)$ for a system involving n generalized coordinates. Any particular generalized coordinate is then designated as q_j. In dealing with a particular mechanical system, for which the specific generalized coordinates might happen to be $\{q\} = \text{col}\,(\theta,\ x,\ z,\ \phi)$, it is often more convenient to use the symbols specific to that problem. The reader should have no difficulty distinguishing the intent of the notation from the context.

8.3 Kinetic Energy for MDOF Machine

In Appendix 6 it is shown that, for any single rigid body, the kinetic energy may be written in the form

$$T = \frac{1}{2} M \{V_c\}^T \{V_c\} + \frac{1}{2} \{\omega\}^T [I_c] \{\omega\} \tag{8.1}$$

where

M = mass of the body

$[I_c]$ = mass moment of inertia matrix for the body with respect to the center of mass

$\{V_c\}$ = velocity vector for the center of mass

$\{\omega\}$ = angular velocity vector for the body

This result is of fundamental importance in the application energy methods as already demonstrated in Chapter 7 and to be further demonstrated in the present chapter. It applies for motion in both two dimensions and three dimensions. If the body is constrained to move in two dimensions only, the expression can be somewhat simplified to

$$T = \frac{1}{2} M \left(\dot{x}_c^2 + \dot{y}_c^2\right) + \frac{1}{2} I_c \omega^2 \tag{8.2}$$

where $\dot{x}_c$ and $\dot{y}_c$ are the in-plane center of mass velocity components, and ω is the (scalar) angular velocity.

Kinetic energy quantities are simple scalars and therefore directly additive. For a multibody system, the total system kinetic energy is simply the sum of the kinetic energies of

the several components, so that

$$\begin{aligned} T = & \frac{1}{2} M_1 \{V_{1c}\}^T \{V_{1c}\} + \frac{1}{2} \{\omega_1\}^T [I_{1c}] \{\omega_1\} \\ & + \frac{1}{2} M_2 \{V_{2c}\}^T \{V_{2c}\} + \frac{1}{2} \{\omega_2\}^T [I_{2c}] \{\omega_2\} \\ & + \cdots \end{aligned} \tag{8.3}$$

The work that follows demonstrates that the kinetic energy expression contains within it all of the system information regarding inertia and acceleration terms. It is absolutely central to the analysis of multidegree of freedom systems.

8.4 Lagrange Equation First Form

The first general form for the Lagrange equation of motion is developed in Appendix 7 where it is written as

$$\frac{d}{dt} \frac{\partial T}{\partial \dot{q}_j} - \frac{\partial T}{\partial q_j} = Q_j \tag{8.4}$$

where

q_j is any of the generalized coordinates of the system;

T is the system kinetic energy;

Q_j is the generalized force associated with the coordinate q_j.

(It may be useful to review Chapter 6 where the concept of the generalized force is discussed in more detail.) This is a parallel to Eksergian's equation (7.21), but this expression applies for any number of degrees of freedom where Eksergian's form only applies to a single degree of freedom system. It also applies to those base excited single degree of freedom systems for which Eksergian's equation did not apply.

8.5 Lagrange Equation Second Form

Just as was true for single degree of freedom systems, there are many multidegree of freedom systems in which some of the forces are derivable from a potential energy function. This is particularly true for systems involving gravitational or spring forces. In that case, the complete generalized force can be separated into two parts, one due to the

potential function and the second due to nonconservative forces. With this separation, the complete generalized force is

$$Q_j = -\frac{\partial V\left(\{q\}\right)}{\partial q_j} + Q_j^{nc} \tag{8.5}$$

where

$V\left(\{q\}\right)$ is the potential function that depends upon some or all of the generalized coordinates;

Q_j^{nc} is the remaining, nonconservative portion of the generalized force that is not representable by the potential function. Note the superscript *nc* to indicate *nonconservative*.

When this form is substituted into the first general form of the Lagrange equation, after some re-arrangement, the result is either of these:

$$\frac{d}{dt}\frac{\partial T}{\partial \dot{q}_j} - \frac{\partial T}{\partial q_j} + \frac{\partial V}{\partial q_j} = Q_j^{nc} \tag{8.6}$$

$$\frac{d}{dt}\frac{\partial \mathcal{L}}{\partial \dot{q}_j} - \frac{\partial \mathcal{L}}{\partial q_j} = Q_j^{nc} \tag{8.7}$$

where $\mathcal{L}$ is called the Lagrangian function, $\mathcal{L} = T - V$. These expressions are equivalent because $\partial\mathcal{L}/\partial\dot{q}_j = \partial T/\partial\dot{q}_j - \partial V/\partial\dot{q}_j$ where the last term is always zero because velocities can not appear in the potential function.

Many people prefer the last, more compact form for the Lagrange equation of motion. This is particularly true among physicists and those concerned with the development of theory; it is less true among engineers whose principal concern is solving specific problems. The first form of the Lagrange equation, or either variation of the second form may be applied to any holonomic system problem. When done correctly, they always produce exactly the same resulting equations of motion.

8.6 Applications of the Lagrange Equation

The real power of the Lagrange formulation is not evident until it is used to work problems. In application, it is clearly more direct and less prone to error than the vector methods of Newton. Several examples follow.

8.6.1 Three Blocks on a Ramp

Consider the motion of three blocks on a ramp, connected by spring and damper assemblies as shown in Figure 8.1. The position reference lines are at (unknown) fixed distances, c_1 and c_2. The two springs are strain free when $x_1 = x_2 = x_3 = 0$.

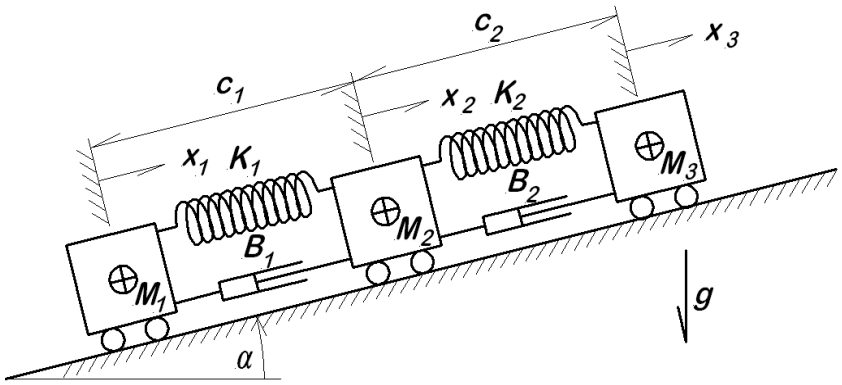

Figure 8.1: Three Blocks on a Ramp

The system has three degrees of freedom, easily associated with the three coordinates x_1, x_2, and x_3. The first step is to deal with the kinematics, specifically the change in length of the two springs. The unstretched lengths of the springs are

$$s_{1o} = c_1 - d_{12} \tag{8.8}$$
$$s_{2o} = c_2 - d_{23} \tag{8.9}$$

where d_{12} and d_{23} are the rigid body portions of the distances c_1 and c_2. With displacement of the bodies, the spring lengths are

$$s_1 = c_1 - d_{12} + x_2 - x_1 \tag{8.10}$$
$$s_2 = c_2 - d_{23} + x_3 - x_2 \tag{8.11}$$

The strain energy of the springs is then

$$\begin{aligned} V_s &= \frac{1}{2}K_1 (s_1 - s_{1o})^2 + \frac{1}{2}K_2 (s_2 - s_{2o})^2 \\ &= \frac{1}{2}K (x_2 - x_1)^2 + \frac{1}{2}K_2 (x_3 - x_2)^2 \end{aligned} \tag{8.12}$$

The complete potential energy expression, including both spring strain energy and gravitational potential terms, is then

$$\begin{aligned} V &= \frac{1}{2}K\left(x_2 - x_1\right)^2 + \frac{1}{2}K_2\left(x_3 - x_2\right)^2 \\ &\quad + g\sin\alpha\left[M_1 x_1 + M_2\left(c_1 + x_2\right) + M_3\left(c_1 + c_2 + x_3\right)\right] \end{aligned} \tag{8.13}$$

The system kinetic energy is T

$$T = \frac{1}{2}\left(M_1\dot{x}_1^2 + M_2\dot{x}_2^2 + M_3\dot{x}_3^2\right) \tag{8.14}$$

There are working forces not taken into account by the potential energy, specifically the dashpot forces, so it is necessary to develop the nonconservative virtual work,

$$\begin{aligned} \delta W^{nc} &= -B_1\left(\dot{x}_2 - \dot{x}_1\right)\delta\left(x_2 - x_1\right) - B_2\left(\dot{x}_3 - \dot{x}_2\right)\delta\left(x_3 - x_2\right) \\ &= -B_1\left(\dot{x}_2 - \dot{x}_1\right)\delta x_2 + B_1\left(\dot{x}_2 - \dot{x}_1\right)\delta x_1 \\ &\quad -B_2\left(\dot{x}_3 - \dot{x}_2\right)\delta x_3 + B_2\left(\dot{x}_3 - \dot{x}_2\right)\delta x_2 \\ &= \delta x_1\left[B_1\left(\dot{x}_2 - \dot{x}_1\right)\right] \\ &\quad +\delta x_2\left[-B_1\left(\dot{x}_2 - \dot{x}_1\right) + B_2\left(\dot{x}_3 - \dot{x}_2\right)\right] \\ &\quad +\delta x_3\left[-B_2\left(\dot{x}_3 - \dot{x}_2\right)\right] \end{aligned} \tag{8.15}$$

from which the generalized nonconservative forces are

$$Q_1^{nc} = B_1\left(\dot{x}_2 - \dot{x}_1\right) \tag{8.16}$$

$$Q_2^{nc} = -B_1\left(\dot{x}_2 - \dot{x}_1\right) + B_2\left(\dot{x}_3 - \dot{x}_2\right) \tag{8.17}$$

$$Q_3^{nc} = -B_2\left(\dot{x}_3 - \dot{x}_2\right) \tag{8.18}$$

For the application of the Lagrange formulation, the necessary derivatives of T and V are

$$\frac{\partial T}{\partial x_1} = 0 \tag{8.19}$$

$$\frac{\partial T}{\partial \dot{x}_1} = M_1\dot{x}_1 \tag{8.20}$$

$$\frac{d}{dt}\frac{\partial T}{\partial \dot{x}_1} = M_1\ddot{x}_1 \tag{8.21}$$

$$\frac{\partial V}{\partial x_1} = -K_1\left(x_2 - x_1\right) + M_1 g\sin\alpha \tag{8.22}$$

$$\frac{\partial T}{\partial x_2} = 0 \tag{8.23}$$
$$\frac{\partial T}{\partial \dot{x}_2} = M_2 \dot{x}_2 \tag{8.24}$$
$$\frac{d}{dt}\frac{\partial T}{\partial \dot{x}_2} = M_2 \ddot{x}_2 \tag{8.25}$$
$$\frac{\partial V}{\partial x_2} = K_1 (x_2 - x_1) - K_2 (x_3 - x_2) + M_2 g \sin\alpha \tag{8.26}$$

$$\frac{\partial T}{\partial x_3} = 0 \tag{8.27}$$
$$\frac{\partial T}{\partial \dot{x}_3} = M_3 \dot{x}_3 \tag{8.28}$$
$$\frac{d}{dt}\frac{\partial T}{\partial \dot{x}_3} = M_3 \ddot{x}_3 \tag{8.29}$$
$$\frac{\partial V}{\partial x_3} = K_2 (x_3 - x_2) + M_3 g \sin\alpha \tag{8.30}$$

When the equations of motion are assembled according to the Lagrange formulation, the results are

$$-M_1 g \sin\alpha = M_1 \ddot{x}_1 + B_1 (\dot{x}_1 - \dot{x}_2) + K_1 (x_1 - x_2) \tag{8.31}$$
$$\begin{aligned} -M_2 g \sin\alpha &= M_2 \ddot{x}_2 - B_1 \dot{x}_1 + (B_1 + B_2)\dot{x}_2 - B_2 \dot{x}_3 \\ &\quad -K_1 x_1 + (K_1 + K_2) x_2 - K_2 x_3 \end{aligned} \tag{8.32}$$
$$-M_3 g \sin\alpha = M_3 \ddot{x}_3 - B_2 \dot{x}_2 + B_2 \dot{x}_3 - K_2 x_2 + K_2 x_3 \tag{8.33}$$

When these results are recast in matrix form, the result is

$$\begin{bmatrix} M_1 & 0 & 0 \\ 0 & M_2 & 0 \\ 0 & 0 & M_3 \end{bmatrix} \begin{Bmatrix} \ddot{x}_1 \\ \ddot{x}_2 \\ \ddot{x}_3 \end{Bmatrix} + \begin{bmatrix} B_1 & -B_1 & 0 \\ -B_1 & B_1 + B_2 & -B_2 \\ 0 & -B_2 & B_2 \end{bmatrix} \begin{Bmatrix} \dot{x}_1 \\ \dot{x}_2 \\ \dot{x}_3 \end{Bmatrix} + \begin{bmatrix} K_1 & -K_1 & 0 \\ -K_1 & K_1 + K_2 & -K_2 \\ 0 & -K_2 & K_2 \end{bmatrix} \begin{Bmatrix} x_1 \\ x_2 \\ x_3 \end{Bmatrix} = -g \sin\alpha \begin{Bmatrix} M_1 \\ M_2 \\ M_3 \end{Bmatrix} \tag{8.34}$$

Note that the distances c_1, c_2, d_{12}, and d_{23} do not appear in the equations of motion, and thus are not required for their formulation. Note also that the extension to a similar system with more blocks is entirely evident from the form shown here.

This example problem involves a chain-like system, one in which the motion of each mass is only influenced by that of its two nearest neighbors. Such a system is said to be *close-coupled*. The form of the stiffness matrix in equation (8.34) is said to be of *triple band diagonal form,* referring to the fact that the only nonzero elements are on the main diagonal, the first super diagonal, and the first subdiagonal. The triple band diagonal form is a direct consequence of the close-coupled nature of the system. In contrast, beam bending vibrations are not close-coupled.

8.6.2 Pendulum Vibration Absorber

The pendulum vibration absorber is a device often used in reciprocating machines (internal combustion engines and reciprocating compressors) to control torsional vibration, the primary topic of Chapter 12. Figure 8.2 shows such an absorber in a simplified form. The primary mass (representing the crank and connected mechanism) turns about a fixed center and has mass moment of inertia I_o. The pendulum is idealized as a point mass (m) on a massless link of length L attached to the primary mass at a radius R. The motion of the primary mass is described by the angle $\Omega t + \theta\,(t)$, where Ω is a relatively large, steady value representing the average speed of the crank. An external torque, $\mathbb{T}\,(t)$, acts on the primary mass causing the motion irregularity, $\theta\,(t)$, that is to eliminated.

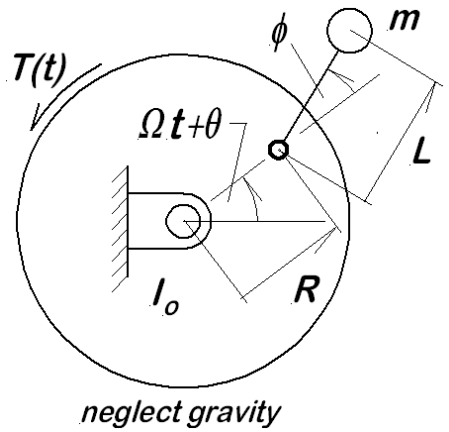

Figure 8.2: Pendulum Absorber on Engine Crank

The position of the point mass pendulum relative to stationary coordinates is given by

$$x_p = R\cos(\Omega t + \theta) + L\cos(\Omega t + \theta + \phi) \tag{8.35}$$

$$y_p = R\sin(\Omega t + \theta) + L\sin(\Omega t + \theta + \phi) \tag{8.36}$$

The velocity components are

$$\dot{x}_p = -R\left(\Omega+\dot{\theta}\right)\sin\left(\Omega t+\theta\right)-L\left(\Omega+\dot{\theta}+\dot{\phi}\right)\sin\left(\Omega t+\theta+\phi\right) \tag{8.37}$$

$$y_p = R\left(\Omega+\dot{\theta}\right)\cos\left(\Omega t+\theta\right)+L\left(\Omega+\dot{\theta}+\dot{\phi}\right)\cos\left(\Omega t+\theta+\phi\right) \tag{8.38}$$

The system kinetic energy is T

$$T=\frac{1}{2}I_o\left(\Omega+\dot{\theta}\right)^2+\frac{1}{2}m\left(\dot{x}_p^2+\dot{y}_p^2\right) \tag{8.39}$$

There is no potential energy involved in this problem because gravity is completely neglected; the motion may be in any plane, but the rotational effects are dominant over the gravitational effects. The virtual work of the external torque is

$$\delta W^{nc}=\mathbb{T}\left(t\right)\,\delta\theta \tag{8.40}$$

from which the generalized forces are

$$Q_\theta = \mathbb{T}\left(t\right) \tag{8.41}$$

$$Q_\phi = 0 \tag{8.42}$$

The application of the Lagrange formulation requires the determination of several derivatives. When all the differentiations are completed, and the results simplified, these give one side of each of the two equations of motion which are then set equal to the two generalized forces. The results are these:

$$\begin{aligned}\mathbb{T}\left(t\right) = {} & \ddot{\theta}\left[I_o+2mRL\cos\phi+m\left(R^2+L^2\right)\right]+\ddot{\phi}m\left(L^2+RL\cos\phi\right)\\ & -m\left[2\left(\Omega\ +\dot{\theta}\right)\dot{\phi}+\dot{\phi}^2\right]RL\sin\phi\end{aligned} \tag{8.43}$$

$$0 = \ddot{\theta}\left(L^2+RL\cos\phi\right)+\ddot{\phi}L^2+L\sin\phi\left(R\Omega^2+R\dot{\theta}^2+2R\Omega\dot{\theta}\right) \tag{8.44}$$

where the common factor m is divided out of the second equation of motion.

As mentioned previously, the primary reason this system is of interest is its application as a vibration absorber. The next step is to show how the pendulum system can be made to function in that role.

If the rotational vibration of the crank is eliminated, $\theta=0$, and the crank angular displacement is simply Ωt; this is the intended result. To achieve that end, it is important that the pendulum acts as a linear device which implies small oscillations only [1]. Assuming all of this to be true, there are three conditions to be imposed at this point: $\theta=0$, $\cos\phi\approx 1$. $\sin\phi\approx\phi$.

Consider first the impact of these conditions on the second equation of motion.

$$\ddot{\phi} + (R/L)\,\Omega^2\phi = 0 \tag{8.45}$$

It is evident that, in linear form, the pendulum has the natural frequency ω_n

$$\omega_n = \Omega\sqrt{R/L} \tag{8.46}$$

Suppose that the disturbing torque is of the form $\mathbb{T}(t) = T_o \sin(n\Omega t)$ where $n = 1, 2, 3, \ldots$. To achieve the intended purpose, it is necessary to tune the pendulum such that the natural frequency of the pendulum coincides with the oscillatory order to be removed. Thus choose R/L such that

$$\begin{aligned} n\Omega &= \Omega\sqrt{R/L} \\ R/L &= n^2 \end{aligned} \tag{8.47}$$

This means that the natural frequency of the pendulum is not constant, but in fact varies directly in proportion to the gross rotational speed of the system. The pendulum motion is then sinusoidal,

$$\phi(t) = \Phi \sin(n\Omega t) \tag{8.48}$$

Turn next to the first of the equations of motion, and again impose the linearization conditions there. The result is an expression for the torque required to cancel the external disturbing torque:

$$\begin{aligned} \mathbb{T}(t) &= T_o \sin(n\Omega t) \\ &= m\left[\ddot{\phi}\left(L^2 + RL\right)\right] \\ &= mL^2\left(1 + n^2\right) n^2\Omega^2\Phi \sin(n\Omega t) \\ &= mR^2\left(1 + n^2\right)\Omega^2\Phi \sin(n\Omega t) \end{aligned} \tag{8.49}$$

or

$$T_o = mR^2\left(1 + n^2\right)\Omega^2\Phi \tag{8.50}$$

Reference [1] makes two important points in regard to this device:

1. The mass of the pendulum has no effect on the tuning;

2. The mass must be correctly sized to effectively remove the intended harmonic.

The first of these points is evident in the expression for ω_n; the mass m does not appear there. The second is seen in the equation of motion that produces the torque on the system. Note that the torque produced by the pendulum is proportional to the product $m \cdot \Phi$, so that a smaller mass results in a larger pendulum amplitude in order to cancel a specified torque harmonic. Reference [1] cautions that the pendulum amplitude must be limited to a maximum value of $\Phi \leq 0.2$ radians for satisfactory results.

8.6.3 Induction Motor Starting a Blower

Consider a system consisting of an induction motor driving a blower through a friction clutch and gear train. Such a system is shown in Figure 8.3. Initially, with the clutch disengaged, the motor is started and brought up to no-load speed. After the motor is up to speed, the clutch begins to engage progressively. As the clutch engages, the motor speed drops due to the imposed load, while the blower train accelerates. During the initial engagement, the clutch slips until it develops sufficient friction to provide the torque required to both (a) accelerate the train, and (b) drive the aerodynamic load of the blower. Eventually the relative motion across the clutch ceases, and the entire machine train rotates together. While the clutch is slipping, the system has two degrees of freedom; after the clutch is locked, the system is reduced to a single degree of freedom. The detailed description and modeling of the system follows below. A computer program is required to solve the equations of motion with a view to answering these questions:

(1) How long does it take for the blower to reach final operating speed?
(2) What is the final operating speed of the motor under load?
(3) What is the minimum motor speed?
(4) What is the maximum torque transmitted by the clutch?
(5) How much energy is dissipated as heat in the clutch?

Motor The electric motor for this system has the following characteristics:

3 Phase Induction Motor

Rated Voltage	460 v	Synch Speed	$\omega_s = 1800$ rpm
Rated Current	59.5 amp	No-load Speed	$\omega_{nl} = 1790$ rpm
Power Factor	0.86 @ 60 Hz	Rated Speed	$\omega_r = 1700$ rpm
Power	37 kW	Rotor MMOI	$J_m = 0.1481$ kg-m^2

The motor is assumed to follow the linear torque speed relation described in Appendix 5.1.4.1,

$$T_m(\omega_m) = c_o + c_1\omega_m \tag{8.51}$$

where the constants are determined to produce the rated and no-load conditions specified for the motor.

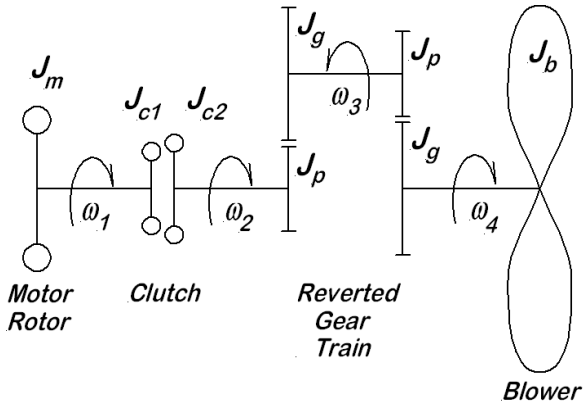

Figure 8.3: Blower Driven Through a Clutch by an Induction Motor

Clutch The clutch for this system is an air-actuated, multiple disk, dry clutch. It consists of two members, with inertias denoted as $J_{c1} = 0.0035$ kg-m^2 on the motor side and $J_{c1} = 0.0117$ kg-m^2 on the output side. To avoid a damaging shock to the mechanical system when the blower is started, the clutch engages gradually over a time interval of $t_{rise} = 0.45$ seconds. According the manufacture's data for this clutch, the torque transmission capacity of the clutch rises with engagement time according to the expression

$$T_{tc}(t) = \begin{cases} \frac{1}{2}T_{cr}\left[1 - \cos\left(\frac{\pi t}{t_{rise}}\right)\right] & t \le t_{rise} \\ T_{cr} & t > t_{rise} \end{cases} \tag{8.52}$$

The torque capacity of the clutch is the actual torque transmitted as long as the clutch is slipping. After slipping ceases, the torque transmitted through the clutch may have any value not exceeding the rated maximum value, $T_{cr} = 230$ N-m.

Gear Set The motor speed is too fast for a large blower, and the necessary speed reduction is accomplished by a two stage, reverted gear train as shown in Figure 8.3. Both stages are identical, and each involves a 29 tooth pinion driving a 114 tooth gear. Thus the gear ratio for each mesh is $N = 29/114$. The inertias for each pinion and gear are $J_p = 0.0023$ kg-m^2 and $J_g = 0.5531$ kg-m^2.

Blower The whole purpose of this train is to drive an industrial blower rated at 12 kW when operating at 110 rpm. In the absence of other data about the power required

at various speeds, the blower is assumed to follow the typical aerodynamic cubic power law

$$P_b = c_b \cdot \omega_4^3 \tag{8.53}$$

where ω_4 is the impeller speed (rad/s). Based on the given data regarding rated power and speed for the blower, the constant $c_b = 185.67288$ kW-s^3. It follows then that the torque required to drive the blower at other speeds is expressible as

$$T_b = c_b \cdot \omega_4^2 \tag{8.54}$$

The blower is quite large, and has far greater mass moment of inertia than the other components in the train, $J_b = 31.0$ kg-m^2.

For the present example, losses in the gears and elsewhere are neglected; in professional practice, these should be included. Similarly, the mass moments of inertia for the various shafts, couplings, and so forth, are neglected here, but should be included in engineering practice.

8.6.3.1 System Equations of Motion

Before developing the equations of motion, it is first necessary to determine the number of degrees of freedom and then define appropriate generalized coordinates. Because this is a rotating machine, the angular positions of the various components are irrelevant; what are significant are the time derivatives of the angular positions, the angular velocity values.

At the end of the start-up process, after the clutch is locked up, the system has only one degree of freedom. In the early part of the start-up, while the clutch is slipping, the system has two degrees of freedom. Throughout the entire start-up process, the motor speed is an appropriate generalized coordinate velocity. Indeed, after the clutch is locked up, it is sufficient to describe all of the system velocities. While the clutch is slipping, it is necessary to have a second generalized coordinate to describe the state of the components to the right of the clutch. The clutch output shaft velocity is a suitable choice for the second coordinate velocity, although it is not the only possible choice. For this example, the generalized coordinate velocities for two degrees of freedom are taken as ω_1 and ω_2, the motor speed and the clutch output shaft speed. When the problem reduces to only a single degree of freedom, ω_1, the motor speed, is used as the single generalized coordinate velocity. The whole matter of the changing number of degrees of freedom is one of the unusual aspects of this problem.

The first step in preparation for applying the Lagrange equation of motion is to develop the system kinetic energy. This is written first in terms of the angular velocities of the individual components, and then revised to include the kinematic constraint conditions that exist:

$$\begin{aligned} T \;=\; & \frac{1}{2}\left(J_m + J_{c1}\right)\omega_1^2 + \frac{1}{2}\left(J_{c2} + J_p\right)\omega_2^2 \\ & + \frac{1}{2}\left(J_g + J_p\right)\omega_3^2 + \frac{1}{2}\left(J_g + J_b\right)\omega_4^2 \end{aligned} \tag{8.55}$$

where

J_m = motor rotor MMOI

J_{c1} = clutch input half MMOI

J_{c2} = clutch output half MMOI

J_p = pinion MMOI

J_g = gear MMOI

J_b = blower MMOI

With the kinematic constraints included, the expression for the kinetic energy is

$$\begin{aligned} T \;=\; & \frac{1}{2}\left(J_m + J_{c1}\right)\omega_1^2 \\ & + \frac{1}{2}\left[\left(J_{c2} + J_p\right) + \left(J_g + J_p\right)N^2 + \left(J_g + J_b\right)N^4\right]\omega_2^2 \end{aligned} \tag{8.56}$$

where $N = 29/114$ is the ratio of a single stage of the gear reduction.

Before assembling the Lagrange equations, it is necessary to develop two derivative relations:

$$\frac{\partial T}{\partial \omega_1} \;=\; \left(J_m + J_{c1}\right)\omega_1 \tag{8.57}$$

$$\frac{\partial T}{\partial \omega_2} \;=\; \left[\left(J_{c2} + J_p\right) + \left(J_g + J_p\right)N^2 + \left(J_g + J_b\right)N^4\right]\omega_2 \tag{8.58}$$

The required further time differentiation of these expressions is trivial, and is not written out here. To avoid the need to write out the mass moment of inertia sums, it is convenient

to define

$$J_1 = J_m + J_{c1} \tag{8.59}$$
$$J_2 = (J_{c2} + J_p) + (J_g + J_p) N^2 + (J_g + J_b) N^4 \tag{8.60}$$

Note that the partial derivatives with respect to the angles are both zero, because as mentioned above, for the rotating machine, the angles are irrelevant.

All that remains for the completion of the Lagrange form is the development of the nonconservative virtual work, leading to the generalized force expressions. The nonconservative virtual work is

$$\begin{aligned} \delta W^{nc} &= T_m \delta\theta_1 - T_c \delta\theta_1 + T_c \delta\theta_2 - T_b \delta\theta_b \\ &= (T_m - T_c)\, \delta\theta_1 + \left(T_c - N^2 T_b\right) \delta\theta_2 \\ &= (T_m - T_c)\, \delta\theta_1 + \left(T_c - N^6 C_b \omega_2^2\right) \delta\theta_2 \end{aligned} \tag{8.61}$$

where

θ_1 = motor shaft rotation angle

θ_2 = clutch output shaft rotation angle

T_m = motor output torque

T_c = torque through the clutch

T_b = blower torque

It is evident that, while there are two degrees of freedom, the nonconservative generalized forces are

$$Q_1^{nc} = T_m - T_c \tag{8.62}$$
$$Q_2^{nc} = T_c - N^6 C_b \omega_2^2 \tag{8.63}$$

When the system reduces to a single degree of freedom, $\delta\theta_2 = \delta\theta_1$, and the single nonconservative generalized force is

$$Q = T_m - N^6 C_b \omega_2^2 \tag{8.64}$$

where the clutch torque is no longer doing work on the system. The final forms for the equations of motion are

2 DOF

$$J_1\dot{\omega}_1 = T_m(\omega_1) - T_c(\omega_1, \omega_2, t) \tag{8.65}$$
$$J_2\dot{\omega}_2 = T_c(\omega_1, \omega_2, t) - N^6 C_b \omega_2^2 \tag{8.66}$$

1 DOF

$$(J_1 + J_2)\dot{\omega}_1 = T_m(\omega_1) - N^6 C_b \omega_1^2 \tag{8.67}$$

Note that, in equations (8.65) and (8.66), the clutch torque is indicated explicitly as a function of the two shaft speeds (as to whether it is slipping or not) and time (as to the clutch torque capacity as the contact force builds). After the reduction to one degree of freedom, the clutch torque is no longer in the equation of motion, but it may be calculated with either of the following expressions:

$$T_c = T_m - J_1\dot{\omega}_1 = J_2\dot{\omega}_1 + N^6 C_b \omega_1^2 \tag{8.68}$$

Looking at equations (8.65) and (8.66), it is evident that these equations are not as fully coupled as one might expect in general. Specifically, there is no mathematical coupling between $\dot{\omega}_1$ and $\dot{\omega}_2$ which would be expected in a more general situation. This makes the present system particularly simple for numerical solution.

8.6.3.2 System Simulation

In the initial phase, with the clutch slipping, the system has two degrees of freedom, represented by two, first order ordinary differential equations, (8.65) and (8.66). The numerical solution for these equations is readily accomplished using the Runge-Kutta algorithms described in Appendix 3. When a numerical simulation of this system is run, the following results are produced:

```
Calculated System Parameters
Motor Coefficients
co=36867.774
c1=196.6823
Blower Coefficient
cb=185.67288

              Engagement History
dof    t      omega1      omega2     Tc
     sec      rad/s       rad/s      N-m
```



```
2   0.00   187.45     0.00     0
2   0.01   187.44     0.01     0
2   0.02   187.42     0.04     1
2   0.03   187.38     0.14     3
2   0.04   187.30     0.33     4
2   0.05   187.21     0.64     7
2   0.06   187.09     1.10    10
2   0.07   186.92     1.74    13
2   0.08   186.78     2.58    17
2   0.09   186.60     3.66    28
2   0.10   186.39     5.00    27
.
.
.
2   0.21   183.06    40.96   103
2   0.22   182.70    46.24   111
2   0.23   182.34    51.81   119
.
.
.
2   0.43   177.19   167.91   229
2   0.44   177.14   171.51   230
2   0.45   177.11   174.77   230
1   0.46   177.39   177.39   203
1   0.47   178.34   178.34   193
1   0.48   178.80   178.80   187
1   0.49   179.02   179.02   185
1   0.50   179.13   179.13   184
1   0.51   179.18   179.18   183
1   0.52   179.21   179.21   183
1   0.53   179.22   179.22   183
1   0.54   179.22   179.22   183
1   0.55   179.23   179.23   183
1   0.56   179.23   179.23   183
1   0.57   179.23   179.23   183
1   0.58   179.23   179.23   183
1   0.59   179.23   179.23   183
1   0.60   179.23   179.23   183
```

The plotted results are shown in Figure 8.4. The speed curves utilize the full range of the vertical axis, but the two torque curves only use the range $0 \rightarrow 100$ to plot the torques as percentages of the clutch rated torque. There are several noteworthy points evident in both the data table and the plotted results.

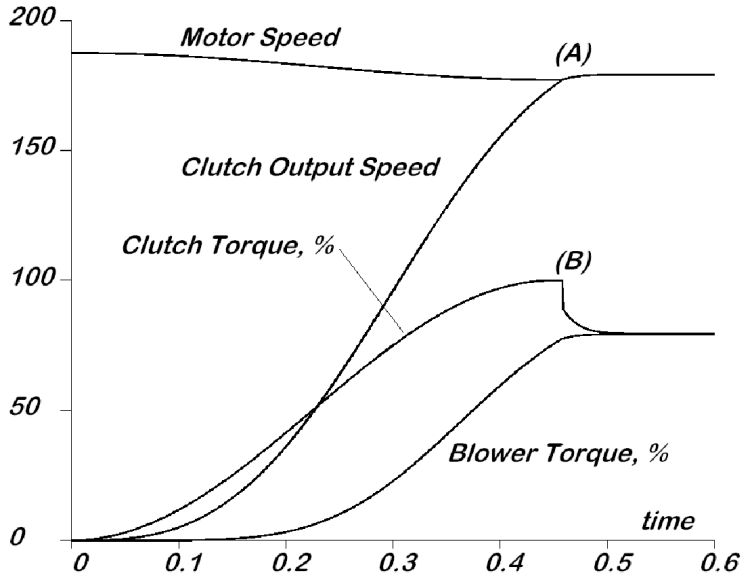

Figure 8.4: Induction Motor Starting A Blower Through A Clutch

1. At time $t = 0$, the motor is at the no-load speed, but as the clutch gradually engages, the motor speed drops to point (A) due to the increased torque load imposed on the motor.

2. At time $t = 0$, the clutch output speed starts at zero and gradually increases as the clutch engages.

3. Time $t_A \approx 0.445$ seconds is where the clutch output speed is finally up to that of the motor shaft and the clutch stops slipping. After the clutch locks up, notice that the curve shows that the system accelerates slightly as a single degree of freedom. This is evident in the numerical data table as well.

4. The blower torque curve, expressed as a percent of the clutch rated torque, is the lowest curve plotted. It rises continuously as the blower speed increases.

5. The clutch torque rises continuously with increasing time up to point (B) where it briefly attains the clutch rated torque level. After point (B), the clutch torque drops suddenly when the clutch stops slipping. But notice that it does not immediately fall all the way to the level of the blower torque. It is this continuation of motor torque in excess of that required to drive the blower that causes the system to accelerate as a single degree of freedom system.

Returning now to the original list of questions that were to be addressed, the answers are evident in the observations above.

1. How long does it take to reach final operating speed? – From the tabulated data, it is evident that the final motor operating speed is $\omega_1 = 179.23$ rad/s first achieved at $t = 0.55$ seconds.

2. What is the final operating speed of the motor under load? – As just mentioned in the previous answer, $\omega_1 = 179.23$ rad/s is the final motor speed.

3. What is the minimum motor speed? – The plotted results show that the minimum motor speed occurs at the point where the clutch locks up, $t_A \approx 0.445$ sec where the motor speed is between 177.11 and 177.14 rad/s.

4. What is the maximum torque transmitted by the clutch? – The tabulated data shows the maximum value is 230 N-m, the clutch rated torque, at the point of lock-up.

5. How much energy is dissipated as heat in the clutch? – This last question requires a little bit more work, as shown below.

The energy lost in the clutch is the work done by the friction torque in the clutch. Consider separately the energy input to the clutch and then the energy out of the clutch, expressed as integrals of the related power expressions:

$$W_{in} = \int T_c \, d\theta_1 = \int T_c \cdot \omega_1 \, dt \tag{8.69}$$

$$W_{out} = \int T_c \, d\theta_2 = \int T_c \cdot \omega_2 \, dt \tag{8.70}$$

The energy lost is the difference of these two work values,

$$\begin{aligned} W_{lost} &= W_{in} - W_{out} \\ &= \int T_c \, (\omega_1 - \omega_2 \,) \, dt \end{aligned} \tag{8.71}$$

where the integration extends over the duration of the clutch slip. In the computer code, after the simulation is completed, it is a simple matter to use the trapezoidal rule to compute the lost energy integral, with the result $W_{lost} = 3807.55$ Joules. This completes the answers to all of the original questions.

There are other questions that could be addressed with the same primary computer program, such as

- What is the effect of increasing the clutch rated capacity?
- What is the effect of a shorter clutch capacity rise time?

- What would be the effect of replacing the gear train with a two-stage belt drive?
- What are the maximum gear tooth forces found in the present system?
- If losses in the gear set are included, how does this change the results?

The reader may wish to consider how the computer program would need to be modified to answer each of these additional questions.

8.7 A More General Approach

The Lagrange form for the equations of motion offers an approach to dealing with all holonomic systems, but the application to specific problems often entails a significant amount of analysis. The desire to circumvent this laborious task has led to the search for approaches that put the labor on a computer, rather than on a human analyst. There have been a number of programs developed, including IMP (**I**ntegrated **M**echanisms **P**rogram, J.J. Uicker), DRAM (**D**ynamic **R**esponse of **A**rticulated **M**achines, M.A. Chase), ADAMS (**A**utomatic **D**ynamic **A**nalysis of **M**echanical **S**ystems, N.V. Orlandea), DADS (**D**ynamic **A**nalysis and **D**esign **S**ystem, E.J. Haug and R. Wehage) [2] and perhaps others as well. The essential ideas of the DADS program are detailed in [3]. The methods of such computer codes are usually relatively unattractive for manual calculation because they forfeit any advantages offered by the details of a specific problem.

As already demonstrated in this chapter, the kinetic energy is the key element in describing the system dynamics. The potential energy may be a useful tool in some cases, but it is never required. This observation regarding the essential nature of the kinetic energy is the fundamental observation behind this more general approach.

8.7.1 Alternate Points of View

The purpose for this section is to present an approach to formulating multidegree of freedom problems in a very general way, suitable for computer implementation. To this end, the familiar slider-crank mechanism is analyzed as a multidegree of freedom mechanism to demonstrate the approach. The system is shown in several forms in Figure 8.5.

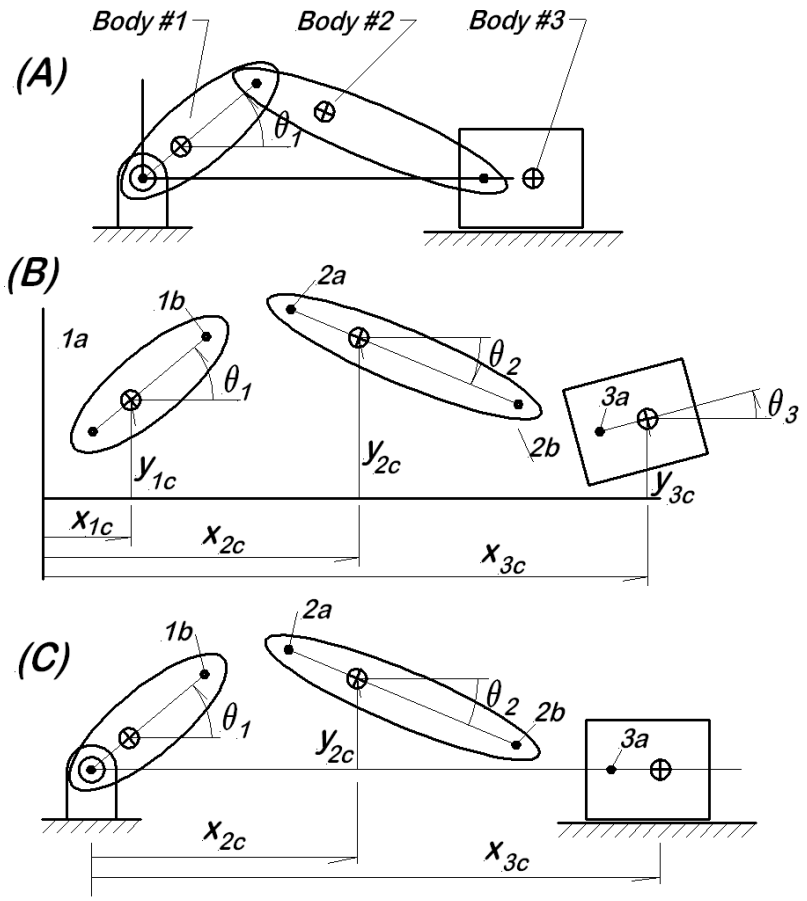

Figure 8.5: Three Approaches to Modeling a Slider-Crank Mechanism

8.7.1.1 (A) – SDOF Model

At the top of the figure, there is the familiar form for the slider-crank mechanism, modeled as a single degree of freedom system. The kinematics for this system are developed in Chapter 2 and the dynamic analysis is detailed in Chapter 7. Knowledge of the one generalized coordinate, θ_1, is sufficient to determine the complete geometry of the system, and θ_1, with its time derivatives, fully describes the system dynamics.

8.7.1.2 (B) – 9 DOF Model

In the middle of the figure, the disassembled slider-crank is shown, consisting of three separate bodies. The system is constrained to move in a plane, so each body has three degrees of freedom. This gives a total of nine degrees of freedom for the model (note that nothing is said as yet about connecting the bodies). Seen is this way, a suitable set

of generalized coordinates is $\{q\} = \text{col}(x_{1c},\, y_{1c},\, \theta_1,\, x_{2c},\, y_{2c},\, \theta_2,\, x_{3c},\, y_{3c},\, \theta_3)$. In terms of these generalized coordinates, the system kinetic energy is

$$\begin{aligned} T \;=\; \frac{1}{2}[&M_1\left(\dot{x}_{1c}^2 + \dot{y}_{1c}^2\right) + J_{1c}\dot{\theta}_{1c}^2 \\ &+M_2\left(\dot{x}_{2c}^2 + \dot{y}_{2c}^2\right) + J_{2c}\dot{\theta}_{2c}^2 \\ &+M_3\left(\dot{x}_{3c}^2 + \dot{y}_{3c}^2\right) + J_{3c}\dot{\theta}_{3c}^2] \end{aligned} \tag{8.72}$$

where

M_1, J_{1c} are the mass and mass moment of inertia of the crank with respect to the crank center of mass;

M_2, J_{2c} are the mass and mass moment of inertia of the connecting rod with respect to the rod center of mass;

M_3, J_{3c} are the mass and mass moment of inertia of the slider with respect to the slider center of mass.

Note that the form for the contribution from each body is exactly the same. This facilitates computer formulation of the problem. When the Lagrange form is applied to this system, the result is nine ordinary differential equations (ODEs), all of the same general form.

The system connectivity is expressed in the form of the loop equations, understood as equations of constraint. For each body, assume a body coordinate system oriented with the $U-$axis along the body and the $V-$axis perpendicular in the usual fashion, but *with the origin in each case at the body center of mass.* Then the left end connection for each body has the body coordinates $(-u_{ic}, 0)$ and the right end connection has body coordinates $(L_i - u_{ic}, 0)$, where L_i is the overall length of the body. The eight equations of constraint, written in terms of the generalized coordinates, are these:

- Crank Pivot Stationary:

$$x_{1c} - u_{1c}\cos\theta_1 \;=\; 0 \tag{8.73}$$

$$y_{1c} - u_{1c}\sin\theta_1 \;=\; 0 \tag{8.74}$$

- Crank and Connecting Rod Joint, Point 1b and Point 2a Must Coincide:

$$[x_{2c} - u_{2c}\cos\theta_2] - [x_{1c} + (L_1 - u_{1c})\cos\theta_1] \;=\; 0 \tag{8.75}$$

$$[y_{2c} - (L_2 - u_{2c})\cos\theta_2] - [y_{1c} + (L_1 - u_{1c})\sin\theta_1] \;=\; 0 \tag{8.76}$$

- Connecting Rod and Slider Joint, Point 2b and Point 3a Must Coincide:

$$[x_{3c} - u_{3c}\cos\theta_3] - [x_{2c} + (L_2 - u_{2c})\cos\theta_2] \;=\; 0 \tag{8.77}$$

$$[y_{3c} - u_{3c}\sin\theta_3] - [y_{2c} - (L_2 - u_{2c})\sin\theta_2] \;=\; 0 \tag{8.78}$$

- Slider Only Translates Without Rotation:

$$y_{3c} = 0 \tag{8.79}$$
$$\theta_3 = 0 \tag{8.80}$$

All of this means that there is a system of nine ODEs and eight algebraic-trigonmetric equations required to describe the system. Such a system is called a system of Differential Algebraic Equations (DAEs), and special methods are required for their solution.

Notice the similarity in form for all the equations of constraint. This similarity is the sort of thing that facilitates computer implementation. But preserving the similarity requires neglecting to take advantage of simplifications that are evident in the particular problem. Computer implementation thrives on uniformity of approach but dies on special cases!

8.7.1.3 (C) – 5DOF Model

Four of the eight equations of constraint simply express lack of motion, either that a point does not move in a particular direction or that a body does not rotate. Constraints of this type can be incorporated into the computer formulation to significantly reduce the problem size, although the fundamental nature of the formulation remains unchanged. For the slider-crank, consider the five degree of freedom model shown in the part C of Figure 8.5 where the generalized coordinate vector is then reduced to $\{q\} = \mathrm{col}\,(\theta_1,\ x_{2c},\ y_{2c},\ \theta_2,\ x_{3c})$. In terms of these five generalized coordinates, the kinetic energy is

$$\begin{aligned} T = \frac{1}{2}[&J_{1o}\dot{\theta}_1^2 \\ &+M_2\left(\dot{x}_{2c}^2+\dot{y}_{2c}^2\right)+J_{2c}\dot{\theta}_{2c}^2 \\ &+M_3\dot{x}_{3c}^2] \end{aligned} \tag{8.81}$$

where all the parameters remain the same as previously, except that the crank mass moment of inertia with respect to the rotation axis is used, rather than the center of mass value. This formulation has the advantage that no data are required for M_1, u_{1c} or for J_{3c}.

In writing the kinetic energy in this form, four of the constraints are directly incorporated in a manner similar to that done in Chapter 2, but the system retains five degrees of freedom. The other four constraints still apply in slightly modified form:

- Crank and Connecting Rod Joint, Point 1b and Point 2a Must Coincide:

$$[x_{2c} - u_{2c}\cos\theta_2] - L_1\cos\theta_1 = 0 \tag{8.82}$$
$$[y_{2c} - (L_2 - u_{2c})\cos\theta_2] - L_1\sin\theta_1 = 0 \tag{8.83}$$

- Connecting Rod and Slider Joint, Point 2b and Point 3a Must Coincide:

$$[x_{3c} - u_{3c}\cos\theta_3] - [x_{2c} + (L_2 - u_{2c})\cos\theta_2] = 0 \tag{8.84}$$
$$[y_{3c} - u_{3c}\sin\theta_3] - [y_{2c} - (L_2 - u_{2c})\sin\theta_2] = 0 \tag{8.85}$$

The result of this formulation is a system of only five ODEs along with four algebraic-trigonometric equations. The benefit is a smaller system, but it is still a system of DAEs.

8.7.2 Comparisons

With either of the constrained systems approaches, the 9 DOF model or the 5 DOF model, the result is a system of equations described by what are called *sparse matrices*, that is, matrices with relatively few nonzero elements. In comparing the loop closure method that is presented throughout this book, with the constrained system technique used in the DADS computer code, Haug, et al. [3, p. 2] say this:

> The loop closure method generates equations that require closure of each independent loop of the linkage. The resulting nonlinear equations are then differentiated to obtain the smallest possible number of independent equations of motion, in terms of a minimum number of system degrees of freedom. Thus, the loop closure method generates a small number of highly nonlinear equations that are solved with standard numerical integration methods. The constrained system modeling method, on the other hand, explicitly treats three degrees of freedom for each element (in the plane). Algebraic equations prescribing constraints between the various bodies are then written and elementary forms of equations of motion for each body are written separately. The constraint equations prescribing assembly of the mechanism are adjoined to the equations of motion through use of Lagrange multipliers *(see below)*. Thus, one treats a large number of equations in many variables. These equations may be solved by an implicit numerical integration method that iteratively solves a linear matrix equation. The saving grace of this technique is that the matrix that arises in the iterative process is sparse. That is, only three to ten percent of the elements of the matrix are different from zero.

They further say "It has been shown that it is usually more efficient to solve large systems of sparse equations, rather than smaller systems with greater percentages of nonzero entries" [3, p. 13]. For a small system, such as the slider-crank, computational efficiency is a minor matter, but for large systems, such as a full automobile suspension or a human body moving in three dimensions, this becomes much more significant.

8.7.3 Lagrange Multipliers

The application of Lagrange multipliers is a widely used technique for incorporating constraints into various systems. In the context of differential equations, the essence of the technique for incorporating constraints is

1. Express the constraints in homogeneous form, as done above;
2. Add the constraint to the differential equation with an unknown multiplier (traditionally denoted λ);
3. Solve the resulting system of equations, to give the generalized coordinates and the Lagrange multiplier values.

This is not a simple process, but it is available in an automated form in some computer program packages such as Matlab^{TM}, GNU Octave, and perhaps others like SciLab and Sage. Carrying this through to application is beyond the scope of the present discussion, but the reader should be aware that there exist methods and software to deal with this approach.

8.8 Conclusion

While there are many useful machines that involve a single degree of freedom only, there are many more that have many degrees of freedom. This becomes especially true when motion in three dimensions is considered. The application of the Lagrange formulation to the whole problem of multidegree of freedom dynamics provides a systematic approach to the equations of motion for such systems. Without the correct equations of motion, all efforts to obtain a solution are pointless.

The whole field of multidegree of freedom dynamics is growing rapidly, particularly in response to increases in available computer power. The ability to model real systems with many degrees of freedom opens up the opportunity to analyze systems of great complexity, systems like complete internal combustion engines, agricultural and construction machinery, and even human and animal body motion.

References

[1] Mitchiner, R.G. and Leonard, R.G., "Centrifugal Pendulum Vibration Absorbers – Theory and Practice," *J. Vibration and Acoustics, Trans. ASME*, Oct. 1991, Vol. 113,

pp. 503 – 507.

[2] Orlandea, N.V., "Multibody Systems History of ADAMS," *J. Computational and Nonlinear Dynamics*, Paper No: CND-16-1275, 2016 (on line).

[3] Haug, E.J., Wehage, R., and Barman, N.C., "Dynamic Analysis and Design of Constrained Mechanical Systems," Interim Report No. 12588, 12 June, 1981, for the US Army Tank-Automotive Command R&D Center (available on line from DTIC).

Problems

For all problems in this set, there are two parts. First, develop all of the kinematic analysis required to compute everything needed for computer solution of the equations of motion. Carry the analysis as far as is practical in closed form. If a computer solution is necessary, determine the type of numerical method to be used and cast the equations in a suitable form. Second, determine the equations of motion for the system. As in the problems of chapter 7, a subscript c on a moment of inertia indicates that the reference point is the center of mass, while a subscript o indicates that the reference point is a fixed pivot.

8-1 The two rollers are connected by links of length L_1 and L_2. All of the geometric dimensions, mass, and mass moment of inertial values shown are assumed to be known. The system is released in the configuration shown and allowed to fall under gravity. Take q_1 and q_2 as generalized coordinates.

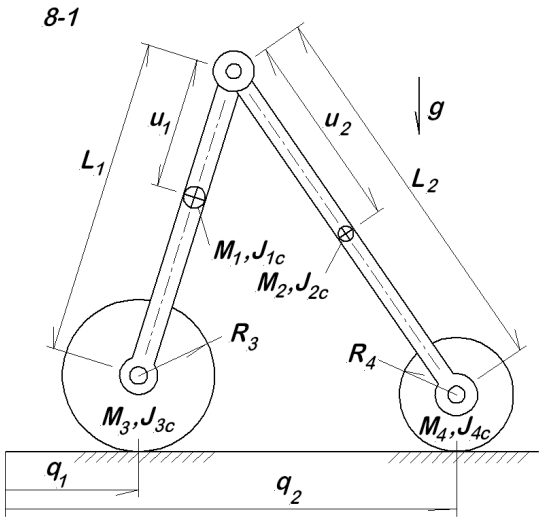

8-2 The mass M_1 moves horizontally under the influence of the force $F(t)$, and the restraining forces due the spring and the damper. The pendulum swings freely from the translating mass under the influence of gravity. The mass M_1 and M_2 are known, as are the mass moment of inertia J_{2c} and the distance D.

8-3 The masses M_1 and M_2 slide without friction, other than the viscous friction of the dashpot with coefficient B. The force $F(t)$ acts on M_2. The spring constant, K, the angle C, and the distance D, are all known.

8-4 The large ring rolls without slipping on the two small rollers, and the small disk rolls without slipping inside the ring. All masses, mass moments of inertia, and radii shown in the figure are known. The mass moment of inertia values are each with respect to the

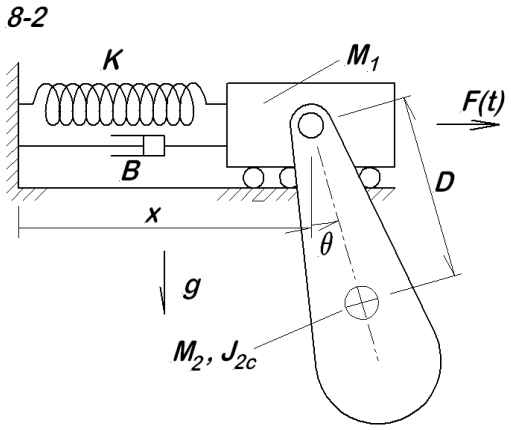

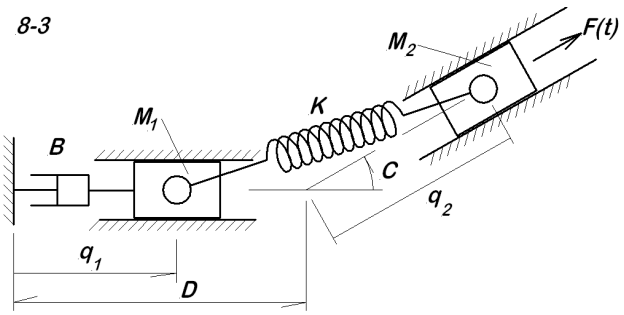

body center of mass. When $\theta = \phi$, the disk contacts the inside of the ring such that points p and q are in contact.

8-5 For the double pendulum, the length of the upper pendulum is L, and it has mass M_1 and mass moment of inertia J_{1o}. For the lower pendulum, the distance from the attachment point to the center of mass is R, the mass is M_2, and the mass moment of inertia is J_{2c}. The torsional spring is relaxed with the two pendula are aligned ($\theta = \phi$).

8-6 The figure shows a large church bell being rung by a small person hanging on the end of the bell rope; the person is completely off the floor. At the center of the wheel, there is the trunnion axel; the bell, bell yoke, and the wheel rotate together about this point. The mass of that complete assembly is M_b, the enter of mass is below the rotation axis by a distance C_1, and the mass moment of inertia for the assembly is J_{bo}. The clapper is supported at distance C_2 above the bell rotation axis, and it has mass $M_{clapper}$ and mass moment of inertia J_{co}. The clapper center of mass is a distance C_3 below the support point. The problem is only concerned with time when the clapper is not in contact with the side of the bell. The impact event that occurs when the clapper strikes the bell requires special handling, a matter beyond the scope of the present problem.

8-7 A bell crank pivots on the slider that moves in a vertical guide (there is no gravity here). The system is driven by the external force $F(t)$ applied to the slider and the

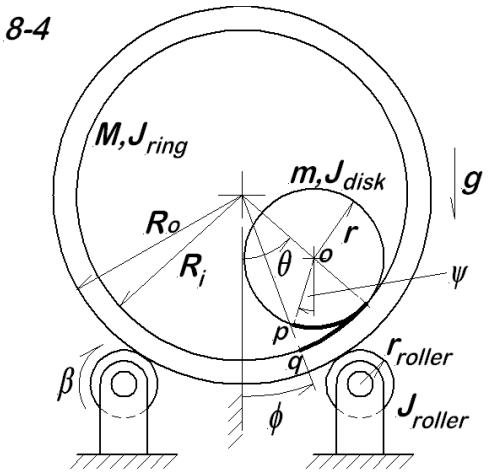

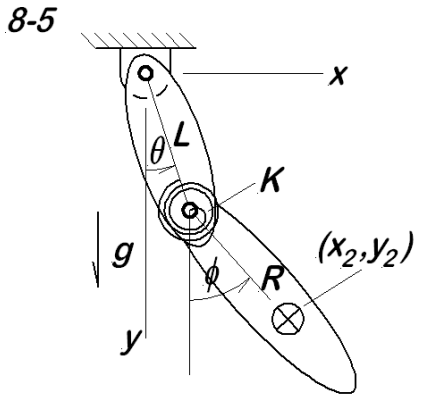

torque T acting on the wheel. As the wheel rotates, the pin on the wheel engages the slot in the bell crank. The significant masses are: (1) the slider, with mass M_S, the wheel with mass moment of inertia J_c, and the bell crank with mass M_b and centroidal mass moment of inertia J_{bc}. The bell crank center of mass is located the the body coordinates (u_c, v_c). The mass of the dashpot is neglected, although its force must be included.

8-8 Torsional vibration is often excited by a prime mover with unsteady torque, such as an internal combustion engine, making it desirable to attempt to torsionally isolate the load from the driving torque oscillations. This topic is examined in much more detail in the last chapter of the current book. The figure shows a rather crude attempt to devise a torsional isolation coupling. The prime mover is station 1, the coupling is stations 2 and 3, and the driven load is station 4. The shaft between the prime mover and the coupling has torsional stiffness K_{12}, and that between the coupling and the load is K_{34}. The coupling springs, K_c, have free length S_o; the spring are attached at radius R on stations 3 and 4. The length of these springs changes due to relative rotation between stations 3 and 4, thus transferring torque to the load. The unsteady torque of the prime mover is $T_1(t)$, and the load torque acting on station 4 is $T_4\left(\theta_4, \dot{\theta}_4\right)$. All stiffness and

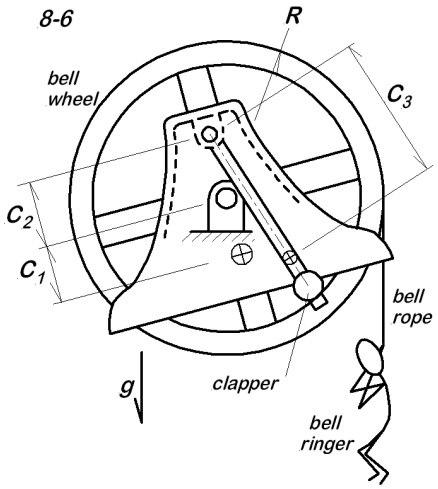

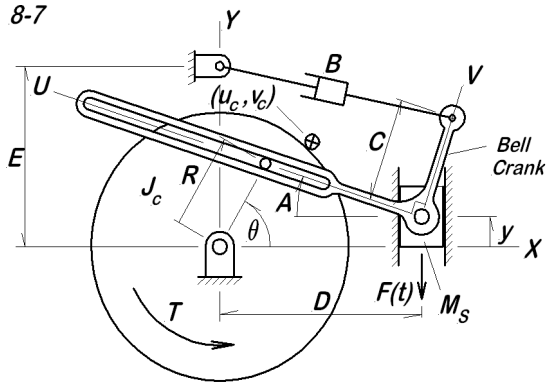

mass moment of inertia values are known.

8-9 The figure shows two sliders in a horizontal guide linked by a spring. The whole assembly is tied to the left support through a dash pot. There are also two links joining the two sliders, and a force $F(t)$ applied at the joint between the two links. There is no gravity to be considered. All geometric dimensions, spring rate, dashpot coefficient, masses, and mass moments of inertia are known.

8-10 The figure shows two sliders with identical mass and mass moment of inertia values, one operating in a straight guide while the other follows a circular arc. A spring of stiffness K connects the two sliders. Take z and θ as generalized coordinates.

8-11 This problem is in some ways similar to the one preceding it, but this time, the straight guide is itself pivoted at the origin. As before, the two sliders have identical mass and mass moments of inertia, while the guide, #3, has mass moment of inertia J_{3o}. The dimensions (R, C, β) and the spring rate, K, are all known. Choose appropriate generalized coordinates to write the equations of motion.

8-8

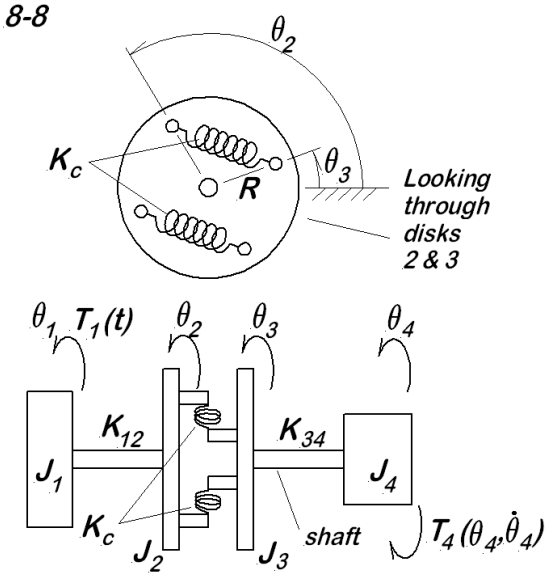

8-9

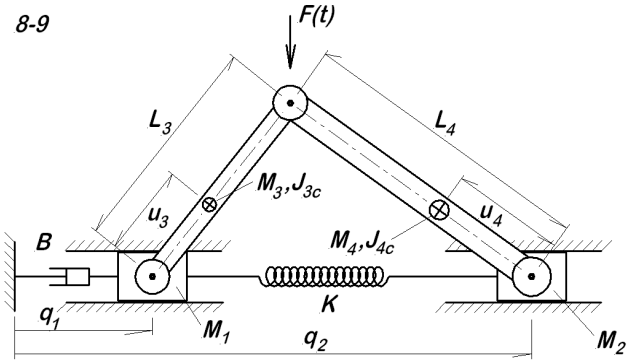

8-10

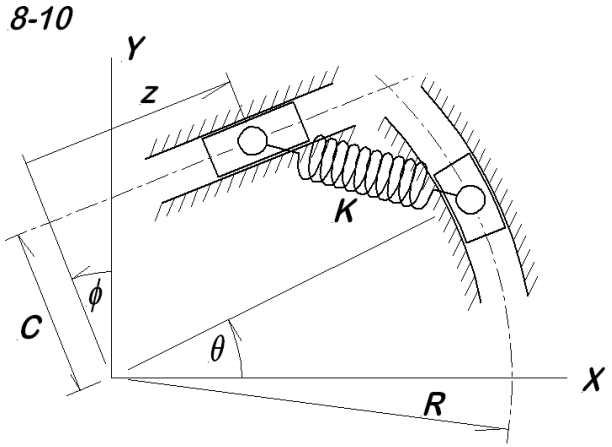

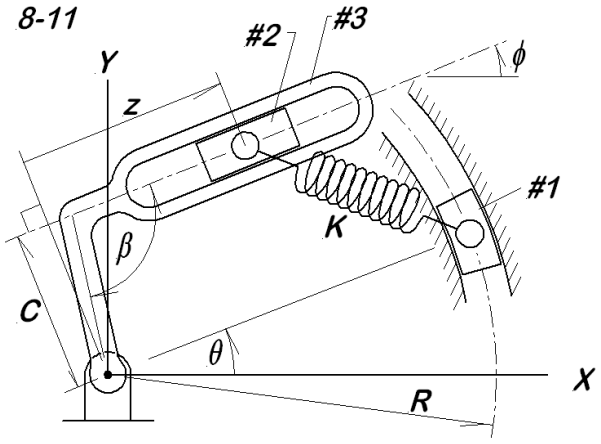

Chapter 9

Internal Forces and Reactions

9.1 General Comments

In previous chapters, the focus is on obtaining the system equations of motion for a machine, and on methods for solving the resulting differential equations. In particular, the emphasis is on avoiding the need to describe and deal with as many of the forces in the system as possible. Energy based scalar formulations, employing either Eksergian's method or the Lagrange equation of motion, are used to (1) avoid the need to deal with the vectorial nature of force relations, and (2) to avoid dealing with often unknowable forces like bearing reactions and internal joint forces. Forces that *cause motion* are included within the energy based formulation, but forces that are the *result of motion* are mostly avoided. In Chapter 6, the forces that cause a body to be in equilibrium (a special state of motion) are analyzed, but nonworking constraint forces do not enter the analysis. In Chapters 7 and 8, system motions are described in terms of external forces that do work on the system, but nonworking external forces and internal forces do not enter the equations of motion. The ability to determine the equations of motion without the need to consider internal forces and nonworking external forces is a great advantage.

When the ultimate objective is engineering design, determination of the forces is often an essential requirement. This is clearly necessary as a first step towards stress analysis, bearing design, deflection evaluation, and other force-based design considerations. When the forces must be evaluated, it is necessary to deal with Newton's Second Law of Motion and the resulting vector equations. In that regard, this chapter is much like the material in elementary statics and dynamics, but with two distinctions: (1) the emphasis is on real machine systems, rather than idealized problems, and (2) a powerful approach to kinematics is available here that is usually not accessible in earlier courses. For the purposes of this chapter, the topic is discussed largely in the context of single degree of freedom systems where it is most easily understood, although the same ideas apply in

general.

An *external force or moment* that bears on the machine system, often through the foundation or other support structure, is called a *reaction*. A knowledge of the reactions is essential for the design of proper supports for a machine. The time-varying component of the reaction is often called a *shaking force* or *shaking moment*, descriptive terms because these reactions tend to shake the supporting structure. A machine designer is often asked to provide information about the reactions for use by the person charged with the design of the support structure. Alternatively, the designer of the supports may find it necessary to determine those reactions.

Forces of interaction between two moving members of a system are called *internal forces*, a term intended to convey the idea that they are internal to the mechanical system. Internal forces are of great concern to a machine designer because they affect the choice of materials and sizes for the components. Stress, deflection, bearing load capacity, wear, and energy consumption are all governed by the internal forces, so a machine design cannot be considered complete until the internal forces are determined and found acceptable for the final design. The term *internal force* is extended to include forces internal to a single member (as shown in the latter part of this chapter) as well as the interaction force between two members.

9.2 Governing Equations

To begin the consideration internal force determination, **consider a rigid body moving in two dimensions** as a part of a single degree of freedom machine, for which Newton's Second Law [1] provides three equations of motion:

$$\sum_i F_{xi} = M\ddot{x}_c = M\left(\ddot{\theta}K_{cx} + \dot{\theta}^2 L_{cx}\right) \tag{9.1}$$

$$\sum_i F_{yi} = M\ddot{y}_c = M\left(\ddot{\theta}K_{cy} + \dot{\theta}^2 L_{cy}\right) \tag{9.2}$$

$$\sum_i M_{ci} = J_c\ddot{\phi} = J_c\left(\ddot{\theta}K_{\phi} + \dot{\theta}^2 L_{\phi}\right) \tag{9.3}$$

where

θ is the generalized coordinate associated with the single degree of freedom,

(x_c, y_c) are the center of mass coordinates,

ϕ is an angular coordinate describing the orientation of the body,

M is the body mass,

J_c is the body mass moment of inertia with respect to the center of mass.

If three dimensional motion were involved, there would be six equations, but the same principles would apply. Now separate each of the force and moment sums into a sum of internal loads ($\sum F^I$) and a sum of external loads ($\sum F^E$), so that after rearrangement, the equations read

$$\sum_i F^I_{xi} - \ddot{\theta} M K_{cx} = \dot{\theta}^2 M L_{cx} - \sum_i F^E_{xi} \tag{9.4}$$

$$\sum_i F^I_{yi} - \ddot{\theta} M K_{cy} = \dot{\theta}^2 M L_{cy} - \sum_i F^E_{yi} \tag{9.5}$$

$$\sum_i M^I_{ci} - \ddot{\theta} J_c K_\phi = \dot{\theta}^2 J_c L_\phi - \sum_i M^E_{ci} \tag{9.6}$$

Three equations of this sort can be written for every rigid body in the system. The left side of each equation contains the unknown internal forces and $\ddot{\theta}$, all to be determined. On the right, there are the centripetal acceleration terms and various externally applied (known) forces and moments that drive the motion. The objective here is to evaluate the internal force, moment, and acceleration terms (on the left side), but this raises the question of what to do with the terms on the right.

Notice also that the eventual solution will provide a value for the acceleration, $\ddot{\theta}$. This last should not be surprising since, in elementary mechanics courses, the application of Newton's Second Law is the usual approach to determining an acceleration. It should be noted, however, that this acceleration determination is independent of acceleration found through either Eksergian's equation or the Lagrange equation, but the two acceleration calculations must be in agreement. Both should be made and compared; this is an important quality check.

In a computer implemented force analysis, the process is that of stepping the system through a sequence of positions representing the full operating cycle of the machine under study, evaluating all of the forces (and the acceleration) at each position. For the case of a rotating machine, this usually means one full crank revolution, although the exact meaning must be determined in the context of each application. In that process, position values are assigned sequentially, perhaps in 1 degree increments of shaft rotation or something similar. But what value should be used for the associated velocity, the value for $\dot{\theta}$? This is the analyst's dilemma.

There are three standard engineering approaches to the problem of determining reactions and internal forces, each of which is appropriate to a particular situation. They are the methods of *Statics*, *Kinetostatics*, and *Dynamics*; their descriptions follow.

Static Analysis As the name implies, this approach assumes that all components are in equilibrium, and the forces are determined on this basis. This method is valid for a mechanism that is motionless under load, and may also be appropriate for very slowly moving (quasistatic) machines. This is the simplest of the three approaches, and this method has been used widely for many years. Unfortunately, it is often applied to situations where it is definitely not valid.

Kinetostatic Analysis Many mechanisms move without great changes in speed. It may be possible to assume an approximate description of the motion, usually the relatively simple expression $\dot{\theta} = \text{constant}$. The kinetostatic method attempts to account for the effects of motion by assuming that an approximate motion is the true motion, and including some of the induced inertial effects. For a single degree of freedom system, a description of the type $\dot{\theta} = \Omega = \text{constant}$ incorporates (approximately) all of the centripetal terms ($\Omega^2 L_j$), but completely neglects the generalized acceleration terms ($\ddot{\theta} K_j$). This topic is discussed briefly by Paul [2] and, in the context of cam systems, by Norton [3] . (There is more to be said about the nature of this process later.)

Dynamic Analysis When speed variation is significant, there is often no adequate, simple approximate description of the motion. In that case, it is necessary first to determine the motion by solving the equation of motion, and then to use that dynamic solution for the determination of the internal forces and reactions. For most systems, the dynamic analysis is the most difficult and time consuming of the three approaches. At the same time, however, it is the most correct and reliable.

In summary, the entire issue is a question of just how to handle the inertial terms. The static analysis is strictly applicable only to systems in equilibrium, which often – but not always – means "motionless." It may be a very reasonable approximation in some other cases involving slow, apparently non-accelerated motion. The kinetostatic analysis is a well known, widely used approximate analysis that gives acceptable results in many cases. The dynamic analysis is consistently the most correct, most difficult, and most time consuming of the three approaches. The choice of an appropriate method of analysis is an engineering judgment. Static analysis is adequately covered in elementary courses; the development below is confined to the kinetostatic and dynamic analysis methods. The discussion continues in terms of specific examples to illustrate the concepts described above.

9.3 Spring-Loaded Trammel

Consider the application of the approaches previously discussed to the determination of the forces in the trammel system shown in Figure 9.1. For this system, there is no meaningful "steady operating condition," and consequently the kinetostatic analysis is not applicable. The dynamic analysis is the only option available.

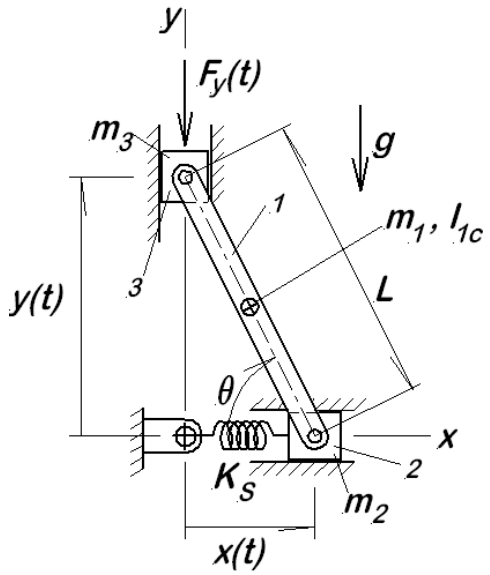

Figure 9.1: Spring Supported Trammel With Impulsive Load

9.3.1 Application of Newton's Second Law

It is necessary to define the force components within the system, and for that purpose, consider Figure 9.2 where Free Body Diagrams are shown for each component.

The equations of motion for the link, body 1 are:

$$-F_1 + F_3 = m_1 \left[\ddot{\theta} \left(-\frac{L}{2} \sin\theta \right) + \dot{\theta}^2 \left(-\frac{L}{2} \cos\theta \right) \right] \tag{9.7}$$

$$F_2 - F_4 - w_1 = m_1 \left[\ddot{\theta} \left(\frac{L}{2} \cos\theta \right) + \dot{\theta}^2 \left(-\frac{L}{2} \sin\theta \right) \right] \tag{9.8}$$

$$\frac{L}{2} \left(F_1 \sin\theta - F_2 \cos\theta + F_3 \sin\theta - F_4 \cos\theta \right) = I_{1c} \left[\ddot{\theta} \cdot (1) + \dot{\theta}^2 \cdot (0) \right] \tag{9.9}$$

Note that positive moments on body 1 are taken clockwise to be consistent with the fact that the angle θ opens clockwise in the positive sense. For the lower slider, body 2, the equations of motion are:

$$F_1 - F_S(x) = m_2 \left[\ddot{\theta} \left(-L \sin\theta \right) + \dot{\theta}^2 \left(-L \cos\theta \right) \right] \tag{9.10}$$

$$R_2 - F_2 - w_2 = m_2 \left[\ddot{\theta} \cdot (0) + \dot{\theta}^2 \cdot (0) \right] \tag{9.11}$$

$$0 = I_{2c} \left[\ddot{\theta} \cdot (0) + \dot{\theta}^2 \cdot (0) \right] \tag{9.12}$$

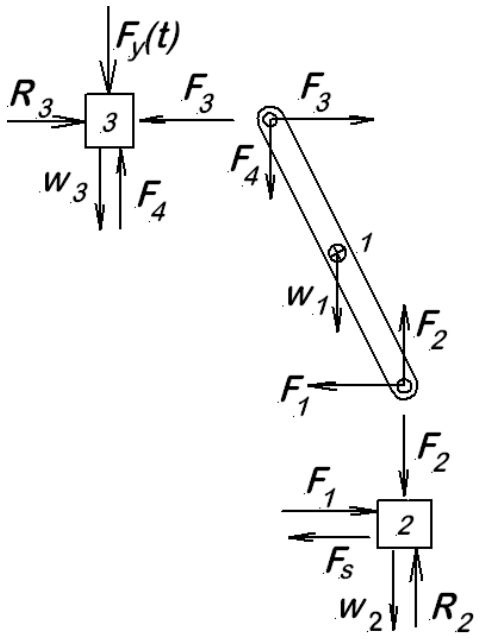

Figure 9.2: Free Body Diagrams for the Trammel Mechanism Components

The second and third equations are static force relations because there is no possibility for motion normal to the guide or for rotational motion. Note that the constitutive equation for the spring, expressing $F_S(x) = K_S(L\cos\theta - x_o)$, is required before this system of equations is complete. Similarly, it is evident that, because of the one dimensional motion of the slider, there is only one actual equation of motion resulting. The other is simply a static equilibrium relation. For the vertical axis slider, body 3:

$$F_4 - w_3 - F_y(t) = m_3\left[\ddot{\theta}(L\cos\theta) + \dot{\theta}^2(-L\sin\theta)\right] \tag{9.13}$$

Collecting all of the nontrivial equations together gives the following matrix equation:

$$\begin{bmatrix} -1 & 0 & +1 & 0 & m_1\frac{L}{2}\sin\theta \\ 0 & +1 & 0 & -1 & -m_1\frac{L}{2}\cos\theta \\ \frac{L}{2}\sin\theta & \frac{-L}{2}\cos\theta & \frac{L}{2}\sin\theta & \frac{-L}{2}\cos\theta & -I_c \\ 1 & 0 & 0 & 0 & m_2 L\sin\theta \\ 0 & 0 & 0 & 1 & -m_3 L\cos\theta \end{bmatrix} \begin{Bmatrix} F_1 \\ F_2 \\ F_3 \\ F_4 \\ \ddot{\theta} \end{Bmatrix}$$

$$= \begin{Bmatrix} 0 \\ w_1 \\ 0 \\ K_S\left(L\cos\theta - x_o\right) \\ w_3 + F_y\left(t\right) \end{Bmatrix} + \dot{\theta}^2 \begin{Bmatrix} -m_1\frac{L}{2}\cos\theta \\ -m_1\frac{L}{2}\sin\theta \\ 0 \\ -m_2 L\cos\theta \\ -m_3 L\sin\theta \end{Bmatrix} \tag{9.14}$$

or

$$[C]\{F\} = \{R_1\} + \dot{\theta}^2\{R_2\} \tag{9.15}$$

As mentioned previously, it is important to note that the system acceleration, $\ddot{\theta}$, is calculated in the system solution, along with the several internal forces. Newton's Second Law has always furnished the acceleration in earlier approaches to dynamic situations, and so it does here again.

In carrying out the force analysis, it is evident that both position and velocity are needed as inputs to the force calculation at each position. What source provides these values? The answer is that the force solution must be combined with, or follow, the motion solution. This situation offers three possible approaches:

1. The complete motion solution can be generated first, based on numerical solution of Eksergian's equation over some suitable time interval with position, velocity, and acceleration computed at each time point and saved for later use. Then the position and velocity values can be employed in the later force solution process to produce forces (and an alternate acceleration value) at each position.

2. The motion solution can be generated by numerical solution of the equation of motion, using acceleration values determined from the Eksergian equation, followed by a force and acceleration calculation made at each time step. In many cases, it is not necessary to make a force calculation for every time step, but rather only at larger time intervals such as, for example, every fifth time step.

3. The motion solution can be generated by numerical solution of the equation of motion, integrating the acceleration as calculated in the force solution. This necessitates a complete force solution at every time step, but that may well be the intent anyway.

The first approach is conceptually least complex, keeping the motion solution and the force solution as entirely separate processes to be applied sequentially. The second approach keeps the two processes separate, but requires applying them alternately as the time integration proceeds. The third approach, using the force solution to develop the acceleration values, is more complex and relatively slow to execute. This is because of (a) the large number of force solutions required, and (b) the overall complexity of the process. For this reason, only the first or second approaches are recommended here. The second approach is presented in flow chart form in Figure 9.3.

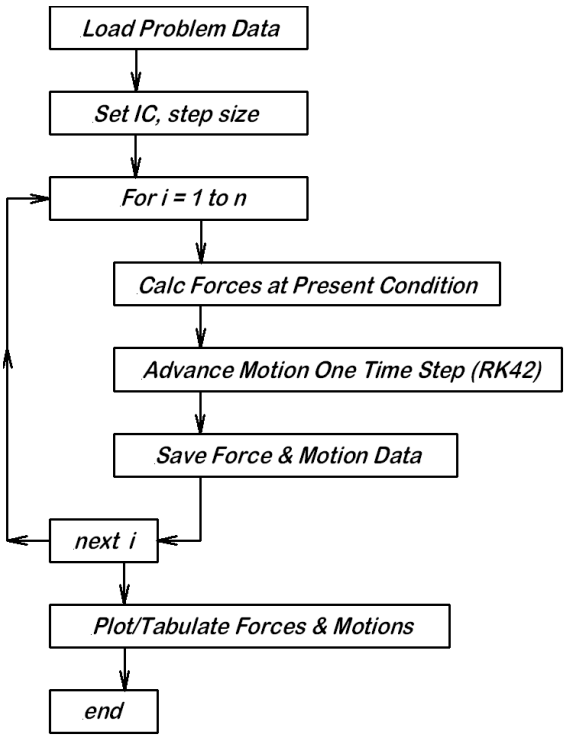

Figure 9.3: Flow Chart for the Second Approach to Force Calculations

In the event that the first or second approach is employed, two values for the system acceleration are available, one obtained from Eksergian's equation, and the other from the force solution. These must be in very close agreement; if not, it indicates either an algebraic or computational error and no confidence should be placed in the computed results. For this reason, automatic checking needs to be built into a computer code to verify that these solutions agree on the acceleration value at each position. Otherwise, the whole exercise is pointless!

Returning to the example of the impact driven trammel, the system data is the same as that used in the motion simulation of Chapter 7. The motion was previously developed in Chapter 7, so it is certainly easiest to simply add the force calculation as an additional step after the motion calculation is complete. A subroutine for the force calculation, implementing the solution of equation (9.12) above follows.

Subroutine for Trammel Dynamic Force Calculations

```
sub force
    if t<tau then
       Fy=Fym*sin(pi*t/tau)
    else
       Fy=0
    end if
    mat coef=zer
    mat R1=zer
    mat R2=zer
    coef(1,1)=-1
    coef(1,3)=+1
    coef(1,5)=m*L/2*sin(theta)
    R2(1)=-m*L/2*cos(theta)

    coef(2,2)=+1
    coef(2,4)=-1
    coef(2,5)=-m*L/2*cos(theta)
    R1(2)=wt1
    R2(2)=-m*L/2*sin(theta)

    coef(3,1)=L/2*sin(theta)
    coef(3,2)=-L/2*cos(theta)
    coef(3,3)=L/2*sin(theta)
    coef(3,4)=-L/2*cos(theta)
    coef(3,5)=-Ic

    coef(4,1)=+1
    coef(4,5)=mx*L*sin(theta)
    R1(4)=K*(L*cos(theta)-xo)
    R2(4)=-mx*L*cos(theta)

    coef(5,4)=1
    coef(5,5)=-my*L*cos(theta)
    R1(5)=wt3+Fy
    R2(5)=-my*L*sin(theta)
```



```
    mat coefi=inv(coef)

    mat S1=coefi*R1
    mat S2=coefi*R2
    mat S2=(dth^2)*S2
    mat Stot=S1+S2

    F1=Stot(1)
    F2=Stot(2)
    F3=Stot(3)
    F4=Stot(4)
    ddthn=Stot(5)

    if abs(Stot(5)-ddthe)>1e-12 then
       print "accel error"
       print "ddthe = ";ddthe;"   Stot(5) = ";Stot(5)
       get key xxx
    end if
    F1sav(ik)=F1
    F2sav(ik)=F2
    F3sav(ik)=F3
    F4sav(ik)=F4
    ddthnsav(ik)=ddthn
    tfsav(ik)=t
end sub
```

Most aspects of the subroutine are self-explanatory; the notation follows closely that used in the theoretical development. It is understood that the motion simulation has been previously completed, and this routine is called for every value of time (t) for which forces are to be calculated. At each of those values, the motion simulation provides values for $\theta(t)$, $\dot{\theta}(t)$, and $\ddot{\theta}(t)$. Note the test near the end of the subroutine to compare the acceleration from the simulation with the acceleration computed along with the forces. If at any point they differ by more than an acceptable amount (10^{-12} in this case), the subroutine pauses; this pause never occurs in actual program execution.

The computed force results are shown in Figures 9.4 and 9.5. Each of these plots shows the two components of force at a joint, plotted one against the other; with time as the implied parameter connecting the values. Thus, in Figure 9.4, the force curve begins with the static forces, approximately $(F_1, F_2) = (20, 80)$ lb (reading from the plot). During the time of the vertical impulse, the forces each increase greatly to maximum values of approximately 600 lb and 550 lb, respectively. As the impact diminishes, the force components also drop, both becoming negative near the end of the impact. This point is marked with an X at approximately $(-70, -110)$. The continued motion is periodic (see

Figure 7.8), and the forces repeat a trajectory that looks like an inclined letter "J." For this example, it is clear that the most severe loading occurs only once, shortly after the beginning of the impulse, but is then followed by a periodic loading-unloading- reverse loading cycle.

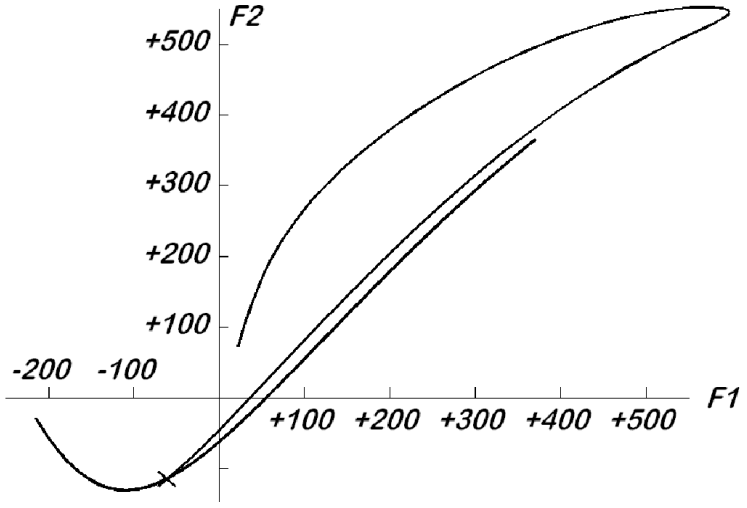

Figure 9.4: Locus of the Force Components F_1 and F_2

Similar comments (with different force values) also apply to Figure 9.5 where, again, the end of the impulse is marked with a letter X.

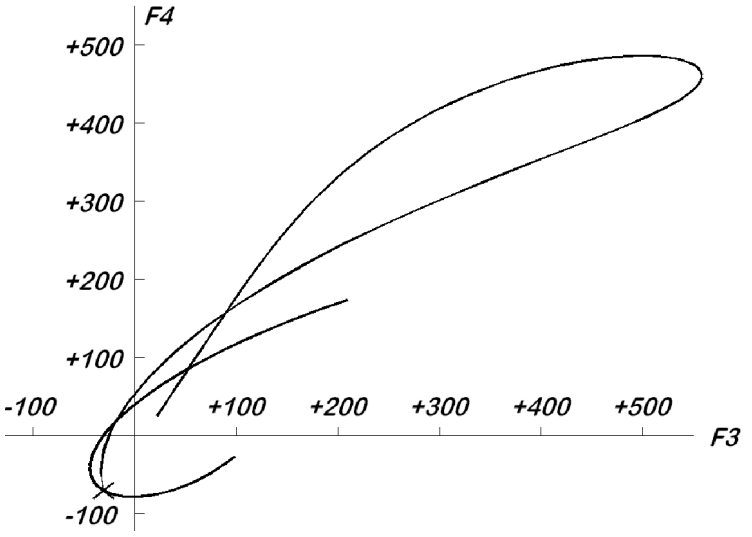

Figure 9.5: Locus of the Force Components F_3 and F_4

It should be noted that, for each of these plots, for any point on the curve, the distance of the point from the origin gives the magnitude of the shear force in the connecting pin,

and the direction of the line to that point provides the direction of the shear force. It is clear that the shear forces varies considerably, both in magnitude and direction, as the system moves through a cycle.

9.4 Slider-Crank Force Analysis

The slider-crank mechanism has been previously discussed in several contexts, but its central role most in internal combustion engines and reciprocating compressors makes it necessary to consider the internal force analysis as well. It also provides an opportunity to compare two approaches to the internal force problem as discussed in section 9.2. In order to keep the problem as simple as possible while still representing a real case, it is presented here in the context of a motor driven, single cylinder reciprocating compressor, operating in steady state. The presentation begins with a system description.

9.4.1 System Description

The system is a reciprocating air compressor driven by an induction motor; there are countless such machines in actual use. The compressor is a typical slider-crank machine, of the sort shown in Figure 2.7 except that here the offset, ε, is zero.

The compressor employs poppet valves that open and close in response to differential pressure across the valves; there are no springs or lifting mechanisms involved. Figure 9.6 that shows a plot of cylinder pressure versus wrist pin position; this is equivalent to a scaled pressure-volume diagram for the compression process. The suction manifold is at atmospheric pressure, 101000 Pa, while the discharge manifold is constant at 687000 Pa. (All pressure references are to absolute pressure, not gauge pressure.) The crank case is vented, so that the underside of the piston is at atmospheric pressure at all times.

Consider the compression process to begin at point (1) which corresponds to crank angle $\theta = -\pi$. The cylinder is already filled with air at atmospheric pressure, so as the piston advances toward the head (θ increasing), the pressure rises according to the polytropic law,

$$PV^{\gamma} = \text{ Constant} \tag{9.16}$$

The polytropic exponent for air is taken as $\gamma = 1.41$.

When the cylinder pressure reaches the discharge manifold pressure, point (2), the discharge valves are assumed to instantly open to allow flow at discharge pressure into the discharge manifold. This is somewhat of an idealization; in reality, the cylinder pressure must rise slightly above the discharge manifold pressure in order to open the valves and

drive the flow; this detail is omitted here. Flow into the discharge manifold continues until the end of the stroke, the minimum cylinder volume condition with $\theta = 0$. At this point, point (3), the discharge valves close and there is no further flow, leaving some air trapped in the cylinder.

As the crank continues to advance, $\dot{\theta} > 0$, the gas previously trapped in the cylinder re-expands. The re-expansion follows the same polytropic law, except that there is a different constant because it is a smaller mass of air. When the pressure of the re-expanding air reaches manifold pressure, (4), the intake valves open to allow a fresh air charge to be drawn in at atmospheric pressure. Again, this is somewhat idealized, but the details of the flow pressure are not the main point of this discussion. This refilling process continues until the piston reaches BDC with $\theta = +\pi$, at which point, the entire cycle is repeated again and again, endlessly.

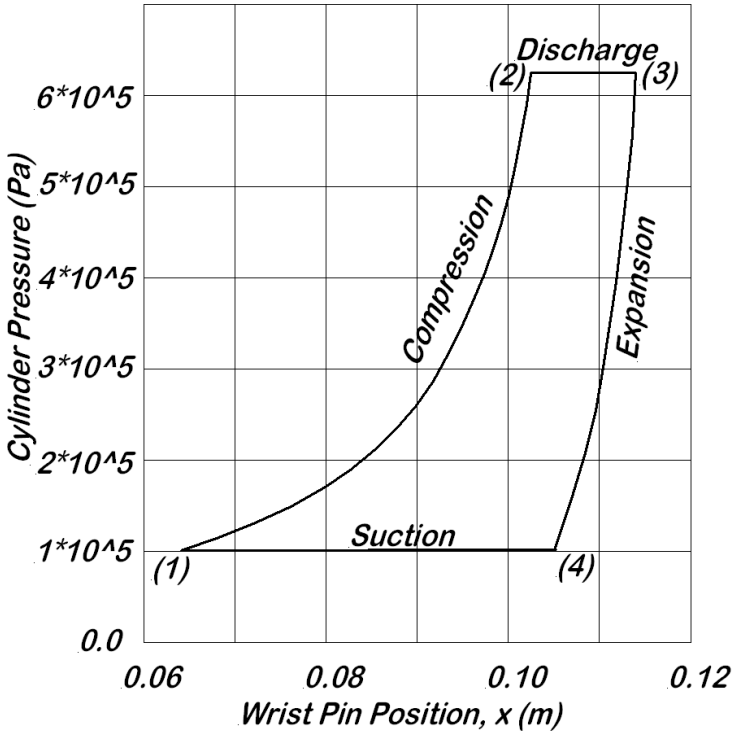

Figure 9.6: Plot of Cylinder Pressure (Pa) versus Wrist Pin Position (m)

The compressor is driven by a three phase induction motor, coupled to the crank through a 3 : 2 speed reduction. For purposes of this problem, only steady state operation is of interest, so the simple, linear torque-speed approximation presented in Appendix 5.1.4.1 is adequate. Better motor models could also be employed, such as that of 5.1.4.3. The necessary system data is given in Tables 9.1, 9.2, and 9.3 below.

Table 9.1 Compressor Mechanical Data		
$R = 0.025$ m		Crank Radius
$L = 0.089$ m		Connecting Rod Length
$D = 0.061$ m		Cylinder Bore Diameter
$u_{1c} = 0.0$ m		Crank CM Location*
$u_{2c} = 0.022$ m		Connecting Rod CM Location*
$W_1 = 47.8$ N		Crank Weight
$W_2 = 1.2$ N		Connecting Rod Weight
$W_3 = 1.9$ N		Piston Ass'y Weight
$J_{1o} = 0.0157$ kg-m^2		Crank MMOI wrt Rotation Axis
$J_{2c} = 0.000339$ kg-m^2		Connecting Rod MMOI wrt CM
$V_{\max} = 1.56352 \cdot 10^{-4}$ m^3		Maximum Cylinder Volume
$*$ Note that $v_{c1} = v_{c2} = 0$		

Table 9.2 Thermodynamic Cycle Data		
$P_1 = 101353$ Pa		Suction Pressure
$P_2 = 618460$ Pa		Discharge Pressure
$\gamma = 1.41$		Polytropic Exponent for Air

Table 9.3 Electric Motor Data		
$P_{Rated} = 750$ W		Rated Power
$N_{Rated} = 1689$ rpm		Rated Speed
$N_{Synch} = 1800$ rpm		Synchronous Speed
$J_{Mtr} = 0.02$ kg-m^2		Motor Rotor MMOI
$n = 3/2$		Speed Reduction to Load

9.4.2 Equations of Motion

The system for analysis is shown in schematic form in Figure 9.7 where the upper part is a schematic diagram of the slider-crank while the lower part shows free body diagrams

for each component. All of the necessary kinematic analysis is available in Chapter 2, so it is not repeated here. The equation of motion, based on Eksergian's equation, is found in Chapter 7. What remains new here is to write the equations of motion for each of the several components, equations that can be solved to give the connection forces.

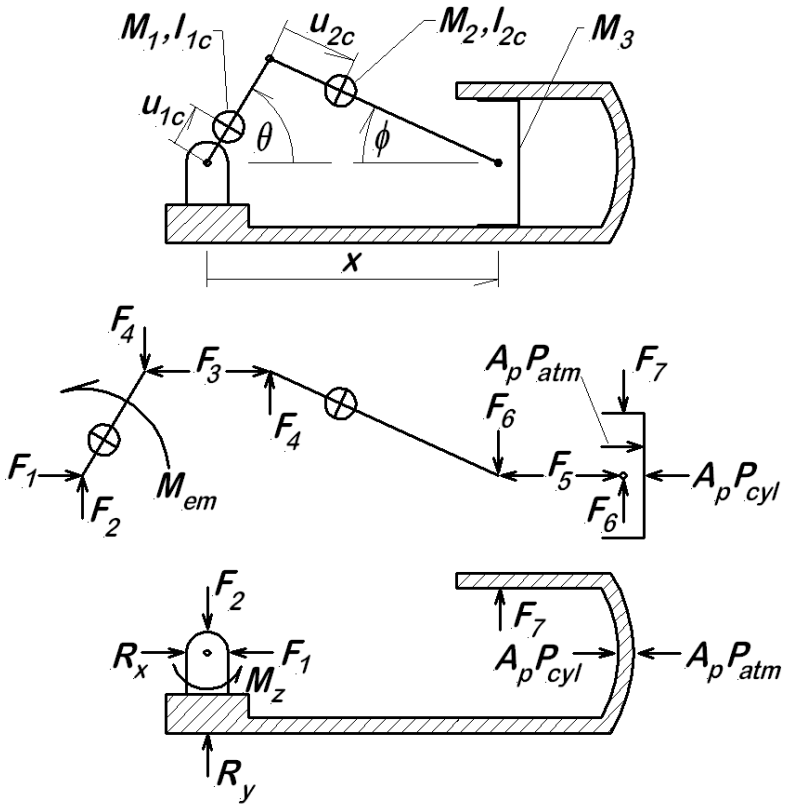

Figure 9.7: Slider-Crank Schematic and Free Body Diagrams

Note that in the naming of the many forces involved, in most cases an odd subscript number indicates a horizontal force while an even subscript denotes a vertical force (with the exception of F_7 that is vertical). The couple M_{em} is the electromagnetic torque from the motor, a function of rotor speed and applied directly to the crank. The frame of the machine is assumed to be supported at rest equilibrium by two external forces and a moment, R_x, R_y, and M_z, all acting at the crank axis of rotation.

The first step is to write Newton's Second Law for each component. Note that, in summing moments on the crank, it is more convenient to sum moments about the crank pivot than about the center of mass. This requires the use of the mass moment of inertia for the crank and motor assembly with respect to the axis of rotation, understanding that J_θ is actually $J_{1o} + J_{Mtr}$. The resulting equations follow below:

Crank:

$$F_1 - F_3 = M_1\left(\ddot{\theta}K_{1cx} + \dot{\theta}^2 L_{1cx}\right) \tag{9.17}$$

$$F_2 - F_4 = M_1\left(\ddot{\theta}K_{1cy} + \dot{\theta}^2 L_{1cy}\right) \tag{9.18}$$

$$F_3 R\sin\theta - F_4 R\cos\theta = J_\theta\ddot{\theta} - n\cdot M_{em}\left(\dot{\theta}\right) \tag{9.19}$$

Connecting Rod:

$$F_3 - F_5 = M_2\left(\ddot{\theta}K_{2cx} + \dot{\theta}^2 L_{2cx}\right) \tag{9.20}$$

$$F_4 - F_6 = M_2\left(\ddot{\theta}K_{2cy} + \dot{\theta}^2 L_{2cy}\right) \tag{9.21}$$

$$\begin{aligned} &F_3 u_{2c}\sin\phi + F_4 u_{2c}\cos\phi \\ &+F_5\left(L - u_{2c}\right)\sin\phi \quad = J_{2c}\left(\ddot{\theta}K_\phi + \dot{\theta}^2 L_\phi\right) \\ &+F_6\left(L - u_{2c}\right)\cos\phi \end{aligned} \tag{9.22}$$

Piston:

$$\begin{aligned} F_5 = \; & M_3\left(\ddot{\theta}K_x + \dot{\theta}^2 L_x\right) \\ & + \left[P_{cyl}\left(\theta\right) - P_{atm}\right]A_p \end{aligned} \tag{9.23}$$

$$F_6 - F_7 = 0 \tag{9.24}$$

Frame:

$$R_x - F_1 + \left[P_{cyl}\left(\theta\right) - P_{atm}\right]A_p = 0 \tag{9.25}$$

$$R_y - F_2 + F_7 = 0 \tag{9.26}$$

$$M_z + x\cdot F_7 = 0 \tag{9.27}$$

Ignoring for the moment the static frame reaction equations, it is useful to recast the

eight dynamic equations in matrix form. When this is done, the result is this:

$$\begin{bmatrix} 1 & 0 & -1 & 0 & 0 & 0 & 0 & -M_1K_{1cx} \\ 0 & 1 & 0 & -1 & 0 & 0 & 0 & -M_1K_{1cy} \\ 0 & 0 & Z_{33} & Z_{34} & 0 & 0 & 0 & -J_\theta \\ 0 & 0 & 1 & 0 & -1 & 0 & 0 & -M_2K_{2cx} \\ 0 & 0 & 0 & 1 & 0 & -1 & 0 & -M_2K_{2cy} \\ 0 & 0 & Z_{63} & Z_{64} & Z_{65} & Z_{66} & 0 & -J_{2c}K_\phi \\ 0 & 0 & 0 & 0 & 1 & 0 & 0 & -M_3K_x \\ 0 & 0 & 0 & 0 & 0 & 1 & -1 & 0 \end{bmatrix} \begin{Bmatrix} F_1 \\ F_2 \\ F_3 \\ F_4 \\ F_5 \\ F_6 \\ F_7 \\ \ddot{\theta} \end{Bmatrix} \tag{9.28}$$

$$= \dot{\theta}^2 \begin{Bmatrix} M_1L_{1cx} \\ M_1L_{1cy} \\ 0 \\ M_2L_{2cx} \\ M_2L_{2cy} \\ J_{2c}L_\phi \\ M_3L_x \\ 0 \end{Bmatrix} + n \cdot M_{em}\left(\dot{\theta}\right) \begin{Bmatrix} 0 \\ 0 \\ -1 \\ 0 \\ 0 \\ 0 \\ 0 \\ 0 \end{Bmatrix} + \left[P_{cyl}\left(\theta\right) - P_{atm}\right] A_p \begin{Bmatrix} 0 \\ 0 \\ 0 \\ 0 \\ 0 \\ 0 \\ 1 \\ 0 \end{Bmatrix}$$

where

$Z_{33} = R\sin\theta$

$Z_{34} = -R\cos\theta$

$Z_{63} = u_{2c}\sin\phi$

$Z_{64} = u_{2c}\cos\phi$

$Z_{65} = (L - u_{2c})\sin\phi$

$Z_{66} = (L - u_{2c})\cos\phi$

In this form, it is fully evident that the internal forces, $F_1 \ldots F_7$ and the crank acceleration, $\ddot{\theta}$ are each functions of:

- crank angular position, θ;

- crank speed, $\dot{\theta}$ (squared);
- motor torque, $n \cdot M_{em}$, modified by the transmission ratio;
- pressure difference acting on the piston, $[P_{cyl}(\theta) - P_{atm}]$.

Every term in the coefficient matrix is either (a) constant, or (b) a function of the angle θ.

As mentioned previously, there are three types of analysis possible. The static analysis is so primitive as to be near worthless, so it is ignored here. The other two types are developed below, but before attending to that, consider particularly the three equations for the frame reactions.

9.4.2.1 External Reactions

Assume for the moment that the internal forces are all known (by whatever means), so that all that remains is to determine the frame reactions. Equations (9.25), (9.26), and (9.27) are readily solved to give

$$R_x = F_1 - [P_{cyl}(\theta) - P_{atm}] A_p \tag{9.29}$$
$$R_y = F_2 - F_7 \tag{9.30}$$
$$M_z = -x \cdot F_7 \tag{9.31}$$

These same three expression apply, no matter how the internal forces are determined, so there is no need to repeat them again here for each analysis type. Note, however, that the values produced for the reactions certainly vary from one analysis type to the next.

9.4.2.2 Kinetostatic Analysis

For the kinetostatic analysis, the system is assumed to be running at an assigned speed (Ω), and then stepped through crank angles from 0 to 2π. Considering equation (9.28) under these conditions, note that:

- At every position, the angle is assigned, so that θ, ϕ, and x are all known through the kinematic calculations, along with all the associated velocity coefficients and velocity coefficient derivatives;

- At the assigned crank angle, the cylinder pressure, $P_{cyl}(\theta)$, is readily evaluated from the cycle description;
- The coefficient of the first right side vector is simply Ω^2, for the kinetostatic analysis considered an assigned value;
- The motor torque at the assigned speed can be evaluated through the linear model as $M_{em}(\Omega)$;

In short then, everything necessary to evaluate the coefficient matrix and the right side vectors is available for the solution of equation (9.28).

Speed Assignment A key element in this analysis is selection of an appropriate value for the assigned speed. Small air compressors of this sort usually appear to run in steady state at a constant speed after going through their initial start-up phase. This evident constant speed would seem to be the appropriate choice for Ω if it were known; usually, it is not. On the other hand, if the motor has been properly selected for this application, the steady operation should be close to the rated speed so that the full rated power is being used. For this reason, the rated speed of the motor is a logical choice for the assigned motor speed. It must be recalled, however, that for this example, crank speed is reduced from motor speed, so the assigned crank speed is

$$\Omega = \omega_{rated}/n = \frac{176.87}{3/2} = 117.91 \text{ rad/s} \tag{9.32}$$

where

ω_{rated} = rated motor speed, rad/s.

Since the motor speed is assigned as the rated value, it is consistent to use the rated torque for the motor torque value.

Cylinder Pressure Modeling Referring back to Figure 9.6, the conditions at the end of the suction stroke are easily determined. At this point, the cylinder volume is a maximum, and the pressure is atmospheric. Thus, for this point, and for every point on the compression curve, there is a single constant value, Λ_c, such that

$$PV^\gamma = P_1 V_1^\gamma = \Lambda_c \tag{9.33}$$

Similarly, conditions at the end of the discharge are readily found. For point (3) and for every point on the re-expansion curve, there exists different constant, Λ_e, different from Λ_c, such that

$$PV^\gamma = P_3 V_3^\gamma = \Lambda_e \tag{9.34}$$

Then the pressure volume relation is described by

$$P(\theta) = \begin{cases} \min\left\{\Lambda_c / \left[V(\theta)\right]^{\gamma}, P_2\right\} & K_x(\theta) \geq 0 \text{ (upward piston motion)} \\ \max\left\{\Lambda_e / \left[V(\theta)\right]^{\gamma}, P_1\right\} & K_x \leq 0 \text{ (downward piston motion)} \end{cases} \tag{9.35}$$

where

Λ_c, Λ_e are as described just above,

$V(\theta)$ is the cylinder volume for crank angle θ

P_1 is the suction pressure

P_2 is the discharge pressure

The above is all easily programmed for computer evaluation, provided there is the means to evaluate $V(\theta)$. The volume swept by the piston is computed as

$$V_{swept} = 2RA_p$$

where A_p is the piston area $= \pi D^2/4$. The maximum cylinder volume is part of the given data for the compressor. The difference between these two values is an irregularly shaped volume close to the cylinder head with clearances for the valves and other irregularities. It is useful to idealize this irregular volume to be considered as a continuation of the cylindrical cylinder wall to a height d_c beyond the extreme piston position. The quantity d_c is called the *clearance distance*. It must be remembered that it is not an actual physical distance and cannot be measured with a micrometer. It is a fictional distance to describe a fictional right circular cylinder with the same volume as the clearance volume above the piston. It is evident that the clearance distance is such that

$$V_{\max} = V_{swept} + A_p d_c \tag{9.36}$$

With the clearance distance known, the cylinder volume for any crank angle is

$$V(\theta) = A_p\left(R + L + d_c - x\right) \tag{9.37}$$

With these comments in effect, there is no difficulty at all in solving the system of equation (9.28) for a sequence of θ values. This has been programmed, and some of the results are shown in Figures 9.9 and 9.10. It should be noted that, although only the results for F_1 and F_2 are presented in those figures, all of the internal forces and the crank acceleration are determined at every position.

9.4.2.3 Dynamic Analysis

The fully dynamic force analysis requires that the complete system of equations (9.28) be solved without assumptions regarding the speed. This means that the actual speed variation, based on the solution of the differential equation of motion, must be employed at every position where force calculations are to be performed. That solution requires a full simulation, with the numerical solution of the differential equation of motion, as discussed in Chapter 7. The equation of motion for the slider-crank is readily developed by means of Eksergian's equation and need not be elaborated here except for a few details. Everything previously said about modeling the cylinder pressure in connection with the kinetostatic analysis applies for this analysis as well.

Motor Torque Modeling The whole purpose of the dynamic model is to reflect the effect of speed variation, so a dynamic model for the motor torque is required. However, since only steady state operation is specified, it is implied that the range of speed variation is limited, not deviating too greatly from the rated speed of 176.87 rad/s. This indicates that the linear torque-speed relation of Appendix 5.1.4.1 can be employed. The constants for that model are determined from the rated (motor rotor) speed and power:

$$c_o = 68.762637 \quad \text{N-m} \tag{9.38}$$

$$c_1 = -0.36479712 \quad \text{N-m-s} \tag{9.39}$$

These two constants describe the electromagnetic torque acting on the motor rotor.

Steady-State Operation The problem statement indicates that only steady state conditions are of interest, but the question remains, "what exactly constitutes steady state?" On the surface, the answer is relatively simple: steady state means that the crank speed varies in a periodic manner over each crank revolution while the total crank angle turned increases without limit. In detail, there is a bit more to it!

To achieve steady state operation, each crank revolution must begin with exactly the same speed. Thus the question comes down to "what is $\dot{\theta}$ when $\theta = 0,\ 2\pi,\ 4\pi,\ \ldots$ such that each cycle will be exactly like every other one? While it is easy to start the integration of the equation of motion with $\theta = 0$, the question remains as to what value to use for $\dot{\theta}$ at the beginning?

There are several possible approaches to this question, each of which will eventually work out.

1. The linear model for the motor torque can be replaced by a more detailed model such that the actual start-up phase can be correctly simulated. When this is done,

the simulation will eventually settle into steady state operation, and the speed variation over a cycle can be extracted from the simulation. This has the drawback of requiring a more detailed model of the motor, but it is entirely feasible. Depending on the particular problem under consideration, it may be necessary to simulate a very long time before steady state is reached, with the attendant problems of computer storage and extended run times.

2. The linear torque-speed model can be used with any reasonably close starting speed, and it too will eventually settle into the steady state operating mode. The early part of this simulation should not be taken as steady state; it is based on an incorrect torque model and differs substantially from the actual physical case. It will, however, eventually become correct as steady state is approached.

3. The simulation may be performed repeatedly for only one crank revolution with the starting speed estimate progressively improved each time. For periodicity, the crank speed at the end of the revolution must exactly match that the beginning. Thus simulating one cycle allows for a correction to the starting speed based on the difference between initial and final speeds in the previous computer run. This approach is attractive because only one crank revolution needs to be simulated and thus each computer run is fairly short. It is less attractive because of the seemingly unpredictable behavior of the final speed with each intended improvement to the initial speed estimate.

The third approach is employed in preparing this example. It should be emphasized that in using this approach, it is important to simulate exactly one crank revolution, stopping exactly at $\theta = 2\pi$ if the cycle is begun at $\theta = 0$. This may well require modifying the integration time step to obtain the required termination point. By iteration, it is determined that the steady state operation is associated with the initial speed $\dot{\theta}\,(t = 0) = 118.29$ rad/s.

9.4.3 Slider-Crank Internal Force Results

The result of the steady state simulation are show in Figure 9.8 where both crank speed and cylinder pressure are plotted against crank angle.

Considering Figure 9.8, the four phases of the compression cycle are clearly evident in the crank forces.

1. During the re-expansion phase, the crank is accelerated by both the motor torque and the pressure of the trapped gas;

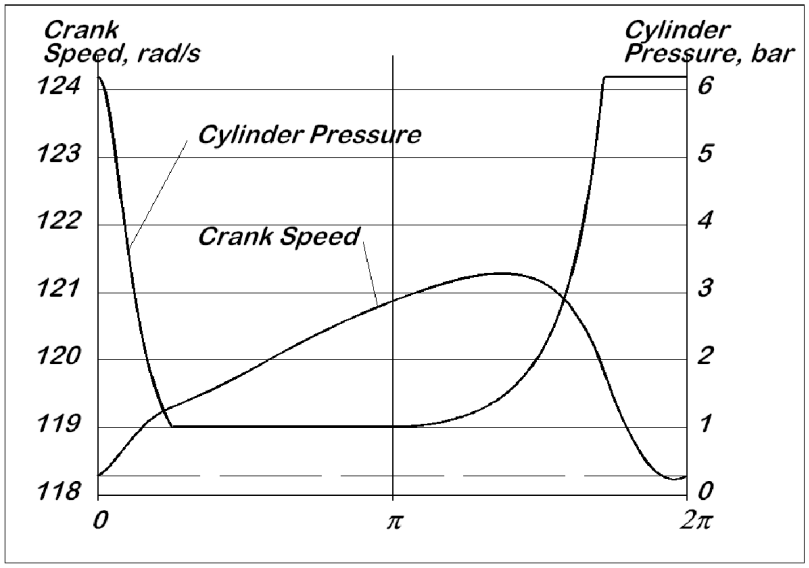

Figure 9.8: Plots of Cylinder Pressure (Pa) and Crank Speed (rad/s) versus Crank Angle θ

2. During the suction phase, the crank continues to accelerate under the influence of the motor torque;

3. As compression begins, the rate of acceleration drops, leading eventually to negative acceleration approaching the discharge stage;

4. During discharge, the crank continues to decelerate, with the speed retarded by the high pressure gas on top of the piston.

Note that the starting crank velocity, $\dot{\theta}_o = 118.29$ rad/s, is near the lowest speed of all; the piston is slowed to a stop at the TDC position due to the gas pressure above the piston.

The main bearing forces, F_1 and F_2 are plotted in Figure 9.9 and 9.10. These two figures show the curves generated by both (a) the kinetostatic analysis, and (b) the dynamic analysis; they appear a a single curve, indistinguishable to the unaided eye. This indicates that, for this example, both methods of analysis give almost identical results for these forces. The same four phases can be seen in these force plots. Note particularly how strongly F_1 is influenced by the cylinder pressure; this is in agreement with intuition.

The other matters of interest here are the external reaction forces, R_x and R_y as the crank goes through a full revolution; these are shown plotted against each other in Figure 9.11. Again, this figure shows the results of both (a) kinetostatic analysis (inner curve) and (b) dynamic analysis (outer curve). This is the only place where there is a visible difference between the two analysis methods. These forces are determined by employing the values

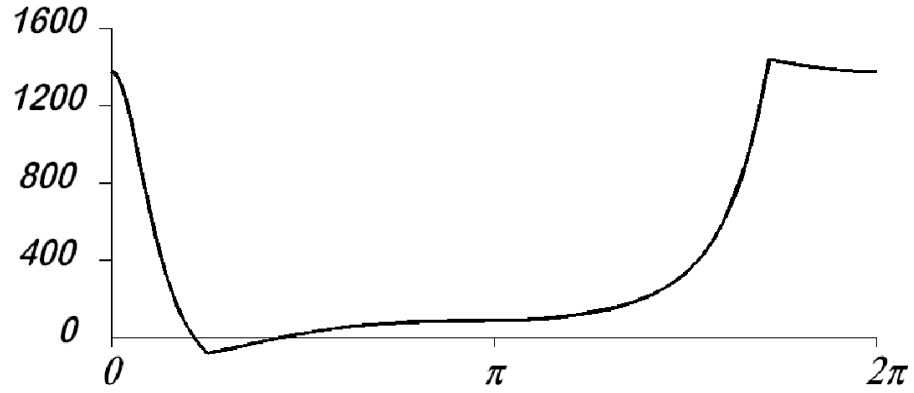

Figure 9.9: Crank Force F_1 (N) as a Function of Crank Angle θ (rad)

of F_1 and F_2 in equations (9.29) and (9.30). The result is the characteristic egg-shaped plot.

9.5 A Second Look at the Two Methods

In the kinetostatic analysis, the velocity is assigned a constant value, $\dot{\theta} = \Omega$. This has often been misconstrued in the past as equivalent to saying that $\ddot{\theta} = 0$, but that is not correct. It is important to distinguish what is actually being done.

For any of the force analysis techniques applied to the slider-crank mechanism, the process ultimately comes down to solving equations (9.28). This solution, for either technique, produces force values and a value for $\ddot{\theta}$, the last usually not equal to zero. Such a result cannot be a solution based on $\ddot{\theta} = 0$. For either technique, evaluating all of the terms in equation (9.28) requires values for both θ and $\dot{\theta}$. The difference between the two approaches is in how these two values are provided.

1. **Kinetostatic Analysis** Both values are assigned at will by the analyst.

   (**a**) The position, θ, is assigned based on interest in a particular position, or simply as a matter of stepping through the whole cycle;

   (**b**) The speed, $\dot{\theta}$ is assigned as a representative value, thought to be reasonably close to the actual value at the particular position;

   (**c**) Using the same value repeatedly, $\dot{\theta} = \Omega =$ constant, is simply an expedient based on lack of better information. It is a matter of choosing the same approximate value time and again, rather than an intention to say that $\ddot{\theta}$ is zero.

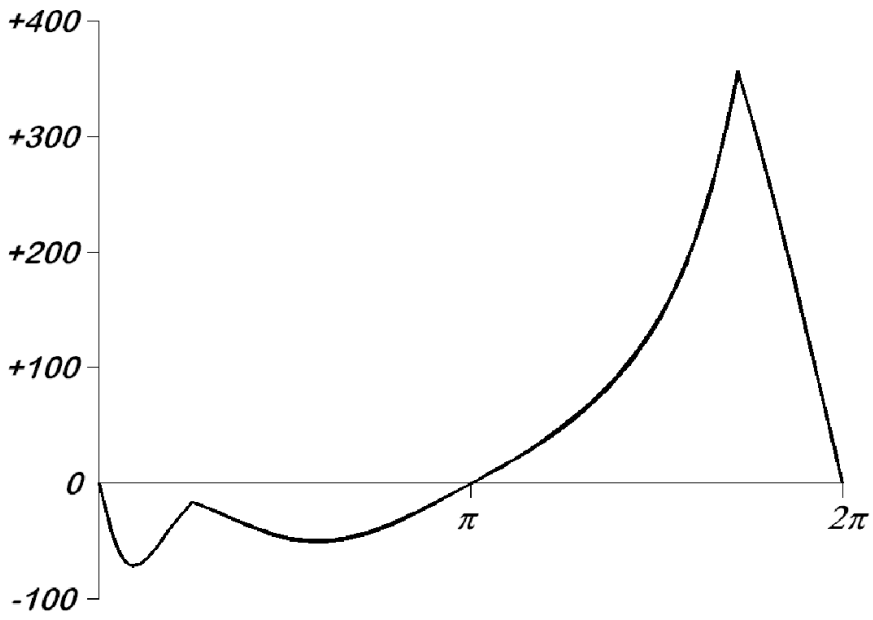

Figure 9.10: Crank Force F_2 (N) as a Function of Crank Angle θ (rad)

(**d**) Each successive position analyzed represents a point on a different natural motion; they are not at all parts of the same continuous motion. The result is an artificial, contrived motion, not one that actually exists in nature.

2. **Dynamic Analysis** Both values are determined by the dynamic simulation, the solution of the governing differential equation of motion. That solution provides values for $\theta(t)$, $\dot{\theta}(t)$, and $\ddot{\theta}(t)$, all controlled by the equation of motion subject to the initial conditions, the result of a true, natural motion of the system. The analyst has no control at all over these values, other than being able to stop the process at will.

The example just presented shows that, for some cases, the results of the two approaches can be quite close. This should not be taken as an indication that this is true in all cases.

9.6 Forces in a Link

The discussion to this point has considered the matter of determining the interconnection forces within a dynamic mechanism. The development of a system of equations, solvable for the connection forces, is discussed, based on the sums of forces and moments, and involving the mass and mass moment of inertia of each member, in each case multiplied by the appropriate acceleration. The only assumptions involved have been that the bodies

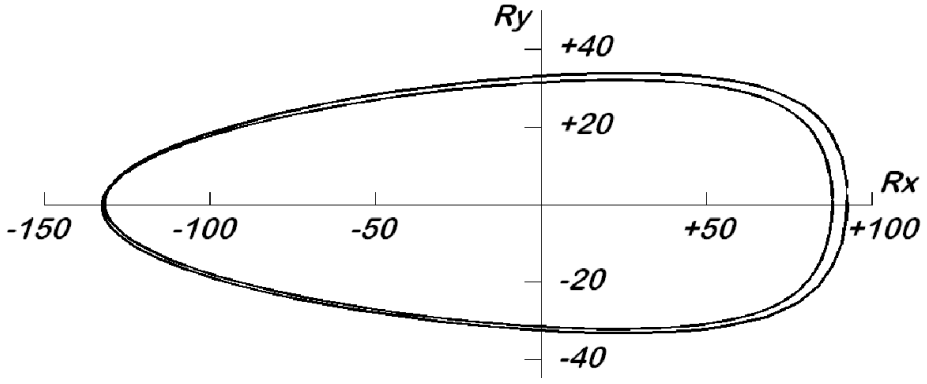

Figure 9.11: External Reactions, R_x and R_y, Through the Crank Cycle

are rigid and moving in planar motion. However, understood more broadly, the forces inside a single machine component are also internal forces. For the ideas developed in this section, a further assumption is made, namely that the body considered is long and slender, like a link or rod, such that the elementary stress analysis for beams is applicable. This then applies to a variety of push rods, connecting rods, and actuator links.

For now, consider that all interconnection forces are known for the member shown in the part shown in Figure 9.12. Note that it is long and slender, as required, and if the section is not entirely uniform, the variation is at most only small. The coordinate ξ locates any section of particular interest. This might be a section where cracks have been found in service, it might be a suspect location for serious stress conditions, or ξ may be varied from 0 to L to describe every point along the length of the link.

To be more specific, consider that, for the link shown, the following items have all been determined: $x(t)$, $y(t)$, $\phi(t)$, $F_x(t)$, and $F_y(t)$. Then consider a cut at the position shown located by the distance ξ. The purpose for this discussion is to determine the internal forces on the section at ξ, specifically $T(\xi)$, $V(\xi)$, and $M(\xi)$, that is, the tension, shear, and bending moment at the cut surface.

9.6.1 Inertial Properties

Since the material and all details of the link geometry are assumed to be known, it is reasonable to assume that the mass per unit length, $\mu(\xi)$, is also known. The distance $\rho_c(\xi)$ locates the center of mass **of the section of the link under consideration** (this is not the entire link, but rather, it is the section to the left of the cut at ξ). The total mass of the section under consideration is $m(\xi)$,

$$m(\xi) = \int_0^{\xi} \mu(\lambda)\ d\lambda \tag{9.40}$$

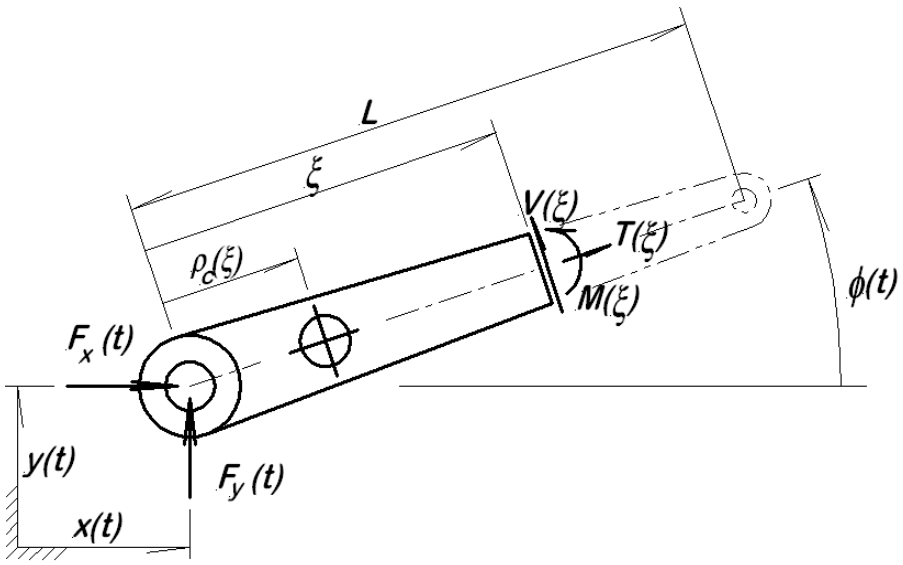

Figure 9.12: Lower Left Part of the Link, Showing the Internal Forces on the Cut at ξ

The location of the center of mass of this segment of the link is calculated as

$$\rho_c(\xi) = \frac{\int_0^\xi \lambda \mu(\lambda)\ d\lambda}{\int_0^\xi \mu(\lambda)\ d\lambda} \tag{9.41}$$

Finally, the mass moment of inertia for this segment, with respect its own center of mass, is calculated as

$$\begin{aligned} J_c(\xi) &= \int_0^\xi [\lambda - \rho_c(\xi)]^2 \mu(\lambda)\ d\lambda \\ &= \int_0^\xi \lambda^2 \mu(\lambda)\ d\lambda - \rho_c^2(\xi)\, m(\xi) \end{aligned} \tag{9.42}$$

as expected from the parallel axis theorem. All of these inertial properties (the mass, center of mass location, and mass moment of inertia with respect to the center of mass) for the segment are required for the analysis to follow. It should be noted that, while these integrals can be evaluated by hand for simple cases, they are also readily evaluated by numerical means for more complex mass distributions, such as tapering links.

9.6.2 Acceleration Components

The acceleration of the center of mass of the segment under consideration is also required. This follows rather simply from a kinematic analysis of the situation, showing the roles of the accelerations of the left end coupled with the effects of the angular motion. Thus the position of the segment center of mass is given by

$$x_c = x(t) + \rho_c \cos\phi \tag{9.43}$$
$$y_c = y(t) + \rho_c \sin\phi \tag{9.44}$$

These equations are then differentiated twice with respect to time to obtain the center of mass acceleration components:

$$\dot{x}_c = \dot{x}(t) - \dot{\phi}(t)\,\rho_c \sin\phi(t) \tag{9.45}$$
$$\dot{y}_c = y(t) + \dot{\phi}(t)\,\rho_c \cos\phi(t) \tag{9.46}$$
$$\ddot{x}_c = \ddot{x}(t) - \ddot{\phi}(t)\,\rho_c \sin\phi(t) - \dot{\phi}^2(t)\,\rho_c \cos\phi(t) \tag{9.47}$$
$$\ddot{y}_c = \ddot{y}(t) + \ddot{\phi}(t)\,\rho_c \cos\phi(t) - \dot{\phi}^2(t)\,\rho_c \sin\phi(t) \tag{9.48}$$

It is convenient to resolve the force sums along axes parallel and perpendicular to the axis of the link. For this purpose, the components of acceleration are

$$\begin{aligned} a_{\parallel} &= \ddot{x}_c \cos\phi + \ddot{y}_c \sin\phi \\ &= \ddot{x}\cos\phi + \ddot{y}\sin\phi - \dot{\phi}^2 \rho_c \end{aligned} \tag{9.49}$$

$$\begin{aligned} a_{\perp} &= -\ddot{x}_c \sin\phi + \ddot{y}_c \cos\phi \\ &= -\ddot{x}\sin\phi + \ddot{y}\cos\phi + \ddot{\phi}\rho_c \end{aligned} \tag{9.50}$$

9.6.3 Force & Moment Equations

The stage is now set for the application of Newton's Second Law. Thus,

$$\sum F_{\parallel} = F_x \cos\phi + F_y \sin\phi + T(\xi) = m(\xi)\, a_{\parallel} \tag{9.51}$$
$$\sum F_{\perp} = -F_x \sin\phi + F_y \cos\phi + V(\xi) = m(\xi)\, a_{\perp} \tag{9.52}$$
$$\begin{aligned} \sum_{+CCW} M_c &= M(\xi) + [\xi - \rho_c(\xi)]\, V(\xi) + F_x \rho_c(\xi) \sin\phi - F_y \rho_c(\xi) \cos\phi \\ &= J_c \ddot{\phi} \end{aligned} \tag{9.53}$$

These equations are solved for the required force components:

$$\begin{aligned} T(\xi) &= m(\xi)\, a_{\parallel} - F_x \cos\phi - F_y \sin\phi \\ &= m(\xi)\left[\ddot{x}(t)\cos\phi + \ddot{y}(t)\sin\phi - \dot{\phi}^2 \rho_c\right] \\ &\quad -F_x \cos\phi - F_y \sin\phi \end{aligned} \tag{9.54}$$

$$\begin{aligned} V(\xi) &= m(\xi)\, a_{\perp} + F_x \sin\phi - F_y \cos\phi \\ &= m(\xi)\left[-\ddot{x}(t)\sin\phi + \ddot{y}(t)\cos\phi + \ddot{\phi}\rho_c\right] \\ &\quad +F_x \sin\phi - F_y \cos\phi \end{aligned} \tag{9.55}$$

$$\begin{aligned} M(\xi) &= J_c\ddot{\phi} - [\xi - \rho_c(\xi)]\, V(\xi) - F_x \rho_c(\xi)\sin\phi + F_y \rho_c(\xi)\cos\phi \\ &= J_c\ddot{\phi} - [\xi - \rho_c(\xi)]\, m(\xi)\left[-\ddot{x}(t)\sin\phi + \ddot{y}(t)\cos\phi + \ddot{\phi}\rho_c\right] \\ &\quad -\xi\left(F_x \sin\phi - F_y \cos\phi\right) \end{aligned} \tag{9.56}$$

This is the intended result, expressions for $T(\xi)$, $V(\xi)$, and $M(\xi)$. The tension, shear, and bending moment for a cut at any position can now be calculated at any time during the motion.

With the shear, tension, and bending moment known at any point, the standard methods of elementary stress analysis may be employed to compute shear, axial, and bending stresses in the link. It should be noted that a gravitational load on the link is not included in the analysis above; it can certainly be added to this work, although it is often not considered significant. These results show, for example, that a uniform bar swinging as a pendulum experiences at every section not only a tension but also shear and bending moment.

9.7 Conclusion

The determination of interconnection forces and moments (and those internal to individual components for limited situations) is demonstrated in this chapter. These values are often essential to a proper design analysis, to assure adequate component strength, bearing size, and a host of other design questions. It is also often necessary to evaluate the forces after the fact for purposes of accident investigation and failure analysis.

While the development of system equations of motion is often best done by means of energy methods (Eksergian's equation or the Lagrange equations), the evaluation of forces and moments is only possible through the use of Newton's Second Law. The application of Newton's Second Law also produces, in addition to the forces, a value for the system acceleration, although usually only at the cost of considerably more computational effort. The energy-derived acceleration and that obtained from the Second Law must be in agreement; failure to agree indicates a computational error.

If static analysis is dismissed for dynamical systems, there remain at most two major approaches to the force analysis. For situations where a the system motion is periodic, exhibiting a steady state oscillation, it may well be possible to obtain a satisfactory force analysis by means of the kinetostatic method. Where it applies, this method should not be dismissed because of its relative ease of application. For those cases where there is no steady state, or where the velocities are thought to vary widely through a cycle, then the dynamic simulation is the only basis available for the force analysis.

References

[1] Beer, F.P. and Johnston, E.R., *Vector Mechanics for Engineers*, 4th ed., McGraw-Hill, New York, 1984.

[2] Paul, B., *Kinematics and Dynamics of Planar Machinery*, Prentice-Hall, Englewood Cliffs, N.J., 1979.

[3] Norton, R.L, *Design of Machinery*, 2nd. ed., McGraw-Hill, New York, 1999.

Problems

9-1 The figure shows a bit over half of a plan view of an aircraft. The aircraft is in level flight with its velocity along the $y-$axis; the $z-$axis is vertically upward. The aircraft velocity at this moment is v_y but it is accelerating in the forward direction in the amount a_y. The lift and drag forces on the elemental wing section (shown shaded) are of the forms $dF_{Lift} = C_L v_y^2\, dx$ (in the positive $z-$direction) and $d_{F_{Drag}} = C_D v_y^2\, dx$ (in the negative $y-$direction). The aerodynamic forces combine to produce four items of concern for this problem. Draw the appropriate free body diagram for the wing, and then, based on aero-loads only, compute:

(a) S_y = horizontal shear force at the wing root;

(b) S_z = vertical shear force at the wing root;

(c) M_y = bending moment at the wing root about the $y-$axis;

(d) M_z = bending moment at the wing root about the $z-$axis.

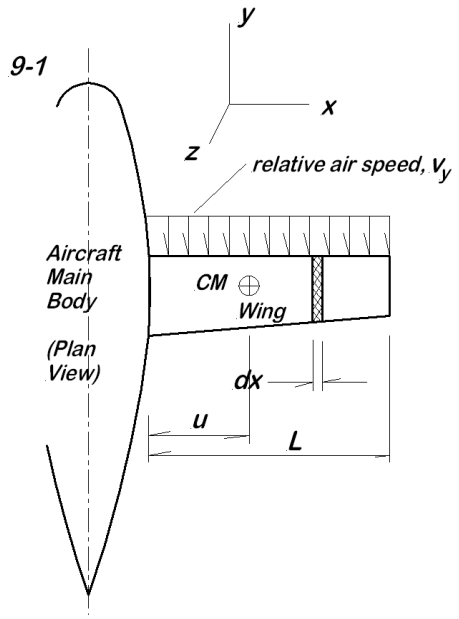

9-2 For the trammel mechanism shown, the center of mass of the connecting link is at the midpoint. All geometric data are known, as are the spring rate and the dashpot coefficient. The spring is relaxed when $x = x_o$, a known value.

(a) Develop all of the kinematic analysis required for later steps;

(b) Determine the guide reactions and the pin connection forces in terms of the geometry and $F(t)$;

(c) Determine the values for all of the forces of (b) at an instant when $x = 155$ mm, $\dot{x} = 85$ mm/s, bases on the parameters below:

$L = 688$ mm $\quad x_o = 77$ mm

$M_L = 1.15$ kg $\quad J_{Lc} = 0.0152$ kg-m^2

$M_x = 0.225$ kg $\quad M_y = 0.272$ kg

$K = 785$ N/m $\quad B = 147$ N-s/m

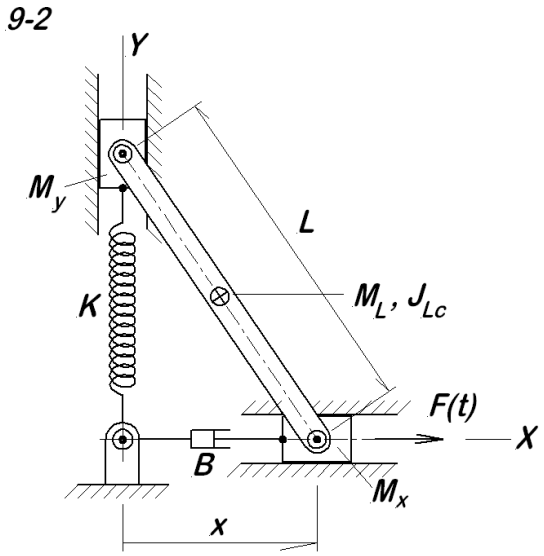

9-3 For the roller-pendulum shown, evaluate the force components on the stationary pivot pin, the roller axle, and the shear and normal forces between the roller and the level surface when $\theta = 0.0287$ rad and $\dot{\theta} = 26.38$ rad/s. This system data is in the following table.

$M_L = 12.86$ kg $\quad J_{LC} = 3.485$ kg-m^2

$M_R = 17.89$ kg $\quad J_{RC} = 0.333$ kg-m^2

$C = 1.255$ m $\quad H = 0.974$ m $\quad R = 0.139$ m

9-4 For the quick return mechanism shown, the flywheel is driven by a motor torque T while the slider motion is opposed by the force F.

(a) Perform all kinematic analysis required for later use;

(b) Determine the system equation of motion;

(c) Determine the slider-guide reaction force;

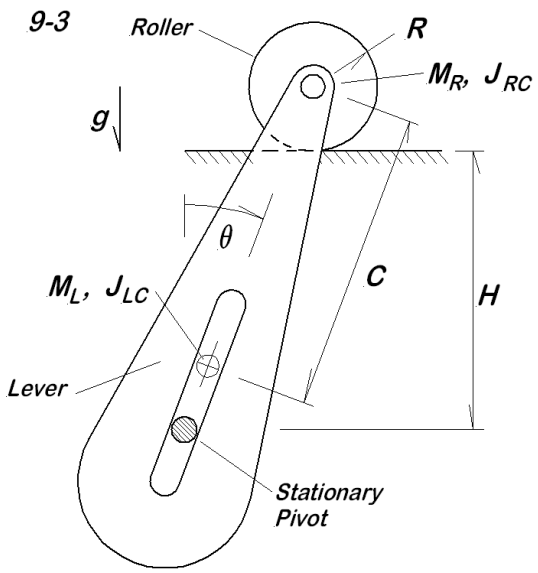

(d) Determine the lever pivot reactions at point O;

(e) Determine the forces on the flywheel pin in the lever slot;

(f) Determine the forces on the slider pin in the lever slot;

(g) Determine the flywheel bearing reactions;

(h) Using the data below, evaluate all of the forces enumerated above for the situations where $\theta = 0.544$ rad, $\dot{\theta} = 22.33$ rad/s, $T = 27.7$ N-m, $F = 587$ N and the following system parameters:

$M_S = 10.7$ kg	$J_c = 0.28$ kg-m^2	$J_o = 5.30$ kg-m^2
$R = 115$ mm	$C = 490$ mm	$D = 710$ mm
$B_S = 185$ N-s/m	$B_P = 126$ N-s/m	

9-5 The cam shown is an eccentric circle with radius R and eccentricity ε. The cam shaft rotates at a constant rate, $\dot{\theta} = const$. The spring tension is F_{ko} when the follower angle ϕ is at its minimum value. All the indicated mass moments of inertia are referenced to the body axis of rotation. The shaft joining the cam follower to the load is considered as massless.

(a) Perform all kinematic analysis required for later parts;

(b) Determine the equation of motion in terms of the cam rotation angle, θ;

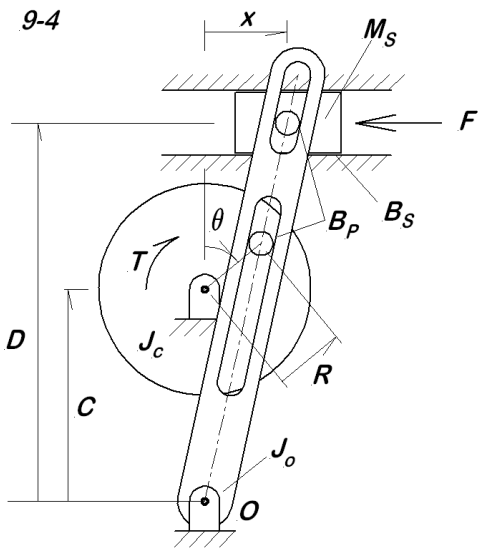

(c) Determine the required driving torque, T_o, for $\dot{\theta}$ = constant;

(d) Determine the contact force between the cam and the follower;

(e) Determine the net cam shaft bearing reactions;

(f) Determine the net bearing reactions on the follower shaft;

(g) Determine the torque in the follower shaft at section G;

(h) For the case where $\theta = 1.378$ rad and $\dot{\theta} = 53.0$ rad/s, evaluate numerically all of the forces and torques enumerated above. Use the following system data for these calculations:

$\varepsilon = 6.33$ mm	$R = 18.0$ mm	$F_{ko} = 125$ N
$D = 135$ mm	$d = 92$ mm	$K = 400$ N/m
$J_o = 1.5 \cdot 10^{-5}$ kg-m^2	$J_1 = 6.3 \cdot 10^{-5}$ kg-m^2	$J_2 = 3.3 \cdot 10^{-5}$ kg-m^2

9-6 The planet carrier motion is the input angle, θ, driven by the torque T_o. The sun gear is stationary, and the planet gear rotation is A. The crank arm is aligned with the reference make on the planet gear. The drive mechanism may be considered as massless, but the load has mass moment of inertia J_c about its rotation axis, $C - C$. The sun gear pitch radius is R_S, the planet pitch radius R_P, and the crank offset is b. The input angular velocity, $\dot{\theta}$, is held constant.

(a) Perform all kinematic analysis required for later use;

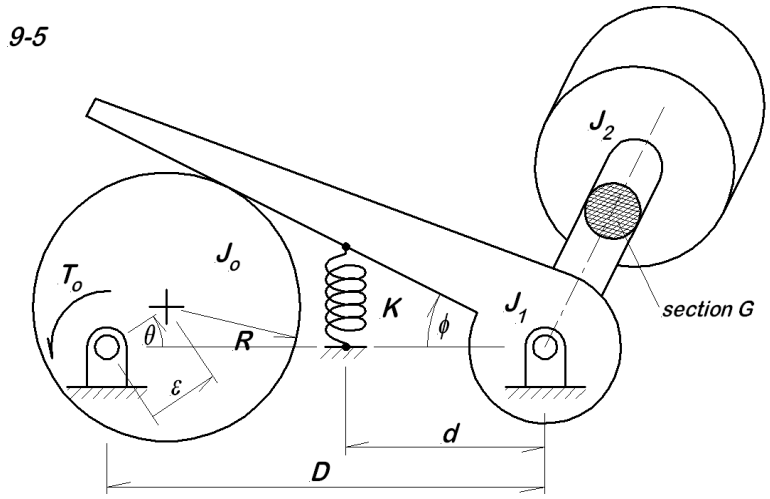

(b) Express the required torque, T_o, as a function of θ and $\dot{\theta}$;

(c) Determine the tangential force between the sun gear and planet;

(d) Determine the contact force between the crank and the slot wall;

(e) Evaluate all the previously enumerated forces and torques for the situation $\theta = 1.122$ rad, $\dot{\theta} = 15.55$ rad/s. Use the following data for the system parameters:

$R_S = 380$ mm $\quad R_P = 123$ mm

$b = 35.0$ mm $\quad J_c = 0.320$ kg-m^2

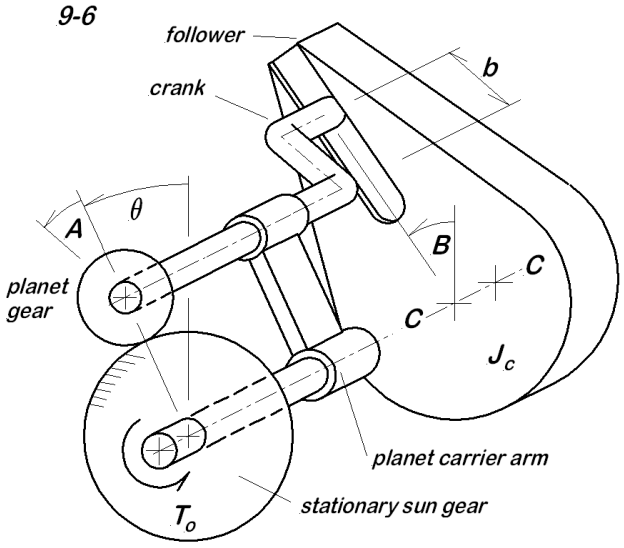

9-7 The figure shows a coil spring used to launch a small block, M. The free length of

the spring is S_o, and prior to launch, it is compressed to the length $S_{\min}$. The spring has mass M_S, assumed to be uniformly distributed over its length. The objective here is to determine the launch velocity for the block, while taking into account the mass of the spring.

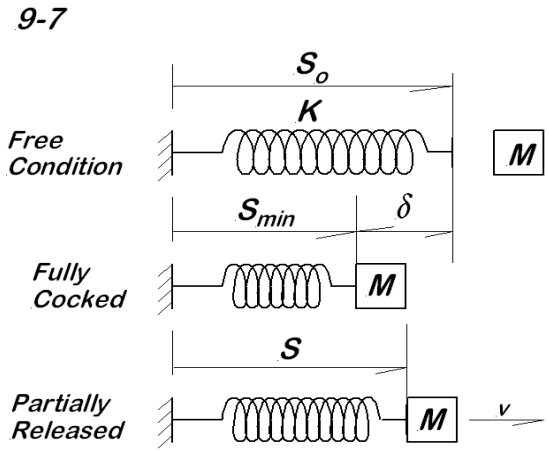

9-8 In the quick return shown, the torque T_o acting on the crank causes reciprocating motion in the slider, resisted only by the inertia of the system. The crank has mass M_1 and mass moment of inertia J_{1o} with respect to the fixed pivot. The coupling link #4 has its center of mass at the center of the link.

(a) Perform all kinematic analysis required for later use;

(b) Determine the equation of motion;

(c) Determine the forces on the stationary pivot pin in the lever slot:

(d) Determine the bearing reactions on the crank;

(e) Determine the slider guide force;

(f) Determine the forces at all connecting pins;

(g) Evaluate all the forces enumerated above for the case where $\theta = 0.858$ rad, $\dot{\theta} = 14.52$ rad/s, using the data below:

$D_1 = 92$ mm	$D_2 = 195$ mm	$D_3 = 198$ mm	$D_4 = 75$ mm
$M_1 = 0.055$ kg	$M_2 = 0.119$ kg	$M_3 = 1.420$ kg	$M_4 = 0.080$ kg
$J_{1o} = 3.4 \cdot 10^{-5}$ kg-m^2	$J_{2c} = 3.8 \cdot 10^{-4}$ kg-m^2		$J_{4c} = 3.8 \cdot 10^{-5}$ kg-m^2
$T_o = 0.72$ N-m	$u = 85$ mm	$R = 37$ mm	

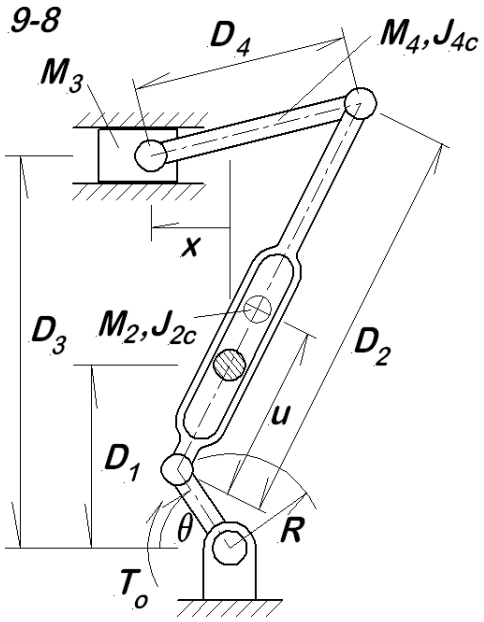

9-9 The device shown is a chain cutter, found in a hardware store. Consider the case when a horizontal force is applied to the lever, $F = 450$ N. Using the data below,

(a) Determine the force available to cut the chain link;

(b) Determine the load on the roller in the lever slot;

(c) Determine the bearing loads at both fixed pivots.

$C = 136$ mm $\quad L = 1067$ mm

$R = 162$ mm $\quad r = 33$mm

9-10 The figure shows a spring-loaded garage door (previously considered in problems **2-15** and **2-16**). The door weighs 940 N, and the center of mass is at the middle of the panel. Both opening and closing motions are very slow, so that dynamics really do not need to be considered. Determine appropriate values for the spring constant, K, and the pre-load in the spring, such that a man lifting on the lower edge never needs to exert more than 30 N upward to raise the door.

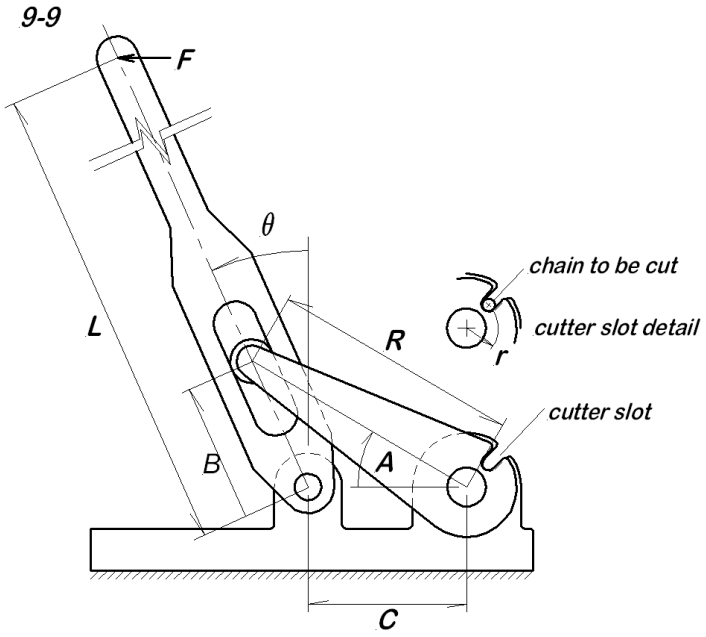

$C_1 = 2134$ mm	$C_2 = 2079$ mm	$C_3 = 274$ mm
$C_4 = 274$ mm	$C_5 = 213$ mm	$C_6 = 90$ mm
$x_A = 1402$ mm	$y_A = 183$ mm	lower pivot location
$x_D = 1402$ mm	$y_D = 975$ mm	upper pivot location
$x_F = 2286$ mm	$y_F = 1066$ mm	spring anchor location

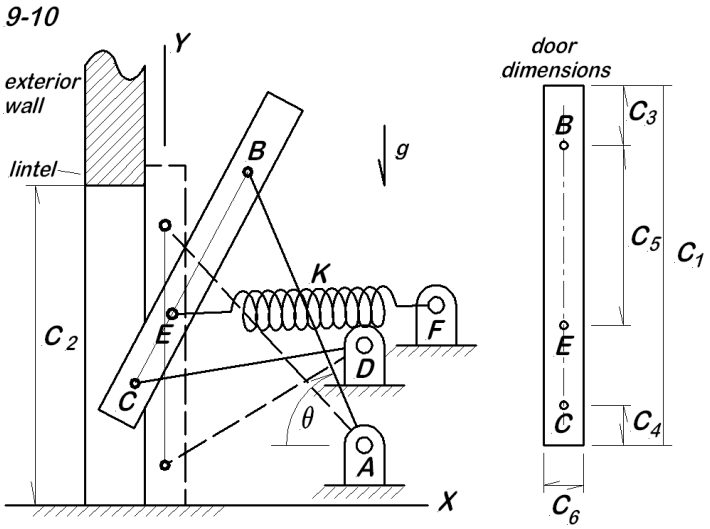

9-11 Consider yet again the air powered press previously encountered in problems **2-20**, **2-21**, and **6-14**. All data provided in those problems, and all analysis done for them, is

understood to apply here as well.

(a) Determine the force acting in each of the simple links L_1, L_2, L_3 and L_4 throughout the piston stroke. Take tension forces as positive and compressive forces as negative.

(b) Identify the extreme values in each link along with the piston position for which those extreme values occur.

Part III

Vibrations of Machines

Chapter 10

SDOF Vibrations

10.1 Introduction

In all of the earlier portion of this book, all bodies are considered to be rigid. The only exceptions have been springs, usually identified with the traditional coil spring or a spiral torsional spring, and assumed to have a linear force-deflection relation. While rigid bodies are an extremely useful idealization for many purposes, they do not perfectly reflect reality. In the physical world, all bodies deform to some degree under load. For systems where the deformation is linearly related to the applied load, the proportionality constant is called the *stiffness*. The reciprocal of the stiffness is called the *compliance* or *flexibility*.

When part deformation is taken into account, the simple rigid body geometric relations used in kinematic analysis are no longer applicable; the distances between points in a single body are no long constant but now change with load on the part. One immediate consequence of this is that the number of degrees of freedom increases drastically. In the most extreme case, every single physical body is considered to have infinitely many degrees of freedom. This is clearly an unmanageable model. Because engineering analysis is about making mathematical models that provide useful descriptions of reality, retaining the essentials without being over burdened by excessive detail, the inclusion of flexibility in the model is something of an art (rather than a science) and must be practiced with skill to obtain good results.

In application, the existence of flexibility in machine parts leads in many cases to small amplitude, high frequency motions. Theses are sometimes called chatter, oscillation, bouncing, noise, or more generally, simply *vibration*. Most machine parts, made from steel or other strong engineering materials, are quite stiff, which means that they do not deform very much under design load levels. This has two consequences: (1) the

motion amplitudes of concern are usually small (larger amplitudes would be associated with extremely large forces), and (2) the motion is usually quite rapid (high frequency) compared to the gross body motion that may also be occurring.

From a mathematical perspective, much of the study of mechanical vibration comes down to dealing with a single family of ordinary differential equations. This family of equations is so widely encountered that the student will do well to simply memorize the solutions and apply them directly, rather than repeatedly working through the solutions time and again.

There are two major cases of common interest. The first is what is called free vibration. *Free vibration* means that the system is set in motion by the initial conditions, either an initial deformation, an initial velocity, or perhaps both of these conditions combined. If an elastic body is suddenly released from a strained position, the resulting vibratory motion is free vibration. Similarly, if an elastic system is subjected to an initial velocity, such as with a hammer blow, the resulting motion is free vibration. The second major case is called *forced vibration*. A forced vibration is the response of the system to a continuing excitation, a source of continued energy input to the system. The general case is, of course, a combination of these two cases, where an elastic system with some initial energy (initial strain and/or kinetic energy) is subject to continuous external excitation from an outside energy source.

10.2 Free Vibration of SDOF Systems

Just as seen in the earlier study of kinematics, the simplest case is that of the single degree of freedom (SDOF) vibrational system. Experience shows that this actually is a useful model for a large number of real systems, as well as providing background for vibrations of multidegree of freedom systems.

10.2.1 Undamped Vibration

For this section, only very simple mechanical systems are considered, although they are in fact representative of a vast number of actual physical systems. The focus is instead on the form of the differential equations of motion and their solutions. To this end, consider first the simple spring-mass system shown in Figure 10.1. This is the prototypical SDOF vibratory system.

The figure shows a simple mass, a block of mass M, connected on the left side to a fixed support through a spring of stiffness K. The position of the mass is indicated by the coordinate $x\,(t)$, and the spring is relaxed (stress free) when $x = 0$. The small circular

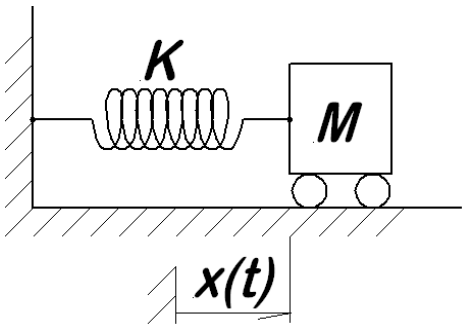

Figure 10.1: Free Vibration of an Undamped Spring-Mass Oscillator

rollers under the mass are intended to indicate that there is no friction in the system. The only force acting on the mass is that of the stretched spring. The equation of motion is immediately obtained through Newton's Second Law as

$$M\ddot{x} + Kx = 0 \tag{10.1}$$

There is nothing at all incorrect about equation (10.1) as written, but it is not quite in the preferred form. *Standard form* for an equation of this sort requires two things:

1. That the coefficient of the highest derivative is normalized to 1.0;

2. The ratio K/M is replaced with the symbol ω_o^2.

Thus, in standard form, the equation of motion is written as

$$\ddot{x} + \omega_o^2 x = 0 \tag{10.2}$$

where ω_o is called the *(undamped) natural frequency.* This is a key parameter of the solution and tells much about the nature of the solution in itself.

Assume the solution and the first derivative in the form

$$x(t) = \alpha \cos \omega_o t + \beta \sin \omega_o t \tag{10.3}$$
$$\dot{x}(t) = -\omega_o \alpha \sin \omega_o t + \omega_o \beta \cos \omega_o t \tag{10.4}$$

The coefficients α and β are to be appropriately chosen to satisfy the initial conditions.

Suppose the given initial conditions are these: $x(0) = x_o$ and $\dot{x}(0) = v_o$. The solution and the derivative, equations (10.3) and (10.4), are evaluated at $t = 0$ to provide a pair

of equations solvable for α and β. When these solutions are substituted into equation (10.3), the result is

$$x(t) = x_o \cos \omega_o t + \frac{v_o}{\omega_o} \sin \omega_o t \tag{10.5}$$

The reader should verify that this expression does indeed satisfy equation (10.2) and the initial conditions.

There is more significance to equation (10.5) than may at first be apparent. It says that the response of any undamped spring-mass system to an initial disturbance (non-zero initial position, velocity, or both) but absent further excitation is (a) harmonic motion, (b) at the frequency ω_o. Consider now two substitutions:

$$x_o = X \sin \phi \tag{10.6}$$
$$v_o = \omega_o X \cos \phi \tag{10.7}$$

which, when solved for X and ϕ, give

$$X = \sqrt{x_o^2 + \left(\frac{v_o}{\omega_o}\right)^2} \tag{10.8}$$
$$\phi = \arctan\left(\frac{\omega_o x_o}{v_o}\right) \tag{10.9}$$

When these substitutions are made in equation (10.5), the result is

$$x(t) = X \sin(\omega_o t - \phi) \tag{10.10}$$

This last form expresses the solution in terms of a single sinusoid of amplitude X with a phase angle ϕ. This form, equation (10.10) and the previous solution, equation (10.5) are completely equivalent.

10.2.2 Damped Free Vibration

Damping is the general term used to describe the several processes by which mechanical energy in the system is converted into heat and thus lost from the motion. Damping may be due to dry friction (Coulomb friction), viscous friction, fluid dynamic drag, and internal hysteresis in the spring. The only damping description that is relatively easy to deal with mathematically is what is called *viscous friction*, that is, a friction force proportional to the first power of the relative velocity between two points (this sort of friction has been previously encountered in dashpots). The system of Figure 10.1 is

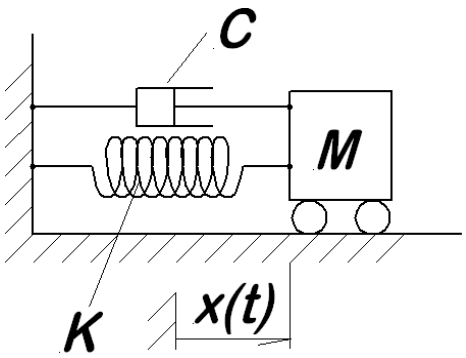

Figure 10.2: Free Vibration of a Spring-Mass Oscillator with Viscous Damping

redrawn in Figure 10.2 with the inclusion of a viscous damper with coefficient C. (Note that both B and C are common symbols for the damper coefficient, and both are used in this work.) The system is otherwise the same as that previously considered.

When the equation of motion for the system of Figure 10.2 is assembled, the result is

$$M\ddot{x} + C\dot{x} + Kx = 0 \tag{10.11}$$

or, in *standard form*, it reads

$$\ddot{x} + 2\zeta\omega_o\dot{x} + \omega_o^2 x = 0 \tag{10.12}$$

where

$\omega_o = \sqrt{K/M}$ = *undamped natural frequency*, as previously

$\zeta = C/\left(2M\omega_o\right)$ = *damping factor* (or *damping ratio*).

Compare standard form for the damped system with that for the undamped system, and note the differences.

While the undamped natural frequency has units of radians/second, the damping factor is dimensionless. The nature of the solution depends strongly on the value of the damping factor.

Assume a solution in the form

$$x\left(t\right) = ae^{\lambda t} \tag{10.13}$$

which is easily differentiated and substituted into equation (10.12) to produce

$$\left(\lambda^2 + 2\zeta\omega_o\lambda + \omega_o^2\right) ae^{\lambda t} = 0 \tag{10.14}$$

This equation is satisfied if either (a) $a = 0$, in which case the result is only the trivial solution, or (b) the coefficient in parentheses is zero. Equating the coefficient to zero gives what is called the *characteristic equation*. Solving the characteristic equation produces here two roots,

$$\lambda_{1,2} = -\zeta\omega_o \pm \omega_o\sqrt{\zeta^2 - 1} \tag{10.15}$$

It is apparent that the size of ζ is extremely important as this will control the sign of the quantity under the radical. There are four cases to be considered.

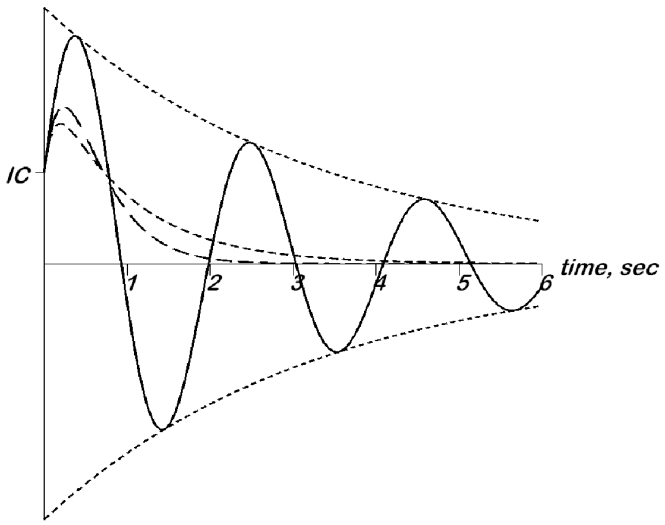

Figure 10.3: Damped Spring-Mass Oscillator Response Curves

Figure 10.3 shows three possible system responses (discussed below) plotted as functions of time and depending upon the damping level. In addition to the three actual motion plots, the graph shows a pair of envelope curves. The same physical system is considered in all three cases ($\omega_o = 3.0$ rad/s), except for the amount of damping that varies from case to case. Note that all three response motions begin from the same point (marked *IC* for **I**nitial **C**ondition) with the same initial slope ($x_o = 0.2$, $v_o = 1.5$).

10.2.2.1 Case 1: Over Damped Solution, $\zeta > 1$

If $\zeta > 1$, the system is said to be *over damped* (the meaning of the term becomes more clear when considered in context with the remaining cases). For this case, the quantity under the radical is greater than zero, so there are two real roots:

$$\lambda_1 = -\zeta\omega_o + \omega_o\sqrt{\zeta^2 - 1} \tag{10.16}$$

$$\lambda_2 = -\zeta\omega_o - \omega_o\sqrt{\zeta^2 - 1} \tag{10.17}$$

and the solution is

$$x(t) = a_1 e^{\lambda_1 t} + a_2 e^{\lambda_2 t} \tag{10.18}$$

The constants a_1 and a_2 must be evaluated to satisfy the initial conditions. This solution does not oscillate, but simply dies away as shown in Figure 10.3 as the curve of shortest broken lines. For the example plotted, $\zeta = 1.6$, which in most circumstances is rather heavy damping. Note that this curve shows the smallest maximum rise, a limitation imposed by the substantial damping value, and the curve rather quickly begins to return to the zero displacement condition. Note also, however, that it does not get to zero most quickly.

10.2.2.2 Case 2: Critically Damped Solution, $\zeta = 1$

In the event that $\zeta = 1$, the system is said to be *critically damped*. When this happens, both roots of the characteristic equation are real and equal; this is said to be a *repeated real root*.

$$\lambda_1 = \lambda_2 = -\omega_o \tag{10.19}$$

For this situation, the originally assumed solution form, equation (10.13) is inadequate, and a different form must be used:

$$x(t) = (a_1 + a_2 t)\, e^{-\omega_o t} \tag{10.20}$$

As before, the constants a_1 and a_2 must be evaluated to satisfy the initial conditions. *In point of fact, this solution dies away in the most rapid manner possible without oscillation,* making this the boundary case between oscillatory and non-oscillatory solutions. This solution is also shown in Figure 10.3 as the longer broken line curve, again originating at the IC mark. It rises to a higher level than the $\zeta = 1.6$ curve due to the lesser amount of damping, but it also returns to the zero displacement level most quickly of all possible solutions.

10.2.2.3 Case 3: Under Damped Solution $\zeta < 1$

By far the most common case in mechanical vibrations is that for which $\zeta < 1$. For this case, the roots of the characteristic equation are complex values,

$$\lambda_1 = -\zeta\omega_o + j\omega_o\sqrt{1-\zeta^2} \tag{10.21}$$

$$\lambda_2 = -\zeta\omega_o - j\omega_o\sqrt{1-\zeta^2} \tag{10.22}$$

where $j = \sqrt{-1}$. Note that the terms under the radical are re-ordered so that the radical represents a real number. Because the quantity $\omega_o\sqrt{1-\zeta^2}$ occurs repeatedly, it is convenient to define the *damped natural frequency*, ω_d, thus:

$$\omega_d = \omega_o\sqrt{1-\zeta^2} \tag{10.23}$$

With this new notation, the solution may be written as

$$x(t) = e^{-\zeta\omega_o t}\left(a_1 e^{j\omega_d t} + a_2 e^{-j\omega_d t}\right) \tag{10.24}$$

or, to avoid the complex exponential functions, it is written in the equivalent form

$$x(t) = e^{-\zeta\omega_o t}\left(\alpha\cos\omega_d t + \beta\sin\omega_d t\right) \tag{10.25}$$

where all factors of the last form are real numbers. This is a very important solution form that should be simply committed to memory. As before, the constants (now α and β) are evaluated from the initial conditions. It is apparent that this is a sinusoid scaled by a decaying exponential function. It may be visualized as a sinusoidal oscillation bounded above and below by decaying exponential *envelope curves*. In Figure 10.3, the actual motion is shown as a solid curve, and the upper and lower envelope curves are shown in very short broken line. Note that, due to the small damping ($\zeta = 0.1$ used for the example), the solution rises to the greatest excursion and it also oscillates repeatedly as it gradually decays to zero.

10.2.2.4 Case 4: Undamped Solution, $\zeta = 0$

In the event that $\zeta = 0$, there is no damping at all. This is the case that was considered in the previous section. It may be considered as the limit of the under damped case for which $\zeta \to 0$. In that limit, two important things happen:

1. The damped natural frequency approaches the undamped natural frequency, that is, $\omega_d \to \omega_o$;
2. The exponential factor approaches unity, so that the envelope does not decay, that is, $e^{-\zeta\omega_o t} \to 1.0$.

This case is not shown in Figure 10.3, but it is just a pure sinusoid passing through the prescribed initial conditions.

10.2.3 Log Decrement

In practice, it is often quite difficult to accurately assess the damping ratio of a physical system. Certainly any deliberate damping, such as a dashpot, makes a contribution, but there are always other small, not easily described, contributions as well. For an under damped physical system that actually exists (as opposed to one that exists on paper only), there is one physical measurement approach that enjoys considerable success. It is called the *log decrement* method.

Consider the physical system to be similar to that shown in Figure 10.2, adequately instrumented to record $x\,(t)$ accurately. Let the mass be set in motion by any combination of initial displacement and/or initial velocity. The *log decrement,* δ, is defined by the simple relation

$$\delta = \frac{1}{n} \ln \left(\frac{x_i}{x_{i+n}} \right) \tag{10.26}$$

where x_i denotes the i^{th} displacement peak value, and n is an integer. The necessary peak values are read from the displacement recording, where x_i and x_{i+n} are two well defined peak values. From equation (10.26), it is evident that the log decrement can be written as

$$\delta = \frac{1}{n} \ln \frac{e^{-\zeta \omega_o t_1}}{e^{-\zeta \omega_o (t_1 + n\tau)}} = \frac{1}{n} \ln e^{\zeta \omega_o n \tau_d} = \zeta \omega_o \tau_d \tag{10.27}$$

where τ_d is the period of damped vibration,

$$\tau_d = \frac{2\pi}{\omega_d} = \frac{2\pi}{\omega_o \sqrt{1-\zeta^2}} \tag{10.28}$$

Combining these two expressions shows that

$$\delta = \frac{2\pi\zeta}{\sqrt{1-\zeta^2}} \approx 2\pi\zeta \tag{10.29}$$

where the last equivalence is true only for small values of ζ. Finally, for small damping factors, the value of the damping factor ζ is related to the directly measurable log decrement thus:

$$\zeta \approx \frac{1}{2\pi}\delta = \frac{1}{2\pi n} \ln \left(\frac{x_i}{x_{i+n}} \right) \tag{10.30}$$

For existing under damped systems, the log decrement provides a readily applicable experimental approach to determining the actual damping factor. This has the advantage of incorporating all damping mechanisms actually present, whether by design or by accident.

10.2.4 Free Vibration Summary

For free vibrations, the mass (M), stiffness (K) and damping (C) values combine into two primary parameters: the undamped natural frequency, $\omega_o = \sqrt{K/M}$, and the damping factor, $\zeta = C/(2M\omega_o)$. These two parameters entirely determine the nature of the solution (over damped, critically damped, under damped, or undamped). Both parameters are easily evaluated without the need to consider initial conditions at all. The initial conditions are necessary only if the full solution is required.

10.3 Transient and Steady State Solutions

In dealing with ordinary differential equations, the terms *homogeneous and particular solutions* are most frequently used by mathematicians, while engineers tend to speak in terms of *transient and steady state solutions*. What is the relation between these terms?

The differential equations describing free vibration, such as equations (10.2) or (10.12), always have a zero on the right side. In mathematical terminology, such an equation is said to be a *homogeneous equation*, and the solution is called a *homogeneous solution*. For systems with viscous damping, the homogeneous solution always includes a factor $e^{-\zeta\omega_o t}$ that progressively reduces the homogeneous solution toward zero.

A dictionary definition for the word *transient* suggest that it describes something that exists only over a limited time; anything that is transient is not permanent or enduring. Thinking about the differential equation solutions demonstrated above, it is evident that this is an appropriate description for terms that decay toward zero amplitude as time becomes large. These are the terms that involve a factor $e^{-\zeta\omega_o t}$, and they arise in the homogeneous solution. **This leads to the common engineering practice of referring to the homogeneous solution as the transient solution in all cases, irrespective of the presence or lack of damping.**

When the right side of the differential equation of motion is nonzero, the complete solution must always include a particular solution, that is, terms included specifically to satisfy the right side. Particular solution terms usually do not tend to zero unless the right side terms also tend to zero, so particular solutions typically continue on without a time limit. This is exactly what is described by the term *steady state,* a term that suggests something that continues following a regular pattern indefinitely, enduring without a time limit. **Thus engineering practice tends to use the term steady state for the particular solution.** For real systems, where damping is always present, it is reasonable and correct to speak of the steady state as the vibration that continues to exist long after damping has eliminated the effects of the initial conditions.

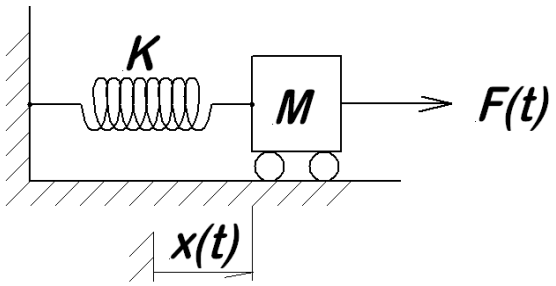

Figure 10.4: Undamped Spring-Mass Oscillator with External Forcing

One of the difficulties with this terminology is in regard to undamped motion. Even in this case, it is common practice to associate the homogeneous solution with the term transient solution. In complicated problems, damping is often neglected in order to simplify other aspects of the problem. When this is done, it is common engineering practice to drop the homogeneous solution, usually with a few words about "damping would eventually removed it from the solution" to justify discarding it. This is frequently done even when damping is omitted from the mathematical model. When the transient (homogeneous solution) terms are discarded, what is left for the solution are the steady state (particular solution) terms.

10.4 Forced Vibrations of SDOF Systems

While free vibration is very common, it is certainly not the only type and often not the most troublesome. Vibration that continues on and on indefinitely, driven by an external energy source, is often the cause of serious wear, fatigue damage, noise, and annoyance to personnel near the equipment. There are three cases of common interest: (1) external forcing, (2) support motion, and (3) rotating unbalance. Each of these are addressed below.

10.4.1 Externally Forced Vibration

This is the situation where an outside agent applies a specified force to the system of interest. A typical system diagram is shown in Figure 10.4. The energy source is considered to be external to the system of interest.

10.4.1.1 Undamped Forced Vibration

For the *forced vibration*, consider the case where there are two nonzero terms on the right side of the equation of motion, specifically the form

$$\ddot{x} + \omega_o^2 x = \frac{1}{M}\left(C + D\sin\Omega t\right) \tag{10.31}$$

Recall that the complete solution requires both the homogeneous solution and a particular solution for each term on the right side. Thus two particular solutions are required for this case. Consider two proposed particular solutions, x_{p1} and x_{p2},

$$\begin{aligned} x_{p1} &= c \\ x_{p2} &= d\sin\Omega t \end{aligned}$$

where c and d are to be determined. Note what is being proposed: the particular solution for a constant term is a constant, and the particular solution for a sinusoid is a sinusoid. But what are the values of the coefficients c and d?

Substitute the first particular solution to obtain

$$\omega_o^2 c = C/M \tag{10.32}$$

which is satisfied provided that $c = C/\left(\omega_o^2 M\right)$. Similarly, substitute the second particular solution to obtain

$$d\left(\omega_o^2 - \Omega^2\right) = D \tag{10.33}$$

which is satisfied by $d = D/\left(\omega_o^2 - \Omega^2\right)$, provided that $\omega_o^2 - \Omega^2 \neq 0$. For the moment, assume the last condition is satisfied. With the two constants c and d now known, the *complete solution* and the first derivative are of the forms

$$\begin{aligned} x_c(t) &= x_h(t) + x_{p1}(t) + x_{p2}(t) \\ &= \alpha\cos\omega_o t + \beta\sin\omega_o t + \frac{C}{\omega_o^2 M} + \frac{D}{\omega_o^2 - \Omega^2}\sin\Omega t \qquad (10.34) \\ \dot{x}_c(t) &= -\alpha\omega_o\sin\omega_o t + \beta\omega_o\cos\omega_o t + \frac{D\,\Omega}{\omega_o^2 - \Omega^2}\cos\Omega t \qquad (10.35) \end{aligned}$$

It is these last two equations, equations (10.34) and (10.35) involving the coefficients α and β that must satisfy the initial conditions, $x(0) = x_o$, $\dot{x}(0) = v_o$.

When the complete solution and its derivative are evaluated for $t = 0$ and the results set equal to the initial conditions, the resulting equations can be solved for the constants α

and β. When those constants are substituted back into equation (10.34) and after some re-arrangement, the final solution is

$$x(t) = \left(x_o - \frac{C}{\omega_o^2 M}\right)\cos\omega_o t + \left[\frac{v_o}{\omega_o} - \frac{\Omega}{\omega_o}\frac{D}{(\omega_o^2 - \Omega^2)}\right]\sin\omega_o t + \frac{C}{\omega_o^2 M} + \frac{D}{\omega_o^2 - \Omega^2}\sin\Omega t \tag{10.36}$$

What does this solution say?

1. If $C = D = 0$, that is, if there is no excitation (right side is zero), then the problem is one of free vibration only, and the solution comes back to the same result as equation (10.5); this is what should be expected.
2. If $C \neq 0$ but $D = 0$, then the solution oscillates forever at the natural frequency ω_o; this is true, irrespective of the values of x_o and v_o.
3. If $C = 0$ but $D \neq 0$, then the solution oscillates forever at two frequencies, ω_o and Ω, again, irrespective of the values of x_o and v_o.

Is endless oscillation realistic? Is this consistent with experience? What has been neglected in this initial formulation of the problem is energy loss through various forms of friction. The simple solution obtained neglecting damping is useful for some purposes, but the user must always be alert to false conclusions based on this very important omission. This is considered in the next section.

10.4.1.2 Damped Forced Vibration

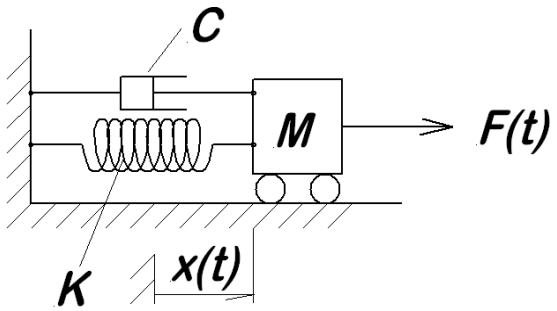

Figure 10.5: Damped Spring-Mass Oscillator with External Forcing

In general, the equation of motion takes the form

$$\ddot{x} + 2\zeta\omega_o\dot{x} + \omega_o^2 x = \frac{1}{M}F(t) \tag{10.37}$$

One case of particular importance occurs when the external force, $F(t)$, is sinusoidal in time. In the case of the undamped motion, the presence of a sine term on the right gave rise to a sine term in the particular solution. The situation is slightly different in the damped case. The presence of either a sine or cosine on the right requires *both* a sine and a cosine term in the particular solution; this is a direct consequence of viscous damping that causes a phase shift between the response and the excitation. Consider then the particular case where $F(t)$ is sinusoidal at frequency Ω, so that equation (10.37) takes the form

$$\ddot{x} + 2\zeta\omega_o\dot{x} + \omega_o^2 x = \frac{F_o}{M}\sin\Omega t \tag{10.38}$$

for which the homogeneous solution is developed earlier. For the particular solution, assume the form

$$x_p = A\cos\Omega t + B\sin\Omega t \tag{10.39}$$

where A and B are to be determined as required for the particular solution. When the form for x_p is differentiated and substituted into equation (10.38), the result is a single equation with A and B as unknowns. Separating the sine and cosine terms gives a pair of equations to be solved for A and B. The result is

$$A = \frac{-2\zeta\omega_o\Omega\frac{F_o}{M}}{\Omega^4 - 2\omega_o^2\Omega^2\left(1-2\zeta^2\right) + \omega_o^4} \tag{10.40}$$

$$B = \frac{-\left(\Omega^2 - \omega_o^2\right)\frac{F_o}{M}}{\Omega^4 - 2\omega_o^2\Omega^2\left(1-2\zeta^2\right) + \omega_o^4} \tag{10.41}$$

With the particular solution in hand, the complete solution is obtained by adding the homogeneous and particular solutions, thus

$$\begin{aligned} x_c(t) &= x_h(t) + x_p(t) \\ &= e^{-\zeta\omega_o t}\left(\alpha\cos\omega_d t + \beta\sin\omega_d t\right) \\ &\quad + A\cos\Omega t + B\sin\Omega t \end{aligned} \tag{10.42}$$

where A and B are now known from above, equations (10.41) and (10.42). It is now necessary to evaluate α and β such that the complete solution satisfies the initial conditions. This is a process of several steps:

1. Differentiate equation (10.42) to obtain $\dot{x}_c(t)$;

2. Evaluate $x_c(0)$ and set it equal to the initial value, x_o;

3. Evaluate $\dot{x}_c(0)$ and set it equal to the initial velocity, v_o;

4. Solve the two resulting equations for α and β to obtain the complete solution, $x_c(t)$.

When all of these steps are carried out, the result is

$$\alpha = x_o + \frac{2\zeta\omega_o\Omega\frac{F_o}{M}}{\Omega^4 - 2\omega_o^2\Omega^2\left(1-2\zeta^2\right)+\omega_o^4} \tag{10.43}$$

$$\beta = \frac{\zeta x_o}{\sqrt{1-\zeta^2}} + \frac{v_o}{\omega_o\sqrt{1-\zeta^2}} + \frac{\left[\Omega^2 - \omega_o^2\left(1-2\zeta^2\right)\right]}{\sqrt{1-\zeta^2}\left[\Omega^4 - 2\omega_o^2\Omega^2\left(1-2\zeta^2\right)+\omega_o^4\right]}\frac{\Omega}{\omega_o}\frac{F_o}{M} \tag{10.44}$$

10.4.1.3 Forced Vibration Solution Summary

It is important to recognize the multi-step nature of this solution process. It is easy for the unwary to get confused as to where they are in the process, and the rather formidable amount of algebra involved makes this confusion a great waste of time. Thus, to review very briefly, the process is this:

1. Start by obtaining the homogeneous solution. This solution must include two arbitrary constants that cannot be evaluated at this point, but must wait until later in the process.

2. Propose an appropriate form for the particular solution. This proposed form may have several constants that must be adjusted in order to satisfy the requirements for the particular solution. Initial or boundary conditions are not involved in this step. Determine all constants required for the particular solution.

3. Add the homogeneous and particular solutions to obtain the complete solution. Differentiate the complete solution in order to obtain a velocity expression.

4. Evaluate the complete solution and the associated velocity expression at time $t = 0$ and set those results equal to the initial position and velocity, respectively. Solve the resulting equations for the two arbitrary constants in the homogeneous solution.

5. Put all evaluated constants in their respective locations to obtain the final, complete solution.

10.4.1.4 Magnification Factor

Engineering interest is often focused particularly on steady state vibration. This is the persistent motion where most fatigue cycles leading to component failure are accumulated. The steady state solution of equation (10.38) involves the two constants, A and B, given in equations (10.40) and (10.41) to express the solution in the form given in equation (10.39). While that form is entirely correct, it is often convenient to express the solution in terms of a single sine term with a phase angle, thus:

$$x_{ss}(t) = \frac{F_o/K}{\sqrt{\left[1-(\Omega/\omega_o)^2\right]^2+(2\zeta\Omega/\omega_o)^2}}\sin(\Omega t-\phi) \tag{10.45}$$

$$= X_{ss}\sin(\Omega t-\phi) \tag{10.46}$$

where the steady state amplitude, X_{ss}, and phase angle, ϕ, are

$$X_{ss} = \frac{F_o/K}{\sqrt{\left[1-(\Omega/\omega_o)^2\right]^2+(2\zeta\Omega/\omega_o)^2}} \tag{10.47}$$

$$\tan\phi = \frac{2\zeta\Omega/\omega_o}{1-(\Omega/\omega_o)^2} \tag{10.48}$$

This is the result of combining the sine and cosine terms (and their coefficients A and B) in a manner similar to that done to obtain equation (10.10).

The amplitude of the exciting force is F_o. If a constant force of that same magnitude were applied statically to the system, the static displacement would be X_{st},

$$X_{st} = F_o/K \tag{10.49}$$

Using this last expression to replace F_o/K in equation (10. 47) allows the ratio X_{ss}/X_{st} to be re-written as

$$\frac{X_{ss}}{X_{st}} = \mathcal{M}(\Omega/\omega_o,\zeta) = \frac{1}{\sqrt{\left[1-(\Omega/\omega_o)^2\right]^2+(2\zeta\Omega/\omega_o)^2}} \tag{10.50}$$

where $\mathcal{M}(\Omega/\omega_o,\zeta)$ is defined as the *magnification factor.* These results, equations (10.48) and (10.50) provide both the vibration amplitude ratio ($\mathcal{M} = X_{ss}/X_{st}$) and the phase angle ($\phi$) expressed in terms of the dimensionless ratios (Ω/ω_o) and ζ.

Figure 10.6 shows both the magnification factor $\mathcal{M}(\Omega/\omega_o)$ and the phase angle (ϕ) plotted as functions of the frequency ratio Ω/ω_o for various values of the damping factor values, ζ. There are several interesting aspects of this plot that bear comment:

1. For both the magnification factor and phase plots, the frequency ratio varies from $\Omega/\omega_o = 0$ up to $\Omega/\omega_o = 5$; the trends beyond that range are evident. Plots are provided for damping factor values $\zeta = 0.1$, 0.2, 0.3, 0.4, 0.5, 1.0, and 2.0.

2. On the magnification factor plot, the smaller the value of the damping factor, the more extreme the peak around $\Omega/\omega_o = 1.0$ becomes. Although the curves exceed the available space, it should be understood that all of these curves close at the top. No curve is shown for $\zeta = 0$, but it is not difficult to understand that (a) it must lie just slightly above the highest magnification factor curve shown, and (b) it does not close at the top. The reader should look to the defining equation (10.50) to understand why the curve does not close at $\Omega/\omega_o = 1.0$ when $\zeta = 0$.

3. All of the phase angle curves shown are smooth, and all pass through 90^o at $\Omega/\omega_o = 1.0$. For the case not shown, $\zeta = 0$, the phase curve is zero for $\Omega/\omega_o < 1$ and then jumps discontinuously to 180^o for $\Omega/\omega_o > 1$.

4. For values of the damping factor $0 < \zeta \leq \sqrt{2}$ the magnification factor has an interior maximum point. For extremely small values of ζ, that maximum occurs very near $\Omega/\omega_o = 1.0$. As the value of ζ is increased, the maximum amplitude point moves down (due to increased damping action) and to the left until it reaches the value 1.0 at $\Omega/\omega_o = 0$. The locus of the maxima is shown in Figure 10.6 as just described here.

5. For values of the damping factor $\zeta > \sqrt{2}$, the maximum value of the magnification factor is 1.0, an end point maximum occurring at $\Omega/\omega_o = 0$.

10.4.2 Displacement Excitation

Displacement excitation refers to a situation where the structure supporting the system of interest is displaced causing vibration of the system. This is often the case with seismic activity, but also occurs near large machinery (like a punch press or a railroad) that shakes the ground or building structure during the course of its operation. A system schematic of this sort is shown in Figure 10.7. The support motion is denoted as $s(t)$. Note that, when $s(t) = x(t) = 0$, there is no force in the spring.

The equation of motion for the damped system with support motion is easily obtained by applying Newton's Second Law to give

$$M\ddot{x} + C\dot{x} + Kx = C\dot{s} + Ks \tag{10.51}$$

This is cast in standard form by dividing by M and using the standard definitions for ω_o and ζ

$$\ddot{x} + 2\zeta\omega_o\dot{x} + \omega_o^2 x = 2\zeta\omega_o\dot{s} + \omega_o^2 s \tag{10.52}$$

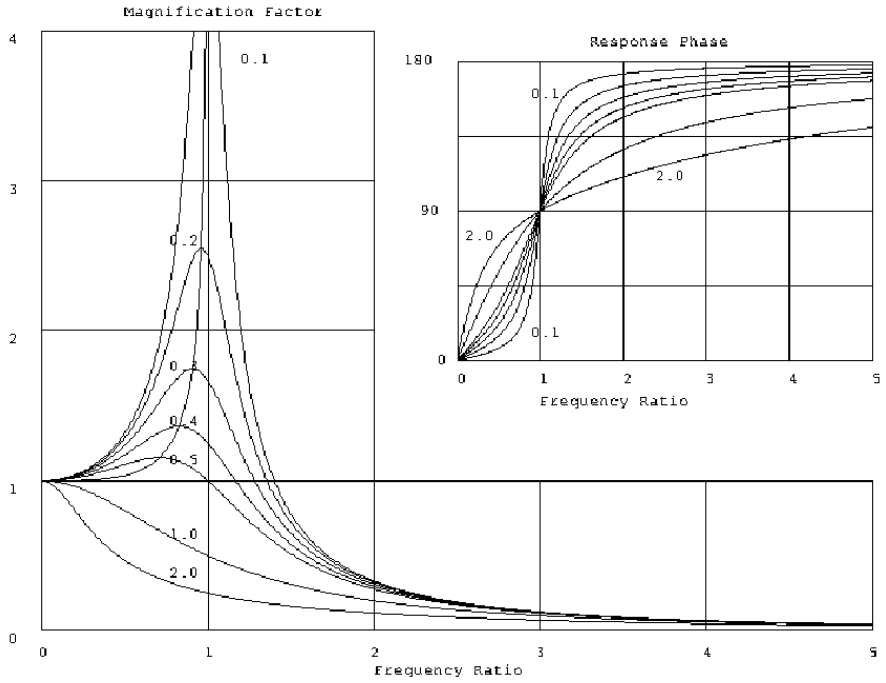

Figure 10.6: Magnification Factor and Response Phase for Sinusoidal Excitation

Note that the right side contains both $s(t)$ and the derivative, $\dot{s}(t)$; this is the only part of this problem that is unusual.

In particular, it is of interest to solve this system for the case where the displacement excitation is sinusoidal, that is,

$$s(t) = S\cos\Omega t \tag{10.53}$$

As before, the steady state response is assumed to be of the form

$$x(t) = A\cos\Omega t + B\sin\Omega t \tag{10.54}$$

which is then differentiated and substituted into the equation of motion. When the sine and cosine terms are separated, the result is a pair of equations to be solved for A and B:

$$\left(\omega_o^2 - \Omega^2\right)A + 2\zeta\omega_o\Omega B = \omega_o^2 S \tag{10.55}$$

$$-2\zeta\omega_o\Omega A + \left(\omega_o^2 - \Omega^2\right)B = -2\zeta\omega_o\Omega S \tag{10.56}$$

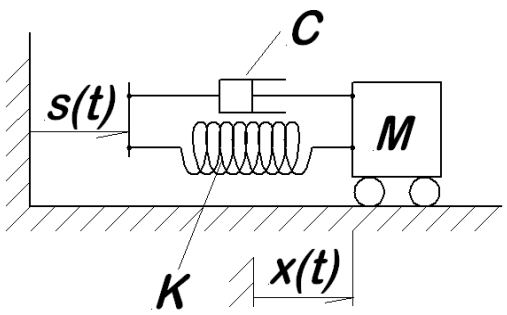

Figure 10.7: Damped SDOF Oscillator Subject to Support Motion

with the solutions

$$A = \frac{1-(\Omega/\omega_o)^2+(2\zeta\Omega/\omega_o)^2}{\left[1-(\Omega/\omega_o)^2\right]^2+(2\zeta\Omega/\omega_o)^2}S \tag{10.57}$$

$$B = \frac{2\zeta\,(\Omega/\omega_o)^3}{\left[1-(\Omega/\omega_o)^2\right]^2+(2\zeta\Omega/\omega_o)^2}S \tag{10.58}$$

This result can be written in the form of a response amplitude ratio and phase angle by the usual process:

$$x\,(t) = X\cos\left(\Omega t-\phi\right) \tag{10.59}$$

where

$$\frac{X}{S} = \frac{\sqrt{1+(2\zeta\Omega/\omega_o)^2}}{\sqrt{\left[1-(\Omega/\omega_o)^2\right]^2+(2\zeta\Omega/\omega_o)^2}} \tag{10.60}$$

$$\phi = \arctan\left[\frac{2\zeta\,(\Omega/\omega_o)^3}{1-(\Omega/\omega_o)^2+(2\zeta\Omega/\omega_o)^2}\right] \tag{10.61}$$

Figure 10.8 shows plots of the amplitude ratio and phase functions as defined by equations (10.60) and (10.61). Each is plotted as a function of the frequency ratio, Ω/ω_o, for a range of damping factors, $\zeta = 0.1$, 0.2, 0.3, 0.5, 1.0, and 1.5. There are several interesting points to note about these curves:

1. As might be expected, the curves are such that the lowest value of the damping factor produces the highest response ratio, X/S, for low values of the frequency ratio, Ω/ω_o. However, exactly the reverse is true for higher frequency ratios where the greatest response is the result of the highest damping ratio. At higher frequencies, damping acts like additional stiffness in the system.

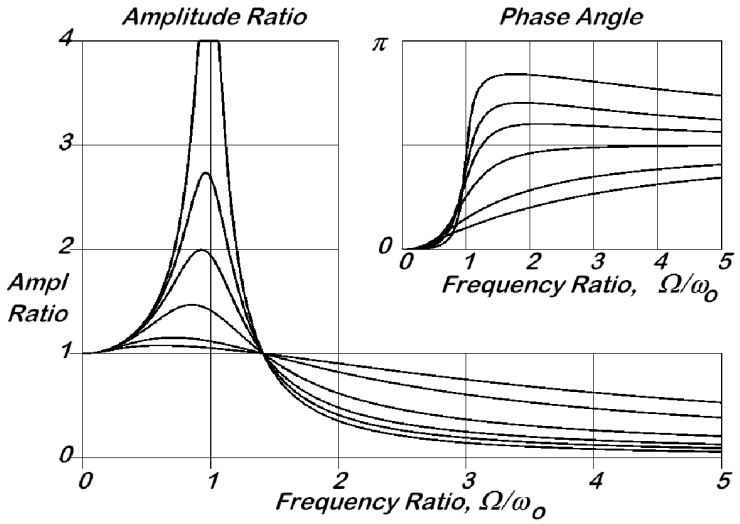

Figure 10.8: Response Amplitude Ratio and Phase for Displacement Excitation

2. All of the response amplitude ratio curves pass through the common point $\left(\sqrt{2}, 1\right)$. This means that the system response is independent of the damping factor for $\Omega = \sqrt{2}\,\omega_o$.

3. Looking at the phase angle plot, it is evident that there is no point where the phase angle is the same for all damping factors. This is unlike the previous case with force excitation where a common phase of $\pi/2$ (90^o) occurs for $\Omega = \omega_o$.

4. For very large values of the frequency ratio, for all damping levels, the phase angle tends slowly toward $\pi/2$ (90^o) due to the dominance of the $(\Omega/\omega_o)^3$ factor in the numerator of the phase angle expression.

10.4.3 Rotating Unbalance

One case of particular importance is unbalance in a rotating part. It is commonly found in electric motors, generators, steam and gas turbines, and various other rotating machinery. Such a system is shown in Figure 10.9, along with free body diagrams for both the housing and the rotor.

Further note that there are two masses involved: (a) M_h is the mass of the housing, and (b) M_r is the mass of the rotor. The rotor is assumed to be slightly unbalanced, so that the center of mass for the entire rotor is a distance ε off the axis of rotation. As drawn, ε appears quite large, but in actual practice it will be some tiny amount, typically less than one millimeter. It is assumed here that the rotor remains centered in the housing at all times, and rotates at a constant angular speed Ω rad/sec. The horizontal displacement

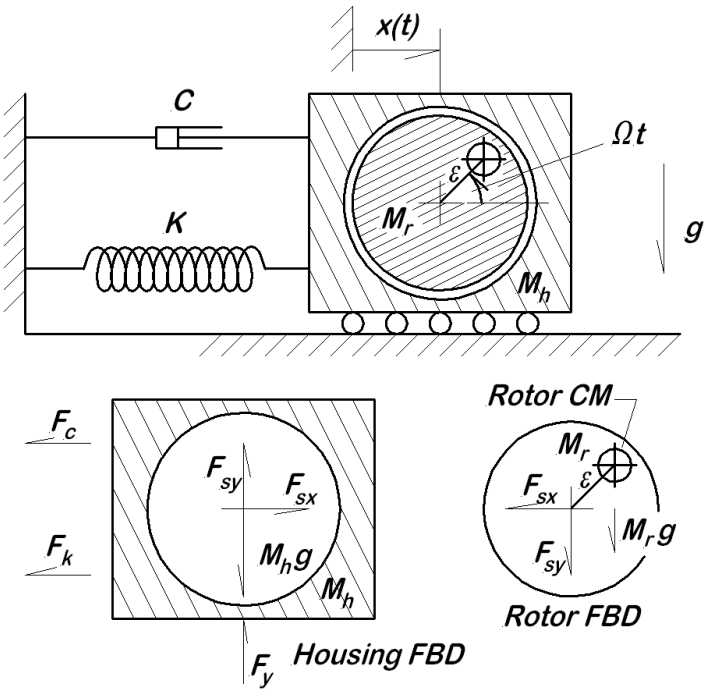

Figure 10.9: Unbalanced Rotor on Damped Supports

of the rotor axis is $x\,(t)$, where $x = 0$ is the stress free state of the spring. Vertical motion is not considered here.

In the lower part of Figure 10.9, free body diagrams are shown for the housing (left) and rotor (right). All forces are shown on each FBD, including gravitational forces, although these last play no role because only horizontal motion is considered.

Notations:

$x\,(t)$ = displacement of shaft center from relaxed spring position

Ωt = angle turned by rotor

ε = rotor eccentricity

M_r = mass of the rotor

M_h = housing mass

F_{sx} = shaft force in horizontal direction

F_{sy} = shaft force in vertical direction

F_y = vertical guide reaction force

F_k = spring force

F_c = damper force

K = spring rate

C = damping rate

g = acceleration of gravity

Begin by forming the horizontal equations of motion for each of the two free bodies:

Housing

$$\sum^{+\rightarrow} F_{horiz} = F_{sx} - F_c - F_k = F_{sx} - C\dot{x} - Kx = M_h\ddot{x} \tag{10.62}$$

Rotor

$$\sum^{+\rightarrow} F_{horiz} = -F_{sx} = M_r \frac{d^2}{d^2t}\left[x + \varepsilon\cos\Omega t\right] \tag{10.63}$$

Notice that the acceleration of the rotor center of mass involves two terms, one expressing the motion of the shaft center and the second expressing the horizontal component of the eccentricity. When these two equations are added together and the derivative expression is expanded, the result is

$$\left(M_h + M_r\right)\ddot{x} + C\dot{x} + Kx = M_r\Omega^2\varepsilon\cos\Omega t \tag{10.64}$$

This is put in standard form by dividing by the coefficient of $\ddot{x}$, with the result

$$\ddot{x} + 2\zeta\omega_o\dot{x} + \omega_o^2 x = \frac{M_r\varepsilon\Omega^2}{M_h + M_r}\cos\Omega t \tag{10.65}$$

where

$\omega_o^2 = \frac{K}{M_h+M_r}$ = square of the undamped natural frequency

$\zeta = \frac{C}{2\omega_o(M_h+M_r)}$ = damping factor

Because the steady state solution is the primary concern, consider a particular solution in the form

$$x = A\cos\Omega t + B\sin\Omega t \tag{10.66}$$

When this is differentiated, substituted, and the sines and cosines separated, two equations for A and B result:

$$\begin{bmatrix} 1-\left(\frac{\Omega}{\omega_o}\right)^2 & 2\zeta\left(\frac{\Omega}{\omega_o}\right) \\ -2\zeta\left(\frac{\Omega}{\omega_o}\right) & 1-\left(\frac{\Omega}{\omega_o}\right)^2 \end{bmatrix} \begin{Bmatrix} A \\ B \end{Bmatrix} = \left(\frac{\Omega}{\omega_o}\right)^2 \frac{M_r\varepsilon}{M_h+M_r} \begin{Bmatrix} 1 \\ 0 \end{Bmatrix} \tag{10.67}$$

This system of equations is easily solved to evaluate the amplitude of the rotor excursion given by $\sqrt{A^2+B^2}$.

$$\sqrt{A^2+B^2} = \frac{\left(\Omega/\omega_o\right)^2 \frac{M_r\varepsilon}{M_h+M_r}}{\sqrt{\left[1-\left(\Omega/\omega_o\right)^2\right]^2 + \left[2\zeta\left(\Omega/\omega_o\right)\right]^2}} \tag{10.68}$$

Now define the dimensionless unbalance response ratio $\mathcal{M}\left(\Omega/\omega_o, \zeta\right)$ as

$$\begin{aligned} \mathcal{M}\left(\Omega/\omega_o, \zeta\right) &= \frac{\left(M_h+M_r\right)\sqrt{A^2+B^2}}{M_r\varepsilon} \\ &= \frac{\left(\Omega/\omega_o\right)^2}{\sqrt{\left[1-\left(\Omega/\omega_o\right)^2\right]^2 + \left[2\zeta\left(\Omega/\omega_o\right)\right]^2}} \end{aligned} \tag{10.69}$$

A typical set of unbalance response ratio curves, $\mathcal{M}$ as a function of Ω/ω_o, are shown in Figure 10.10 for the sequence of damping ratio values, $\zeta = 0.1, 0.2, 0.3, 0.5, 0.7, 1.0, 1.5$ from top to bottom.

From equation (10.69), it is evident that for $\Omega \ll \omega_n$, the response ratio $\mathcal{M}\left(\Omega/\omega_o, \zeta\right)$ goes to 0 for all values of the damping ratio. Again, from equation (10.69), as the shaft speed becomes very large, in a similar fashion $\mathcal{M}\left(\Omega/\omega_o, \zeta\right)$ goes to 1, again for all values of ζ.

The unbalance response curve actually tells a bit of industrial history. Toward the left end ($\Omega/\omega_o \ll 1$), the response to unbalance is very small. This means that if the operating speed is far below the natural frequency, the response is essentially zero, as mentioned above. At the beginning of the industrial revolution in Europe, machines using wind and water power ran slowly, and unbalance was not much of a problem. Moving slightly to the right on the plot, it is clear that as operating speed increases to approach the natural frequency ($\Omega/\omega_o \to 1$), the response amplitude rises drastically, and ultimately is limited only by the damping present in the system. This led many people in the 19th century

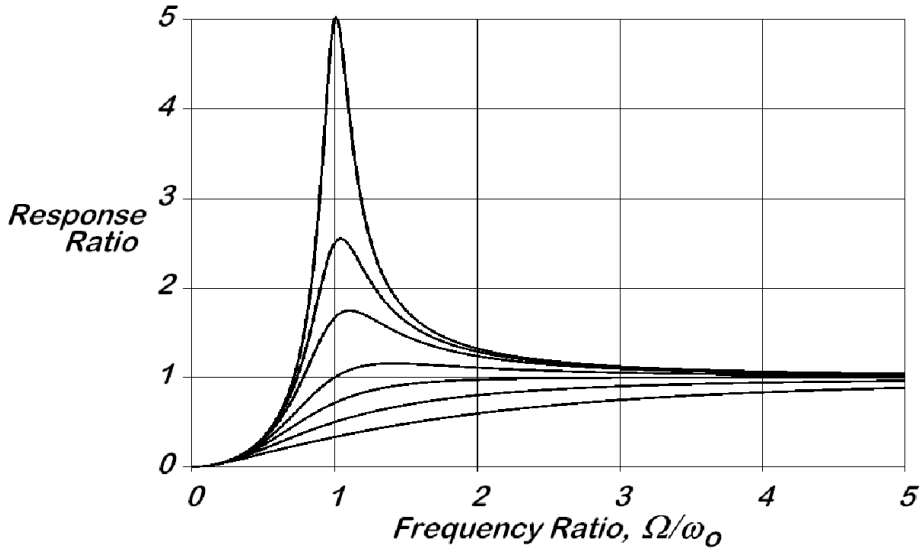

Figure 10.10: Unbalance Response Ratio versus Frequency Ratio

to believe that there was a natural limit for machinery speed. Whenever attempts were made to operate a machine faster than its natural frequency, the amplitude became large and there would be a machine wreck. Understanding this was a matter of major concern in the 19^{th} and early 20^{th} centuries. Today, many machines operate well above their natural frequency (aircraft jet engines have many natural frequencies, and it is common for them to pass through several as they run up to operating speed). This is out on the far right end of the curve or beyond. In the very high speed range ($\Omega/\omega_o \gg 1$), it is evident that the amount of damping makes little difference; all of the curves approach the same value. In the limit for extremely high operating speed, the analysis above shows that $\mathcal{M} \to 1$ and the displacement approaches $\varepsilon M_r / (M_h + M_r)$. This indicates that the displacement can be reduced by reducing ε, i.e. by better balancing, and by increasing the housing mass in proportion to the rotor mass. This is common sense. If there is better balancing, then the centrifugal forces are reduced, and they are the driving force for this system. If the housing is made more massive compared to the rotor, this says that the rotating element is simply anchored to a more massive block which intuition indicates must have a smaller response.

10.4.4 Other Periodic Excitations

The reader may properly wonder why so much attention is paid to the response to sinusoidal excitations when there are many non-sinusoidal excitations. The full answer to such a question is beyond the scope of the present effort, but a partial explanation is offered here.

Under rather broad mathematical conditions, a periodic excitation function can be expressed in terms of a Fourier series of the form

$$y(t) = a_o + \sum_{n=1}^{\infty} [a_n \cos(n\Omega t) + b_n \sin(n\Omega t)] \tag{10.70}$$

where

$y(t)$ is a periodic excitation of whatever sort, perhaps a force or maybe a support displacement

Ω is the fundamental excitation frequency

a_o is the mean value of the excitation

Consider then a single degree of freedom system subject to a general periodic excitation, where the equation of motion is

$$M\ddot{x} + C\dot{x} + Kx = a_o + \sum_{n=1}^{\infty} [a_n \cos(n\Omega t) + b_n \sin(n\Omega t)]$$

or, in standard form,

$$\ddot{x} + 2\zeta\omega_o\dot{x} + \omega_o^2 x = \frac{a_o}{M} + \frac{1}{M}\sum_{n=1}^{\infty} [a_n \cos(n\Omega t) + b_n \sin(n\Omega t)] \tag{10.71}$$

Recall now what the solution process is:

1. Determine the homogeneous solution, if the transient response if of interest;
2. Determine a particular solution for each term, or pair of terms, on the right.

For engineering purposes, sums that run to infinity are rarely useful, so it is appropriate to assume in most cases that there is an upper limit, N, such that all terms past that point may be neglected. It may be difficult to determine an appropriate value for N, and it may be rather large in some cases, but with computer implementation, finite series of hundreds of terms are quite feasible. Thus it is assumed that the series can be truncated to a finite number of terms so the problem is

$$\begin{aligned} \ddot{x} + 2\zeta\omega_o\dot{x} + \omega_o^2 x \;=\; & \frac{a_o}{M}a_o + \frac{1}{M}[a_1 \cos(\Omega t) + b_1 \sin(\Omega t) \\ & + \cdots a_n \cos(n\Omega t) + b_n \sin(n\Omega t) \\ & + \cdots a_N \cos(N\Omega t) + b_N \sin(N\Omega t)] \end{aligned} \tag{10.72}$$

The solution for the constant term on the right presents no difficulty, and the solution for each pair of terms on the right side has been discussed previously in isolation. All that remains is to find all of the required particular solutions and add them together. This idea is not developed further in the present text, but it is simple enough to employ whenever required, only tedious and requiring careful attention to detail and bookkeeping.

10.4.5 Force Transmission

To this point, the discussion has focused on the motion resulting from various types of excitation. For most vibration problems, this is the beginning, but it often not the end, of the inquiry. If the primary concern is with the motion of the mass, then this much analysis tells about all that is necessary; it provides the motion amplitude and phase, and by differentiation also the velocity and accelerations. From a design perspective there are two other questions of major concern:

1. What is the force transferred through each of the supports to the structure? This is a serious question for the design of the spring-damper system supporting the mass, for the anchors that support the spring and the damper, and most important of all, for component fatigue evaluation.

2. What can be done to reduce (or in a few cases, to maximize) the force transmitted to the supports?

Considering first the second question, it is fairly easily addressed if it is understood that the total transmitted force is the issue of concern. The total force transmitted to the structure consists of all the terms in the equation of motion other than the mass $\times$ acceleration term. Often system stiffness is assigned based on other considerations, particularly the allowable deflections for the system. In many cases, the damping can be adjusted to minimize (or maximize) the total force transmitted to the structure.

For the first issue, the force through an elastic element, a spring, depends upon the relative displacement of the ends, the elongation or deformation of the component. This is only a part of the total force transmitted, but it should be easy enough to multiply the stiffness into the relative displacement to obtain this force in most cases. The force through a viscous connection, such as a dashpot, depends upon the relative velocity of the two ends. Evaluation of this force requires that the displacement solution be differentiated and used to express the relative velocity. Then the force through the viscous element is simply the product of the viscous coefficient with the relative velocity.

10.5 Laplace Transform Solutions

The Laplace transform technique is a popular means for dealing with the differential equations frequently found in vibration and control system problems. A full exposition is beyond the scope of the present book, but a brief introduction is offered here for those who may not have encountered the topic previously. At its heart, the Laplace transform approach converts a differential equation in the time domain into an algebraic equation in the complex plane. After the algebraic problem is solved, the results must then be transformed back to the time domain to obtain the solution for the original problem.

Consider a time function, $x(t)$, for which the Laplace transform is formally defined as $X(s)$,

$$X(s) = \mathcal{L}\{x(t)\} = \int_0^\infty e^{-st}\, x(t)\, dt \tag{10.73}$$

where

s = Laplace variable, a complex value

$\mathcal{L}\{-\}$ denotes the Laplace transform operation

The notational convention *used in this section of the book only* is that lower case letters typically denote time functions (with the exception of s), while the same letter in upper case denotes the Laplace transform of the time function. Thus, in equation (10.73), $x(t)$ is the time function, while $X(s)$ is the Laplace transform of $x(t)$. Not all functions have Laplace transforms, but fortunately transforms do exist for a wide variety of the functions commonly found in engineering practice.

Laplace transformation is linear, which implies two things:

1. The transform of a function multiplied by a constant is simply that same constant multiplied by the transform of the function: $\mathcal{L}\{c \cdot x(t)\} = c \cdot \mathcal{L}\{x(t)\} = c \cdot X(s)$;

2. The transform of the sum of two functions is the sum of their respective transforms: $\mathcal{L}\{x(t) + y(t)\} = \mathcal{L}\{x(t)\} + \mathcal{L}\{y(t)\} = X(s) + Y(s)$.

These two properties follow directly from the properties of integration as used in the definition of the transform.

The utility of Laplace transforms in dealing with differential equations arises from the way that time derivatives transform. In particular, note the two following transformation

rules:

$$\mathcal{L}\{\dot{x}(t)\} = sX(s) - x(0) \tag{10.74}$$
$$\mathcal{L}\{\ddot{x}(t)\} = s^2X(s) - sx(0) - \dot{x}(0) \tag{10.75}$$

Notice that the transforms of the derivatives involve the initial values of the time function and derivatives of lower order. This makes the Laplace technique attractive for *initial value problems* (IVPs) where the initial conditions are specified, but much less attractive for *two-point boundary values problems* that involve specified initial and final values (BVPs).

When the solution is obtained in the Laplace domain, the task remains to transform it back to the time domain. There exists formal methods for doing this operation, referred to as *inverse transformation*, but these formal methods are not often really necessary. The more common approach is to examine the Laplace domain solution and find the individual pieces one by one in a table of Laplace transforms, of which there are many available. An short table of Laplace transforms is provided here as Table 10.1, with more extensive tables to be found elsewhere [1, 2]. While many problems can be solved with even a short table, the availability of a larger table often facilitates problem solving.

Table 10.1 Laplace Transform Pairs

	$x(t)$	$X(s)$
1	$c = \text{constant}$	c/s
2	e^{at}	$1/(s-a)$
3	$\sin(kt)$	$k/(s^2+k^2)$
4	$\cos(kt)$	$s/(s^2+k^2)$
5	$e^{-at}\sin(kt)$	$k/\left[(s+a)^2+k^2\right]$
6	$e^{-at}\cos(kt)$	$(s+a)/\left[(s+a)^2+k^2\right]$
7	$\frac{1}{a}\sin(at) - \frac{1}{b}\sin(bt)$	$\frac{b^2-a^2}{(s^2+a^2)(s^2+b^2)}$
8	$\frac{1}{a-b}\left(e^{at}-e^{bt}\right)$	$1/[(s-a)(s-b)]$
9	$\frac{1}{a-b}\left(ae^{at}-be^{bt}\right)$	$s/[(s-a)(s-b)]$
10	$\frac{1}{2a^3}(\sin at - at\cos at)$	$1/(s^2+a^2)^2$
11	$\frac{t}{2a}\sin at$	$s/(s^2+a^2)^2$
12	$\frac{1}{2a}(\sin at + at\cos at)$	$s^2/(s^2+a^2)^2$
13	$t\cos at$	$(s^2-a^2)/(s^2+a^2)^2$

10.5.1 Example Problem: Free Vibration

Consider the damped spring-mass-damper system shown in Figure 10.2 in free vibration, described by the equation of motion and initial conditions shown here:

$$\ddot{x} + 2\zeta\omega_o\dot{x} + \omega_o^2 x = 0 \tag{10.76}$$

$$x(0) = x_o \tag{10.77}$$

$$\dot{x}(0) = v_o \tag{10.78}$$

Applying the Laplace transformation to both sides of the equation gives the algebraic equation

$$\begin{aligned} 0 &= s^2 X(s) - s \cdot x_o - v_o \\ &+ 2\zeta\omega_o \left[sX(s) - x_o \right] \\ &+ \omega_o^2 X(s) \end{aligned} \tag{10.79}$$

or, after some manipulation,

$$\left(s^2 + 2\zeta\omega_o s + \omega_o^2 \right) X(s) = sx_o + v_o + 2\zeta\omega_o x_o \tag{10.80}$$

The quadratic coefficient expression on the left is always factorable, provided complex numbers are admitted. With this provision, the solution for $X(s)$ is

$$\begin{aligned} X(s) = &\frac{sx_o}{\left(s + \zeta\omega_o - j\omega_o\sqrt{1-\zeta^2} \right)\left(s + \zeta\omega_o + j\omega_o\sqrt{1-\zeta^2} \right)} \\ &+ \frac{v_o + 2\zeta\omega_o x_o}{\left(s + \zeta\omega_o - j\omega_o\sqrt{1-\zeta^2} \right)\left(s + \zeta\omega_o + j\omega_o\sqrt{1-\zeta^2} \right)} \end{aligned} \tag{10.81}$$

Despite the somewhat complicated appearance of equation (10.81), it is invertible by application of transforms #8 and #9 in the Table 10.1. Applying these two transform pairs allows the time function to written immediately in the form of complex exponential functions. After some tedious algebra and employing the definition of sine and cosine in terms of complex variables, the final result is simply

$$x(t) = e^{-\zeta\omega_o t}\left[x_o \cos\left(\sqrt{1-\zeta^2}\omega_o t \right) + \frac{(\zeta\omega_o x_o + v_o)}{\sqrt{1-\zeta^2}\omega_o} \sin\left(\sqrt{1-\zeta^2}\omega_o t \right) \right] \tag{10.82}$$

Note that this is the complete solution for the free vibration of a single degree of freedom damped oscillator for any possible initial conditions. Compare this last result with equation (10.25).

10.5.2 Unit Step Function

There are interesting features associated with one function already introduced in the short table of Laplace Transform Pairs, Table 10.1. The Laplace transform process assumes that all functions are zero before $t = 0$; this is implied in the lower limit of the integral that defines the transformation, equation (10.72). Thus the transform of the constant c, given as item #1 in Table 10.1, is the transformation of a function that is zero for all time before $t = 0$ and has the value c for all time after $t = 0$. It is useful to consider specifically the value $c = 1$, and to call that the *unit step function* because it represents a step change of unit value at $t = 0$. The notation $u(t)$ is used here for the unit step at time t.

Consider now a unit step that is delayed until $t = a$, where $a > 0$, denoted as $u(t - a)$. The value a is called the *trigger point,* the location where the step change occurs. Then applying the definition of the Laplace transformation gives

$$\begin{aligned} U(s) &= L\{u(t-a)\} = \int_0^\infty e^{-st}\, u(t-a)\, dt \\ &= \int_0^a e^{-st} \cdot 0\, dt + \int_a^\infty e^{-st} \cdot 1\, dt \\ &= -\frac{1}{s}\, e^{-st}\Big|_a^\infty \\ &= e^{-as}/s \end{aligned} \tag{10.83}$$

When a function is multiplied by a delayed unit step, this is often described as activating (or "turning on") the function at $t = a$. Thus a function can be initiated at $t = a$ and terminated at $t = b$ by the use of a pair of unit step functions triggered at a and b.

10.5.3 Functions Shifted in Time

One of the useful properties of the Laplace transform is its ability to deal with functions translated in time, the sort of shift shown in Figure 10.11 (c).

Consider a time function, $g(t)$ for which the Laplace transform is known, $G(s) = \mathcal{L}\{g(t)\}$. If it is necessary to shift the time function an amount a while activating it at $t - a$, to become $g(t-a) \cdot u(t-a)$, the transform is defined by

$$\mathcal{L}\{g(t-a) \cdot u(t-a)\} = \int_0^\infty e^{-st}\, g(t-a)\; u(t-a)\, dt \tag{10.84}$$

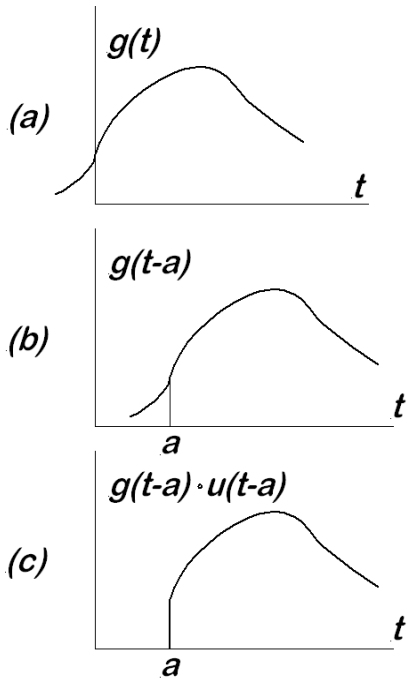

Figure 10.11: Time Shifted Function: (a) Original Function, (b) Shifted Function. (c) Shifted and Multiplied by Unit Step

At this point, make a change of variable such that $\tau = t - a$ in the integral,

$$\begin{aligned}\mathcal{L}\left\{g\left(t-a\right)\cdot u\left(t-a\right)\right\} &= \int_{-a}^{\infty} e^{-s(\tau+a)} g\left(\tau\right) u\left(\tau\right) d\tau \\ &= \int_{0}^{\infty} e^{-s(\tau+a)} g\left(\tau\right) d\tau \\ &= e^{-as} G\left(s\right) \end{aligned} \tag{10.85}$$

The lower limit is changed from $-a$ to 0 because $u\left(\tau\right) = 0$ for $\tau < 0$. This development makes evident that shifting and multiplying by the unit step has the effect of multiplying the transform by e^{-as}. The usefulness of this capability is demonstrated in the following example.

10.5.4 Example Problem: SDOF Response to a Rectangular Pulse

Consider the undamped spring-mass oscillator of Figure 10.4, initially at rest ($x(0) = 0$, $\dot{x}(0) = 0$) acted upon by the rectangular force pulse $F(t)$:

$$F(t) = \begin{cases} 0 & t < 0 \\ F_o & 0 < t < a \\ 0 & a < t \end{cases} \tag{10.86}$$

The system equation of motion is

$$\ddot{x} + \omega_o^2 x = \frac{1}{M} F(t) \tag{10.87}$$

When the Laplace transformation is applied to each term, the result is

$$\left(s^2 + \omega_o^2\right) X(s) = \frac{F_o}{M}\left(\frac{1}{s} - \frac{e^{-as}}{s}\right) \tag{10.88}$$

Notice the way the translational capability is used to initiate the pulse at $t = 0$ and again to terminate the pulse at $t = a$. Solving for the transform of the displacement gives

$$X(s) = \frac{F_o}{M}\left[\frac{1}{s\left(s^2 + \omega_o^2\right)} - \frac{e^{-as}}{s\left(s^2 + \omega_o^2\right)}\right] \tag{10.89}$$

Consider at first only the first term of the expression just above, here denoted as $X_1(s)$, which can itself be separated into two terms as

$$X_1(s) = \frac{F_o}{M}\frac{1}{s\left(s^2 + \omega_o^2\right)} = \frac{F_o}{M}\left[\frac{1/\omega_o^2}{s} - \frac{s/\omega_o^2}{\left(s^2 + \omega_o^2\right)}\right] \tag{10.90}$$

Each of the two terms in $X_1(s)$ can be readily inverted to give

$$x_1(t) = \frac{F_o}{M\omega_o^2}\left(1 - \cos\omega_o t\right) \tag{10.91}$$

Thus the first term in $X(s)$ leads to a displaced cosine term, $(1 - \cos\omega_o t)$. Notice also that the second term in $X(s)$ is of the same form, except that it is multiplied by a $-e^{-as}$.

The exponential factor shifts the solution to the right and triggers it at $t = a$, so the complete solution is

$$x(t) = \frac{F_o}{M\omega_o^2}\left\{(1-\cos\omega_o t) - u(t-a)\left[(1-\cos\omega_o(t-a))\right]\right\} \tag{10.92}$$

The result is that the response to the initial application of the force initiates a sinusoidal response that is to some extent negated by the response to the force removal. The most interesting case is $a = 2\pi/\omega_o$ for which the entire response consists of a single cycle of sinusoidal motion with the mass returning to rest in the initial position.

10.5.5 Dirac Delta Function

Consider now the derivative of the unit step function. It is obviously zero for all time before the trigger point, and also for all time after the trigger point. Even so, something happens at the trigger point such that integration across that location changes the function value. This is expressed mathematically as

$$\begin{aligned} u\left(a^+\right) - u\left(a^-\right) &= \int_{a^-}^{a^+} \frac{d}{dt}\left[u(t-a)\right]\,dt \\ &= \int_{a^-}^{a^+} \delta(t-a)\,dt = 1 \end{aligned} \tag{10.93}$$

The integrand here is what is called the *Dirac Delta* function, denoted as $\delta(t-a)$. According the rigorous definitions of Riemann integration, the value of a function at a single point cannot affect the integration, but the delta function is actually a mathematical device called a *distribution*, and the integral is not strictly a Riemann integral. For engineering purposes, it is sufficient to consider it an ordinary integral that obeys the unique property indicated in equation (10.93).

Although the Dirac delta is called a function, *no value can be assigned to it at the trigger point*. It may useful to consider another approach to understanding the Dirac delta, as the limit of a more easily described proper function, For that purpose, consider a rectangular pulse defined by the function $f(t-a)$ defined as

$$f(t-a) = \begin{cases} 0 & t < a \\ 1/w & a < t < a+w \\ 0 & a+w < t \end{cases} \tag{10.94}$$

The function $f(t-a)$ is a pulse of width w and height $1/w$. If the area A under this pulse is expressed formally by integration, the result is

$$A = \int_{-\infty}^{+\infty} f(t-a)\, dt = \int_{a}^{a+w} \left(\frac{1}{w}\right) dt = 1 \tag{10.95}$$

Now consider what happens to A in the limit as $w \to 0$. It is clear that the function $f(t-a)$ becomes unbounded, but it does so in such a way that the area under the curve is always 1.0. *Unit value for this integration is a fundamental property of the Dirac delta.*

Looking at the definition of the Laplace transform, it follows that the transform of the Dirac delta is

$$\mathcal{L}\{\delta(t-a)\} = \int_{0}^{\infty} e^{-st}\, \delta(t-a)\, dt = e^{-as} \tag{10.96}$$

Further, for some other function, $g(t)$, the Laplace transform of its product with a Dirac delta is readily established,

$$\mathcal{L}\{\delta(t-a)\cdot g(t)\} = \int_{0}^{\infty} e^{-st}\, \delta(t-a)\; g(t)\; dt = g(a)\, e^{-as} \tag{10.97}$$

10.5.6 Impulse Response

Consider again the simple damped spring-mass system shown in Figure 10.5. The system is initially at rest with no energy stored in the spring when a sudden, very brief force is applied to the mass. Such a force might be the result of a hammer blow, or a vehicle collision with the mass; the source of the force does not matter. All that is important is the *impulse of the force*, that is, the time integral of the force taken over the duration of the impact event; the *impulse* is as $\mathfrak{I}$.

$$\mathfrak{I} = \int_{0^-}^{0^+} F(t)\; dt \tag{10.98}$$

In writing this expression for the impulse, it is understood that the impact occurs at $t = 0$, so the limits are from the instant before impact to the instant after impact. In view of what has been said about the Dirac delta, it is clear that the impulsive force can be written as

$$F(t) = \mathfrak{I} \cdot \delta(t) \tag{10.99}$$

Observe that this last expression is zero for all time before and after $t = 0$, but when integrated across $t = 0$, the result is the required value for the impulse of the force. It is important to note that nothing has been said about the actual shape of the force pulse.

It could be rectangular, it could be triangular, it could be half of a sine pulse, it could be any shape at all. The only thing that is significant is the value of the impulse, the area under the force-time curve. The units of impulse are [Force] · [time] which in SI is N-s or in USC units it is lb-s.

With the impulsive force substituted for $F(t)$ in the equation of motion, equation (10.36) becomes

$$\ddot{x} + 2\zeta\omega_o\dot{x} + \omega_o^2 x = \frac{1}{M}\mathfrak{I}\cdot\delta(t) \tag{10.100}$$

Taking Laplace transforms of all terms with all zero initial conditions gives

$$X(s) = \frac{\mathfrak{I}/M}{s^2 + 2\zeta\omega_o s + \omega_o^2} = \frac{\mathfrak{I}/M}{(s+\zeta\omega_o)^2 + \left(1-\zeta^2\right)\omega_o^2} \tag{10.101}$$

Performing the inverse Laplace transformation using # 5 in Table 10.1 gives

$$x(t) = \frac{\mathfrak{I}}{M\omega_o\sqrt{1-\zeta^2}}e^{-\zeta\omega_o t}\sin\left(\sqrt{1-\zeta^2}\omega_o t\right) \tag{10.102}$$

The reader should check the units of this result to verify that the final result has proper displacement units. Thus the response to an impulse $\mathfrak{I}$ at time $t = 0$ is a damped sinusoid at the damped natural frequency.

The Dirac delta is the ideal description for an impact event in a mechanical system. Instrumented hammers are commercially available that can measure the actual force-time characteristic by electronic means and compute the impulse. When the response is similarly measured, either by a displacement transducer or an accelerometer, the impulse response can calculated directly from measured data. This provides a powerful connection between experimental measurements and theoretical calculations. There are methods available (see Chapter 11) to relate all of this to systems far more complicated than the simple system of Figure 10.5.

10.6 Linearization About an Equilibrium Point

Many mechanical system are described by nonlinear differential equations, as seen in Chapters 7 and 8. When such a system executes small oscillations near an equilibrium point, it is usually possible to *linearize the equation of motion*, that is, to substitute a linear approximation to the exact equation of motion. Here this process is considered for a single degree of freedom system only, although similar, but more complicated processes, apply with multiple degrees of freedom.

10.6.1 General SDOF Equation of Motion

Recall from Chapter 7 that the equation of motion for a single degree of freedom system can be written, using Eksergian's formulation, as

$$\mathbb{I}(q)\,\ddot{q} + \mathbb{C}(q)\,\dot{q}^2 + \frac{dV}{dq} = Q^{nc}(t, q, \dot{q}) \tag{10.103}$$

where q is the generalized coordinate describing the system, and $Q^{nc}(t, q, \dot{q})$ is the generalized nonconservative force acting on the system (see Chapters 6 and 7 for the development). The coefficients are the generalized inertia, $\mathbb{I}(q)$ and the centripetal coefficient, $\mathbb{C}(q)$, given by

$$\mathbb{I}(q) = \sum_i \left[m_i\left(K_{icx}^2 + K_{icy}^2\right) + J_{ic}K_{i\theta}^2\right] \tag{10.104}$$

$$\mathbb{C}(q) = \sum_i \left[m_i\left(K_{icx}L_{icx} + K_{icy}L_{icy}\right) + J_{ic}K_{i\theta}L_{i\theta}\right] \tag{10.105}$$

and the potential energy term is

$$V(q) = V\left[S_1(q), S_2(q), \ldots\right] \tag{10.106}$$

$$\frac{dV}{dq} = \sum_j \frac{\partial V}{\partial S_j}\frac{dS_j}{dq} = \sum_j \frac{\partial V}{\partial S_j}K_{S_j}(q) \tag{10.107}$$

where the $S_j(q)$ are the various secondary variables as required and the K_{S_j} are the associated velocity coefficients.

10.6.2 Equilibrium

For steady load conditions, there often are one or more static equilibrium positions. Let such a position be denoted as q_e. The condition for static equilibrium is then

$$\left.\frac{dV}{dq}\right|_{q=q_e} = Q^{nc} = \text{ constant} \tag{10.108}$$

where Q^{nc} is the generalized nonconservative force.

10.6.2.1 Linearization

Consider now the small motion of the system near the equilibrium position q_e. The small deviation from equilibrium is denoted as $z(t)$, and a change of variables is made such that

$$q \longrightarrow q_e + z \tag{10.109}$$
$$\dot{q} \longrightarrow \dot{z} \tag{10.110}$$
$$\ddot{q} \longrightarrow \ddot{z} \tag{10.111}$$

Taylor series expansions are made for each of the nonlinear terms in the equation of motion, retaining only terms of orders zero and one in the small quantity z:

$$\mathbb{I}(q_e + z) = \mathbb{I}(q_e) + \left.\frac{d\mathbb{I}(q)}{dq}\right|_{q=q_e} z + \cdots \tag{10.112}$$
$$\mathbb{C}(q_e + z) = \mathbb{C}(q_e) + \cdots \tag{10.113}$$

No further terms in are needed in the expansion of $\mathbb{I}(q)$ and $\mathbb{C}(q)$ because any additional coefficients are second and higher order terms in both cases. Continuing the Taylor expansion for the potential energy gives

$$\begin{aligned}\left.\frac{dV}{dq}\right|_{q_e+z} = & \left.\frac{dV}{dq}\right|_{q_e} \\ & + z \cdot [\underbrace{\sum_j \frac{\partial^2 V}{\partial^2 S_j} K_{S_j}^2}_{\text{Term \#1}} + \underbrace{\sum_j \frac{\partial V}{\partial S_j} L_{S_j}}_{\text{Term \#2}} \\ & + \underbrace{\sum_{j,r} \frac{\partial^2 V}{\partial S_r \partial S_j} K_{S_r} K_{S_j}}_{\text{Term \#3}}]_{q_e} + \cdots\end{aligned} \tag{10.114}$$

$$Q^{nc}(t, q_e + z, \dot{z}) = Q_e^{nc} + \left.\frac{\partial Q^{nc}}{\partial q}\right|_{q_e} z + \left.\frac{\partial Q^{nc}}{\partial \dot{q}}\right|_{q_e} \dot{z} + \cdots \tag{10.115}$$

Regarding the expression for the potential energy derivative, note that Term #1 and Term #2 are present in all cases. The presence or absence of Term #3 depends somewhat on the choice of secondary variables. To clarify, consider a spring for which the left end is located by the secondary variable $S_1(q)$ while the right end is located by the secondary variable $S_2(q)$. An additional secondary variable might be defined, $S_3(q) = S_2(q) - S_1(q)$. If the potential energy is formulated directly in terms of S_1 and S_2 (without reference to S_3), Term #3 is present; if the potential energy is formulated in terms of S_3, then Term #3 is absent. The results are fully equivalent [3].

10.6.3 Linearized Equation of Motion

When all the Taylor series are substituted into the equation of motion and (1) higher order terms are dropped and (2) the equilibrium expression is removed, the linearized result is

$$\begin{aligned} \ddot{z}\,\mathbb{I}\,(q_e) + z\,[\underbrace{\sum_j \frac{\partial^2 V}{\partial^2 S_j} K_{S_j}^2}_{\text{Term \#1}} + \underbrace{\sum_j \frac{\partial V}{\partial S_j} L_{S_j}}_{\text{Term \#2}} \\ + \underbrace{\sum_{j,r} \frac{\partial^2 V}{\partial S_r \partial S_j} K_{S_r} K_{S_j}}_{\text{Term \#3}}]_{q_e} \\ = \left.\frac{\partial Q^{nc}}{\partial q}\right|_{q_e} z + \left.\frac{\partial Q^{nc}}{\partial \dot{q}}\right|_{q_e} \dot{z} \end{aligned} \tag{10.116}$$

This is the intended result. Notice that the "stiffness" of the system involves several combinations of derivatives of the potential energy, along with velocity coefficients and velocity coefficient derivatives and a contribution from the nonconservative generalized force. It is not recommended that this analysis ever be used simply as a formula; rather, for each case, the full analysis should be conducted to be sure that everything appropriate to the specific case is properly taken into account.

10.6.4 Spring-Loaded Trammel Example

At this point, consider again the spring-loaded trammel, nominally at rest equilibrium but actually executing small oscillations about the equilibrium position. From Chapter 7, the exact equation of motion without the exciting force is

$$\begin{aligned} 0 &= \ddot{\theta}\,\mathbb{I} + \dot{\theta}^2\,\mathbb{C} + \frac{dV}{d\theta} \\ &= \ddot{\theta}\,\left[\frac{1}{4}m_1 + I_{1c} + m_2 L^2 \sin^2\theta + m_3 L^2 \cos^2\theta\right] \\ &\quad + \dot{\theta}^2\,\left[(m_2 - m_3)\,L^2 \sin\theta\cos\theta\right] \\ &\quad + \left(\frac{1}{2}m_1 + m_3\right) gL\cos\theta - K_S L \sin\theta\,(L\cos\theta - x_o) \end{aligned} \tag{10.117}$$

The numerical solution presented in Chapter 7 shows that this represents an oscillatory motion, but the evident nonlinearity puts it beyond the scope of linear vibration theory.

As mentioned above, the intent here is linearize the equation of motion for small motions about the equilibrium condition. This requires making a linear approximation to each term in the equation of motion by means of Taylor series expansions.

From Chapter 7, the generalized inertia and the centripetal coefficient are

$$\mathbb{I}(\theta) = \frac{1}{4}m_1 + I_{1c} + m_2 L^2 \sin^2\theta + m_3 L^2 \cos^2\theta \tag{7.58}$$

$$\mathbb{C}(\theta) = \frac{1}{2}\frac{d\mathbb{I}}{d\theta} = (m_2 - m_3) L^2 \sin\theta\cos\theta \tag{7.59}$$

$$\frac{dV}{d\theta} = \left(\frac{1}{2}m_1 + m_3\right) gL\cos\theta - K_S L \sin\theta\,(L\cos\theta - x_o) \tag{7.61}$$

Making the Taylor series expansions gives

$$\mathbb{I}(\theta) \approx \mathbb{I}(\theta_e) + 2\mathbb{C}(\theta_e)\, z + \cdots \tag{10.118}$$

$$\mathbb{C}(\theta) \approx \mathbb{C}(\theta_e) + \left.\frac{d\mathbb{C}(\theta)}{d\theta}\right|_{\theta_e} z + \cdots \tag{10.119}$$

$$\begin{aligned}\frac{dV}{d\theta} &\approx \left.\frac{dV}{d\theta}\right|_{\theta_e} + \left.\frac{d^2V}{d^2\theta}\right|_{\theta_e} z + \cdots \\ &\approx \left(\frac{1}{2}m_1 + m_3\right) gL\cos\theta_e - K_S L\sin\theta_e\,(L\cos\theta_e - x_o) \\ &\quad -z\left[\left(\frac{1}{2}m_1 + m_3\right) gL\sin\theta_e + K_S L\cos\theta_e\,(L\cos\theta_e - x_o) - K_S L^2\sin^2\theta_e\right] \\ &\quad +\cdots \\ &\approx z\left[-\left(\frac{1}{2}m_1 + m_3\right) gL\sin\theta_e - K_S L\cos\theta_e\,(L\cos\theta_e - x_o) + K_S L^2\sin^2\theta_e\right]\end{aligned} \tag{10.120}$$

Now, substitute these results into the equation of motion, dropping all terms of order two and higher in z and its derivatives, to obtain the linearized approximation:

$$\begin{aligned}0 = \ddot{z}\,\mathbb{I}(\theta_e) + z[&-\left(\frac{1}{2}m_1 + m_3\right) gL\sin\theta_e \\ &-K_S L\cos\theta_e\,(L\cos\theta_e - x_o) + K_S L^2\sin^2\theta_e]\end{aligned} \tag{10.121}$$

From the final form for the linearized equation of motion, it is evident that the effective values of inertia and stiffness are

$$I_{Eff} = \mathbb{I}(\theta_e) \tag{10.122}$$

$$K_{Eff} = -\left(\frac{1}{2}m_1 + m_3\right) gL\sin\theta_e - K_S L\cos\theta_e\,(L\cos\theta_e - x_o) + K_S L^2\sin^2\theta_e \tag{10.123}$$

When the numerical values from Chapter 7 are substituted into these expressions, the results are

$$I_{Eff} = 80.319043 \text{ lb-s}^2\text{-in} \tag{10.124}$$
$$K_{Eff} = 44542.726 \text{ in-lb/rad} \tag{10.125}$$

from which, for a linear system the natural frequency and period are

$$\begin{aligned} \omega_o &= \sqrt{44542.726/80.319043} = 23.549 \text{ rad/s} \\ f_o &= \frac{\omega_o}{2\pi} = 3.7479 \text{ Hz} \\ \text{Period} &= 1/f_o = 0.26682 \text{ sec} \end{aligned} \tag{10.126}$$

Now, compare this result with that from the numerical simulation developed in Chapter 7. There the simulation was based on a vertical blow with a magnitude of 450 pounds, resulting in a rather large motion. The period of that motion after the end of the initial impact is $P_{450} = 0.28219818$ s. If however, the same simulation is repeated except that the magnitude of the blow is reduced to 2 pounds, so as to excite only a very small motion, the period is $P_2 = 0.27092$ sec. The fact that the period is amplitude dependent is a result of the system nonlinearity. The result from the linearization was $P_{\text{Linearized}} = 0.26682$ sec which compares rather closely with the period from complete simulation with the 2 pound excitation, roughly a four millisecond difference in the period.

The advantage of the linearization is evident; the period (or frequency) for small amplitudes is obtained without the labor of the full nonlinear simulation. The limitation is also evident; the effects of nonlinearity are not seen at all, and the results are valid only for very small motions.

10.7 Dynamic Stability

In the previous discussion of stability, near the end of Chapter 6, the systems involved were considered to be at rest equilibrium. Stability was presented there in terms of returning to the original equilibrium state, but it is necessary to broaden the concept of stability to include dynamic systems. This is an immense subject, and a full treatment is beyond the scope of the present work. Thus the concept is extended here only by means of an example. This example is also important because of what it says about the role of friction.

Consider a simple pendulum (a point mass on a massless shaft), supported on a spinning support, as shown in Figure 10.12. The support rotates clockwise at angular speed Ω,

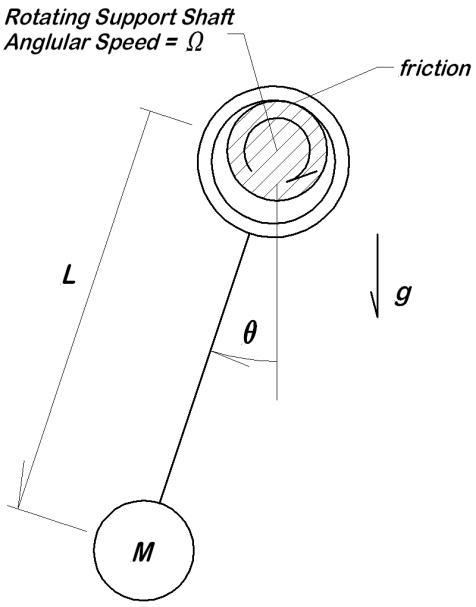

Figure 10.12: Simple Pendulum on Rotating Support

and friction at the support causes the pendulum to assume an equilibrium position as shown. The equilibrium angle is θ_e, expressed as

$$\theta_e = \arcsin\left(\frac{T_{fo}}{MgL}\right) \tag{10.127}$$

where T_{fe} = equilibrium value of friction torque at the sliding contact.

It is reasonable to assume that the friction torque depends upon the relative velocity at the point of contact, $f\left(\Omega - \dot{\theta}\right)$, where the functional form for f is yet to be specified. Whatever the specific form may be, it is here expanded in a Taylor series and truncated,

$$\begin{aligned} T_f &= f\left(\Omega - \dot{\theta}\right) \\ &= f(\Omega) - \dot{\theta} f'(\Omega) + \frac{1}{2}\dot{\theta}^2 f''(\Omega) + \cdots \\ &\approx T_{fe} - \dot{\theta} f'(\Omega) \end{aligned} \tag{10.128}$$

After noting that $MgL\sin\theta_e = T_{fe}$, the equation of motion for the pendulum is

$$ML^2\ddot{\theta} + \dot{\theta}\cdot f'(\Omega) + MgL\cos\theta_e \cdot \theta = 0 \tag{10.129}$$

There are three cases to be considered:

1. If $f'(\Omega) > 0$, which is to say that the friction torque increases with relative velocity, then the motion is a damped sinusoid. The response of the system to a disturbance is to oscillate, but it will eventually return to the original equilibrium position. The system is *stable*. This is the case most people expect, but it is not universally true.

2. If $f'(\Omega) = 0$, which means that the friction torque is independent of the relative velocity, then the motion is an undamped sinusoidal oscillation. The oscillation does not grow with time, but neither does it damp out. Thus the system oscillates about the initial position, but does not return to rest there. This case is *neutrally stable*.

3. If $f'(\Omega) < 0$, so that the friction torque decreases with increasing relative velocity, the system motion is a growing oscillation. The amplitude of the oscillation grows without limit, so that the system departs more and more from the initial state. This system is *unstable*.

All three cases exist in real systems of various sorts, so friction can be a major determining factor in system stability. Note how the concept of stability is here extended to include systems that remain in motion for an extended time when disturbed, but are still unstable or stable depending on whether or not completely depart from their initial state.

10.8 Conclusion

The subject of SDOF vibrations is a vast landscape of fairly well explored physical problems. The discussion above has only presented a few of the salient points that have found wide application in engineering. If these topics are mastered, so that they are readily available for application, they are a sufficient foundation for the many variations that will be encountered in actual engineering work.

The reduction to standard form in terms of the undamped natural frequency (ω_o) and the damping ratio (ζ) is a vitally important first step. The solutions for the relevant differential equations are already known when the describing differential equation is written in standard form. Time spent re-solving these differential equations for each particular case is simply time wasted.

The response formulations in terms of the dimensionless parameters (Ω/ω_o) and ζ make it possible to deal with a wide range of problems of the same general form. For any physical problem, described using any consistent units system, these same expressions apply. They are easily solved to give correct results for any particular units system.

The discussion of SDOF vibrations also serves as background for the next discussion to follow dealing with multi-degree of freedom vibrations, although major differences are

soon apparent.

References

[1] Churchill, R.V., *Operational Mathematics*, 2nd. ed, McGraw-Hill, 1958.

[2] Ogata, K., *System Dynamics*, Prentice-Hall, 1978.

[3] Doughty, S., "Single Degree of Freedom Mechanism Vibration Near Equilibrium," *Mech. Mach. Theory*, Vol. 31, No. 3, pp. 339 - 344, 1996.

Problems

10-1 The figure shows a cylindrical body with cross section in the form of a greater circular segment (a) (see Appendix 4.4 for the properties of this shape). The body rolls without slipping on a flat horizontal surface as shown at (b).

The known data are

$d = 377$ mm	diameter of the circle
$w = 162$ mm	width of the chordal flat
$L = 140$ mm	length of the cylinder
$\rho = 7800.55$ kg/m^3	mass density of the cylinder material

(a) Determine the mass, center of mass location, and mass moment of inertia for the cylindrical body;

(b) Formulate the nonlinear equation of motion for the rocking vibration that results from an initial displacement and/or velocity;

(c) Linearize the equation of motion and determine the natural frequency for the rocking motion.

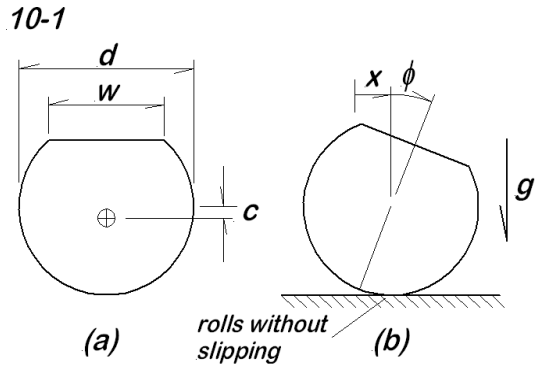

10-2 A submersible vehicle for deep sea exploration is being lowered from a winch on an exploration ship. Suddenly there is a breakdown in the winch mechanism, causing the winch drum to stop abruptly; call the time when the winch stops $t = 0$. At $t = 0$, the vehicle is located at $y(0) = y_o$, and dropping at a rate $\dot{y}(0) = \dot{y}_o > 0$. This causes a bouncing motion of the submersible. The submersible has a total mass of 5700 kg, and a volume of 10.2 m^3. The elasticity of the cable is described by the compliance per unit length, $c = 0.238 \cdot 10^{-10}$ N^{-1}. The mass density of sea water is $\rho_{H_2O} = 1026$ kg/m^3. Damping due to fluid drag is to be neglected.

(a) Determine the amplitude and frequency of the bouncing motion if the sudden stop occurs for $y_o = 700$ m, $\dot{y}_o = 1.7$ m/s;

(b) Determine the amplitude and frequency of the bouncing motion if the sudden stop occurs for $y_o = 1400$ m, $\dot{y}_o = 1.7$ m/s;

(c) Determine the amplitude and frequency of the bouncing motion if the sudden stop occurs for $y_o = 2100$ m, $\dot{y}_o = 1.7$ m/s;

(d) Determine the amplitude and frequency of the bouncing motion if the sudden stop occurs for $y_o = 2800$ m, $\dot{y}_o = 1.7$ m/s;

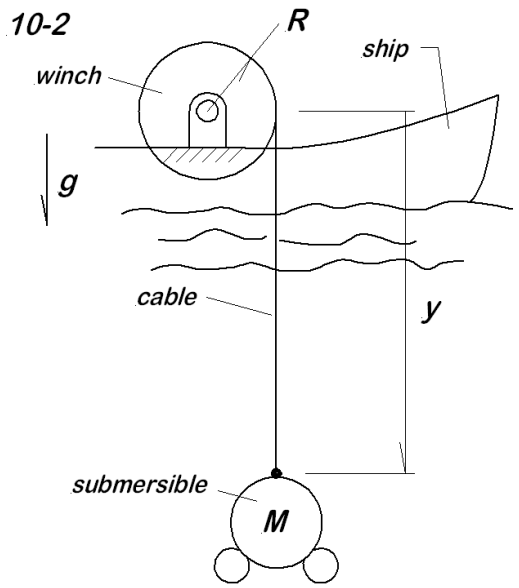

10-3 The figure shows a mass M supported against gravity by a spring and a viscous damper; three different positions are shown for the mass. In the position $y = 0$, there is no strain in the spring.

(a) Develop the system equation of motion in terms of y and cast it in standard form (in terms of ω_o and ζ);

(b) Determine the equilibrium position, y_e;

(c) Modify the equation of motion to eliminate y in favor of z;

(d) State in words the advantages of expressing the equation of motion in terms of z.

(e) Using the data below, evaluate numerically ω_o, ζ, ω_d, and y_e.

$M = 3.77$ kg $\quad K = 21750$ N/m $\quad B = 280$ N-s/m

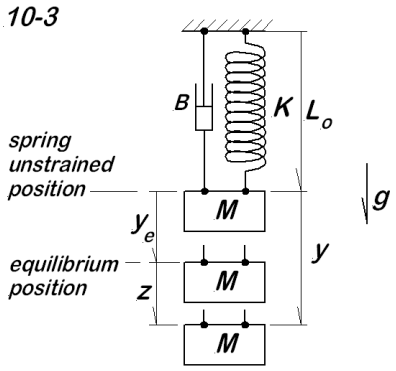

10-4 The figure shows a simple torsional oscillator. The entire assembly is constructed of the same material for which physical properties follow below.

(a) Assuming at first that the shaft torsional stiffness K_t and the disk mass moment of inertia J_c are both known, write the equation of motion for small oscillations;

(b) Use a mechanics of materials approach to determine

(1) the disk mass polar moment of inertia;

(2) the shaft stiffness;

(c) Evaluate numerically ω_o, ζ, and ω_d for this system.

$D = 23$ mm	$\rho g = 76000$ N/m^3	material specific weight
$R = 97$ mm	$E = 190$ GPa	Young's modulus
$H = 12$ mm	$G = 73.1$ GPa	shear modulus
$L = 322$ mm	$\mu = 0.305$	Poisson's ratio
$B = 160$ N-s/m		

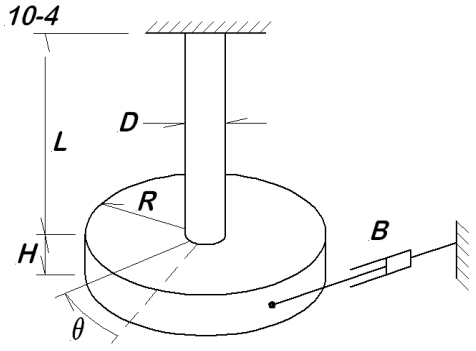

10-5 Consider a simple spring-mass oscillator such as that shown in Figure 10.1 or, because it is a real system, it is actually more like that in Figure 10.2. It is known that the effective system mass is $M = 3.27$ kg. The system is displaced and given an initial velocity, and the motion is recorded as shown in the figure. By reading data from the figure, obtain estimates for:

(a) the damping factor, ζ;

(b) the damped natural frequency, ω_d;

(c) the undamped natural frequency, ω_o;

(d) the spring stiffness, K.

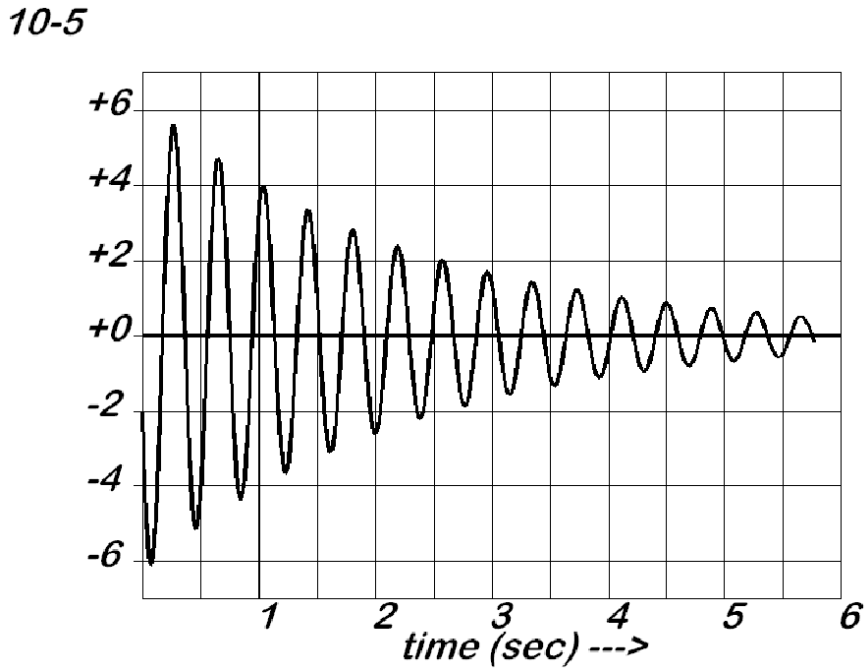

10-6 The figure shows a wedge cam with a roller follower rigidly connected to a mass M_3. The horizontal spring may operate in either tension or compression while the vertical spring is always in compression to maintain contact between the cam and the follower. The system is preloaded such that, when the roller makes contact on the tip of the cam, the vertical spring is at 85% of its free length, L_{2o}. Before using the numerical data provided, assume that all dimensions and physical parameters (K_1, K_2, B, M_1, M_2, M_3, J_{2c}) are known, as is the free length for the horizontal spring, L_{1o}.

(a) Develop any kinematic relations required later;

(b) Calculate J_{2c} assuming the roller is a simple disk of radius R and thickness $t = 8$ mm;

(c) Determine the free length of the vertical spring;

(d) Write the system equation of motion (be sure to include the follower rotation);

(e) In terms of the known system parameters, express ω_o, ζ, and ω_d;

(f) Using the data below, calculate numerical values for ω_o, ζ, and ω_d.

(g) What is the equilibrium value of x?

$K_1 = 18500$ N/m	$L_{1o} = 122$ mm	$C = 165$ mm
$K_2 = 4350$ N/m	$H = 45$ mm	$L = 92$ mm
$M_1 = 1.3$ kg	$Y = 210$ mm	$R = 20$ mm
$M_2 = 0.8$ kg	$B = 25$ N-s/m	$H = 8$ mm
$M_3 = 2.4$ kg		$\alpha = 20^o$

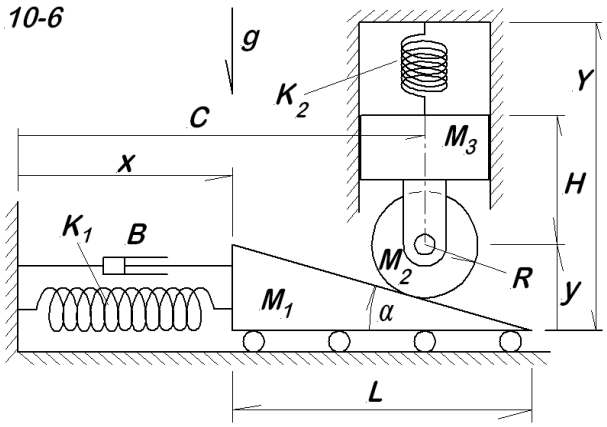

10-7 The figure shows a point mass (the block) on the end of a massless pivoted lever. The rotation of the block is to be neglected, so the mass moment of inertia of the block does not matter. Assume that the spring is relaxed when $\theta = 0$ and that $|\theta|$ remains small at all times.

(a) Develop the equation of motion for this system;

(b) Express the undamped natural frequency and the damping factor;

(c) Using the numerical data below, evaluate ω_o, ζ, and ω_d for this system.

$M = 7.26$ kg $\quad a_1 = 275$ mm

$K = 165$ N/m $\quad a_2 = 410$ mm

$B = 57.3$ N-s/m $\quad a_3 = 883$ mm

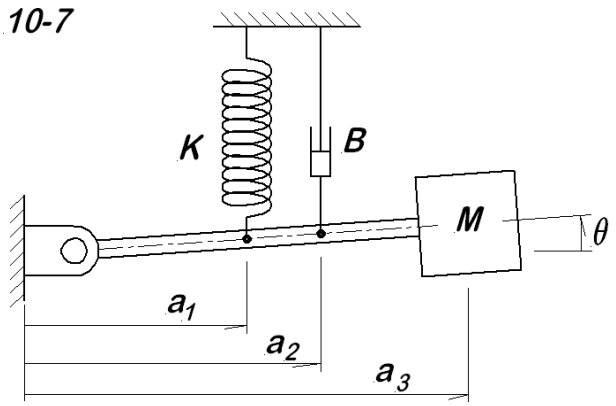

10-8 In Section 10.4, when discussing the response to a sinusoidal excitation applied to an undamped system, the solution was developed with the explicit constraint that the forcing frequency must not coincide with the system natural frequency. When the excitation frequency is the same as the system natural frequency, the system said to be in *resonance*, a condition usually associated with eventual catastrophic failure. Consider now an undamped spring-mass oscillator such as that shown in Figure 10.4, where $F(t) = F_o \sin \omega_o t$. Assume that $x(0) = \dot{x}(0) = 0$.

(a) Use the Laplace transform technique to obtain the solution for this case;

(b) Describe in words the nature of the solution;

(c) Based on the data below, how long does it take for the envelope of the motion to reach 350 mm?

(d) How many cycles of system oscillations are required for the envelop to reach 350 mm?

$M = 7.35$ kg $\quad K = 1520000$ N/m $\quad F_o = 520$ N

10-9 In Section 10.4 based on Figure 10.5, the response of a damped spring-mass oscillator to sinusoidal excitation is formulated. In that development, there was no need to exclude resonant forcing, and thus it is included in the solution given, equation (10.42).

(a) For resonant excitation, that is $\Omega = \omega_o$, what does equation (10.42) say about the nature of the response?

(b) Using the data from problem **10-8**, with the additional value $C = 17200$ N-s/m, what

is the eventual steady state amplitude of the response?

(c) Develop a computer generated plot for the system response. Does this agree with your answer to part (a)?

10-10 In Section 10.5.4, the response to a single rectangular pulse is developed my means of Laplace transforms and unit step functions. The undamped period is $\tau_o = 2\pi/\omega_o$. Use the system data from problems **10-8** and **10-9** (b) for the questions below. Development of computer code is necessary for this problem.

(a) For the pulse magnitude constant at $F_o = 520$ N, develop computer plots of the solution for $a = \frac{1}{2}\tau_o$, $\frac{7}{10}\tau_o$, $\frac{9}{10}\tau_o$. $\frac{95}{100}\tau_o$, $\frac{98}{100}\tau_o$, and τ_o out to $t = 5\tau_o$;

(b) For the constant impulse value 1000 N-s, develop computer plots of the solution for $a = \frac{1}{2}\tau_o$, $\frac{2}{10}\tau_o$, $\frac{1}{10}\tau_o$. $\frac{5}{100}\tau_o$, and $\frac{2}{100}\tau_o$ out to $t = 5\tau_o$.

Chapter 11

MDOF Vibrations

11.1 Introductory Comments

Most machines may readily be seen to consist of parts in two categories: (1) the moving mechanism, and (2) the stationary supporting structure. The reader is referred back to the first page of Chapter 1 for the distinction between a mechanism and a structure. Understanding this distinction is important at this point because the present chapter is mostly about structures. The vibration of mechanisms, particularly the slider-crank mechanism, is the subject of Chapter 12.

The modeling and analysis of multidegree of freedom systems was discussed in Chapter 8. In that chapter, the major new tool introduced was the Lagrange formulation of the equations of motion. For the purposes of this chapter, it is assumed that the reader is familiar with that approach and also with the classical Newton's Second Law approach to formulating equations of motion. The choice as to which one to use depends to a degree upon the nature of the problem, but the eventual results should be the same no matter which approach is employed.

11.2 Introductory Example

To begin this chapter, the simple single degree of freedom spring-mass oscillator is extended to include a second spring and a second mass. This changes the required approach in several ways. The new system is shown in Figure 11.1

In the upper part of the figure, (a), the system is shown at equilibrium rest with no strain in either spring. In the lower part, (b), the system is displaced x_1 and x_2 under the

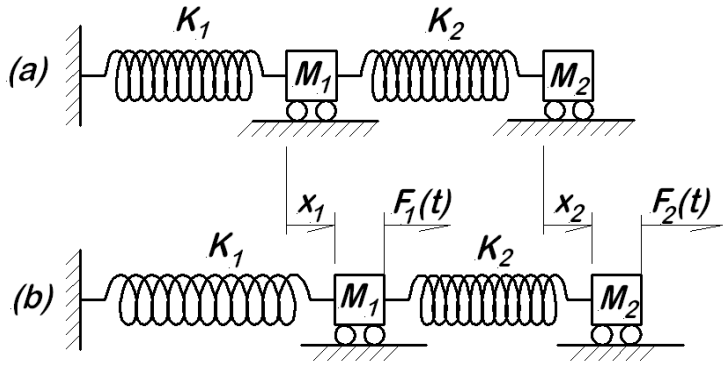

Figure 11.1: Two Degree of Freedom Vibratory System

action of the applied external forces $F_1(t)$ and $F_2(t)$. The problem to be addressed here is the determination of the vibratory response of the system under the time dependent forces. Note that there is no damping included; this matter is addressed later.

11.3 Equations of Motion

In order to write the equations of motion, Newton's Second Law is applied to each block separately:

$$M_1\ddot{x}_1 = -K_1x_1 + K_2(x_2 - x_1) + F_1(t) \tag{11.1}$$
$$M_2\ddot{x}_2 = -K_2(x_2 - x_1) + F_2(t) \tag{11.2}$$

The difficulty is immediately evident; the equations of motion are *coupled*. This means that they must be solved together, rather than separately. Think about what that means for a system with many degrees of freedom and an equal number of equations of motion!

It is convenient to re-cast these equations in matrix form. In that way, what is done to solve this simple system will also serve as a model for more complicated systems involving a greater number of degrees of freedom.

$$\underbrace{\begin{bmatrix} M_1 & 0 \\ 0 & M_2 \end{bmatrix}}_{\text{Mass Matrix}} \begin{Bmatrix} \ddot{x}_1 \\ \ddot{x}_2 \end{Bmatrix} + \underbrace{\begin{bmatrix} K_1 + K_2 & -K_2 \\ -K_2 & K_2 \end{bmatrix}}_{\text{Stiffness Matrix}} \begin{Bmatrix} x_1 \\ x_2 \end{Bmatrix} = \underbrace{\begin{Bmatrix} F_1(t) \\ F_2(t) \end{Bmatrix}}_{\text{Excitation Vector}} \tag{11.3}$$

Note that the mass matrix is diagonal; this is emphasized in the form of the brackets enclosing $\lceil M \rfloor$ that point to the ends of the main diagonal. The diagonal mass matrix is

typical for system equations formulated based on lumped mass models. The user should be aware, however, that this is not the case with most finite element codes which usually employ a device called a *consistent mass matrix*, a topic beyond the scope of the present discussion. Note also that the stiffness matrix is symmetric; this is to be expected.

In many respects, the approach to MDOF vibration follows the same process as that used for SDOF systems, specifically dealing first with the homogeneous solution, then the particular solution, and finally the application of initial conditions. These steps are developed below.

11.4 Homogeneous Solution

For the homogeneous solution, the excitation vector is set to zero, thus:

$$\begin{bmatrix} M_1 & 0 \\ 0 & M_2 \end{bmatrix} \begin{Bmatrix} \ddot{x}_1 \\ \ddot{x}_2 \end{Bmatrix} + \begin{bmatrix} K_1 + K_2 & -K_2 \\ -K_2 & K_2 \end{bmatrix} \begin{Bmatrix} x_1 \\ x_2 \end{Bmatrix} = \begin{Bmatrix} 0 \\ 0 \end{Bmatrix} \tag{11.4}$$

A solution is assumed in sinusoidal form at frequency ω_n,

$$\{x\} = \{A\} \sin(\omega_n t) \tag{11.5}$$

where $\{A\}$ is a vector of constants to be determined. When this assumed form is differentiated and substituted back into equation (11.4), the result is

$$\begin{bmatrix} K_1 + K_2 - \omega_n^2 M_1 & -K_2 \\ -K_2 & K_2 - \omega_n^2 M_2 \end{bmatrix} \begin{Bmatrix} A_1 \\ A_2 \end{Bmatrix} = \begin{Bmatrix} 0 \\ 0 \end{Bmatrix} \tag{11.6}$$

Equation (11.6) is called the *algebraic eigenproblem*[1]. It represents a system of simultaneous, homogeneous, linear algebraic equations. Because they are homogeneous, a nontrivial solution exists *if and only if* the determinant of the coefficients is zero. Thus, because only a nontrivial solution is of interest, it is necessary to require that

$$\begin{vmatrix} K_1 + K_2 - \omega_n^2 M_1 & -K_2 \\ -K_2 & K_2 - \omega_n^2 M_2 \end{vmatrix} = 0 \tag{11.7}$$

[1] The algebraic eigenproblem is discussed here in Section 11.4 in a physical context. Most of the same ideas are presented from a mathematical perspective in Appendix 1.7 and Appendix 1.8. The reader should consider reading these two presentations together.

which can be solved to determine the suitable values of ω_n^2 (eigenvalues). Equation (11.7) is called the *characteristic equation*. For this example, the characteristic equation is a *(bi)quadratic* form

$$M_1 M_2 \omega_n^4 - \left[K_2 M_1 + (K_1 + K_2)\, M_2\right] \omega_n^2 + K_1 K_2 = 0 \tag{11.8}$$

The term *biquadratic* means that it is an equation of degree four, but may be considered as being simply quadratic in the variable ω_n^2 because the terms of degree one and three in ω_n are absent. From the quadratic formula, the solution is

$$\begin{aligned} \omega_n^2 \;=\; & \frac{1}{2M_1M_2}(K_1M_2 + K_2M_1 + K_2M_2 \\ & \pm\sqrt{K_1^2M_2^2 + K_2^2M_1^2 + K_2^2M_2^2 + 2K_1K_2M_2^2 + 2K_2^2M_1M_2 - 2K_1K_2M_1M_2}) \end{aligned} \tag{11.9}$$

Completing the calculation gives two nonzero values, denoted as ω_1 and ω_2 that are the two system natural frequencies. These are assumed known from this point on. The symbolic solution shown is not very meaningful, but the whole process is easily carried out with numeric values.

It is important to note that while the characteristic equation is simply a biquadratic for the 2DOF system, for systems with more degrees of freedom, the degree of the polynomial grows rapidly. In general, for n degrees of freedom, the characteristic equation is of degree $2n$. Such larger systems cannot be solved in closed form, but there has been a vast amount of work done in developing numerical methods for solving this problem, usually found under the label the *algebraic eigenvalue problem*. *Eigen-* is a German adjective prefix that translates roughly as the proper, appropriate, acceptable, or correct solution.

For the values of $\omega_n = \omega_1$ and $\omega_n = \omega_2$, the existence theorem assures the existence of nontrivial solutions, but it does not say how to find them. In actual fact, the solutions are not fully determined; the meaning of this statement becomes more clear below.

Let $\omega_n = \omega_1$ and assume $A_1 = 1.0$. Then the first equation reads

$$\left(K_1 + K_2 - \omega_1^2 M_1\right)(1.0) - K_2 A_2 = 0 \tag{11.10}$$

so that

$$A_2 = \frac{K_1 + K_2 - \omega_1^2 M_1}{K_2} \tag{11.11}$$

The solution vector (called an *eigenvector*) associated with ω_1 is $\{A\}_1 = \text{col}\left(1.0,\ \frac{K_1+K_2-\omega_1^2 M_1}{K_2}\right)$. The solution vector associated with the second natural frequency is found by an similar process.

Does the reader notice a degree of arbitrariness about the eigenvector? The first element is simply chosen to be +1.0. It could just as easily have been chosen as $A_1 = 3.0$, $A_1 = -1.0$, or $A_1 = -37.2$. It really does not matter; any nonzero value is satisfactory. The result of another choices is to scale the second element accordingly. Thus, if we choose $A_1 = -1.0$, the resulting eigenvector is col $\left(-1.0, -\frac{K_1+K_2-\omega_1^2 M_1}{K_2}\right)$. This scalability is what was meant when it was noted that the solutions are not fully determined. *In general, any constant (real or complex) multiplier applied to an eigenvector produces another version of that same eigenvector.* An eigenvalue and its associated eigenvector are known as an *eigensolution*, ω_j and $\{A\}_j$.

The eigenvector is often called a *mode vector* or more graphically, a *mode shape*. The term "shape" may initially sound strange, but it is actually very descriptive. In the example above, the first mode vector (first mode shape) says two things about the first mode motion: (1) the two masses move in the same direction at all times, and (2) for any displacement of M_1, the displacement of M_2 in this mode is $\left(K_1 + K_2 - \omega_1^2 M_1\right)/K_2$ times as great. Similar statements can be made regarding the second mode shape. This description of the motion, in terms of directions and relative magnitudes, is the reason for the term *mode shape*. The concept of a mode shape is extremely important and must be considered very carefully. The mode shape concept is encountered repeatedly in what follows.

At this point, the homogeneous problem is put on hold, even though it has not been fully solved. The entire solution process is addressed below in terms of the forced response, for which the free vibration is simply a special case. For now, consider a numeric example of the process discussed above.

11.4.1 Numerical Example

For the sake of an example, consider the system of Figure 11.1 with the following data:

$M_1 = 1.5$ kg $\quad K_1 = 275$ N/m

$M_2 = 2.1$ kg $\quad K_2 = 124$ N/m

The homogeneous equation (11.6), above, takes the form

$$\begin{bmatrix} 399 - 1.5\omega^2 & -124 \\ -124 & 124 - 2.1\omega^2 \end{bmatrix} \begin{Bmatrix} A_1 \\ A_2 \end{Bmatrix} = \begin{Bmatrix} 0 \\ 0 \end{Bmatrix} \tag{11.12}$$

so that the characteristic determinant is

$$\begin{vmatrix} 399 - 1.5\omega^2 & -124 \\ -124 & 124 - 2.1\omega^2 \end{vmatrix} = 0 \tag{11.13}$$

When this is expanded, the characteristic equation is

$$3.15\omega^4 - 1023.9\omega^2 - 34100 = 0 \tag{11.14}$$

The positive roots of the characteristic equation are

$$\begin{aligned} \omega_1 &= 6.13755 \text{ rad/s} \\ \omega_2 &= 16.95223 \text{ rad/s} \end{aligned} \tag{11.15}$$

Note that, because the equation was a quartic, there are two more roots, the negatives of these two values. For this problem, the negative roots are meaningless.

When the first root is substituted back with $A_1 = 1.0$, the result is $A_2 = 2.76206$. When the second root is substituted back, again with $A_1 = 1.0$, the result is $A_2 = -0.258606$. Thus the complete set of eigensolutions are

$$\begin{aligned} \omega_1 = 6.13755 \text{ rad/s} \qquad & \omega_2 = 16.95223 \text{ rad/s} \\ \{A\}_1 = \begin{Bmatrix} 1.0 \\ 2.76206 \end{Bmatrix} \quad & \{A\}_2 = \begin{Bmatrix} 1.0 \\ -0.258606 \end{Bmatrix} \end{aligned} \tag{11.16}$$

These results are typical. For free vibration, in the low frequency mode, both masses move in phase as indicated by the same sign on all elements of the first mode vector (first eigenvector); in this example, when M_1 moves one unit, M_2 moves 2.79206 units in the same direction. In the high frequency mode, the opposite is true as indicated by the sign difference in the eigenvector elements; again in this example, when M_1 moves one unit, M_2 moves 0.258606 in the opposite direction.

11.4.2 Systems of Higher Order

For the simple system of the example above with two degrees of freedom, the characteristic equation is of fourth degree, i.e., $2n$, where n is the number of degrees of freedom. This facilitates the solution considerably. When the system order is relatively small, say no more than 20, there are a number of techniques commonly taught in numerical

analysis courses for determining the eigensolution. These include such methods as the Jacobi method and various iteration schemes that are usually not too difficult for an average engineer to program. When the system becomes large, perhaps $n \gg 20$, then the problem falls into the domain of the numerical analyst and the computer scientist. Virtually all finite element programs incorporate highly sophisticated eigensolvers that are carefully designed and coded for speed and control of rounding errors.

It should be mentioned that an equation of the form

$$\left([K] - \omega_n^2 \lceil M \rfloor\right) \{A\} = \{0\} \tag{11.17}$$

is called a *generalized eigenvalue problem*. The term *generalized* is used to distinguish it from the *classical eigenvalue problem* of the form

$$\left([G] - \lambda \lceil I \rfloor\right) \{\phi\} = \{0\} \tag{11.18}$$

There are methods for converting the generalized eigenvalue problem into the classical form; one such method is the *Choleski transformation*. As long as the mass matrix is diagonal, this is a simple process. With that assumption, define the Choleski transformation matrix $[T_C]$ such that

$$\lceil T_C \rfloor = \lceil M \rfloor^{1/2} \tag{11.19}$$

Note that

- $\lceil T_C \rfloor$ is diagonal;
- $\lceil T_C \rfloor = \left\lceil \sqrt{m_{ii}} \right\rfloor$, the diagonal elements are the square roots of the mass values;
- $\lceil T_C \rfloor^T = \lceil T_C \rfloor$, the transformation matrix is its own transpose;
- $\lceil T_C \rfloor^{-1} = \left\lceil 1/\sqrt{m_{ii}} \right\rfloor$, a diagonal matrix with $1/\sqrt{m_{ii}}$ on the main diagonal;
- $\lceil T_C \rfloor^T \lceil T_C \rfloor = \lceil M \rfloor$, the products of the square roots reproduce the original mass values.

Now replace $\lceil M \rfloor$ in equation (11.17) with the product $\lceil T_C \rfloor^T \lceil T_C \rfloor$, to obtain

$$\left([K] - \omega^2 \lceil T_C \rfloor \lceil T_C \rfloor^T\right) \{A\} = \{0\} \tag{11.20}$$

and then premultiply by the inverse of the transformation matrix,

$$\begin{aligned} \lceil T_C \rfloor^{-1} [K] \{A\} &= \omega^2 \lceil T_C \rfloor^{-1} \lceil T_C \rfloor \lceil T_C \rfloor^T \{A\} \\ &= \omega^2 \lceil T_C \rfloor^T \{A\} \end{aligned} \tag{11.21}$$

Define a new eigenvector, $\{\phi\}$ and a new coefficient matrix $[G]$ such that

$$\{\phi\} = \lceil T_C \rfloor^T \{A\} \tag{11.22}$$
$$[G] = \lceil T_C \rfloor^{-1} [K] [T_C]^{-T} \tag{11.23}$$

which results in the classical eigenvalue problem

$$\begin{aligned} \lceil T_C \rfloor^{-1} [K] [T_C]^{-T} \lceil T_C \rfloor^T \{A\} - \omega^2 \lceil T_C \rfloor^T \{A\} &= \{0\} \\ \left([G] - \omega^2 [I] \right) \{\phi\} &= \{0\} \end{aligned} \tag{11.24}$$

Note particularly that the eigenvector is transformed while the eigenvalue remains the same before and after the transformation. If the computer subroutine Jacobi.Tru (given in Appendix 1.9 as a part of ChoJac.Tru) is used to solve the classical eigenvalue problem when the generalized problem is the actual objective, it is necessary to execute the inverse transformation in order to obtain the eigenvectors for the generalized problem. A single computer code implementing (a) the Choleski Transformation, (b) the Jacobi Eigensolution, and (c) the inverse transformation is provided as ChoJac.Tru (see Appendix 1.9). All of this is demonstrated later in regard to shaft vibration.

11.5 Forced Response Calculation

Everything in this chapter to this point has considered only the free vibration problem, that is, the homogeneous response, even though that solution was not completed above. The discussion now continues in terms of the forced response, remembering that the free vibration response is simply the special case where there is no external forcing of the system.

11.5.1 Modal Transformation

The original problem had an external force acting on each mass, and the equations of motion were

$$\begin{bmatrix} M_1 & 0 \\ 0 & M_2 \end{bmatrix} \begin{Bmatrix} \ddot{x}_1 \\ \ddot{x}_2 \end{Bmatrix} + \begin{bmatrix} K_1 + K_2 & -K_2 \\ -K_2 & K_2 \end{bmatrix} \begin{Bmatrix} x_1 \\ x_2 \end{Bmatrix} = \begin{Bmatrix} F_1(t) \\ F_2(t) \end{Bmatrix} \tag{11.3}$$

The homogeneous solutions found in the previous section provide a device to simplify the solution of the problem. It begins with the eigenvectors, assembled to form what is

called the *modal transformation matrix*, $[A]$, (or simply the *modal matrix*), thus

$$[A] = [\{A\}_1 | \{A\}_2] = \left[\left\{ \begin{array}{c} 1.0 \\ A_{21} \end{array} \right\} \left\{ \begin{array}{c} 1.0 \\ A_{22} \end{array} \right\} \right] = \left[\begin{array}{cc} 1.0 & 1.0 \\ A_{21} & A_{22} \end{array} \right] \tag{11.25}$$

Define the *modal coordinate vector*, $\{\xi(t)\}$, such that

$$\{x(t)\} = [A]\{\xi(t)\} \tag{11.26}$$

Note that, while $\{x(t)\}$ and $\{\xi(t)\}$ are each time dependent, the modal matrix is composed entirely of constants. This transformation of variables is the key that unlocks the multidegree of freedom response.

With the transformation defined, it is differentiated and substituted it back into the equations of motion, in abbreviated form thus:

$$\begin{aligned} \lceil M \rfloor \{\ddot{x}\} + [K]\{x\} &= \{F(t)\} \\ \lceil M \rfloor [A] \left\{\ddot{\xi}\right\} + [K][A]\{\xi\} &= \{F(t)\} \\ [A]^T \lceil M \rfloor [A] \left\{\ddot{\xi}\right\} + [A]^T [K][A]\{\xi\} &= [A]^T \{F(t)\} \end{aligned} \tag{11.27}$$

The premultiplication by $[A]^T$ has an astonishing effect; the results is that $[A]^T \lceil M \rfloor [A]$ and $[A]^T [K][A]$ each reduce to diagonal matrices:

$$\lceil \mathbb{M} \rfloor = [A]^T [M][A] \tag{11.28}$$

$$\lceil \mathbb{K} \rfloor = [A]^T [K][A] \tag{11.29}$$

where the notation $\lceil .. \rfloor$ denotes a diagonal matrix. The matrices $\lceil \mathbb{M} \rfloor$ and $\lceil \mathbb{K} \rfloor$ are called *modal mass* and *modal stiffness* matrices, respectively. This process of reducing the coefficient matrices to diagonal form is called a *similarity transformation*. It is discussed at length in texts on linear algebra where the mode vectors are shown to satisfy certain *orthogonality relations*.

With this final step, the equations of motion are

$$\lceil \mathbb{M} \rfloor \left\{\ddot{\xi}\right\} + \lceil \mathbb{K} \rfloor \{\xi\} = [A]^T \{F(t)\} \tag{11.30}$$

Because the coefficient matrices are now diagonal, *the equations are decoupled* (separated) and may be re-written as

$$\mathbb{M}_{11}\ddot{\xi}_1 + \mathbb{K}_{11}\xi_1 = A_{11}F_1(t) + A_{21}F_2(t) \tag{11.31}$$

$$\mathbb{M}_{22}\ddot{\xi}_2 + \mathbb{K}_{22}\xi_2 = A_{12}F_1(t) + A_{22}F_2(t) \tag{11.32}$$

The modal transformation trades the original problem, involving coupled differential equations, for an equal number of decoupled, single degree of freedom problems. This is a huge step forward because the solution of single degree of freedom problems is known from previous work. Further, these equations can be written in the familiar standard form

$$\ddot{\xi}_1 + \frac{\mathbb{K}_{11}}{\mathbb{M}_{11}}\xi_1 = \frac{1}{\mathbb{M}_{11}}\left[A_{11}F_1(t) + A_{21}F_2(t)\right] \tag{11.33}$$

$$\ddot{\xi}_2 + \frac{\mathbb{K}_{22}}{\mathbb{M}_{22}}\xi_2 = \frac{1}{\mathbb{M}_{22}}\left[A_{12}F_1(t) + A_{22}F_2(t)\right] \tag{11.34}$$

or, better yet,

$$\ddot{\xi}_1 + \omega_1^2\xi_1 = \frac{1}{\mathbb{M}_{11}}\left[A_{11}F_1(t) + A_{21}F_2(t)\right] \tag{11.35}$$

$$\ddot{\xi}_2 + \omega_2^2\xi_2 = \frac{1}{\mathbb{M}_{22}}\left[A_{12}F_1(t) + A_{22}F_2(t)\right] \tag{11.36}$$

Thus the equations are not only separated, they are also in standard form with the coefficients ω_1^2 and ω_2^2 as previously determined. The somewhat amazing thing about this transformation is that it works every time, no matter what the parameter values are, no matter how many degrees of freedom are involved. This is very powerful!!

At this point, the process is to solve this last set of equations to produce $\xi_1(t)$ and $\xi_2(t)$. These are called the *modal responses*. After the modal responses are known, it is a simple matter to go back through the modal transformation to produce the physical responses.

11.5.2 Numerical Example

For this example, the previous numeric problem, based on Figure 11.1, is continued with the excitation in the form

$$\{F(t)\} = \begin{Bmatrix} 22\sin(8t) \\ 0.0 \end{Bmatrix} \tag{11.37}$$

This means that an external force of 22 Newtons, varying sinusoidally at 8 rad/s, is applied to the mass M_1 while there is no external force acting directly on M_2.

11.5.2.1 Transformation to Modal Coordinates

The first step is to form the modal matrix using the eigensolutions found previously:

$$[A] = \begin{bmatrix} 1.0 & 1.0 \\ 2.76206 & -0.258606 \end{bmatrix} \tag{12.30}$$

The *modal mass* and *modal stiffness* matrices are then calculated:

Modal Mass Matrix

$$\begin{aligned} \lceil \mathbb{M} \rfloor &= [A]^T [M] [A] \\ &= \begin{bmatrix} 1.0 & 1.0 \\ 2.76206 & -0.258606 \end{bmatrix}^T \begin{bmatrix} 1.5 & 0 \\ 0 & 2.1 \end{bmatrix} \begin{bmatrix} 1.0 & 1.0 \\ 2.76206 & -0.258606 \end{bmatrix} \\ &= \begin{bmatrix} 17.521 & 8.944\,4 \cdot 10^{-7} \\ 8.944\,4 \cdot 10^{-7} & 1.6404 \end{bmatrix} \\ &\approx \begin{bmatrix} 17.521 & 0 \\ 0 & 1.6404 \end{bmatrix} \end{aligned} \tag{11.38}$$

Modal Stiffness Matrix

$$\begin{aligned} \lceil \mathbb{K} \rfloor &= [A]^T [K] [A] \\ &= \begin{bmatrix} 1.0 & 1.0 \\ 2.76206 & -0.258606 \end{bmatrix}^T \begin{bmatrix} 399 & -124 \\ -124 & 124 \end{bmatrix} \begin{bmatrix} 1.0 & 1.0 \\ 2.76206 & -0.258606 \end{bmatrix} \\ &= \begin{bmatrix} 660.0 & 3.282\,4 \cdot 10^{-4} \\ 3.282\,4 \cdot 10^{-4} & 471.43 \end{bmatrix} \\ &\approx \begin{bmatrix} 660.0 & 0 \\ 0 & 471.43 \end{bmatrix} \end{aligned} \tag{11.39}$$

The observant reader will notice immediately that the off-diagonal terms in each product are small, but not quite zero; why? This is a result of the unavoidable numerical rounding that happens in the calculation. The calculation is theoretically exact, but always fails to this minor extent in actual application. The solution is simply to round the results, dropping the small off-diagonal terms and replacing them with zeros. As a check, verify

that the ratios of the diagonal terms are indeed the squares of the natural frequencies as expected:

$$\frac{\mathbb{K}_{11}}{\mathbb{M}_{11}} = \frac{660.0}{17.521} = 37.669 \sim \omega_1^2 = (6.13755)^2 = 37.670 \tag{11.40}$$

$$\frac{\mathbb{K}_{22}}{\mathbb{M}_{22}} = \frac{471.43}{1.6404} = 287.39 \sim \omega_2^2 = (16.95223)^2 = 287.38 \tag{11.41}$$

These values check, as expected, to within small rounding errors.

The equations of forced motion, expressed in modal coordinates, are

$$\begin{aligned} \ddot{\xi}_1 + (6.13755)^2 \xi_1 &= \frac{1}{17.521}\left[(1.0)\,22\sin(8t) + (2.76206)\,(0)\right] \\ \ddot{\xi}_1 + 37.670\xi_1 &= 1.2556\sin(8t) \end{aligned} \tag{11.42}$$

$$\begin{aligned} \ddot{\xi}_2 + (16.95223)^2 \xi_2 &= \frac{1}{1.6404}\left[(1.0)\,22\sin(8t) + (-0.258606)\,(0)\right] \\ \ddot{\xi}_2 + 287.38\xi_2 &= 13.411\sin(8t) \end{aligned} \tag{11.43}$$

11.5.2.2 Solution in Modal Coordinates

As always, the complete solution consists of both homogeneous and particular solutions, so the homogeneous solution forms are

$$\xi_{1h}(t) = a_1\cos(6.13755\cdot t) + b_1\sin(6.13755\cdot t) \tag{11.44}$$

$$\xi_{2h}(t) = a_2\cos(16.95223\cdot t) + b_2\sin(16.95223\cdot t) \tag{11.45}$$

The particular solution is

$$\xi_{1p}(t) = X_1\sin(8t) \tag{11.46}$$

$$\xi_{2p}(t) = X_2\sin(8t) \tag{11.47}$$

which must satisfy

$$X_1\left[-8^2 + (6.13755)^2\right] = 1.2556 \tag{11.48}$$

$$X_2\left[-8^2 + (16.95223)^2\right] = 13.411 \tag{11.49}$$

The final result for the particular solutions is

$$X_1 = -4.7687\cdot 10^{-2} \tag{11.50}$$

$$X_2 = 6.0037\cdot 10^{-2} \tag{11.51}$$

and the modal particular solution is

$$\left\{\xi_p(t)\right\} = \left\{ \begin{array}{c} -4.7687 \\ 6.0037 \end{array} \right\} \cdot 10^{-2} \cdot \sin(8t) \tag{11.52}$$

11.5.2.3 Initial Conditions

At this point, a decision must be made. The choices are: (1) to transform the initial conditions through the modal transformation, so that they can be applied directly to the modal solution, or (2) to pass back through the modal transformation with several undetermined coefficients, so that the initial conditions can be applied directly to the physical coordinates. Either process will work, and they are fully equivalent. For this example, the first process is selected.

For the example problem, assume that the initial conditions are: $x_1(0) = \dot{x}_1(0) = x_2(0) = \dot{x}_2(0) = 0$. The modal transformation matrix is nonsingular (this is usually true, but not in all cases. It is true in this case.) Then the all zero physical initial conditions imply all zero modal initial conditions also. If there were nonzero initial values, then the system of simultaneous equations would be solved to give the nonzero modal initial conditions.

The forms for the complete solutions, in modal coordinates, are

$$\begin{aligned} \xi_1(t) &= a_1 \cos(6.13755 \cdot t) + b_1 \sin(6.13755 \cdot t) \\ &\quad -4.7687 \cdot 10^{-2} \cdot \sin(8t) \end{aligned} \tag{11.53}$$

$$\begin{aligned} \xi_2(t) &= a_2 \cos(16.95223 \cdot t) + b_2 \sin(16.95223 \cdot t) \\ &\quad +6.0037 \cdot 10^{-2} \cdot \sin(8t) \end{aligned} \tag{11.54}$$

Taking derivatives gives

$$\begin{aligned} \dot{\xi}_1(t) &= -6.137\,6a_1 \sin(6.3755t) + 6.13755b_1 \cos(6.13755t) \\ &\quad -0.38150 \cos(8.0t) \end{aligned} \tag{11.55}$$

$$\begin{aligned} \dot{\xi}_2(t) &= -16.952a_2 \sin(16.952t) + 16.952b_2 \cos(16.952t) \\ &\quad +0.48030 \cos(8.0t) \end{aligned} \tag{11.56}$$

When all four of these expression are evaluated at $t = 0$, the solved results are

$a_1 = 0.0$

$b_1 = 6.2158 \cdot 10^{-2}$

$a_2 = 0.0$

$b_2 = -2.833\,3 \cdot 10^{-2}$

The complete solution, in modal coordinates, is

$$\xi_1(t) = 6.2158 \cdot 10^{-2} \sin(6.13755 \cdot t) - 4.7687 \cdot 10^{-2} \cdot \sin(8t) \tag{11.57}$$

$$\xi_2(t) = -2.833\,3 \cdot 10^{-2} \sin(16.95223 \cdot t) + 6.0037 \cdot 10^{-2} \cdot \sin(8t) \tag{11.58}$$

To recover the physical coordinates, the modal transformation is employed once again,

$$\begin{aligned}
\{x(t)\} &= [A]\{\xi(t)\} \\
&= \begin{bmatrix} 1.0 & 1.0 \\ 2.76206 & -0.258606 \end{bmatrix} \\
&\quad \times \begin{Bmatrix} 6.2158 \cdot 10^{-2} \sin(6.13755 \cdot t) - 4.7687 \cdot 10^{-2} \cdot \sin(8t) \\ -2.833\,3 \cdot 10^{-2} \sin(16.95223 \cdot t) + 6.0037 \cdot 10^{-2} \cdot \sin(8t) \end{Bmatrix} \\
&= \begin{Bmatrix} 6.215\,8 \cdot 10^{-2} \sin(6.1376t) \\ -2.833\,3 \cdot 10^{-2} \sin(16.952t) \\ +0.01235 \sin(8.0t) \\ \\ 0.17168 \sin(6.1376t) \\ +7.3271 \cdot 10^{-3} \sin(16.952t) \\ -0.14724 \sin(8.0t) \end{Bmatrix}
\end{aligned} \tag{11.59}$$

The final expression for the physical response shows that the motion of each mass includes a terms (1) at the first natural frequency, (2) at the second natural frequency, and (3) at the forcing frequency. Physical intuition says that, in a real system where damping is unavoidable, the first two terms in each response must eventually die out, leaving only the steady state (particular) solution. Since damping was omitted in the original formulation, there is nothing in the mathematical solution to cause the natural frequency terms to decay.

The initial reaction of the reader may well be, "That is an exhausting process to solve a small, simple system. It must be terrible to solve a larger, more complicated system." There are several responses to this reaction:

1. Many real problems do not require that the solution be carried all the way through as was done in this example. In some cases, it is sufficient to determine only the undamped natural frequencies to assure that they are well removed from any

excitation frequencies. In that situation, it is often enough to state that there will be no amplification of the vibratory motion (no resonance), and therefore the response is considered safe.

2. In many cases, there is no interest in the transient response but only in the steady state response. For such a case, there is no need to consider initial conditions (steady state is so far removed in time that initial conditions no longer matter), and it is sufficient to determine only the forced response.

3. For systems with many degrees of freedom, computer methods employing matrix methods (just as shown here) are really no more difficult to code than for a simple system. They do require more computer time to execute (usually very little more), but they operate in exactly the same way.

4. It is simply foolhardy to attack a larger, more complex, physical system problem without using a computer to handle the large number of arithmetic calculations involved. The complexity of the example problems given above points to the sort of difficulties that will be encountered.

11.6 Modal Analysis With Damping

Someone not familiar with this whole problem might reasonably assume that viscous damping could be readily incorporated by simply modifying equation (11.3) to read

$$\lceil M \rfloor \{\ddot{x}\} + [C] \{\dot{x}\} + [K] \{x\} = \{F(t)\} \tag{11.60}$$

where $[C]$ would include coefficients representing viscous coupling directly to ground and also between the several masses. Indeed, there is nothing incorrect about such an equation, but the problem is how to proceed past this point.

It has been demonstrated above how the modal transformation decouples the equations of motion and thereby greatly facilitates their solution. This is the result of the similiarity transformation that is able to simultaneously diagonalize two coefficient matrix. The difficulty lies in the fact that the similarity transformation is not able to diagonalize three matrices, and hence cannot, in general, decouple equation (11.60). There are three approaches to dealing with this difficulty, each of which has proved useful in engineering practice.

11.6.1 Proportional Damping

If the eigensolution is known for the undamped system, there is certainly the hope that a modal transformation based on those eigenvectors will also decouple the damped problem. In truth, this is possible for only a rather particular damping matrix $[C]$. If it is true that the damping matrix is the sum of a matrix proportional to the stiffness matrix and a second matrix proportional to the mass matrix, then the decoupling process works as desired. Thus consider the equations of motion in the form

$$\lceil M \rfloor \{\ddot{x}\} + (\alpha [K] + \beta \lceil M \rfloor) \{\dot{x}\} + [K] \{x\} = \{F(t)\} \tag{11.61}$$

where α and β are known constants. This approach is commonly called *proportional damping*, referring to the fact that the damping matrix is a sum of matrices proportional to $[K]$ and $\lceil M \rfloor$.

When the modal transformation is performed, the result is

$$\lceil \mathbb{M} \rfloor \left\{\ddot{\xi}\right\} + (\alpha \lceil \mathbb{K} \rfloor + \beta \lceil \mathbb{M} \rfloor) \left\{\dot{\xi}\right\} + \lceil \mathbb{K} \rfloor \{\xi\} = [A]^T \{F(t)\} \tag{11.62}$$

This is a system of completely decoupled, damped, second order differential equations, solvable by the methods of the previous chapter. Only in rare circumstances is there any real basis for assuming the damping matrix to be in the required form. For this reason, this method is used primarily when there is a demand for a rationalization for including some degree of viscous damping.

11.6.2 Modal Damping

It has previously been demonstrated that the modal transformation is able to decouple the undamped multidegree of freedom vibration problem. The decoupled problem is then equation (11.30):

$$\lceil \mathbb{M} \rfloor \left\{\ddot{\xi}\right\} + \lceil \mathbb{K} \rfloor \{\xi\} = [A]^T \{F(t)\} \tag{11.30}$$

There are situations where this form is simply modified by adding a damping term,

$$\lceil \mathbb{M} \rfloor \left\{\ddot{\xi}\right\} + \lceil \mathbb{D} \rfloor \left\{\dot{\xi}\right\} + \lceil \mathbb{K} \rfloor \{\xi\} = [A]^T \{F(t)\} \tag{11.63}$$

where the $\lceil \mathbb{D} \rfloor$ matrix is a diagonal matrix of damping values arbitrarily assigned by the analyst. It should be emphasized that this is the *art of engineering*, something to be done only by those highly skilled in the particular subject area where this is to be applied. There is little science and a lot of experience involved in assigning the damping values, so this is not a useful form for beginners to use.

11.6.3 FDC Formulation

The term *FDC Formulation* is here used to describe a formulation of the viscously damped multidegree of freedom problem that seems to have first appeared in the work of Frazer, Duncan and Collar [1], where term *FDC Formulation* is a reference to their names. It was largely unnoticed until it was revived in a technical report by Foss in 1956 [2] and appears again in later works such as Tse, Morse, and Hinkle [3].

Frazer, Duncan and Collar begin with the typical form for a linear, viscously damped system with n degrees of freedom,

$$\lceil M \rfloor \{\ddot{x}\} + [C]\{\dot{x}\} + [K]\{x\} = \{F\} \tag{11.64}$$

which is then put into something like standard form by premultiplying by the inverse of the mass matrix to give

$$\{\ddot{x}\} + \lceil M \rfloor^{-1}[C]\{\dot{x}\} + \lceil M \rfloor^{-1}[K]\{x\} = \lceil M \rfloor^{-1}\{F\} \tag{11.65}$$

Consider first only the homogeneous problem, and introduce a new variable, $\{z\}$ that is $(2n \times 1)$, defined as

$$\{z\} = \begin{Bmatrix} \{x\} \\ \{\dot{x}\} \end{Bmatrix} \tag{11.66}$$

The system differential equations are then re-written if first order form in terms of $\{z\}$ and a partitioned coefficient matrix:

$$\frac{d}{dt}\{z\} = \begin{bmatrix} [0] & [I] \\ -\lceil M \rfloor^{-1}[K] & -\lceil M \rfloor^{-1}[C] \end{bmatrix} \{z\}$$

where

$[0] = (n \times n)$ null partition;

$[I] = (n \times n)$ identity partition;

$\lceil M \rfloor = (n \times n)$ diagonal mass matrix;

$[C] = (n \times n)$ damping matrix;

$[K] = (n \times n)$ stiffness matrix.

The reader should multiply out this expression to verify that it is true and contains the original equations of motion. This is all written in compact form as

$$\{\dot{z}\} = [U]\{z\} \tag{11.67}$$

where

$$[U] = \begin{bmatrix} [0] & [I] \\ -\lceil M \rfloor^{-1}[K] & -\lceil M \rfloor^{-1}[C] \end{bmatrix} \tag{11.68}$$

At this point, assume a solution of the form

$$\{z\} = \{A\}e^{\lambda t} \tag{11.69}$$

and substitute to obtain the classical eigenvalue problem.

$$([U] - \lambda[I])\{A\} = \{0\} \tag{11.70}$$

Note that, in most cases, λ and the elements of $\{A\}$ are complex numbers.

11.6.4 Numerical Examples

For a numeric example, the same two degree of freedom system considered previously is considered, but now with damping included.

11.6.4.1 Proportional Damping

For the numeric inclusion of proportional damping, consider $\alpha = 0.02$ and $\beta = 0.01$. The system matrices are

$$\begin{aligned} \lceil M \rfloor &= \begin{bmatrix} 1.5 & 0 \\ 0 & 2.1 \end{bmatrix} \\ [C] &= \begin{bmatrix} 7.9950 & -2.4800 \\ -2.4800 & 2.5010 \end{bmatrix} \\ [K] &= \begin{bmatrix} 399 & -124 \\ -124 & 124 \end{bmatrix} \end{aligned} \tag{11.71}$$

These are the same $\lceil M \rfloor$ and $[K]$ that were used previously; only $[C]$ is new here. Since the proportional damping approach is based on the eigensolution for the undamped problem, the eigenvalues and eigenvectors remain as they were previously,

$$\begin{array}{cc} \omega_1 = 6.13755 \text{ rad/s} & \omega_2 = 16.95223 \text{ rad/s} \\ \{A\}_1 = \left\{ \begin{array}{c} 1.0 \\ 2.76206 \end{array} \right\} & \{A\}_2 = \left\{ \begin{array}{c} 1.0 \\ -0.258606 \end{array} \right\} \end{array} \tag{11.16}$$

11.6.4.2 Modal Damping

As mentioned earlier, the application of modal damping is very closely tied to the nature of the specific physical system being modeled. Since there is no actual system for this example (it is only two generic masses connected with spring and damper elements), then there is no basis for assuming any values at all. Consequently, there is no numeric example for this approach.

11.6.4.3 FDC Formulation

As a numeric example of the FDC Formulation, consider the same system used for the proportional damping system, so that the $\lceil M \rfloor$, $[C]$ and $[K]$ matrices are the same as given just above in equation (11.71). When the matrix $[U]$ is formed, it is

$$[U] = \left[\begin{array}{cccc} 0 & 0 & 1 & 0 \\ 0 & 0 & 0 & 1 \\ -266.0 & 82.66667 & -5.33000 & 1.65333 \\ 59.04762 & -59.04762 & 1.18095 & -1.19095 \end{array} \right] \tag{11.72}$$

With the classical eigenproblem is solved for $[U]$, the results are:

$$\lambda_{1,2} = -2.87878 \pm j16.70601 \tag{11.73}$$

$$\lambda_{3,4} = -0.38170 \pm j6.12567 \tag{11.74}$$

$$\{A\}_{1,2} = \left\{ \begin{array}{c} -0.00968 \mp j0.05618 \\ 0.00250 \pm j0.01453 \\ 0.96647 + j0.0 \\ -0.24993 \mp j0.33412 \cdot 10^{-15} \end{array} \right\} \tag{11.75}$$

$$\{A\}_{3,4} = \left\{ \begin{array}{c} 0.00340 \pm j0.05464 \\ 0.00940 \pm j0.15091 \\ -0.33599 + 0.54416 \cdot 10^{-15} \\ -0.92803 + j0.0 \end{array} \right\} \tag{11.76}$$

where $j = \sqrt{-1}$. The numeric results shown here were produced by Maple®. There are several points in this example worthy of comment.

1. All the eigenvalues and the components of the eigenvectors are complex numbers.

2. The eigensolutions are randomly ordered, probably not the way the user would prefer to have them, but they can be re-ordered.

3. Recalling that the $\lambda-$values correspond to $-\zeta\omega_o + j\sqrt{1-\zeta^2}\omega_o$ for a damped single degree of freedom, it is evident that the first eigensolution found corresponds to the high frequency mode (here 16.70601 rad/s compared to 16.95223 rad/s for the undamped case) while the second eigensolution corresponds with the low frequency mode. The reduction in oscillatory frequency is what is usually expected with the addition of damping, so this is consistent with experience.

4. Looking at the real parts of the two eigenvalues, it is evident that they represent damping factors $\zeta_{1,2} = 2.87878/16.95233 = 0.16982$ and $\zeta_{3,4} = 0.38170/6.13755 = 6.2191 \cdot 10^{-2}$, relatively light damping in both modes.

5. No particular nomalization is here applied to the eigenvectors. The complex entries make it difficult to visualize the mode shapes. This difficulty is even more significant for systems with many degrees of freedom.

As a final comment on the matter of including damping in multidegree of freedom vibrations, it is safe to say that there is no easy way. The FDC Formulation is mathematically correct, but the results are very difficult to interpret because of the complex values. The other two methods involve a lot of guess work and are therefore suspect to some degree.

11.7 Beam Vibrations & Whirling

Beam-like structures are very common in machinery, both in the frames that hold the machine component in their proper places, and in the shafting used to transfer motion

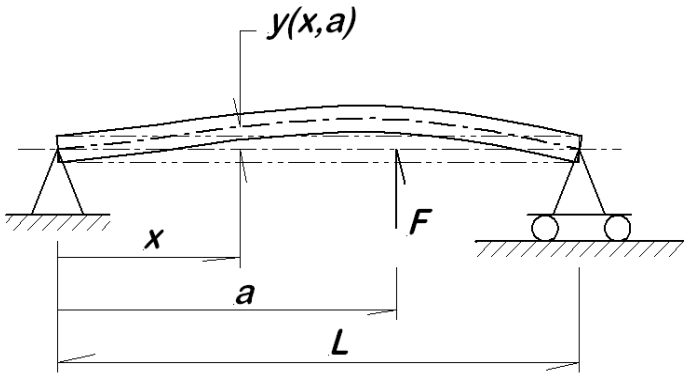

Figure 11.2: Simply Supported Uniform Beam With Point Load

and power from one part to another. Consider first the typical simply supported uniform beam shown in Figure 11.2.

When considering Figure 11.2, one of the first questions that needs to be asked is "how many degrees of freedom does the bending beam have?" It should not be too difficult to realized that there are infinitely many degrees of freedom. For every particle in the beam, there is a vertical motion, $y(x,t)$, and there are infinitely many particles in the beam. Moreover, there are also infinitely many rotations, a rotation at every cross section in the beam, so the total number of degrees of freedom is a double infinity. The beam is what is called a *continuous system*, meaning that there are infinitely many masses continuously distributed in the interval $[0, L]$.

The mathematically completely correct method for dealing with continuous systems involves writing the equations of motion as partial differential equations and then solving those equations in a manner consistent with the boundary conditions. For very simple systems, this is entirely possible, but most real systems involve complications that render this approach impractical for engineering practice. One such complication that occurs frequently is geometric nonuniformity. It the beam cross section varies along the length, then the partial differential equations must reflect that variation, substantially increasing the problem difficulty. A model formulated in this manner is called a *continuum model*, referring to the continuous distribution of both mass and flexibility.

The alternative to the continuous system model is to approximate the beam with a finite number of degrees of freedom. This approach is widely used in engineering practice, and it can be carried to a high degree of refinement, essentially capturing all of the significant aspects of the beam vibration while employing only a large but finite number of degrees of freedom. This approach is called a *discrete mass model*, or more commonly a *lumped mass model* or *lumped parameter model*. Only this second approach is developed for this book.

11.7.1 Flexibility and Stiffness

Before getting into the process of developing a lumped mass model, it is necessary to introduce an extended understanding of stiffness. In earlier parts of this book, it is assumed that readers are familiar with the typical coiled spring, usually a helical wire form, that deforms axially with far less resistance than a straight piece of wire of similar length. But now, what of a shaft or beam? In what way does it behave like a spring?

For the simple coiled spring, it is common to speak of the stiffness as the slope of the force-deflection curve. However, if that force-deflection relation is inverted to show deflection as a function of force, the slope of that modified graph is called the *compliance* or *flexibility*. In general, it is appropriate to think of flexibility (or compliance) as the inverse of stiffness.

With that idea in mind, look again at Figure 11.2. Let the applied load F be one unit of force; it does not matter whether this is 1 N, 1 lb, 1 dyne, etc., so long as consistent units are used for all calculations. **For a simply supported, uniform beam**, with one unit load applied at position a as shown in Figure 11.2, the ordinary mechanics of materials approach to beam deflections makes it possible to calculate the deflection at any point x between the supports [4],

$$y(x,a) = -\frac{(L-a)}{6EIL}\left\{x^3 - x\left[L^2-(L-a)^2\right]\right\} \qquad x \le a \tag{11.77}$$

$$= -\frac{(L-a)}{6EIL}\left\{x^3 - \frac{L(x-a)^3}{L-a} - x\left[L^2-(L-a)^2\right]\right\} \qquad a \le x \tag{11.78}$$

where

$y(x,a)$ = deflection at x due to unit load at a;

L = bearing span (distance between supports);

a = load location;

E = Young's Modulus for the beam material;

I = area moment of inertia of the cross section about the neutral axis.

Note that these expressions are **deflection per unit load**, not simply deflection (there is no force factor).

Now consider the length of the beam be subdivided at n locations, x_i, where i = 1, 2, ... n; these may be evenly or unevenly spaced. Each division mark is called a *station*

or *node*. The stations are simply placed at whatever locations are useful for later work, as becomes evident below. Next, consider that equation (11.77) or (11.78), whichever equation is appropriate to the location, is evaluated at each of these n locations. This gives a list of n values of deflection per unit load; consider this list as a column vector. This list is called a set of *influence coefficients* for a load located at $x = a$.

Now revise the previous step, to locate the unit load at the first station, and calculate the influence coefficients for that location. Repeat this process of calculating the influence coefficients for the unit load at each station in turn, arranging all the as columns within a square $(n \times n)$ matrix, denoted as $[S]$. Then for the same beam subject to a system of n loads of various values F_i located at the n stations, the total deflections y_i at each of the stations can be calculated by superposition as

$$\begin{Bmatrix} y_1 \\ y_2 \\ \vdots \\ y_n \end{Bmatrix} = \begin{bmatrix} S_{11} & S_{12} & \cdots & S_{1n} \\ S_{21} & S_{22} & \cdots & S_{2n} \\ \vdots & \vdots & \ddots & \vdots \\ S_{n1} & S_{n2} & \cdots & S_{nn} \end{bmatrix} \begin{Bmatrix} F_1 \\ F_2 \\ \vdots \\ F_n \end{Bmatrix} \tag{11.79}$$

where the F_i are no longer unit loads, but whatever actual applied load values. The matrix of influence coefficients is the *flexibility* or *compliance matrix*. It is symmetric ($S_{ij} = S_{ji}$), and for the typical beam problem can easily be inverted to give the stiffness matrix, $[K] = [S]^{-1}$. The inverse equation is easily recognized as a force–deflection relation,

$$\{F\} = [K]\{y\} \tag{11.80}$$

11.7.2 Example Calculation

Consider the simply supported shaft shown in Figure 11.3. Note that the simple supports are at the ends; this is only necessary for equations (11.77) and (11.78) to be applicable for the calculation of the flexibility matrix. The shaft is 1.0 m in length, with a uniform diameter $d = 65$ mm. The material is steel, for which Young's Modulus is $E = 2.07 \cdot 10^{11}$ Pa and the specific weight is $\gamma = 76500$ N/m^3.

11.7.2.1 Construction of the Model

As long as the entire system consists of only the uniform shaft, there is no reason to space the nodes other than uniformly. With this assumption, the segments between the nodes are $\Delta x = 166.67$ mm. If there were other elements on the shaft, such as wheels, disks,

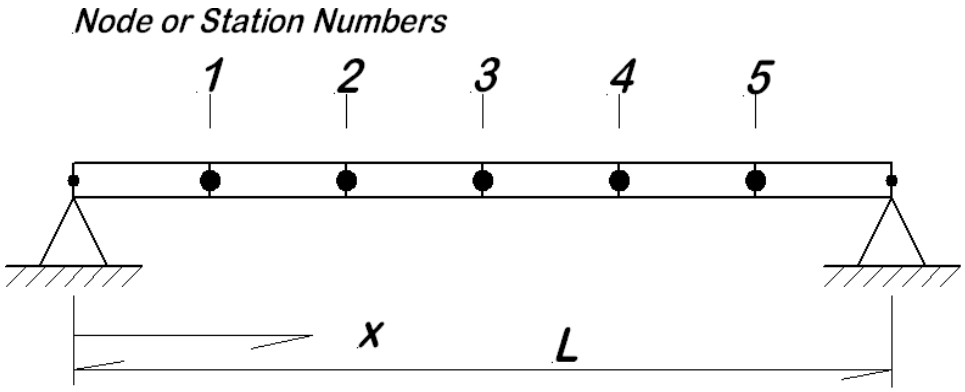

Figure 11.3: Lumped Mass Model for Uniform Shaft on Simple Supports

or diameter changes, then certainly it would make sense, indeed it would be completely necessary, to locate a node at each such point.

The total shaft mass is computed as $M_{total} = 25.8846$ kg. One of the most critical issues is how this mass should be distributed to the nodes. The method proposed here is simply that half of the mass of each segment be distributed to each end of the segment. Since all of the segments are of equal length in this example, this means that for the active nodes (those that are able to move vertically) the mass at each node is $m_i = M_{total}/6 = 4.3141$ kg. This distribution of mass only includes 5/6 of the total mass in the vibratory model because the half segment mass at each end does not move. This is clearly only an approximation; it is not a perfect model. The approximation can be improved by choosing a larger number of segments. With this approximation, the resulting lumped mass matrix is

$$\lceil M \rfloor = diag\,(m_1, m_2, \ldots) = 4.3141\, diag\,(1, 1, 1, 1, 1) \tag{11.81}$$

Note that the end nodes are not included; this is because they do not move as a result of the supports.

The flexibility matrix is developed by sequentially placing a unit load at each of the active nodes and then calculating the displacement at all of them. When this is done, the resulting flexibility matrix $[S]$ is

$$[S] = 10^{-8} \begin{bmatrix} 3.5450 & 5.3884 & 5.5302 & 4.3958 & 2.4106 \\ 5.3884 & 9.0753 & 9.7843 & 7.9409 & 4.3958 \\ 5.5302 & 9.7843 & 11.4859 & 9.7843 & 5.5302 \\ 4.3958 & 7.9409 & 9.7843 & 9.0753 & 5.3884 \\ 2.4106 & 4.3958 & 5.5302 & 5.3884 & 3.5450 \end{bmatrix} \text{ m/N} \tag{11.82}$$

This is inverted to produce the stiffness matrix, $[K]$:

$$[K] = 10^8 \begin{bmatrix} 3.8696 & -3.7250 & 1.6274 & -0.4340 & 0.0108 \\ -3.7250 & 5.4970 & -4.1589 & 1.7359 & -0.4340 \\ 1.6274 & -4.1589 & 5.6055 & -4.1589 & 1.6274 \\ -0.4340 & 1.7359 & -4.1589 & 5.4970 & -3.7250 \\ 0.0108 & -0.4340 & 1.6274 & -3.7250 & 3.8696 \end{bmatrix} \text{ N/m} \tag{11.83}$$

Note that both the flexibility and stiffness matrices are symmetric; this is to be expected. While these flexibility and stiffness matrices were developed using equations (11.77) and (11.78), the same result could be obtained with the proper data applied in program Shaft.Tru found in Appendix 8. That computer program applies to both uniform and nonuniform shafts.

11.7.2.2 Eigensolutions

Provided the computer solution is written with sufficient generality, it is a simple matter to change n, the number of active nodes, so that various levels of detail can be tested. The 5 station model (developed above) and a similar model employing 26 stations have both been computed, and the results are tabulated in Table 11.1. When the eigensolutions are obtained (whether by means of the program ChoJac.Tru (Appendix 1.9) or some other method), it is necessary to extract the square roots to obtain the system natural frequencies. The natural frequencies for the simply supported uniform beam as given by the continuum model are easily evaluated as $\omega_n = \left(\frac{n\pi}{L}\right)^2 \sqrt{EI/\mu}$ where μ = mass per unit length [5]; this gives a basis for comparison to evaluate the quality of the discrete model. When the calculations are carried out for the five station model, the results are these:

The results shown in Table 11.1 indicate that the5 station model gives an excellent value for the first natural frequency, a rather good value for the second natural frequency, and less than adequate values for the higher frequencies. This is exactly what the should be expected with so few node points. The 26 node model is in very close agreement with the continuum model for the first five modes. It should be noted that the model with 26 active nodes produces 26 natural frequencies, and that at higher mode numbers, the computed natural frequencies diverge from the continuum model just as the 5 station model results diverge. The only difference is that the larger model gives much better agreement for more of the low frequency modes.

Table 11.1 Five Station Model			
Computed Natural Frequencies			
	5 Node	26 Node	Continuum
	Discrete	Discrete	Model
	Model	Model	
	rad/s	rad/s	rad/s
$\omega_1 =$	826.1	827.8	826.2
$\omega_2 =$	3301.2	3304.7	3304.7
$\omega_3 =$	7381.6	7435.4	7435.6
$\omega_4 =$	12785	13218	13218
$\omega_5 =$	18293	20653	20655

The quality of the eigenvectors is also a matter of interest. The continuum model shows that, for the simply supported uniform beam, the mode shapes are simply sinusoids. When the mode vectors from the 5 node model are plotted, they are very jagged; there are too few points to describe a smooth sinusoid. When the first four modes from the 26 node model are plotted, the results are as shown in Figure 11.4.

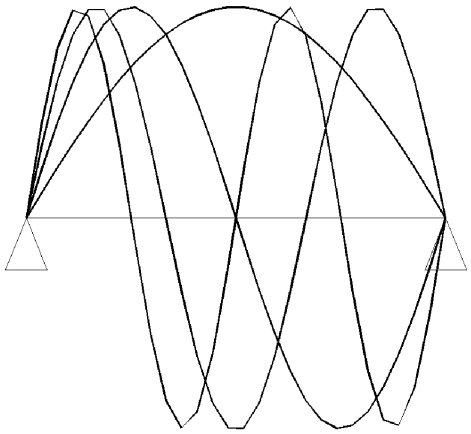

Figure 11.4: First Four Mode Shapes From 26 Node Model

It is evident that the more finely the shaft model is divided, the more nearly the results approach those from the continuum model. If the reader is wondering why the continuum model is not simply used in place of the lumped mass model, it would be well to recall (a) it was only applicable to a uniform shaft, and (b) that the lumped mass model applies equally well to stepped shafts. There are few uniform shafts found in actual machinery.

11.7.3 Whirling

In the discussion above, bending vibration of the nonrotating shaft (or shaft with mounted rotors) is considered. Bending vibration necessarily implies alternating stress and strain in the shaft. Imagine now instead a scenario in which:

- the shaft is bent, perhaps in a plane curve or perhaps in a complicated, three dimensional space curve, but continuing to pass through the fixed bearing locations;
- the bent shaft simply whirls about the line of centers while maintaining the same bent form at all times;
- the shaft may also be rotating as well, and the rotational speed and the whirling speed may be the same or different;
- the whirling may be in the same direction as the shaft rotation (forward whirl) or it may be opposite the shaft rotation (backward whirl).

Consider a horizontal, simply supported shaft (or shaft and rotor system) where the $x-$axis runs between the two supports, with the $y-$axis vertical, and the $z-$ axis horizontal and perpendicular to both x and $y-$ axes. The shaft rotates as speed Ω. A lumped mass model is required for the lateral motion of this system in response to slight unbalance at every station. Specifically, assume that the center of mass at station i is eccentric by an amount ε_i at an angular position ψ_i. The vertical and horizontal equations of motion are of the form

$$\lceil M \rfloor \{\ddot{y}\} + [K]\{y\} = \Omega^2 \lceil M \rfloor \{\varepsilon_i \cos(\Omega t - \psi_i)\} \tag{11.84}$$

$$\lceil M \rfloor \{\ddot{z}\} + [K]\{z\} = \Omega^2 \lceil M \rfloor \{\varepsilon_i \sin(\Omega t - \psi_i)\} \tag{11.85}$$

These may be combined into a single matrix differential equation of twice the size by defining $\{\xi\} = \mathrm{col}\,(y_1, \ldots y_n, z_1, \ldots z_n)$ to read

$$\begin{bmatrix} \lceil M \rfloor & [0] \\ [0] & \lceil M \rfloor \end{bmatrix} \left\{ \ddot{\xi} \right\} + \begin{bmatrix} [K] & [0] \\ [0] & [K] \end{bmatrix} \{\xi\}$$
$$= \Omega^2 \begin{bmatrix} \lceil M \rfloor & [0] \\ [0] & \lceil M \rfloor \end{bmatrix} \begin{Bmatrix} \{\varepsilon_i \cos(\Omega t - \psi_i)\} \\ \{\varepsilon_i \sin(\Omega t - \psi_i)\} \end{Bmatrix} \tag{11.86}$$

Now assume a solution of the form $\{\xi\} = \{X\} \sin \omega_n t$ to give the equation

$$\left(\begin{bmatrix} [K] & [0] \\ [0] & [K] \end{bmatrix} - \omega_n^2 \begin{bmatrix} \lceil M \rfloor & [0] \\ [0] & \lceil M \rfloor \end{bmatrix} \right) \{X\} = \Omega^2 \begin{bmatrix} \lceil M \rfloor & [0] \\ [0] & \lceil M \rfloor \end{bmatrix} \begin{Bmatrix} \{\varepsilon_i \cos(\Omega t - \psi_i)\} \\ \{\varepsilon_i \sin(\Omega t - \psi_i)\} \end{Bmatrix} \tag{11.87}$$

It is apparent that this brings up the eigenproblem again, and that solutions exist only when the eigenvalue problem is satisfied. Note that the eigenvalues, ω_n^2, are are determined by the eigenvalue problem only, and are completely independent of the rotational speed Ω.

There are two significant omissions in the formulation above that should be noted:

1. Gyroscopic effects are not included. To be fully correct, these effects should also be incorporated into the problem, although experience shows that they are important only at higher speeds.
2. It has been implicitly assumed that the bearings are infinitely stiff and that all deformation is in the shaft; this is never entirely true. There is always some compliance in the bearing supports, and in the bearings themselves. Additionally, fluid film bearings show a complicated "cross-coupling" wherein a load in one direction results in a displacement at right angles to the load.

There is a vast literature related to the whirling problem, usually found under the headings *rotordynamics* or *shaft whirling* for the reader who may wish to pursue this topic further. This has been a topic of vigorous engineering research for many years, and continues to be so to this day.

11.8 Lateral Rotordynamic Stability

The discussion of the previous section touches lightly on the vast area of rotordynamic stability. This has been a subject of interest for many years, as mentioned in the historical comment at the end of Section 10.4.3. The increased use of turbomachinery (turbocompressors, jet engines, and similar machines) have focused even more attention on this area in the past half century.

In considering simple planar beam vibrations, there is no evident question of stability. Such a beam simply vibrates in plane motion, but internal frictional loses always limit the

amplitude of the motion. It is clear, however, that if the vibrational motion causes the beam to collide with the surrounding structure, there is the potential for damage. When the scope of the discussion is expanded to include whirling, a three dimensional motion, the potential for collisions is even greater. In machinery with very tight clearances, this is a major concern.

Recall that the whole concept of stability is based on whether or not a system returns to its previous operating state following a disturbance. If the excitations do not change, other than a momentary disturbance, then the particular solution of the governing differential equations should not change. Thus the question of stability hinges upon the transient response which is the homogeneous solution.

A homogeneous solution is stable if it dies away with the passage of time, and unstable if it grows. Which of these behaviors occurs depends upon the sign of the real part of the eigenvalue for each mode. If the real part of an eigenvalue is negative, that particular mode dies away. How rapidly it dies away depends upon the magnitude of the negative real part. If the real part of the eigenvalue is positive, the mode grows in amplitude with the passage of time; this is clearly an instability. If the real part of the eigenvalue is zero, indicating no damping at all, system stability is neutral, and must be considered unstable because it does not return to the undisturbed state.

The eigenproblems of rotordyanamics are extremely complicated due to several factors. In previous parts of this book, the only place that complex eigenvalues have been encountered is in connection with damped systems. In those examples, involving viscous damping of relatively simple systems, the real part of the eigenvalue is negative in every case, resulting in solutions that decay with time. In high-speed turbomachinery, the fluid-structure interaction creates a peculiar phenomenon of cross coupling. This means that a force in a particular direction results in a displacement in the direction of the force and also a displacement at right angles to the force. The result of this is that *both stiffness and damping in such cases are cross-coupled*. Further, at the very high speeds often involved, gyroscopic effects must be included leading to additional cross-coupling. Finally it should be mentioned that the stiffness and damping characteristics of the supporting structure also participate in the rotor motion, further complicating the picture.

The interested reader will find countless technical papers on the internet related to this subject. It remains a topic of aggressive research that will continue for years to come.

11.9 Rayleigh's Method

In the bending vibration of shafts (or in whirling), there is very slow energy loss; to a good approximation, energy is conserved over short time intervals. This is the basis for Rayleigh's Method. The development of Rayleigh's Method in several forms is given

in Appendix 9. The present discussion is limited to showing its application to beam vibration and shaft critical speed calculations.

It should be noted that Rayleigh's Method is limited to approximating the lowest natural frequency of a vibratory system. In many cases, the first natural frequency is sufficient for engineering purposes, but other methods must be employed if higher natural frequencies and mode shapes are required.

11.9.1 Rayleigh Example 1

Consider the simply supported shaft used as an example of Section 11.7.2 for which good results are already available, by both the discrete mass model and from the continuum model. The shaft has $L = 1.0$ m, and a diameter $d = 65$ mm. The material is steel, for which Young's modulus is $E = 2.07 \cdot 10^{11}$ Pa and the specific weight is $\gamma = 76500$ N/m^3. Assume for the present that the previous results are not known. An integral expression for one of the alternate forms of Rayleigh's Method is used here to obtain an approximate fundamental frequency.

Assume for $Y(x)$ the form of a simply supported uniform shaft sagging under its own weight

$$Y(x) = \frac{\mu g x}{24EI}\left(L^3 - 2Lx^2 + x^3\right) \tag{11.88}$$

where

μ = mass per unit length of the shaft;

L = length between the simple supports.

The two integrals involved are

$$\int_0^L \mu g Y(x)\, dx = \frac{\mu g W L^4}{120EI} \tag{11.89}$$

$$\int_0^L \mu Y^2 dx = \frac{31\mu W^2 L^7}{362880E^2I^2} \tag{11.90}$$

Taking the square root of the ratio gives the natural frequency

$$\omega = \frac{9.877}{L^2}\sqrt{\frac{EI}{\mu}} \tag{11.91}$$

compared to the continuum model result $\omega = \frac{\pi^2}{L^2}\sqrt{\frac{EI}{\mu}} \approx \frac{9.8696}{L^2}\sqrt{\frac{EI}{\mu}}$.

11.9.2 Rayleigh Example 2

Consider again the same simply supported, uniform shaft already examined several times previously. The total weight of the shaft is 253.8505 N. To see the effect of varying the number of nodes, let n = number of active nodes, be considered as a variable. For the uniform shaft, the location of the stations and the weight applied at each is then

$$x_i = i\frac{L}{n+1} \tag{11.92}$$

$$W_i = \frac{W_{Total}}{n+1} \tag{11.93}$$

The deflections at each station are estimated based on the deflections of the uniformly loaded beam, equation (11.86), used in earlier examples.

With 5 active nodes, the calculation details are as follows:

Table 11.2 Details of Rayleigh Calculation

Node	Weight	Deflection	Product	Product
Number	W_i	$Y_i \cdot 10^6$	$W_i Y_i \cdot 10^4$	$W_i Y_i^2 \cdot 10^9$
	N	m	N-m	N-m^2
1	42.308	9.2240	3.90255	3.59974
2	42.308	15.8384	6.70097	10.61325
3	42.308	18.2231	7.70992	14.04989
4	42.308	15.8384	6.70097	10.61325
5	42.308	9.2240	3.90255	3.59974

$\sum W_i Y_i = 2.8916962 \cdot 10^{-3}$

$\sum W_i Y_i^2 = 4.2475865 \cdot 10^{-8}$

$\omega_{Rayleigh} = \sqrt{g \sum W_i Y_i / \sum W_i Y_i^2}$

$= \sqrt{(9.807)\,(2.8916962 \cdot 10^{-3}) \,/\, (4.2475865 \cdot 10^{-8})}$

$= 817.096$ rad/s

This is the result of the 5 node model, compared to the

(1) the Jacobi eigenvalue for the 5 node model, $\omega = 826.1$ rad/s;

(2) the continuum model for the uniform shaft, $\omega = 826.2$ rad/s.

It is evident that the Rayleigh approximation is only fair with this small number of active nodes. As simple as the Rayleigh calculation is, it is easily extended to a greater number of active nodes. The results tend to improve with the number of nodes.

Table 11.3 Rayleigh Results	
For Different Numbers of Nodes	
n	$\omega_{Rayleigh}$
	rad/s
5	817.09642
10	823.91579
15	825.42457
20	825.99049
25	826.26246
30	826.41375
35	826.50648
40	826.56739
45	826.60954
50	826.63990

When these results are compared to the value from the continuum model, $\omega = 826.18186$ rad/s, it is evident that the Rayleigh values are both above and below the continuum model, depending upon the number of active nodes. It appears that two phenomena are at work here as the number of nodes increases:

1. The higher the number of active nodes, the more nearly the discrete mass distribution approximates the actual continuous mass distribution, thus bringing the Rayleigh model closer to physical reality.
2. The approximate mode shape is not the actual dynamic mode shape; the approximation is based on a static deflection calculation. For the system to vibrate in the form described by this approximation, there must be additional constraints present that stiffen the system and tend to raise the natural frequency.

The general conclusion then is this: *when the number of active nodes is large enough to give a close approximation to the physical mass distribution, the Rayleigh natural*

frequency estimate will err on the high side, that is, the Rayleigh frequency value will be larger than the true value. Can the reader say why this happens?

11.9.3 Rayleigh Example 3

As a final example of the application of Rayleigh's Method, consider the cantilever beam with a rigid mass attached at the tip as shown in Figure 11.5. The length of the beam is L, the EI product is known, and the total mass of the beam is M_B. The block at the end has mass M_T and mass moment of inertia J_c with respect to the center of mass that is located a distance a from the end of the beam. The problem is to estimate the first natural frequency for this system, taking into account the mass of the beam, the tip mass, and the tip mass rotary inertia.

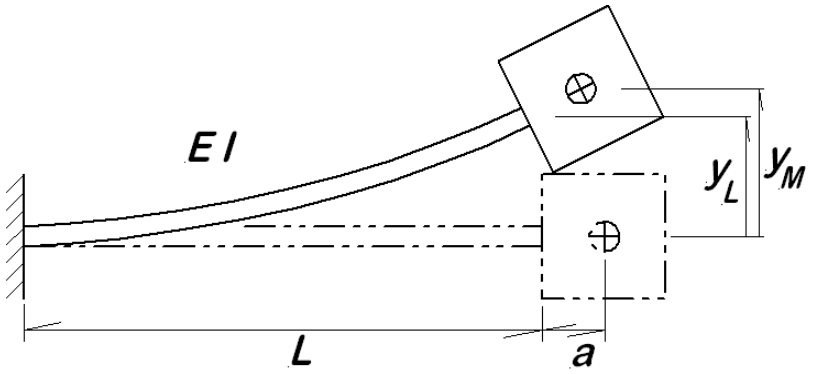

Figure 11.5: Cantilever Beam With Rigid Mass at Tip

In order to apply Rayleigh's Method, an approximation for the beam deflection is assumed,

$$y\left(x,t\right)=y_L\left[1-\cos\left(\frac{\pi x}{2L}\right)\right]\sin\omega t \tag{11.94}$$

Den Hartog notes [6, p.153] that this form has no moment at the right end, $x = L$. In that respect, this is a less than ideal choice for the approximate form because a moment is required to rotate the block. Nevertheless, it has simplicity to recommend it.

Note that two vertical coordinates are indicated; there is y_L is the deflection of the end of the beam, and y_M is the displacement of the center of mass for the rigid block. These two are related kinematically as

$$y_M=y_L+ay_L' \tag{11.95}$$

Using the original form for Rayleigh's Method (see Appendix 9), the potential energy of

bending is

$$\begin{aligned} V &= \frac{EI}{2}\int_0^L \left[y''(x,t)\right]^2 dx \\ &= \frac{EI}{2}\left(\frac{\pi^2}{4L^2}\right)^2 y_L^2 \sin^2\omega t \int_0^L \cos^2\left(\frac{\pi x}{2L}\right) dx \\ &= \frac{y_L^2 \pi^4 EI}{64L^3}\sin^2\omega t \end{aligned} \tag{11.96}$$

The kinetic energy is a combination of discrete and continuum terms,

$$\begin{aligned} T &= \frac{1}{2}M_T \dot{y}_M^2 + \frac{1}{2}J_c\left(\dot{y}'\right)^2 + \frac{1}{2}\frac{M_B}{L}\int_0^L \left[\dot{y}(x,t)\right]^2 dx \\ &= \frac{\omega^2 y_L^2 \cos^2\omega t}{2}\left[M_T\left(1+\frac{\pi a}{2L}\right)^2 + J_c\frac{\pi^2}{4L^2} + M_B\left(\frac{3}{2}-\frac{4}{\pi}\right)\right] \end{aligned} \tag{11.97}$$

Note that y_L^2 is a factor common to all terms in both T and V; y_L plays the role of a single, generalized coordinate for the entire system. When the maximum values are taken for each of V and T and the two are set equal, the result is then solved for the square of the natural frequency

$$\omega^2 = \frac{\pi^4 EI}{32L^3\left[M_T\left(1+\frac{\pi a}{2L}\right)^2 + J_c\left(\frac{\pi}{2L}\right)^2 + M_B\left(\frac{3}{2}-\frac{4}{\pi}\right)\right]} \tag{11.98}$$

It is a straight-forward matter to substitute numbers and compute a numerical result at this point.

One of the principal points of this example is to demonstrate the ability to combine different element models in a single analysis. In this case, the continuum beam model is combined with the discrete model for the solid block. Further, that model for the solid block takes into account both translation and rotation of the block, all with remarkable ease.

11.9.4 Final Comment on Rayleigh's Method

One of the most significant aspects of Rayleigh's Method is that it essentially converts a problem with infinitely many degrees of freedom into a single degree of freedom problem. This is most evident in the third example above where y_L, the displacement at the end of the beam, becomes the single generalized coordinate with all other displacements related

to it. This is at once very powerful, but also limiting in that the method cannot model more than a single degree of freedom and hence can only give a single natural frequency.

As demonstrated above, Rayleigh's Method is only an approximation, and as such can never be considered as exact. Even in applications where a rather exact analysis is eventually required, it is often useful to make a quick approximation by means of Rayleigh's Method to assure that the more detailed study is justified. It has served engineers well for many years, and will no doubt continue to do so in the future.

11.10 Case Study – Frahm Absorber

One of the major concerns of engineering is control of vibration levels. Two types of control are usually considered: vibration dampers and vibration absorbers. *Vibration dampers* are systems that convert vibrational energy into heat and are thus limited by their ability to reject heat. *Vibration absorbers* are systems that generate counteracting forces to limit motion at the point of interest in the system by absorbing it in the motion of the absorber. In the ideal absorber there is no heat generated and therefore no heat limitation, but of course internal friction in a real absorber must generate heat.

By far the best known vibration absorber is the "Frahm Damper," invented by H. Frahm in the early 20^{th} century (the dates 1909 and 1911 are both cited for his patent and it is not clear which applies). The theory of this device is detailed in many places, notably by Den Hartog [6, pp.$87-92$]. It has has often been applied in both translational and torsional forms with great success. There is one particular application of the Frahm absorber that is of particular interest and is the subject of this case study from a real engineering problem.

The Newington Station is a 400 MW cycling fossil fuel electrical generating plant in Newington, NH. To be a cycling plant means that it must go from low to high output power levels at least once (and perhaps more often) each day. This is relatively hard duty for a power plant, the easier duty being to be "base loaded" which means to have a steady load all the time. Cycling duty puts the entire system through severe thermal cycles and associated fatigue and this adversely affects the expected life of the plant. Fatigue of components is a major consideration in the operation of a power plant.

The Newington plant has two induced draft fans (ID fans) driven by 4500 horsepower, three phase induction motors at 890 rpm (synchronous speed would be 900 rpm, so these motors have only slightly over 1% slip). The fans are mounted on concrete block foundations as shown in the end view, Figure 11.6, and the motors (not shown in the figure) are directly coupled to the fans. In the original configuration, the absorber masses shown in the figure were not present.

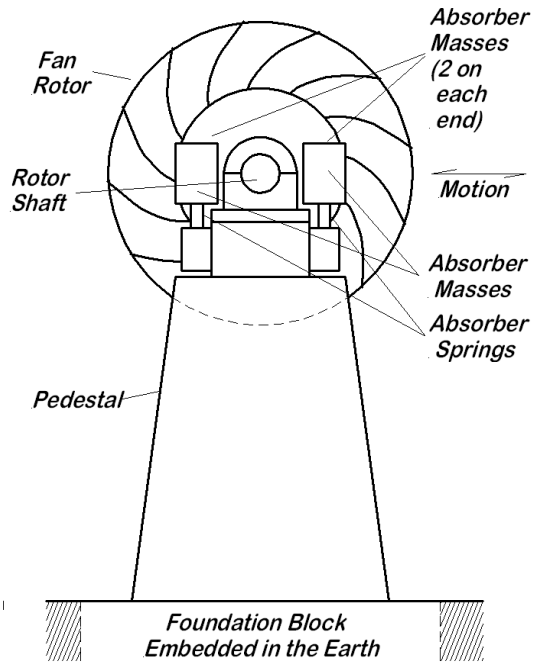

Figure 11.6: End View of Fan Showing Two Mounted Vibration Absorbers

When the plant was initially put into operation, severe vibrations were found in the fans. The fans could not be balanced in both the hot and cold conditions simultaneously, although hot balancing allowed the system to operate in steady state after that condition was reached. Ramp rates (the rate of change of the electrical load on the generator) were another matter, however, and this is a critical issue for a cycling plant. Ramp rates above 2 MW/min produced severe vibrations and thus limited the ability of the plant to perform its primary function as a cycling plant.

In January, 1976, Brewer Engineering Laboratories, Inc. (BEL), under the direction of Mr. Given A. Brewer, P.E., began work at the plant. They made measurements resulting in a dynamic model for the fan and foundation system, and they presented three possible alternatives for solutions. One of those alternatives was the design and fitting of dynamic vibration absorbers (known as Frahm dampers, even though this is not strictly correct terminology) for the fans, and the owner elected to have BEL proceed with that approach. This was successful, and eventually the plant was able to accept increased electrical load at rates of 20 MW/min without problems.

This project eventually involved not only BEL and Mr. Brewer, but also the noted Prof. S.H. Crandall of MIT and a student, A.T. Guillen, who wrote an MIT BS thesis on the problem [7]. Guillen's paper is the source for the parameter values used in the analysis given here, although the model and analysis here differs slightly from his.

Mr. Brewer was a successful business man, and he publicized his work on this project with

a number of articles [8]. He also received a patent on the system (US Patent 4,150,588, Apr. 24, 1979). Mr. Brewer sold his company, BEL, to Teledyne Engineering Services and then remained on with them in a senior consulting capacity for some time.

11.10.1 Vibration Analysis

The motion of concern is the horizontal motion at the bearing level; vertical and angular motions are neglected. For this motion, the system is thought of as having two inertias (before the absorbers are added): the pedestal and the rotor, that are elastically coupled, and the pedestal is elastically coupled to ground. When the absorbers are added, if all four of them are acting in phase as they are intended to act, then this is effectively a single additional mass, so that a total of three elastically coupled masses comprise the system model. This model is shown in Figure 11.7.

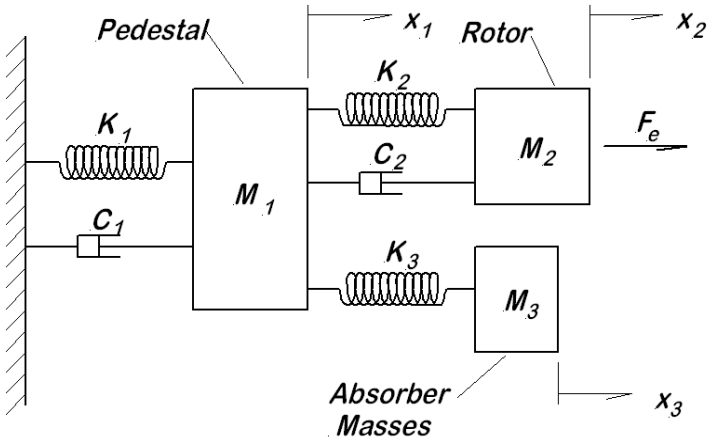

Figure 11.7: System Model, Including Absorbers, for Horizontal Motion

The actual construction of the absorbers uses vertical rectangular beams in bending as the spring elements. These beams are cantilevered upwards from the steel pedestal just below the actual bearing. The absorber masses are constructed as a stack of flat plates. The majority of the absorber stack is welded into a solid mass, but there is provision to add or remove thin plates at the top (these are simply bolted on) to adjust the mass for system tuning purposes.

Now consider the system equations of motion with the absorbers included:

$$\begin{aligned} \sum F_1 &= -K_1 x_1 - C_1 \dot{x}_1 + K_2 (x_2 - x_1) + C_2 (\dot{x}_2 - \dot{x}_1) + K_3 (x_3 - x_1) \\ &= M_1 \ddot{x}_1 \end{aligned} \tag{11.99}$$

$$\sum F_2 = -K_2 (x_2 - x_1) - C_2 (\dot{x}_2 - \dot{x}_1) + F_e = M_2 \ddot{x}_2 \tag{11.100}$$

$$\sum F_3 = -K_3 (x_3 - x_1) = M_3 \ddot{x}_3 \tag{11.101}$$

where the external force on the rotor, F_e, is the force of unbalance, $F_e = -M_2\varepsilon\Omega^2\cos\Omega t$ where ε = eccentricity and Ω is the shaft speed. These equations are recast in matrix form as

$$\begin{aligned}
&\begin{bmatrix} M_1 & 0 & 0 \\ 0 & M_2 & 0 \\ 0 & 0 & M_3 \end{bmatrix} \begin{Bmatrix} \ddot{x}_1 \\ \ddot{x}_2 \\ \ddot{x}_3 \end{Bmatrix} \\
&+ \begin{bmatrix} C_1 + C_2 & -C_2 & 0 \\ -C_2 & C_2 & 0 \\ 0 & 0 & 0 \end{bmatrix} \begin{Bmatrix} \dot{x}_1 \\ \dot{x}_2 \\ \dot{x}_3 \end{Bmatrix} \\
&+ \begin{bmatrix} K_1 + K_2 & -K_2 & -K_3 \\ -K_2 & K_2 & 0 \\ -K_3 & 0 & K_3 \end{bmatrix} \begin{Bmatrix} x_1 \\ x_2 \\ x_3 \end{Bmatrix} \\
&= M_2\varepsilon\Omega^2\cos\Omega t \begin{Bmatrix} 0 \\ 1 \\ 0 \end{Bmatrix}
\end{aligned} \tag{11.102}$$

From Guillen's paper, the system parameters are as follows:

Table 11.4 Case Study System Parameters		
$M_1 = 8.321 \cdot 10^4$ kg	$C_1 = 2.72 \cdot 10^6$ N–s/m	$K_1 = 1.454 \cdot 10^9$ N/m
$M_2 = 2.153 \cdot 10^4$ kg	$C_2 = 4.97 \cdot 10^4$ N–s/m	$K_2 = 2.874 \cdot 10^8$ N/m
$M_3 = 7.26 \cdot 10^3$ kg	—	$K_3 = 6.3035 \cdot 10^7$ N/m

For purposes of calculation, it is assumed that the eccentricity is $\varepsilon = 0.5$ mm.

It is useful to investigate the response of this system for different shaft speeds, in effect, a frequency response analysis. For this purpose, assume that all of the responses are sinusoidal at the excitation frequency,

$$\begin{Bmatrix} x_1 \\ x_2 \\ x_3 \end{Bmatrix} = \begin{Bmatrix} a_1 \\ a_2 \\ a_3 \end{Bmatrix} \cos\Omega t + \begin{Bmatrix} b_1 \\ b_2 \\ b_3 \end{Bmatrix} \sin\Omega t$$

Now substitute into the differential equation to get

$$\begin{aligned} &\lceil M \rfloor \left\langle -\Omega^2 \{a\} \cos \Omega t - \Omega^2 \{b\} \sin \Omega t \right\rangle \\ &+ [C] \left\langle -\Omega \{a\} \sin \Omega t + \Omega \{b\} \cos \Omega t \right\rangle \\ &+ [K] \left\langle \{a\} \cos \Omega t + \{b\} \sin \Omega t \right\rangle \\ = \; & M_2 \varepsilon \Omega^2 \cos \Omega t \left\{ \begin{array}{c} 0 \\ 1 \\ 0 \end{array} \right\} \end{aligned} \tag{11.103}$$

Separating sine and cosine terms gives

Cosines

$$\left\langle [K] - \Omega^2 \lceil M \rfloor \right\rangle \{a\} + \Omega [C] \{b\} = M_2 \varepsilon \Omega^2 \operatorname{col}(0, 1, 0) \tag{11.104}$$

Sines

$$-\Omega [C] \{a\} + \left\langle [K] - \Omega^2 \lceil M \rfloor \right\rangle \{b\} = \{0\} \tag{11.105}$$

This system can be written in terms of (6×6) matrices by partitioning them so that

$$\left[\begin{array}{cc} [K] - \Omega^2 \lceil M \rfloor & \Omega [C] \\ -\Omega [C] & [K] - \Omega^2 \lceil M \rfloor \end{array} \right] \left\{ \begin{array}{c} \{a\} \\ \{b\} \end{array} \right\} = M_2 \varepsilon \Omega^2 \operatorname{col}(0, 1, 0, 0, 0, 0) \tag{11.106}$$

As long as the $[C]$ matrix is nonzero, the coefficient matrix on the left is nonsingular and can be inverted to solve for the a's and the b's. For the full system, including the absorbers, there is a (6×6) coefficient matrix; if the absorbers are not present, then the system collapses to a (4×4) system of the same form with the vector on the right becoming simply $\operatorname{col}(0, 1, 0, 0)$. Only the steady state solution is of interest, so there is no need to find a homogeneous solution. Once the a's and b's are known, the amplitude of the displacement for each component is simply

$$displ\ ampl = \sqrt{a^2 + b^2} \tag{11.107}$$

When the system parameters are substituted into the equations, it is interesting to compare the original (two mass model) displacement amplitudes (Figure 11.8) with those for the modified (three mass model) system (Figure 11.9). The intended shaft speed is 890 rpm, so that $\Omega = 14.833$ Hz. Notice that, for the original system configuration, the worst

possible condition happens at a frequency higher than the actual operating frequency, between 15 and 16 Hz where the rotor displacement is calculated as approximately 4 mm. Figure 11.9 shows that, at the operating frequency, the motion of the support is completely stopped, but this only happens at that one particular shaft speed. Notice also in Figure 11.9 that at the operating speed, the motion of the absorber mass is quite large; this large motion is how the absorber develops the force required to stop the motion of the support. It also shows that, at the operating frequency, the shaft motion is not zero, but is roughly 1 mm.

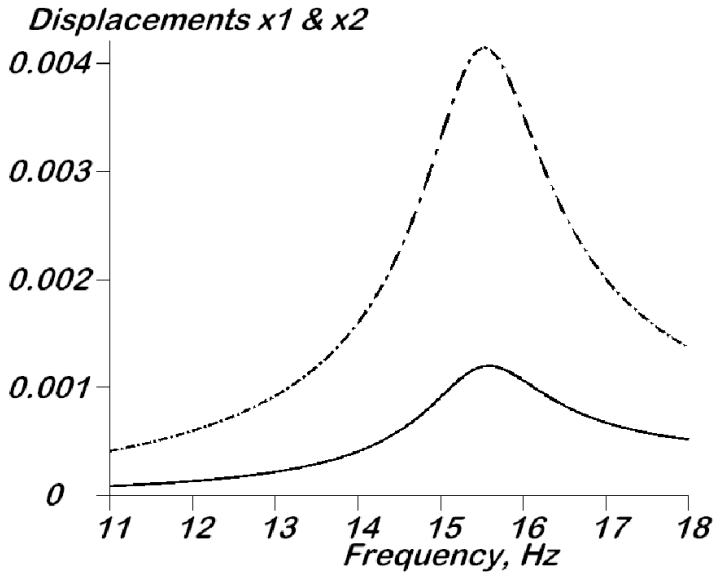

Figure 11.8: Modified (Three Mass Model) Displcement Amplitudes as Functions of Frequency ($x1$ - solid line, $x2$ - dash-dot)

11.10.2 Internal Forces

A second question of concern, both with and without the absorbers, is, "what is the force transferred at through each of the connections?" After the motions of the several points are known, that question can be addressed as well. Consider two points i and j moving with displacements x_i and x_j and joined by a spring-damper combination (if the damper is absent, that only simplifies things; if one point does not move, that further simplifies things). Then,

$$\begin{aligned} x_i &= a_i \cos \Omega t + b_i \sin \Omega t \\ \dot{x}_i &= -\Omega a_i \sin \Omega t + \Omega b_i \cos \Omega t \end{aligned} \tag{11.108}$$

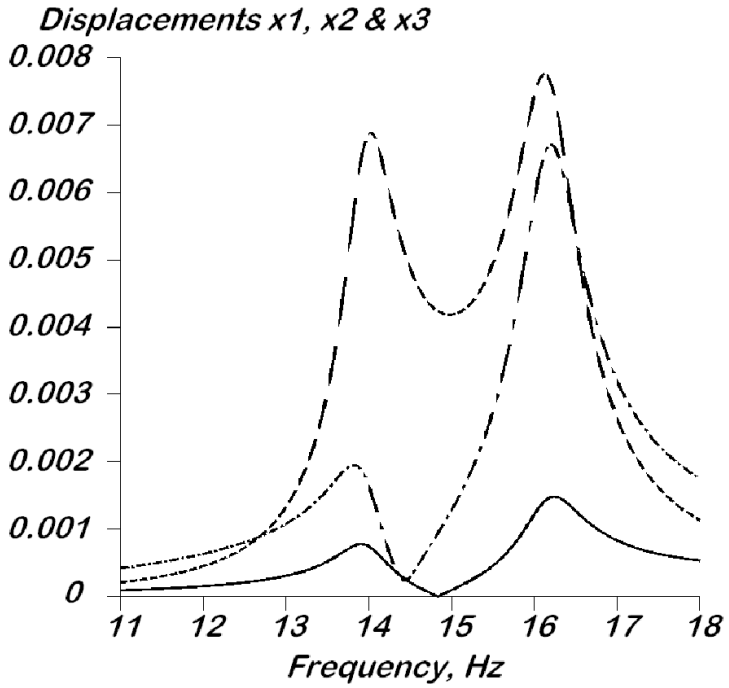

Figure 11.9: Modified (Three Mass Model) Displcement Amplitudes as Functions of Frequency ($x1$ - solid line, $x2$ - dash-dot, $x3$ - broken line)

$$\begin{aligned} x_j &= a_j \cos\Omega t + b_j \sin\Omega t \\ \dot{x}_j &= -\Omega a_j \sin\Omega t + \Omega b_j \cos\Omega t \end{aligned} \tag{11.109}$$

The force through the connection is

$$\begin{aligned} F &= K\left(x_j - x_i\right) + C\left(\dot{x}_j - \dot{x}_i\right) \\ &= K\left[\left(a_j - a_i\right)^2 + \left(b_j - b_i\right)^2\right]^{1/2} \underbrace{\left(\cos\psi\cos\Omega t + \sin\psi\sin\Omega t\right)}_{\cos(\Omega t - \psi)} \\ &\quad + C\Omega\left[\left(a_j - a_i\right)^2 + \left(b_j - b_i\right)^2\right]^{1/2} \underbrace{\left(\sin\psi\cos\Omega t - \cos\psi\sin\Omega t\right)}_{-\sin(\Omega t - \psi)} \end{aligned} \tag{11.110}$$

where

$$\cos\psi = \frac{a_j - a_i}{\left[\left(a_j - a_i\right)^2 + \left(b_j - b_i\right)^2\right]^{1/2}} \tag{11.111}$$

$$\sin\psi = \frac{b_j - b_i}{\left[\left(a_j - a_i\right)^2 + \left(b_j - b_i\right)^2\right]^{1/2}} \tag{11.112}$$

Continuing then to get the total force,

$$\begin{aligned} F &= K\left[(a_j-a_i)^2+(b_j-b_i)^2\right]^{1/2}\cos(\Omega t-\psi) \\ &\quad -C\Omega\left[(a_j-a_i)^2+(b_j-b_i)^2\right]^{1/2}\sin(\Omega t-\psi) \\ &= \left[(a_j-a_i)^2+(b_j-b_i)^2\right]^{1/2}\left(K^2+C^2\Omega^2\right)^{1/2}\cos(\Omega t+\gamma-\psi) \end{aligned} \tag{11.113}$$

where

$$\cos\gamma = \frac{K}{(K^2+C^2\Omega^2)^{1/2}} \tag{11.114}$$

$$\sin\gamma = \frac{C\Omega}{(K^2+C^2\Omega^2)^{1/2}} \tag{11.115}$$

Finally, the magnitude of the force through the connection is

$$|F| = \left[(a_j-a_i)^2+(b_j-b_i)^2\right]^{1/2}\left(K^2+C^2\Omega^2\right)^{1/2} \tag{11.116}$$

This is the basis for calculating the force through all connections in the system.

Again, when numerical values are substituted into the connection force relation, the magnitudes of those forces can be considered as functions of the shaft speed, Ω. In many respects, the force amplitude plots, Figures 11.10 and 11.11, tell the same story as that of the displacement amplitude plots. In the original system, the force transferred to the support is approximate $1.2\cdot10^6$ N at the operating shaft speed. At the operating speed, in the modified system, all three forces are reduced. With the modification in effect, the force to the support is zero. This is what should be expected since, at this speed only, there is no displacement of the base as shown in Figure 11.9. But note that this is a very localized matter, limited very narrowly to the design speed. Away from the design speed, the force transferred to the support becomes very large. This is typical for such systems, and explains why tuned absorbers can only be used for constant speed machinery, except for the torsional pendulum absorber discussed in Chapter 8.

There are two important points to notice regarding the application of the Frahm damper (technically the Frahm absorber):

1. While the motion of the primary object is completely stopped at the frequency of interest (running speed for the machine), the other bodies in the system are still vibrating. In point of fact, they are moving out of phase with each other so as to cancel the forces transferred to the primary body.

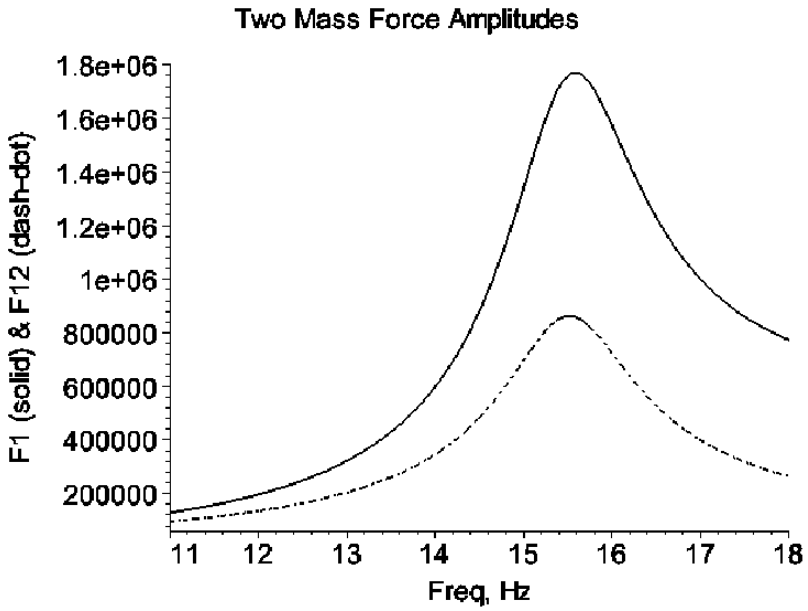

Figure 11.10: Force Amplitudes For the Original System, Force Amplitudes F_1 and F_{12} as Functions of Shaft Speed

2. This is clearly a "tuned system" and is designed to function at a specific frequency. At frequencies other than the design point, the results are likely to be worse than if the absorber were not present.

The second point is of considerable importance in terms of choosing applications where the Frahm absorber may be applied. The power plant fan in this application is just about ideal because the fan speed is always very close to the design speed, 890 rpm. Utility generator shafts are another place where shaft speed is very constant and Frahm absorbers can be used well.

11.11 Conclusion

The whole field of multidegree of freedom vibration is vast and rapidly growing. All that has been presented here is a short introduction. One of the technological advances that has promoted this growth is the Fast Fourier Transform Analyzer that has played a major role in connecting theory and experiment. While this chapter has leaned in the direction of structures, in the next chapter the topic of multidegree of freedom torsional vibrations of machine trains is explored in some detail.

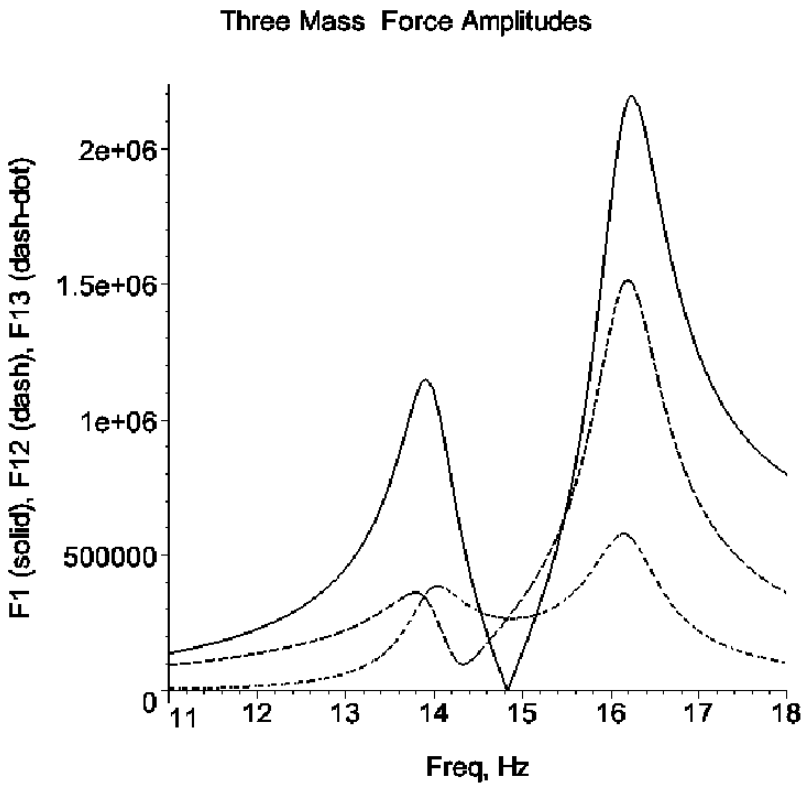

Figure 11.11: For the Modified System, Force Amplitudes F_1, F_{12}, and F_{13} as Functions of Shaft Speed

References

[1] Frazer, R.A, Duncan, W.J., and Collar, A.R., *Elementary Matrices*, Cambridge University Press, 1938, p. 327.

[2] Foss, K.A., "Coordinates Which Uncouple the Equations of Motion of Damped Linear Dynamic Systems," Technical Report 25-20, ONR Project NR 064-259, March, 1956.

[3] Tse, F.S., Morse, I.E., and Hinkle, R.T., *Mechanical Vibrations*, 2nd ed., Allyn and Bacon, 1978.

[4] Harris, C.O., *Introduction to Stress Analysis*, Macmillan, 1959, p. 10.

[5] Young, D., "Continuous Systems," p. 61-7 in *Handbook of Engineering Mechanics*, W. Flugge, ed., McGraw-Hill, 1962.

[6] Den Hartog, J.P., *Mechanical Vibrations*, 4th ed., McGraw–Hill, 1956.

[7] Guillen, A.T., "Control of Machine Vibration by Tuned Absorber," MIT,1980.

[8] Brewer, G.A., "Power Plant Fan Vibration –Absorber Systems, *Sound and Vibration*, April, 1983, pp. 20 – 22.

Problems

11-1 The figure shows three blocks on a ramp, able to move without friction except for the viscous dampers shown. All the physical parameters are known ($M_1, M_2, M_3, K_1, K_2, K_3, B_1, B_2$) and the geometric data (α, c_1, c_2, c_3).

(a) Determine the equilibrium position of the system;

(b) Write the equations of motion for the system in matrix form;

(c) Using the data below, evaluate the equilibrium position values;

(d) Neglecting the damping, evaluate the system natural frequencies and mode shapes.

$M_1 = 2.1$ kg	$B_1 = 27$ N-s/m	$K_1 = 205$ N/m	$L_{1o} = 40$ mm	$c_1 = 62$ mm
$M_2 = 1.75$ kg	$B_2 = 15$ N-s/m	$K_2 = 180$ N/m	$L_{2o} = 55$ mm	$c_2 = 60$ mm
$M_3 = 2.6$ kg		$K_3 = 225$ N/m	$L_{3o} = 37$ mm	$c_3 = 44$ mm
$\alpha = 16^o$				

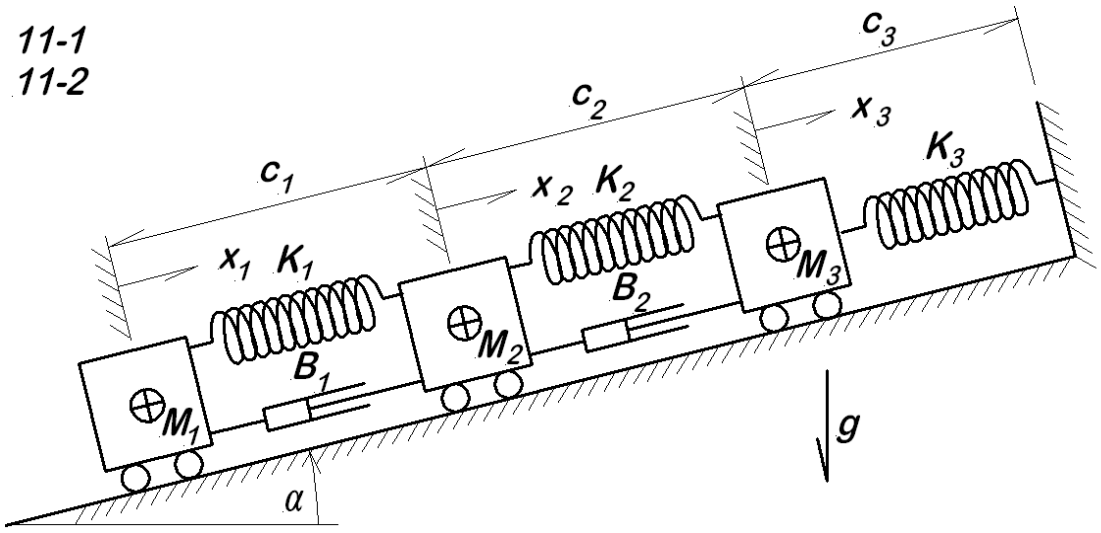

11-2 For the same system studied in problem **11-1** without damping and building on the solution from that problem, make use of the modal transformation to answer the questions below. All data and results from the previous problem may be used here.

(a) Define the modal matrix;

(b) Determine the modal mass and stiffness matrices;

(c) Determine the modal solutions for each modal coordinate, using the initial conditions given below;

(d) Transform the results of (c) back into the physical coordinates.

$$x_1(0) = 5 \text{ mm} \quad x_2(0) = -12 \text{ mm} \quad x_3(0) = 0 \text{ mm}$$
$$\dot{x}_1(0) = 0 \text{ m/s} \quad \dot{x}_2(0) = 0 \text{ m/s} \quad \dot{x}_3(0) = 0.52 \text{ m/s}$$

11-3 The figure shows the same system of three blocks described in problem **11-1**, with one exception. The upper spring, K_3, has been removed.

(a) Is there an equilibrium position for this system? Why, or why not?

(b) Write the equations of motion for this system in matrix form;

(c) Using the data provided in problem **11-1** and again neglecting damping, determine the natural frequencies and mode shapes for this system;

(d) What is unusual about the eigensolutions?

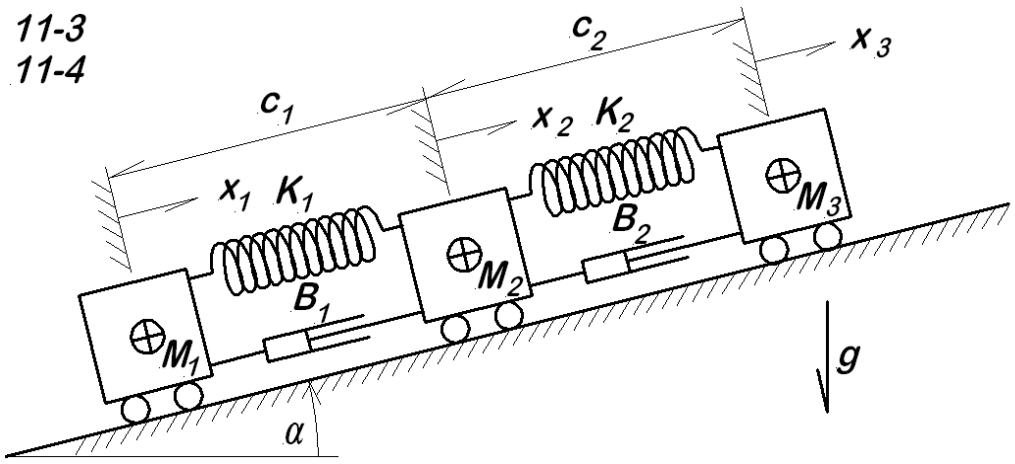

11-4 For the system of three blocks on a ramp considered in problem **11-3**, assume that there is a force $F_o + F_s \sin \Omega$ acting up slope on the middle block.

(a) Write the system equations of motion in matrix form;

(b) Using the system data from the two previous problems while neglecting damping, and assuming the values of F_o and F_s given below, determine the full solution for the system motion.

$F_o = 32$ N	$x_1(0) = 0.077$ m	$\dot{x}_1(0) = -0.15$ m/s
$F_s = 9$ N	$x_2(0) = 0.283$ m	$\dot{x}_2(0) = -0.75$ m/s
	$x_3(0) = 0.006$m	$\dot{x}_3(0) = +0.25$ m/s

11-5 The figure shows a block on three vibration isolation mounting springs, K_1, K_2, and K_3. The block is only able to move in the y and θ directions; there is no lateral displacement. The dimensions $c_1, c_2,$ and c_3 are all known, positive constants. It is assumed that the springs all have the same free length, L_o.

(a) Determine equilibrium values of y and θ;

(b) Write the equations of motion for small vibratory displacements from the equilibrium position;

(c) Using the data below, determine numerical values for the natural frequencies and mode shapes.

$K_1 = 3500$ N/m	$c_1 = 850$ mm	$M = 120$ kg
$K_2 = 4200$ N/m	$c_2 = 150$ mm	$J_c = 32$ kg-m^2
$K_3 = 2500$ N/m	$c_3 = 1200$ mm	

11-5

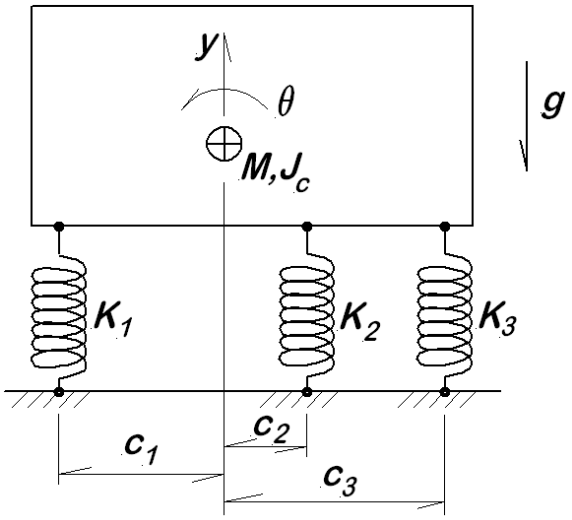

11-6 The figure shows a point mass, M, suspended in the gravitational field from two supports at different elevations. The spring constants, spring free lengths, dimensions shown, and the mass are all known. Resolve motions on the inclined $Y - Z$ coordinate system shown. *For this problem, there is no out-of-plane motion;* the motion is only in

the $Y - Z$ plane.

(a) Develop any kinematic relations required for later use;

(b) Develop the nonlinear equations of motion for this system;

(c) Determine (in symbols) the equilibrium position of the mass;

(d) Linearize (in symbols) the equations of motion for small displacements from equilibrium;

(e) Use the data below to evaluate numerically the equilibrium coordinates for the mass;

(f) Use the data below to determine numerically the equilibrium loads in each spring;

(g) Use the data below to determine numerically the natural frequencies and mode shapes for this system.

$K_1 = 18500$ N/m $\quad K_2 = 8500$ N/m $\quad M = 6.1$ kg

$L_{1o} = 250$ mm $\quad L_{2o} = 600$ mm

$D_H = 800$ mm $\quad D_V = 200$ mm

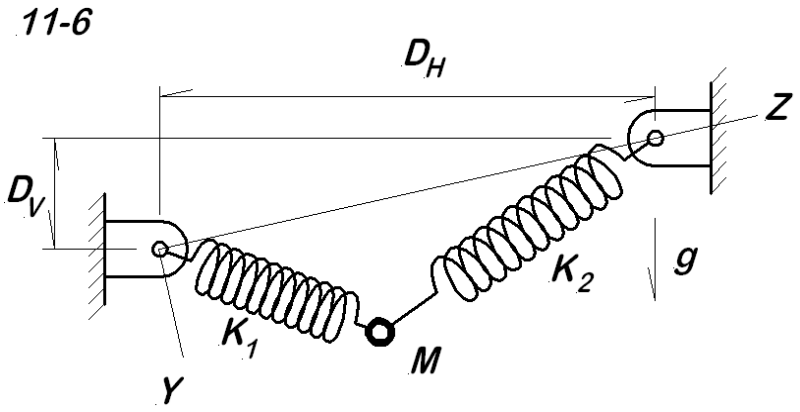

10-7 The figure shows a large ring supported on small rollers with a small solid disk rolling inside the ring. The small disk rolls inside the ring without slipping, and the ring rolls on the small rollers without slipping. The two small rollers are identical.

(a) Develop any kinematic results required later;

(b) Write the nonlinear equations of motion for this system;

(c) Determine the equilibrium configuration for the system;

(d) Linearize the system equations of motion.

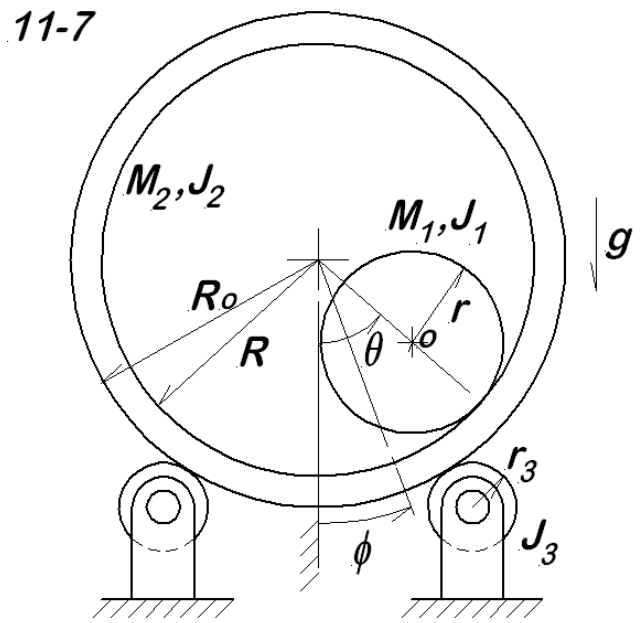

11-8 The figure shows two blocks, each having mass M and connected by a spring of stiffness K. The two blocks are free to move without friction on a horizontal surface, and when $x_1 = x_2 = 0$ the spring is relaxed.

(a) Write the equations of motion for this system in matrix form;

(b) Develop the characteristic equation, and solve for the natural frequencies;

(c) Using the data below, numerically evaluate the natural frequencies;

(d) Using the data below, numerically determine the eigenvectors (make the first element 1 for each eigenvector);

(e) Using the data below, determine the modal mass values and modal stiffness values;

(f) What is unusual about the modal equations? What impact does this have?

(g) Solve the modal equation using the initial conditions given below;

(h) Transform the solution back into the physical coordinates.

$K = 1492$ N/m $\quad x_1(0) = 0$ m $\quad x_2(0) = 0$ m

$M = 3.45$ kg $\quad \dot{x}_1(0) = 0.12$ m/s $\quad \dot{x}_2(0) = -0.18$ m/s

11-9 The figure shows two rotors on a shaft that is fixed at the left end. The mass

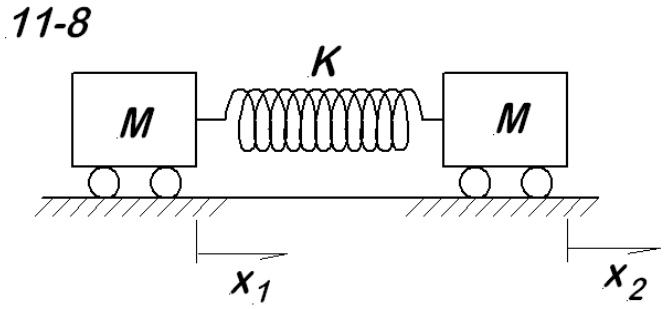

moments of inertia are related such that $J_1 = 2J_2$.

(a) Write the system equations of motion in matrix form;

(b) Develop the characteristic equation, and solve for the natural frequencies in terms of the ratio K/J_2, including a numerical coefficient for each one;

(c) Obtain numerical values for the eigenvectors for each mode.

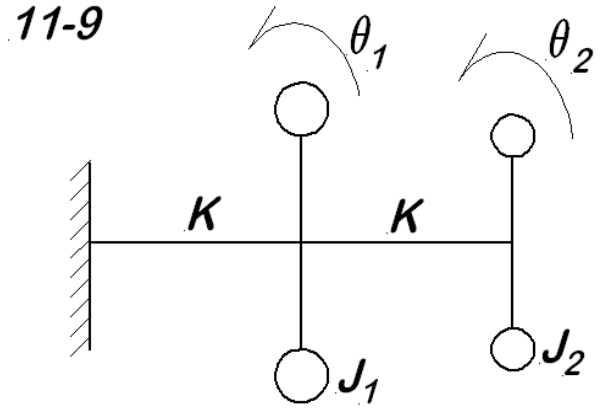

11-10 For this problem, the system appears exactly the same as that shown for problem **11-6**. What is new here is that out-of-plane motion is now considered, so that there is motion in three dimensions. All of the data given in connection with problem **11-6** applies here. Answer all of the same questions posed for problem **11-6** again, this time allowing for out-of-plane motion.

11-11 Although the sketch for this problem looks somewhat like that for problem **11-9**, they are significantly different systems. The figure shows a torsional system comprised of two stations, representing a prime mover and a synchronous generator, and a third station denoted as a steadily rotating reference[2]. For purposes of this problem, the third

[2]The figure represents, in simplified form, a situation that has been a major concern for the electric power generation industry. The left-most station is the prime mover, typically a steam or gas turbine, or in some cases a diesel engine. The second station is the rotor of a synchronous generator while the

station may be considered as an infinite flywheel, rotating at constant angular speed, Ω; it does not participate in the torsional vibration. Consider the parameters J_1, J_2, K_{shaft}, and K_{mag} as known.

(a) Write the equations of motion for the torsional system in matrix form;

(b) Using the parameter values below, determine numerically the system natural frequencies and mode shapes;

(c) Explain the significance of each mode shape.

---

shaft between them, with stiffness K_{shaft}, is the physical shaft that connects the two machines. This much is all that would be seen if the system were inspected while out of service. This suggests that, in operation, the system will function as a free-free vibratory system, but that is not the case.

Commercial electric power generation always connects many generators in parallel through an electric power grid. This gives improved reliability in the event of an accident that takes one generator out of service, and it provides for load sharing so that the demand for power is distributed over all of the generators in the grid.

In a synchronous machine, the magnetic field that couples the rotor and stator windings transfers torque across the air gap between the rotating and stationary parts. The torque transfer is proportional to the vector cross product of the magnetic flux density (B-field) from the rotor winding with the B-field from the stator winding. If the two fields were perfectly aligned, there would be no torque transfer and hence no power transferred. In operation, they are somewhat out of alignment, by an angle called the *torque angle* and denoted as δ. Thus the torque transferred across the air gap may be written as

$$T_{\text{air gap}} = kB_{\text{rotor}}B_{\text{stator}} \sin\delta$$

For steady operation, there is an equilibrium value for the torque angle, δ_{eq}, such that the previous equation is satisfied by the equilibrium values. If the torque on the rotor is varied mechanically, due to torsional oscillation while the field factors remain constant, this results in a displacement of the torque angle. For this situation, the change in the air gap torque is

$$\begin{aligned}
\Delta T_{\text{air gap}} &= kB_{\text{rotor}}B_{\text{stator}} \left[\sin\left(\delta_e + \Delta\theta\right) - \sin\delta_e\right] \\
&= kB_{\text{rotor}}B_{\text{stator}} \left(\cos\Delta\theta \sin\delta_e + \sin\Delta\theta \cos\delta_e - \sin\delta_e\right) \\
&\approx kB_{\text{rotor}}B_{\text{stator}} \cos\delta_e \cdot \Delta\theta
\end{aligned}$$

This says that, for small angular displacements from the equilibrium position, the air gap acts like a torsional spring with stiffness

$$K_{mag} = kB_{\text{rotor}}B_{\text{stator}} \cos\delta_e$$

Thus when the system is in operation and connected to a semi-infinite external electrical system, the external system acts like a flywheel, rotating at constant speed and connected to the present system by a torsion spring with stiffness K_{mag}.

As with any oscillatory system, there is the possibility of resonance, and torsional resonance leads, in many cases, to shaft failure or other mechanical damage. This was first noted in the US power industry in the early 1970s, and became the subject of intensive study. Most of the work is reported under the heading *Subsynchronous Resonance* (SSR), and there is much published work available on the internet for those who wish to pursue the topic further.

$J_1 = 17$ kg-m^2 $\quad K_{shaft} = 1.375 \cdot 10^7$ N-m

$J_2 = 18.5$ kg-m^2 $\; K_{mag} = 3.65 \cdot 10^5$ N-m

11-11

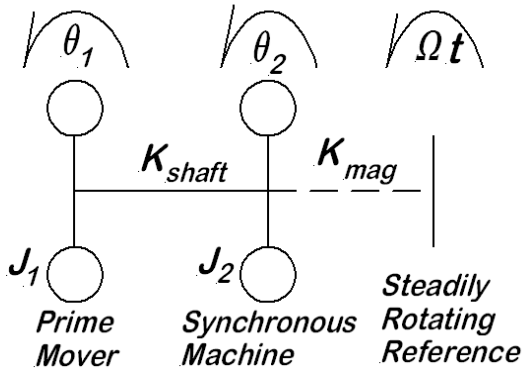

Chapter 12

Torsional Vibrations

12.1 Introduction

The previous chapter dealt with multidegree of freedom vibrations, and from one perspective, that includes the topic of torsional vibration. Seen from an alternate point of view, torsional vibration is a unique topic, presenting many problems in modeling and analysis not found in the typical structural multidegree of freedom problem. Because the design of machinery is a uniquely mechanical engineering task, the latter point of view is taken here, and special care is taken to develop the unique aspects of torsional vibration of machinery.

There are many machinery situations in which torsional vibration is of engineering concern. One in particular stands out, and that is systems that involve slider-crank machines, either as prime movers (internal combustion engines, steam engines) or as driven machinery (reciprocating compressors). Slider-crank machines are given particular emphasis in this chapter because of (1) their wide application in engineered systems, and (2) their close connection with the earlier material of this text.

One point that needs to be clear from the beginning is that everything in this chapter relates to what is commonly called steady state operation of machines, as opposed to transient operations such as start-up or shut-down. The specific meaning of steady state is discussed in more detail in the chapter, but it is important to start with this idea at least roughly in mind.

The subject is rather complicated, and requires the analyst to draw upon knowledge in kinematics and dynamics of mechanisms, mechanics of materials, thermodynamics, and numerous topics in applied mathematics. The physical phenomena involved are rather subtle, and often difficult to visualize. Because of the diversity of ideas involved, it is

useful for the reader to have an overall outline of the chapter in mind before proceeding, lest he become lost in the details. To that end, consider the following short chapter outline:

1. Introduction;
2. Introductory example, showing in some detail the types of motion to be encountered;
3. Component modeling, with particular attention to shaft stiffness, variable inertia in slider-crank mechanism, and damping estimation, and internal combustion engine cylinder pressure evaluation;
4. System equations of motion, first in the complete nonlinear form and then with linearization and periodic excitation;
5. Discussion of the several approaches to the solution;
6. Development of the Holzer technique for both free and forced vibrations;
7. Detailed torsional vibration analysis for a simple three station system;
8. Closing comments.

The length of this short outline underscores the complexity of the subject matter; the reader may need to refer back to this frequently to keep a clear vision of the process. In addition to the material within this chapter, the reader should be aware of the discussion in Appendix 5.2 dealing with internal combustion engine thermodynamic cycles and cylinder pressure modeling and data for the final example.

12.2 Introductory Example

Consider a very simple system, consisting of two disks, with mass moments of inertia J_1 and J_2, joined by a shaft with torsional stiffness K, all as shown in Figure 12.1. There are any number of real systems that are approximated by such a simple system, including (1) a ship's engine, shaft and propeller system; (2) a steam or gas turbine driven generator set; (3) an engine driven saw at a logging camp saw mill; (4) an aircraft engine, shaft, and propeller; (5) a diesel engine driven generator or pump. Assume for this example that there is no damping in the system. The angular positions of the two disks are described by angular coordinates, θ_1 and θ_2, both positive in the same sense. The external torques

acting on the two disks are T_1 and T_2, taken positive in the same sense as the two angles, θ_1 and θ and are assumed to be of the form:

$$\left\{ \begin{array}{c} T_1 \\ T_2 \end{array} \right\} = \left\{ \begin{array}{c} T_0 \\ -T_0 \end{array} \right\} + \left\{ \begin{array}{c} T_{C1} \\ T_{C2} \end{array} \right\} \cos \Omega t + \left\{ \begin{array}{c} T_{S1} \\ T_{S2} \end{array} \right\} \sin \Omega t \tag{12.1}$$

The value T_0 is the useful torque, while all of the other terms have zero average value and serve only to excite torsional vibration in the system. The frequency Ω is often the shaft speed as is assumed here, but that is not essential. Excitations also arise at other frequencies associated with multiples of the shaft speed, gear mesh frequencies, van passing frequencies, and other phenomena within the system. The system equation of motion is

$$\begin{aligned} &\left[\begin{array}{cc} J_1 & 0 \\ 0 & J_2 \end{array} \right] \left\{ \begin{array}{c} \ddot{\theta}_1 \\ \ddot{\theta}_2 \end{array} \right\} + \left[\begin{array}{cc} K & -K \\ -K & K \end{array} \right] \left\{ \begin{array}{c} \theta_1 \\ \theta_2 \end{array} \right\} \\ &= \left\{ \begin{array}{c} T_0 \\ -T_0 \end{array} \right\} + \left\{ \begin{array}{c} T_{C1} \\ T_{C2} \end{array} \right\} \cos \Omega t + \left\{ \begin{array}{c} T_{S1} \\ T_{S2} \end{array} \right\} \sin \Omega t \end{aligned} \tag{12.2}$$

The solution is made by modal analysis, but there is a twist involved.

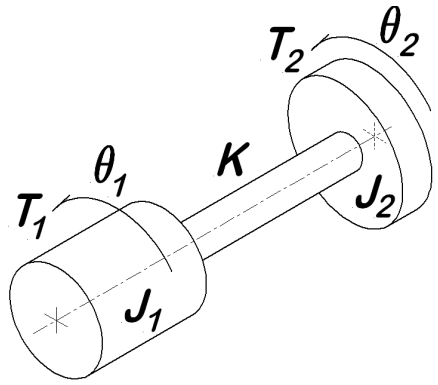

Figure 12.1: Two Station Model for the Introductory Example

12.2.1 Free Vibration Analysis - Eigensolutions

For the free vibration analysis, all of the exciting torques are ignored, and the system natural frequencies and mode shapes, the eigensolutions, are determined. Following the example of Section 11.4, for this system, the characteristic equation is

$$\omega^2 \left[\omega^2 J_1 J_2 - K \left(J_1 + J_2 \right) \right] = 0 \tag{12.3}$$

with solutions

$$\omega_0^2 = 0 \qquad \omega_1^2 = \frac{K\left(J_1 + J_2\right)}{J_1 J_2} \tag{12.4}$$

The associated mode vectors are

$$\{A\}_0 = \left\{ \begin{array}{c} 1 \\ 1 \end{array} \right\} \qquad \{A\}_1 = \left\{ \begin{array}{c} 1 \\ -J_1/J_2 \end{array} \right\} \tag{12.5}$$

The alert reader may notice several new things about these eigensolutions. The first, perhaps, is the use of the zero subscript, but much more important is the $\omega_0 = 0$ value. Associated with these there is the mode shape consisting of $\{A\}_0 = \mathrm{col}\left(1, 1\right)$, with no sign changes. None of these were seen in Chapter 11, but here they appear immediately.

The unique character of torsional vibrations is evident in the zero modal stiffness for the first mode as implied by the zero natural frequency. This reflects the fact that the system is *positive semidefinite*, rather than *positive definite. A system is positive definite if every possible displacement results in positive potential energy; a system is positive semidefinite if some displacements result in positive potential energy but there exists other displacements for which the potential energy remains zero.* Because of the free-free nature of the shaft, a rigid body rotation of the entire system does not store any strain energy.

12.2.2 Modal Transformation

The eigensolutions found above form the basis for the modal transformation. The modal matrix, $[A]$, is composed of the mode vectors in the usual fashion:

$$[A] = [\{A\}_0 \,|\, \{A\}_1] = \left[\begin{array}{cc} 1 & 1 \\ 1 & -J_1/J_2 \end{array} \right] \tag{12.6}$$

As introduced in Section 11.5.1, the modal transformation uses the modal matrix as a transformation matrix, such that

$$\{\theta\} = [A]\{\xi\} \tag{12.7}$$

where $\{\xi\} = col\left(\xi_1(t), \xi_2(t)\right)$ is the column vector of modal coordinates. Applying this transformation to the equation of motion gives

$$\begin{aligned} \lceil J \rfloor \left\{ \ddot{\theta} \right\} + [K]\{\theta\} &= \{T(t)\} \\ [A]^T \lceil J \rfloor [A] \left\{ \ddot{\xi} \right\} + [A]^T [K][A]\{\xi\} &= [A]^T \{T\} \end{aligned} \tag{12.8}$$

all exactly as done in Chapter 11. As before, the triple matrix products are of particular interest, because each of them results in a diagonal matrix:

$$\begin{aligned}
[A]^T \lceil J \rfloor [A] &= \begin{bmatrix} 1 & 1 \\ 1 & -J_1/J_2 \end{bmatrix} \begin{bmatrix} J_1 & 0 \\ 0 & J_2 \end{bmatrix} \begin{bmatrix} 1 & 1 \\ 1 & -J_1/J_2 \end{bmatrix} \\
&= \begin{bmatrix} J_1 + J_2 & 0 \\ 0 & (J_1/J_2)(J_1 + J_2) \end{bmatrix} \\
&= \lceil \mathbb{M} \rfloor
\end{aligned} \tag{12.9}$$

$$\begin{aligned}
[A]^T [K] [A] &= \begin{bmatrix} 1 & 1 \\ 1 & -J_1/J_2 \end{bmatrix} \begin{bmatrix} K & -K \\ -K & K \end{bmatrix} \begin{bmatrix} 1 & 1 \\ 1 & -J_1/J_2 \end{bmatrix} \\
&= \begin{bmatrix} 0 & 0 \\ 0 & K\left[(J_1 + J_2)/J_2\right]^2 \end{bmatrix} \\
&= \lceil \mathbb{K} \rfloor
\end{aligned} \tag{12.10}$$

The $[A]^T$ also multiplies the right side of the equation, so it is necessary to see how this affects the torque terms.

$$\begin{aligned}
[A]^T \{T\} &= \begin{bmatrix} 1 & 1 \\ 1 & -J_1/J_2 \end{bmatrix} \begin{Bmatrix} T_1 \\ T_2 \end{Bmatrix} \\
&= \begin{Bmatrix} 0 \\ T_0\left[1 + (J_1/J_2)\right] \end{Bmatrix} + \cos \Omega t \begin{Bmatrix} T_{C1} + T_{C2} \\ T_{C1} - (J_1/J_2) T_{C2} \end{Bmatrix} \\
&\quad + \sin \Omega t \begin{Bmatrix} T_{S1} + T_{S2} \\ T_{S1} - (J_1/J_2) T_{S2} \end{Bmatrix}
\end{aligned} \tag{12.11}$$

It is significant that the useful torque, T_0, is not a part of the excitation in the first modal equation of motion; the only contributions there are from the sinusoidal terms. All of the original excitation torques appear in the excitation for the second mode.

12.2.3 Modal Response Solutions

The solution proceeds by next solving the modal differential equations, to obtain the modal responses as functions of time, $\xi_1(t)$ and $\xi_2(t)$. After this is complete, the physical displacements are reconstructed through the modal transformation.

12.2.3.1 Zero Frequency Mode Forced Response

The term *zero frequency mode* refers to the first mode of a free-free system, pointing to the fact that the modal stiffness in this mode is zero. The equation of motion for the first mode is

$$\mathbb{M}_{00}\ddot{\xi}_0 = (J_1 + J_2)\,\ddot{\xi}_0 = (T_{C1} + T_{C2})\cos\Omega t + (T_{S1} + T_{S2})\sin\Omega t \tag{12.12}$$

This is simply the equation of motion for the system considered as a rigid body, which is exactly what the zero frequency mode represents. The equation can be solved by direct integration to give,

$$\begin{aligned}\xi_0(t) \;=\; & -\frac{1}{(J_1 + J_2)\,\Omega^2}[(T_{C1} + T_{C2})\cos\Omega t \\ & + (T_{S1} + T_{S2})\sin\Omega t + C_1\Omega t + C_2]\end{aligned} \tag{12.13}$$

This is the full solution for the first mode, and it includes two arbitrary constants, C_1 and C_2, to be evaluated later to satisfy the initial conditions.

12.2.3.2 Twisting Mode Forced Response

For the simple system considered here, there is only one twisting mode, the second mode of the system. The equation of motion governing this mode is

$$\begin{aligned}\mathbb{M}_{11}\ddot{\xi}_1 + \mathbb{K}_{11}\xi_1 \;=\; & T_0\,[1 + (J_1/J_2)] \\ & + [T_{C1} - (J_1/J_2)\,T_{C2}]\cos\Omega t \\ & + [T_{S1} - (J_1/J_2)\,T_{S2}]\sin\Omega t\end{aligned} \tag{12.14}$$

where the modal mass and stiffness are

$$\mathbb{M}_{11} \;=\; (J_1/J_2)\,(J_1 + J_2) \tag{12.15}$$

$$\mathbb{K}_{11} \;=\; K\,[(J_1 + J_2)/J_2]^2 \tag{12.16}$$

There may be some confusion regarding the subscripts. To emphasize the zero natural frequency of the first mode, the subscript 0 is assigned to the mode vector and associated properties; that is the rigid body mode. The subscript 1 then refers to what is actually the second mode, which is also the *first twisting mode*. Thus $\mathbb{M}_{11}$ and $\mathbb{K}_{11}$ are actually taken from the $(2,2)$ positions of their respective matrices.

The homogeneous and particular solutions are found in the usual manner. The complete solution for the second mode is the sum of the homogeneous and particular solutions,

$$\begin{aligned}\xi_1(t) &= \alpha_1 \cos\omega_1 t + \beta_1 \sin\omega_1 t + T_0 \cdot \frac{J_2}{K(J_1+J_2)} \\ &+ \frac{[T_{C1} - (J_1/J_2)\,T_{C2}]}{M_{11}(\omega_1^2 - \Omega^2)} \cos\Omega t + \frac{[T_{S1} - (J_1/J_2)\,T_{S2}]}{M_{11}(\omega_1^2 - \Omega^2)} \sin\Omega t\end{aligned} \tag{12.17}$$

12.2.4 Physical Response Reconstruction

In order to reconstruct the physical responses, the modal transformation is applied to the two expressions above. Thus,

$$\begin{aligned}\left\{\begin{array}{c}\theta_1(t)\\ \theta_2(t)\end{array}\right\} &= [A]\left\{\begin{array}{c}\xi_0(t)\\ \xi_1(t)\end{array}\right\} \\ &= \left\{\begin{array}{c}\xi_0(t) + \xi_1(t)\\ \xi_0(t) - (J_1/J_2)\,\xi_1(t)\end{array}\right\}\end{aligned} \tag{12.18}$$

The detailed expressions are then

$$\begin{aligned}\theta_1(t) = &-\tfrac{1}{(J_1+J_2)\Omega^2}[C_1\Omega t + C_2] && \text{Uniform, Steady Rotation}\\ &-\tfrac{1}{(J_1+J_2)\Omega^2}[(T_{C1}+T_{C2})\cos\Omega t + (T_{S1}+T_{S2})\sin\Omega t] && \text{Rigid Body Rolling}\\ &+\alpha_1\cos\omega_1 t + \beta_1 \sin\omega_1 t && \text{Free Vibration Response}\\ &+T_0 \cdot \tfrac{J_2}{K(J_1+J_2)} && \text{Steady Twist}\\ &+\tfrac{[T_{C1}-(J_1/J_2)T_{C2}]}{M_{11}\left(\omega_1^2-\Omega^2\right)}\cos\Omega t + \tfrac{[T_{S1}-(J_1/J_2)T_{S2}]}{M_{11}\left(\omega_1^2-\Omega^2\right)}\sin\Omega t && \text{Dynamic Twist}\end{aligned} \tag{12.19}$$

$$\begin{aligned}
\theta_2(t) = & -\tfrac{1}{(J_1+J_2)\Omega^2}\left[C_1\Omega t + C_2\right] && \text{Uniform, Steady Rotation}\\
& -\tfrac{1}{(J_1+J_2)\Omega^2}\left[(T_{C1}+T_{C2})\cos\Omega t + (T_{S1}+T_{S2})\sin\Omega t\right] && \text{Rigid Body Rolling}\\
& -(J_1/J_2)\left[\alpha_1\cos\omega_1 t + \beta_1\sin\omega_1 t\right] && \text{Free Vibration Response}\\
& -T_0\cdot\tfrac{J_1}{K(J_1+J_2)} && \text{Steady Twist}\\
& -(J_1/J_2)\left[\tfrac{[T_{C1}-(J_1/J_2)T_{C2}]}{M_{11}\left(\omega_1^2-\Omega^2\right)}\cos\Omega t + \tfrac{[T_{S1}-(J_1/J_2)T_{S2}]}{M_{11}\left(\omega_1^2-\Omega^2\right)}\sin\Omega t\right] && \text{Dynamic Twist}
\end{aligned} \tag{12.20}$$

It is important to note that the terms identified as *Uniform, Steady Rotation* and *Rigid Body Rolling* are identical in both expressions. This means that there is no twisting associated with these parts of the motion, only rigid body rotation.

Rigid body rolling has confused many experimental studies because it occurs at the forcing frequency and appears at both stations, and yet it does not involve dynamic elastic deformation because it represents a rigid body motion. It is for this reason, that it is important to be aware that the rigid body rolling mode is present, in order to properly interpret experimental data taken on actual operating machinery. It does not cause any dynamic strain in the shaft, although there is usually static strain involved.

No damping is included in the mathematical model above, but it should be understood that there is always damping in real physical systems. For this reason, all of the free vibration response terms eventually disappear in the actual physical motion while all of the other terms continue on indefinitely.

The appearance of solution terms involving Ωt suggests that it is useful to consider a rotating reference mark, a line that rotates about the shaft axis at the nominal shaft speed, Ω. The angle from a fixed reference to the rotating mark is then simply Ωt, where t is the time. The reference mark rotates at constant speed, and all stations vibrate torsionally about this rotating reference. This idea appears several times in what follows.

12.3 Component Modeling

In the introductory example of the previous section, it was assumed that the system had been previously modeled as a two degree of freedom system, and that the stiffness and mass moment of inertia values were known. That is rarely the case in practice. The analysis usually starts from drawings of the piece parts and some overall system assembly drawings; the mathematical model must be extracted from these drawings and the data contained in them. Perhaps the first decision to be made is which components to consider

as rigid bodies with mass and which to treat as elastic members without mass. This is largely a matter of experience applied to each specific case, since all real bodies have both mass and flexibility.

12.3.1 Mass Moments of Inertia

Because rotational motion is the primary concern, the physical property characteristic of each rigid body is its mass moment of inertia (MMOI). In some cases, the mass moment of inertia value will be provided by a component manufacturer and specified on the drawing. When this is available, this data should always be used.

At times, this manufacturer supplied value is given indirectly as a quantity called Wk^2; this usage is particularly common in the electrical machinery industry (motors, generators). This quantity is the product of the weight with the square of the *radius of gyration*. All that is necessary to obtain the mass moment of inertia is to divide Wk^2 by the acceleration of gravity,

$$J = \frac{1}{g}\left(Wk^2\right) = \frac{W}{g}k^2 = Mk^2 \tag{12.21}$$

12.3.1.1 Simple Rotor Station

Where there is no manufacturer provided data, the analyst often needs to calculate a moment of inertia value based on the part drawing. For simple, flat disk-like devices mounted on the shaft, this is easily done using the well known formula from elementary dynamics,

$$J = \frac{1}{2}MR^2 \tag{12.22}$$

where

M = mass of the flat disk

R = outer radius of the disk

Many shaft mounted devices have more complicated shapes than a simple disk, but they often remain axisymmetric. In such cases, the methods of Appendix 4 may prove useful. See for example the gear blank calculation in Appendix 4.4. The schematic representation of a simple station is primarily symbolic of its mass moment of inertia, as indicated in Figure 12.2.

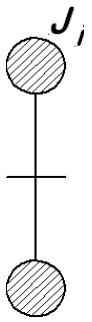

Figure 12.2: Station Mass Moment of Inertia Representation

The short horizontal line along the axis of rotation is representative of the shaft that connects this station to those on either side. The shaded circular areas at the ends of the vertical line are intended to symbolically indicate mass at a radial distance from the axis of rotation. (When drawn in haste or by hand, the circles are often left unshaded.) The notation J_i simply indicates that there is a specific value for the mass moment of inertia associated with the i^{th} station.

12.3.1.2 Slider-Crank Station

Modeling of a single engine cylinder is more complicated. It is a single degree of freedom system fully defined by the crank angle θ, so the Eksergian's equation from Chapter 7 is applicable. The slider-crank system for analysis is shown in schematic form in Figure 12.3 where the mechanism is shown inclined away from the vertical. The necessary kinematic analysis for determining all secondary coordinates in terms of the primary variable, the crank angle θ, is developed in Chapter 2.

The kinetic energy of the complete slider-crank system is

$$\begin{aligned} T_{SliderCrank} &= T_{Crank} + T_{ConRod} + T_{WristPin} + T_{Piston} \\ &= \frac{1}{2}\dot{\theta}^2\{J_{1o} + M_2\left[K_{2cx}^2(\theta) + K_{2cy}^2(\theta)\right] \\ &\quad + (J_{wp} + J_{2c})\,K_\phi^2(\theta) + (M_{wp} + M_3)\,K_x^2(\theta)\} \end{aligned} \tag{12.23}$$

This is a slight extension of equation (7.8). Note that for this particular engine construction, the wrist pin is assumed to be a press fit in the connecting rod and thus to rotate with it. For this reason, the mass moment of inertia of the wrist pin is included with that of the connecting rod, while the mass of the wrist pin is included with the piston with which it travels. If the wrist pin were fixed in the piston, its mass would still be included with the piston, but there would be no rotational energy associated with the wrist pin. In the event that the wrist pin is floating, that is, neither fixed in the connecting rod nor

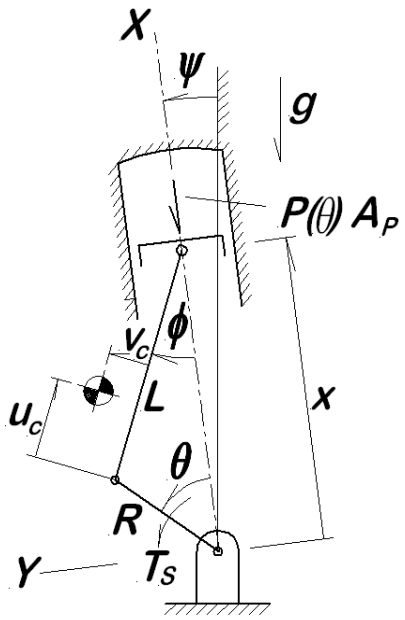

Figure 12.3: Slider-Crank Schematic

the piston, its motion is indeterminate and a correct model requires a considerably more detailed analysis.

From the kinetic energy, the generalized inertia is extracted in a form parallel to that of equation (7.9),

$$\begin{aligned} \mathbb{I}(\theta) \;=\; & J_{1o} + M_2 \left[K_{2cx}^2(\theta) + K_{2cy}^2(\theta) \right] \\ & + (J_{wp} + J_{2c})\; K_\phi^2(\theta) + (M_{wp} + M_3)\, K_x^2(\theta) \end{aligned} \tag{12.24}$$

The centripetal coefficient is calculated by differentiation,

$$\begin{aligned} \mathbb{C}(\theta) \;=\; & M_2[K_{2cx}(\theta)\; L_{2cx}(\theta) + K_{2cy}(\theta)\; L_{2cy}(\theta)] \\ & + (J_{wp} + J_{2c})\; K_\phi(\theta)\; L_\phi(\theta) + (M_{wp} + M_3)\; K_x(\theta)\; L_x(\theta) \end{aligned} \tag{12.25}$$

If the objective is only to prepare the nonlinear equations of motion for a simulation, the results above are sufficient. Since the objective here is to prepare the problem for the application of linear vibration theory, the variable inertia requires further consideration. When the variable generalized inertia and the centripetal coefficient are plotted for a typical slider-crank, the results are as in Figure 12.4.

The function $\mathbb{I}(\theta)$ is always positive (never zero), which suggests that it can be replaced, at least approximately, by an average value. But the function of actual importance is $1/\mathbb{I}(\theta)$, rather than $\mathbb{I}(\theta)$ itself. Therefore, it is this function that should be averaged.

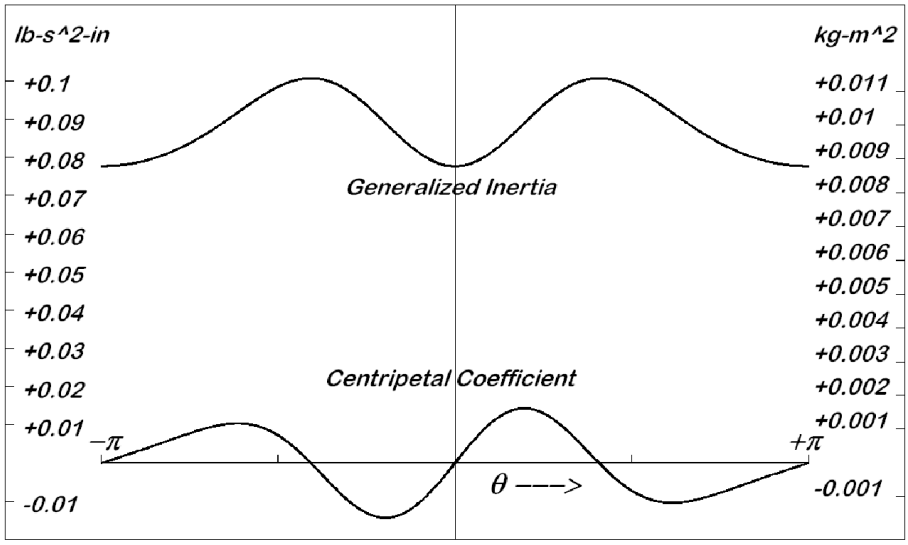

Figure 12.4: Generalized Inertia and Centripetal Coefficient for Typical Crank Station

Biezeno and Grammel [1] indicate that the preferred average value of $\mathbb{I}(\theta)$ is J_1,

$$J_1 = \left[\frac{1}{2\pi} \int_0^{2\pi} \frac{1}{\mathbb{I}(\theta)} d\theta \right]^{-1} \tag{12.26}$$

Thus the value J_1 is thus used in place of $\mathbb{I}(\theta)$ as a step toward linearizing the equations of motion. Appropriate means for dealing with the centripetal coefficient arise later when the equations of motion are assembled.

12.3.2 Stiffness

Torsional stiffness is a property of the shaft connecting two stations. The simplest possible shaft is just a circular rod of constant diameter. For such a simple shaft of length L and diameter d, it is known from mechanics of materials that the application of a torque T produces a twist $\Delta\theta$ from end to end that can be computed according to

$$\Delta\theta = \frac{TL}{J_A G} \tag{12.27}$$

where

J_A = area polar moment of inertia of the cross section = $\pi d^4/32$

G = shear modulus of the shaft material

The reader should be alert to avoid confusion between J_A meaning the *area polar moment of inertia of the shaft* and J_i meaning the *axial mass moment of inertia of a station.* This is an unfortunate overuse of the symbol J, but is is a long established engineering convention.

12.3.2.1 How Long Is A Shaft?

From equation (12.27), the torsional stiffness and compliance are evidently

$$K = \frac{T}{\Delta\theta} = \frac{J_A G}{L} \tag{12.28}$$

$$C = 1/K = \frac{L}{J_A G} \tag{12.29}$$

This seems to suggest that the calculation of shaft stiffness is a simple matter, but consider the situation shown in Figure 12.5 where a gear is mounted on a motor shaft.

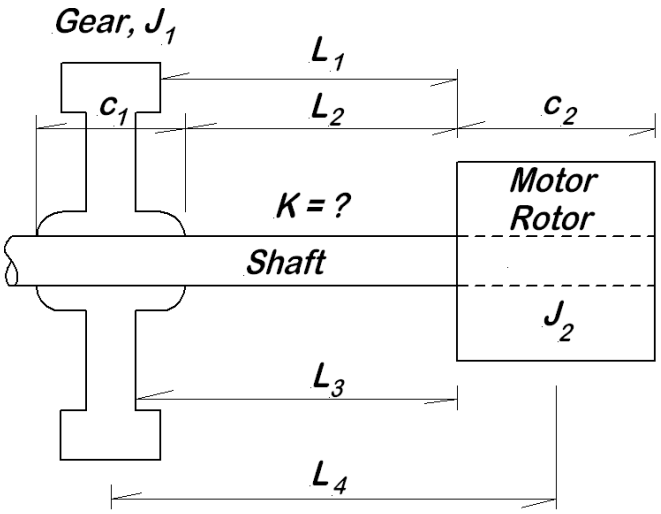

Figure 12.5: What is the effective shaft length?

It is assumed that the shaft material is known (so that the shear modulus is also known from tabulated data), the shaft is uniform in diameter so there is no difficulty in determining the area polar moment of inertia, but what is the appropriate length to use? Would the reader use L_1, or L_2, perhaps L_3, or maybe L_4? Or maybe yet some other length? This is one of the many perplexing problems in modeling torsional vibration problems, and there are no sharply defined answers. Obtaining good results is very much an art! Even a detailed finite element analysis does not provide a valid answer because so much depends upon the unknowable details regarding the fit of the parts on the shaft, the amount of friction developed at the interface.

Consider how torque is transferred from a station (the motor rotor or the gear) onto the shaft. Where does this torque transfer occur? The transfer must happen in the lengths where the station and the shaft are in contact. This means that the effective length, L_{eff} must be greater than L_2, because the L_2 section of the shaft is not in contact with either station and is thus exposed to the full torque. Somewhere, in the contact zone, the frictional shear stress between the shaft and the station must gradually transfer the torque from one to the other.

For the situation shown in Figure 12.5, the two contact zones are of length c_1 and c_2 (assuming that the shaft extends completely through the motor rotor as is typical). A rough rule of thumb, to be used only in the absence of better information, is to say that the complete torque transfer occurs 1/3 of the way through the contact zone. Thus, for this example, the effective length and the estimated stiffness are

$$L_{eff} = L_2 + \frac{1}{3}(c_1 + c_2) \tag{12.30}$$

$$K_{est} = \frac{J_A G}{L_{eff}} \tag{12.31}$$

In particular cases, there may be better estimates available or actual measurements, in which case they should certainly be used.

12.3.2.2 Stepped Shafts

Unfortunately, this is not the end of difficulties in stiffness modeling. Uniform shafts are relatively rare in actual machinery, while stepped shafts are very common. Steps are often used to locate mounted structures (motor rotors, turbine wheels, gears, flywheels, etc.). It is therefore necessary to consider how steps affect shaft stiffness. For this purpose, consider the shaft shown in Figure 12.6. Note that a fillet radius at the step is shown in the figure. Sharp steps are always to be avoided, and the size of the fillet radius, r_f, is an important parameter of the stepped shaft stiffness.

The complete shaft is composed of two cylindrical segments, lengths L_1 and L_2, with diameters D_1 and D_2, where $D_1 < D_2$; *in the discussion of this topic only, the smaller diameter is always denoted* D_1. With all dimensions and material properties known, it is a simple matter to compute the compliance (reciprocal of stiffness) for each segment alone:

$$C_1 = \frac{\Delta\theta_1}{T} = \frac{L_1}{J_{A1}G} = \frac{32L_1}{\pi G D_1^4} \tag{12.32}$$

$$C_2 = \frac{\Delta\theta_2}{T} = \frac{L_{l2}}{J_{A2}G} = \frac{32L_2}{\pi G D_2^4} \tag{12.33}$$

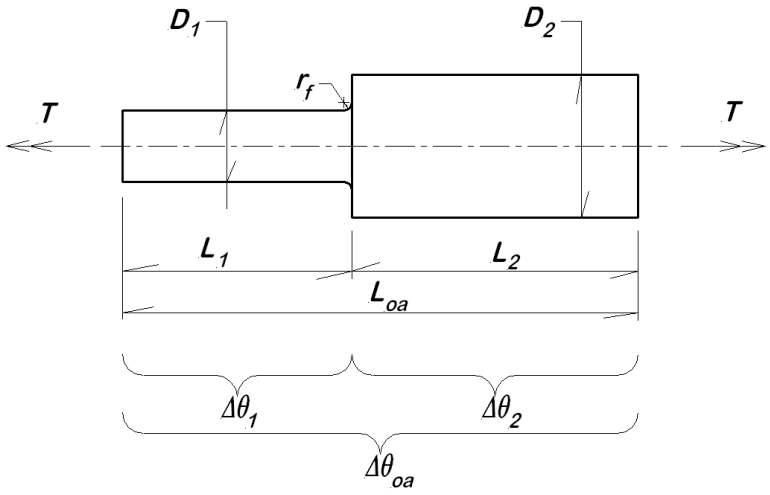

Figure 12.6: Stepped Shaft With Fillet

where the use of the same value of G implies that both segments are made of the same material. Note that $\Delta\theta_1$ and $\Delta\theta_2$ are the twist angles for the individual segments, and $\Delta\theta_{oa}$ is the overall twist. The same torque T passes through both segments, and the twist angles are additive, so the overall torque-twist relation appears to be

$$\begin{aligned} \Delta\theta_{oa} &= \Delta\theta_1 + \Delta\theta_2 \\ &= T\,(C_1 + C_2) \end{aligned} \tag{12.34}$$

Equation (12.34) indicates that the apparent compliance is simply the sum of the individual compliance values. This is exactly the result developed in elementary mechanics for springs in series, so many are surprised to learn that the analysis above is in error. The compliance value computed in this manner is too small, because the effect of the step is not properly taken into account.

The error lies in assuming that the full length L_2 has effective diameter D_2. Although this is geometrically true, the material at the shoulder is not effective in supporting the transmitted torque because no shear stress develops near the shoulder of the step. In progressing along the shaft length, the shear stress pattern transitions smoothly from the smaller to larger diameter, as shown in Figure 12.7. The material close to the exterior corner is a "dead zone," a volume of material that is ineffective for torque transfer.

With this understanding, it becomes evident that the size of the fillet radius is very significant; a larger fillet radius provides a smoother transition. The effect of the shoulder is to increase the overall compliance because the transition from D_1 to D_2 effectively occurs gradually inside the length L_2.

Because of the extreme importance of this topic for internal combustion engines, it was the subject of extensive experimental investigations long before finite element analysis

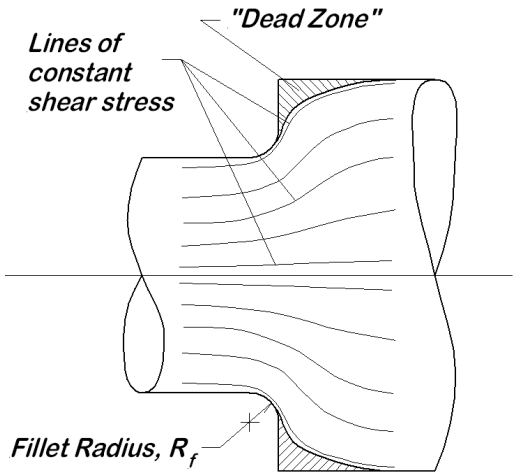

Figure 12.7: Shear Stress Distribution at a Step

became available. Much of that work was reported by BICERA [2] and by W.K. Wilson [3]. Although their approaches differ slightly, their results are similar. The approach followed here is that of BICERA, namely to express the increased compliance as an additional length to be added to L_1 at diameter D_1. If the additional effective length is denoted as ΔL, the experimental results can be presented in graphical form showing $\Delta L/D_1$ as a function of the diameter ratio D_2/D_1 with the fillet radius ratio r_f/R_1 as a parameter, as shown in Figure 12.8, where $R_1 = D_1/2$.

In order to apply the results shown in Figure 12.8, the ratios D_2/D_1 and R_f/R_1 are first evaluated. Note that, if $D_2/D_1 < 1.3$, there is no data available, but reason suggests that the curves should pass through the point $(1, 0)$. Similarly, for $D_2/D_1 > 3$, there is no data available, but the curves are fairly flat by that point. If $R_f/R_1 > 0.5$, the fillet is very large and no data are available. Provided D_2/D_1 and R_f/R_1 are within the ranges of the available data, the ratio $\Delta L/D_1$ is either read directly from the graph or estimated by interpolation for R_f/R_1 values not shown. The additional compliance due to the step is computed as

$$\Delta C = \frac{32\left(\frac{\Delta L}{D_1}\right)D_1}{\pi G D_1^4} = \frac{32}{\pi G D_1^3}\left(\Delta L/D_1\right) \tag{12.35}$$

The overall compliance of the stepped shaft is then

$$C_{oa} = C_1 + \Delta C + C_2 \tag{12.36}$$

and the overall stiffness is the reciprocal of this value. Although this process is conceptually quite simple, accurately reading the data from the plotted curves and interpolating for a final value of $\Delta L/D_1$ is rather tedious. In order to make the data more useful, each

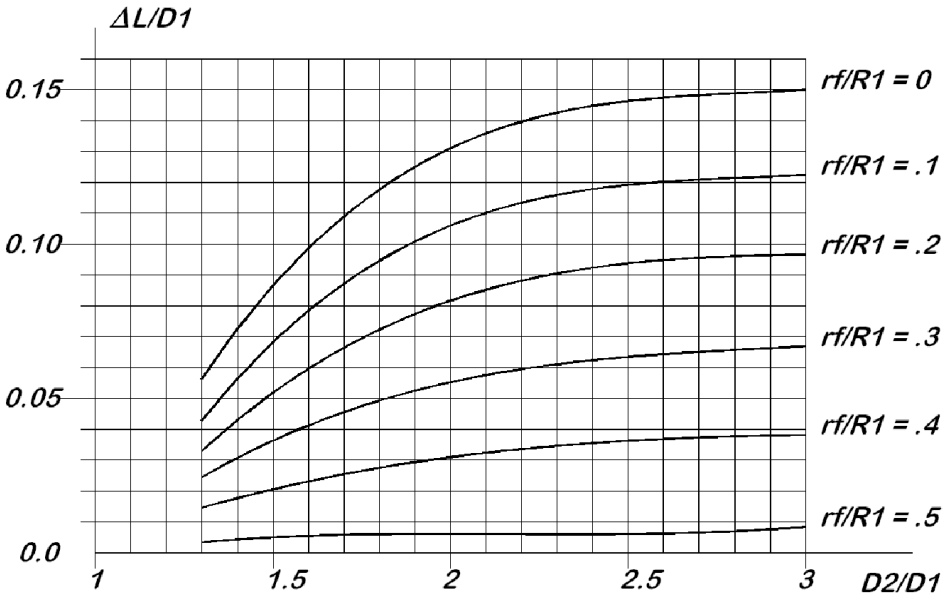

Figure 12.8: Effective Additional Length of a Shaft Step

of the curves is fitted (in the least squares sense) by a cubic polynomial of the form

$$\frac{\Delta L}{D_1} \approx c_o + c_1 \left(\frac{D_2}{D_1}\right) + c_2 \left(\frac{D_2}{D_1}\right)^2 + c_3 \left(\frac{D_2}{D_1}\right)^3 \tag{12.37}$$

For each value of the ratio R_f/D_1, the required polynomial coefficients are given in Table 12.1:

Table 12.1 Polynomial Coefficients for Shaft Step Compliance

R_f/R_1	c_o	c_1	c_2	c_3
0.5	−0.04120449	+0.06629457	−0.03078916	+0.00473217
0.4	−0.05880530	+0.08379197	−0.02406529	−0.00230211
0.3	−0.14435611	+0.20611966	−0.02406529	+0.00793266
0.2	−0.22942227	+0.31729433	−0.10358512	+0.01135170
0.1	−0.34024899	+0.47824631	−0.16669651	+0.01956535
0.0	−0.39996364	+0.57104651	−0.19986226	+0.02354454

The curves in Figure 12.8 are generated using these polynomial fits; for the original curves, the reader is referred to Reference [2].

12.3.2.3 Numerical Example

For a numerical example of the application of the stepped shaft calculations, consider the roller shaft shown in Figure 12.9. The torsional compliance of the complete shaft is to be computed. Note that D_1, D_2 , L_1 and L_2 for this example are not the same as their meaning in the previous example and must be properly interpreted to use the results of that analysis.

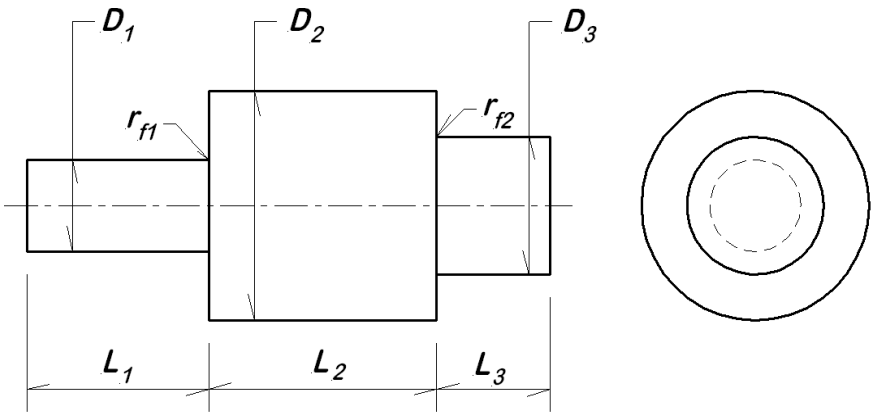

Figure 12.9: Roller Shaft

The following dimensional data apply to Figure 12.9.

$L_1 =$ 2050 mm $\quad D_1 =$ 280 mm

$L_2 =$ 2125 mm $\quad D_2 =$ 650 mm

$L_3 =$ 1850 mm $\quad D_3 =$ 320 mm

$r_{f_1} =$ 35 mm $\quad r_{f_2} =$ 25 mm

$G =$ 79.3 GPa

Breaking this problem down into parts, there are compliances to be calculated for five segments:

1. A simple cylinder of diameter D_1 and length L_1;

2. A shoulder increment for the transition from D_1 to D_2 with fillet radius r_{f_1};

3. A simple cylinder of diameter D_2 and length L_2;

4. A shoulder increment for the transition from D_2 to D_3 with fillet radius r_{f_2};

5. A simple cylinder of diameter D_3 and length L_3.

The calculations follow below, where all dimensions are expressed in meters:

1. For the first simple cylinder, the compliance is

$$C_1 = \frac{32L_1}{\pi G D_1^4} = \frac{32 \cdot 2.050}{\pi \cdot 79.3 \cdot 10^9 (0.280)^4} = 4.28399 \cdot 10^{-8} \text{ rad/(N-m)}$$

2. For the left shoulder increment, two ratios are first required:

$$D_2/D_1 = 0.650/0.280 = 2.32143$$

$$r_{f_1}/R_1 = 2\,(0.035)\,/\,(0.280) = 0.25$$

Going to the curves of Figure 12.8, the fillet radius ratio lies between two of the curves plotted, so interpolation is required. The result is

$$\frac{\Delta L}{D_1} = 0.07615065$$

$$\Delta L = (0.07615065)\,(0.280) = 2.13222 \cdot 10^{-2}$$

$$\Delta C_{12} = \frac{32 \cdot \Delta L}{\pi G D_1^4} = \frac{32 \cdot 2.13222 \cdot 10^{-2}}{\pi \cdot 79.3 \cdot 10^9 (0.280)^4} = 4.45581 \cdot 10^{-10} \text{ rad/(N-m)}$$

3. For the large diameter cylinder in the center,

$$C_3 = \frac{32 \cdot 2.125}{\pi \cdot 79.3 \cdot 10^9 (0.650)^4} = 1.52909 \cdot 10^{-9} \text{ rad/(N-m)}$$

4. For the right shoulder increment, beginning with the ratios

$$D_2/D_3 = 0.650/0.320 = 2.03125$$

$$r_{f_2}/R_3 = 2\,(0.025)\,/0.320 = 0.15625$$

Going again to the curves of Figure 12.8, interpolation is again required. The results are

$$\frac{\Delta L}{D_3} = 9.3569407 \cdot 10^{-2}$$

$$\Delta L = (9.3569407 \cdot 10^{-2})\,(0.320) = 2.99422 \cdot 10^{-2} \text{ m}$$

$$\Delta C_{23} = \frac{32 \cdot \Delta L}{\pi G D_3^4} = \frac{32 \cdot 2.99422 \cdot 10^{-2}}{\pi \cdot 79.3 \cdot 10^9 (0.320)^4} = 3.66784 \cdot 10^{-10} \text{ rad/(N-m)}$$

5. For the final simple cylinder, the compliance is

$$C_5 = \frac{32 \cdot 1.850}{\pi \cdot 79.3 \cdot 10^9 (0.320)^4} = 2.2662 \cdot 10^{-8} \text{ rad/(N-m)}$$

6. Finally, the overall compliance is the sum of the compliances,

$$\begin{aligned} C_{oa} &= C_1 + C_{12} + C_2 + C_{23} + C_3 \\ &= 4.45581 \cdot 10^{-10} + 4.45581 \cdot 10^{-10} + 1.52909 \cdot 10^{-9} \\ &\quad +3.66784 \cdot 10^{-10} + 2.2662 \cdot 10^{-8} \\ &= 2.544\,9 \cdot 10^{-8} \text{ rad/(N-m)} \end{aligned}$$

The overall stiffness is then found as the inverse of overall compliance:

$$K_{oa} = 1/C_{oa} = \tfrac{1}{2.544\,9 \cdot 10^{-8}} = 3.92943 \cdot 10^7 \text{ N-m/rad}$$

12.3.3 Damping

Energy losses come about in many forms, including viscous friction, Coulomb (dry) friction, internal material hysteresis, air drag, and other loss mechanisms. The only one of these phenomena that lends itself to mathematical analysis is viscous friction, so it is common practice to treat all losses as viscous losses. This is clearly a compromise, but it is a well established engineering practice with generally good results. Damping is considered in many previous problems, so the discussion here is limited to internal combustion engines, motors, and generators in particular. There are two fundamental types of damping to be considered: (1) internal damping, and (2) external damping.

Internal damping exists between adjacent stations in the torsional system, and is often called *station-to-station damping*. In the absence of specific damping devices included in the rotating assembly, station-to-station damping is usually only very slight in machinery components (steel shafts, etc.), and is largely due to internal material hysteresis. As such, it is very difficult to correctly model this type of damping. It is often neglected entirely, or only a small nominal viscous damping value is assigned.

External damping is often called *station-to-ground damping*, a term that describes the fact that it exists directly between the rotating station and the stationary ground. Station-to-ground damping includes torques such as the viscous friction in a fluid-film bearing, air-drag (windage) on the rotating assembly, and both viscous and dry friction in an engine piston cylinder.

Figure 12.10 shows two adjacent stations in a damped torsional system, numbered stations 1 and 2 for this discussion. The inertias at these two stations are J_1 and J_2, and the stiffness between them is denoted as K_{12}. Station-to-station damping is indicated with the coefficient c_{12}. Finally, station-to-ground damping is denoted with coefficient d_2, indicating that the damping at station 2 acts directly to ground.

There are other vibration limiting devices as well. Usually these involve additional iner-

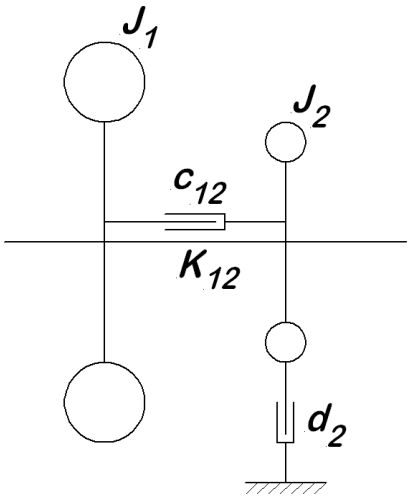

Figure 12.10: Schematic Representation for a Damped Torsional System

tias (with additional degrees of freedom) coupled to the station primary inertia, either by elastic or viscous action, or as a pendulum. The theory of the pendulum absorber is sketched as an example in Section 8.6.2. A detailed discussion of other damping mechanisms is beyond the scope of the present development, but the reader should be aware of their existence.

12.3.3.1 Theoretical Approach

Viscous friction is to be expected at every moving contact within the slider-crank mechanism. This includes

1. Main journal friction between the crank journal and the bearing,
2. Crank pin friction between the crank and the connecting rod,
3. Wrist pin friction between the connecting rod and the piston, and
4. Piston friction against the cylinder wall.

The virtual work of the viscous friction forces accounts for all of these,

$$\begin{aligned}
\delta W_{vf} &= -B_{cj}\dot{\theta}\,\delta\theta - B_{cp}\left(\dot{\theta}+\dot{\phi}\right)\,\delta\left(\theta+\phi\right) - B_{wp}\dot{\phi}\,\delta\phi - B_{cb}\dot{x}\,\delta\dot{x} \\
&= -\delta\theta\,\dot{\theta}\{B_{cj} + B_{cp}\left[1+K_{\phi}\left(\theta\right)\right]^2 + B_{wp}K_{\phi}^2\left(\theta\right) + B_{cb}K_x^2\left(\theta\right)\} \\
&= -B\left(\theta\right)\dot{\theta}\,\delta\theta
\end{aligned} \tag{12.38}$$

where the subscripts denote these quantities:

vf = total viscous friction in the slider-crank

cj = crank journal

cp = crank pin

wp = wrist pin

cb = cylinder bore

The final result is,

$$B(\theta) = B_{cj} + B_{cp}\left[1 + K_{\phi}(\theta)\right]^2 + B_{wp}K_{\phi}^2(\theta) + B_{cb}K_x^2(\theta) \tag{12.39}$$

where $B(\theta)$ is the overall, effective viscous coefficient for the slider-crank mechanism. In most cases it is exceedingly difficult to assign the individual values for B_{cj}, B_{cp}, B_{wp}, and B_{cb}, but in any event, the expression for $B(\theta)$, shows that the net viscous coefficient is position dependent, and identifies the weighting factors associated with each individual coefficient.

12.3.3.2 Engine Cylinder Damping

At a more practical level, for an engine cylinder, the station-to-ground losses are usually more significant than internal shaft losses. If internal shaft damping is neglected, it is reasonable to assign all losses to station-to-ground damping. In an internal combustion engine, the power available before friction losses is the *indicated power*, $P_{indicated}$, obtained from the $P-V$ diagram. The friction losses *at each engine cylinder* absorb some power, and from this a damping coefficient for the station-to-ground damping at each crank can be estimated according to

$$\begin{aligned} P_{loss-eng-cyl} &= \left(1-\eta_{eng}\right)P_{indicated} = \left(\Omega \cdot d_{eng}\right)\cdot\Omega = \Omega^2 \cdot d_{eng} \\ d_{eng-cyl} &= \frac{\left(1-\eta_{eng}\right)}{\Omega^2}P_{indicated} \end{aligned} \tag{12.40}$$

where η_{eng} is the mechanical efficiency of the engine, the ratio of shaft power to indicated power, and d_{eng} is the station-to-ground damping coefficient associated with the particular station representing the power cylinder. "Typical values for a modern automotive engine at wide-open or full throttle are 90 percent at speeds below about 30 to 40 rev/s (1800 to 2400 rev/min), decreasing to 75 percent at maximum rated speed. As the engine is throttled, mechanical efficiency decreases eventually to zero at idle operation" [4].

12.3.3.3 Generator Damping

Internal combustion engines are often used to drive electrical generators, making this a good place to discuss station-to-ground damping in generators. For a generator with electromechanical conversion efficiency η_{gen} (typically $\eta_{gen} \approx 95\%$.), the electromechanical losses (friction, windage, etc.) appear as station-to-ground damping with coefficient d_{gen}

$$\begin{aligned} P_{loss} &= \left(1 - \eta_{gen}\right) P_{shaft\,in} = (\Omega \cdot d_{gen}) \cdot \Omega = \Omega^2 \cdot d_{gen} \\ d_{gen} &= \frac{\left(1 - \eta_{gen}\right)}{\Omega^2} P_{shaft\,in} \end{aligned} \tag{12.41}$$

12.3.3.4 Electric Motor Damping

Although electric motors are rarely involved in parallel with internal combustion engines, they are often used to power equipment similar to that driven by engines. For an electric motor, typical efficiency is around $\eta_{mtr} \approx 96\%$, and the electromechanical losses (friction, windage, etc.) appear as a station to ground damper with coefficient d_{mtr},

$$\begin{aligned} P_{loss} &= (1 - \eta_{mtr})\, P_{elec\,in} = \Omega \cdot (\Omega\, d_{gen}) = d_{gen} \cdot \Omega^2 \\ d_{mtr} &= \frac{(1 - \eta_{mtr})}{\Omega^2} P_{elec\,in} \end{aligned} \tag{12.42}$$

The final example of this chapter describes a transient torsional vibration in an induction motor driven system during startup. This is a situation where the motor provides both positive and negative damping during different parts of the system acceleration. See Section 12.7 and Appendix A5.1 for more information regarding motor torque curves and associated damping.

12.3.4 Geared Systems

The use of gears is extremely common in mechanical systems, and their impact on torsional vibration analysis must be considered. To this end, consider Figure 12.11 (a) where a geared shaft system is shown. An equivalent single shaft system is shown in the Figure 12.11 (b), but how is this equivalent system developed?

In the two shaft system, the station rotations are all denoted by θ_i. The gear pair are J_{31} and J_{32}, with tooth numbers n_1 and n_2, respectively. Assuming completely rigid gears, the gear pair imposes a kinematic constraint between the two shaft rotations such that

$$n_1 \theta_{31} = n_2 \theta_{32} \tag{12.43}$$

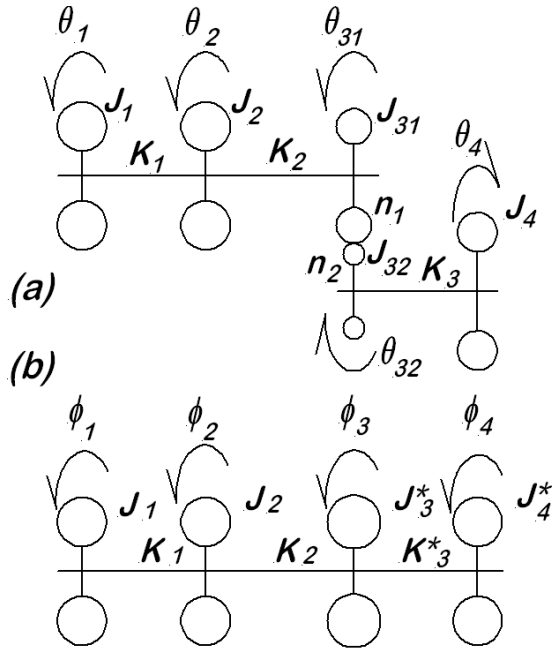

Figure 12.11: (a) Geared Shaft System, and (b) Equivalent Single Shaft System

because the pitch radii are proportional to the tooth numbers.

The analysis begins by writing the kinetic and strain energy expressions in the original coordinates, θ_i

$$\begin{aligned} T &= \frac{1}{2}\left(J_1\dot{\theta}_1^2 + J_2\dot{\theta}_2^2 + J_{31}\dot{\theta}_{31}^2 + J_{32}\dot{\theta}_{32}^2 + J_4\dot{\theta}_4^2\right) \\ &= \frac{1}{2}\left\{J_1\dot{\theta}_1^2 + J_2\dot{\theta}_2^2 + \dot{\theta}_3^2\left[J_{31} + J_{32}\left(\frac{n_1}{n_2}\right)^2\right] + J_4\dot{\theta}_4^2\right\} \\ &= \frac{1}{2}\left\{J_1\dot{\phi}_1^2 + J_2\dot{\phi}_2^2 + \dot{\phi}_3^2\left[J_{31} + J_{32}\left(\frac{n_1}{n_2}\right)^2\right] + J_4\left(\frac{n_1}{n_2}\right)^2\dot{\phi}_4^2\right\} \\ &= \frac{1}{2}\left\{J_1\dot{\phi}_1^2 + J_2\dot{\phi}_2^2 + J_3^*\dot{\phi}_3^2 + J_4^*\dot{\phi}_4^2\right\} \end{aligned} \tag{12.44}$$

$$\begin{aligned} V &= \frac{1}{2}\left[K_1\left(\theta_2 - \theta_1\right)^2 + K_2\left(\theta_{31} - \theta_2\right)^2 + K_3\left(\theta_4 - \theta_{32}\right)^2\right] \\ &= \frac{1}{2}\left\{K_1\left(\theta_2 - \theta_1\right)^2 + K_2\left(\theta_3 - \theta_2\right)^2 + K_3\left[\theta_4 - \theta_3\left(\frac{n_1}{n_2}\right)\right]^2\right\} \\ &= \frac{1}{2}\left[K_1\left(\phi_2 - \phi_1\right)^2 + K_2\left(\phi_3 - \phi_2\right)^2 + K_3\left(\frac{n_1}{n_2}\right)^2\left(\phi_4 - \phi_3\right)^2\right] \\ &= \frac{1}{2}\left[K_1\left(\phi_2 - \phi_1\right)^2 + K_2\left(\phi_3 - \phi_2\right)^2 + K_3^*\left(\phi_4 - \phi_3\right)^2\right] \end{aligned} \tag{12.45}$$

where the new angular variables, ϕ_i, are defined as

$$\phi_1 = \theta_1 \quad \phi_3 = \theta_{31}$$
$$\phi_2 = \theta_2 \quad \phi_4 = \frac{n_2}{n_1}\theta_4$$

and the new, equivalent single shaft system inertia and stiffness values are

$$J_1 = J_1 \qquad K_1 = K_1$$
$$J_2 = J_2 \qquad K_2 = K_2$$
$$J_3^* = J_{31} + J_{32}\left(\frac{n_1}{n_2}\right)^2 \qquad K_3^* = K_3\left(\frac{n_1}{n_2}\right)^2$$
$$J_4^* = J_4\left(\frac{n_1}{n_2}\right)^2$$

It is apparent that the final forms for the kinetic and potential energy functions, equations (12.44) and (12.45), describe exactly the system shown in Figure 12.11 (b). The effect of changing the variables as shown is to reduce the two shaft system to a single shaft system. Note that the parameters of the second shaft of the original system are multiplied by the square of the ratio of the tooth numbers in both instances. After this change of variables, every thing said about a single shaft system applies directly to the two shaft system.

12.3.5 Excitations

Excitations for torsional vibration may be broadly classified into two categories:

1. Start-up transients such as the torque required to begin rotation on a previously stopped machine, or the change in driving torque required when the load torque changes.

2. Periodic torque irregularities that continue through out the period of machine operation.

For most machinery that runs for extended time periods, the first is rarely a matter of engineering concern, but the second is far more important. This is because the underlying concern that motivates interest in torsional vibrations is usually fatigue. Events that happen only a few times cause relatively little fatigue damage. It is events that occur once per shaft revolution on a machine that runs day and night for months or even years that are cause for concern; these can rapidly accumulate a large number of fatigue cycle and result in failure.

In machinery driven by internal combustion engines (Diesel or gasoline), the pulsating torque applied to the crankshaft due to both combustion in the cylinder and inertial reactions in the slider-crank mechanism is a major exciter of torsional vibrations. In a steam or gas turbine, the flow interruptions that happen every time a rotor blade and stator blade pass causes torque pulsations, but these are usually small. Motion irregularities associated with imperfect gearing can also drive torsional vibrations. In the category of start-up transients, the torque developed in large synchronous motors during start-up is highly oscillatory and can be damaging.

Returning specifically to the pulsating torques acting on the crankshaft of an internal combustion engine, note first that in Appendix 5.2 there is a discussion of the thermodynamic cycle for the engine. Cylinder pressure modeling is discussed there, with a means provided to compute the cylinder pressure at every crank position. With that as background, the virtual work of the cylinder gas pressure and the resulting shaft torque are

$$\begin{aligned} \delta W_{\text{CylPress}} &= -P(\theta) A_P \, \delta x \\ &= -P(\theta) A_P K_x(\theta) \, \delta\theta \qquad (12.46) \\ T_{\text{CylPress}}(\theta) &= -P(\theta) A_P K_x(\theta) \qquad (12.47) \end{aligned}$$

where $P(\theta)$ is the net pressure acting on the piston (upper and lower faces combined), and A_P is the piston area.

There is a second effect that acts as a periodic torque on the crank due to the centripetal terms; this is evident below when the equations of motion are assembled, specifically equation (12.55). Typical gas pressure torque and the centripetal term are shown separately and in combination in Figure 12.12 for a two stroke cycle.

In Figure 12.12, the gas pressure torque is shown in broken line, the centripetal term is shown in dotted line, and the combined effects are shown in solid line. Note the negative torque on the crank as the piston moves toward the head, compressing the charge. This is followed by a very high positive torque pulse as the charge burns, producing high pressure in the cylinder.

Figure 12.12 is drawn for a two stroke engine cycle, for which both excitations have crank period 2π. If a four stroke engine were involved, the full thermodynamic period would be 4π. In either case, the combination of gas pressure torque and the centripetal term is

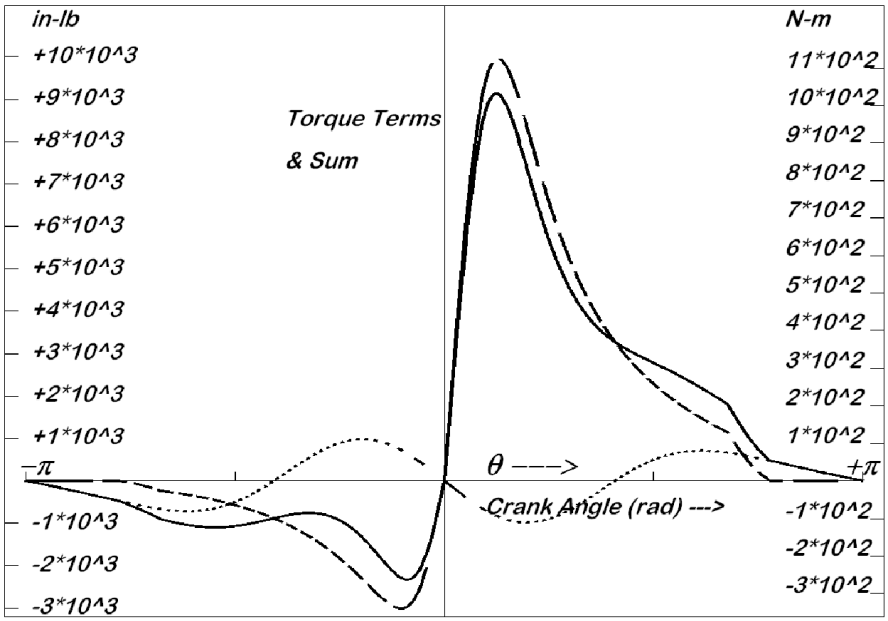

Figure 12.12: Gas Pressure Torque and Centripetal Term, Shown Separately and Combined

periodic and can be expanded in a finite Fourier series[1] of the form

$$\begin{aligned} f(\theta,\Omega) &= -\mathbb{C}(\theta)\,\Omega^2 - P(\theta)\,A_P K_x(\theta) \\ &= a_o + \sum_{n=1}\left[a_n\cos\left(\frac{2n\theta}{N_S}\right) + b_n\sin\left(\frac{2n\theta}{N_S}\right)\right] \end{aligned} \tag{12.48}$$

where, $N_S = 2$ for a two stroke cycle or $N_S = 4$ for a four stroke cycle. Note that $f(\theta,\Omega)$ depends on both the crank angle, θ, and the nominal crank speed, Ω. This is due to the $\Omega-$dependence of the centripetal term, and also due to the fact that the cylinder pressure is dependent on operating speed and load. The Fourier series coefficients, a_n and b_n, are determined numerically by direct application of the definitions:

$$a_o(\Omega) = \frac{1}{2\pi}\int_{-\pi}^{+\pi} f(\theta,\Omega)\,d\theta \tag{12.49}$$

$$a_n(\Omega) = \frac{1}{\pi}\int_{-\pi}^{+\pi} f(\theta,\Omega)\cos(n\theta)\,d\theta \tag{12.50}$$

$$b_n(\Omega) = \frac{1}{\pi}\int_{-\pi}^{+\pi} f(\theta,\Omega)\sin(n\theta)\,d\theta \tag{12.51}$$

[1]Fourier series is a mathematical method for the representation of periodic functions by an infinite series of sine and cosine functions. Interest here is in the truncated form of the series. It is a standard topic in advanced calculus, and the interested reader is referred to any familiar textbook for such a course.

These integrals can all be evaluated numerically without difficulty by modern computational techniques. The results for the present case are given in nondimensional form in Table 12.2. The series must converge (all finite series converge), but an inspection of the coefficients shows that it does not converge very rapidly at all. This is why so many terms are carried in the expansion. Calculations for other engines and different operating conditions may require more or fewer terms.

Table 12.2 (a) Nondimensional Fourier Series for Total Torque, $T/\left(A_p R P_{atm}\right)$ for $\Omega = 2500$ rpm

a_n	b_n
$a\left(0\right) = +3.04470 \cdot 10^{0}$	——
$a\left(1\right) = +3.67816 \cdot 10^{0}$	$b\left(1\right) = +6.68862 \cdot 10^{0}$
$a\left(2\right) = +4.15868 \cdot 10^{-1}$	$b\left(2\right) = +6.47618 \cdot 10^{0}$
$a\left(3\right) = -4.00345 \cdot 10^{-1}$	$b\left(3\right) = +4.26634 \cdot 10^{0}$
$a\left(4\right) = -7.89819 \cdot 10^{-1}$	$b\left(4\right) = +3.33233 \cdot 10^{0}$
$a\left(5\right) = -1.11116 \cdot 10^{0}$	$b\left(5\right) = +2.06466 \cdot 10^{0}$
$a\left(6\right) = -8.49334 \cdot 10^{-1}$	$b\left(6\right) = +1.19997 \cdot 10^{0}$
$a\left(7\right) = -7.60042 \cdot 10^{-1}$	$b\left(7\right) = +8.79285 \cdot 10^{-1}$
$a\left(8\right) = -6.43551 \cdot 10^{-1}$	$b\left(8\right) = +3.75118 \cdot 10^{-1}$
$a\left(9\right) = -3.99197 \cdot 10^{-1}$	$b\left(9\right) = +2.14287 \cdot 10^{-1}$
$a\left(10\right) = -3.51232 \cdot 10^{-1}$	$b\left(10\right) = +1.61168 \cdot 10^{-1}$
$a\left(11\right) = -2.51886 \cdot 10^{-1}$	$b\left(11\right) = -5.14934 \cdot 10^{-3}$
$a\left(12\right) = -1.49366 \cdot 10^{-1}$	$b\left(12\right) = +2.38505 \cdot 10^{-2}$

Table 12.2 (b) Nondimensional Fourier Series for Total Torque, $T/(A_p R P_{atm})$ for $\Omega = 2500$ rpm

a_n	b_n
$a(13) = -1.49592 \cdot 10^{-1}$	$b(13) = +1.15206 \cdot 10^{-2}$
$a(14) = -9.69245 \cdot 10^{-2}$	$b(14) = -3.70592 \cdot 10^{-2}$
$a(15) = -6.83833 \cdot 10^{-2}$	$b(15) = +3.80683 \cdot 10^{-3}$
$a(16) = -7.49451 \cdot 10^{-2}$	$b(16) = -7.62766 \cdot 10^{-3}$
$a(17) = -5.12380 \cdot 10^{-2}$	$b(17) = -1.82137 \cdot 10^{-2}$
$a(18) = -4.46764 \cdot 10^{-2}$	$b(18) = +1.34230 \cdot 10^{-3}$
$a(19) = -4.71629 \cdot 10^{-2}$	$b(19) = -3.33606 \cdot 10^{-3}$
$a(20) = -3.88422 \cdot 10^{-2}$	$b(20) = -7.56337 \cdot 10^{-3}$
$a(21) = -3.31780 \cdot 10^{-2}$	$b(21) = -5.89669 \cdot 10^{-4}$
$a(22) = -3.57665 \cdot 10^{-2}$	$b(22) = +2.41530 \cdot 10^{-3}$
$a(23) = -3.26035 \cdot 10^{-2}$	$b(23) = -6.29426 \cdot 10^{-3}$
$a(24) = -2.47499 \cdot 10^{-2}$	$b(25) = +4.01337 \cdot 10^{-4}$
$a(25) = -3.05082 \cdot 10^{-2}$	$b(25) = +4.50032 \cdot 10^{-3}$

12.4 System Equations of Motion

There are three distinct approaches to developing the system equations of motion, each with its own advantages. When properly applied, all are exactly equivalent, so it really makes no difference which method is used. The possibilities are these:

1. Application of the Lagrange form for the equations of motion is a rigorously correct approach to developing the system equations of motion for a multidegree of freedom torsional system. It is a bit cumbersome in terms of the required algebra, but it correctly develops all of the necessary terms. Note particularly that, where a slider-crank machine is involved, the Lagrange approach does correctly develop the centripetal term, although it is somewhat round about in doing so.

2. Because of the close-coupled nature of the typical crankshaft connected engine, it is feasible to consider each crank throw and the associated mechanism as a single degree of freedom mechanism. This permits the application of Eksergian's form

for the equation of motion for each single crank. The station-to-station coupling through the shaft must then be properly taken into account.

3. Newton's Second Law can be used to formulate the equations of motion, although this can be very awkward when slider-cranks are involved because all of the internal forces remain in the formulation. This method is not recommended.

12.4.1 Nonlinear Equations of Motion

In order to be more specific, consider a rotating assembly comprised of many stations, each station being one of three types. Assume that station type i represents a slider-crank station with associated station-to-ground damping, station type j represents a rotating mass such as a coupling or flywheel that has no connection to ground, and station type k represents a driven load with station-to-ground damping. No station-to-station damping is included here. Then the equations of motion are generally of the form

$$\mathbb{I}(\theta_i)\,\ddot{\theta}_i + \mathbb{C}(\theta_i)\,\dot{\theta}_i^2 + d_i\dot{\theta}_i + K_{i-1}(\theta_i - \theta_{i-1}) + K_i(\theta_i - \theta_{i+1}) = Q_i \tag{12.52}$$

$$J_j\ddot{\theta}_j + K_{j-1}(\theta_j - \theta_{j-1}) + K_j(\theta_j - \theta_{j+1}) = 0 \tag{12.53}$$

$$J_k\ddot{\theta}_k + d_k\dot{\theta}_k + K_{k-1}(\theta_k - \theta_{k-1}) + K_k(\theta_k - \theta_{k+1}) = Q_k \tag{12.54}$$

The generalized forces for each type are;

- Station type i, the gas pressure torque term, T_{CylPress};
- Station type j there is no generalized force because this station does not couple to the outside; and
- Station type k, the generalized force is whatever form is required to specify the load torque.

The total number of equations of motion is always equal to the number of degrees of freedom.

12.4.2 Linearization

As discussed previously, the variable generalized inertia in the first type of equation is replaced with an average value, determined as described by Biezeno and Grammel [1].

Thus $\mathbb{I}(\theta_i)$ becomes simply J_i. The other step necessary for this approach to linearization is to move the centripetal term to the right side of the equation of motion. All of this has no impact on the second and third equation types above, but the equation of motion for the slider-crank station becomes

$$J_i\ddot{\theta}_i + d_i\dot{\theta}_i + K_{i-1}(\theta_i - \theta_{i-1}) + K_i(\theta_i - \theta_{i+1}) = T_{\text{CylPress}}(\theta_i) - \mathbb{C}(\theta_i)\Omega^2 \tag{12.55}$$

Return to an idea introduced at the end of the introductory example, the concept of the rotating reference mark and the nominal angle turned by the shaft, Ωt. The instantaneous angular position of any station, $\theta_i(t)$ is

$$\theta_i(t) = \Omega t + \vartheta_i(t) \tag{12.56}$$

where

Ωt is the gross (or average) angle turned by the shaft, and

$\vartheta_i(t)$ is the oscillatory rotational motion.

(The Greek letter ϑ is known as *script theta,* an alternate form for the usual θ.) The gross angle is ever increasing with time, while the oscillatory term always remains small. In places where the difference of station angles (or their time derivatives) is important, such as the stiffness torque term, the gross rotations cancel, leaving only the oscillatory terms. On the other hand, in places where it is only the station rotation that is used, such as in calculating the cylinder pressure torque or the centripetal coefficient, the gross rotation is dominant and the oscillatory terms are insignificant. For this reason, after dropping small quantities, it is appropriate to write the equation of motion for the slider-crank station as

$$\begin{aligned} & J_i\ddot{\vartheta}_i + d_i\dot{\vartheta}_i + K_{i-1}(\vartheta_i - \vartheta_{i-1}) + K_i(\vartheta_i - \vartheta_{i+1}) \\ = \; & P_{\text{CylPress}}(\Omega t) - \mathbb{C}(\Omega t)\Omega^2 - d_i\Omega \\ = \; & a_o - d_i\Omega + \sum_{n=1}\left[a_n\cos\left(\frac{2n\theta}{N_S}\right) + b_n\sin\left(\frac{2n\theta}{N_S}\right)\right] \end{aligned} \tag{12.57}$$

In the last line, the cylinder pressure and the centripetal term are indicated as expanded in a single Fourier series. With these modifications, the linearized equations of motion (for any number of stations) are cast in matrix form as

$$\lceil J \rfloor \left\{\ddot{\vartheta}\right\} + \lceil D \rfloor \left\{\dot{\vartheta}\right\} + [K]\{\vartheta\} = \{T(\Omega t)\} \tag{12.58}$$

where

$\lceil J \rfloor$ is the diagonal matrix of constant mass moment of inertia values

$\lceil D \rfloor$ is the diagonal matrix of station-to-ground damping coefficients

$[K]$ is the triple band diagonal matrix of stiffness values

$\{T(\Omega t)\}$ is the column vector of all terms required to make up the excitation.

The direct proportionality between the gross angle turned and time means that the right side may be considered as a function of either the gross angle or the time.

12.4.3 Steady State Motion

It is necessary to say a few words about the meaning of the term *steady state* in the machinery context. In the more common context of structural vibrations, the term steady state implies that the displacements involved in the motion are periodic. In view of the ever increasing rotation angles involved in a rotating machine experiencing torsional vibration, such an understanding of steady state has no meaning. Instead, the term must be re-interpreted.

In the machinery torsional vibration context, the angles do not repeat, but the angular velocities do. Thus, in the machinery torsional context, *the term steady state must be understood to imply periodicity in the angular velocities.* This is a fundamental distinction, and without it, the whole concept is meaningless.

If the system is periodic in the angular velocities, then the average value of the angular velocity must be constant. Constant average angular velocity means that the average torque on the system must be zero. Momentarily the system may experience either positive or negative acceleration so long as the long term average is exactly zero. This has implications for the balance of energy flowing into and out of the system.

Carefully considered, the statements above indicate that steady state motion involves a combination of two types of motion:

1. Steady rotation, that is rotation at constant speed, and

2. Oscillatory motion, meaning rotation that fluctuates, sometimes positive and sometimes negative, but always about a zero average value.

These two cases are explored further below.

12.4.3.1 Steady Twist

A part of the steady state motion occurs at constant speed, the nominal shaft speed Ω. If all parts of the system are rotating with the same speed, then the system is rotating like a rigid body. However, this does not mean that it has the undeformed shape. Typically it is a twisted form, because power is being transferred from the prime mover to the driven load. Transmission of power requires both speed and torque, and transmission of torque requires a twist to develop the necessary internal stresses to carry the torque. In short then, this means that the twist in each section of the shaft must carry the torque transferred through that section. But how much is that torque? Consider a simple example.

Imagine an induction motor connected through a length of shafting to a fan with the system running in steady state. Exactly how fast does it run, and how much power is delivered to the fan? The motor has a known rated speed (the speed at which it develops rated power), and the fan is rated for a specified flow rate and power at a given speed. There are characteristic torque-speed curves available for both the motor and the fan, and if they are overlaid, the running speed is, at least approximately, the speed at which the fan torque demand curve intersects the motor torque-speed curve. This is approximate only because system friction losses are not taken into account, but it serves to demonstrate the idea of power balance. If the system is properly engineered, the running speed is near the rated speed for both machines, but it is always the system power flow that determines the actual operating speed.

For a typical machinery torsional vibration analysis, the operating speed is specified, but the steady torques must still be exactly balanced. In words, this means that the input torque from the prime mover (internal combustion engine, electric motor, etc.) must be exactly equal to the sum of the load torque and all friction torques at the specified operating speed. Note that only station-to-ground damping torques needs to be taken into account here; the static form of the rotating assembly means that station-to-station damping has no effect on the twisted shape.

If the shaft nominal speed is specified, all of the station-to-ground torques can be immediately evaluated. The zero net torque condition then provides a relation between the (1) the input torque from the prime mover, (2) the output torque(s) to the driven load(s), and (3) the total station-to-ground friction torques. For each specific problem, the analyst must choose a value for either the input or output torque, with the other determined by the torque sum relation. With the shaft speed and input and output torques assigned, the torque in each shaft segment is then readily evaluated. From this, the angle of twist in each shaft segment is determined. This is described in more detail in connection with the damped forced solution by the Holzer method and then demonstrated later in an extended example problem in Section 12.5.

12.4.3.2 Oscillatory Motion

The remaining portion of the steady state motion is periodic with zero mean value. As such, it is expanded in a Fourier series as

$$\{\vartheta_{osc}(t)\} = \sum_{n=1}^{N_{ord}} \left[\{A_n\} \cos\left(\frac{2n\Omega t}{N_S}\right) + \{B_n\} \sin\left(\frac{2n\Omega t}{N_S}\right) \right] \tag{12.59}$$

where

N_{ord} is the maximum order number

N_S is the number of strokes in the thermodynamic cycle.

The pair of solutions associated with each value of n result from excitation terms at that same frequency. The methods from Chapter 11 are then applicable to the solution.

12.4.4 Pendulum Vibration Absorber

In the case study of Section 11.10, the Frahm vibration absorber was demonstrated. As shown there, the motion of the primary mass can be completely stopped by proper tuning, but proper tuning requires a specific combination of mass and stiffness for the absorber. For rotating systems that operate at variable speeds, and for internal combustion engines in particular, the required stiffness must vary with speed, a capability not found in typical elastic systems. However, the effective stiffness of a rotating pendulum proves to be ideal as demonstrated below.

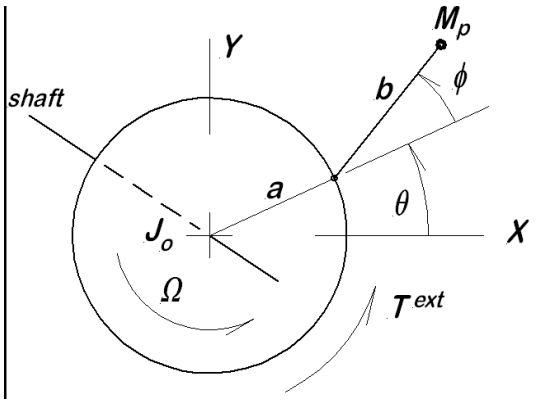

Figure 12.13: Pendulum Torsional Absorber

Figure 12.13 shows a primary inertia (J_o) fitted with a pendulum torsional absorber. The pendulum is considered as a point mass (M_p) with length b from the point of attachment at radius a. With proper choices for a and b, this relatively small mass, M_p, can dramatically alter the effective inertia of the station as shown below. Attention here is focused on this one station with the associated pendulum, a system with two degrees of freedom (θ, ϕ), but it must be realized that this station also interacts with adjacent stations through the shafting to either side.

Consider first the kinematics of the pendulum mass. The position equations are

$$x_p = a\cos\theta + b\cos(\theta+\phi) \tag{12.60}$$
$$y_p = a\sin\theta + b\sin(\theta+\phi) \tag{12.61}$$

The velocity components are obtained by differentiation,

$$\dot{x}_p = -a\dot{\theta}\sin\theta - b\left(\dot{\theta}+\dot{\phi}\right)\sin(\theta+\phi) \tag{12.62}$$
$$\dot{y}_p = a\dot{\theta}\cos\theta + b\left(\dot{\theta}+\dot{\phi}\right)\cos(\theta+\phi) \tag{12.63}$$

Now write the system kinetic energy as

$$\begin{aligned} T &= (1/2)\,J_o\dot{\theta}^2 + (1/2)\,M_p\left(\dot{x}_p^2+\dot{y}_p^2\right) \\ &= (1/2)\,J_o\dot{\theta}^2 + (1/2)\,M_p\{\left[-a\dot{\theta}\sin\theta - b\left(\dot{\theta}+\dot{\phi}\right)\sin(\theta+\phi)\right]^2 \\ &\quad + \left[a\dot{\theta}\cos\theta + b\left(\dot{\theta}+\dot{\phi}\right)\cos(\theta+\phi)\right]^2\} \end{aligned} \tag{12.64}$$

At this point, the stage is set for the development of the left side of the Lagrange equations of motion. The process is lengthy but straight forward; the details are left as an exercise.

The virtual work expression is required in order to establish the generalized forces associated with this system. Note that while there may well be an external torque applied (such as through a slider-crank in an internal combustion engine), there are no external forces acting directly on the pendulum since gravity is ignored. Thus the virtual work expression is

$$\delta W = T^{ext}\delta\theta \tag{12.65}$$

From this, it is evident that the generalized forces are

$$Q_\theta = T^{ext} \tag{12.66}$$
$$Q_\phi = 0 \tag{12.67}$$

The complete system equations of motion are then developed by the process of linearization described previously. The Lagrange equation involving derivatives with respect to

ϕ and $\dot{\phi}$ is of particular interest first. With the understanding that ϕ is always small, it is true that $\sin\phi \approx \phi$, $\cos\phi \approx 1$, and terms of higher order in ϕ and $\dot{\phi}$ may be dropped, so the equation reduces to

$$\ddot{\theta}(a+b) + \ddot{\phi}b + \dot{\theta}^2 a\phi = 0 \tag{12.68}$$

(The zero on the right is because $Q_\phi = 0$.) Notice that this is a differential equation describing the pendulum motion in relation to the motion of the primary station.

In describing absorber operation, the focus is on steady state conditions are rather than transient operation. As shown in previous sections, the externally exciting torque may be a periodic function with terms at frequencies that are many multiples of the shaft operating speed. For simplicity, and because the absorber is only effective against a single frequency, the exciting torque is here taken as

$$T^{ext}(t) = T_n \sin(n\Omega t) \tag{12.69}$$

where Ω is the shaft speed and n is a multiplier, usually an integer or half-integer. Recall that, for linear systems such as considered here, the response to a sinusoid is a sinusoid at the same frequency. If there is no damping, the response is in phase (or directly out of phase) with the excitation. Thus the form assumed for the excitation implies that steady state motions for the primary station and for the pendulum will be of the forms

$$\theta(t) = \Omega t + \Theta \sin(n\Omega t) \tag{12.70}$$

$$\phi(t) = \Phi \sin(n\Omega t) \tag{12.71}$$

where both Θ and Φ are always small. When these form are substituted back into the reduced equation of motion, equation (12.68), and again dropping terms of higher order in small quantities, the result can be solved for Φ in terms of Θ

$$\Phi = \Theta \frac{n^2(a+b)}{a - n^2 b} \tag{12.72}$$

This provides the amplitude of the pendulum motion, relative to the primary station, in terms of the amplitude of motion at the primary station. This is a very important result; notice what it says about the possibility of making Φ very large by the choice of a and b.

Now, return to the equation of motion for the primary mass, the Lagrange equation based on derivatives with respect to θ and $\dot{\theta}$. After linearization similar to that done for the $\phi-$equation, the equation of motion is

$$\left[J_o + M_p(a+b)^2\right]\ddot{\theta} + M_p b(a+b)\ddot{\phi} = T^{ext} \tag{12.73}$$

The first term suggest that the pendulum acts as simply clamped to the primary station in the fully extended position, but further exploration is required. When the motions are

again assumed sinusoidal at frequency $n\Omega$, the station equation of motion is

$$-n^2\Omega^2 \left[J_o + M_p \frac{a\,(a+b)^2}{a - n^2 b} \right] \Theta = T_n \tag{12.74}$$

This last expression, equation (12.74) is solvable for the amplitude of motion of the primary mass **at the frequency nΩ only.**

Look at the possibilities presented by the pendulum absorber, depending on the choices for a and b:

1. If the a and b are such that $a = n^2 b$, the effect is to make the pendulum appear to the overall system at the frequency $n\Omega$ as an infinite inertia. This must completely stop motion at this frequency at the primary station at the expense of violent motion of the pendulum.

2. If $a > n^2 b$, the pendulum appears to the remainder of the system like a large positive inertia added to the primary station.

3. If $a < n^2 b$, the pendulum appears to the rest of the system like a large **negative inertia** added to the primary station inertia.

Consider an example for which the order of concern is $n = 5$ with $a = 50$ mm. The system is then tuned to completely stop motion at that frequency when $b = a/n^2 = 50/5^2 = 2.0$ mm. (Such a short pendulum length may present problems in itself, but that is not the focus of this example). With the parameters fixed, $a = 50$ mm and $b = 2$ mm, then consider what happens for $n = 4$ and $n = 6$. At $n = 4$, the factor $a - n^2 b = 50 - 4^2 \cdot 2 = 18.0$ appears in the denominator. At $n = 6$, the factor $a - n^2 b = 50 - 6^2 \cdot 2 = -22.0$ appears in the denominator. Since the actual excitation, in most cases, includes all orders, all three of these cases are included. Thus the single pendulum will affect the system steady state response in different ways, depending upon which excitation order is being considered. In order to block motion in several orders at a particular station, several pendula can be located at that station. The overall effect can be quite complicated.

12.4.5 Systems With Many Degrees of Freedom

By this point, the reader should be concerned about more complicated systems, rotating machinery systems with many degrees of freedom. The modal method of Chapter 11 seems to offer a solution approach, but with many degrees of freedom, this could get very complicated. Such systems have characteristic polynomials of very high degree, and

while there is always the zero root pair, the degree of the remaining polynomial remains very large. How are such systems to be analyzed?

To gain a greater appreciation for the nature of the problem, consider the following Figure 12.14 that shows a torsional schematic for an actual small, portable, two cylinder diesel engine driven generator.

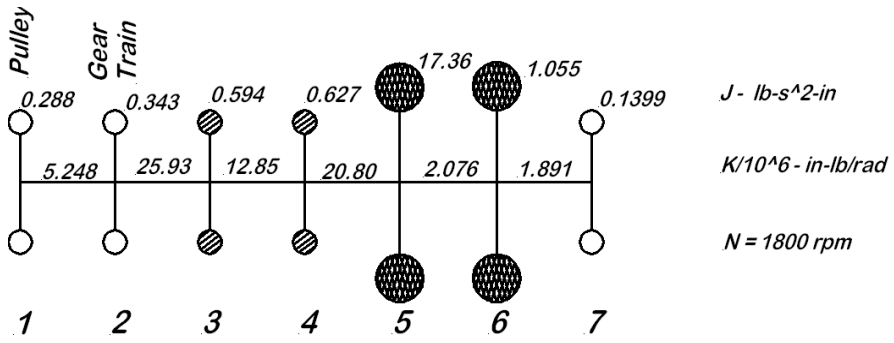

Figure 12.14: Torsional Schematic for Two Cylinder Diesel Generator Set

Note that there are seven stations, indicating seven degrees of freedom. These components are as follows:

1. Front Pulley – This pulley powers a belt driving the cooling fan, water pump, and perhaps a small alternator for battery charging.
2. Gear Train – The gear train drives the cam shaft and the fuel injection system.
3. Crank Throw – This is the first crank station, representing the slider-crank mechanism for the first cylinder.
4. Crank Throw – This is the second crank station, representing the slider-crank mechanism for the second cylinder.
5. Flywheel – Note the flywheel mass moment of inertia in comparison to others in the system.
6. Generator Rotor – This is the main generator rotor that carries the rotating field winding.
7. Exciter Rotor – This is the rotor of a small permanent magnet generator that generates DC power for the main field winding.

For even this relatively simple machine, the characteristic polynomial is of degree seven in ω_n^2. Then think about a large engine-generator set with a V-type twenty cylinder engine

with many details (fan, water pump, oil pump, cam shaft drive, supercharger, etc.) to be modelled. Detailed torsional models as large as 250 stations are required for major machinery trains. Such detailed models are created for very expensive machines to be built and operated at great expense and risk. How can they be analyzed for torsional natural frequencies and other significant torsional motion aspects?

Consider a brief digression to look at the history of this problem. In the early history of mankind, all work was done by human effort. This was then supplemented by the use of animal power (horses, oxen, etc.). Eventually water power and wind power were incorporated. With all of these power sources, movement remained relatively slow. This situation began to change in late 17^{th} century Europe with the application of steam power. Initially speeds remained quite low, but it was not long before they began to increase. With increasing speeds, there were many industrial accidents. Some were things like boiler explosions, but there were also unexplained machines wrecks. In these latter, it seemed that when certain natural speed limits were exceeded, the machines would simply vibrate wildly and self-destruct. Of course, in retrospect, it is evident that the machines were being pushed to approach a resonance condition in which vibration grows rapidly until something breaks.

There are two primary modes of vibration for any machine: (1) torsional vibration, such as that being discussed here, and (2) lateral vibration. Lateral vibration is associated with motion perpendicular to a shaft axis of rotation. It transmits great oscillating forces to the bearings which in turn cause the machine structure and supports to vibrate. Human beings usually sense lateral vibration simply by feel; they become aware of the shaking. In contrast, torsional vibration is usually not felt at all, and people rarely sense it until there is a failure. The major exception to this last statement occurs when there is a gear set involved which causes the torsional motion to drive lateral vibration that can be detected.

There was little progress in understanding torsional resonance until the early 20^{th} century. The tachometers of German U-boats examined after WW I were marked with red zones, speed ranges where the engine must not be permitted to operate for any extended time period; these evidently marked torsional critical speeds. Evidently the engines were able to pass through these zones, provided they accelerated through rapidly, but they must not be permitted to dwell at those speeds. Shortly after WW I, in 1921, Heinrich Holzer published the first solid mathematical analysis of torsional vibrations [5]. In that book, he showed a tabular calculation that could predict the critical speeds (natural frequencies) of rotating machinery, and also how to calculate the forced response. Holzer's original work was in tabular form for hand calculation, but it has since been cast in matrix form by others. It remains significant to the present day because (1) it is applicable to both free and forced vibration, (2) it can readily include viscous damping, and (3) it is easily adapted to computer implementation.

With the linearized equations of motion in hand, consider the means available for solving

these equations. There are three major possibilities: (1) simulation, (2) direct eigensolution and modal analysis, and (3) the Holzer technique. The first two are presented in Chapters 7, 8, and 11. The Holzer technique is developed in the next section, and demonstrated in the final example of this chapter.

12.5 Holzer Response Calculations

Holzer presented an approach applicable to both the free and forced torsional analysis of machine trains. The inclusion of viscous damping does not significantly complicate the forced vibration analysis, which is an added benefit. There is some difference between the free and forced analyses, with the forced analysis conceptually more involved.

12.5.1 Holzer Free Vibration Analysis

In the form presented in this section, the Holzer method is applicable only to free vibration (a more general form, applicable to the damped, forced problem is presented in the following section). In this formulation, the Holzer calculation is a process for determining the natural frequencies of a close-coupled chain such is found in many machinery trains. (Close coupled means that each element is connected only to its nearest neighbors to either side. This concept was previously introduced in Section 8.6.1. It should be kept in mind that close-coupling always implies a triple band diagonal stiffness matrix.) The necessary equations are derived below, with the associated figures as needed. A schematic for the system under consideration is shown in Figure 12.15.

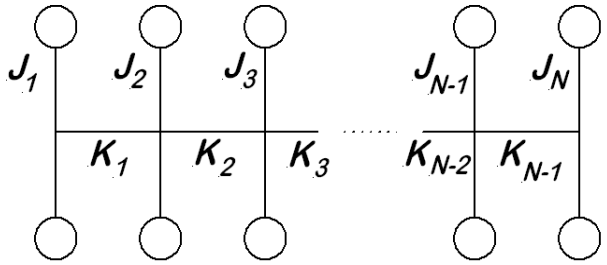

Figure 12.15: N-Station Rotating System

Note at this point that there is no torque to the left of station 1 and no torque to the right of station N; these are the free ends of the system. *These two observations are the essential boundary conditions that determine the natural frequencies of the system as shown below.*

In Figure 12.16, the system is shown broken in three places, to create two free body diagrams. On the left, isolating the first rotor, and several stations to the right, where the i^{th} shaft segment and the $(i+1)^{th}$ rotor are isolated.

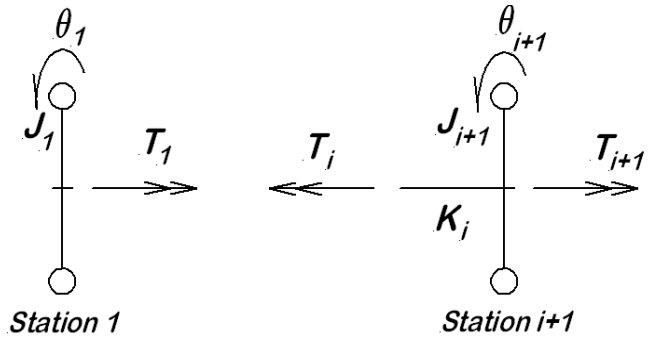

Figure 12.16: Free Body Diagrams for Stations 1 and $i+1$

Looking at the typical station, $i+1$, and the shaft to the left of it, it is evident that

$$T_i = K_i\left(\theta_{i+1} - \theta_i\right) \tag{12.75}$$

$$J_{i+1}\ddot{\theta}_{i+1} = T_{i+1} - T_i \tag{12.76}$$

The first of these can be solved for θ_{i+1} in terms of θ_i and T_i, while the second is solved for T_{i+1} in terms of θ_i and T_i, with the assumption that all motion is sinusoidal in time at frequency Ω:

$$\theta_{i+1} = \theta_i + \frac{1}{K_i}T_i \tag{12.77}$$

$$\begin{aligned} T_{i+1} &= T_i - \Omega^2 J_{i+1}\theta_{i+1} \\ &= \left(1 - \Omega^2 J_{i+1}/K_i\right)T_i - \Omega^2 J_{i+1}\theta_i \end{aligned} \tag{12.78}$$

These two results are cast in what is called *transfer matrix* form,

$$\left\{\begin{array}{c}\theta_{i+1}\\ T_{i+1}\end{array}\right\}^R = \left[\begin{array}{cc}1 & \frac{1}{K_i}\\ -\Omega^2 J_{i+1} & 1-\Omega^2 J_{i+1}/K_i\end{array}\right]\left\{\begin{array}{c}\theta_i\\ T_i\end{array}\right\}^R \tag{12.79}$$

The subscripts i and $i+1$ denote the station numbers involved while the superscript R is a reminder that these are values to the right side of each station. The torque to the right of the last station is often called the *residual*, a name that indicates that this is a quantity to be driven to zero. Using this matrix equation, if θ_i and T_i^R are known, then the calculation of those same quantities at the next station is easily accomplished to give θ_{i+1} and T_{i+1}^R.

The only question remaining is how to start the process, to obtain the first station vector, col $\left(\theta_1, T_1^R\right)$. Referring back to the image on the left side of Figure 12.15, consider the free body diagram for the first station. Note that there is no shaft extending to the left, and hence **no torque applied to the left side of the first station**. For this station, the applicable equations are

$$\theta_1 = \theta_1 \tag{12.80}$$
$$J_1\ddot{\theta}_1 = T_1 \tag{12.81}$$

where the first equation, $\theta_1 = \theta_1$, simply means that θ_1 has whatever value is assigned for it; it is an arbitrary choice. The first station vector can be readily constructed from these equations as

$$\left\{ \begin{array}{c} \theta_1 \\ T_1 \end{array} \right\}^R = \theta_1 \left\{ \begin{array}{c} 1 \\ -\Omega^2 J_1 \end{array} \right\} \tag{12.82}$$

The usual practice is to take $\theta_1 = 1.0$, however any nonzero constant will work just as well. From this point forward, assume that $\theta_1 = 1.0$. The application of these equations is as follows:

1. Assume a value for the frequency, Ω, that is thought to be below the natural frequency, and calculate the station rotations and right side torques for the entire train by repeated application of the equations above (this is well suited to computer implementation);
2. If the residual is zero, then the assumed value for Ω is in fact a natural frequency ω_n because all the boundary conditions are satisfied; this rarely happens. If the residual is nonzero, make note of the sign of the residual and repeat step 1 above for a greater value of Ω. **This process is continued until there is a change in the sign of the residual;**
3. When the residual changes sign, this indicates that the last frequency step has crossed one or more natural frequencies. If this happens on the j^{th} trial value for frequency, then there are one or more natural frequencies in the interval $[\Omega_{j-1}, \Omega_j]$. The root is then said to be *bracketed,* so go to step 4 below.
4. With the root bracketed, all that remains is to refine the bracket to whatever degree is required. This is usually done using the method of bisection or by linear interpolation.
5. With the root refined to the required degree, the rotations calculated for that final, refined natural frequency estimate are the components of the eigenvector for that mode.

This calculation is demonstrated in an example later in this chapter.

12.5.1.1 Why Does the Holzer Calculation Work?

A reader may inquire just why the Holzer calculation described above produces the system natural frequencies. What does this sequence of matrix multiplications to evaluate a residual torque have to do with finding the roots of the characteristic equation?

Consider a rotating system consisting of a shaft in bearings with several mounted inertias (stations). It has been established, both in this and the previous chapters that the *free vibration of an elastic system occurs at the system natural frequencies*. It is important to note that the phrase *at the system natural frequencies* is actual saying that **free vibration is at, and only at, the system natural frequencies**. It does not include motion at any frequencies other than the system natural frequencies, ω_n, where $n = 0, 1, 2, \ldots$.

Now it is also true that **systems can be forced to vibrate at any frequency**. The key word there is *forced*, as opposed to *free*, vibrations. Suppose a particular system is observed to be vibrating at a frequency $\Omega \neq \omega_n$. Then it must immediately be concluded that an external agent is driving the system at the frequency Ω; *this cannot be a free vibration*. In the Holzer calculation, the initial torque is specified to be zero to the left of the first station. The calculation process leads to an evaluation of the residual torque, the torque that must be present on the second free end of the shaft to cause the system to vibrate at the assumed frequency. If, and only if, the residual torque happens to be zero, then (1) the motion is a free vibration, and (2) the frequency of motion is a natural frequency.

The Holzer calculation is a method for evaluating the residual torque, which is equivalent to evaluating a polynomial expression in Ω. The Holzer calculation evaluates a polynomial of the form

$$\begin{aligned} T_{resid}(\Omega) &= c_0 + c_1\Omega + c_2\Omega^2 + \cdots + c_m\Omega^m \\ &= C_H(\Omega - r_1)(\Omega - r_2)(\cdots)(\Omega - r_m) \end{aligned} \tag{12.83}$$

where the $r_1, r_2, \ldots r_m$ are the values of Ω for which T_{resid} is zero. Now return to the process for evaluating the characteristic polynomial (which is the result of expanding the characteristic determinant). The value of the characteristic polynomial is P,

$$P(\Omega) = C_C(\Omega - \omega_1)(\Omega - \omega_2)(\cdots)(\Omega - \omega_m) \tag{12.84}$$

The polynomials $P(\Omega)$ and $T_{resid}(\Omega)$ are of the same degree, and they have the same roots (remember, $T_{resid}(\Omega) = 0$ at $\Omega = \omega_n$ which is the necessary condition for a free vibration), so they are essentially the same polynomial, with the exception of the constant scale factors C_H and C_C, which have no effect on the root locations. This is why the Holzer calculation, focused on finding the frequency value associated with zero residual torque, is effectively a method for finding the roots of the characteristic polynomial.

12.5.2 Damped Forced Analysis

To obtain the maximum information about the system response requires that a forced response calculation be made. Only the steady state solution is of interest; it is understood that the transient solution disappears from the motion rather rapidly. In engine driven systems, damping plays a major role in limiting the torsional vibration response, so it is included in the formulation given here. If damping is to be omitted, it is only necessary to set all of the damping coefficients to zero, but this does not change the nature of the calculation at all.

The forced Holzer calculation is limited to periodic excitations, so it is here assumed that the equations of motion can be written in terms of a Fourier series with vector coefficients:

$$\begin{aligned} & \lceil J \rfloor \left\{ \ddot{\theta} \right\} + \left([C] + \lceil D \rfloor \right) \left\{ \dot{\theta} \right\} + [K] \{\theta\} \\ = \; & \{a_o\} - \Omega \{d\} \\ & + \sum_{n=1} \left[\{a_n\} \cos\left(\frac{2n\Omega t}{N_S} \right) + \{b_n\} \sin\left(\frac{2n\Omega t}{N_S} \right) \right] \end{aligned} \tag{12.85}$$

where

$\lceil J \rfloor$ is a diagonal matrix of mass moment of inertia values;

$[C]$ is a triple band diagonal matrix of station-to-station damping coefficients;

$\lceil D \rfloor$ is a diagonal matrix of station-to-ground damping coefficients;

$[K]$ is a triple band diagonal matrix of stiffness values;

$\{a_n\}$ is a vector of torque cosine coefficients;

$\{b_n\}$ is a vector of torque sine coefficients;

$\{a_o\}$ is a vector of constant torque terms;

$\{d\}$ is a vector of the station-to-ground damping coefficients.

The right side consists of two constant vectors and also of many vectors with sinusoidal time dependence. This form is chosen with the implicit understanding that one or more slider-crank machines are involved, and that N_S is the number of strokes in the thermodynamic cycle. Separate solutions are required for (1) the constant vector, and (2) each pair of sinusoidal vectors.

Consider for a moment the right side vector $\{a_o\}$. This vector consists of all the externally applied steady torques acting on the system, both driving and driven. In the typical

situation, one of the first entries is the driving torque from the prime mover (T_{PM}) and the one of the last entries is the load torque from the driven load ($-T_L$). If the prime mover is a multicylinder engine, then there are several driving torques, one for each crank station in the engine. These torques, and those arising from station-to-ground damping, are the only steady torques that act on the system.

At every station, the complete rotation consists of several terms, one of which is always the rotation of the reference mark. Thus for the steady forced response, the complete rotation vector, $\{\theta(t)\}$, is written as

$$\{\theta(t)\} = \Omega t \begin{Bmatrix} 1 \\ 1 \\ 1 \\ \vdots \end{Bmatrix} + \begin{Bmatrix} 0 \\ -\phi_2 \\ -\phi_3 \\ \vdots \end{Bmatrix} + \sum_{n=1}^{N} \{A_n\} \cos\left(\frac{2n\Omega t}{N_S}\right) + \{B_n\} \sin\left(\frac{2n\Omega t}{N_S}\right) \tag{12.86}$$

The first term is the steady rotation of the entire system with the rotating reference mark. The second term describes the static twists required to transmit the steady torque required at each shaft section. The first two terms are comprised entirely of constants, and often called the *static solution*. The remaining terms, those in the summation, are called the *dynamic response*.

12.5.2.1 Static Solution

After the transient solution is decayed to zero, the particular solution that remains is non-oscillatory; it is simply a twisted form rotating at the nominal shaft speed Ω:

$$\{\theta_{static}\} = \Omega t \begin{Bmatrix} 1 \\ 1 \\ 1 \\ \vdots \end{Bmatrix} + \begin{Bmatrix} 0 \\ -\phi_2 \\ -\phi_3 \\ \vdots \end{Bmatrix} \tag{12.87}$$

It is important to understand what is being said here about the nature of the steady solution. In particular, note that

1. All stations have the same speed, Ω; there are no angular accelerations associated with this part of the solution.

2. For a system comprised of N_{sta}, there are really only $N_{sta}-1$ angular displacement variables to be determined, the steady twist angles ϕ_2, $\phi_3, \ldots$.

The first point means that there is no dynamic twisting (only steady twist), and hence no possibility for fatigue damage except as the result of a nonzero mean stress superimposed on the oscillatory stresses. As indicated, in the form for the static solution, there is nothing unknown about the steady position of the first station in the static solution. This leaves only the twist angles for the remaining stations to be determined.

When the assumed solution form is substituted and the equations rearranged, the result is

$$[K]\begin{Bmatrix} 0 \\ \phi_2 \\ \phi_3 \\ \vdots \end{Bmatrix} = \begin{Bmatrix} T_{PM} - d_1\Omega \\ -d_2\Omega \\ \vdots \\ -T_L - d_3\Omega \end{Bmatrix} \tag{12.88}$$

If the prime mover steady torque is assumed known, this is a system N_{sta} equations with unknowns including the load torque and the $N_{sta}-1$ angles ϕ_2, $\phi_3, \ldots$. If the load torque is assumed to be specified, then the prime mover torque becomes one of the N_{sta} unknowns. Note that this equation cannot be solved by simply inverting the stiffness matrix $[K]$ because it is singular. Even so, the system is solvable algebraically for the unknowns indicated.

12.5.2.2 Dynamic Solution

Recall the way steady state solutions were obtained in Chapter 11 for sinusoidal excitation terms; a similar process is used here. The solution for a typical pair of excitation terms is developed in some detail, and then the complete set of solutions is indicated by summation.

For the forced solution, including excitation torques and the possibility of damping, the Holzer transfer relations are developed a second time with those additional considerations included. For that purpose consider Figure 12.17.

Figure 12.17 (a) shows a shaft segment that has both stiffness (k_i) and viscous damping (c_i); the same total torque, T_i, acts on both ends of the shaft. On the right, Figure 12.17 (b), the typical inertia has station–to–ground viscous damping, indicated by the coefficient d_{i+1}, and there is also the external torque $T_{i+1}^E(t)$ acting on the station.

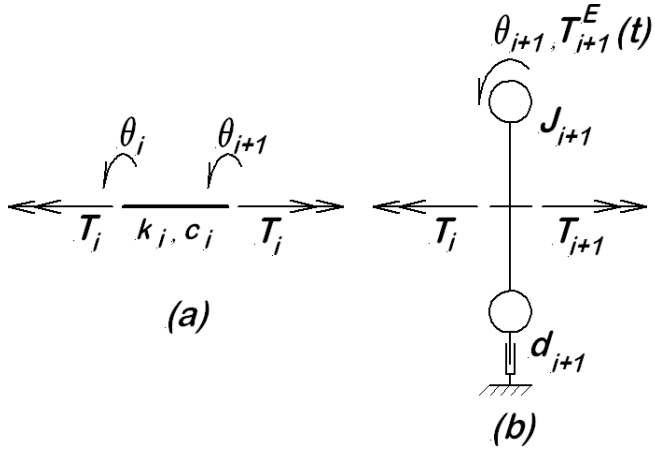

Figure 12.17: Typical Damped Shaft Segment and Station

12.5.2.3 Shaft Equations

Consider first the shaft segment from station i to station $i+1$ as shown in Figure 12.17 (a). The governing equations for this shaft segment are often called *field equations*. This shaft is characterized by the stiffness k_i and the station–to–station damping coefficient c_i. The internal torque in this shaft is T_i,

$$T_i = k_i \left(\theta_{i+1} - \theta_i\right) + c_i \left(\dot{\theta}_{i+1} - \dot{\theta}_i\right) \tag{12.89}$$

All variables are assumed to have sinusoidal time dependence at frequency $n\Omega$, so that

$$T_i = T_{i_C} \cos\left(n\Omega t\right) + T_{i_S} \sin\left(n\Omega t\right) \tag{12.90}$$
$$\theta_i = \theta_{i_C} \cos\left(n\Omega t\right) + \theta_{i_S} \sin\left(n\Omega t\right) \tag{12.91}$$
$$\theta_{i+1} = \theta_{i+1_C} \cos\left(n\Omega t\right) + \theta_{i+1_S} \sin\left(n\Omega t\right) \tag{12.92}$$

When these forms are substituted into the torque relation for the shaft, the cosine and sine terms separate to give two relations:

$$T_{i_C} = k_i \left(\theta_{i+1_C} - \theta_{i_C}\right) + n\Omega c_i \left(\theta_{i+1_S} - \theta_{i_S}\right) \tag{12.93}$$
$$T_{i_S} = k_i \left(\theta_{i+1_S} - \theta_{i_S}\right) - n\Omega c_i \left(\theta_{i+1_C} - \theta_{i_C}\right) \tag{12.94}$$

Considering for present T_{i_C}, T_{i_S}, θ_{i_C}, and θ_{i_S} as known values, the next step is to determine θ_{i+1_C} and θ_{i+1_S}. Equations (12.93) and (12.94) are re–arranged to read

$$\begin{bmatrix} k_i & n\Omega c_i \\ -n\Omega c_i & k_i \end{bmatrix} \begin{Bmatrix} \theta_{i+1_C} \\ \theta_{i+1_S} \end{Bmatrix} = \begin{bmatrix} k_i & n\Omega c_i \\ -n\Omega c_i & k_i \end{bmatrix} \begin{Bmatrix} \theta_{i_C} \\ \theta_{i_S} \end{Bmatrix} + \begin{Bmatrix} T_{i_C} \\ T_{i_S} \end{Bmatrix} \tag{12.95}$$

Solving for the θ_{i+1} components gives

$$\left\{ \begin{array}{c} \theta_{i+1_C} \\ \theta_{i+1_S} \end{array} \right\} = \left\{ \begin{array}{c} \theta_{i_C} \\ \theta_{i_S} \end{array} \right\} + \frac{1}{Det_1} \left[\begin{array}{cc} k_i & -n\Omega c_i \\ n\Omega c_i & k_i \end{array} \right] \left\{ \begin{array}{c} T_{i_C} \\ T_{i_S} \end{array} \right\} \tag{12.96}$$

where $Det_1 = k_i^2 + n^2\Omega^2 c_i^2$. Finally, separating these two equations gives

$$\theta_{i+1_C} = \theta_{i_C} + \frac{1}{Det_1}\left(k_i T_{i_C} - n\Omega c_i T_{i_S}\right) \tag{12.97}$$

$$\theta_{i+1_S} = \theta_{i_S} + \frac{1}{Det_1}\left(k_i T_{i_S} + n\Omega c_i T_{i_C}\right) \tag{12.98}$$

This completes the development of the transfer relation for this shaft segment.

12.5.2.4 Station Equations

The second part, Figure 12.17 (b), shows the $i+1^{th}$ station, having mass moment of inertia J_{i+1}, angular displacement θ_{i+1}, station–to–ground damping d_{i+1}, and an external torque T^E_{i+1}. The relations governing this element are often called *point relations* in the literature. The equation of motion for this station is

$$J_{i+1}\ddot{\theta}_{i+1} = T^E_{i+1} + T_{i+1} - T_i - d_{i+1}\dot{\theta}_{i+1} \tag{12.99}$$

This equation is solved for the internal torque to the right of the station,

$$T_{i+1} = J_{i+1}\ddot{\theta}_{i+1} + T_i + d_{i+1}\dot{\theta}_{i+1} - T^E_{i+1} \tag{12.100}$$

As before, all quantities are sinusoidal in time, so that the equation separates into two equations, one in cosine terms and the second in sine terms. The final result is

$$T_{i+1_C} = -n^2\Omega^2 J_{i+1}\theta_{i+1_C} + T_{i_C} + n\Omega d_{i+1}\theta_{i+1_S} - T^E_{i+1_C} \tag{12.101}$$

$$T_{i+1_S} = -n^2\Omega^2 J_{i+1}\theta_{i+1_S} + T_{i_S} - n\Omega d_{i+1}\theta_{i+1_C} - T^E_{i+1_S} \tag{12.102}$$

Summary of Shaft and Station Relations

$$Det_1 = k_i^2 + n^2\Omega^2 c_i \tag{12.103}$$

$$\theta_{i+1_C} = \theta_{i_C} + \frac{1}{Det_1}\left(k_i T_{i_C} - n\Omega c_i T_{i_S}\right) \tag{12.104}$$

$$\theta_{i+1_S} = \theta_{i_S} + \frac{1}{Det_1}\left(k_i T_{i_S} + n\Omega c_i T_{i_C}\right) \tag{12.105}$$

$$T_{i+1_C} = -n^2\Omega^2 J_{i+1}\theta_{i+1_C} + T_{i_C} + n\Omega d_{i+1}\theta_{i+1_S} - T^E_{i+1_C} \tag{12.106}$$

$$T_{i+1_S} = -n^2\Omega^2 J_{i+1}\theta_{i+1_S} + T_{i_S} - n\Omega d_{i+1}\theta_{i+1_C} - T^E_{i+1_S} \tag{12.107}$$

In application, starting with values for θ_{i_C}, θ_{i_S}, T_{i_C}, and T_{i_S}, the first two equations are used to evaluate θ_{i+1_C} and θ_{i+1_S}. Then these values are used in the last two equations to evaluate T_{i+1_C} and T_{i+1_S}. In this way the Holzer calculation is propagated down the length of the machine train.

A simple subroutine for implementing the Holzer process for a forced, damped solution is shown below. Note that the first station requires separate handling for reasons presented in the discussion following the code.

```
SUB HOLZER

    ! Holzer calculation routine
    ! nord = n-order, 1,2,...NNord
    ! n   = station number, 1,2, ... NNsta
    ! Values of rc(1) and rs(1) must be previously assigned
    ! tc,ts = cosine & sine components of shaft internal torque
    ! rc,rs = cosine & sine components of station rotations
    ! Tec,Tes = cosine & sine components of external torque on station
    ! First Station ...
    tc(1)=-Tec(1)+nord*Omega*DD(1)*rs(1)-(nord*Omega)^2*JJ(1)*rc(1)
    ts(1)=-Tes(1)-nord*Omega*DD(1)*rc(1)-(nord*Omega)^2*JJ(1)*rs(1)
    ! All Other Stations ...
    FOR n=2 to NNsta
        n1=n-1
        det1=KK(n1)^2+(nord*Omega*CC(n1))^2
        rc(n)=rc(n1)+(KK(n1)*tc(n1)-nord*Omega*CC(n1)*ts(n1))/det1
        rs(n)=rs(n1)+(nord*Omega*CC(n1)*tc(n1)+KK(n1)*ts(n1))/det1
        tc(n)=tc(n1)-Tec(n)+nord*Omega*DD(n)*rs(n)&
              &-(nord*Omega)^2*JJ(n)*rc(n)
        ts(n)=ts(n1)-Tes(n)-nord*Omega*DD(n)*rc(n)&
              &-(nord*Omega)^2*JJ(n)*rs(n)
    NEXT n
END SUB
```

12.5.2.5 Boundary Conditions

The boundary conditions of interest for machinery problems are that there is no shaft torque to the left of the first station and no shaft torque to the right of the last station. Consider the first station where there is no torque to the left of the station. The equation of motion is

$$J_1\ddot{\theta}_1 = T_1 + T_1^E - d_1\dot{\theta}_1 \tag{12.108}$$

After substitution of the harmonic forms and separation this becomes

$$T_{1_C} = -n^2\Omega^2 J_1\theta_{1_C} + n\Omega d_1\theta_{1_S} - T^E_{1_C} \tag{12.109}$$
$$T_{1_S} = -n^2\Omega^2 J_1\theta_{1_S} - n\Omega d_1\theta_{1_C} - T^E_{1_S} \tag{12.110}$$

The question that remains is how the initial values, θ_{1_C} and θ_{1_S}, are to be assigned.

The first boundary condition is immediately satisfied in the way that equation (12.93) is formulated because no torque from the left is included. The boundary condition that remains to be satisfied is the vanishing of the torque on the right side of the last station. To that end, consider three cases:

1. $\theta_{1_C} = 1.0$ and $\theta_{1_S} = 0.0$ and *with all externally applied torques set to zero.* When the Holzer calculation process is executed for the entire system with these starting conditions, the residual torques are saved as $T_{N_C} = \widehat{T}_1$ and $T_{N_S} = \widehat{T}_4$.
2. $\theta_{1_C} = 0.0$ and $\theta_{1_S} = 1.0$ and *with all externally applied torques set to zero.* The Holzer calculation is made a second time for the whole assembly, this time with these revised starting conditions, and the residual torques saved as $T_{N_C} = \widehat{T}_2$ and $T_{N_S} = \widehat{T}_5$.
3. $\theta_{1_C} = 0.0$ and $\theta_{1_S} = 0.0$ and *with all externally applied torques set to their actual values.* When the Holzer calculation is made the third time with these starting values, the residual torques are saved as $T_{N_C} = \widehat{T}_3$ and $T_{N_S} = \widehat{T}_6$.

For any nonzero values of θ_{1_C} and θ_{1_S} and with the externally applied torques at their actual values, the combined residual torque values are linear combinations of the residual torques for each case, thus

$$T_{N_C} = \theta_{1_C}\widehat{T}_1 + \theta_{1_S}\widehat{T}_2 + \widehat{T}_3 \tag{12.111}$$
$$T_{N_S} = \theta_{1_C}\widehat{T}_4 + \theta_{1_S}\widehat{T}_5 + \widehat{T}_6 \tag{12.112}$$

The second boundary condition requirement is that the residual torques be zero, so that

$$0 = \theta_{1_C}\widehat{T}_1 + \theta_{1_S}\widehat{T}_2 + \widehat{T}_3 \tag{12.113}$$
$$0 = \theta_{1_C}\widehat{T}_4 + \theta_{1_S}\widehat{T}_5 + \widehat{T}_6 \tag{12.114}$$

This is a system of equations solvable for θ_{1_C} and θ_{1_S}. The solution is

$$\begin{Bmatrix} \theta_{1_C} \\ \theta_{1_S} \end{Bmatrix} = \frac{1}{Det\widehat{T}} \begin{bmatrix} -\widehat{T}_5 & \widehat{T}_2 \\ \widehat{T}_4 & -\widehat{T}_1 \end{bmatrix} \begin{Bmatrix} \widehat{T}_3 \\ \widehat{T}_6 \end{Bmatrix} \tag{12.115}$$

where $Det\widehat{T} = \widehat{T}_1\widehat{T}_5 - \widehat{T}_2\widehat{T}_4$. This calculation gives the required values for the initial angular displacements, and the actual angular displacement column can then be generated by applying the initial values thus determined simultaneously with the externally applied torques. Note that this process requires a total of four applications of the Holzer calculation to the system model for the complete process. A block of code implementing these steps, including all four calls to subroutine Holzer, is shown below:

Code For Application of Forced, Damped Holzer Calculation

```
FOR nord=1 to NNord
    MAT Tec=zer                   ! externally applied torque-cosine comp
    MAT Tes=zer                   ! externally applied torque-sine comp
    !  ********* Case 1 **********
    rc(1)=1
    rs(1)=0
    CALL HOLZER
    T1=tc(NNsta)
    T4=ts(NNsta)
    !  ********* Case 2 **********
    rc(1)=0
    rs(1)=1
    CALL HOLZER
    T2=tc(NNsta)
    T5=ts(NNsta)
    !  ********* Case 3 **********
    rc(1)=0
    rs(1)=0
    ! Any external excitations (Tec,Tes) present should be evaluated here,
    ! such as excitations due to slider crank machines, etc.
    Tec(1)=Tcoefa(nord)
    Tes(1)=Tcoefb(nord)
    CALL HOLZER
    T3=tc(NNsta)
    T6=ts(NNsta)
    ! Evaluate initial conditions
    detT=T1*T5-T2*T4
    rc(1)=(T2*T6-T3*T5)/detT
    rs(1)=(T3*T4-T1*T6)/detT
    PRINT  "Computed initial values"
    PRINT  "      rc(1) = ";rc(1);" radians"
    PRINT  "      rs(1) = ";rs(1);" radians"
    !  ********* Case 4 **********
    CALL HOLZER
```



```
    ! uses rc(1) & rs(1) computed as above, with whatever
    ! external torques act as well to return actual dynamic shape
    FOR jsta=1 to NNsta     ! cos & sin coef for dynamic ang displ at each station
        LET sc(nord,jsta)=rc(jsta)
        LET ss(nord,jsta)=rs(jsta)
    NEXT jsta
    hd1$="   Station              Angular Displacements"
    hd2$="      No.       Cos Coeff          Sin Coeff       Magnitude"
    img$="      ##      +#.#####^^^^+#.#####^^^^#.#####^^^^<##########"
    PRINT  hd1$
    PRINT  hd2$
    FOR n=1 to NNsta              ! output shape for this order
        PRINT using img$: n,rc(n),rs(n),sqr(rc(n)^2+rs(n)^2)"
    NEXT n
NEXT nord
```

In the code above,

`nord` = typical order number, n

`NNord` = maximum order number, N_{ord}

`jsta` = a typical station number, j

`NNsta` = maximum station number, N_{sta}

`rc(), rs()` = cosine and sine rotation coefficients (θ_{j_C}, θ_{j_S})

`tc(), ts()` = cosine and sine torque coefficients (T_{i+1_C}, T_{i+1_S})

This completes the development of the Holzer forced response calculation. With this technique, the forced response of models of essentially any size can be calculated with modest computer resources. It remains a valuable engineering tool in the 21^{st} century, despite advances in other numerical approaches related to the eigenproblem and modal analysis.

12.6 Three Station Example Problem

To demonstrate the Holzer forced response calculation, consider a three station example consisting of a single cylinder internal combustion engine, a flywheel, and a generator load. While this is a relatively small system, it provides and opportunity to exercise all

aspects of the Holzer solution. The detailed data for this system are given in Appendix 5.2.1., Tables A5.2, A5.3, and A5.4.

12.6.1 Model

The complete three station example system is shown in Figure 12.18, and includes:

(1) an internal combustion engine cylinder operating on a two stroke thermodynamic cycle with variable effective moment of inertia $\mathbb{I}(\theta_1)$;

(2) a flywheel with constant mass moment of inertia J_{2o};

(3) a passive load, the generator rotor with mass moment of inertia J_{3o} that only absorbs steady torque without developing any oscillatory torques.

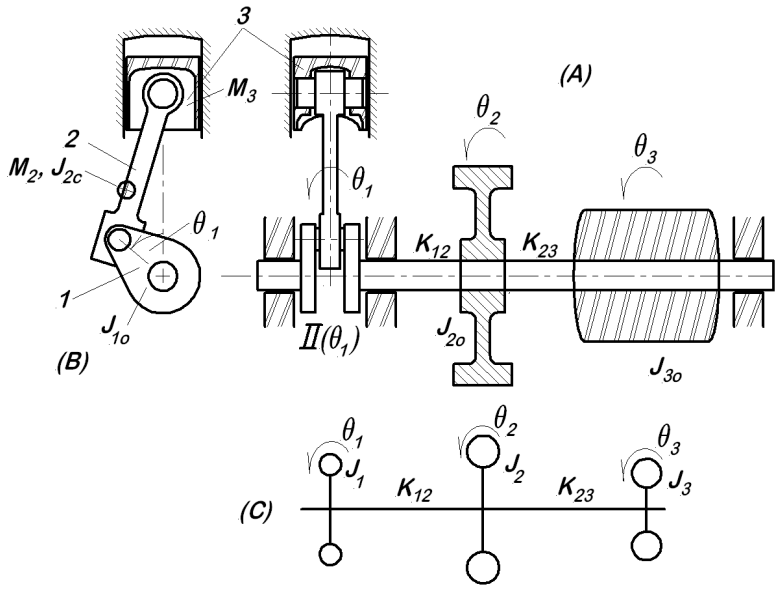

Figure 12.18: System Pictorial & Schematic

There are three views in Figure 12.18:

(A) At the upper right, the main system pictorial side view showing all three components much as they actually appear in section views;

(B) At the upper left, a pictorial detail of the engine cylinder (slider-crank) mechanism;

(C) At the lower right, the simple schematic representation used for torsional vibration analysis.

Note that, in (A), the inertia of the engine cylinder mechanism is denoted as $\mathbb{I}(\theta_1)$, a reminder that this is a variable inertia system. However, in (C), that same station is identified with J_1, a constant mass moment of inertia. This approximation is accomplished using the average value calculation given in equation (12.26). The data for that calculation are all listed in Table A5.2. This transformation from a variable inertia to a fixed average value is one of the important insights in this example.

The primary components of the engine (the slider-crank mechanism) are shown in Figure 12.18 (A). The subscripts used are **1** for quantities related to the crank, **2** for the connecting rod, and **3** for items related to the piston. All of the usual assumptions and notations used regarding slider-crank mechanisms in Chapter 2 are assumed to apply here. The crank rotation θ_1 describes the motion of all components in the slider-crank mechanism through the appropriate kinematic relations. The flywheel rotation is θ_2 and the rotation of the load inertia is given by the angle θ_3. The three bearings play no role other than supporting the system. The system physical data are summarized in Table 12.3, and the graphic results shown previously in Figures 12.4 and 12.12 are specific to this example problem.

Table 12.3 Three Station System Parameters

	USC Units		SI Units	
$K_{12} =$	$2.1550 \cdot 10^6$	in-lb/rad	$2.4348 \cdot 10^5$	N-m/rad
$K_{23} =$	$1.2400 \cdot 10^6$	in-lb/rad	$1.4010 \cdot 10^5$	N-m/rad
$J_{1o} =$	0.0876605414	lb-s^2-in	$9.9043 \cdot 10^{-3}$	kg-m^2
$J_{2o} =$	15.320	lb-s^2-in	1.7131	kg-m^2
$J_{3o} =$	1.020	lb-s^2-in	0.11524	kg-m^2
$d_1 =$	0.56333	in-lb-s	0.063647	N-m-s
$d_2 =$	0.0	in-lb-s	0.0	N-m-s
$d_3 =$	0.30160	in-lb-s	0.03475	N-m-s

$N = 2500$ rpm $\longrightarrow \Omega = 261.79939$ rad/s

12.6.2 Free Vibration Analysis - Holzer

In the search for the system natural frequencies using USC units, first assume a starting frequency estimate $\Omega = 10$ rad/s (this value is assumed only to make the calculations

easy). Then for the first station, the station vector is

$$\left\{ \begin{array}{c} \theta_1 \\ T_1 \end{array} \right\}^R = \left\{ \begin{array}{c} 1 \\ -(10)^2 (0.0876605414) \end{array} \right\} = \left\{ \begin{array}{c} 1 \\ -8.76605414 \end{array} \right\} \tag{12.116}$$

and for the second and third stations, the station vectors are

$$\begin{aligned} \left\{ \begin{array}{c} \theta_2 \\ T_2 \end{array} \right\}^R &= \left[\begin{array}{cc} 1 & \frac{1}{2.1550 \cdot 10^6} \\ -10^2 (15.320) & 1 - 10^2 \frac{15.320}{2.1550 \cdot 10^6} \end{array} \right] \left\{ \begin{array}{c} 1 \\ -8.76605414 \end{array} \right\} \\ &= \left\{ \begin{array}{c} 0.99999593 \\ -1540.76 \end{array} \right\} \end{aligned} \tag{12.117}$$

$$\begin{aligned} \left\{ \begin{array}{c} \theta_3 \\ T_3 \end{array} \right\}^R &= \left[\begin{array}{cc} 1 & \frac{1}{1.24 \cdot 10^6} \\ -10^2 (1.020) & 1 - 10^2 \frac{1.020}{1.24 \cdot 10^6} \end{array} \right] \left\{ \begin{array}{c} 0.99999593 \\ -1540.76 \end{array} \right\} \\ &= \left\{ \begin{array}{c} 0.99875 \\ -1642.6 \end{array} \right\} \end{aligned} \tag{12.118}$$

Since the final torque is negative (-1642.6), it is evident that $\Omega = 10$ rad/s is **not** a system natural frequency. Further searching starting at $\Omega = 50$ rad/s and increasing in steps of $\Delta\Omega = 50$ rad/s shows sign changes in the intervals shown in Table 12.4.

Table 12.4 Natural Frequencies for Three Station Example

Holzer Search Results			Refined Natural Frequency Estimate rad/s
$\Omega = 1100$ rad/s	residual $= -1256387.3$	$\longrightarrow$	$\omega_1 \approx 1137.5133$
$\Omega = 1150$ rad/s	residual $= +418202.24$		
$\Omega = 4950$ rad/s	residual $= +64743506$	$\longrightarrow$	$\omega_2 \approx 4971.8142$
$\Omega = 5000$ rad/s	residual $= -83654251$		

These are close to the results found by solving for the roots of the characteristic polynomial, but the agreement is not exact. This is due to the fact that only a single step

of root refinement is used for this example. Here the root is estimated by linear interpolation between the two points where the sign change is noted. A more detailed and exact refinement is possible by simply using the Holzer process to repeatedly evaluate the residual while projecting a new estimate at each iteration of the refinement. It should be emphasized that the same values for the natural frequencies are obtained (to within rounding errors) no matter which system of units is used for the calculation.

12.6.3 Integrity Check

The running speed of the machine was given as $N = 2500$ rpm ($\Omega = 261.79939$ rad/s), so there is a temptation to say that the two nonzero natural frequencies are well above the running speed so there is no possibility for resonance. To say this is, however, short sighted. Recall that the principal source of torsional excitation in this machine is an engine operating on the pulsating torque from a slider-crank mechanism, and that there are resultant excitations at integer multiples of the operating speed all the way to infinity. Can the system be resonant with any of these higher order excitations from the slider-crank mechanism? *(In the case of the two stroke cycle considered here, only integer multiples of the crank speed need to be considered, that is,* 1Ω, 2Ω, 3Ω, *... . For a four stroke cycle, there are also half orders to be considered, so that the potentially resonant speeds are* $\frac{1}{2}\Omega$, 1Ω, $\frac{3}{2}\Omega$, 2Ω, *...)* Thus the question comes down to, "Are any of the multiples of the crank speed close to the natural frequencies?"

A search for excitation orders that coincide, either exactly or approximately, can be readily added to the computer code for this calculation. Based on a window width of 10% of the calculated natural frequency, the results are as shown in Table 12.5.

Table 12.5 Excitation Order Coincidence Table

Natural Frequency rad/s	Order Number	Excitation Frequency rad/s	Frequency Ratio
$\omega_1 = 1138.4816$	$4 \times$ shaft speed =	1047.1976	$4 \cdot \Omega/\omega_1 = 0.9199$
$\omega_2 = 4972.3856$	$18 \times$ shaft speed =	4712.3890	$18 \cdot \Omega/\omega_2 = 0.9477$
$\omega_2 = 4972.3856$	$19 \times$ shaft speed =	4974.1884	$19 \cdot \Omega/\omega_2 = 1.0004^*$
$\omega_2 = 4972.3856$	$20 \times$ shaft speed =	5235.9878	$20 \cdot \Omega/\omega_2 = 1.0530$

$*$ As the table shows, there is one extremely high risk situation associated with the 19^{th} order excitation that is almost exactly resonant.

At this point, there are two questions that the analyst must ask:

(1) What is the strength of the 19^{th} order excitation?

(2) What is the significance of being even slightly off the natural frequency?

The first question is fairly easy to address. Returning to the nondimensional Fourier series coefficient list, Table 12.2, it is clear that the two components of the 19^{th} harmonic torque are $a\,(19) = -4.71629 \cdot 10^{-2}$ and $b\,(19) = -3.33606 \cdot 10^{-3}$. For comparison, the average torque is $a\,(0) = +3.04470 \cdot 10^{0}$, so the 19^{th} harmonic is considerably smaller, but how to evaluate the significance of this is not entirely clear at this point.

Regarding the second question, the answer depends to some extent as to how much damping is thought to be in the system. If the system is extremely lightly damped, the resonance peak will be very sharp and narrow, and an excitation a few percent away from the natural frequency will have only a small effect. On the other hand, if there is more damping present, while the peak response is reduced, the width of the peak is significantly increased. This means that the same degree of separation between the excitation and the natural frequency is less effective in reducing the response.

Faced with the facts that the excitation is not negligible, the coincidence is almost exact, and the amount of damping completely indeterminate, the conscientious analyst must choose to go on to do a forced response calculation to determine just how significant this coincidence is in this case. Similar considerations apply to the other coincidences listed in Table 12.5. If there were no significant coincidences, the system would, in many cases, be declared acceptable at this point without further analysis.

12.6.4 Damped Forced Response Calculation

The forced response solution is where the real information about dynamic stresses and strains in the shafting is determined. It is vital to include all sources of excitation and all damping in order to obtain a realistic result. This is the real basis for evaluating the design integrity, but it requires additional effort.

12.6.4.1 Static Solution

For this example, the steady term in the prime mover torque is the term a_o in the the Fourier series expansion of the engine torque. For this example, the engine power is specified, so that $a_o = 1136.1$ in-lb $= 128.36$ N-m is a known value which leaves the load torque and the static twists to be determined by the equilibrium conditions by applying

equation (12.88).

$$[K]\left\{\begin{array}{c}0\\-\phi_2\\-\phi_3\end{array}\right\}=\left\{\begin{array}{c}a_o-d_1\Omega\\0\\-T_L-d_3\Omega\end{array}\right\} \tag{12.119}$$

This is a system three equations in the three unknowns ϕ_2, ϕ_3, and T_L. As noted previously, this cannot be solved by simply inverting the $[K]$ matrix; $[K]$ is singular and has no inverse. Even so, the system of three equations is solvable for the indicated unknowns. When the numbers are substituted and the solutions developed, the results are

$$\phi_2 = 4.58778\cdot 10^{-4} \text{ rad} \tag{12.120}$$
$$\phi_3 = 1.25609\cdot 10^{-3} \text{ rad} \tag{12.121}$$
$$T_L = 909.707 \text{ in-lb } = 102.78 \text{ N-m} \tag{12.122}$$

With these results, the generator output is

$$P_{gen-out}=\Omega T_L = 2.3816\cdot 10^5 \text{ in-lb/s} = 26.908 \text{ kW} \tag{12.123}$$

12.6.4.2 Dynamic Solution

When the Holzer calculation is applied to the three station example with damping and the full 25 orders of excitation included, the results for the dynamic solution are as shown in Table 12.6.

Table 12.6 Holzer Results by Orders

		Dynamic Angular Displacement (rad)		
Order Number (A)	Station Number (B)	Cosine Coeff (C)	Sine Coeff (D)	Order Response Magnitude (E)
1	1	$-5.82856 \cdot 10^{-4}$	$-1.11051 \cdot 10^{-3}$	$1.25417 \cdot 10^{-3}$
	2	$-1.21821 \cdot 10^{-3}$	$-2.32152 \cdot 10^{-3}$	$2.62173 \cdot 10^{-3}$
	3	$-1.29083 \cdot 10^{-3}$	$-2.46031 \cdot 10^{-3}$	$2.77838 \cdot 10^{-3}$
2	1	$+3.81604 \cdot 10^{-5}$	$+4.19546 \cdot 10^{-4}$	$4.21278 \cdot 10^{-4}$
	2	$-3.42186 \cdot 10^{-5}$	$-3.75754 \cdot 10^{-4}$	$3.77309 \cdot 10^{-4}$
	3	$-4.41027 \cdot 10^{-5}$	$-4.85174 \cdot 10^{-4}$	$4.8717 \cdot 10^{-4}$
3	1	$-5.66188 \cdot 10^{-5}$	$+4.63561 \cdot 10^{-4}$	$4.67005 \cdot 10^{-4}$
	2	$+1.42199 \cdot 10^{-5}$	$-1.16535 \cdot 10^{-4}$	$1.17399 \cdot 10^{-4}$
	3	$+2.89594 \cdot 10^{-4}$	$-2.36564 \cdot 10^{-4}$	$2.38330 \cdot 10^{-4}$
⋮	⋮	⋮	⋮	⋮

Table 12.6 is the beginning of a tabulation that must run through all 25 orders, with the number of each new order listed in turn in column (A). In column (B), for each order number, the three station numbers are repeated, so that each station appears for each order number.

The key results are in columns (C) and (D) where the cosine and sine coefficients for the response at each station are listed for each order. It is evident here that the process produces the Fourier series coefficients for the dynamic motion at each station for each order. To be able to compare the response in different orders, it is useful to have the magnitude of the response in each order, computed as the square root of the sum of the squares of the coefficients; this is tabulated in column (E).

Recall that the Fourier series coefficients generated by the Holzer process give rise to a series that is a function of time (alternatively, it may be considered a function of the steadily rotating crank reference angle, Ωt) of the form

$$\begin{aligned} \theta_i(t) \;=\; & \theta_{i_{1C}} \cos(\Omega t) + \cdots + \theta_{i_{nC}} \cos(n\Omega t) + \cdots \\ & \theta_{i_{1S}} \sin(\Omega t) + \cdots + \theta_{i_{nS}} \sin(n\Omega t) + \cdots \end{aligned} \tag{12.124}$$

To visualize the dynamic motion of the station, it is necessary to sum this series for many crank angles (or time values) and plot the resulting vibratory angular displacements. This

result is shown in Figure 12.19.

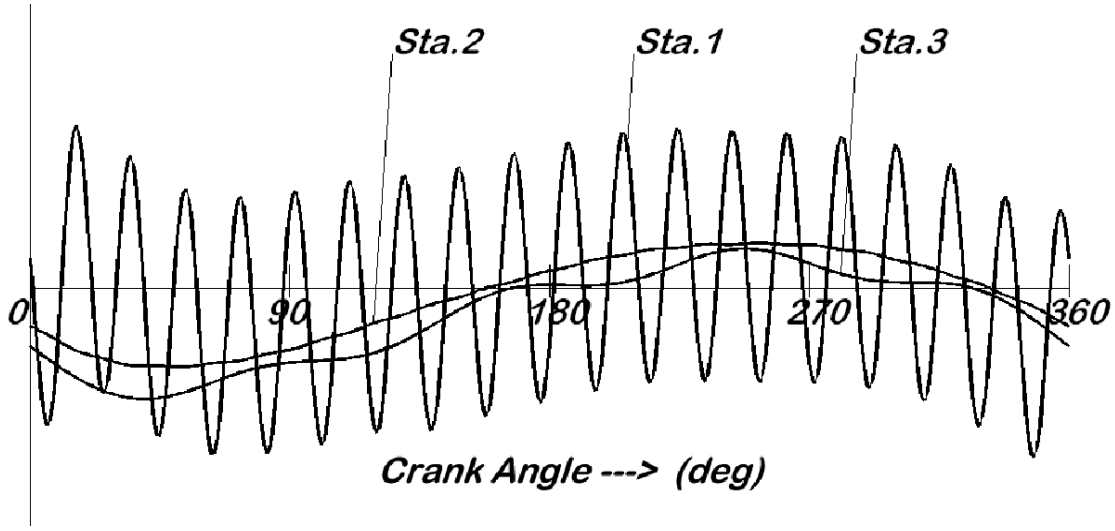

Figure 12.19: Motion Reconstuction Using 25 Orders

The plot in Figure 12.19 represents one full crank revolution at nominal crank speed. The jagged, highly oscillatory curve that tends to dominate the whole picture is the motion of the engine crank, station 1. If the reader will count the peaks on this curve, it will be observed that there are exactly 19 peaks. The large response at this high frequency is the result of the coincidence of 19 times shaft speed with the second nonzero natural frequency. The resulting resonance is very real, and is likely to result in the necessity for redesign to remove the resonance condition or add sufficient damping to control the motion. That all depends upon the findings of a torsional fatigue analysis, a topic beyond the scope of the present work.

12.6.5 Length of the Series: A Caution

In any forced response calculation, there is always a question as to how many orders must be included. In the example used here, 25 orders were used, which for many purposes is more than adequate, but it is difficult to be certain. While developing computer code, it is common practice to make certain simplifications in order to assist development. These simplifications include:

1. Omitting damping;

2. Using only a few excitation orders.

Omitting damping allows the computed solutions to be easily checked by other means such as the classical solution approach. Checking results is an important part of the process, so this can be very useful.

Using only a few excitation orders makes the computer code execute faster, and this is useful when it must be executed many times during code development. However, the results can be misleading. Recall that the system integrity check, based solely on the undamped free vibration analysis, pointed to a possible resonance condition, so it is no surprise when that condition is actually found. However, during code development, many solutions were generated based on only 10 orders. A typical result from such a computer run is shown in Figure 12.20. The response for each station is identified on the figure.

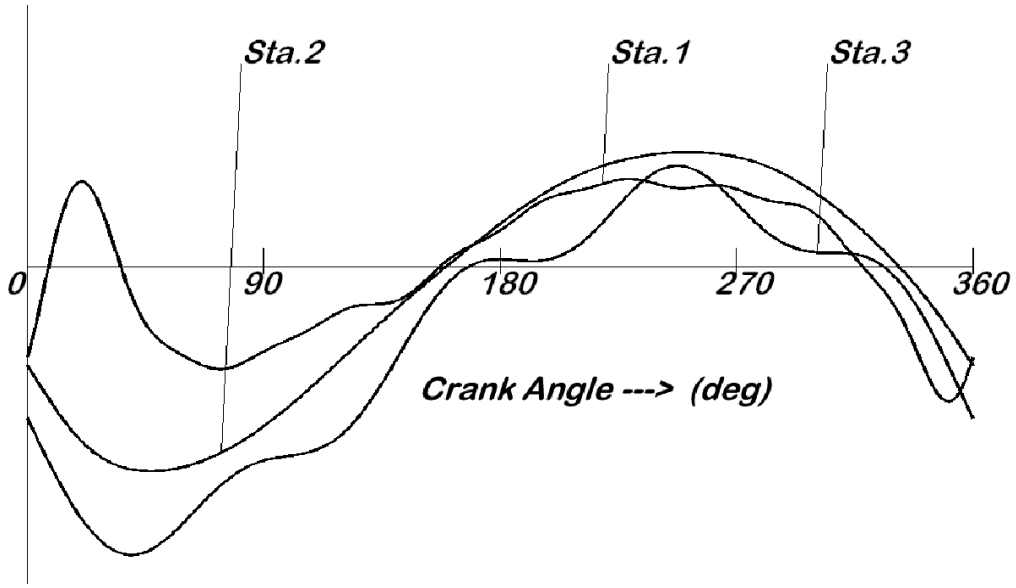

Figure 12.20: Reconstruction Using Only 16 Orders (vertical scale is not the same as in Figure 12.19.)

Note the difference in appearance between this and Figure 12.19. One might easily think that they represent two different physical systems, but the only actual difference is the number of excitation orders included in the computed solution. This makes it evident that the full series must be used for valid final results.

12.7 Transient Torsional Instability Example

In the previous example, both the gas pressure excitation and the inertial reaction arising from the variable system inertia play a major roles in the system response. The example that follows is at the other extreme, a self-excited torsional vibration, with no obvious

excitation at all. Even though no damping is explicitly included in the models that are developed, damping, both positive and negative, plays a key role.

12.7.1 Background

The first super highway in America was the Pennsylvania Turnpike which was engineered and built in the late 1930s and opened in October, 1940. The original section was 160 miles long and included several tunnels. Large exhaust fans were required to remove noxious gases from the tunnels, and these fan systems were built by Westinghouse in East Pittsburgh, PA. Each fan was provided with two drive motors (on a common shaft) coupled through a speed reduction gear to a centrifugal blower. The two motors were powered such that the more powerful motor was used to accelerate the fan while the less powerful motor powered steady operation.

In testing, it was observed that there was a torsional instability, a self-excited torsional vibration, that occurred during the acceleration phase and disappeared in steady operation. Because the fans would be re-started countless times, this was cause for concern with respect to both fatigue and noise. The investigation into this problem and its resolution are reported in a paper by Wahl and Fischer [6]. The present example is adapted from that paper using system parameters that approximate those of the original systems. A simplified system sketch, showing only the acceleration motor is presented in Figure 12.21. While the original paper went into much detail regarding the design of appropriate dampers, the purpose here is simply to explore the torsional instability. Wahl and Fischer did not provide complete numerical data for this system, so it is necessary to fill in some of the gaps by reverse engineering. All the numerical values used are summarized in a table at the end of this discussion.

The original paper by Wahl and Fischer does not go very far in terms of analysis, focusing more on experimental measurement and the application of simple damped vibration theory for the design of the dampers required. At the time of the original design work, computation was entirely by pencil and paper, and the numerical solution of differential equations was in its infancy. Today, we have tools not available then, and they are useful here.

The process of analysis that follows is rather lengthy, and it is useful to outline it in advance. The major steps are these:

1. Mathematical models for the torques of both the induction motor and the fan;

2. SDOF model development and simulation results;

3. 2DOF model development and simulation results;

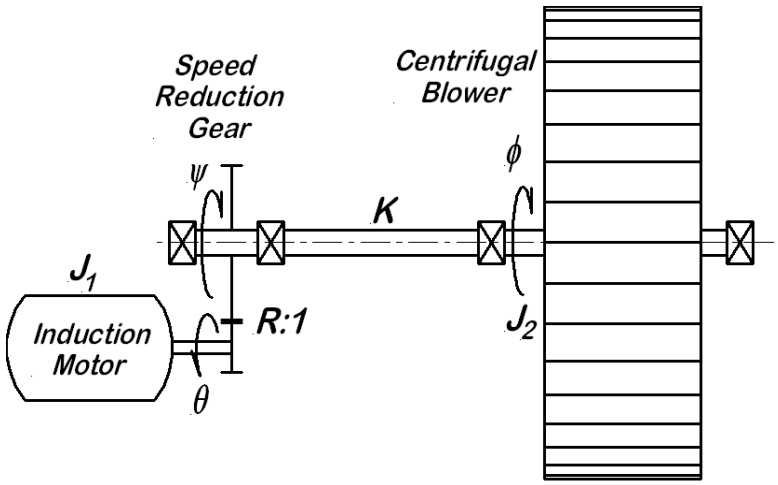

Figure 12.21: Turnpike Exhaust Fan System

4. Transformation to an equivalent single shaft system;

5. Single shaft equivalent system eigensolution;

6. Modal transformation and simulation;

7. Twisting mode oscillations.

8. Conclusions

This example is particularly useful at this point because it illustrates several of the multidegree of freedom analysis techniques previously discussed.

12.7.2 Torque Models

The problem at hand is a dynamical systems problem in that the whole system is accelerating during the time interval of interest. It is also a vibrations problem because the instability observed manifest itself as a torsional vibration. The key elements in this study are the two torque sources that cause the systems motion.

12.7.2.1 Motor Torque

In the Appendix Section 5.1, an approximate model for the torque-speed relation of a three phase, squirrel cage induction motor is given. The Gärtner-Kloss relation [7] is

$$T_{em}(s) = 2T_{\mathrm{m}}\left(1 + s_{\mathrm{m}}e^{As}\right) / \left(\frac{s_{\mathrm{m}}}{s} + \frac{s}{s_{\mathrm{m}}} + 2s_{\mathrm{m}}e^{As}\right) \tag{12.125}$$

where

s = slip $= (N_{synch} - N_{rpm})/N_{synch} = \left(\dot{\theta}_{synch} - \dot{\theta}\right)/\dot{\theta}_{synch}$

N_{synch} = synchronous speed, rpm

N_{rpm} = motor speed, rpm

T_{em} = electromagnetic motor shaft torque (air-gap torque)

T_{m} = maximum torque (pull-out torque)

s_{m} = slip at maximum torque (slip at pull-out torque)

A = Gärtner coefficient, typically $1.3 \leq A \leq 3.0$

The values of s_{m}, T_{m}, and A are adjusted to approximate the particular motor of interest.

For later work, the derivative of this torque is also required. Note first that the Gärtner-Kloss model expresses the electromagnetic torque as a function of only one variable, the slip, s. Thus any required derivatives of T_{em} are obtained by applying the chain rule for derivatives. While the resulting expression is unwieldy, it is not difficult to evaluate numerically.

12.7.2.2 Fan Torque

As a first approximation, for any aerodynamically loaded system such as a fan, the power required varies as the third power of the rotational speed. For the case at hand, where the fan rotation is described by ϕ, this means that fan power may be expressed as

$$P_{fan}\left(\dot{\phi}\right) = B\dot{\phi}^3 \tag{12.126}$$

where B is a suitable constant coefficient. Since power is the product of torque and rotational speed, the fan torque is

$$T_{fan}\left(\dot{\phi}\right) = B\dot{\phi}\left|\dot{\phi}\right| \tag{12.127}$$

where the absolute value is used to insure that this term always opposes the motion.

12.7.2.3 Torque Balance

While computational capability was lacking at the time of the Wahl and Fischer investigation, they did have measured torque-speed curves for both the motor and the blower. A typical pair of curves are shown in Figure 12.22 with both torques plotted as positive. In this figure, the fan torque is as seen at the motor shaft, decreased by the reduction ratio to account for the increased speed at the motor shaft. The intersection of these two curves at the motor rated speed $N_{\text{rated}} = 1173.9$ rpm shows that the motor and fan are exactly matched for steady operation at rated power. The fact that the motor torque curve is well above the fan curve for all speeds to the left of the intersection assures that the motor is entirely capable of accelerating the fan up to speed.

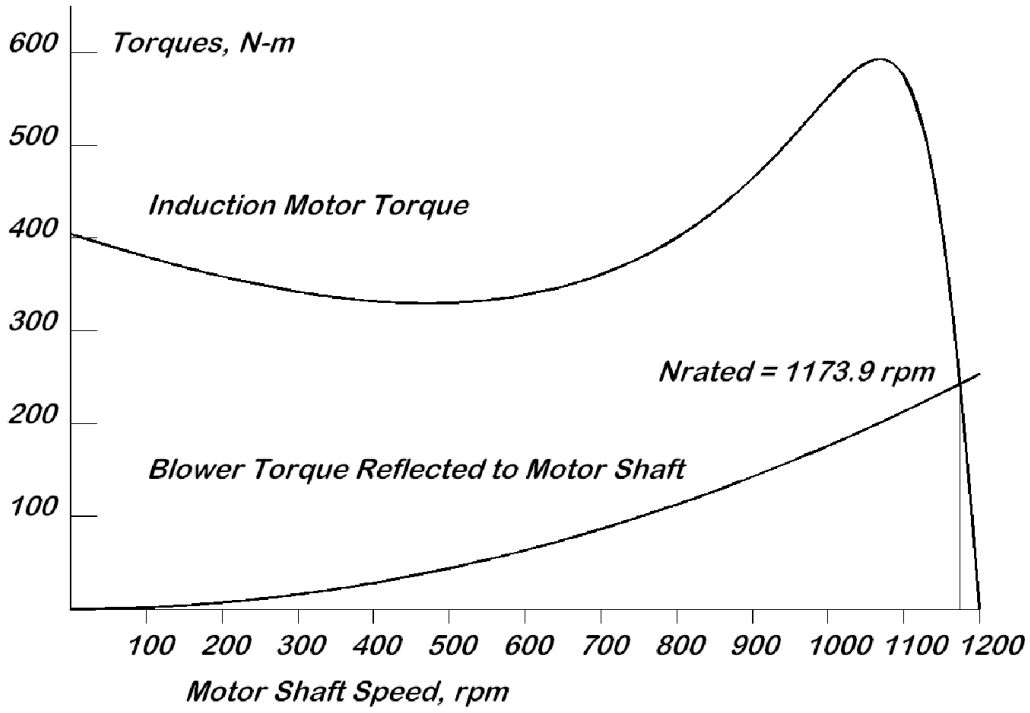

Figure 12.22: Torque-Speed Curves for Motor & Fan at Motor Shaft Speed

12.7.3 Single Degree of Freedom Model

In all likelihood, Wahl and Fischer based their analysis on a single degree of freedom model. It is certainly attractive as a starting point, and is investigated here for a simplified

understanding of the system response.

12.7.3.1 Kinematics & Kinetic Energy

For the single degree of freedom model, all system compliance is neglected and the shaft rotation angle, θ, serves as a suitable generalized coordinate. The undeformable nature of the system implies two constraints:

$$\theta = R \cdot \psi \tag{12.128}$$
$$\psi = \phi \tag{12.129}$$

where R is the dimensionless reduction ratio $(R:1)$.

The second constraint equation eliminates the shaft twist from the problem, leaving only the kinetic energy to be considered:

$$\begin{aligned} T &= \frac{1}{2}\dot{\theta}^2 \left[J_{mtr} + J_{pin} + \left(J_{gear} + J_{fan} \right) / R^2 \right] \\ &= \frac{1}{2}\dot{\theta}^2 \left(J_1 + J_{fan}/R^2 \right) \end{aligned} \tag{12.130}$$

where $J_1 = J_{mtr} + J_{pin} + J_{gear}/R^2$.

12.7.3.2 Generalized Force

The virtual work done on the system is

$$\begin{aligned} \delta W^{nc} &= T_{em}\delta\theta - B\dot{\phi}\left|\dot{\phi}\right|\delta\phi \\ &= \delta\theta \left[T_{em} - \left(\frac{B}{R^3} \right) \dot{\theta}\left|\dot{\theta}\right| \right] \end{aligned} \tag{12.131}$$

12.7.3.3 SDOF Equation of Motion

The equation of motion for the SDOF model is simply

$$\left(J_1 + J_{fan}/R^2 \right) \ddot{\theta} = T_{em} - \left(\frac{B}{R^3} \right) \dot{\theta}\left|\dot{\theta}\right| \tag{12.132}$$

Before leaving this equation, it is significant to note that, although it is written in terms of $\ddot{\theta}$ on the left side, it is actually only a first order differential equation. To see this, let $\dot{\theta} = \omega$, and then re-write the equation in the form

$$\left(J_1 + J_{fan}/R^2\right)\dot{\omega} = T_{em}\left(\omega\right) - \left(\frac{B}{R^3}\right)\omega\left|\omega\right| \tag{12.133}$$

Thus it is evident that the angle θ does not enter into the equation at all, and the equation is actually a first order equation in ω.

12.7.3.4 SDOF Simulation Results

When this differential equation is solved numerically, the results are as shown in the plot of motor speed versus time, Figure 12.23. In most respects, the plot is unremarkable. There is a smooth, almost linear, acceleration from zero up to a smooth transition near the final operating speed. Notice that the final speed is reached after approximately 54 seconds (as read from the graph).

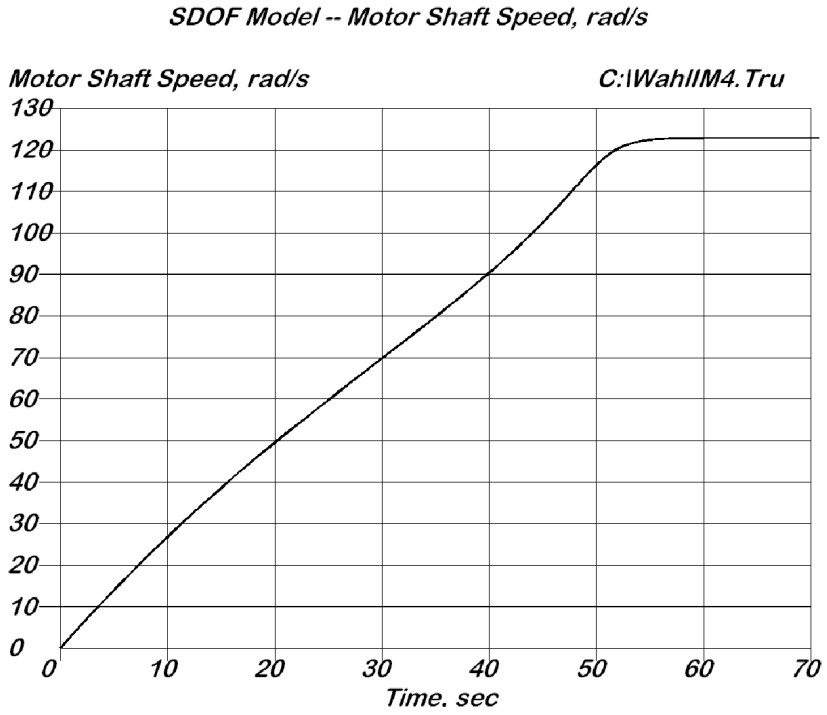

Figure 12.23: Motor Speed versus Time for SDOF Model

12.7.4 Two Degree of Freedom Model

It is immediately evident that (1) the SDOF model does not fully capture the dynamics of this system because the flexibility of the long drive shaft is omitted, and (2) a better model must involve multiple degrees of freedom.

12.7.4.1 Coordinates

Figure 12.21 shows three angular coordinates (θ, ϕ, ψ) which suggests that the system model may require three degrees of freedom. However, for a simple model, it is sufficient to treat the gearing as rigid and introduce the single constraint equation

$$\theta = R \cdot \psi \tag{12.134}$$

This same constraint appeared previously in the SDOF model, but the absence of a second constraint enables this model to include the shaft flexibility. Thus, only two degrees of freedom remain, suitably described by θ and ϕ.

12.7.4.2 Energy Expressions

The system kinetic energy is T,

$$\begin{aligned} T &= \frac{1}{2}\left(J_{mtr} + J_{pin}\right)\dot{\theta}^2 + \frac{1}{2}J_{gear}\dot{\psi}^2 + \frac{1}{2}J_{fan}\dot{\phi}^2 \\ &= \frac{1}{2}\dot{\theta}^2\left(J_{mtr} + J_{pin} + J_{gear}/R^2\right) + \frac{1}{2}J_{fan}\dot{\phi}^2 \\ &= \frac{1}{2}J_1\dot{\theta}^2 + \frac{1}{2}J_2\dot{\phi}^2 \end{aligned} \tag{12.135}$$

where

J_{mtr} = motor mass moment of inertia

J_{pin} = pinion mass moment of inertia

J_{gear} = gear mass moment of inertia

with

$J_1 = J_{mtr} + J_{pin} + J_{gear}/R^2$

$J_2 = J_{fan}$

The only potential energy involved is that of the twisted shaft,

$$V = \frac{1}{2}K\left(\phi - \psi\right)^2 = \frac{1}{2}K\left(\phi - \theta/R\right)^2 \tag{12.136}$$

12.7.4.3 Equations of Motion

The equations of motion are developed using the Lagrange formulation, again using the motor torque and fan torque models discussed above. The Lagrange formulation begins with the formation of various derivatives of the kinetic energy, potential energy, and generalized force expressions. For this purpose, consider:

$$\frac{d}{dt}\frac{\partial T}{\partial \dot{\theta}} = J_1\ddot{\theta} \tag{12.137}$$

$$\frac{\partial V}{\partial \theta} = -\frac{K}{R}\left(\phi - \theta/R\right) \tag{12.138}$$

$$\frac{d}{dt}\frac{\partial T}{\partial \dot{\phi}} = J_2\ddot{\phi} \tag{12.139}$$

$$\frac{\partial V}{\partial \phi} = K\left(\phi - \theta/R\right) \tag{12.140}$$

The general form for the Lagrange equation is

$$\frac{d}{dt}\frac{\partial T}{\partial \dot{q}} - \frac{\partial T}{\partial q} + \frac{\partial V}{\partial q} = Q^{nc} \tag{12.141}$$

For this particular system, the results are

$$J_1\ddot{\theta} - \frac{K}{R}\left(\phi - \theta/R\right) = T_{em}\left(s\right) \tag{12.142}$$

$$J_2\ddot{\phi} + K\left(\phi - \theta/R\right) = -T_{fan}\left(\dot{\phi}\right) \tag{12.143}$$

For some purposes, it is desirable to look at this system of equations in matrix form as

$$\begin{bmatrix} J_1 & 0 \\ 0 & J_2 \end{bmatrix}\begin{Bmatrix} \ddot{\theta} \\ \ddot{\phi} \end{Bmatrix} + \begin{bmatrix} K/R^2 & -K/R \\ -K/R & K \end{bmatrix}\begin{Bmatrix} \theta \\ \phi \end{Bmatrix} = \begin{Bmatrix} T_{em}\left(s\right) \\ -T_{fan}\left(\dot{\phi}\right) \end{Bmatrix} \tag{12.144}$$

Cast in the form most suited for programming, the equations of motion are

$$\ddot{\theta} = \frac{1}{J_1}\left[-\frac{K}{R^2}\theta + \frac{K}{R}\phi + T_{em}(s)\right] \tag{12.145}$$

$$\ddot{\phi} = \frac{1}{J_2}\left[\frac{K}{R}\theta - K\phi - T_{fan}\left(\dot{\phi}\right)\right] \tag{12.146}$$

Note this is actually a fourth order system of equations, because θ, $\dot{\theta}$, ϕ, and $\dot{\phi}$ all enter into the equations. This is a direct consequence of taking the system flexibility into account.

12.7.4.4 Two DOF Simulation Results

The result of numerically solving the coupled system is shown in Figure 12.24 where the motor speed ($\dot{\theta}$) is plotted as a function of time. The result is rather startling. Note that Figure 12.24 shows both the curve of Figure 12.23 and also the motor shaft speed plot resulting from the solution of the two degree of freedom problem. There are several points worthy of comment:

- Over the time interval from about 5 seconds to 34 seconds, the models agree as closely as the eye can see. They also agree on the final speed after the acceleration is ended.
- In the time interval roughly 34 seconds up to 52 seconds, the motor speed from the two degree of freedom model shows a wild, self-excited oscillation. This is a torsional instability. The oscillation disappears, just as it began, for no obvious reason.
- The motor shaft speed at 52 seconds from the second simulation is approximate 5 rad/s less than that for the single degree of freedom simulation. In the 2DOF simulation, part of the energy put into the system is expended in the oscillatory motion, rather than in the rigid body acceleration.
- The SDOF simulation shows the system reaching steady state about 4 seconds sooner than the 2DOF simulation indicates. This is because of the waste of energy in oscillations shown in the 2DOF model.
- The 2DOF simulation also shows some oscillation when the motor first starts, between 0 and 5 seconds. More discussion about this is provided later.

- The double amplitude of the major $\dot{\theta}$ oscillation appears to be approximately 78.0 rad/s. Wahl and Fischer report a measured displacement (single) amplitude of approximately 85^o for the motor staff oscillation with a natural frequency of 5.8 Hz [6]. The amplitude values are not directly comparable since the values here are for velocity oscillation amplitude while the Wahl and Fischer data is a displacement amplitude. Both results indicate large amplitude motion, cause for considerable concern.

- As shown later, and using the system data for this study, the undamped twisting natural frequency is computed as $\omega_1 = 6.49$ Hz. The natural frequency observed in the simulation (based on counting a large number of peaks) is $f = 6.47$ Hz. It is reasonable, therefore, to conclude that this is in fact simply a free vibration response.

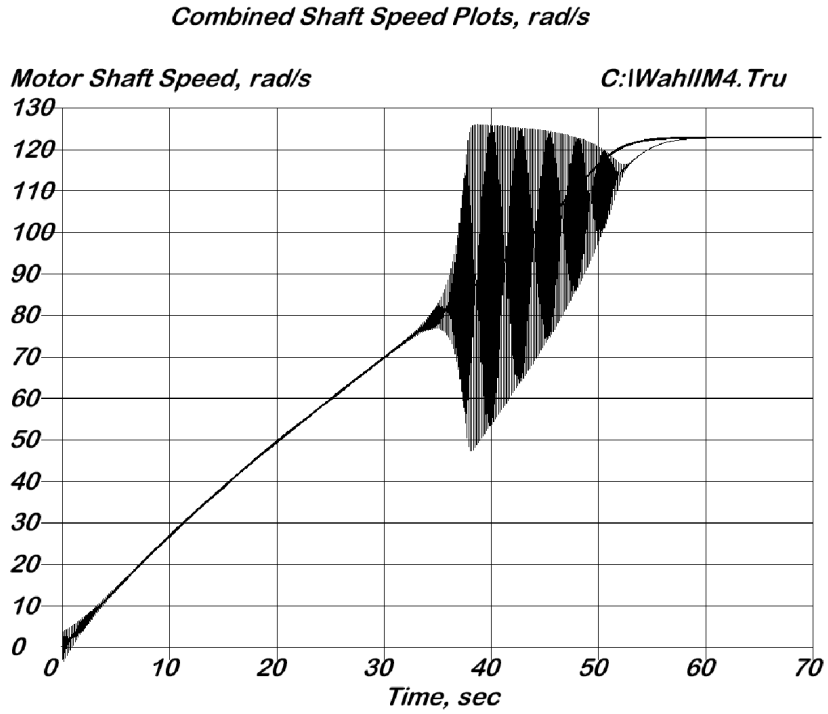

Figure 12.24: Combined Plots of Motor Speed versus Time for SDOF and 2DOF Models

12.7.5 Single Shaft Equivalent System

One of the techniques previously introduced to simplify dealing with geared systems is the introduction of a single-shaft equivalent system (Section 12.3.4). This technique is applied here with the objective of creating an equivalent single shaft system at motor

speed. This is conceptually equivalent of mounting the blower directly on the end of the motor shaft.

If the new variables for the equivalent system are denoted with Greek capitals, the transformation is defined in this way:

$$\Theta = \theta \tag{12.147}$$
$$\Phi = R\phi \tag{12.148}$$

The transformed single shaft equivalent equations of motion are

$$R^2 J_1 \ddot{\Theta} + K(\Theta - \Phi) = R^2 T_{em}(s) \tag{12.149}$$
$$J_2 \ddot{\Phi} + K(\Phi - \Theta) = -R T_{fan}\left(\dot{\phi}\right) \tag{12.150}$$

Casting these in matrix form gives

$$\begin{bmatrix} R^2 J_1 & 0 \\ 0 & J_2 \end{bmatrix} \begin{Bmatrix} \ddot{\Theta} \\ \ddot{\Phi} \end{Bmatrix} + K \begin{bmatrix} 1 & -1 \\ -1 & 1 \end{bmatrix} \begin{Bmatrix} \Theta \\ \Phi \end{Bmatrix} = \begin{Bmatrix} R^2 T_{em}(s) \\ -R T_{fan}\left(\dot{\phi}\right) \end{Bmatrix} \tag{12.151}$$

Notice that the inertia and stiffness matrices of the transformed system are symmetric; this is an essential requirement for the later modal transformation. While there are no identifiable damping terms included, this is, in fact, a damped system as demonstrated below.

12.7.6 Eigensolutions for Single Shaft Equivalent

To look at the free vibration of the equivalent system, it is necessary to deal with the eigenproblem. For this purpose, assume a homogeneous solution of the form $\mathrm{col}(\Theta, \Phi) = \{A\} e^{j\omega t}$. The homogeneous solution must satisfy the equation

$$\begin{bmatrix} K - \omega^2 R^2 J_1 & -K \\ -K & K - \omega^2 J_2 \end{bmatrix} \{A\} = \{0\} \tag{12.152}$$

This leads to the characteristic equation,

$$\begin{aligned} 0 &= \det \begin{bmatrix} K - \omega^2 R^2 J_1 & -K \\ -K & K - \omega^2 J_2 \end{bmatrix} \\ &= -\omega^2 \left(K J_2 + K R^2 J_1 - R^2 \omega^2 J_1 J_2\right) \end{aligned} \tag{12.153}$$

for which the roots are

$$\omega_o = 0 \tag{12.154}$$

$$\omega_1 = \frac{1}{R}\sqrt{\frac{K\left(J_2 + R^2 J_1\right)}{J_1 J_2}} \tag{12.155}$$

The complete eigensolutions are as follows:

$$\begin{gathered} \omega_o = 0 \qquad \omega_1 = \tfrac{1}{R}\sqrt{\tfrac{K(J_2+R^2J_1)}{J_1J_2}} \\ \{A_o\} = \left\{ \begin{array}{c} 1 \\ 1 \end{array} \right\} \quad \{A_1\} = \left\{ \begin{array}{c} 1 \\ -R^2\frac{J_1}{J_2} \end{array} \right\} \end{gathered} \tag{12.156}$$

12.7.7 Modal Transformation

The modal transformation for the equations of motion is based on the eigensolutions found previously, starting with the previous equations of motion for the single shaft equivalent system:

$$\begin{gathered} \left[\begin{array}{cc} R^2 J_1 & 0 \\ 0 & J_2 \end{array} \right] \left\{ \begin{array}{c} \ddot{\Theta} \\ \ddot{\Phi} \end{array} \right\} + K \left[\begin{array}{cc} 1 & -1 \\ -1 & 1 \end{array} \right] \left\{ \begin{array}{c} \Theta \\ \Phi \end{array} \right\} = \left\{ \begin{array}{c} R^2 T_{em}(s) \\ -R T_{fan}\left(\dot{\phi}\right) \end{array} \right\} \\ [J]\left\{\ddot{X}\right\} + [S]\{X\} = \{T\} \end{gathered} \tag{12.151}$$

where $\{X\} = \mathrm{col}\left(\Theta, \Psi\right)$, the single shaft equivalent variables, $[J]$ is the equivalent single shaft inertia matrix, and $[S]$ is the associated stiffness matrix.

12.7.7.1 Modal Equation Development

Define the modal response $\{\xi\}$ such that $\{X\} = [A]\{\xi\}$, which leads to the transformed equations below:

$$\begin{aligned} [J]\left\{\ddot{X}\right\} + [S]\{X\} &= \{T\} \\ [J][A]\left\{\ddot{\xi}\right\} + [S][A]\{\xi\} &= \{T\} \\ [A]^T[J][A]\left\{\ddot{\xi}\right\} + [A]^T[S][A]\{\xi\} &= [A]^T\{T\} \\ [\mathbb{M}]\left\{\ddot{\xi}\right\} + [\mathbb{K}]\{\xi\} &= \{\mathbb{T}\} \end{aligned} \tag{12.157}$$

Because the coefficient matrices $[\mathbb{M}]$ and $[\mathbb{K}]$ are each diagonal, the equations have the appearance of completely decoupling the two modes. In fact, this is not entirely true, because they remain coupled through the right side torque components. The indicated matrix products are:

$$[\mathbb{M}] = [A]^T [J] [A] = \begin{bmatrix} J_1 R^2 + J_2 & 0 \\ 0 & R^2 \frac{J_1}{J_2} (J_1 R^2 + J_2) \end{bmatrix} \tag{12.158}$$

$$[\mathbb{S}] = [A]^T [S] [A] = \begin{bmatrix} 0 & 0 \\ 0 & \frac{K}{J_2^2} (J_1 R^2 + J_2)^2 \end{bmatrix} \tag{12.159}$$

$$\{\mathbb{T}\} = [A]^T \{T\} = \begin{Bmatrix} R^2 T_{em}(s) - R T_{fan}\left(\dot{\phi}\right) \\ R^2 T_{em}(s) + R^3 (J_1/J_2) T_{fan}\left(\dot{\phi}\right) \end{Bmatrix} \tag{12.160}$$

The modal equations of motion are readily assembled from the transformed terms in the previous section. For the single shaft equivalent system, the modal equations of motion are:

$$\left(J_1 R^2 + J_2\right) \ddot{\xi}_o = R^2 T_{em}(s) - R T_{fan}\left(\dot{\phi}\right) \tag{12.161}$$

$$R^2 \frac{J_1}{J_2} \left(J_1 R^2 + J_2\right) \ddot{\xi}_1 + \frac{K}{J_2^2} \left(J_1 R^2 + J_2\right)^2 \xi_1 = R^2 T_{em}(s) + R^3 (J_1/J_2) T_{fan}\left(\dot{\phi}\right) \tag{12.162}$$

These equations are solved numerically with the initial conditions $\dot{\xi}_o(0) = \xi_1(0) = \dot{\xi}_1(0) = 0$. Only three initial conditions are provided because the first equation is only a first order differential equation in $\dot{\xi}_o$ and its derivative. Thus the numerical simulation is reduced to solving only a total third order system.

Note that, for each equation, the right side is dependent on both s and $\dot{\phi}$, even though the numerical solution generates $\dot{\xi}_o$, ξ_1 and $\dot{\xi}_1$. To evaluate the right side at each time step, it is necessary, therefore, to work back through the transformations to produce $\dot{\theta}$, $\dot{\phi}$ and finally s.

$$\dot{\theta} = \dot{\xi}_1 + \dot{\xi}_o \tag{12.163}$$

$$\dot{\phi} = \frac{1}{R}\dot{\xi}_o - R\frac{J_1}{J_2}\dot{\xi}_1 \tag{12.164}$$

$$s = \left(\dot{\theta}_{synch} - \dot{\theta}\right) / \dot{\theta}_{synch} \tag{12.165}$$

This is not difficult to code in the computer simulation, but it is an important observation for the discussion to follow regarding positive and negative damping.

12.7.7.2 Modal Simulation Results

The results of simultaneously solving equations (12.161) and (12.162) are shown in the upper part of Figure 12.25. It is immediately evident that the sum of these two curves, $\dot{\xi}_o + \dot{\xi}_1$, is the $\dot{\theta}$ curve of Figure 12.24. The modal decomposition very neatly separates the two aspects of the motion, so that each may be considered separately. All of the features found in Figure 12.24 can be seen broken out separately in Figure 12.25.

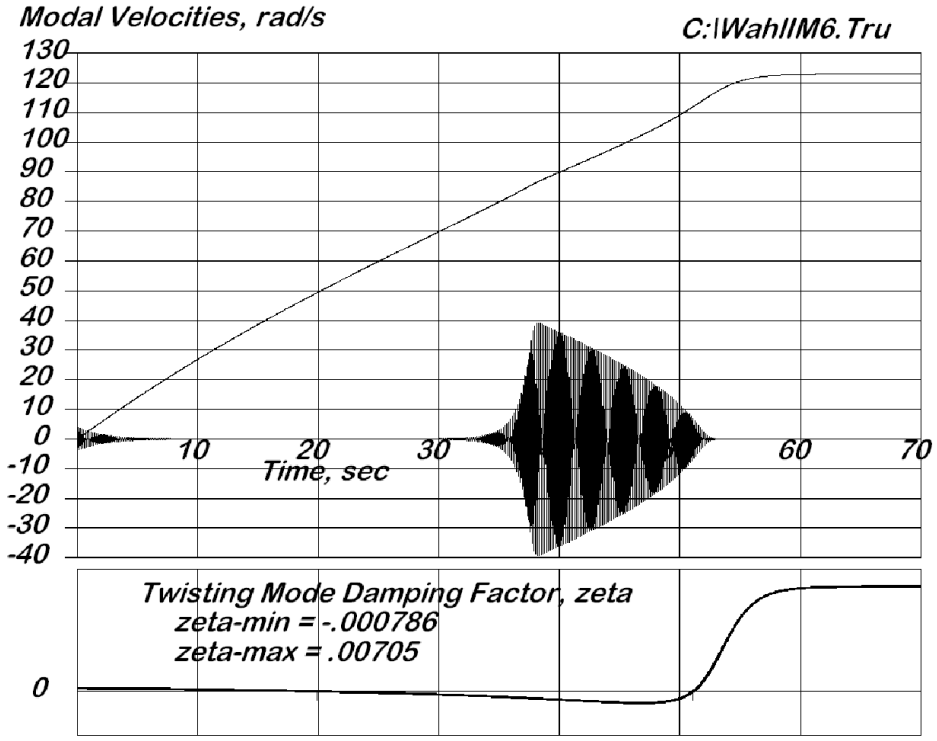

Figure 12.25: Modal Simulation Results and Computed Damping Factor

12.7.8 Twisting Mode Oscillations

Before dealing specifically with the oscillations, it is well to exclude the rigid body mode from consideration. As noted previously, although the rigid body equation of motion appears to be second order, it is not. There are no terms that are functions of the rotations, only the rotational velocities. Hence, it is only a first order equation, not subject to the typical negative damping instability. **All of the observed oscillation is only in the twisting mode.** The right side of the first equation shows the forward torque of the motor in opposition to the fan torque, exactly as expected. But note, that in the second equation, both terms act in the same sense.

12.7.8.1 Negative Damping

Various authors have suggested that the positive slope of the induction motor torque-speed curve, roughly in the range one half synchronous speed up to the point of maximum torque, is a region of unstable operation [8, 9]. Unfortunately, they only offer vague, non-rigorous mathematical support for these assertions. The intent here is to provide something more definite.

Consider again the twisting equation of motion,

$$R^2\frac{J_1}{J_2}\left(J_1R^2+J_2\right)\ddot{\xi}_1+\frac{K}{J_2^2}\left(J_1R^2+J_2\right)^2\xi_1=R^2T_{em}\left(s\right)+R^3\left(J_1/J_2\right)T_{fan}\left(\dot{\phi}\right) \quad (12.162)$$

The left side is recognized as a typical undamped oscillator. The objective here is to focus on the right side of this equation, so define T_{RHS}

$$T_{RHS}=R^2T_{em}\left(s\right)+R^3\left(J_1/J_2\right)T_{fan}\left(\dot{\phi}\right) \quad (12.166)$$

Suppose that, at a particular instant, the solution has the specific values $\left(\underline{\xi}_o,\,\underline{\xi}_1,\,\underline{\dot{\xi}}_o,\,\underline{\dot{\xi}}_1\right)$. In order to to project the solution to a nearby state $\left(\xi_o,\xi_1,\dot{\xi}_o,\dot{\xi}_1\right)$, consider a Taylor series expansion in the two variables $\dot{\xi}_o$ and $\dot{\xi}_1$,

$$\begin{aligned}T_{RHS}\left(\dot{\xi}_o,\dot{\xi}_1\right) &= T_{RHS}\left(\underline{\dot{\xi}}_o,\underline{\dot{\xi}}_1\right)+\left(\underline{\dot{\xi}}_o-\dot{\xi}_o\right)\left.\frac{\partial T_{RHS}}{\partial\dot{\xi}_o}\right|_{\left(\underline{\dot{\xi}}_o,\underline{\dot{\xi}}_1\right)}+\left(\underline{\dot{\xi}}_1-\dot{\xi}_1\right)\left.\frac{\partial T_{RHS}}{\partial\dot{\xi}_1}\right|_{\left(\underline{\dot{\xi}}_o,\underline{\dot{\xi}}_1\right)}+\cdots\\ &= T_{RHS}\left(\underline{\dot{\xi}}_o,\underline{\dot{\xi}}_1\right)-\underline{\dot{\xi}}_o\left.\frac{\partial T_{RHS}}{\partial\dot{\xi}_o}\right|_{\left(\underline{\dot{\xi}}_o,\underline{\dot{\xi}}_1\right)}-\underline{\dot{\xi}}_1\left.\frac{\partial T_{RHS}}{\partial\dot{\xi}_1}\right|_{\left(\underline{\dot{\xi}}_o,\underline{\dot{\xi}}_1\right)}\\ &\quad+\dot{\xi}_o\left.\frac{\partial T_{RHS}}{\partial\dot{\xi}_o}\right|_{\left(\underline{\dot{\xi}}_o,\underline{\dot{\xi}}_1\right)}+\dot{\xi}_1\left.\frac{\partial T_{RHS}}{\partial\dot{\xi}_1}\right|_{\left(\underline{\dot{\xi}}_o,\underline{\dot{\xi}}_1\right)}+\cdots\end{aligned} \quad (12.167)$$

With a slight re-arrangement, the twisting mode equation, equation (12.162), now reads as

$$\begin{aligned}&R^2\frac{J_1}{J_2}\left(J_1R^2+J_2\right)\ddot{\xi}_1-\dot{\xi}_1\left.\frac{\partial T_{RHS}}{\partial\dot{\xi}_1}\right|_{\left(\underline{\dot{\xi}}_o,\underline{\dot{\xi}}_1\right)}+\frac{K}{J_2^2}\left(J_1R^2+J_2\right)^2\xi_1 \quad (12.168)\\ &= T_{RHS}\left(\underline{\dot{\xi}}_o,\underline{\dot{\xi}}_1\right)-\underline{\dot{\xi}}_o\left.\frac{\partial T_{RHS}}{\partial\dot{\xi}_o}\right|_{\left(\underline{\dot{\xi}}_o,\underline{\dot{\xi}}_1\right)}-\underline{\dot{\xi}}_1\left.\frac{\partial T_{RHS}}{\partial\dot{\xi}_1}\right|_{\left(\underline{\dot{\xi}}_o,\underline{\dot{\xi}}_1\right)}+\dot{\xi}_o\left.\frac{\partial T_{RHS}}{\partial\dot{\xi}_o}\right|_{\left(\underline{\dot{\xi}}_o,\underline{\dot{\xi}}_1\right)}+\cdots\end{aligned}$$

It is the last term, proportional to $\dot{\xi}_1$, that has the potential to provide either positive or negative damping. The required partial derivative, $\partial T_{RHS}/\partial\dot{\xi}_1$, can be produced by chain rule differentiation.

What is needed is a clear indicator of when the damping is positive and when it is negative. This is most easily done by returning to the definition of the damping factor, ζ, for a damped SDOF system. Equation (12.168) is of the typical second order form that may be written as

$$\ddot{\xi}_1 + \frac{\mathbb{C}}{\mathbb{M}_{11}}\dot{\xi}_1 + \frac{\mathbb{S}_{11}}{\mathbb{M}_{11}}\xi_1 = \frac{1}{\mathbb{M}_{11}}\mathbb{T}_1 \tag{12.169}$$

from which the damping factor is extracted as

$$\zeta_1 = \frac{\mathbb{C}}{2\omega_1 \mathbb{M}_{11}} \tag{12.170}$$

The damping factor varies with speed as the partial derivative terms change. Where ζ is positive, the usual damped response applies. Where it is negative, the solution becomes unstable and tends to grow with increasing time.

The effective damping factor has been computed, moment by moment, and is plotted in the lower part of Figure 12.25. It is negative from about 19 seconds up to 52 seconds, roughly the same time interval where the major torsional instability is observed. It is true that the positive slope of the induction motor torque-speed curve is a significant factor, but the slope of the load curve (in this case, the blower torque-speed curve) is also important.

12.7.8.2 Start-up Oscillations

Wahl and Fischer measured oscillations during the first few seconds of the acceleration. In Figure 12.24, there is an evident small oscillation during the first five seconds of the acceleration. While it is known that induction motors do in fact produce oscillatory torques during starting (see Appendix Section A5.1.4.5), these oscillatory torques are only described in detailed electromagnetic models; this is beyond the capability of the Gärtner-Kloss model. Even so, the torque-speed models used here support the observed start-up oscillations.

The damping factor described in the previous section is positive over the time interval zero to 19 seconds. As reported above in relation to the eigensolution, the undamped natural frequency of this system is $f_1 = 6.490$ Hz, and where the peak counting approach is applied to the early part of the simulated acceleration, the oscillation frequency is observed to be $f = 6.486$ Hz, based on the first three seconds. Thus it is apparent that this early damped oscillation is simply the natural "ringing" response of a damped oscillator following the application of an initial torque step when power is applied to the system. It decays away because the effective damping factor in that time interval is positive.

12.7.9 System Data

The intention here is to replicate the observations of Wahl and Fischer. Fortunately, their original paper [1] provides a significant amount of data, some of it expressed exactly and some as only approximate. The approximate values are here taken as exact, and a certain amount of reverse engineering is used to fill in the remaining gaps.

Motor

$f = 60$ Hz	line power frequency
$N_p = 6$	number of poles
$N_{synch} = 1200$ rpm	synchronous speed
$P_{rated} = 40$ Hp $= 29827.996$ W	rated power
$N_{rated} = 1173.936212$ rpm	rated speed
$T_{rated} = 242.6336092$ N-m	rated torque
$s_{rated} = 0.02171982302$	slip at rated speed
$T_{start} = 404.2145593$ N-m	starting torque
$T_m = 592.8992401$ N-m	maximum torque
$s_m = 0.10933333333$	slip at max torque
$A = 4.126124876$	Gärtner torque-speed parameter

Mechanical System

$R = 7$	gear reduction ratio
$J_1 = 1$ kg-m^2	assumed effective value for station 1
$J_2 = 4410 \cdot J_1$	consistent inertia for station 2
$P_{fan} = 40$ Hp $= 29827.996$ W	fan rated power
$N_{\text{fan rated}} = N_{\text{motor rated}}/R = 167.71$ rpm	fan rated speed
$B = 5.506794171$	fan coefficient
$K = 200000$ N-m/rad	fan drive shaft stiffness

12.8 Conclusion

The final example provides a basis for understanding of all of the transient torsional oscillations originally observed by Wahl and Fischer on the Pennsylvania Turnpike blowers. The inclusion of torsional flexibility in the model is clearly essential for this demonstration. The changing signs on the damping factor is directly related to the varying slope of the induction motor torque-speed curve, as well as the relative slope magnitudes of the motor and fan torque-speed relations. Thus a quantifiable approach to predicting the region of instability is presented.

The transformation to a single-shaft equivalent system is shown to be useful way to visualize the system and to prepare for the later modal analysis. The transformation to modal coordinates accomplished the decoupling of the left sides of the two differential equations, but does not result in complete system decoupling. Despite that, the separation into rigid body and twisting motions greatly facilitates understanding of the nature of the system motions. While this partial decoupling would be of only limited value if a closed form solution were sought, it is sufficient to enable the computer modal simulation to be conducted. The reader might be inclined to view this problem as having historical interest only, but that is not the case. The literature shows several very similar studies regarding torsional vibration problems in cooling tower fans used.

Understanding torsional vibration of machines remains a matter of vital importance in the successful design of machinery of all sorts. It is one of the most broadly based problems that mechanical engineers face, being intimately connected with kinematics, dynamics of variable inertia systems, mechanics of materials, higher mathematics, and thermodynamics. In this short introduction, only the surface elements are exposed, but this is sufficient to provide a start for further study and application should the need arise for the reader.

Understanding of the problem was delayed because of the computational complexity involved for most real systems. Holzer's original tabular calculation was a major break through, but even so, it was a huge computing task. The availability of digital computation to do the massive amount of arithmetic involved has helped immeasurably. The computational complexity is often given as an excuse for avoiding the subject in the classroom, but this is no longer valid since the advent of the personal computer. The necessary computational power is now within reach of every engineer, and this vital topic must be well developed at the college level to enable the continued application of machines to do man's work.

References

[1] Biezeno, C.B. and Grammel, R., *Engineering Dynamics*, *Internal Combustion Engines* (Vol. 4), Wiley, 1954.

[1] BICERA (British Internal Combustion Engine Research Association), *A Handbook on Torsional Vibration*, E.J. Nestorides, ed., Cambridge University Press, 1958, p. 44 ff.

[3] Wilson, W.K., *Practical Solution of Torsional Vibration Problems*, vol. 1, 3rd ed. revised, Wiley, 1956, p. 570 ff.

[4] Heywood, J.B., *Internal Combustion Engine Fundamentals*, McGraw-Hill, 1988, p. 49.

[5] Holzer, H., *Die Berechnung der Drehschwingungen*, Springer, Berlin, 1921.

[6] Wahl, A.M. and Fischer, E.G., "Investigation of Self-Excited Torsional Oscillations and Vibration Damper for Induction-Motor Drives," *J. Applied Mechanics, Trans. ASME,* Dec., 1942, pp. A-175 through A-183.

[7] Gärtner, J., Halámka, Z., Pavelka, J., "The Speed Control of Induction Motors by the Change of Suply (sic) Voltage," *Silnoproudá Elektro Technika A Electro Energetika,* 2001, pp. D-41 through D-44.

[8] San Andres, Luis, "Notes 9 Torsional Vibrations – A Twisted Overview," 2018, found on line at https//rotorlab.tamu.edu.

[9] Adachi, A., and Murphy, B., "Torsional Instability of Cooling Tower Fan During Induction Motor Startup,"*45*$^{\text{th}}$ *Turbomachinery and 32*$^{\text{nd}}$ *Pump Simposia*, Houston, TX, 12-15 Sept., 2016.

Problems

12-1 The figure shows a simple shaft with five stations designated at diameter changes. The shaft is made of steel ($\gamma = 76.5$ kN/m^3, $G = 79.3$ GPa), and all dimensions shown are in millimeters. Be sure to note the fillet radii indicated for each diameter change.

(a) Lumping half of the segment mass moment of inertia at each end of the segment, develop an inertia matrix, $[M]$, for the shaft alone;

(b) Taking proper account of the several fillet radii, develop a torsional stiffness matrix, $[K]$, for the shaft;

(c) What is the overall, end-to-end, stiffness of the shaft?

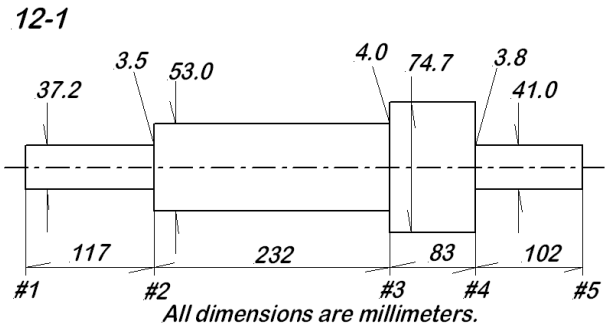

12-2 Table 12.2 (parts a and b) provide Fourier series for an internal combustion engine torque curve, the graph of torque as a function of crank angle. Consider this data applied to an engine cylinder for which the data is given below.

(a) Develop computer code to evaluate this function at every point throughout the crank cycle in two degree increments. Take great care to correctly enter all of the data;

(b) Use this computer program to evaluate and plot the torque curve over a full cycle;

(c) What is the maximum torque, and at what crank angle does it occur, according to the plot?

(d) What is the minimum torque, and at what crank angle does it occur, again according to the plot?

Crank Radius	$R = 35$ mm
Cylinder Bore	$Diam = 65$ mm

12-3 The figure shows a three station torsional model without damping. External excitation torques are also indicated, but they are for a later problem and do not apply

here.

(a) Write the system equations of motion in matrix form without external excitations;

(b) Develop the characteristic equation and numerically solve the polynomial for the natural frequencies using the data below;

(c) Obtain the system eigenvectors, and normalize each to unit value for the first station.

$J_1 = 15$ kg-m^2 $J_2 = 75$ kg-m^2 $J_3 = 50$ kg-m^2

$K_1 = 2.5 \cdot 10^6$ N-m $K_2 = 5.5 \cdot 10^6$ N-m

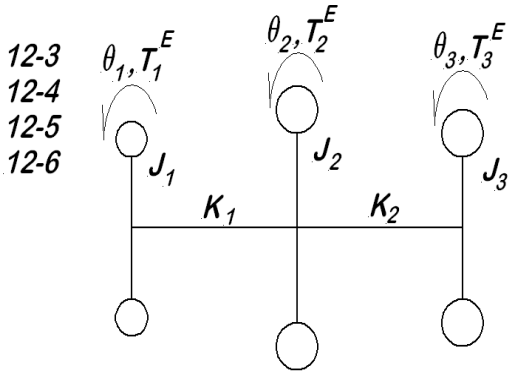

12-4 Consider again the same system studied in problem **12-3**. The system parameters given there are applicable to this problem as well.

(a) Develop computer code to implement the Holzer calculation of natural frequencies and mode shapes;

(b) Employ that code to numerically determine the system natural frequencies and mode shapes for the system;

(c) Compare the results with those obtained by directly solving the characteristic polynomial (they should be quite close, but rarely are they exactly the same).

12-5 For the same system considered in problem **12-3**, let the shaft speed be $\Omega = 439.8$ rad/s, and assume that the unstrained system is rotating at constant speed Ω when the following system of external torques are initiated: $T_1^E(t) = 8.856 \cdot 10^4 (1 - \cos \Omega t)$, $T_2^E = 0$, and $T_3^E(t) = -8.856 \cdot 10^4$, all in N-m units. For the questions below, use the modal method of analysis. Where the mode vectors are used, normalize the first element in each to 1.0.

(a) Calculate the steady twist of the system;

(b) Second (first twisting) mode vibratory angular displacements at each station;

(c) Third (second twisting) mode vibratory angular displacements at each station.

(d) No damping is indicated in the problem statement, therefore whatever motion ensues continues without decay. Knowing that a real system is intended, one for which there must always be damping in reality, what terms are expected to decay and which are not?

12-6 Consider again the same system considered in problem **12-5**, this time using the Holzer forced response calculation.

(a) Does the Holzer forced response calculation provide the steady shaft twists? If not, is there an alternate way to determine it? If either is true, evaluate them.

(b) Does the Holzer forced response calculation provide the uniform rotation terms?

(c) Does the Holzer calculation provide the response at the system natural frequencies?

(d) Compare the forced response values obtained by the Holzer calculation with those from the modal analysis of problem **12-5**.

12-7 The effects of two different types of damping are demonstrated here. Each step of the analysis should be formulated in symbols before numbers substituted and the arithmetic completed. Where numerical values are required, use the data tabulated below. While working this problem, the reader should bear in mind what was learned in Chapters 10 and 11 regarding the significance of (i) a zero root, and (ii) a complex root, and (iii) a pure imaginary root.

(a) Formulate the system equations of motion in matrix form, first in full detail and then rewritten in more compact form using the notations

$$\lceil J \rfloor = diag\,(J_1, J_2)$$

$$[C] = \begin{bmatrix} C & -C \\ -C & C \end{bmatrix}$$

$$\lceil D \rfloor = diag\,(D_1, D_2)$$

$$[K] = \begin{bmatrix} K & -K \\ -K & K \end{bmatrix};$$

(b) Assume a solution of the form $\{\theta\} = \{A\}\, e^{\lambda t}$, and develop the characteristic equation in detail;

(c) Formulate and solve numerically for the λ values for Case 1: $[C] = \lceil D \rfloor = [0]$;

(d) Formulate and solve numerically for the λ values for Case 2: $[C] \neq [0]$, $\lceil D \rfloor = [0]$;

(e) Formulate and solve numerically for the λ values for Case 3: $[C] = [0]$, $\lceil D \rfloor \neq [0]$;

(f) Formulate and solve numerically for the λ values for Case 4: $[C] \neq [0]$, $\lceil D \rfloor \neq [0]$;

(g) Accumulate all the results in a table with the following headings: column 1 is the case number, column 2 is the condition description (what is zero), column 3 is the list of root values, and column 4 is a brief comment about the nature of the motion;

(h) Based on what is observed in these solutions, extrapolate to make a general statement about the effects of the two types of damping.

$J_1 = 1 \quad D_1 = 0.05 \quad K = 1000$

$J_2 = 1.5 \quad D_2 = 0.05 \quad C = 0.1$

(Note that no units are given. It is to be assumed that they are in a consistent system of units, either SI or USC.)

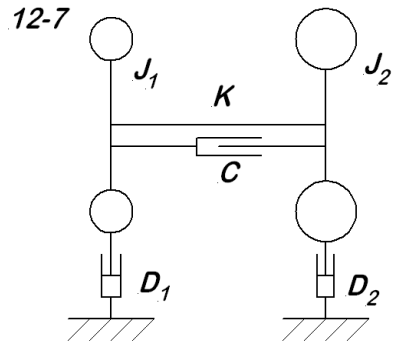

12-8 One of the application areas where torsional vibration is of great concern is the driveline of a ship; a shaft failure at sea can be catastrophic. For this reason, ships propulsion systems are always given a rigorous torsional analysis. The figure shows a ship's drive line model with the engine at the left and the propeller at the right. The parameter values used here are taken from a technical paper concerned with this problem[2].

(a) Calculate the three lowest twisting mode natural frequencies for this system, along with the mode vectors for each (normalize the mode vectors to 1.0 at the first station;

[2]Murawski, L., "Some Aspects of Torsional Vibration Analysis Methods of Marine Power Transmission Systems," *J. of Polish CIMAC*, Vol. 7, No. 1, Gdansk, 2012, pp. 175-182.

(b) Plot the mode shapes (mode vector value versus station number) for the first three modes;

(c) How is the number of axis crossings related to the mode number?

Mass Moments of Inertia		Shaft Stiffness Values	
kg-m^2	kg-m^2	N-m/rad	N-m/rad
$J_1 = 2.2462 \cdot 10^4$	$J_7 = 1.1161 \cdot 10^4$	$K_1 = 1.3120 \cdot 10^9$	$K_7 = 1.8800 \cdot 10^9$
$J_2 = 1.1161 \cdot 10^4$	$J_8 = 4.8020 \cdot 10^3$	$K_2 = 1.3720 \cdot 10^9$	$K_8 = 2.7400 \cdot 10^9$
$J_3 = 1.1161 \cdot 10^4$	$J_9 = 6.3420 \cdot 10^3$	$K_3 = 1.380 \cdot 10^9$	$K_9 = 1.1145 \cdot 10^8$
$J_4 = 1.1161 \cdot 10^4$	$J_{10} = 4.4500 \cdot 10^2$	$K_4 = 1.3460 \cdot 10^9$	$K_{10} = 1.08677 \cdot 10^8$
$J_5 = 1.1161 \cdot 10^4$	$J_{11} = 7.7800 \cdot 10^2$	$K_5 = 1.3790 \cdot 10^9$	$K_{11} = 1.29662 \cdot 10^8$
$J_6 = 1.1161 \cdot 10^4$	$J_{12} = 8.4537 \cdot 10^4$	$K_6 = 1.4390 \cdot 10^9$	

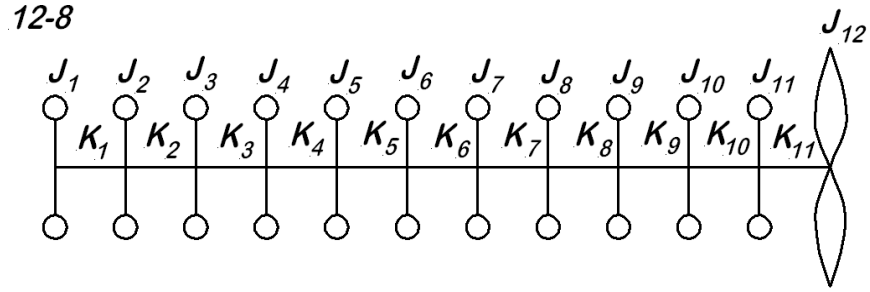

12-9 The figure shows the system previously considered in problem **12-7** with the addition of a viscously coupled ring damper ($C_d = 40$, $J_d = 0.3$). The numerical data given there apply for this problem as well. The damper ring is contained in a hollow cavity connected to the main shaft, and the space between the ring and housing is filled with a viscous fluid. Assume that the external torques are of the forms $T_1(t) = a_{1o} + a_{1n}\cos(n\Omega t) + b_{1n}\sin(n\Omega t)$ and $T_2(t) = a_{2o} + a_{2n}\cos(n\Omega t) + b_{2n}\sin(n\Omega t)$ where station 1 is the load and station 2 is the prime mover. The nominal shaft speed is $\Omega = 40$ rad//s.

(a) Develop the system equations of motion in matrix form;

(b) Develop an expression for a_{2o} in terms of a_{1o}, D_1, D_2 and Ω;

(c) Using the available numerical data, for steady state in the specific case where $n = 1$. $a_1 = 0$, $a_2 = 50$, $b_1 = b_2 = 0$, determine:

(i) the motion amplitude at frequency Ω for each station, including the damper rotor;

(ii) the slip amplitude in the damper (slip is the difference in component speeds).

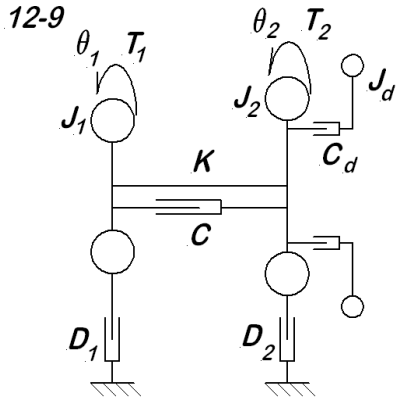

12-10 The figure shows two primary stations, a slider-crank engine and a driven load. The cylinder pressure force, $A \cdot P(\Omega t)$, is considered as known in Fourier series form.

(a) Develop any kinematic analysis required for later use;

(b) Formulate the full, nonlinear system equations for this machine;

(c) Linearize the slider-crank portion using the method of Biezeno and Grammel as described in the text. The crank motion is of the form $\theta(t) = \Omega t + \vartheta(t)$ where Ω is a relatively large value, and $|\vartheta(t)|$ is always relatively small.;

(d) Determine the system twisting mode natural frequency.

	Engine Data	Other System Data
$R = 50.8$ mm	$J_{1o} = 0.0094$ kg-m^2	$K = 2700$ N-m/rad
$L = 168.3$ mm	$M_2 = 0.8508$ kg	$J_2 = 2.6$ kg-m^2
$u_{2c} = 55.1$ mm	$J_{2c} = 0.0043$ kg-m^2	
$a = 46$ mm	$M_3 = 1.0143$ kg	
Power = 26.845196 MW	Avg Torque = 106814 N-m	Speed = 2400 rpm

12-11 The figure shows a two station torsional system, with a pendulum absorber fitted to station #1. The pendulum is to be considered as a point mass, M_p, with length b, supported at a distance a off the axis of rotation. There are external torques applied to each station, and the interest is in the steady state response at each station. Most of the system data is given below, but the user must determine one dimension.

(a) Ignoring the pendulum, determine the system twisting natural frequency;

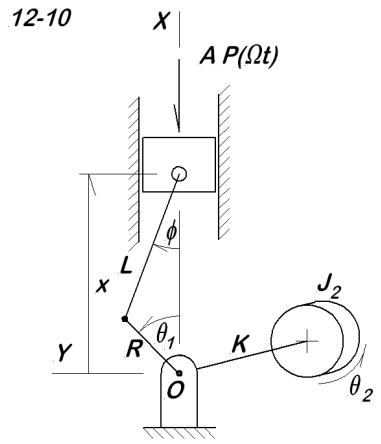

(b) Determine the pendulum length, b, such as to completely stop motion at station #1 for $n = 3$;

(c) Using the length b determined in part (b), determine the amplitude of the system response at each station for orders $n = 1, 2, 3, 4, 5, 6$;

(d) Develop a computer plot for the system response at each station through one full revolution.

$J_1 = 1.5$ kg-m^2	$a = 165$ mm	$M_p = 0.2$ kg
$J_2 = 2.5$ kg-m^2	$K = 10000$ N-m/rad	$\Omega = 35$ rad/s
$A_1 = 110$ N-m	$A_3 = 195$ N-m	$A_5 = -135$ N-m
$B_2 = 140$ N-m	$B_4 = 207$ N-m	$B_6 = 45$ N-m

$T_1^e = A_1 \cos(\Omega t) + A_3 \cos(3\Omega t) + A_5 \cos(5\Omega t)$

$T_2^e = B_2 \sin(2\Omega t) + B_4 \sin(4\Omega t) + B_6 \sin(6\Omega t)$

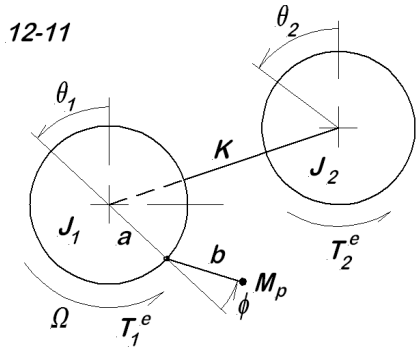

Appendix 1

Matrices

The ability to use matrix notation and to manipulate matrices is an essential skill for many scientific endeavors, particularly including the kinematics, dynamics, and vibration of machines. This short review is intended as an aid to those who have not seen this material before or who have become rusty on its use.

A1.1 Matrix Notation

A matrix is a *rectangular array of numbers*. A typical matrix with r rows and c columns may be denoted $[A]$, and represents the following array:

$$[A] = \begin{bmatrix} A_{11} & A_{12} & A_{13} & \cdots & A_{1c} \\ A_{21} & A_{22} & A_{23} & \cdots & A_{2c} \\ A_{31} & A_{32} & A_{33} & \cdots & A_{3c} \\ \vdots & \vdots & \vdots & & \vdots \\ A_{r1} & A_{r2} & A_{r3} & \cdots & A_{rc} \end{bmatrix}$$

Note that the subscripts refer to the location of the element within the array. In general, A_{ij} denotes the element in row i and column j. The range of the row index (1 to r) is the row dimension of the matrix. Similarly, the range of the column index (1 to c) is the column dimension of the matrix. If $r = c$, the matrix is said to be *square*. There is no requirement that a matrix be square, although many of interest are in fact square.

Two types of matrices are of particular interest: (1) square matrices, and (2) column (or row) matrices. A column matrix consists of a single column of n numbers and is denoted

by braces, {.}, such as

$$\{V\} = \left\{ \begin{array}{c} V_1 \\ V_2 \\ V_3 \\ \vdots \\ V_n \end{array} \right\}$$

This may be thought of as a single column of the general rectangular matrix form just given above. Because there is only one column, there is no need for a column index and the single index given serves to denote the row in which the element is located. The dimensions of the preceding column matrix are $(n \times 1)$, which keeps the column matrix in context as a special case of the rectangular matrix. A column matrix is often termed a *vector* and, conversely, a vector is usually understood to mean a column matrix. If there are only two or three elements, this may be considered to represent a physical vector in two- or three-dimensional space. At other times, there will be more than three elements, and the matrix may be considered as a vector in a space of higher dimensions. To conserve space, it is common practice to write the elements on one line, with the prefix col, so that the preceding vector would be written as $\{V\} = \text{col}\,(V_1, V_2, V_3, \ldots, V_n)$. The hybrid term *column vector* is used when it is necessary to distinguish it from the *row vector* to be discussed shortly.

One of the common matrix operations used is the *transpose*. Applied to a rectangular matrix, this operation consists of exchanging rows for columns. The result is that those elements that were originally in the j^{th} row of the original matrix are now found in the j^{th} column of the transposed matrix. The transpose of a matrix is denoted by the same name as the original matrix with the addition of a superscript T. Thus, for the preceding rectangular matrix, the transpose would be

$$[A]^T = \left[\begin{array}{ccccc} A_{11} & A_{21} & A_{31} & \cdots & A_{c1} \\ A_{12} & A_{22} & A_{33} & \cdots & A_{c2} \\ A_{13} & A_{23} & A_{33} & \cdots & A_{c3} \\ \vdots & \vdots & \vdots & & \vdots \\ A_{1r} & A_{2r} & A_{3r} & \cdots & A_{rc} \end{array} \right]$$

Note that the subscripts as used here are those of the original array. Thus, A_{23} from the original $[A]$ matrix is found in the transpose in the $(3, 2)$ position. If the transpose operation is applied to a column matrix, the result is to move the single column into a single row. This is often called a *row vector*. The dimensions for the row vector are

$(1 \times n)$. For the preceding column matrix $\{V\}$, the transpose is

$$\{V\}^T = (V_1, V_2, V_3, \ldots V_n)$$

A1.2 Matrix Addition and Subtraction

Addition and subtraction of two matrices are each defined to produce a new matrix, the elements of which are the sums, or differences, of corresponding elements in the two original matrices. However, addition and subtraction can be defined only when the two matrices have the same dimensions. If $[A]$ and $[B]$ are two rectangular matrices to be added,

$$[A] = \begin{bmatrix} A_{11} & A_{12} & A_{13} & \cdots \\ A_{21} & A_{22} & A_{23} & \cdots \\ A_{31} & A_{32} & A_{33} & \cdots \\ \vdots & \vdots & \vdots & \ddots \end{bmatrix} \qquad [B] = \begin{bmatrix} B_{11} & B_{12} & B_{13} & \cdots \\ B_{21} & B_{22} & B_{23} & \cdots \\ B_{31} & B_{32} & B_{33} & \cdots \\ & & & \ddots \end{bmatrix}$$

then the sum is $[C]$

$$[C] = [A] + [B] = \begin{bmatrix} A_{11} + B_{11} & A_{12} + B_{12} & A_{13} + B_{13} & \cdots \\ A_{21} + B_{21} & A_{22} + B_{22} & A_{23} + B_{23} & \cdots \\ A_{31} + B_{31} & A_{32} + B_{32} & A_{33} + B_{33} & \cdots \\ \vdots & \vdots & \vdots & \ddots \end{bmatrix}$$

Subtraction can be illustrated in a similar manner simply by changing the sign on the second term of each element in $[C]$. If $[A]$ and $[B]$ are of dimension $(r \times c)$, then the sum or difference, $[C]$, is also of dimension $(r \times c)$.

A1.3 Matrix Multiplication

The product of two matrices is another matrix, the elements of which are sums of products of the elements of the two original matrices. Formally, if the matrices to be multiplied are $[A] = [A_{ij}]$, $(n_1 \times n_2)$, and $[B] = [B_{jk}]$ $(n_2 2 \times n_3)$, the matrix product

$$\begin{array}{ccccc} [C] & = & [A] & & [B] \\ (n_1 \times n_3) & & (n_1 \times n_2) & & (n_2 \times n_3) \end{array}$$

has, as the typical element of $[C]$,

$$C_{ik} = \sum_{j=1}^{j=n_2} A_{ij} B_{jk}$$

Notice that the dimensions for each matrix are indicated in parentheses below the matrix name in the displayed matrix product. The results matrix, $[C]$, will be $(n_1 \times n_3)$, as indicated there. *An essential condition for the existence of the matrix product is also indicated that the column dimension of the first factor must be the same value as the row dimension of the second factor.* In this illustration, this dimension is n_2. The need for this condition is seen in the expression for the typical term; if this condition is not satisfied, there will not be an equal number of A_{ij} and B_{jk} factors to be multiplied together. Furthermore, the matrix product $[A][B]$ is, in general, not equal to the matrix product $[B][A]$, The order of the matrix factors is significant and *must* be maintained.

For manual evaluation of matrix products, the following approach is useful. A specific example serves to present the manual method. Consider the product of two matrices $[A]$ and $[B]$:

$$[C] = [A]\,[B]$$

To form the $(i,j)^{th}$ element of the product, the steps are as follows:

1. Locate the i^{th} row of the first factor ($[A]$) and the j^{th} column of the second factor ($[B]$);
2. Consider the i^{th} row to be rotated 90 degrees clockwise and placed adjacent to the elements of the j^{th} column, forming three indicated products;
3. Sum the three indicated products and store the result in the $(i,j)^{th}$ position of the result.

For the case $i = 2$, $j = 1$ just identified, this produces

$$\begin{aligned} C_{21} \;=\; & A_{21}B_{11} \\ & +A_{22}B_{21} \\ & +A_{23}B_{31} \end{aligned}$$

At times, the transpose operation may be applied to an indicated matrix product. The transpose of a product is the reversed product of the individual factors transposed:

$$([A]\,[B])^T = [B]^T\,[A]^T$$

For the proof of this statement, consult any standard text on matrix theory.

A1.4 Matrix Inversion

Addition, subtraction, and multiplication are each defined for both real numbers and matrices. At this point the similarity ends because there is no division operation defined for matrices. Instead, there is an operation known as *inversion* that produces a matrix called the *inverse of the original matrix*. Inversion is only distantly related to the idea of division, and the two must not be considered in any sense the same.

Before beginning the explanation of the matrix inverse, it is convenient to define the terms diagonal matrix and identity matrix. For a square matrix, the elements on the diagonal from the upper left corner to the lower right corner make up what is called the *main diagonal*. Some special matrices have all elements zero except for the elements on the main diagonal. Such matrices are called *diagonal matrices* and are sometimes written as

$$\lceil D \rfloor = diag\,(D_{11}, D_{22}, D_{33}, \cdots)$$

where only the elements on the main diagonal are written out. One very important diagonal matrix is the *identity matrix*, for which the elements on the main diagonal are each 1.0. A typical identity matrix of dimensions (3×3) is

$$\lceil I \rfloor = diag\,(1,1,1) = \begin{bmatrix} 1 & 0 & 0 \\ 0 & 1 & 0 \\ 0 & 0 & 1 \end{bmatrix}$$

The symbol $\lceil I \rfloor$ is often used for the identity matrix, although it also has other meanings such as the area or mass moment of inertia matrix. Care should be taken to make clear what is meant in each case.

One important characteristic of the identity matrix is seen when it is multiplied with a second matrix. The product is simply the second matrix; multiplication by the identity matrix changes nothing at all. This is indicated by the following statement:

$$\lceil I \rfloor\,[A] = [A]\,\lceil I \rfloor = [A]$$

This is comparable to multiplying a scalar by the value 1.0.

If $[A]$ is a square matrix for which $[B]$ is the inverse, this relation is expressed as

$$[B] = [A]^{-1}$$

where the superscript -1 is reminiscent of the exponent -1 that is used to denote the inverse of a scalar. Because $[B]$ is the inverse of $[A]$, this means that

$$[A][B] = [B][A] = \lceil I \rfloor$$

Notice that the matrix product taken in either order, $[A][B]$ or $[B][A]$, results in the identity matrix. This defines the inverse, $[B]$, in terms of the result when $[B]$ is multiplied with $[A]$; it does not tell how to determine $[B]$. There are many methods to determine the inverse of a matrix, and for these a suitable text on matrix algebra or numerical methods should be consulted. Most commercial computer codes provide a subroutine for matrix inversion, or equivalently, for the solution of a set of simultaneous linear algebraic equations.

One of the major concerns in dealing with the inverse of a particular matrix is whether or not an inverse actually exists for that matrix. To investigate, let $[A]$ be a square matrix for which $[B]$ is postulated to be the inverse. The matrix $[B]$ exists if, and only if, the determinant of $[A]$ is nonzero. Testing the value of the determinant of $[A]$ becomes a necessary part of assuring that subsequent analysis using $[B]$ will in fact be valid.

There are occasions when the inverse of a matrix product is indicated. For further analysis, this inverse can be replaced by the reversed product of the individual factor inverses:

$$([A]\,[B]) = [B]^{-1}\,[A]^{-1}$$

demonstrating a property much like the rule for the transpose of a product. The proof of this relation is available in many texts on matrices.

A1.5 Solution of Linear Algebraic Equations

One application of the matrix inverse is the formal solution of a system of linear simultaneous algebraic equations. The system of N equations in N unknown variables, which can be represented as

$$\begin{aligned} C_{11}x_1 + C_{12}x_2 + C_{13}x_3 + \ldots &= B_1 \\ C_{21}x_1 + C_{22}x_2 + C_{23}x_3 + \ldots &= B_2 \\ C_{31}x_1 + C_{32}x_2 + C_{33}x_3 + \ldots &= B_3 \\ &\vdots \end{aligned}$$

can be written very compactly in matrix form as

$$[C]\{x\} = \{B\}$$

where $[C]$ is $(N \times N)$ while $\{x\}$ and $\{B\}$ are each $(N \times 1)$. The formal solution for this system of equations is obtained by premultiplying by the inverse of $[C]$ (this presumes that such an inverse exists):

$$[C]^{-1}[C]\{x\} = [C]^{-1}\{B\}$$

or

$$\{x\} = [C]^{-1}\{B\}$$

This shows that the solution, $\{x\}$, is obtained from the product of the inverse of the coefficient matrix $[C]$ with the column matrix of constants, $\{B\}$. This is entirely correct and, from an analytic point of view, is the manner in which the solution is usually indicated a matrix inversion followed by a matrix product.

From the numerical standpoint, this is not the best way to compute the solution, $\{x\}$. It involves an unnecessary multiplication that slows the process and an unnecessary matrix inversion with associated numerical round-off errors. In writing computer programs to solve a system of linear equations, the direct solution should always be preferred; the inverse of the coefficient matrix should be computed only when the inverse itself is required. That said, True BASIC provides an excellent matrix inversion routine but no routine for the direct solution of a system of equations. Thus, if working in True BASIC, the matrix inversion is the recommended way to approach such problems.

There are times when the system to be solved consists of rectangular arrays for both the unknowns and the right side.

$$\begin{array}{ccccc} [C] & & [x] & = & [B] \\ (n \times n) & & (n \times m) & & (n \times m) \end{array}$$

Consider both $[x]$ and $[B]$ to be partitioned into columns:

$$[C][x_1|x_2|x_3|\ldots] = [B_1|B_2|B_3\cdots]$$

Then, the vectors $\{x_1\}$, $\{x_2\}$, and so forth, are the solutions associated with the various right-side vectors $\{B_1\}$, $\{B_2\}$, and so on, so that

$$[C]\{x_i\} = \{B_i\}$$

There will be m such solution vectors, each defining a column in the solution matrix $[x]$.

A1.6 Special Case: (2×2) Matrix

In many of the examples of the analysis of machines, a (2×2) matrix must be inverted or a system of two simultaneous linear equations must be solved. These special solutions are tabulated here for use when needed. They apply only for the inversion of a (2×2) matrix or the solution of two simultaneous linear equations.

A1.6.1 Analytical Inverse for (2×2) Matrix

Consider the (2×2) matrix $[C]$:

$$[C] = \begin{bmatrix} C_1 & C_2 \\ C_3 & C_4 \end{bmatrix}$$

The determinant of $[C]$ is $\det[C]$,

$$\det(C) = C_1 C_4 - C_2 C_3$$

and the inverse of $[C]$ is

$$[C]^{-1} = \frac{1}{\det[C]} \begin{bmatrix} C_4 & -C_2 \\ -C_3 & C_1 \end{bmatrix}$$

A1.6.2 Solution of Two Simultaneous Linear Equations

For the system of two linear equations,

$$\begin{bmatrix} C_1 & C_2 \\ C_3 & C_4 \end{bmatrix} \begin{Bmatrix} x_1 \\ x_2 \end{Bmatrix} = \begin{Bmatrix} B_1 \\ B_2 \end{Bmatrix}$$

the solution is

$$\left\{ \begin{array}{c} x_1 \\ x_2 \end{array} \right\} = \frac{1}{\det[C]} \left[\begin{array}{cc} C_4 & -C_2 \\ -C_3 & C_1 \end{array} \right] \left\{ \begin{array}{c} B_1 \\ B_2 \end{array} \right\}$$
$$= \frac{1}{\det[C]} \left\{ \begin{array}{c} C_4 B_1 - C_2 B_2 \\ -C_3 B_1 + C_1 B_2 \end{array} \right\}$$

These special cases occur so often in this book that the reader may wish to simply commit them to memory.

A1.7 Classical Eigenvalue Problem

This discussion is complementary to that presented in Section 11.4 because both look at the eigenproblem. There the discussion is approached from a physical view point

, while here and in the next section, it is looked at from a more mathematical perspective.

One of the most common linear algebra problems is the matter of solving the equation

$$[W]\{x\} = \{B\}$$

This is encountered countless times in this text, and usually presents no difficulty at all. That is, it presents no difficulty provided $\{B\}$ is not the zero vector. If in fact $\{B\} = \{0\}$, then considering the system of equations as a transformation matrix $[W]$ operating on a vector $\{x\}$, the equation says that $[W]$ transforms $\{x\}$ into the zero vector, a singular operation (one that cannot be reversed).

Consider then the equation

$$[W]\{x\} = \{0\}$$

There is always the trivial solution $\{x\} = \{0\}$, but that is of little interest. The real question is, "when are there nontrivial solutions?" The answer is that nontrivial solutions exist if and only if the determinant of $[W]$ is zero. Note that this does not say anything about how to find the nontrivial solutions; it only gives the conditions under which they exist.

All the above is by way of introduction to the *classical eigenvalue problem*, usually written as

$$[A]\{x\} = \lambda\{x\}$$

or

$$([A] - \lambda \lceil I \rfloor) \{x\} = \{0\}$$

where

$[A]$ is the matrix of interest, $n \times n$

$\{x\}$ is called the *eigenvector,* $n \times 1$

λ is the scalar *eigenvalue*

$\lceil I \rfloor$ is the diagonal identity matrix of the same order as $[A]$, $(n \times n)$

The German prefix *eigen-* is usually translated as *characteristic* although the older word in English was *proper*. The intent of the prefix is to indicate that the result correctly satisfies the characteristic equation. These proper solution elements exist only provided that

$$\det([A] - \lambda \lceil I \rfloor) = 0$$

which is the defining relation, usually called the *characteristic equation.* When the determinant is expanded, it is a polynomial of degree n, called the *characteristic polynomial. The number of eigenvalues and associated eigenvectors is equal to the order of the system*, n.

Example: Determine the eigenvalues of the following matrix:

$$[A] = \begin{bmatrix} 1 & 2 \\ 3 & 4 \end{bmatrix}$$

First the characteristic equation is written

$$\begin{aligned} 0 &= \det([A] - \lambda \lceil I \rfloor) \\ &= \det \begin{bmatrix} 1-\lambda & 2 \\ 3 & 4-\lambda \end{bmatrix} \\ &= \lambda^2 - 5\lambda - 2 \\ &= \left[\lambda - \left(\frac{5}{2} + \frac{1}{2}\sqrt{33}\right)\right] \left[\lambda - \left(\frac{5}{2} - \frac{1}{2}\sqrt{33}\right)\right] \end{aligned}$$

Since the equation is satisfied if either factor is zero, the eigenvalues are

$$\begin{aligned} \lambda_1 &= \frac{5}{2} - \frac{1}{2}\sqrt{33} \approx -0.37228 \\ \lambda_2 &= \frac{5}{2} + \frac{1}{2}\sqrt{33} \approx 5.3723 \end{aligned}$$

Observe (without proof) several statements that are true in general for all matrices of any order:

1. The product of the eigenvalues is $\det[A]$; in this example, the determinant is -2.0;

2. The sum of the eigenvalues is the sum of main diagonal entries, called the *trace*; in this example, $tr[A] = 5$;

3. A square matrix can be inverted if, and only if, none of its eigenvalues is zero.

With the eigenvalues in hand, the next question to address is the determination of the associated eigenvectors. Let λ_n be the n^{th} eigenvalues for a particular matrix. Then $\{x_n\}$ is an associated eigenvector if, and only if, it is true that

$$([A] - \lambda_n \lceil I \rfloor) \{x_n\} = \{0\}$$

It should be noted that *the eigenvector is not unique. Any nonzero constant multiplier (including complex number multipliers) applied to an eigenvector produces an alternate form of the same eigenvector.* There are infinitely many such multiples. This indicates that eigenvectors may be correctly be scaled in any convenient manner.

Example: Continuing the example just above where the two eigenvalues for a matrix $[A]$ were determined, with that same matrix $[A]$, assume that $\{x\}_j = \mathrm{col}(a, b)$ is an eigenvector associated with the eigenvalue λ_j. Then it is true that

$$\begin{bmatrix} 1-\lambda_j & 2 \\ 3 & 4-\lambda_j \end{bmatrix} \begin{Bmatrix} a_j \\ b_j \end{Bmatrix} = \begin{Bmatrix} 0 \\ 0 \end{Bmatrix}$$

$$\begin{aligned} (1-\lambda_j)\, a_j + 2b_j &= 0 \\ 3a_j + (4-\lambda_j)\, b_j &= 0 \end{aligned}$$

For $j = 1$, the first eigenvalue is $\lambda_1 \approx -0.37228$, both equations produce the same result, namely, $b = 0.68615a$. This means that one component of the eigenvector can be chosen at will, and then the second must be in this proportion. Choose for this example $a_1 = +1.0$, which leads to $b_1 = 0.68615$, which gives the eigenvector $\{x\}_1 = \mathrm{col}(1.0, 0.68615)$ associated with the first eigenvalue $\lambda_1 \approx -0.37228$.

For $j = 2$, the second eigenvalue is $\lambda_2 \approx 5.3723$, again both equations agree, $b_2 = 2.1862a_2$. It the first element of the second eigenvector is also chosen as $+1.0$, then the

result is $b_2 = 2.1862$. With this same scaling (choosing the first element as +1.0), the associated eigenvector is $\{x\}_2 = \text{col}\,(1.0, 2.1862)$ for the eigenvalue $\lambda_2 \approx 5.3723$.

On reflection, it should be evident that while there is nothing unduly complicated in the theory presented here, the numerical work can be daunting for systems of high order. For this reason, computer implementation is generally considered a necessity for systems of any significant size.

A1.8 Generalized Eigenproblem

The classical eigen problem is defined with respect to a single matrix (denoted above as $[A]$), but in engineering applications, a similar problem often appears in terms of two matrices in the form

$$\left([K] - \omega_j^2 \lceil M \rfloor\right) \{x\}_j = \{0\}$$

where

$[K] = (n \times n)$ stiffness matrix

$\lceil M \rfloor = (n \times n)$ diagonal mass or inertia matrix

$\{x\}_j = j^{th}$ $(n \times 1)$ eigenvector

$\omega_j^2 = j^{th}$ eigenvalue

This is called the *generalized eigenvalue problem*. While there are evident similarities with the classical form, there are significant differences as well. In general, the stiffness matrix reflects the connectivity of the system, and hence is not diagonal. The mass matrix is diagonal when a lumped mass formulation is developed (as is done in this book), although the reader should be aware that many finite element programs use a different, nondiagonal form called a *consistent mass matrix*; the last is not discussed further here.

There are two major options for dealing with the generalized eigenproblem. They are:

1. Find a way to convert it into the classical eigenproblem; such a process exists for many cases; or
2. Deal directly with it as it stands.

Consider here the first option, to convert the problem into the classical eigenproblem

form. The approach is based on the idea of finding a matrix, $[C]$ such that

$$\lceil M \rfloor = [C]^T [C]$$

where

1. $\lceil M \rfloor$ is diagonal, as supposed for all cases considered in this book;
2. $[K]$ is positive definite.

Then the Cholesky matrix $[C]$ is diagonal with the square roots of the diagonal elements of $\lceil M \rfloor$ for its entries. Use this to replace $\lceil M \rfloor$ in the original expression to obtain

$$\left([K] - \omega^2 [C] [C]^T \right) \{x\} = \{0\}$$

and then premultiply by $[C]^{-1}$ to get

$$\begin{aligned} [C]^{-1} [K] \{x\} &= \omega^2 [C]^{-1} [C] [C]^T \{x\} \\ &= \omega^2 [C]^T \{x\} \end{aligned}$$

Define a new eigenvector,

$$\{X\} = [C]^T \{x\}$$

and substitute in terms of $\{X\}$ to obtain

$$[C]^{-1} [K] [C]^{-T} \{X\} = \omega^2 \{X\}$$

If a matrix $[A]$ is now defined such that $[A] = [C]^{-1} [K] [C]^{-T}$, the problem is again in the classical eigenproblem form,

$$\left([A] - \omega^2 \lceil I \rfloor \right) \{X\} = \{0\}$$

This enables methods previously developed for the classical problem (such as the Jacobi method) to be applied to the generalized problem. Note, however, that while the eigenvalue remains unchanged in the Choleski transformation, the eigenvector is transformed and must be transformed back to solve the original problem. The inverse transformation of the eigenvectors is accomplished by

$$\{x\} = \left[[C]^T \right]^{-1} \{X\}$$

A1.9 Generalized Eigensolution Computer Code

The two section above discussed the Classical Eigenproblem and the Generalized Eigenproblem, the latter in terms of converting the generalized problem into the classical problem. Here the process is demonstrated in terms of a computer program that consists of three steps:

1. Problem data input and calculation of the Choleski transformation matrix;
2. Iterative solution of the classical problem by Jacobi's method;
3. Transformation of the modal matrix back to that of the original generalized problem.

The problem for this demonstration involves mass and stiffness matrices as follow:

$$\lceil M \rfloor = \begin{bmatrix} 2 & 0 & 0 \\ 0 & 1 & 0 \\ 0 & 0 & 2.2 \end{bmatrix}$$

$$[K] = \begin{bmatrix} 4.0 & -1.0 & 0.0 \\ 1.0 & 2.0 & -1.0 \\ 0.0 & -1.0 & 4.1 \end{bmatrix}$$

These matrices appear as `DATA` statements near the beginning of Program ChoJac.Tru and they are echoed back as the first part of the output from the program. This is useful in order to verify that the correct problem is solved. The first new results then follow, the computed natural frequencies which are the square roots of the eigenvalues determined by Subroutine Jacobi.Tru. This is then followed by (a) the modal matrix for the original problem, (b) the modal mass matrix for the original problem, and (c) the modal stiffness matrix for the original problem. The final output is a summary of the modal results for the original problem and a statement regarding the diagonalization process. The figure on the next page is a screen capture of the results.

All of the matrices are printed in scientific notation, and this is particularly significant for the modal mass and stiffness matrices. Note that neither one is exactly diagonal, but that both are very close to being diagonal, as indicated by the exponents on the off-diagonal terms. This demonstrates the quality of the Jacobi iteration process. If the off-diagonal terms are ever found to be significant, then the process fails and must be investigated further. The computer code for ChoJac.Tru is listed following the program output.


```
Mass Matrix
 +2.0000000e+00   +0.0000000e+00   +0.0000000e+00
 +0.0000000e+00   +1.0000000e+00   +0.0000000e+00
 +0.0000000e+00   +0.0000000e+00   +2.2000000e+00

Stiffness Matrix
 +4.0000000e+00   -1.0000000e+00   +0.0000000e+00
 -1.0000000e+00   +2.0000000e+00   -1.0000000e+00
 +0.0000000e+00   -1.0000000e+00   +4.1000000e+00

omega 1  =    .99369795  rad/s
omega 2  =   1.3888546  rad/s
omega 3  =   1.7167655  rad/s


Modal Matrix
 +1.0000000e+00   +1.0000000e+00   +1.0000000e+00
 +2.0251288e+00   +1.4216603e-01   -1.8945675e+00
 +1.0505733e+00   -9.8989441e-01   +7.9469305e-01



Modal Mass Matrix
 +8.5292957e+00   -1.3322676e-15   -4.4408921e-16
 -1.3322676e-15   +4.1759713e+00   -4.4408921e-16
 -6.6613381e-16   -4.4408921e-16   +6.9787676e+00

Modal Stiffness Matrix
 +8.4221304e+00   -1.3322676e-15   +1.3897772e-12
 -1.7763568e-15   +8.0551019e+00   -8.8817842e-16
 +1.3908874e-12   -8.8817842e-16   +2.0568408e+01

         Modal Mass   Modal Stiffness   Square Root
 index    Diagonal       Diagonal      Ratio = wn r/s
    1     8.529e+00      8.422e+00            .994
    2     4.176e+00      8.055e+00           1.389
    3     6.979e+00      2.057e+01           1.717
Modal Mass Max Abs Off-diagonal Element  =  1.3322676e-15
Modal Stiff Max Abs Off-diagonal Element =  1.3908874e-12

This demonstrates that the modal matrix, found through the
forward and inverse Choleski transformations, does in fact
diagonalize the mass and stiffness matrices to produce the
diagonal modal mass and modal stiffness matrices
```


Computer Program ChoJac.Tru

```
!      ChoJac.Tru
! Eigenproblem solution by Choleski transformation & Jacobi's method
! Solution of Generalized Eigenproblem by ----
!   (1) transforming the generalized problem to the classical problem
!       by the Choleski transformation
!   (2) solving the classical problem by Jacobi's method
!   (3) transforming back by the inverse Choleski transformation
!   [C] is the Choleski transformation matrix
OPTION NOLET
OPTION BASE 1
SET WINDOW 1,2,3,4
DIM A(3,3),evect(3,3),AIK(3),eval(3),MM(3,3),KK(3,3),SS(3,3)
DIM C(3,3),Ci(3,3),Ct(3,3),order(3),cit(3,3)
DIM sc1(3,3),sc(3),omega(3),modal(3,3),x(3),mdiag(3),kdiag(3)
e1=0.1e-11
e2=0.1e-11
e3=0.1e-5
itmax=50
CLEAR
! Problem data
DATA 3                          ! number of degrees of freedom
DATA  2,  1,  2.2               ! diag of mass matrix
DATA  4, -1,  0                 ! stiffness matrix by rows
DATA -1,  2, -1
DATA  0, -1,  4.1
READ ndof
MAT c=zer
MAT ci=zer
MAT MM=zer
MAT KK=zer
FOR i=1 to ndof                 ! read the diag of the mass matrix
    READ MM(i,i)
NEXT i
FOR i=1 to ndof                 ! read the stiffness matrix by rows
    FOR j=1 to ndof
        READ KK(i,j)
    NEXT j
NEXT i
img$="    +#.#######^^^^+#.#######^^^^+#.#######^^^^"
PRINT
PRINT
PRINT "   Mass Matrix"
```



```
MAT PRINT using img$: MM
PRINT "   Stiffness Matrix"
MAT PRINT using img$: KK
! Calculate the Choleski transformation
MAT c=zer
MAT ci=zer
FOR i=1 to ndof
    c(i,i)=sqr(MM(i,i))
    ci(i,i)=1/c(i,i)
NEXT i
MAT cit=trn(ci)
MAT sc1=ci*KK
MAT A=sc1*ci
! Send only the upper triangle for [A] to Jacobi!
FOR i=2 to ndof                    ! null the lower triangle
    FOR j=1 to i-1
        A(i,j)=0
    NEXT j
NEXT i

CALL jacobi

FOR i=1 to ndof
    ww=sqr(eval(i))                ! compute frequencies from omega^2 values
    omega(i)=ww
    PRINT "   omega";i;" = ",ww;" rad/s"
NEXT i
MAT modal=cit*modal                ! inverse Choleski transformation
FOR j=1 to ndof                    ! normalize first element to 1.0
    FOR i=ndof to 1 step -1
        modal(i,j)=modal(i,j)/modal(1,j)
    NEXT i
NEXT j
PRINT
PRINT
PRINT "   Modal Matrix"
MAT PRINT using img$: modal
! Calculate modal mass matrix = [A]t[M][A]
MAT sc1=trn(modal)
MAT sc1=sc1*MM
MAT sc1=sc1*modal
PRINT
PRINT
PRINT "  Modal Mass Matrix"
```



```
MAT PRINT using img$: sc1
mmod=0
FOR i=1 to ndof
    mdiag(i)=sc1(i,i)             ! diag element of modal mass matrix
    FOR j=1 to ndof
        ! mmod is max off diag of modal mass matrix
        IF i<>j then mmod=max(mmod,abs(sc1(i,j)))
    NEXT j
NEXT i
! Calc Modal Stiff Matrix = [A]t[K][A]
MAT sc1=trn(modal)
MAT sc1=sc1*KK
MAT sc1=sc1*modal
PRINT "   Modal Stiffness Matrix"
MAT PRINT using img$: sc1
kmod=0
FOR i=1 to ndof
    kdiag(i)=sc1(i,i)             ! diag element of modal stiffness matrix
    FOR j=1 to ndof
        IF i<>j then kmod=max(kmod,abs(sc1(i,j)))
    NEXT j
NEXT i
hdr1$="            Modal Mass   Modal Stiffness   Square Root"
hdr2$="    index    Diagonal       Diagonal      Ratio = wn r/s"
ivg$= "      ##     #.###^^^^#.###^^^^######.###"
PRINT hdr1$
PRINT hdr2$
FOR i=1 to ndof
    wn=sqr(kdiag(i)/mdiag(i))
    PRINT using ivg$: i,mdiag(i),kdiag(i),wn
NEXT i
PRINT "   Modal Mass Max Abs Off-diagonal Element  = ";mmod
PRINT "   Modal Stiff Max Abs Off-diagonal Element = ";kmod
PRINT
PRINT "   This demonstrates that the modal matrix, found through the"
PRINT "   forward and inverse Choleski transformations, does in fact"
PRINT "   diagonalize the mass and stiffness matrices to produce the"
PRINT "   diagonal modal mass and modal stiffness matrices"
GET KEY xxx

SUB jacobi
    ! Assume upper triangular [A] matrix as input
    ! Set up initial evector matrix, compute s1 and s
    FOR i=1 to ndof
```



```
        s1=s1+A(i,i)^2
        evect(i,i)=1
        FOR j=i+1 to ndof
            odsq=odsq+A(i,j)^2
        NEXT j
    NEXT i
    s=2*odsq+s1

    ! Begin Jacobi iteration ...
    FOR iter=1 to itmax
        FOR i=1 to ndof-1
            FOR j=i+1 to ndof
                q=abs(A(i,i)-A(j,j))
                ! Compute sine and cosine of rotation angle
                IF q<=e1 then
                   cang=1/sqr(2)
                   sang=cang
                ELSE IF abs(A(i,j))<=e2 then
                   EXIT FOR
                ELSE
                   p=2*A(i,j)*q/(A(i,i)-A(j,j))
                   spq=sqr(p^2+q^2)
                   cang=sqr((1+q/spq)/2)
                   sang=p/(2*cang*spq)
                END IF
                ! Update columns i and j of evect
                FOR k=1 to ndof
                    holdki=evect (k,i)
                    evect(k,i)=holdki*cang+evect(k,j)*sang
                    evect(k,j)=holdki*sang-evect(k,j)*cang
                NEXT k
                ! Compute new elements of [A] in rows i and j
                FOR k=i to ndof
                    IF k<=j then
                       aik(k)=A(i,k)
                       A(i,k)=cang*aik(k)+sang*A(k,j)
                       IF k=j then A(j,k)=sang*aik(k)-cang*A(j,k)
                    ELSE IF k>j then
                       holdik=A(i,k)
                       A(i,k)=cang*holdik+sang*A(j,k)
                       A(j,k)=sang*holdik-cang*A(j,k)
                    END IF
                NEXT k
                ! Compute new elements of [A] in columns i and j
```



```
          aik(j)=sang*aik(i)-cang*aik(j)
          FOR k=1 to j
              IF k>i then A(k,j)=sang*aik(k)-cang*A(k,j)
              IF k<=i then
                 holdki=A(k,i)
                 A(k,i)=cang*holdki+sang*A(k,j)
                 A(k,j)=sang*holdki-cang*A(k,j)
              END IF
          NEXT k
          A(i,j)=0
      NEXT j
NEXT i
! Find s2 and test for convergence
s2=0
FOR i=1 to ndof
    eval(i)=A(i,i)
    s2=s2+eval(i)^2
NEXT i
IF abs(1-s1/s2)<=e3 then
   flag=1
   ! Re-order eigensolutions
   FOR i=1 to ndof
       order(i)=i
   NEXT i
   FOR i=1 to ndof
       sa=eval(i)
       sb=order(i)
       si=i
       FOR j=i+1 to ndof
           IF eval(j)<sa then
              sa=eval(j)
              sb=order(j)
              si=j
           END IF
       NEXT j
       eval(si)=eval(i)
       order(si)=order(i)
       eval(i)=sa
       order(i)=sb
   NEXT i
   FOR j=1 to ndof        ! construct ordered modal matrix
       jj=order(j)
       FOR i=1 to ndof
           modal(i,j)=evect(i,jj)
```



```
                NEXT i
             NEXT j
          ELSE
          END IF
          s1=s2
          IF flag=1 then
             EXIT FOR
          END IF
      NEXT iter

      IF flag=0 then
         PRINT "   Solution Failed to Converge"
         STOP
      END IF
END SUB
END
```

References

[1] Hildebrand, F.B, *Introduction to Numerical Analysis*, New York: McGraw-Hill, 1956.

[2] Hohn, F.E, *Elementary Matrix Algebra*, New York: Macmillan, 1964.

Appendix 2

Newton-Raphson Solution

The Newton-Raphson solution method is a technique for numerically solving systems of simultaneous, nonlinear equations. Such systems of equations are frequently encountered in kinematic position analysis, and a clear understanding of the method is essential.

Consider the system of equations to be solved as

$$\begin{aligned} f_1(q_1, q_2, \ldots q_m, s_1, s_2, \ldots s_n) &= 0 \\ f_2(q_1, q_2, \ldots q_m, s_1, s_2, \ldots s_n) &= 0 \\ &\vdots \\ f_n(q_1, q_2, \ldots q_m, s_1, s_2, \ldots s_n) &= 0 \end{aligned}$$

where

- $q_1, q_2, \ldots q_m$ are primary variables, values either assigned at will or determined by means outside this system of equations,
- $s_1, s_2, \ldots s_n$, are secondary variables to be determined by the solution of these equations.

It is convenient to consider the s_i and the f_i values as column vectors,

$$\begin{aligned} \{S\} &= \text{col}(s_1, s_2, \ldots s_n) \\ \{F\} &= \text{col}(f_1, f_2, \ldots f_n) \end{aligned}$$

The solution process begins with an initial estimate for the solution, denoted as $\{S\langle 1\rangle\}$, where the $\langle 1\rangle$ indicates the first estimate. It is up to the user to provide this initial

estimate; Newton-Raphson is really only a process for refining estimates to approach the true solution. The initial estimate may be determined from a scale drawing, by an approximate calculation neglecting some factors, or simply a good guess. The better the initial estimate is, the quicker the process will converge to the true solution. On the other hand, if the initial estimate is too far removed from the desired solution, either the process may not converge at all, or it may converge to another solution. (It is common for these systems of equations to have many solutions in addition to the one desired.) For most kinematics problems, there is little difficulty in making a reasonable starting estimate.

If the vector function $\{F\}$ is evaluated at $\{S\langle 1\rangle\}$, in almost all cases, it will not be the zero vector. In the exceptional case where it is exactly $\{0\}$, then $\{S\langle 1\rangle\}$ is the exact solution, but this case is exceedingly rare! Assuming the usual case, where the function values are not all zero (these nonzero values are usually called the *residual*, indicating the values that remain nonzero), the problem becomes that of attempting to adjust the solution estimate so as to reduce the residuals. To this end, consider a Taylor series expansion of the vector function $\{F(\{S\})\}$ about the initial estimate, $\{S\langle 1\rangle\}$:

$$\{F(\{S\langle 2\rangle\})\} = \{F(\{S\langle 1\rangle\})\} + \left[\frac{\partial\{f\}}{\partial\{S\}}\right]\Bigg|_{\{S\langle 1\rangle\}} (\{S\langle 2\rangle\} - \{S\langle 1\rangle\}) + \cdots$$

The objective is to find $\{S\}$ that makes $\{F\} = \{0\}$, so suppose that $\{S\langle 2\rangle\}$ is the argument vector that achieves this goal. If that is true, then (1) the left side of the equation above is zero, and (2), the higher order terms in the equation may be dropped (terms indicated by the $\cdots$), to give an expression that is solvable for the *adjustment*, $\{S\langle 2\rangle\} - \{S\langle 1\rangle\}$, that is required to make this happen. The adjustment is

$$\{S\langle 2\rangle\} - \{S\langle 1\rangle\} = -\left[\frac{\partial\{f\}}{\partial\{S\}}\right]^{-1}\Bigg|_{\{S\langle 1\rangle\}} \{F(\{S\langle 1\rangle\})\}$$

If the adjustment is added to $\{S\langle 1\rangle\}$, the result will be $\{S\langle 2\rangle\}$, the improved estimate of the solution. It will not, in fact, be exactly the true solution because the higher order terms were neglected, but it will be closer to the solution than the previous estimate. It should be evident that this process can be repeated as many times as required to make the residual vector, $\{F(S\langle i\rangle)\}$, as small as desired.

The square matrix, $[\partial\{f\}/\partial\{S\}]$, is the *Jacobian matrix* for this system of equations. The solution for the adjustment requires the inverse of the Jacobian. If for any reason this inverse does not exist, the process cannot proceed. In terms of mechanism position analysis, this is called a *singular point*, and such conditions must be handled by special means on a case-by-case basis. Note that this is precisely the same Jacobian matrix that appears again in the expression for the velocity coefficients and velocity coefficient derivatives; this is no accident.

The development above shows the calculation of the adjustment as the product of the Jacobian inverse with the existing residual vector. This is equivalent to solving a system of linear equations. From a numerical standpoint, and depending on the software in use, solving the system of equations may be preferable in terms of computation speed and error control to inverting the matrix. When working in True BASIC, the process above is best implemented exactly as shown. A flow chart for the computer implementation is shown in Figure A2.1.

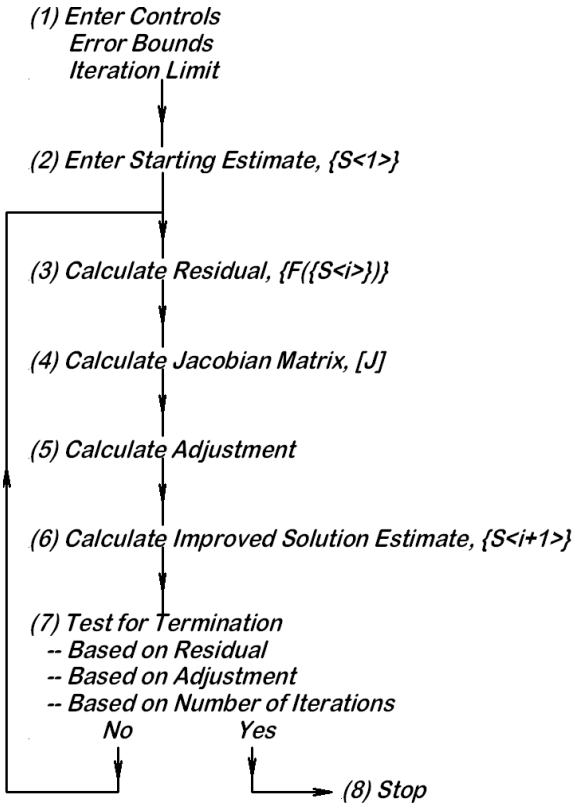

Figure A2.1: Newton-Raphson Solution Sequence

If the process described above is to be done manually, the decision to terminate the process will undoubtedly be made by the person performing the calculations at the earliest possible moment. If the process is to be done by a computer, then it is necessary to tell the computer when to stop iterating. There are three possible circumstances that indicate iteration should end:

1. Iteration should stop when every element of the residual has been reduced to a sufficiently small value to be considered (approximately) zero;

2. Iteration should end when the solution ceases to move, as indicated by adjustments below some specified threshold level. The solution may not be truly satisfactory, but further iteration is not going to improve the estimate;

3. Iteration should stop when the solution appears to simply wander, exceeding a specified number of steps, and indicating that the process is not converging.

The residual is a vector function, so it is necessary to assign a meaning to the idea of reducing the residual to a suitably small value. From a conceptual point of view, the simplest measure of the size of the residual is the absolute value of the largest element in the residual vector. Using this approach, iteration should continue until the residual element of maximum absolute value is less than an assigned error bound, typically 10^{-4} to 10^{-6} times a representative length for the mechanism. This representative length identifies the scale of the problem, thus connecting the allowable error to the system dimensions.

The process in the previous paragraph is conceptually simple, but it requires a bit more programming and more computer time to execute than a termination based on the sum of the squares of the residual components. This sum of squares is

$$|\{F\}|^2 = f_1^2 + f_2^2 + \cdots + f_n^2$$

In most computer codes, this can be calculated very quickly with a minimum of effort. It should be evident that no single element in the residual can be larger than the square root of the sum of the squares, so this single calculation essentially accounts for all residual elements in a single calculation. Because it is squared, and the values are much less than 1.0, the error criteria must be squared as well. Thus, for a termination criteria comparable to that of the previous approach, the sum of squares should be less than 10^{-8} to 10^{-12} times the square of the representative length. The sum of squares criterion is recommended because of its speed and ease of execution.

There are certainly circumstances when the process appears to hover near the solution without finally meeting the error criterion. If the magnitude of the adjustment vector is small, say 10^{-5}, then further iteration is unlikely to change the solutions in the first four digits to the right of the decimal point, and it may be necessary to terminate the iteration. The sum of squares approach can be used to measure the size of the adjustment vector just as recommended for the residual.

The iteration should always be placed in a counted loop (usually a `FOR-NEXT` or similar type loop) so that it does not go on endlessly, hanging the computer in an endless loop. With good starting estimates, it is common to have the Newton-Raphson converge quickly to very precise solutions, often within less than five iterations. Thus it is good practice to limit the number of iterations to no more than 20 unless careful study of the process indicates otherwise. In the event that the process is terminated for exceeding the allowed number of iterations, it is important that the solution produced be marked as suspect and not used further without examination. Thus, when the loop counter terminates a solution, a flag must be set to print a warning message and stop the whole computer program to examine the results.

The Newton-Raphson process is a powerful numerical technique, extraordinarily well suited for the solution of kinematic position equations. It also has many other applications in engineering and science, and the reader will do well to keep this very useful tool ready at hand.

Appendix 3

Numerical ODE Solutions

For most mechanisms, the differential equations of motion are nonlinear, coupled, ordinary differential equations with variable coefficients. Generally, closed-form solutions are not possible, but numerical solutions are readily available. The purpose of this appendix is to provide a numerical method of solution, the fourth-order Runge-Kutta method, without attempting to provide a comprehensive survey of available methods. The Runge-Kutta method is relatively reliable and is suitable for all of the problem types addressed in this text. There are many variations on the Runge-Kutta algorithm, and the particular forms presented here are those given by Abramowitz and Stegun (see References). For those who wish to pursue the topic further, there is a large body of literature available, often referenced under such headings as *Numerical Solution of Ordinary Differential Equations, Runge-Kutta,* or *Simulation.*

A3.1 The Marching Solution

Before discussing the Runge-Kutta algorithm, it is useful to consider the basic philosophy for the numerical solution of differential equations. This is presented most simply in terms of the Euler method applied to a single differential equation of the form

$$\dot{y} = f(t, y)$$

with the initial condition $y(0) = y_o$. The slope of the solution at $t = 0$ can be determined by using the initial condition to evaluate the slope as expressed by the differential equation evaluated at the initial conditions; this information is indicated in Figure A3.1(a).

To obtain an estimate of the solution at $t = h$, where h is a small time step, the tangent

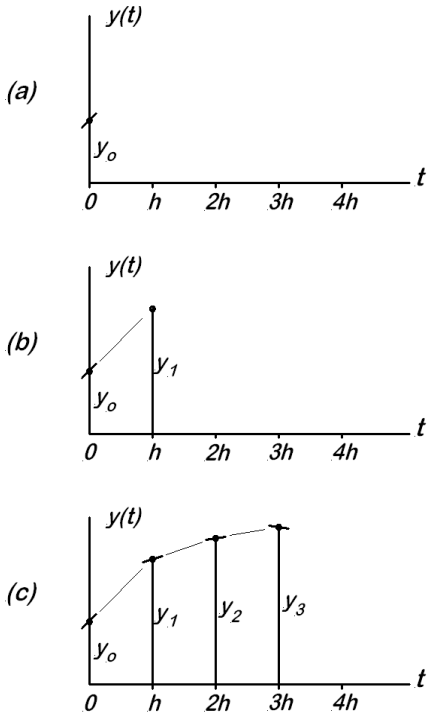

Figure A3.1: The Marching Solution: (a) Initial Conditions, (b) The First Step, (c) After Three Steps

line at $t = 0$ is projected to the right to intersect the line $t = h$. That intersection defines the new (approximate) solution point, Y_1, as shown in Figure A3.1(b).

The slope of the solution curve for $t = h$ is evaluated from the differential equation, using $t = h$ and $y = y_1$. A tangent line is then projected to intersect the line $t = 2h$, which defines a new solution point, Y_2. This process of projecting a tangent line repeatedly, called the *Euler method*, can be continued indefinitely and generates an approximate solution for the differential equation in the form of a table of values. From the description of the process, it is seen that the approximate solution is "marched out" from the initial condition under the guidance of the differential equation. **The Euler method is not recommended for actual application**, but it serves as a good basis for understanding the general idea of a "marching solution." The Runge-Kutta algorithm, presented below, operates in a similar manner. The major difference is that a more involved and more stable procedure is used to project each new solution point from the previous point.

It should be noted that the computed solution is really only a list of values, $Y_o, Y_1, Y_2, \ldots$ associated with the time values $0, h, 2h, \ldots$. Although it is common practice to plot a continuous line through these points, in fact, there is simply no function value information available between the tabulation points. It is only because the physical process is assumed to be *smooth* and *continuous* that there is some justification for drawing the continuous

solution curve.

A3.2 Fourth Order Runge-Kutta Method

There is a well–known family of stable solutions called Runge–Kutta solutions, named for Carl Runge (1856–1927) and M.W. Kutta (1867–1944). Runge was associated with the University of Göttingen from 1904 to 1925. Kutta is otherwise known for his work in aerodynamics (the Kutta–Joukowski theory of lift). Probably the most widely used single version of the Runge–Kutta algorithm is the fourth order algorithm. The term **fourth order** means that it agrees at each step with a Taylor series expansion as far as the fourth order difference term. The fourth order Runge–Kutta involves the calculation of several intermediate quantities before making the actual time step, all as follows, for the differential equation:

$$\dot{y} = f(t, y)$$

$$\begin{aligned} k_1 &= f(t, y_i) \\ k_2 &= f\left(t + \frac{h}{2}, y_i + \frac{h}{2}k_1\right) \\ k_3 &= f\left(t + \frac{h}{2}, y_i + \frac{h}{2}k_2\right) \\ k_4 &= f(t + h, y_i + hk_3) \\ y_{i+1} &= y_i + \frac{h}{6}(k_1 + 2k_2 + 2k_3 + k_4) \end{aligned}$$

It is obvious from their definitions that these quantities must be calculated in sequence, beginning with k_1 and continuing down through k_4, then all four of them (k_1, k_2, k_3 and k_4) are used to advance the solution one time step from t_i to t_{i+1}. On the one hand, this process is very similar to the Euler step, but it differs in that a more complex group of estimates is used to project the solution forward across the time step.

A3.3 Systems of ODE

Multidegree of freedom systems give rise to systems of second-order differential equations. It is notationally awkward to present the application of the Runge-Kutta algorithm to a general system of N differential equations, so the process is illustrated here in terms of

two second-order differential equations. The extension to any larger number of equations is then evident.

Consider the following system of differential equations:

$$\begin{aligned} \ddot{q}_1 &= f_1(t, q_1, q_2, \dot{q}_1, \dot{q}_2) \\ \ddot{q}_2 &= f_2(t, q_1, q_2, \dot{q}_1, \dot{q}_2) \end{aligned}$$

The first step is to replace this system with an equivalent system of first-order differential equations, based on the substitutions

$$\begin{aligned} u_1 &= q_1 \quad v_1 = \dot{q}_1 \\ u_2 &= q_2 \quad v_2 = \dot{q}_2 \end{aligned}$$

so that the equivalent system of differential equations is

$$\begin{aligned} \dot{u}_1 &= v_1 \\ \dot{u}_2 &= v_2 \\ \dot{v}_1 &= f_1\left(t, u_1, u_2, v_1, v_2\right) \\ \dot{v}_2 &= f_2\left(t, u_1, u_2, v_1, v_2\right) \end{aligned}$$

Applying the Runge-Kutta algorithm to this system, the new solution values are given by

$$\begin{aligned} u_{1,n+1} &= u_{1,n} + (1/6)\left(k_{11} + 2k_{12} + 2k_{13} + k_{14}\right) \\ u_{2,n+1} &= u_{2,n} + (1/6)\left(k_{21} + 2k_{22} + 2k_{23} + k_{24}\right) \\ v_{1,n+1} &= v_{1,n} + (1/6)\left(k_{31} + 2k_{32} + 2k_{33} + k_{34}\right) \\ v_{2,n+1} &= v_{2,n} + (1/6)\left(k_{41} + 2k_{42} + 2k_{43} + k_{44}\right) \end{aligned}$$

The new values are based on the following derivative evaluations:

$$\begin{aligned} k_{11} &= h\, v_{1,n} \\ k_{21} &= h\, v_{2,n} \\ k_{31} &= h\, f_1\left(t_n, u_{1,n}, u_{2,n}, v_{1,n}, v_{2,n}\right) \\ k_{41} &= h\, f_2\left(t_n, u_{1,n}, u_{2,n}, v_{1,n}, v_{2,n}\right) \end{aligned}$$

$$
\begin{aligned}
k_{12} &= h\left(v_{1,n} + \frac{1}{2}k_{11}\right) \\
k_{22} &= h\left(v_{2,n} + \frac{1}{2}k_{21}\right) \\
k_{32} &= h\, f_1\left(t_n + \frac{1}{2}h, u_{1,n} + \frac{1}{2}k_{11}, u_{2,n} + \frac{1}{2}k_{21}, v_{1,n} + \frac{1}{2}k_{31}, v_{2,n} + \frac{1}{2}k_{41}\right) \\
k_{42} &= h\, f_1\left(t_n + \frac{1}{2}h, u_{1,n} + \frac{1}{2}k_{11}, u_{2,n} + \frac{1}{2}k_{21}, v_{1,n} + \frac{1}{2}k_{31}, v_{2,n} + \frac{1}{2}k_{41}\right)
\end{aligned}
$$

$$
\begin{aligned}
k_{13} &= h\left(v_{1,n} + \frac{1}{2}k_{12}\right) \\
k_{23} &= h\left(v_{2,n} + \frac{1}{2}k_{22}\right) \\
k_{33} &= h\, f_1\left(t + \frac{1}{2}h, u_{1,n} + \frac{1}{2}k_{12}, u_{2,n} + \frac{1}{2}k_{22}, v_{1,n} + \frac{1}{2}k_{32}, v_{2,n} + \frac{1}{2}k_{42}\right) \\
k_{43} &= h\, f_2\left(t + \frac{1}{2}h, u_{1,n} + \frac{1}{2}k_{12}, u_{2,n} + \frac{1}{2}k_{22}, v_{1,n} + \frac{1}{2}k_{32}, v_{2,n} + \frac{1}{2}k_{42}\right)
\end{aligned}
$$

$$
\begin{aligned}
m_{14} &= h\left(v_{1,n} + m_{13}\right) \\
m_{24} &= h\left(v_{2,n} + m_{23}\right) \\
m_{34} &= h\, f_1\left(t + h, u_{1,n} + m_{13}, u_{2,n} + m_{23}, v_{1,n} + m_{33}, v_{2,n} + m_4\right) \\
m_{44} &= h\, f_2\left(t + h, u_{1,n} + m_{13}, u_{2,n} + m_{23}, v_{1,n} + m_{33}, v_{2,n} + m_4\right)
\end{aligned}
$$

The need for repeated evaluations of the second derivative expressions makes it clear that these evaluations should be programmed as a subroutine. This subroutine can then be called with the various argument combinations required. The actual application of these equations is not as difficult as might first appear. An example of this approach for a multidegree of freedom system is given in Section 8.6.3.

A3.4 Runge-Kutta for Second Order ODE

The general fourth order Runge–Kutta, presented above, is certainly applicable to second order ordinary differential equations. However, because second order differential equations arise so frequently in connection with the study of physical systems, it is convenient

to have a particular form uniquely suited to their solution. In this context, consider the second order differential equation

$$\ddot{y} = f\left(t, y, \dot{y}\right)$$

A fourth order Runge–Kutta specifically adapted to this equation is given by the following sequence of derivative evaluations and variable update statements:

$$\begin{aligned}
k_1 &= h \cdot f\left(t_i, y_i, \dot{y}_i\right) \\
k_2 &= h \cdot f\left(t_i + \frac{1}{2}h, y_i + \frac{h}{2}\dot{y}_i + \frac{h}{8}k_1, \dot{y}_i + \frac{1}{2}k_1\right) \\
k_3 &= h \cdot f\left(t_i + \frac{1}{2}h, y_i + \frac{h}{2}\dot{y}_i + \frac{h}{8}k_1, \dot{y}_i + \frac{1}{2}k_2\right) \\
k_4 &= h \cdot f\left(t_i + h, y_i + h\dot{y}_i + \frac{h}{2}k_3, \dot{y}_i + k_3\right)
\end{aligned}$$

$$\begin{aligned}
y_{i+1} &= y_i + h\left[\dot{y}_i + \frac{1}{6}\left(k_1 + k_2 + k_3\right)\right] \\
\dot{y}_{i+1} &= \dot{y}_i + \frac{1}{6}\left(k_1 + 2k_2 + 2k_3 + k_4\right) \\
t_{i+1} &= t_i + h
\end{aligned}$$

In the computer implementation that follows below, each variable is prefaced with `rk42`, so that the current value of y becomes `rk42y`, etc.

```
SUB RK42(rk42t,rk42y,rk42dy,rk42h)
 ! A fourth order Runge-Kutta routine for a single second order ODE
 ! Based on the formulation in Abramowitz & Stegun, Handbook of
 ! Mathematical Functions, NBS AMS 55, #25.5.20, p. 897
 ! This routine assumes that the derivative evaluation is done by DERIV.
 ! The ODE is ddy = f(t,y,dy) = DERIV(tt,yy,yp,ypp)
 ! h is the step size
 ! First derivative evaluation ...
 rk42tt=rk42t
 rk42yy=rk42y
 rk42yp=rk42dy
 CALL DERIV(rk42tt,rk42yy,rk42yp,rk42ypp)
 rk42k1=rk42h*rk42ypp
 ! Second derivative evaluation ...
 rk42tt=rk42t+rk42h/2
```



```
 rk42yy=rk42y+rk42h/2*rk42dy+rk42h/8*rk42k1
 rk42yp=rk42dy+rk42k1/2
 CALL DERIV(rk42tt,rk42yy,rk42yp,rk42ypp)
 rk42k2=rk42h*rk42ypp
 ! Third derivative evaluation ...
 rk42tt=rk42t+rk42h/2
 rk42yy=rk42y+rk42h/2*rk42dy+rk42h/8*rk42k1
 rk42yp=rk42dy+rk42k2/2
 CALL DERIV(rk42tt,rk42yy,rk42yp,rk42ypp)
 rk42k3=rk42h*rk42ypp
 ! Fourth derivative evaluation ...
 rk42tt=rk42t+rk42h
 rk42yy=rk42y+rk42h*rk42dy+rk42h/2*rk42k3
 rk42yp=rk42dy+rk42k3
 CALL DERIV(rk42tt,rk42yy,rk42yp,rk42ypp)
 rk42k4=rk42h*rk42ypp
 ! Update the solution ...
 rk42t=rk42t+rk42h ! new solution time
 rk42y=rk42y+rk42h*(rk42dy+(rk42k1+rk42k2+rk42k3)/6) ! new solution value
 rk42dy=rk42dy+(rk42k1+2*rk42k2+2*rk42k3+rk42k4)/6 ! new solution velocity
END SUB
```

In reading through the code above, it is evident that a subroutine called `DERIV` must be available to provide the required derivative values. The above mostly demonstrates the repeated calls to such a subroutine with varying arguments to accomplish the Runge-Kutta step for a second order differential equation. The last three lines show the solution updates, and the whole process should be enclosed in a loop to step the solution out.

A3.5 Simulation Languages

There are a number of *simulation languages* in the market today. These are programs which have built into them all of the details shown above (or something similar), so that the user needs only to specify the differential equations to be solved, along with the initial conditions, and then the program generates the numerical solution. Some of these simulation languages allow input in block diagram form, such that the user does not even have to completely formulate the differential equations of motion. Matlab® is famous for their popular Simulink® program that is block diagram oriented, and there are several others in the market, such as CSMP®, ACSL®, and MIMIC® There is no doubt that these programs are useful in engineering environments, particularly when they need to be used by technicians who do not fully understand the mathematics of their problems. One of the greatest difficulties with such programs is that they are often

difficult to check. The user does not have access to all of the details of the program, and consequently may wonder whether particular aspects of the problem have been correctly entered into the simulation language.

References

[1] Abramowitz, M. and Stegun, L. A., eds., *Handbook of Mathematical Functions*, Washington, D.C.: National Bureau of Standards, Applied Mathematics Series 55, US Government Printing Office, 1964 (9th printing, earlier printings had a few errors).

[2] Hildebrand, F. B., *Introduction to Numerical Analysis*, New York: McGraw-Hill, 1956.

Appendix 4

Geometric Property Calculations

A4.1 Introduction

In many of the problems discussed in this book, the mass properties of the various rigid bodies are assumed known. For actual engineering practice, this raises the question, "Where does this information come from?" How are the mass, location of center of mass, and mass moments of inertia determined for actual machine components? There are several possible answers to this question, including:

1. They can be determined by experiment, provided the physical parts already exist. The mass is determined by weighing the object, the center of mass is determined (at least in principle) by finding the balance point, and the mass moments of inertia can be determined by appropriate pendulum experiments.
2. For simple shapes, the mass properties can be calculated directly, often making use of the parallel axis theorem in order to combine calculations for different regions.
3. Some high end CAD programs are able to compute these properties after the part has been modeled in that CAD environment.
4. For a number of cases of interest, the mass properties can be calculated using Green's Theorem.

The subject of this appendix is the fourth item in the list above, the applications of Green's Theorem, to determine properties for plate-like bodies and for bodies of revolution, particularly when the boundaries are irregular in shape.

The calculations discussed below are essentially geometric in nature (hence the title for this appendix), but they are adaptable to the determination of the mass properties by the

inclusion of a density factor, ρ, and in some cases, the a thickness factor, t, for plate-like bodies. For most purposes, ρ should be considered to be the mass density, mass/volume. If the value of the specific weight (weight/volume) is used for ρ, then the properties calculated are weight based, rather than mass based. If the factor $\rho = 1$ is used, then purely geometric properties result.

A4.2 Green's Theorem

One of the topics often discussed in an Advanced Calculus course is called Green's Theorem [1, 2]. In the abstract, the value of this theorem is often unclear, but as will be seen here, it is particularly useful for the numerical evaluation of certain double integrals. The theorem states:

> Let D be a domain of the x-y plane and let Γ be a piece-wise smooth simple closed curve in D whose interior is also in D. Let $P(x, y)$ and $Q(x, y)$ be functions defined and continuous and having continuous first partial derivatives in D. Then
>
> $$\oint_\Gamma P\,dx + Q\,dy = \iint_A \left(\frac{\partial Q}{\partial x} - \frac{\partial P}{\partial y}\right)\,dx\,dy$$
>
> where A is the closed region bounded by Γ. The integration process proceeds around the boundary curve with positive area on the left, that is, in a counter clockwise sense.

For present purposes, this theorem is used to convert double integrals into cyclic line integrals. The cyclic line integrals lend themselves to numerical evaluation in a computer code. The conversion is accomplished by finding appropriate functions $P(x, y)$ and $Q(x, y)$, such that the integrand of the double integral is in the form of the right side of the expression above. Then Green's Theorem provides the equivalent in the form of a line integral. The problem then becomes on of numerical evaluation of the line integral along the appropriate boundary. Provided that the boundary of the domain of integration can be reasonably approximated by a sequence of straight line segments drawn between a set of node points on the boundary, the integration is usually straight forward.

Consider the closed boundary curve broken into n segments by n nodes. For the cyclic integral, the integration may be taken as n line integrals, comprising the complete path of integration, Γ:

$$\oint_\Gamma (\cdots)\ ds = \int_{x_1,y_1}^{x_2,y_2} (\cdots)\ ds + \int_{x_2,y_2}^{x_3,y_3} (\cdots)\ ds + \cdots + \int_{x_n,y_n}^{x_1,y_1} (\cdots)\ ds$$

As mentioned just above, for numerical evaluation of the cyclic integral, the boundary curve Γ is replaced by an irregular n-sided polygon defined by the n nodes, numbered in the sense of positive motion along Γ and approximating the boundary curve. The sequence must enclose the area on the left when the boundary is traversed in the counter clockwise sense.

To prepare for numerical evaluation of the cyclic integrals, the contribution of a boundary segment from (x_i, y_i) to (x_{i+1}, y_{i+1}) for each of three cases is required. These expressions are developed by substituting the forms appropriate to each of the three cases in the integral and evaluating the integral between the two end points for each case. The resulting expressions for the contribution of each increment can then be implemented in a subroutine for the numerical evaluation.

A4.3 Planar Area Properties

The area, centroidal coordinates, and area moments of inertia for a planar area are properties defined by the following double integrals:

$$\begin{aligned} A &= \iint_A 1 \, dx \, dy \\ x_c &= \tfrac{1}{A} \iint_A x \, dx \, dy \\ y_c &= \tfrac{1}{A} \iint_A y \, dx \, dy \\ I_{xx} &= \iint_A y^2 \, dx \, dy \\ I_{xy} &= -\iint_A xy \, dx \, dy \\ I_{yy} &= \iint_A x^2 \, dx \, dy \end{aligned}$$

In order to apply the ideas presented above regarding Green's Theorem, it is necessary to consider the integrand of each of the double integrals as being in the form $\frac{\partial Q}{\partial x} - \frac{\partial P}{\partial y}$ and then to devise appropriate functions $P(x, y)$ and $Q(x, y)$. The choices for P and Q are not unique, but, in fact, there are many satisfactory choices. For this discussion, the decision is made to take $Q(x, y) \equiv 0$, and then chose an appropriate function for $P(x, y)$ for each case. This has the effect of making the $\oint Q \, dy = 0$, and thus eliminating that part of the calculation.

The fundamental approximation to be made is that the boundary curve, Γ, may be approximated by an $n-$sided, irregular polygon. For the polygonal approximation, there

are basically three cases:

Case 0 a vertical line, $x = constant$

Case 1 a horizontal line, $y = constant$

Case 2 an inclined line, $y = s_i\,(x - x_i) + y_i$

The first of these cases (number 0) is of no further concern, because the integral $\int P\,dx$ is zero along a vertical line segment. For the other two cases, it is necessary to consider them in detail for each of the properties to be determined. Note that, before using the expressions developed for Case 2, it is necessary to evaluate s_i = slope of the line segment between points i and $i + 1$,

$$s_i = \frac{y_{i+1} - y_i}{x_{i+1} - x_i}$$

Note: if $|s_i|$ is very large (say, $|s_i| > 10^{10}$), it is necessary to treat such a segment as a vertical section and set all contributions to zero.

A4.3.1 Area

For the area calculation, $P = -y$ is a satisfactory choice. With this choice, $\frac{\partial P}{\partial y} = -1$, and the double integral is

$$\begin{aligned} A &= \iint 1\,dx\,dy \\ &= -\iint \frac{\partial P}{\partial y}\,dx\,dy \\ &= \iint \left(\frac{\partial Q}{\partial x} - \frac{\partial P}{\partial y}\right)\,dx\,dy \\ &= \oint P\,dx + Q\,dy \\ &= \oint P\,dx \\ &= -\oint y\,dx \end{aligned}$$

The negative sign may appear out of place here, but recall that the boundary curve is traversed with positive area on the left. Thus, for an area bounded by $x = a$, the x-axis, $x = b$, and a curve $y = f\,(x) > 0$ for $a \leq x \leq b$, in order to enclose the area on the left, the integration may be considered to begin at $(a, 0)$, move to the right along the x-axis,

up along the line $x = b$, right to left along the curve $y = f(x)$, and down along the line $x = a$. On three legs of the circuit, the integral is zero (either $y = 0$, or $dx = 0$) and the expression for the area comes down to

$$A = -\oint y\, dx = -\int_b^a y\, dx = \int_a^b y\, dx$$

This is of course the familiar expression for the area, and the previous form is seen to be compatible with the more familiar form for this situation.

For Case 1, the value of y is a constant and can be taken out of the integration. For Case 2, the integral can be evaluated along the inclined line segment. The results are, for the area,

$$\begin{aligned} &\text{Case 1} \quad \Delta A = -y_i \left(x_{i+1} - x_i\right) \\ &\text{Case 2} \quad \Delta A = -\left[\tfrac{1}{2} s_i \left(x_{i+1}^2 - x_i^2\right) + \left(y_i - s_i x_i\right)\left(x_{i+1} - x_i\right)\right] \end{aligned}$$

The two formulae above, giving ΔA for Cases 1 and 2, are referred to as *increments in A*, or more simply just as *increments*. They are the incremental contributions to the cyclic integral from the segment i to $i+1$. As noted previously, there is no increment when the line segment is vertical because of the way in which the function $Q(x, y)$ was chosen.

A4.3.2 Centroidal Coordinates

For the calculation of x_c, the horizontal coordinate of the centroid, a suitable choice is $P = -xy$, for which $\frac{\partial P}{\partial y} = -x$. For the calculation of y_c, the vertical coordinate of the centroid, a suitable choice is $P = -\frac{1}{2}y^2$, for which $\frac{\partial P}{\partial y} = -y$. The further development parallels that above, and is presented below in a parallel format.

$$\begin{aligned} x_c &= \tfrac{1}{A}\iint x\, dx\, dy & y_c &= \tfrac{1}{A}\iint_A y\, dx\, dy \\ &= \tfrac{1}{A}\iint \left(-\tfrac{\partial P}{\partial y}\right) dx\, dy & &= \tfrac{1}{A}\iint \left(-\tfrac{\partial P}{\partial y}\right) dx\, dy \\ &= \tfrac{1}{A}\iint \left(\tfrac{\partial Q}{\partial x} - \tfrac{\partial P}{\partial y}\right) dx\, dy & &= \tfrac{1}{A}\iint \left(\tfrac{\partial Q}{\partial x} - \tfrac{\partial P}{\partial y}\right) dx\, dy \\ &= \tfrac{1}{A}\oint (P\, dx + Q\, dy) & &= \tfrac{1}{A}\oint (P\, dx + Q\, dy) \\ &= \tfrac{1}{A}\oint P\, dx & &= \tfrac{1}{A}\oint P\, dx \\ &= -\tfrac{1}{A}\oint xy\, dx & &= -\tfrac{1}{2A}\oint y^2\, dx \end{aligned}$$

As before, the incremental contributions for Cases 1 and 2 must be determined for each of these integrals. The process is illustrated above for ΔA, and the results for Δx_c and

Δy_c follow:

$$\begin{aligned}
&\text{Case 1} \quad \Delta x_c = \tfrac{-1}{2A} y_i \left(x_{i+1}^2 - x_i^2\right) \\
&\text{Case 2} \quad \Delta x_c = \tfrac{-1}{A} \left[\tfrac{1}{3} s_i \left(x_{i+1}^3 - x_i^3\right) + \tfrac{1}{2} \left(y_i - s_i x_i\right) \left(x_{i+1}^2 - x_i^2\right)\right]
\end{aligned}$$

$$\begin{aligned}
&\text{Case 1} \quad \Delta y_c = \tfrac{-1}{2A} y_i^2 \left(x_{i+1} - x_i\right) \\
&\text{Case 2} \quad \Delta y_c = \tfrac{-1}{2A} [\tfrac{1}{3} s_i^2 \left(x_{i+1}^3 - x_i^3\right) + s_i \left(y_i - s_i x_i\right) \left(x_{i+1}^2 - x_i^2\right) \\
&\qquad\qquad + \left(y_i^2 + s_i^2 x_i^2\right) \left(x_{i+1} - x_i\right)]
\end{aligned}$$

A4.3.3 Area Moments of Inertia

The integrals involved for the area moments of inertia are

$$\begin{aligned}
I_{xx} &= \iint_A y^2 \, dx \, dy \\
I_{xy} &= \iint_A xy \, dx \, dy \\
I_{yy} &= \iint_A x^2 \, dx \, dy
\end{aligned}$$

A4.3.3.1 I_{xx} – X-axis Moment of Inertia

Following the line of development given above, for the moment of inertia with respect to the x-axis, a suitable choice for P is $P = -\frac{1}{3} y^3$ with the partial derivative $\frac{\partial P}{\partial y} = -y^2$. When carried through to the final form, the expression for I_{xx} is

$$\begin{aligned}
I_{xx} &= \iint_A y^2 \, dx \, dy \\
&= -\iint_A \frac{\partial P}{\partial y} \, dx \, dy \\
&= \oint P dx \\
&= -\frac{1}{3} \oint y^3 \, dx
\end{aligned}$$

The incremental expressions for this integral are

$$\begin{aligned}
&\text{Case 1 } \Delta I_{xx} = -\tfrac{1}{3} y_i^3 \left(x_{i+1} - x_i\right) \\
&\text{Case 2 } \Delta I_{xx} = -\tfrac{1}{3}[\tfrac{1}{4} s_i^3 \left(x_{i+1}^4 - x_i^4\right) + s_i^2 \left(y_i - s_i x_i\right) \left(x_{i+1}^3 - x_i^3\right) \\
&\qquad\qquad + \tfrac{3}{2} s_i \left(y_i - s_i x_i\right)^2 \left(x_{i+1}^2 - x_i^2\right) + \left(y_i - s_i x_i\right)^3 \left(x_{i+1} - x_i\right)]
\end{aligned}$$

A4.3.3.2 I_{xy} – Product of Inertia

For the product of inertia, one suitable choice is $P\left(x, y\right) = \left(1/2\right) xy^2$ with the derivative $\frac{\partial P}{\partial y} = xy$. Then the equivalent line integral is

$$\begin{aligned}
I_{xy} &= -\iint_A xy \, dx \, dy \\
&= -\iint_A \left(\frac{\partial P}{\partial y}\right) \, dx \, dy \\
&= \oint_\Gamma P dx \\
&= \oint_\Gamma \left(\frac{1}{2} xy^2\right) dx
\end{aligned}$$

For Case 1, $y = constant$, the contribution to the integral is

$$\begin{aligned}
\Delta I_{xy} &= \int_{x_i}^{x_{i+1}} \left(\frac{1}{2} xy^2\right) dx \\
&= \frac{1}{4} x^2 y_i^2 \Big|_{x_i}^{x_{i+1}} \\
&= \frac{1}{4} y_i^2 \left(x_{i+1}^2 - x_i^2\right)
\end{aligned}$$

For Case 2, $y = s_i \left(x - x_i\right) + y_i$, the contribution to the integral is

$$\begin{aligned}
\Delta I_{xy} &= \int_{x_i}^{x_{i+1}} \left(\frac{1}{2}xy^2\right) dx \\
&= \frac{1}{2}\int_{x_i}^{x_{i+1}} x\left[s_i\left(x-x_i\right)+y_i\right]^2 dx \\
&= \frac{1}{2}\int_{x_i}^{x_{i+1}} x\left[s_i^2\left(x-x_i\right)^2+2s_iy_i\left(x-x_i\right)+y_i^2\right] dx \\
&= \frac{1}{2}\int_{x_i}^{x_{i+1}} x\left[s_i^2\left(x^2-2xx_i+x_i^2\right)+2s_iy_i\left(x-x_i\right)+y_i^2\right] dx \\
&= \frac{1}{2}\int_{x_i}^{x_{i+1}} \left[s_i^2\left(x^3-2x^2x_i+xx_i^2\right)+2s_iy_i\left(x^2-xx_i\right)+xy_i^2\right] dx \\
&= \frac{1}{2}\left[s_i^2\left(\frac{x^4}{4}-\frac{2x^3x_i}{3}+\frac{x^2x_i^2}{2}\right)+2s_iy_i\left(\frac{x^3}{3}-\frac{x^2x_i}{2}\right)+\frac{x^2y_i^2}{2}\right]_{x_i}^{x_{i+1}} \\
&= s_i^2\left[\frac{1}{8}\left(x_{i+1}^4-x_i^4\right)-\frac{1}{3}x_i\left(x_{i+1}^3-x_i^3\right)+\frac{1}{4}x_i^2\left(x_{i+1}^2-x_i^2\right)\right] \\
&\quad +s_iy_i\left[\frac{1}{3}\left(x_{i+1}^3-x_i^3\right)-\frac{1}{2}x_i\left(x_{i+1}^2-x_i^2\right)\right]+\frac{1}{4}y_i^2\left(x_{i+1}^2-x_i^2\right)
\end{aligned}$$

A4.3.3.3 I_{yy} – Y-axis Moment of Inertia

In the determination of I_{yy}, an appropriate choice for P is $P=-x^2y$ with the partial derivative $\frac{\partial P}{\partial y}=-x^2$. This leads to the expression for I_{yy} as

$$\begin{aligned}
I_{yy} &= \iint_A x^2\, dx\, dy \\
&= -\iint_A \frac{\partial P}{\partial y}\, dx\, dy \\
&= \oint_\Gamma P dx \\
&= -\oint x^2y\, dx
\end{aligned}$$

The incremental expressions for I_{yy} are

$$\begin{aligned}
&\text{Case 1 } \Delta I_{yy} = -\tfrac{1}{3}y_i\left(x_{i+1}^3-x_i^3\right) \\
&\text{Case 2 } \Delta I_{yy} = -\tfrac{1}{4}s_i\left(x_{i+1}^4-x_i^4\right)-\tfrac{1}{3}\left(y_i-s_ix_i\right)\left(x_{i+1}^3-x_i^3\right)
\end{aligned}$$

The calculations described above are implemented in a simple program, PlnArea.Tru, for which a listing follows below. Following the listing, there are two recommended test cases to verify the program and a few comments on the quality of the results.

A4.3.4 Program PlnArea.Tru

```
!                     PlnArea.Tru
! Geometric properties for a planar area
! of arbitrary shape
OPTION NOLET
OPTION BASE 1
DIM x(0),y(0)
s1$="   Nodes must enclose the area,"
s11$="positive area on the left"
s2$="   This is sometimes described as"
s22$=" counter clockwise"
s3$="   Enter the total number of nodes to be used"
CLEAR
PRINT
PRINT "                         PlnArea.Tru"
PRINT
PRINT s1$&s11$
PRINT s2$&s22$
PRINT
PRINT  s3$
INPUT n
MAT redim x(n),y(n)
PRINT
PRINT "   Enter the node coordinates in pairs, xi,yi"
FOR i=1 to n
    PRINT "x(";i;"), y(";i;") = ?"
    INPUT x(i),y(i)
NEXT i
CALL PAcalcs
PRINT
PRINT "                Results"
PRINT
PRINT "         Area = ";area
PRINT "         xc   = ";xc
PRINT "         yc   = ";yc
PRINT "        Ixx   = ";ixx
PRINT "        Ixy   = ";ixy
```



```
PRINT "        Iyy   = ";iyy

SUB PAcalcs
    asum=0                          ! initialize sum for area
    xcsum=0                         ! initialize sum for Xc
    ycsum=0                         ! initialize sum for Yc
    ixxsum=0                        ! initialize sum for Ixx
    ixysum=0                        ! initialize sum for Ixy
    iyysum=0                        ! initialize sum for Iyy
    x1=x(1)
    y1=y(1)
    FOR i=1 to n
        i2=i+1
        IF i2<=n then               ! usual case
           x2=x(i2)
           y2=y(i2)
        ELSE IF i2>n then           ! last side
           x2=x(1)                  ! close the polygon
           y2=y(1)
        END IF
        IF x2=x1 then
           da=0                     ! vertical edge
           dxc=0
           dyc=0
           dixx=0
           dixy=0
           diyy=0
           EXIT IF
        ELSE IF y2=y1 then
           CALL cas1                ! horizontal segment
        ELSE IF y2<>y1 then
           CALL cas2                ! sloping segment
        END IF
        ! Add increments ...
        asum=asum+da
        xcsum=xcsum+dxc
        ycsum=ycsum+dyc
        ixxsum=ixxsum+dixx
        ixysum=ixysum+dixy
        iyysum=iyysum+diyy
        x1=x2
        y1=y2
    NEXT i
    ! Final evaluations ...
```



```
    area=asum
    xc=xcsum/area
    yc=ycsum/area
    ixx=ixxsum/3
    ixy=ixysum
    iyy=iysum
END SUB
SUB cas1
    da=-y1*(x2-x1)
    dxc=-y1*(x2^2-x1^2)/2
    dyc=-y1^2*(x2-x1)/2
    dixx=-y1^3*(x2-x1)
    dixy=y1^2*(x2^2-x1^2)/4
    diyy=-y1*(x2^3-x1^3)/3
END SUB
SUB cas2
    s=(y2-y1)/(x2-x1)
    if abs(s)>1e7 then            !treat like a vertical section
        da=0
        dxc=0
        dyc=0
        dixx=0
        dixy=0
        diyy=0
        exit sub
    end if
    da=-(s/2*(x2^2-x1^2)+(y1-s*x1)*(x2-x1))
    dxc=-(s/3*(x2^3-x1^3)+.5*(y1-s*x1)*(x2^2-x1^2))
    dyc=(s^2/3)*(x2^3-x1^3)+s*(y1-s*x1)*(x2^2-x1^2)
    dyc=-.5*(dyc+(y1-s*x1)^2*(x2-x1))
    dixx=s^3/4*(x2^4-x1^4)+s^2*(y1-s*x1)*(x2^3-x1^3)
    dixx=dixx+3*s/2*(y1-s*x1)^2*(x2^2-x1^2)
    dixx=-(dixx+(y1-s*x1)^3*(x2-x1))
    dixy=s^2*((x2^4-x1^4)/8-x1*(x2^3-x1^3)/3+x1^2*(x2^2-x1^2)/4)
    dixy=dixy+s*y1*((x2^3-x1^3)/3-x1*(x2^2-x1^2)/2)
    dixy=dixy+y1^2*(x2^2-x1^2)/4
    diyy=-s/4*(x2^4-x1^4)-(y1-s*x1)*(x2^3-x1^3)/3
END SUB
END
```


A4.3.4.1 Test Cases

It is useful to have a few test cases to validate a program such as this after it has been coded for the computer. The two test cases below will exercise all aspects of the program, and they are sufficiently simple to allow an exact calculation.

1. Rectangle: vertices at $(2,1)$, $(4,1)$, $(4,3)$, and $(2,3)$;
2. Triangle: vertices at $(2,0)$, $(3,0)$, and $(2,3)$.

	Rectangle	Triangle
Area =	4.0	1.5
x_C =	3.0	2.333333
y_C =	2.0	1.0
I_{xx} =	17.33333	2.25
I_{xy} =	−24.0	−3.375
I_{yy} =	37.33333	8.25

The validity of the results when this program is applied to a complicated area with curved boundaries is dependent on the degree of approximation achieved by the $n-$sided polygon for which the program is exact (other than round-off and the inherent truncation errors of finite arithmetic). If the polygon deviates significantly from the intended curved boundary, the results are not very good. Dividing the curved boundary into a greater number of parts will improve the results, and, in the limit as infinitely many divisions are used, the program result approaches the exact result, although the execution time becomes unacceptable! If a part of the boundary is straight, the program computes the contribution of that part of the boundary exactly; there is no benefit to dividing a straight edge into several segments.

A4.3.5 Rocker Mass Properties Example

In Chapter 7, one of the simulation examples involves a rocker that rolls around a circular support. The rocker is a flat plate, bounded by five circular arcs and two straight lines. It is shown in the adjacent figure, the same as Figure 7.4. The purpose of this example is to illustrate the application of the Planar Area program to the determination of the inertial properties of such a body.

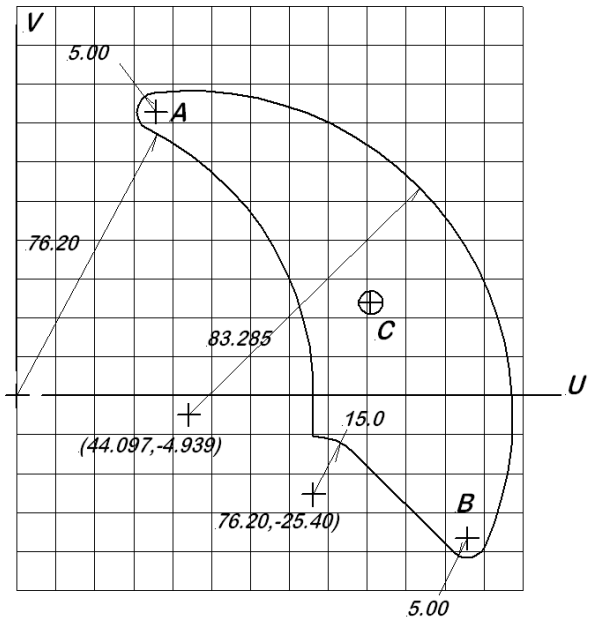

Figure A4.1: Rocker Geometry on a 10 mm Grid (All Dimensions in Millimeters)

The rocker geometry is shown in Figure 7.5 on a 10 mm grid, and the rocker thickness is 21 mm. Note that the origin of the body coordinate system is the center of the inside radius at the level of the beginning of the arc (below that point, the profile is straight). This choice is made because of the circular form of the body inner boundary, most easily expressed with this coordinate system choice. Using the Planar Area Program of this Appendix, the following properties are determined for the planar area of the part profile:

Property	As Calculated	Converted to SI Units
Area	$A = 5044.6$ mm^2	$A = 5.0446 \cdot 10^{-3}$ m^2
Centroid	$u_c = 91.879$ mm	$u_c = 9.1879 \cdot 10^{-2}$ m
Coordinates	$v_c = 23.306$ mm	$v_c = 2.3306 \cdot 10^{-2}$ m
Area	$I_{\text{uu}} = +7.4286 \cdot 10^6$ mm^4	$I_{\text{uu}} = +7.4286 \cdot 10^{-6}$ m^4
Moments	$I_{uv} = -8.5492 \cdot 10^6$ mm^4	$I_{uv} = -8.5492 \cdot 10^{-6}$ m^4
of Inertia	$I_{vv} = +4.4664 \cdot 10^7$ mm^4	$I_{vv} = +4.4664 \cdot 10^{-5}$ m^4

All the data in the table above is purely geometrical in nature, but what is required is inertial data for the rocker. Thus the obvious question is, "How are these two related?"

In the given data, there was $\rho = 7800.6$ kg/m^3 and thickness $t = 0.021$ m. The mass of the body is expressible as

$$\begin{aligned} M &= \iiint_V \rho \, dxdydz = \rho t \iint_A dxdy = \rho t A \\ &= (7800.6)\,(0.021)\left(5.0446 \cdot 10^{-3}\right) \\ &= 0.8264 \text{ kg} \end{aligned}$$

The center of mass coordinates, (x_{cm}, y_{cm}) are the same as the centroid, (x_c, y_c). For the mass moments of inertia, the process is similar to that for the mass:

$$\begin{aligned} J_{\text{uu}} &= \iiint_V \rho y^2 \, dxdydz = \rho t \iint_A y^2 \, dxdy = \rho t I_{\text{uu}} \\ &= (7800.6)\,(0.021)\left(7.4286 \cdot 10^{-6}\right) \\ &= 1.2169 \cdot 10^{-3} \text{ kg-m}^2 \end{aligned}$$

The parallel axis theorem is then employed to find the corresponding value at the center of mass,

$$\begin{aligned} J_{\text{uuc}} &= J_{\text{uu}} - M v_c^2 \\ &= 1.2169 \cdot 10^{-3} - (0.8264)\,(0.023306)^2 \\ &= 7.6804 \cdot 10^{-4} \text{ kg-m}^2 \end{aligned}$$

For the problem where this example originated, the mass moment of inertia with respect to an axis at the center of mass and perpendicular to the plate is required. This is what is often called the polar mass moment of inertia, J_{zzc}.

$$J_{zzc} = J_{\text{uuc}} + J_{vvc}$$

This completes the process of finding mass properties from the area properties. The final results are summarized here:

$$\begin{aligned} M &= 0.826367 && \text{kg} \\ u_c &= 0.091879 && \text{m} \\ v_c &= 0.023306 && \text{m} \\ J_{xxc} &= 0.00076804 && \text{kg-m}^2 \\ J_{yyc} &= 0.00036907 && \text{kg-m}^2 \\ J_{zzc} &= 0.00110864 && \text{kg-m}^2 \end{aligned}$$

The other important data required for that problem are the locations of the several attachment points. This is all summarized in the following list:

$u_A = +0.035795$ m $\qquad v_A = +0.072885$ m

$u_B = +0.115676$ m $\qquad v_B = -0.036593$ m

$x_D = +0.083976$ m $\qquad y_D = -0.086593$ m

This completes all of the required geometrical and inertial data for this example.

A4.4 Circular Segments

There are two closely related plane figures derived from a circle that occur with some frequency. As shown in Figure A4.2, consider a chordal line $A - A'$ dividing a circle into two regions. The smaller area, I, is the *lesser circular segment* (ruled area), while the larger area, II, is the *greater circular segment*. While their area properties can certainly be determined numerically by the methods of the previous section, they are also expressible in closed form as given below. All results are expressed with respect to the $X - Y$ coordinate system shown.

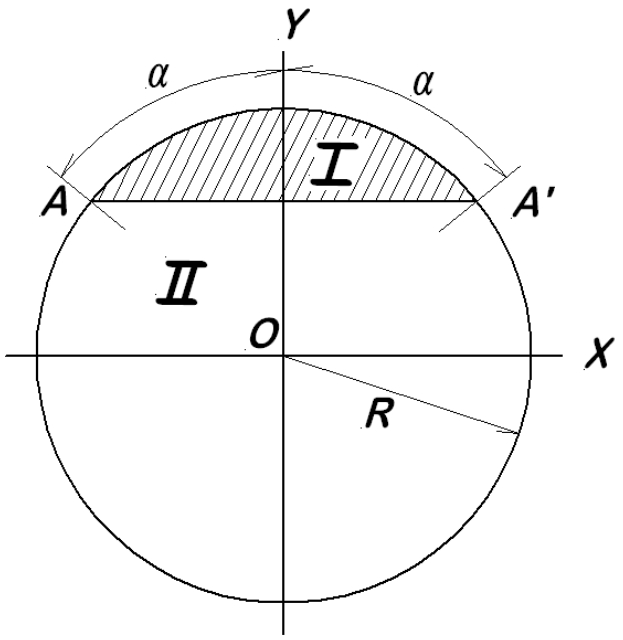

Figure A4.2: Circular Segments

A4.4.1 Lesser Circular Segment, I

For the lesser circular segment, the area properties are expressed as

$\text{Area}_I = R^2 (\alpha - \sin\alpha\cos\alpha)$	Enclosed Area
$x_{cI} = 0$	Centroid Location
$y_{cI} = \frac{R}{3}\frac{[-3\sin\alpha+\sin(3\alpha)]}{\sin(2\alpha)-2\alpha}$	Centroid Location
$I_{xxoI} = \frac{R^4}{4}(\alpha + \sin\alpha\cos\alpha - 2\cos^3\alpha\sin\alpha)$	X-axis Area MOI
$I_{yyoI} = \frac{R^4}{12}\left(-3\sin\alpha\cos\alpha - 2\sin^3\alpha\cos\alpha + 3\alpha\right)$	Y-axis Area MOI
$J_{ooI} = \frac{R^4}{6}(3\alpha - 2\cos^3\alpha\sin\alpha - \sin\alpha\cos\alpha)$	Area Polar MOI

A4.4.2 Greater Circular Segment, II

$\text{Area}_{II} = R^2 (\pi - \alpha + \sin\alpha\cos\alpha)$	Enclosed Area
$x_{cII} = 0$	Centroid Location
$y_{cII} = -\left(\frac{2R}{3}\right)\frac{\sin^3\alpha}{\pi-\alpha+\sin\alpha\cos\alpha}$	Centroid Location
$I_{xxoII} = \frac{R^4}{4}(\pi - \alpha - \sin\alpha\cos\alpha + 2\cos^3\alpha\sin\alpha)$	X-axis Area MOI
$I_{yyoII} = \frac{R^4}{12}(3\pi - 3\alpha + 5\sin\alpha\cos\alpha - 2\cos^3\alpha\sin\alpha)$	Y-axis Area MOI
$J_{ooII} = \frac{R^4}{6}(3\pi - 3\alpha + \sin\alpha\cos\alpha + 2\cos^3\alpha\sin\alpha)$	Area Polar MOI

A4.5 Properties for Solids of Revolution

Another application of the use of cyclic integrals is found in the determination of the surface area, volume, and inertial properties of a solid of revolution. Each of these quantities is describable as an integration over the area of the section; as before, such an integration can be converted into a cyclic integral on the boundary of the section by means of Green's Theorem [3].

A4.5.1 Basic Definitions

Consider a solid of revolution defined by the z-axis and a plane figure in the $r-z$ plane bounded by the curve Γ. For this solid, the surface area, volume, and axial position of the centroid are

$$A_S = 2\pi \oint_\Gamma r \, ds \qquad \text{Surface Area}$$

$$V = 2\pi \iint_A r \, dr \, dz \qquad \text{Volume}$$

$$z_c = \tfrac{2\pi}{V} \iint_A rz \, dr \, dz \qquad \text{Axial Position of Centroid}$$

where ds is differential arc length along the curve Γ, and A is the total cross section area with differential element $dr\,dz$.

The body is assumed to be homogeneous with mass density ρ, so the total mass is simply

$$M = \rho V$$

and the center of mass coincides with the centroid of the volume. The cylindrical polar coordinate system, r-θ-z, is a *principal coordinate system* for this body, and the two transverse moments of inertia are equal. There are, therefore, only two distinct mass moments of inertia to be determined:

$$I_{rr} = \pi\rho \iint_A r^3 \, dr \, dz + 2\pi\rho \iint_A rz^2 \, dr \, dz \qquad \text{Transverse MMOI}$$

$$I_{zz} = 2\pi\rho \iint_A r^3 \, dr \, dz \qquad \text{Axial MMOI}$$

Note that while the integral for the surface area is expressed directly in terms of a cyclic integral on Γ, all of the other properties require a double integration over the section area.

A4.5.2 Application of Green's Theorem

With the application of Green's Theorem, these double integrals may be rewritten as cyclic integrals on Γ. As mentioned in the previous application, the choice of functions $P(x,y)$ and $Q(x,y)$ is not unique, and this application is not been handled in quite the

same manner as the previous application. There are four basic integrals required, and after these are evaluated the expressions above for surface area, volume, axial position of the centroid, and moments of inertia are easily evaluated. The four basic integrals are

$$\begin{aligned}
M_r &= \iint_A r \, dr \, dz &&= \oint_\Gamma (rz \, dr + r^2 \, dz) \\
M_{rz} &= \iint_A rz \, dr \, dz &&= \oint_\Gamma \left(rz^2 \, dr + \tfrac{3}{2} r^2 z \, dz\right) \\
M_{rz^2} &= \iint_A rz^2 \, dr \, dz &&= -\oint_\Gamma (rz^3 \, dr + r^2 z^2 \, dz) \\
M_{r^3} &= \iint_A r^3 \, dr \, dz &&= \oint_\Gamma (3r^3 z \, dr + r^4 \, dz)
\end{aligned}$$

Through these integrals, the properties of interest may be considered as determined by a contribution from each segment of the boundary curve Γ. In the evaluation of these integrals, it is necessary (as before) that the boundary be traversed in the counter clockwise sense, that is, with positive area lying on the left of the boundary curve.

A4.5.3 Polygonal Approximation

As in the previous application, the boundary curve is approximated by an irregular n-sided polygon, and any particular side falls into one of three categories:

Case 1 a cylinder, $r = constant$

Case 2 a flat, annular disk, $z = constant$

Case 3 a conical surface, $z = s_i \, (r - r_i) + z_i$

Because of the manner in which Green's Theorem is applied, all three cases can contribute to the value of the integral.

The incremental contribution for each case is determined as in the previous application. It is necessary to compute a slope, s_i, before applying any of the Case 3 increment formulae. The several incremental expressions are summarized in the following table:

Incremental Contributions

	Case 1 Cylindrical Section $r = constant$	Case 2 Annular Disk $z = constant$	Case 3 Conical Section $z = s_i (r - r_i) + z_i$
$s_i =$	——	——	$(z_{i+1} - z_i) / (r_{i+1} - r_i)$
$\Delta\left(\frac{A_s}{2\pi}\right) =$	$r_i \lvert z_{i+1} - z_i \rvert$	$\frac{1}{2}\left\lvert r_{i+1}^2 - r_i^2 \right\rvert$	$\frac{1}{2}\sqrt{1+s_i^2}\left\lvert r_{i+1}^2 - r_i^2 \right\rvert$
$\Delta(M_r) =$	$r_i^2 (z_{i+1} - z_i)$	$\frac{1}{2} z_i \left(r_{i+1}^2 - r_i^2\right)$	$\frac{2}{3} s_i \left(r_{i+1}^3 - r_i^3\right)$ $-\frac{1}{2}(s_i r_i - z_i)\left(r_{i+1}^2 - r_i^2\right)$
$\Delta(M_{rz}) =$	$\frac{3}{4} r_i^2 \left(z_{i+1}^2 - z_i^2\right)$	$\frac{1}{2} z_i^2 \left(r_{i+1}^2 - r_i^2\right)$	$\frac{5}{8} s_i^2 \left(r_{i+1}^4 - r_i^4\right)$ $-\frac{7}{6} s_i (s_i r_i - z_i)\left(r_{i+1}^3 - r_i^3\right)$ $+\frac{1}{2}(s_i r_i - z_i)^2 \left(r_{i+1}^2 - r_i^2\right)$
$\Delta(M_{rz^2}) =$	$-\frac{1}{3} r_i^2 \left(z_{i+1}^3 - z_i^3\right)$	$-\frac{1}{2} z_i^3 \left(r_{i+1}^2 - r_i^2\right)$	$-\frac{2}{5} s_i^3 \left(r_{i+1}^5 - r_i^5\right)$ $+\frac{5}{4} s_i^2 (s_i r_i - z_i)\left(r_{i+1}^4 - r_i^4\right)$ $-\frac{4}{3} s_i (s_i r_i - z_i)^2 \left(r_{i+1}^3 - r_i^3\right)$ $+\frac{1}{2}(s_i r_i - z_i)^3 \left(r_{i+1}^2 - r_i^2\right)$
$\Delta(M_{r^3}) =$	$r_i^4 (z_{i+1} - z_i)$	$\frac{3}{4} z_i \left(r_{i+1}^4 - r_i^4\right)$	$\frac{4}{5} s_i \left(r_{i+1}^5 - r_i^5\right)$ $-\frac{3}{4}(s_i r_i - z_i)\left(r_{i+1}^4 - r_i^4\right)$

The theory developed above can be readily implemented in computer code. After this is done, the most complicated cross sections become tractable in numerical form. A program incorporating these ideas is listed below followed by a few comments on the program and the results for an example calculation.

A4.5.4 Program SolRev.Tru

```
!                    SolRev.Tru
! Geometric properties for a Solid of Revolution
```



```
! with an arbitrary cross section
OPTION NOLET
OPTION BASE 1
DIM r(0),z(0),x(0),y(0)
s1$="    Nodes must enclose the section area"
s2$="    counter clockwise in the R-Z plane"
s3$="Enter the total number of nodes "
s4$="to be used to define the section"
CLEAR
SET WINDOW 1,2,3,4
PRINT  "                    SolRev"
PRINT
PRINT s1$
PRINT s2$
PRINT  "    (Positive area on the left.)"
PRINT
PRINT s3$&s4$
INPUT n
MAT redim r(n),z(n),x(n),y(n)
PRINT  "Enter the material density."
INPUT p
PRINT
PRINT  "Enter section node coordinates, (Ri, Zi)"
FOR i=1 to n
    PRINT  "R(";i;"), Z(";i;") = ?"
    INPUT r(i),z(i)
NEXT i
CALL SRcalcs
CALL table
SUB SRcalcs
    g1=0             ! sum for perimeter
    g2=0             ! sum 1st radial moment of boundary
    g3=0             ! sum for sect area
    g4=0             ! sum 1st radial moment of area
    g5=0             ! sum 1st axial moment of area
    g6=0             ! sum product moment of area
    g7=0             ! sum mr^3 - axial moment of inertia
    g8=0             ! sum mrz^2 - transverse moment of inertia
    FOR i=1 to n
        i2=i+1
        IF i2>n then  i2=1
        r1=r(i)
        z1=z(i)
        r2=r(i2)
```



```
        z2=z(i2)
        d1=sqr((r2-r1)^2+(z2-z1)^2)
        IF r1=r2 then
           CALL cas1
        ELSEIF z1=z2 then
           CALL cas2
        ELSE
           CALL cas3
        END IF
        ! Form sums
        g1=g1+d1
        g2=g2+d2
        g3=g3+d3
        g4=g4+d4
        g5=g5+d5
        g6=g6+d6
        g7=g7+d7
        g8=g8+d8
    NEXT i
END SUB
SUB cas1              ! R=const
    d2=r1*abs(z2-z1)
    d3=0.5*r1*(z2-z1)
    d4=r1^2*(z2-z1)
    d5=-0.5*r1*(z2^2-z1^2)
    d6=0.75*r1^2*(z2^2-z1^2)
    d7=r1^4*(z2-z1)
    d8=-r1^2*(z2^3-z1^3)/3
END SUB
SUB cas2              ! Z=const
    d2=0.5*abs(r2^2-r1^2)
    d3=-0.5*z1*(r2-r1)
    d4=0.5*z1*(r2^2-r1^2)
    d5=-z1^2*(r2-r1)
    d6=0.5*z1^2*(r2^2-r1^2)
    d7=0.75*z1*(r2^4-r1^4)
    d8=-0.5*z1^3*(r2^2-r1^2)
END SUB
SUB cas3              ! Z=C(R-Ri)+Zi
    c=(z2-z1)/(r2-r1)
    f=c*r1-z1
    d2=0.5*sqr(1+c^2)*abs(r2^2-r1^2)
    d3=0.5*f*(r2-r1)
    d4=2*c/3*(r2^3-r1^3)-0.5*f*(r2^2-r1^2)
```



```
    t1=-2/3*c^2*(r2^3-r1^3)
    t2=1.5*c*f*(r2^2-r1^2)
    t3=-f^2*(r2-r1)
    d5=t1+t2+t3
    d6=5/8*c^2*(r2^4-r1^4)-7/6*c*f*(r2^3-r1^3)
    d6=d6+0.5*f^2*(r2^2-r1^2)
    t1=0.8*c*(r2^5-r1^5)
    t2=-0.75*f*(r2^4-r1^4)
    d7=t1+t2
    t1=-0.4*c^3*(r2^5-r1^5)
    t2=1.25*c^2*f*(r2^4-r1^4)
    t3=-4/3*c*f^2*(r2^3-r1^3)
    t4=0.5*f^3*(r2^2-r1^2)
    d8=t1+t2+t3+t4
END SUB
SUB table
    hdr$="    ###         ####.####     +####.####"
    CLEAR
    PRINT  "Print the data?    y/n"
    INPUT g$
    IF g$="y" then
       PRINT  "          input Data"
       PRINT  "      i            R(i)           Z(i)"
       FOR i=1 to n
           PRINT using hdr$: i,r(i),z(i)
       NEXT i
       PRINT
       PRINT "Strike any key to continue"
       GET KEY xxx
    END IF
    blk$="    "
    PRINT
    PRINT  "         Section Area Properties"
    PRINT  blk$&"Perimeter = ";g1
    PRINT  blk$&"Perimeter 1st moment = ";g2
    PRINT  blk$&"Cross section area = ";g3
    PRINT  blk$&"Section area radial 1st moment = ";g4
    PRINT  blk$&"Section area axial 1st moment = ";g5
    PRINT  blk$&"Centroid radius = ";g4/g3
    PRINT  blk$&"Centroid axial position = ";g5/g3
    PRINT
    PRINT  blk$&"        Solid of Revolution Properties"
    PRINT  blk$&"Surface area = ";2*pi*g2
    PRINT  blk$&"Volume = ";2*pi*g4
```



```
    PRINT  blk$&"Mass = ";2*pi*g4*p
    PRINT  blk$&"Axial position of body centroid = ";g6/g4
    PRINT
    PRINT  blk$&"   Principal Mass Moments of Inertia"
    PRINT  blk$&"Irr = ";p*pi*(2*g8+g7)
    PRINT  blk$&"Izz = ";2*pi*p*g7
    SET CURSOR "off"
    GET KEY xxx
END SUB
END
```

The program begins with a data entry portion, and then the main calculation is done in a subroutine named `SRcalcs` and subroutines that it calls, `cas1`, `cas2`, and `cas3`. These last three routines implement the detailed formulae given before the program listing for each of the three cases. The determination of which case applies is made in `calcs`, using a sequence of `if`-statements. The very last calculations and formatting of the printed results is done in the subroutine `table`. It is recommended that the user consider plotting of the data after entering the node coordinates (r_i, z_i) that define the cross section. This will facilitate checking the data to assure that the correct section is calculated.

A4.5.4.1 Test Case

Consider the triangular section defined by the following nodes:

Node	r_i	z_i
1	1.00	0.50
2	3.00	0.00
3	2.00	2.00

When this section is revolved about the $z-$axis, the result is a ring with triangular section, having an edge on the inside, the outside, and the top. The mass density is taken as 1.0 for this example.

The computed results for this body of revolution are as follows:

Section Area Properties

Perimeter	= 6.1003964
Perimeter 1st Moment	= 12.417439
Cross Section Area	= 1.75
Section Area Radial 1st Moment	= 3.50
Section Area Axial 1st Moment	= 1.4583333
Centroid Radius	= 2.00
Centroid Axial Position	= 0.8333333

Solid of Revolution Properties

Surface Area	= 78.02107
Volume	= 21.991149
Mass	= 21.991149
Axial Position of Body Centroid	= 0.8125

Principal Mass Moment of Inertia

$$I_{rr} = 68.172561$$

$$I_{zz} = 98.960169$$

While only a simple cross section (a triangle) is involved here, the problem quickly becomes very complicated and quite laborious by manual methods. More complicated cross sections simply make the situation worse.

A4.5.5 Gear Blank Example

In Figure 4.1 a gear blank is shown, both in half section and in cross section views. This body is described in the following data table:

Gear Blank Cross Section Data

All dimensions in millimeters.

Node	r_i	z_i	Node	r_i	z_i
1	12.70	0.00	7	63.50	25.40
2	24.33	0.00	8	50.80	25.40
3	24.33	12.70	9	50.80	21.28
4	49.48	12.70	10	24.33	21.28
5	50.80	7.70	11	24.33	25.40
6	63.50	7.70	12	12.70	24.40

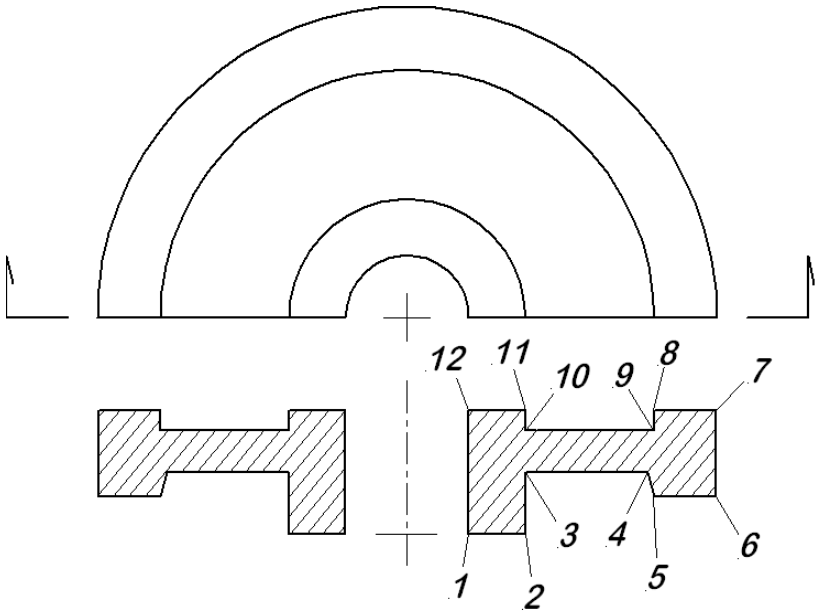

Figure A4.3: Gear Blank

The material for this has mass density $\rho = 7.8005506 \cdot 10^{-6}$ kg/mm^3. Using the Sol-Rev.Tru program, the computed results are

Gear Blank Section Area Properties

Perimeter	=	169.491	mm
Perimeter 1st Moment	=	6129.121	mm^2
Cross Section Area	=	750.605	mm^2
Section Area Radial 1st Moment	=	27013.789	mm^3
Section Area Axial First Moment	=	11366.933	mm^3
Centroid Radius	=	35.989	mm
Centroid Axial Location	=	15.144	mm

Gear Blank Solid of Revolution Properties

Surface Area	=	38510.403	mm^2
Volume	=	169732.644	mm^3
Mass	=	1.324	kg
Axial Position of Body Centroid	=	15.876	mm

Principal Mass Moments of Inertia

I_{rr}	=	1804.231	kg-mm^2
I_{zz}	=	2866.823	kg-mm^2

References

[1] Kaplan, W., *Advanced Calculus*, Addison-Wesley, 1952, p. 239.

[2] Courant, R. *Differential and Integral Calculus*, Vol. II, John Wiley & Sons, 1936.

[3] Doughty, S., "Calculating Properties for Solids of Revolution," *Machine Design*, 10 Dec., 1981, pp. 184 – 186.

Appendix 5

Prime Mover Modeling

Relatively few mechanical systems function without some external power source. Certainly there are a few gravity driven machines (such as a weight driven mechanical clock), but the vast majority of machines are driven either by an internal combustion engine or an electric motor. The detailed description of both of these is beyond the scope of this book, but some ability to model these prime movers will considerably extend the user's ability to model and analyze actual machine systems.

A5.1 Three Phase Induction Motors

Electric motors come in a vast assortment of types, from direct current (DC) motors to alternating current (AC) motors, stepper motors, and more. A complete discussion of these various types is far beyond the scope of this book, with the detailed mathematical analysis even more so. That said, the fact remains that electric motors are integral parts of many machines, and some understanding of them is necessary to understand the dynamics of those machine systems. The discussion here is limited to what is called the *induction motor*, a very common AC motor type. The other major AC motor type is the *synchronous motor*, but it is far less frequently encountered.

The three phase induction motor is the workhorse of modern industry, providing the power for a vast assortment of industrial machines. In comparable power sizes, they are considerably less costly than synchronous motors. The single phase induction motor is common only in the fractional horsepower range, and it is considerably more complex mathematically than the three phase motor. In the discussion below, only across-the-line operation is considered, thus excluding variable frequency drives (VFD) and various "soft-start" mechanisms. Even for the basic three phase machine powered directly by line current, modeling can be approached at several levels, as demonstrated below.

Commercial electric power generation is done with three windings all on the same stationary element (called the *armature*), resulting in three sinusoidal voltages. Each phase has the same amplitude, but they differ from each other in time by a phase shift. If the three phases are denoted as A, B, and C, then the voltages will be $v_A(t) = V\sin(2\pi ft)$, $v_B(t) = V\sin(2\pi ft + 2\pi/3)$, and $v_C(t) = V\sin(2\pi ft - 2\pi/3)$. These voltages exist between a common neutral point and the outer end of each armature winding, so that there are usually four wires extending out from the generator (the three phase ends and the neutral terminal). The factor f is called the *line frequency*, and is typically either 60 Hz or 50 Hz, although other frequencies are used for some situations. The rotating element of a generator carries a winding supplied with DC power and called the *field winding*. Electric power taken from the armature is called *three-phase power*, referring to the three sinusoidal voltages generated. When an external circuit is completed between the end of one phase and the neutral point, this is called a *single phase circuit*. Most fractional horsepower motors use single phase power. If all three phases are fed to a motor, this is an application of three-phase power. The vast majority of industrial machinery is driven by three-phase induction motors, and that is the principal focus of this discussion.

A5.1.1 Induction Motor Construction

From a mechanical perspective, any motor or generator consists of two major parts, identified with their motions. The rotating element is always called the *rotor*, no matter whether it carries the armature or field windings. The stationary element (usually but not always on the outside) is called the *stator*, again no matter which type of windings are attached to it. The stator supports the bearings that in turn support the weight of the rotor. The rotor typically includes the shaft that transmits mechanical power to or from the rotor and supports the weight of the rotor.

To those of a mechanical mind-set, the operation of the induction motor is often a mystery because there is no visible connection to the rotor. In the very common "squirrel cage" motor construction (more about this terminology below), there is no electrical or mechanical power connected to the rotor other than the load, and the means by which torque between the rotor and stator is created is not visible. This is because the torque is developed through *electromagnetic induction*, that is, by magnetic field coupling.

Because time varying magnetic fields are involved in both the stator and the rotor, all of the components in the magnetic circuit components are subject to *eddy currents* which induce power losses through heating. To minimize eddy current losses, the magnetic structures (rotor, stator) are each constructed as laminated stacks, which is to say that they are stacks of thin sheet steel (or iron), each layer with the same outline but insulated electrically from each other. Thus the stator and the rotor each are laminated structures, even though they appear to the eye to be solid blocks of magnetic material. The electrical current carrying elements are embedded in slots in these structures.

A5.1.1.1 Stator Circuits

The magnetic material of the stator is a stack of thin rings, with slots in the axial direction on the inner surface. The stator windings are embedded in these slots in such a way as to form three distinct magnetic windings. This is shown schematically in Figure A5.1, although the actual winding pattern may be difficult to discern by visual inspection of the hardware.

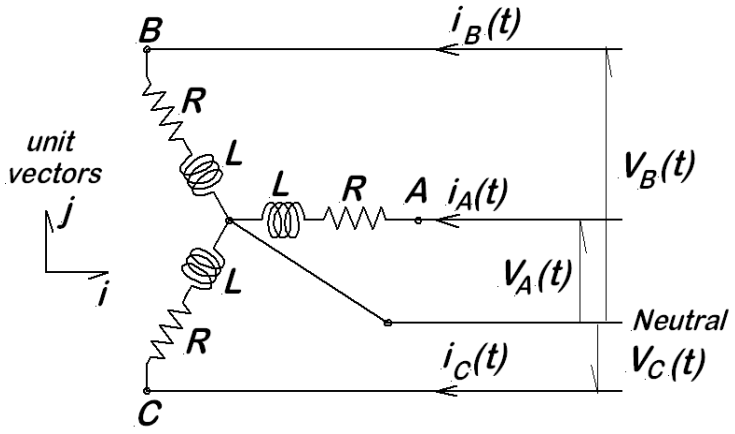

Figure A5.1: Y-connected Stator Circuits for an Induction Motor

Figure A5.1 shows the three windings, oriented 120^o apart in space, each with an inductance (L) and a resistance (R); it is assumed that all three windings are identical. The four connection points (A, B, C, and Neutral) are shown along with the three applied voltages $V_A(t), V_B(t)$, and $V_C(t)$. The currents ($i_A(t)$, $i_B(t)$, and $i_C(t)$) flowing in these windings develop magnetic fields oriented along the axis of each winding. The magnetic fields of the individual windings are:

$$\begin{aligned}
\mathbf{B}_A(t) &= [\mathbf{i}\cos(0) + \mathbf{j}\sin(0)] \cdot B_{\text{single phase}}[\cos(2\pi f t)] \\
\mathbf{B}_B(t) &= [\mathbf{i}\cos(2\pi/3) + \mathbf{j}\sin(2\pi/3)] \cdot B_{\text{single phase}}[\cos 2\pi f t + 2\pi/3] \\
\mathbf{B}_C(t) &= [\mathbf{i}\cos(2\pi/3) - \mathbf{j}\sin(2\pi/3)] \cdot B_{\text{single phase}}[\cos 2\pi f t - 2\pi/3]
\end{aligned}$$

where, in each case, the factor ahead of the dot is a unit vector giving the spatial orientation of the winding while the factor following the dot gives the amplitude and the time dependence of the magnetic field in the winding. The total field due to stator currents ($\mathbf{B}_S$) is simply the sum of the three winding contributions. After some rather tedious

vector arithmetic and trigonometry, the result is

$$\mathbf{B}_S(t) = \frac{3}{2} B_{\text{single phase}} \left[\mathbf{i}\cos(2\pi f t) - \mathbf{j}\sin(2\pi f t)\right]$$

There are two important points to note here:

- The resultant field has constant magnitude equal to 1.5 times the maximum field of a single phase winding;
- The quantity in brackets is simply a unit vector rotating at the electrical supply line frequency.

One final comment is required regarding the stator windings. As presented above, every thing is described in terms of a "two pole" motor stator structure. This means that the stator winding is arranged to create a field comparable to that of a simple bar magnet (one north pole, one south pole) rotating about the shaft axis. In this case, the circular frequency of the magnetic field is simply

$$\omega_e = 2\pi f$$

It is common to employ more complicated winding arrangements to create a rotating magnetic field with four poles, six poles, or more. For a stator structure with n_p poles (remembering that n_p is always a positive even integer), the circular frequency of the stator field is

$$\omega_e = \frac{2\pi f}{n_p/2} = 4\pi f/n_p$$

The circular frequency of the stator field defines an important quantity usually called the *synchronous frequency* or *synchronous speed*. This term becomes quite important later. It is the angular velocity of the combined stator magnetic field vector ($\mathbf{B}_S$).

A5.1.1.2 Rotor Structure

As mentioned previously, the rotating element is a stacked structure such as shown in Figures A5.2 and A5.3. Looking at Figure A5.2, the structure, composed of many laminas, is show, with aligned slots permitting the rotor bars to be embedded axially. The rotor shaft (non shown) is pressed through the axis of the entire stack to rigidly connect the shaft and stack.

Figure A5.3 shows the same structure shown previously in Figure A5.2, with the addition of the end rings. The end rings are electrically conductive material connected to all of

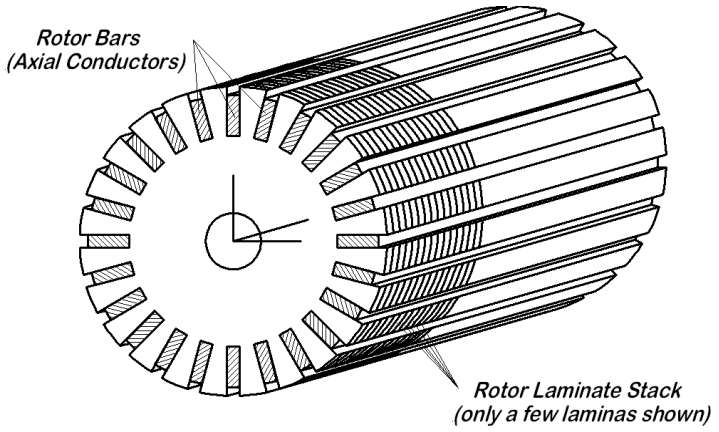

Figure A5.2: Squirrel Cage Induction Motor Rotor Before End Rings Are Added

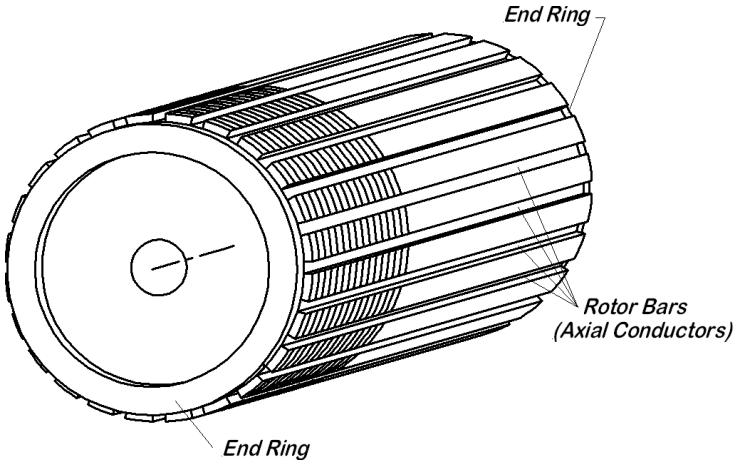

Figure A5.3: Squirrel Cage Induction Motor Rotor Including End Rings

the adjacent rotor bar ends. The rotor bars and the end rings are electrically isolated from the laminations. The result is to create a large number of shorted electrical circuits running from one end of the rotor to the other and back again. The end rings may be brazed or silver soldered to the ends of the rotor bars in large machines where production volumes are limited, or the entire conductive assembly (end rings and rotor bars) may be cast in place in the laminate stack when large production volumes justify the cost of establishing the casting process. Either way, the result is electromagnetically equivalent.

Looking at Figure A5.3, if it is imagined that the laminate stack is removed (an action physically impossible to accomplish), what would be left would be the shaft and the rotor bar/end ring structure. This is very similar to the "squirrel cage," a type of treadmill commonly used for exercise of small animals such as squirrels and hamsters in captivity. This is the source of the term *squirrel cage induction motor*; it describes the electrical

conduction paths in the rotor.

The electrical circuits of the squirrel cage rotor have very low, but finite, resistance. For some purposes, it is desirable to vary the rotor resistance during motor starting. When this is required, the rotor is wire wound in a manner similar to the stator windings, instead of having the rotor bar cage circuits. The ends of the rotor winding are brought off the rotating assembly by means of slip rings. A variable resistor is then added externally to complete the rotor circuit. This form of the induction motor called a *wound-rotor induction motor*. The wound-rotor machine has only limited application and is not discussed further here.

A5.1.2 Slip

When the entire machine is assembled and line power is applied to the stator terminals, the rotating magnetic field of the stator interacts with the many circuits of the rotor, causing current to flow in the rotor circuits. This is the same as the action of a transformer, except that the rotor windings are movable with respect to the stator windings.

Recall that the stator field is rotating with angular velocity $\omega_e = 4\pi f/n_p$. The rotor is, in general, turning at a different angular velocity, ω_m. It is customary to define a quantity called *slip* (s) as

$$s = \frac{\omega_e - \omega_m}{\omega_e}$$

It is evident that, when the machine is functioning as an induction motor, the slip is a dimensionless fraction, $0 \leq s \leq 1$. When $s = 0$, the rotor speed is the same as that of the stator magnetic field vector, and the machine is said to be at *synchronous speed*. If $s = 1$, this means that the rotor is not moving ($\omega_m = 0$). It is clear that the rotor mechanical speed is

$$\omega_m = \omega_e (1 - s)$$

so that knowing the slip implies knowing the mechanical shaft speed and vice versa.

When slip is zero ($s = 0$), the shaft speed is equal to the synchronous speed and there is no torque generated in the motor. It is not possible for an induction motor to run steadily at zero slip, even with no external load torque. Some small amount of torque is required to provide for the motor internal losses due to bearing friction and windage on the rotor.

It should be mentioned that when $s < 0$, the machine is functions as an *induction generator*. Such machines have become interesting in recent times as the preferred generator

type for wind power applications.

A5.1.3 Terminology and Standards

There are two fundamentally different ways to look at induction motor characteristics. One is the very detailed model, based on very accurate modeling of both the electrical and magnetic characteristics. This approach requires a lot of information, but can give very accurate results. The second is the more common engineering approach, often termed the "static" torque-speed characteristic. This requires less information, but it fails to show the high frequency oscillations in the torque response (more on this later). For the present, only the static torque-speed curve is described, but the more detailed models are briefly discussed later. A typical "static" induction motor characteristic is shown in Figure A5.4.

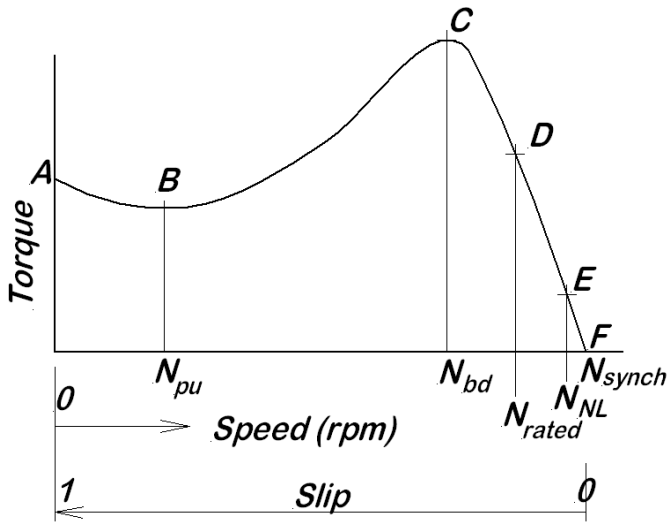

Figure A5.4: Typical "Static"Torque-Speed Curve for An Induction Motor

Induction motors are described by a number of standard terms (some of which are identified in Figure A5.4), and by various industrial standards that establish acceptable ranges for particular characteristics. The most important of these are described below:

- Rated Power (P_{rated}) – the nominal steady power output of the motor, expressed in horsepower or Watts.
- Rated Speed (N_{rated}) – the speed at which the motor produces rated output power, point D in Figure A5.4, usually expressed in revolutions per minute (rpm). This is necessarily somewhat less than synchronous speed because of the slip required to support the rated load.

- No-Load Speed (N_{NL}) – speed at which the motor runs with no external load, point E in Figure A5.4, in units of revolutions per minute (rpm). This is slightly less than synchronous speed because of the small slip required to support the motor internal losses.

- Rated Voltage (V_{rated}) – the root-mean-square (rms) line voltage for which the machine is designed, expressed in volts. This is the safe operating condition for the winding insulation.

- Supply Frequency (f) – the electrical power supply frequency for which the machine is designed to operate, usually in Hz.

- Rated Torque (Full Load Torque) (T_{rated}) – torque developed when the machine is operating at rated voltage, frequency, and power, point D in Figure A5.4, expressed in foot-pounds or meter-Newtons.

- Starting Torque (T_{start}) – the torque developed by the machine at stand-still, point A on the curve of Figure A5.4. This is an important design parameter describing the motor's ability to overcome system static friction and inertia. The units are either foot-pounds or meter-Newtons.

- Pull-up Torque (T_{pu}) – typically the motor torque drops slightly as the motor begins to accelerate, point B in Figure A5.4. The minimum value during this drop is called the pull-up torque, expressed in either foot-pounds or meter-Newtons.

- Breakdown Torque (T_{m}) – point C in Figure A5.4, the maximum torque developed by an induction motor. This occurs at a speed greater than the pull-up point and before torque drops to zero at synchronous speed. This is the absolute maximum torque the machine can develop, and is never exceeded. The units are either foot-pounds or meter-Newtons. For most induction motors, this typically occurs at 80% to 95% of synchronous speed, although it may happen at higher or lower speeds for special designs.

- Breakdown Slip (s_{m}) – the slip at the breakdown torque point. It has no dimensions.

In the USA, the most commonly used standards for electric motors are those published by the National Electrical Manufacturers Association, NEMA. The standards provide typical ranges for most of the parameters above, based on rated power level and application type. One of the most common standards for industrial motors is the NEMA-B design standard. Similar standards exist, no doubt, in other nations. It is important to be aware of these standards as a potential source for modeling information in the absence of more specific information for a particular motor.

A5.1.4 Approaches to Modeling

For mechanical engineering purposes, the primary objective in modeling an induction motor is to describe the motor torque under various operating conditions. Heat generation, motor currents, and other considerations may also be important, but the focus here is on motor torque. Several approaches to modeling are available, and the choice should be governed by these two questions:

1. What is the purpose for the model? This includes the results that are required and the level of accuracy necessary.
2. What information is available about the motor? This can range from the most brief reference to a motor design standard (such as one of the NEMA standards) all the way to the fully detailed design (rarely available to any other than the motor manufacturer).

In almost all cases, there are compromises and trade-offs required in choosing a modeling approach. Rarely ever is all of the desired data available. Even the motor manufacturer, who certainly has the greatest detail about the motor itself, usually lacks the detailed information about the load. With these comments in mind, consider the following approaches to modeling a squirrel cage induction motor where the objective is the torque-speed relationship.

A5.1.4.1 Linear Model

As indicated in Figure A5.4, for situations where the motor is already running at near rated conditions, the torque-speed relation is nearly linear. For torques from zero up to a bit above the rated torque, it is easy to fit this portion of the curve with a straight line that passes through two points:

$$T(\omega_m) = c_o + c_1 \omega_m$$

where

If no-load torque & speed are known –	If no-load torque & speed are unknown –
$c_o = \left(T_{\text{rated}}\omega_{\text{NL}} - T_{\text{NL}}\omega_{\text{rated}}\right) / \left(\omega_{\text{NL}} - \omega_{\text{rated}}\right)$	$c_o = T_{\text{rated}}\omega_{\text{synch}} / \left(\omega_{\text{synch}} - \omega_{\text{rated}}\right)$
$c_1 = -\left(T_{\text{rated}} - T_{\text{NL}}\right) / \left(\omega_{\text{NL}} - \omega_{\text{rated}}\right)$	$c_1 = -T_{\text{rated}} / \left(\omega_{\text{synch}} - \omega_{\text{rated}}\right)$

All of this has the advantage of requiring only minimum information about the motor, but at the same time there are three disadvantages:

1. The linear fit is not exactly correct; there is some curvature to the torque-speed function. This is usually not a serious defect. However, the linear fit is only applicable over a relatively narrow speed range.

2. There is no clear indication as to the upper torque limit for which the model is valid. If the dynamic torque range is very wide, there is the likelihood of using the linear fit beyond the applicable range with no indication that an error has been made.

3. If the actual torque exceeds the breakdown torque, the motor will stall and operation is unstable. This model cannot show that effect at all.

A5.1.4.2 Basic Kloss Model

The basic Kloss model is a formula for the motor torque over the full motor operating range, based on an observation thought to be first made by Dr. Max Kloss [1] and noted again soon afterward by Catterson-Smith [2] , both a bit over a century ago. It features prominently in an on-line lecture by Prof. A. Binder [3]. It seems to be well known in Eastern Europe and Russia, but is not so in the English speaking world. It requires very little information about the motor for a model applicable over the full range of motor slip.

The basic Kloss model assumes that

- The stator resistance is zero (the R values in Figure A5.1);
- The breakdown torque and slip (T_{m} and s_{m}) are known.

With these bits of information, the motor torque-speed curve is approximated by the expression

$$T\left(s\right) = 2T_{\mathrm{m}} / \left(\frac{s_{\mathrm{m}}}{s} + \frac{s}{s_{\mathrm{m}}} \right)$$

In application, to estimate the motor torque at any particular shaft speed, ω, first the slip at that speed is determined and then the formula is evaluated for that slip value. This expression widely used, but it tends to under estimate the torque at high slip. Typical results are shown in Figure A5.5 where it is assumed that $T_{\mathrm{m}} = 48$ N-m and $s_{\mathrm{m}} = 0.2$.

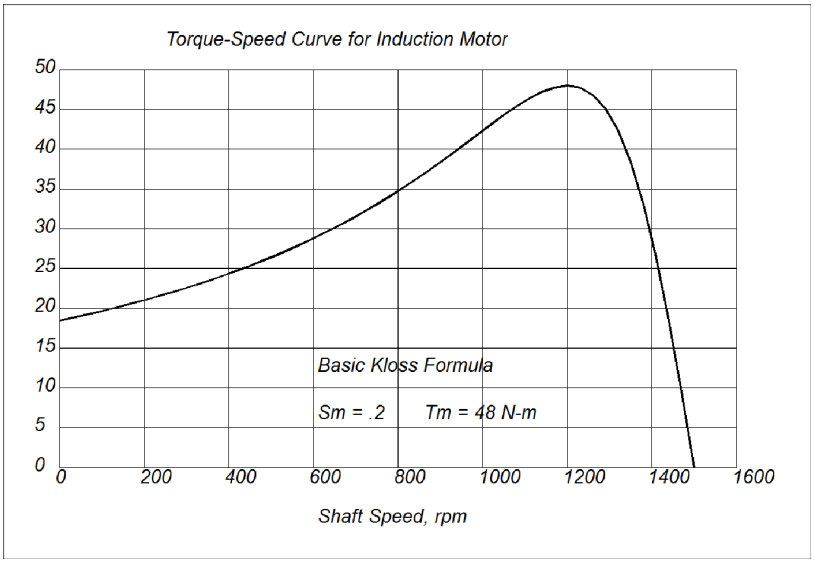

Figure A5.5: Squirrel Cage Motor Torque-Speed Curve per Kloss Equation

A5.1.4.3 Improved Gärtner-Kloss Model

The currents induced in the rotor bars of the squirrel cage induction motor occur at slip frequency, that is $s \cdot \omega_e$. At start-up, the slip is $s = 1$ and the slip frequency is at its maximum value. Conversely, when the rotor is running at near synchronous speed, the slip frequency is quite small. Due to an electrical phenomenon called the *skin effect*, the effective resistance of a rotor bar depends on the frequency of the current. The bar resistance is least when the slip frequency is zero (rotor at synchronous speed), and is greatest when the slip frequency is maximum (rotor stationary). This topic is explored in some detail in [4].

In [5], Gärtner, et al. have proposed an empirical correction to the basic Kloss formula to compensate for the variation in rotor bar resistance. Their proposed form is

$$T_m(s) = 2T_{\mathrm{m}} \left(1 + s_{\mathrm{m}}\, e^{As}\right) / \left(\frac{s_{\mathrm{m}}}{s} + \frac{s}{s_{\mathrm{m}}} + 2s_{\mathrm{m}}\, e^{As}\right)$$

where A is a parameter such that $1.3 \leq A \leq 3.0$. The Gärtner-Kloss equation torque-speed curve is shown plotted in Figure A5.6, along with that of the basic Kloss formula (as previously shown in Figure A5.5). Gärtner, et al. show a measured torque-speed curve that is almost in exact agreement with that computed using their empirical formula with $A = 2.8$.

There are several points of interest regarding the improved relation:

1. The predicted starting torque is considerably higher than that given by the basic

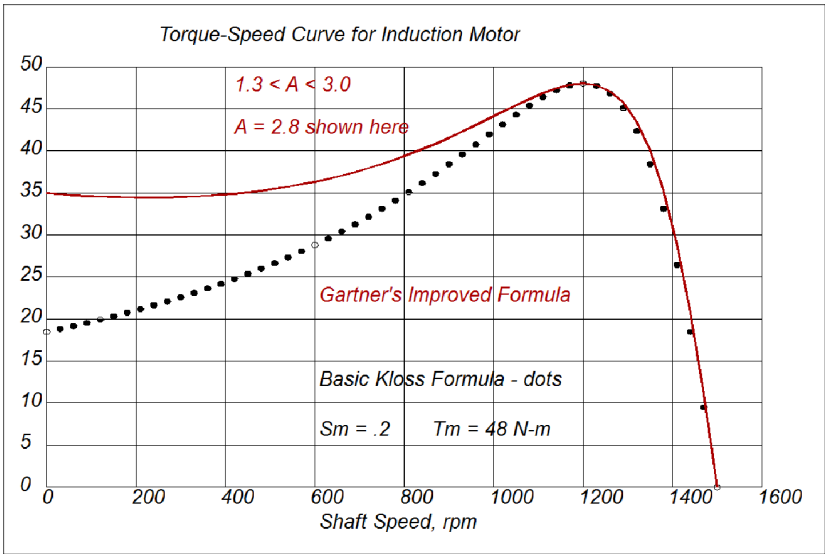

Figure A5.6: Improved Gartner Model

Kloss formula; this is generally in accord with experience.

2. The improved formula shows the torque drop from the starting value out to the pull-up speed. This dip is always absent from the torque-speed curve predicted by the basic Kloss formula.

3. The improved formula and the basic Kloss formula are in close agreement at speeds above the breakdown point.

4. Only one additional parameter is required (A) to apply the improved formula beyond the two required for the basic Kloss formula ($s_{\mathrm{m}}, T_{\mathrm{m}}$). If the pull-up torque value is available, it can guide the choice of A to be used.

A5.1.4.4 Approximate Model Application

The whole point of the Kloss or Gärtner-Kloss models is to provide a useful torque-speed representation, based on information that is readily available. A brief survey of three phase induction motors available from a number of manufacturers shows that the items usually tabulated are: (1) rated power (P_{rated}), (2) rated torque (T_{rated}), (3) starting torque ($T\,(s=1)$), (4) maximum torque (T_{m}), (5) number of poles (n_{p}), and (6) rated speed (N_{rated}). The most obviously missing parameter is s_{m}, the slip at maximum torque, a value required for either the Kloss or Gärtner-Kloss model. It is perhaps less surprising that the Gärtner parameter, A, is not given, but he question remains, "how can either of the approximate models be used with essential parameters absent?"

On preliminary inspection, it appears that there are four conditions available to evaluate the unknown parameters:

1. Torque at $s = s_{\mathrm{m}}$ must have the known value T_{m};
2. Torque at rated speed must have the known value T_{rated};
3. Torque at $s = s_{\mathrm{m}}$ must be an interior maximum value ($dT/ds = 0$);
4. Torque at $s = 1$ must have the known value T_{start}.

All four of these are true and must be satisfied, but they are not all useful for determining the unknown parameters. More careful investigation shows that #1 and #3 are identically satisfied by the Gärtner-Kloss model. This leaves only #2 and #4 available for determination of the two unknown parameters. The process is illustrated in the following example.

A5.1.4.5 Parameter Determination Example

Consider a three phase squirrel cage induction motor operating on a 60 Hz electrical supply. The catalog parameters available for this motor are:

$P_{\mathrm{rated}} = 15$ kW $\qquad T_{\mathrm{m}}/T_{\mathrm{rated}} = 2.15$

$N_{\mathrm{rated}} = 1723.5$ rpm $\qquad T_{\mathrm{start}}/T_{\mathrm{rated}} = 1.5$

The information that the electrical supply frequency is $f = 60$ Hz, combined with the given rated speed, indicates that this is a four pole motor for which $N_{\mathrm{synch}} = 1800$ rpm. Further, the rated speed expressed in radians per second is

$$\omega_{\mathrm{rated}} = (1723.5)\,(2\pi/60) = 180.48 \text{ rad/s}$$

from which the rated torque is

$$T_{\mathrm{rated}} = P_{\mathrm{rated}}/\omega_{\mathrm{rated}} = 15000/180.48 = 83.112 \text{ N-m}$$

With the value for ω_{rated} known, the rated slip is

$$s_{\mathrm{rated}} = (N_{\mathrm{synch}} - N_{\mathrm{rated}})\,/N_{\mathrm{synch}} = (1800 - 1723.5)\,/1800 = 0.0425$$

The unknown parameters of the Gärtner-Kloss model are s_{m} and A, to be determined from these two equations:

$$T_{\mathrm{rated}} = T\,(s = s_{\mathrm{rated}}) = 2T_{\mathrm{m}}s_{\mathrm{m}}s_{\mathrm{rated}}\left(1 + s_{\mathrm{m}}e^{A\cdot s_{\mathrm{rated}}}\right) / \left(s_{\mathrm{rated}}^2 + 2s_{\mathrm{m}}^2 s_{\mathrm{rated}}e^{A\cdot s_{\mathrm{rated}}} + s_{\mathrm{m}}^2\right)$$

$$T_{\text{start}} = T\left(s=1\right) = 2T_{\text{m}}s_{\text{m}}\left(1+s_{\text{m}}e^{A}\right)/\left(1+s_{\text{m}}^{2}+s_{\text{m}}^{2}e^{A}\right)$$

With numerical values substituted, these are

$$\begin{aligned} 83.112 &= 2\cdot 2.15\cdot 83.112\cdot s_{\text{m}}\left(1+s_{\text{m}}e^{0.0425A}\right)/\left(0.0425^{2}+2\cdot 0.0425\cdot s_{\text{m}}\cdot e^{0.0425A}+s_{m}^{2}\right) \\ 1.5\cdot 83.112 &= 2\cdot 2.15\cdot 83.112\cdot s_{\text{m}}\left(1+s_{\text{m}}e^{A}\right)/\left(1+s_{\text{m}}^{2}+2s_{m}^{2}e^{A}\right) \end{aligned}$$

While there is no simple algebraic solution for s_{m} and A, there is no difficulty in obtaining a numerical solution. When this is done (using 20 digit arithmetic in Maple®), the results are

$s_{\text{m}} = 0.194819 \qquad A = 2.67940$

Using these values in the Gärtner-Kloss model results in a torque-speed curve that satisfies all four conditions identified at the beginning of this discussion.

A5.1.4.6 Detailed Models

Because of their immense important in a wide variety of applications, induction motors have been extensively studied for many years. The evolution of the squirrel cage induction motor to its modern form is built on the work of many investigators and investors, including but not limited to Tesla, Westinghouse, Steinmetz, etc. in the 19^{th} century. It seems that Steinmetz originated the equivalent circuit model that served as the principle schematic model for the early analysis.

The application of Kirchoff's voltage law to each circuit appears to be a mid-20^{th} century development, although the originator is unknown to this writer. For a three phase squirrel cage induction machine, the result is a set of six ordinary differential equations in six unknown currents [6]. These are most easily comprehended if cast in matrix form, but they do not admit of closed form solutions. Effective solutions had to wait for the development of computational capability and suitable numerical solution techniques.

In the late 20^{th} century, finite element techniques were applied to the motor problem, providing very detailed information about the magnetic fields and the electrical aspects of such machines; this is where the state of the art stands today.

In the earlier section on Terminology and Standards, the modifier "static" was applied to the torque-speed curves being discussed; the significance of that modifier now becomes evident. Figure A5.7 shows a torque-speed curve developed by a detailed circuit model for a squirrel cage motor starting under load from a reciprocating compressor [7]. The highly oscillatory nature of the starting torque is inescapable. Thus the concept of "static" is

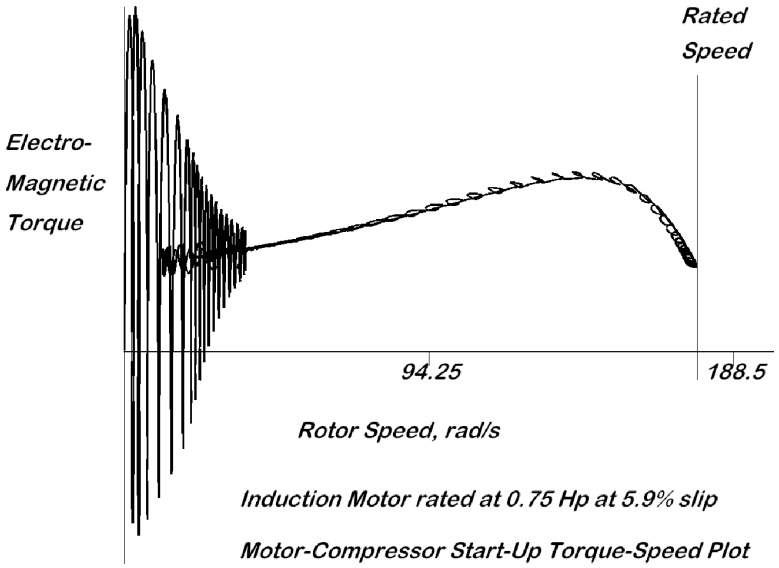

Figure A5.7: Torque-Speed Curve for Induction Motor Starting Under Load From a Detailed Circuit Model

intended to indicate that high frequency oscillations are absent, leaving only the moving average value of the torque. For some engineering purposes, such as determining the time required to bring a machine up to operating speed, the "static" torque-speed curve is entirely adequate; many mechanical systems show little response to the high frequency torque oscillations.

On the other hand, large amplitude, high-frequency oscillations in the motor torque during start-up is found in the detailed models and also observed in engineering practice. A computed oscillatory torque-speed response for the start-up of an induction motor driven compressor is shown in Figure A5.7. Similar oscillations are presented by P.C. Krause [6, pp. 195 - 202]. The high frequency oscillation of the starting torque means that the mechanical system, understood as a collection of rigid bodies, cannot significantly respond, and only the mean torque (such as described by the Kloss or Gärtner-Kloss models above) is available for gross acceleration of the load. However, it must be remembered that the mechanical system is never actually comprised of rigid bodies; there is always flexibility involved. Thus the high frequency torque oscillations during start-up excite severe transient torsional oscillations in the driven machinery. For this reason, the Kloss or Gärtner-Kloss models must never be used to investigate vibratory response; they are only appropriate for the rigid body response.

All of this is particularly important in one surprising situation, the start-up of large synchronous motors. Synchronous motors do not start in synchronous operating mode; at standstill, they are simply too far out of synchronism. Instead, they always start as induction motors, where the damper windings of the synchronous motor (physically similar to the squirrel cage windings of an induction motor) function like an induction

motor rotor. When the motor is almost up to synchronous speed after accelerating as an induction motor, only then is the field current is applied to lock the rotor into synchronism. Thus during start-up, a machine train, nominally driven by a synchronous motor, is subject to the same sort of high frequency torque oscillations as an induction motor driven train. During the world-wide oil shortage of the 1980s, many industries wanted to shift to synchronous motors because they are more efficient than induction motors. This led to serious torsional vibration problems in some cases when synchronous machines were substituted for induction motors.

A5.2 Internal Combustion Engines

Internal combustion engines are widely used to power machines, particularly in situations where electrical power is not readily available. They include both gasoline and diesel powered engines, employing both two and four stroke thermodynamic cycles. Such engines are important parts of the system under analysis in many cases, and it is necessary to have the tools to describe them. Such engines employ slider-crank mechanisms, often several such mechanisms, for which the kinematic and dynamic modeling is described in Chapters 2 and 7. The topic comes up again in Chapter 12 regarding torsional vibrations, specifically Section 12.6 where an example problem is presented involving a three station torsional model for an engine–generator set. Thus in this Appendix, the discussion is focused specifically on (1) the parameters of a particular diesel engine driven generator set used for that example, and (2) the approximate thermodynamic description of the combustion process and the resulting cylinder pressure.

A5.2.1 A Particular Diesel Generator System

The physical parameters of a particular engine driven generator system of Section 12.6 are summarized here. The details of the slider-crank are identified in Figure A5.8. Notice that, in the drawing, Figure A5.8, the centers of mass for both the crank and connecting rod are show as off the body $U-$axis. In the data table below, on the connecting rod is given a displacement from the $U-$axis, but other data could be used equally well.

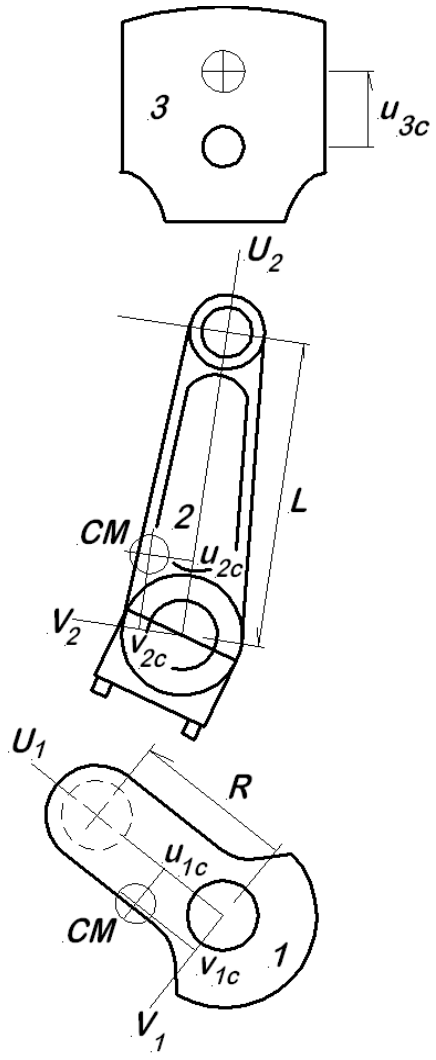

Figure A5.8: Slider-Crank Piece Parts.

Table A5.2 IC Engine Slider-Crank Physical Properties

	USC Value & Units			SI Value & Units	
Crank					
$m_1 =$	$2.2202 \cdot 10^{-2}$	lb-s^2/in	=	3.8882	kg
$u_{c1} =$	0.0	in	=	0.0	mm
$v_{c1} =$	0.0	in	=	0.0	mm
$J_{1o} =$	$6.6745 \cdot 10^{-2}$	lb-s^2-in	=	$7.5412 \cdot 10^{-3}$	kg-m^2
Connecting Rod					
$m_2 =$	$3.5753 \cdot 10^{-3}$	lb-s^2/in	=	0.62613	kg
$u_{2c} =$	1.4898	in	=	37.841	mm
$v_{2c} =$	0.0	in	=	0.0	mm
$J_{2c} =$	$2.5470 \cdot 10^{-2}$	lb-s^2-in	=	$2.877\,7 \cdot 10^{-3}$	kg-m^2
Wrist Pin					
$m_{wp} =$	$8.3429 \cdot 10^{-4}$	lb-s^2/in	=	0.14611	kg
$J_{wpc} =$	$1.2581 \cdot 10^{-4}$	lb-s^2-in	=	$1.4215 \cdot 10^{-5}$	kg-m^2
Piston					
$m_3 =$	$3.517\,3 \cdot 10^{-3}$	lb-s^2/in	=	0.61597	kg

Table A5.3 Linearized Three Station System Parameters

	USC Units			SI Units	
$K_{12} =$	$2.1550 \cdot 10^6$	in-lb/rad	=	$2.4348 \cdot 10^5$	N-m/rad
$K_{23} =$	$1.2400 \cdot 10^6$	in-lb/rad	=	$1.4010 \cdot 10^5$	N-m/rad
$J_{1o} =$	0.0876605414	lb-s^2-in	=	$9.9043 \cdot 10^{-3}$	kg-m^2
$J_{2o} =$	15.320	lb-s^2-in	=	1.7131	kg-m^2
$J_{3o} =$	1.020	lb-s^2-in	=	0.11524	kg-m^2

Table A5.4 Diesel Engine & Generator Parameters

		USC Units			SI Units	
Bore	$d_p =$	4.020	in	=	102.11	mm
Crank Radius	$R =$	2.000	in	=	50.8	mm
Connecting Rod Length	$L =$	6.105	in	=	155.07	mm
Crank Pin Diameter	$d_{cp} =$	1.980	in	=	50.292	mm
Main Journal Diameter	$d_{mj} =$	2.000	in	=	50.8	mm
Indicated Power	$IP =$	297000	$\frac{\text{in-lb}}{\text{s}}$	=	33.556	kW
Shaft Power	$SP =$	258390	$\frac{\text{in-lb}}{\text{s}}$	=	29.194	kW
Mechanical Efficiency	$\eta_{\text{Mech}} =$	87%		=	87%	
Engine Cylinder Damping	$d_1 =$	0.56333	in-lb-s	=	0.063647	N-m-s^2
Generator Efficiency	$\eta_{gen} =$	92%		=	92%	
Generator Damping	$d_3 =$	0.30160	in-lb-s	=	0.03475	N-m-s^2

A5.2.2 Eigensolution for the Three Station System

The free vibration response for the three station example of Section 12.6 can be obtained just as for any other multidegree of freedom vibration, namely by assuming a solution of the form $\{\theta\} = \{A\} \sin \omega_n t$ and then substituting into the equations of motion. This leads to the characteristic equation and generalized eigenproblem. When the numeric values are substituted into the characteristic polynomial and the roots are determined by the quadratic formula, the results are these: $\omega_n = -0, +0, -1138.48, +1138.48, -4972.39, +4972.39$ rad/s. Following the procedures described in Chapter 11, the mode vectors (mode shapes) can also be determined as well, so the complete solution set for non-negative eigenvalues are:

Table A5.5 Eigensolution for Example Problem

$\omega_o = 0$ r/s	$\omega_1 = 1138.48$ r/s	$\omega_2 = 4972.39$ r/s
$\begin{Bmatrix} 1.0 \\ 1.0 \\ 1.0 \end{Bmatrix}$	$\begin{Bmatrix} 1.00000 \\ 0.94728 \\ -14.30365 \end{Bmatrix}$	$\begin{Bmatrix} 1.00000 \\ -0.00574 \\ 0.00030 \end{Bmatrix}$

A5.2.3 Thermodynamic Cycle

In describing the thermodynamic cycle, it is useful to introduce a new variable, s, the piston displacement away from TDC such that

$$s = x_{Max} - x = R + L - x$$

and a related, nondimensional variable, the *stroke fraction*, denoted as sf,

$$sf = \frac{s}{s_{Max}} = \frac{R + L - x}{2R}$$

where it is assumed that there is no cylinder centerline offset. The variable s is such that $0 \leq s \leq 2R$, while $0 \leq sf \leq 1$. Both of these are useful in the description of the thermodynamic cycle.

The ultimate goal for this thermodynamic discussion is to be able to describe the torque acting on the crank due to the gas pressure in the engine cylinder. The virtual work of the gas pressure is:

$$\begin{aligned} \delta W_{GasPressure} &= -P(\theta)\ A_P\, \delta x \\ &= -P(\theta)\ A_P\, K_x(\theta)\ \delta\theta \end{aligned}$$

where $P(\theta)$ is the net pressure acting on the combined top and lower sides of the piston and A_P is the piston area. It is clear that the gas pressure acts as a generalized force (a torque) on the system in the amount $-P(\theta)\ A_P\, K_x(\theta)$.

The period of the gas pressure torque depends upon the number of strokes in the engine thermodynamic cycle (two stroke or four stroke cycle). The time period of the torque is

$$\tau = N_S \pi / \Omega$$

where

N_S is the number of strokes in the cycle (either 2 or 4)

Ω is the nominal crank speed, rad/s.

Thermodynamic discussions of an idealized engine cycle (Diesel or Otto) are often presented as a sequence of straight line segments on a log-log plot; these translate into exponential curves on a linear graph. Such a plot omits the details of the valve opening and closing events. While this is certainly one approach to estimating the cylinder pressure, actual measured data, taken from an operating engine under load, is a much better source. Figure A5.9 represents such a plot for the two stroke engine considered here.

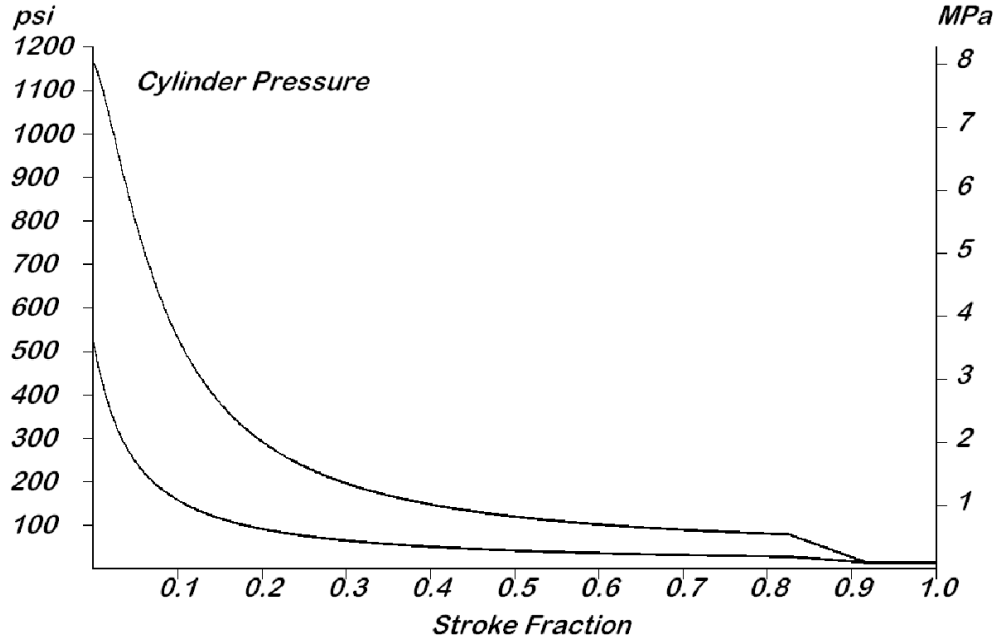

Figure A5.9: Pressure-Stroke Fraction Diagram for Engine Cylinder

Consider the details of the process:

1. With the piston at BDC ($\theta = -\pi$), the system point is at the far lower right corner of the diagram. The cylinder is vented, and the internal pressure is atmospheric, P_{atm}. The starting value is $sf = 1.0$.

2. As the crank moves forward, the piston advances toward the cylinder head. During this interval, the stroke fraction varies from 1.0 to 0.0. At $sf \approx 0.92$, the valves begin to close, an operation that is complete at $sf \approx 0.84$. Cylinder pressure remains atmospheric until the valves begin to close.

3. After the valves close, the pressure begins to rise according to polytropic rule, PV^n = constant. This is the lower curve in Figure A54. This curve is followed until $sf = 0.0$ and the cylinder pressure is just over 500 lb/in^2 (roughly 3.8 MPa).

4. With the piston at TDC, the fuel ignites and the pressure rises suddenly to about 1170 lb/in^2 (roughly 8 MPa).

5. As the piston moves away from the head, s increasing, the fuel continues to burn for a while, and following that, the exhaust gases continue a polytropic expansion until $sf \approx 0.84$ when the exhaust valves begin to open.

6. As the exhaust valves open, the pressure drops rapidly, a drop that be described at least approximately as a linear drop until the valves are fully open at $sf = 0.92$.

7. After the exhaust valves are fully open, the cylinder pressure is approximately atmospheric, P_{atm}, until the piston reaches BDC, $sf = 1$.

There are two curves shown in Figure A5.9. The lower curve is common to all operating conditions; there is no chemical reaction taking place in the cylinder, and the cylinder contains only the fuel/air mixture (or air alone, depending on the method for introducing the fuel). The upper curve, describing the expansion process, is specific to the operating condition that produces the indicated power listed in Table A5.4. For a different operating condition, producing more or less indicated power, the upper curve has a similar shape but has different values from that shown.

A5.2.4 Cylinder Pressure Modeling

It is tempting to use exponential expressions to describe the polytropic curves, but experience suggests that a better fit is obtained with the symmetric sigmoidal curve, a function of the form

$$P = d + \frac{a - d}{1 + \left(\frac{s}{c}\right)^b}$$

where a, b, c, and d are parameters to be adjusted to fit the particular data set. The short block of computer code below gives the approach to generating both the compression and expansion curves of interest here. Note that the necessary coefficient values are embedded in the code.

```
SUB PressFrac(j,sf,pr)
    ! input is stroke fraction, output is  cyl abs pressure ratio
    ! j = 1 is the expansion curve
    ! j = 2 is the compression curve
    ! sf = stroke fraction
    ! sf1 is the point at which valves are fully sealed
    ! sf2 is the point at which valves are fully opened
    IF sf<=sf1 then
       IF j=1 then                     ! IMEP = 140 psi
          pr=2.499803+(79.10112-2.499803)/(1+(sf/0.08461697)^1.421193)
       ELSE IF j=2 then                ! Compression Stroke
          pr=0.4376185+(35.61922-0.4376185)/(1+(sf/0.0439023)^1.067053)
       END IF
    ELSE IF sf>sf1 and s<sf2 then       ! Valves in motion
       pr=(pr2-pr1)/(sf2-sf1)*(sf-sf1)+pr1
    ELSE IF sf>sf2 then
       pr=1
```



```
    END IF
END SUB
```

The subroutine inputs are the choice of curve (1 or 2) and the stroke fraction, denoted as `sf`. The output is the pressure ratio, `pr` $= P(s)/P_{atm}$, a nondimensional value applicable in any system of units. The value of `pr1` is determined by an initial call to this subroutine with `sf=sf1`, the point where the polytropic expansion ends and the linear decline begins. The value of `pr` determined from that call is then `pr1`. The value of `pr2` is `1.0`; at this point, the valves are fully open and the cylinder is vented.

The reason for wanting to describe the cylinder pressure is to be able to calculate the gas pressure torque acting on the crank. Applying the results above to the example engine gives the results shown in Figure A5.10. Note that, as previously, the compression phase is the lower curve while the expansion phase results in the higher values. As must be expected, the crank torque is zero at TDC, despite the very high cylinder pressure at that point.

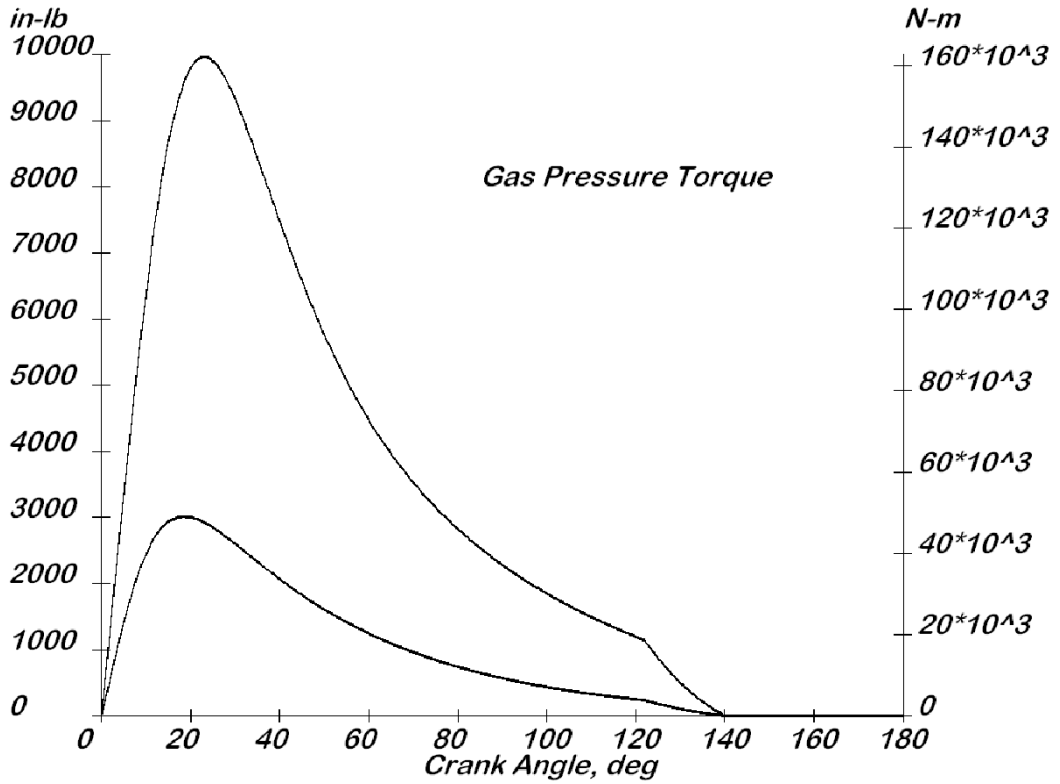

Figure A5.10: Gas Pressure Torque Versus Crank Angle

A5.2.5 Summary

This appendix presents a description of topics normally considered outside the Theory of Machines, but nevertheless closely connected to it. Electric motors and internal combustion engines are the prime movers that drive most of the machinery in use in the world today (with due respect to steam and gas turbines, water power, wind power, etc.). An awareness of how they can be modeled is essential to developing a broad capability in the mechanics of machinery.

References

[1] Kloss, M., "Starting Torque of Three-phase Motors," *The Electron*, vol. 2, p. 18, 1908.

[2] Catterson-Smith, J.K., "Induction Motor Design," *Proceedings of the Institution of Electrical Engineers*, Vol. 49, 1912, pp. 635 - 650.

[3] Binder, A.,"5. The Slip-Ring Induction Machine," Institut fur Elektrische Energiewandlung, Technische Universitat Darmstadt, slide number 18 (on line).

[4] Maddi, Z, Aouzellag, D, and Laddi, T., "Influence of the Skin Effect and the Form of Slot on the Starting Characteristics of Induction Motor Squirrel Cage," *Recent Advances in Mechanics, Mechatronics, and Civil, Chemical, and Industrial Engineering*, pp. 125 - 129 (on line, no date).

[5] Gärtner, J., Halámka, Z., and Pavelka, J., "The Speed Control of the Induction Motors by Change of Suply (sic) Voltage," *Silnoprouda Electroteknika a Electroenergetika 2001*, Brno, Czech Republic, 26.4.2001, pp. D-41 – D-44.

[6] Krause, P.C., *Analysis of Electric Machinery*, McGraw-Hill, 1989.

[7] Doughty, S., "Modeling of Induction Motor Driven Systems," *Sixth International Conference on Control, Automation, Robotics, and Computer Vision, ICARCV 2000*, 6–8 Dec 2000, Singapore.

Appendix 6

Rigid Body Kinetic Energy

Much of this book is built upon the application of energy methods, and of necessity this often requires the ability to describe the kinetic energy of rigid bodies. The derivation given here is quite general and is applicable to motion in both two and three dimensions.

A6.1 Kinematics

Consider the rigid body shown in Figure A6.1, and in particular the differential element of mass, dm. This mass element is located by the position vector $\mathbf{R}$ relative to an inertial coordinate system. The position may also be expressed in terms of the position of the center of mass, $\mathbf{R}_c$, and the relative position of the mass element with respect to the center of mass, $\mathbf{R}'$,

$$\mathbf{R} = \mathbf{R}_c + \mathbf{R}'$$

Next consider the velocity of the mass element, dm. Because the body is rigid, the length of $\mathbf{R}'$ cannot change. The only change that can occur in the relative position vector $\mathbf{R}'$ is a change in direction. The velocity of the mass element is

$$\mathbf{V} = \mathbf{V}_c + \boldsymbol{\omega} \times \mathbf{R}'$$

where $\mathbf{V}_c$ is the velocity vector for the center of mass, and $\boldsymbol{\omega}$ is the angular velocity vector of the rigid body.

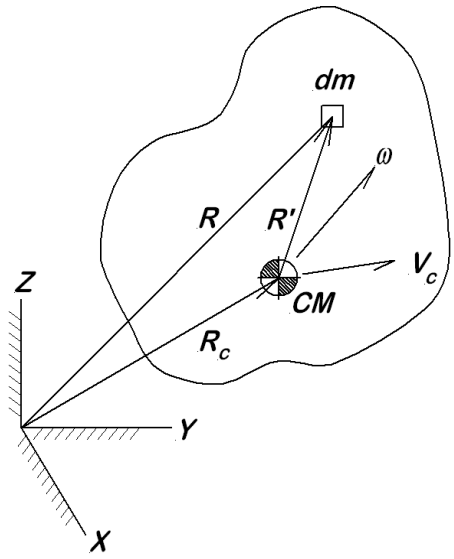

Figure A6.1: Rigid Body Moving In Three Dimensions

A6.2 Kinetic Energy

With this information available, the kinetic energy of the mass element can be written as

$$\begin{aligned} dT &= \frac{1}{2}\mathbf{V}\cdot\mathbf{V}\,dm \\ &= \frac{1}{2}\left(\mathbf{V}_c+\boldsymbol{\omega}\times\mathbf{R}'\right)\cdot\left(\mathbf{V}_c+\boldsymbol{\omega}\times\mathbf{R}'\right)\,dm \\ &= \frac{1}{2}\left[\mathbf{V}_c\cdot\mathbf{V}_c+2\mathbf{V}_c\cdot\boldsymbol{\omega}\times\mathbf{R}'+(\boldsymbol{\omega}\times\mathbf{R}')\cdot(\boldsymbol{\omega}\times\mathbf{R}')\right] \end{aligned}$$

To obtain the total kinetic energy of the rigid body, the contributions from every element are summed in an integration over the total mass.

$$\begin{aligned} T &= \int_M dT \\ &= \frac{1}{2}\mathbf{V}_c\cdot\mathbf{V}_c\int_M dm \\ &\quad +\mathbf{V}_c\cdot\boldsymbol{\omega}\times\int_M \mathbf{R}'dm \\ &\quad +\frac{1}{2}\int_M(\boldsymbol{\omega}\times\mathbf{R}')\cdot(\boldsymbol{\omega}\times\mathbf{R}')\,dm \end{aligned}$$

The first integral simply gives the mass of the body. The second integral vanishes. (Why?)

The third integral requires rearrangement of the integrand using the vector identity:

$$\mathbf{A} \cdot \mathbf{B} \times \mathbf{C} = \mathbf{B} \cdot (\mathbf{C} \times \mathbf{A})$$

where the first factor in parentheses, $(\boldsymbol{\omega} \times \mathbf{R}')$, is taken for A, $\boldsymbol{\omega}$ is taken for $\mathbf{B}$, and $\mathbf{R}'$ is taken for $\mathbf{C}$. The result makes to the leading factor that can be taken outside the integral; for the remaining integrand, the integral is the angular momentum with respect to the center of mass. To justify this statement, consider a motion consisting only of rotation about the center of mass, in which case the product $(\boldsymbol{\omega} \times \mathbf{R}')\ dm$ is the linear momentum of the mass element. When $\mathbf{R}'$ is crossed into the linear momentum, the result is the angular momentum of the mass element with respect to the center of mass. The integral then expresses the summation of the angular momentum contributions from each mass element. Including a non-zero velocity for the center of mass modifies the linear momentum for the mass element, but the additional term contributes nothing to the final angular momentum because the integral is zero.

$$\begin{aligned} \int_M (\boldsymbol{\omega} \times \mathbf{R}') \cdot (\boldsymbol{\omega} \times \mathbf{R}')\ dm &= \boldsymbol{\omega} \cdot \int_M \mathbf{R}' \times (\boldsymbol{\omega} \times \mathbf{R}')\ dm \\ &= \boldsymbol{\omega} \cdot \mathbf{H}_c \\ &= \{\omega\}^T [I_c] \{\omega\} \end{aligned}$$

In the final line, the angular momentum with respect to the center of mass is written as the matrix product of the mass moment of inertia with respect to the center of mass multiplied with the angular velocity vector. The final result is then:

$$T = \frac{1}{2} M\, \mathbf{V}_c \cdot \mathbf{V}_c + \frac{1}{2} \{\omega\}^T [I_c] \{\omega\}$$

For plane motion, where the angular velocity vector must be normal to the plane of motion, the final term reduces to a scalar product:

$$T = \frac{1}{2} M\, \mathbf{V}_c \cdot \mathbf{V}_c + \frac{1}{2} I_c \omega^2$$

In the event that the body is pinned at some point, a similar analysis applies. For that case, the velocity of the mass element with respect to the fixed point is expressed first as the cross product of the angular velocity with the relative position vector. The result is expressed in a single term that involves the angular velocity vector and the mass moment of inertia matrix referred to the *fixed reference point o*. The final result in that case is

$$T = \frac{1}{2} \{\omega\}^T [I_o] \{\omega\}$$

Again, for the case of plane motion, this reduces to the single scalar product

$$T = \frac{1}{2} I_o \omega^2$$

These two cases are sufficient for all kinetic energy expressions that are required.

References

[1] Beer, F.P., and Johnston, E.R., *Vector Mechanics for Engineers*, 4th ed. New York: McGraw-Hill, 1984.

[2] Goldstein, H., *Classical Mechanics*, Reading, MA: Addison-Wesley, 1959.

[3] Lass, H., *Vector and Tensor Analysis*, New York: McGraw-Hill, 1950.

Appendix 7

Lagrange Equations Derivation

The Lagrange form for the equations of motion is an energy based method applicable to multidegree of freedom systems. Because of being energy based, there are no vector expressions to be handled, with only scalar quantities used instead. It is often much more simple to apply than a Newton's Second Law approach, particularly for complicated systems.

A7.1 Derivation By Virtual Work

This appendix deals with the derivation of the Lagrange form for the equation of motion by means of the Principle of Virtual Work [1]. The problem is formulated in terms of N particles, subject to external forces and internal constraint forces. The constraints are limited to what are called *workless constraints*, that is, forces of constraint that do no work as the motion progresses. These are the common type of constraints, and this is not a severe limitation. Including constraint forces makes the result applicable to rigid bodies, because a rigid body may be considered as a collection of a large number of individual particles with a similarly large number of constraint forces.

Consider a collection of N particles, each with a position vector of the form

$$\mathbf{R}_i = \mathbf{R}_i \left(q_1, q_2, q_3, \ldots \right) \qquad\qquad i = 1, 2, \ldots N$$

where q_1, q_2, q_3, ... are generalized coordinates. The total force on the i^{th} particle is composed of the externally applied force and the force of constraint (which may be a rigid body internal force):

$$\mathbf{F}_i = \mathbf{F}_{ei} + \mathbf{F}_{ci}$$

The motion of the particle is described by Newton's second law:

$$M_i\dot{\mathbf{V}}_i = \mathbf{F}_i = \mathbf{F}_{ei} + \mathbf{F}_{ci}$$

or

$$\mathbf{F}_{ei} + \mathbf{F}_{ci} - M_i\dot{\mathbf{V}}_i = \mathbf{0}$$

The virtual work of the terms in the preceding line is necessarily zero, and the sum of such terms over all of the particles remains zero:

$$\delta W = \sum_{i=1}^{N} \left(\mathbf{F}_{ei} + \mathbf{F}_{ci} - M_i\dot{\mathbf{V}}_i\right) \cdot \delta\mathbf{R}_i = 0$$

Now, because the constraints are assumed to be workless, the sum of the virtual work of the constraints is zero:

$$\sum_{i=1}^{N} \mathbf{F}_{ci} \cdot \delta\mathbf{R}_i = 0$$

In writing the remaining expression, the subscript e is dropped, as external forces are understood to be the only forces of interest:

$$\delta W = \sum_{i=1}^{N} \mathbf{F}_i \cdot \delta\mathbf{R}_i - \sum_{i=1}^{N} M_i\dot{\mathbf{V}}_i \cdot \delta\mathbf{R}_i = 0$$

Now focus on the latter term, the virtual work of the momentum derivative. The virtual displacement of the i^{th} particle is

$$\delta\mathbf{R}_i = \sum_j \frac{\partial\mathbf{R}_i}{\partial q_j}\delta q_j$$

where the sum extends over all of the generalized coordinates. The virtual work of the momentum derivative is then

$$\begin{aligned}\sum_{i=1} M_i\dot{\mathbf{V}}_i \cdot \delta\mathbf{R}_i &= \sum_{i=1} M_i\dot{\mathbf{V}}_i \cdot \sum_j \frac{\partial\mathbf{R}_i}{\partial q_j}\delta q_j \\ &= \sum_j \sum_i M_i\dot{\mathbf{V}}_i \cdot \frac{\partial\mathbf{R}_i}{\partial q_j}\delta q_j\end{aligned}$$

Look at the inner sum, and consider it as one term of the derivative of a product, so that

$$\sum_i M_i\dot{\mathbf{V}}_i \cdot \frac{\partial\mathbf{R}_i}{\partial q_j} = \frac{d}{dt}\sum_i M_i\mathbf{V}_i \cdot \frac{\partial\mathbf{R}_i}{\partial q_j} - \sum_i M_i\mathbf{V}_i \cdot \frac{d}{dt}\left(\frac{\partial\mathbf{R}_i}{\partial q_j}\right)$$

Two substitutions are needed for use in this expression for the virtual work of the momentum derivative. The position of the i^{th} particle is

$$\mathbf{R}_i = \mathbf{R}_i\left(q_1, q_2, q_3, \ldots\right)$$

and the velocity is obtained by a time differentiation:

$$\mathbf{V}_i = \sum_j \frac{\partial \mathbf{R}_i}{\partial q_j}\dot{q}_j$$

If the partial derivative of $\mathbf{V}_i$ is then taken with respect to $\dot{q}_j$, all terms of the sum are zero except for one, by the independence of the generalized coordinates:

$$\frac{d\mathbf{V}_i}{d\dot{q}_j} = \frac{\partial \mathbf{R}_i}{\partial q_j}$$

In the expression for the virtual work of the momentum derivative, this will replace the first term on the right-hand side.

For the second substitution, consider once again the expression for the position of the i^{th} particle and differentiate:

$$\begin{aligned}
\mathbf{R}_i &= \mathbf{R}_i\left(q_1, q_2, q_3, \ldots\right) \\
\frac{d}{dt}\frac{\partial \mathbf{R}_i}{\partial q_j} &= \sum_k \frac{\partial^2 \mathbf{R}_i}{\partial q_k \partial q_j}\dot{q}_k \\
&= \frac{\partial}{\partial q_j}\sum_k \frac{\partial \mathbf{R}_i}{\partial q_k}\dot{q}_k \\
&= \frac{\partial \mathbf{V}_i}{\partial q_j}
\end{aligned}$$

This is used as a replacement in the final term of the virtual work of the momentum derivative. When these substitutions are made, the momentum derivative factor becomes

$$\begin{aligned}
\sum_i M_i \dot{\mathbf{V}}_i \cdot \frac{\partial \mathbf{R}_i}{\partial q_j} &= \frac{d}{dt}\sum_i M_i \mathbf{V}_i \cdot \frac{d\mathbf{V}_i}{d\dot{q}_j} - \sum_i M_i \mathbf{V}_i \cdot \frac{\partial \mathbf{V}_i}{\partial q_j} \\
&= \frac{d}{dt}\frac{\partial}{\partial \dot{q}_j}\left(\frac{1}{2}\sum_i M_i \mathbf{V}_i \cdot \mathbf{V}_i\right) - \frac{\partial}{\partial q_j}\left(\frac{1}{2}\sum_i M_i \mathbf{V}_i \cdot \mathbf{V}_i\right) \\
&= \frac{d}{dt}\frac{\partial T}{\partial \dot{q}_j} - \frac{\partial T}{\partial q_j}
\end{aligned}$$

The virtual work of the momentum derivative is then simply

$$\sum_{i=1} M_i \dot{\mathbf{V}}_i \cdot \delta \mathbf{R}_i = \sum_j \left(\frac{d}{dt} \frac{\partial T}{\partial \dot{q}_j} - \frac{\partial T}{\partial q_j} \right)$$

This is the most significant part of the derivation; it shows the relation of the momentum derivative (the mass $\times$ acceleration term of Newton's Second Law) to be a combination of derivatives of the kinetic energy.

The virtual work of the external forces is expressed in the usual manner, leading to the definition of the generalized forces Q_j (see Section 6.2):

$$\begin{aligned}
\mathbf{R}_i &= \mathbf{R}_i \left(q_1, q_2, q_3, \ldots \right) \\
\delta \mathbf{R}_i &= \sum_j \frac{\partial \mathbf{R}_i}{\partial q_j} \delta q_j \\
\sum_i \mathbf{F}_i \cdot \delta \mathbf{R}_i &= \sum_i \mathbf{F}_i \cdot \sum_j \frac{\partial \mathbf{R}_i}{\partial q_j} \delta q_j \\
&= \sum_j \sum_i \mathbf{F}_i \cdot \frac{\partial \mathbf{R}_i}{\partial q_j} \delta q_j \\
&= \sum_j Q_j \, \delta q_j
\end{aligned}$$

where

$$Q_j = \sum_i \mathbf{F}_i \cdot \frac{\partial \mathbf{R}_i}{\partial q_j}$$

After the virtual work of the workless constraints is dropped, the virtual work equation reads

$$\delta W = \sum_i \mathbf{F}_i \cdot \delta \mathbf{R}_i - \sum_i M_i \dot{\mathbf{V}}_i \cdot \delta \mathbf{R}_i = 0$$

The several results developed earlier in this section can then be used in this equation to give

$$\sum_i Q_i \delta q_i - \sum_j \left(\frac{d}{dt} \frac{\partial T}{\partial \dot{q}_j} - \frac{\partial T}{\partial q_j} \right) \delta q_j = 0$$

or

$$\sum_j \left(Q_j - \frac{d}{dt} \frac{\partial T}{\partial \dot{q}_j} - \frac{\partial T}{\partial q_j} \right) \delta q_j = 0$$

The generalized coordinates are independent, so the coefficient of each δq_j must vanish to assure the vanishing of the sum. This gives the first form for the Lagrange equation of motion, which is written as follows:

$$\frac{d}{dt}\frac{\partial T}{\partial \dot{q}_j} - \frac{\partial T}{\partial q_j} = Q_j$$

In the preceding development, the generalized coordinates are considered as independent, as they are throughout this book. This is true for holonomic systems, which are systems that involve only holonomic constraints (discussed in Section 2.7). The extension of the Lagrange equation to nonholonomic systems is accomplished using the Lagrange multiplier technique [2]. This technique involves introducing the nonholonomic constraint equations, each with an unknown multiplier. When the solution is obtained, the multiplier values are determined, and they can be interpreted as the forces required to enforce the constraints.

References

[1] Goldstein, H., *Classical Mechanics*, Reading, MA.: Addison-Wesley, 1959.

[2] D'Souza, A.F. and Garg,V.K. *Advanced Dynamics*, Prentice-Hall, Englewood Cliffs, NJ, 1984, pp. 139-141

Appendix 8

Shaft Bending Deflections

A8.1 Introduction

The Euler-Bernoulli differential equation for the deformed neutral fiber of a beam in bending is commonly presented in elementary courses in mechanics of materials. In such courses, the EI product (=Young's Modulus Area $\times$ Moment of Inertia of the cross section) appearing in that differential equation is nearly always assumed to be constant over the length of the beam. In real machines, a constant value is rarely found in power transmission shafts or bean structures. Such shafts frequently involve a sequence of different diameters to provide shoulders for locating bearing, mounted components, etc. Such shafts are definitely a part of the present study, and their deflection analysis is an essential part of the study of shaft vibration and whirl. For this reason, it is appropriate that Mischke's method be developed for use in this context. While the development below is in terms of a nonuniform solid circular shaft, it should be kept in mind that it is easily extended to nonuniform hollow shafts or to nonuniform beams.

Consider a shaft of length L on simple supports and subject to discreet loads only (distributed loads can easily be approximated as a sequence of several discrete loads). The left end is located at $x = 0$, and the right end is at $x = L$. The two simple supports can be at any locations; they need not be at the ends. The beam is modelled as a sequence of n node locations, x_i, such that

- there is a node at each end;
- there is a node at each support;
- there is a node at every discrete load location;
- there is a node at every change in diameter.

It is further assumed that there is no externally applied load on the shaft at a support node, so that the support reaction is the only force acting at a support.

The externally applied loads are denoted as F_i, where i is the index for the node where the load acts. All forces are taken positive in which ever direction is assumed for positive deflections.

A8.2 External Reactions

The shaft is understood to be simply supported, so let the support locations be denoted as x_L and x_R and the support reactions R_L and R_R are determined by taking moments about the supports:

$$R_L = \frac{-1}{(x_R - x_L)} \sum_{i=1}^{n} (x_R - x_i) F_i$$

$$R_R = \frac{-1}{(x_R - x_L)} \sum_{i=1}^{n} (x_i - x_L) F_i$$

With the reactions known, they can be included in the list of F_i, and treated like any other external load acting on the beam; this is understood to be done.

A8.3 Beam Theory

The Euler-Bernoulli beam bending description says

$$EI(x) \frac{d^2y}{d^2x} = m(x)$$

where

E = Young's modulus for the shaft material

$I(x) = \frac{\pi}{64} [d(x)]^4$ = area moment of inertia of the cross section

$y(x)$ = shaft deflection at x

$m(x)$ = internal bending moment at x

For a shaft loaded by only a set of discrete forces (including the support reactions), the shear diagram is a sequence of positive and negative steps. When the shear is integrated to express the bending moment, the result is a series of linear ramps, rising and falling as dictated by the shear diagram. The application of the trapezoidal rule for numerical integration of the bending diagram is exact, and has long been advocated [1]. Mischke's insight was to observe that while the trapezoidal rule is inexact for the necessary second integration to obtain the deflection, Simpson's rule integration can be done exactly [2, 3]. He proposed a simple way to evaluate the function at the middle of each interval and thus facilitated the application of Simpson's rule.

A8.3.1 Details of the Process

The problem is to solve the ordinary differential equation

$$y''(x) = \frac{m(x)}{EI(x)}$$

subject to the boundary conditions

$$\begin{aligned} y(x_L) &= 0 \\ y(x_R) &= 0 \end{aligned}$$

At least in principle, this can be done by direct integration,

$$\begin{aligned} y'(x) &= \int_0^x \frac{m(x)}{EI(x)} dx + c_1 \\ &= I_1(x) + c_1 \end{aligned}$$

where $I_1(x)$ is the indicated definite integral. Then a second integration give the deflection function,

$$\begin{aligned} y(x) &= \int_0^x [I_1(x) + c_1] dx \\ &= I_2(x) + c_1 x + c_2 \end{aligned}$$

where c_1 and c_2 are constants yet to be determined to match the boundary conditions. The boundary conditions require that

$$\begin{aligned} I_2(x_L) + c_1 x_L + c_2 &= 0 \\ I_2(x_R) + c_1 x_R + c_2 &= 0 \end{aligned}$$

This gives the constants as

$$\begin{aligned} c_1 &= -\left[I_2\left(x_R\right) - I_2\left(x_L\right)\right] / \left(x_R - x_L\right) \\ c_2 &= \left[x_L I_2\left(x_R\right) - x_R I_2\left(x_L\right)\right] / \left(x_R - x_L\right) \end{aligned}$$

What remains is to determine the functions $I_1(x)$ and $I_2(x)$. Consider the integration from x_{i-1} to x_i, where $I_1(x_{i-1})$ and $I_2(x_{i-1})$ are known. Trapezoidal integration is exact for integration of y'' to obtain $I_1(x_i)$ and also to obtain $I_1^* = I_1\left[\left(x_1 + x_2\right)/2\right]$, the mid-point value. Thus

$$\begin{aligned} I_1^* &= I_1\left(x_{i-1}\right) + \left(x_i - x_{i-1}\right)\left(\frac{3}{2}y''_{i-1} + \frac{1}{2}y''_i\right)/4 \\ I_1\left(x_i\right) &= I_1\left(x_{i-1}\right) + \left(x_i - x_{i-1}\right)\left(y''_{i-1} + y''_i\right)/2 \end{aligned}$$

With values now available for $I_1\left(x_{i-1}\right), I_1^*$, and $I_1\left(x_i\right)$, Simpson's Rule is then applied to produce $I_2\left(x_i\right)$

$$I_2\left(x_i\right) = I_2\left(x_{i-1}\right) + \left[I_1\left(x_{i-1}\right) + 4I_1^* + I_1\left(x_i\right)\right]/6$$

Finally, the deflection is

$$y_i = y\left(x_i\right) = I_2\left(x_i\right) + c_1 x_i + c_2$$

Doughty applied this method to the calculation of rotor shaft flexibility matrices and showed how it could be employed to incorporate additional supports (the statically indeterminate shaft) [4].

A8.3.2 Example

Consider the simply supported shaft shown in Figure A8.1. Note that all dimensions shown are in millimeters, but all calculations are made with lengths in meters. The material is steel, $E = 2.07 \cdot 10^{11}$ Pa. For the application of the ideas above, the model requires eleven node points. The working loads are $F_3 = 76225\ N$ (downward) and $F_9 = 86450\ N$ (downward).

A program implementing Mischke's method is given below. When applied to the system as given, the bearing support loads are $R_L = 74454$ N and $R_R = 91221\ N$. The right bearing load is considered unacceptably high for the smaller shaft diameter at that location, so the engineers want to consider the possible application of a third bearing at station B (station 6). This will provide a larger diameter for the bearing, and also relieve some of the mid-span sag in the initial design.

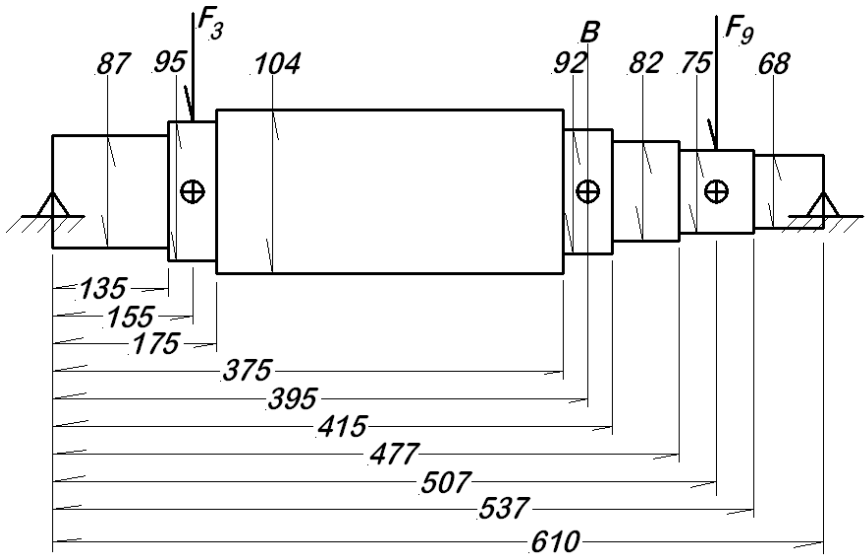

Figure A8.1: Simply Supported Steel Shaft

In order to evaluate a possible additional bearing, the shaft is analyzed without the working loads, but only with a 1 N load applied at station 6. With the 1 N load at station 6 (section B), the deflection at that station is $y_{61} = -5.6050297 \cdot 10^{-9}$ m. With only the normal working loads (F_3 and F_9), the deflection at station 6 was $y_{62} = -5.9221548 \cdot 10^{-4}$ m, so this is the amount that a mid-span bearing will have to lift the shaft at station 6 in order to properly align the shaft. To do so, the load on the proposed bearing at 6 is F_6

$$F_6 = y_{62}/y_{61} = 105657.87 \text{ N}$$

The analysis program can only deal with simply supported shafts, but the case with three bearings can be evaluated by running the program with the force F_6 added to the externally applied loads, in effect applying the bearing force as a known load rather than as a reaction to be determined. When this is done, the results are as shown in Table A8.1.

Note that the application of the bearing load at B decreases the displacement at that point effectively to zero (calculated as $4 \cdot 10^{-19}$ m) which is what should be expected. This also relieves the bearing load on both of the two outboard bearings, with the new bearing picking up the major part of the load.

A program listing for computing the deflections of a simply supported nonuniform shaft by Mischke's Method, program Shaft.Tru, follows. The built-in data are for the example problem just above with only the working loads included on two bearings. It is easily

modified to other purposes

Table A8.1 Mischke Beam Deflection					
Calculation for Three Bearing Shaft					
node	$x\,(i)$	$y\,(i)\cdot 10^5$	$y'\,(i)\cdot 10^4$	$F\,(i)$	
i	m	m	–	N	
1	0.000	+0.0000	−6.2824	34214	Bearing
2	0.135	−6.0711	−0.9266		
3	0.155	−6.1393	+0.2722	−76225	Applied Load
4	0.175	−5.9635	+1.4522		
5	0.375	−0.2626	+1.8926		
6	0.395	$+4.33\cdot 10^{-14}$	+0.6948	105658	Bearing Load
7	0.415	+0.0192	−0.4436		
8	0.477	−1.1725	−2.5133		
9	0.507	−1.7759	−1.2125	−86450	Applied Load
10	0.537	−1.8428	+0.6600		
11	0.610	0.0000	3.4567	22804	Bearing

```
!                    Shaft.Tru
! Stepped shaft deflection calculations by Mischke's Method
OPTION BASE 1
OPTION NOLET
DIM x(20),y(20),yp(20),diam(20),EI(20),Fext(20),mom(20)
DIM MEIL(20),MEIR(20),Int1(20),Int2(20)
CLEAR
! x(i)      node axial position
! y(i)      deflection at node i
! yp(i)     slope at node i
! diam(i)   shaft diameter to right of node i
! EI(i)     EI(x) for shaft to right of node i
! Fext(i)   externally applied load values
! MEIL(i)   moment to left of node i
! MEIR(i)   moment to right of node i
! xL        left bearing node location
! iL        left bearing node number
```



```
! iR        right bearing node number
! xR        right bearing node location
! RL        left bearing reaction force
! RR        right bearing reaction force
! Int1      first integral of M/EI
! Int2      second integral of M/EI

! Data for Example Problem
E=2.07e11                          ! Young's modulus
n=11                               ! number of nodes
x(1)=0.0                           ! node A
x(2)=0.135                         ! node B, shoulder
x(3)=0.155                         ! node C, load Fc
x(4)=0.175                         ! node D, shoulder
x(5)=0.375                         ! node E, load Fe
x(6)=0.395                         ! node F, shoulder
x(7)=0.415                         ! node G, end of shaft
x(8)=0.477
x(9)=0.507
x(10)=0.537
x(11)=0.610
diam(1)=0.087
diam(2)=0.095
diam(3)=0.095
diam(4)=0.104
diam(5)=0.092
diam(6)=0.092
diam(7)=0.082
diam(8)=0.075
diam(9)=0.075
diam(10)=0.068
MAT Fext=zer
Fext(3)=-76225                     ! load at 3, down
Fext(9)=-86450                     ! load at 9, down
xL=x(1)                            ! left support location
xR=x(11)                           ! right support location
iL=1
iR=11

! Calculate Reactions
FOR i=1 to n
    sL=sL+(xR-x(i))*Fext(i)        ! right end moment sum
    sR=sR+(x(i)-xL)*Fext(i)        ! left end moment sum
NEXT i
```



```
RL=-sL/(xR-xL)                    ! reaction force left
RR=-sR/(xR-xL)                    ! reaction force right
Fext(iL)=RL                       ! add reactions to force list
Fext(iR)=RR

! Computer M(x)/EI(x) ...
FOR i=1 to n-1
    AMOI=pi/64*diam(i)^4          ! area MOI for circular shaft
    EI(i)=E*AMOI                  ! EI to the right of x(i)
NEXT i

! Develop moment values
! MEIL   moment/EI left of node
! MEIR   moment/EI right of node
mom(1)=0                          ! actual moment function
shear=Fext(1)
FOR i=2 to n
    deltaX=x(i)-x(i-1)
    mom(i)=mom(i-1)+shear*deltaX  ! moment at node i
    shear=shear+Fext(i)           ! shear force to right of i
NEXT i
FOR i=2 to n
    MEIR(i-1)=mom(i-1)/EI(i-1)
    MEIL(i)=Mom(i)/EI(i-1)
NEXT i

! Compute Int1 and Int2
Int1(1)=0
Int2(1)=0
FOR i=2 to n
    deltaX=x(i)-x(i-1)
    Int1(i)=Int1(i-1)+deltaX*(MEIR(i-1)+MEIL(i))/2
    Istar=Int1(i-1)+deltaX*(3*MEIR(i-1)/2+MEIL(i)/2)/4
    Int2(i)=Int2(i-1)+deltaX*(Int1(i-1)+4*Istar+Int1(i))/6
NEXT I
! Compute integration constants c1 and c2
c1=-(Int2(iR)-Int2(iL))/(xR-xL)
c2=-xR*Int2(iL)-xL*Int2(iR)/(xR-xL)
! Compute Slopes and Deflections
FOR i=1 to n
    yp(i)=Int1(i)+c1              ! slope
    y(i)=Int2(i)+c1*x(i)+c2       ! deflection
NEXT i
```



```
PRINT
PRINT "   Stepped Shaft Deflection Calculations by Mischke's Numerical Method"
PRINT
hdr$="    node     x(i)     Defl          Slope         Fext(i)"
PRINT
img$="     ##   ###.####  +#.####^^^^ +#.####^^^^ +#.####^^^^ ############"
PRINT hdr$
FOR i=1 to n
    com$=""
    IF i=iL or i=iR then com$="Reaction"
    PRINT using img$: i,x(i),y(i),yp(i),Fext(i),com$
NEXT i
END
```

References

[1] Shigley, J.E. and Mitchell, L.D., *Mechanical Engineering Design*, 4th ed., McGraw-Hill, 1983, pp. 123-129.

[2] Mischke, C.R. "An Exact Numerical Method for Determining the Bending Deflection and Slope of Stepped Shafts," *Advances in Reliability and Stress Analysis*, Proceeding of the Winter Annual Meeting of ASME, San Francisco, Dec. 1978, pp. 101-115.

[3] Shigley, J.E. and Mischke, C.R., *Mechanical Engineering Design*, 5th ed., McGraw-Hill, 1989, pp. 98-105.

[4] Doughty, S., "Flexibility Matrix Calculation for a Stepped Rotor Shaft," ASME DE-Vol-18-1, 1989, pp. 35-4.

Appendix 9

Rayleigh's Method

A9.1 Introduction

Rayleigh's Method is a device for approximating the lowest natural frequency of a vibratory system. As Rayleigh's Method was originally presented [1] the potential energy of the system was calculated using the common expression for beam bending strain energy based on the square of the bending moment function

$$V = \frac{1}{2}\int_0^L EI\left[y''\left(x,t\right)\right]dx$$

where

V = strain energy

E = Young's modulus

I = section area moment of inertia

$y\left(x,t\right)$ = transverse displacement of the beam at location x and time t

The kinetic energy was similarly based on summing the incremental contributions

$$T = \frac{1}{2}\int_0^L \mu\left[\dot{y}\left(x,t\right)\right]^2 dx$$

where

μ = mass per unit length of the beam

If it is assumed that

$$y(x,t) = \xi(x)\sin\omega t$$

these two integral expressions become

$$V = \frac{1}{2}\sin^2\omega t\int_0^L EI\left[\xi''(x)\right]^2 dx$$
$$T = \frac{1}{2}\omega^2\cos^2\omega t\int_0^L \mu\left[\xi(x)\right]^2 dx$$

By conservation of energy, $V_{Max} = T_{Max}$ gives Rayleigh's result

$$\omega^2 = \frac{\displaystyle\int_0^L EI\left[\xi''(x)\right]^2 dx}{\displaystyle\int_0^L \mu\left[\xi(x)\right]^2 dx} \tag{A}$$

This is the classic form for the Rayleigh Quotient, an expression for the square of the natural frequency.

In application, the user is required to make an educated guess for the form for $\xi(x)$, choosing a function that satisfies the *essential boundary conditions.* In most applications, there are multiple possible choices for $\xi(x)$, some better than others.

A9.2 Objections

There are, however, difficulties in the application of Rayleigh's original formulation. A function that superficially appears to be a satisfactory approximation to the dynamic mode shape may have serious errors when differentiated twice and used in the numerator integral. This has led a number of authors [2, 3, 4, 5] to propose an alternate form for Rayleigh's method. Consider a beam for which either (a) a lumped mass model has been defined, or (b) the beam mass is considered negligible in comparison to a set of discrete loads W_i acting on the beam. The modified form is equation (B):

$$\omega^2 = \frac{g\left(W_1y_1 + W_2y_2 + \cdots W_ny_n\right)}{W_1y_1^2 + W_2y_2^2 + \cdots W_ny_n^2} \tag{B}$$

If the acceleration of gravity is moved to the denominator as a divisor, the denominator sum is readily seen as the finite approximation to the denominator integral in equation (A) above, assuming that the factor 1/2 has been canceled with a similar factor in the numerator. But how is the numerator sum justified? The numerator sum looks nothing at all like the numerator integral above.

A9.3 Alternate Forms Justified

There are at least two alternative forms commonly used for Rayleigh's method. The first is equation (B) above, and the second is a related form often used with matrix formulations.

A9.3.1 First Alternative Form, Equation (B)

The numerator represents the maximum value of the work done by the loads that deform the beam. Because of the nature of beam behavior, a load at one location results in deflections at most other points in the beam, so this is not the simple case of loading individual springs. Considering a lumped mass model, the force-deflection relation is of the form

$$\begin{aligned} \{f\} &= [K]\{y\} \\ \{y\} &= [S]\{f\} \end{aligned}$$

where

$\{f\}$ is any set of discrete loads

$\{y\}$ the set of deflections associated with $\{f\}$

$[K]$ is the stiffness matrix

$[S]$ is the flexibility matrix

Suppose that the actual loads to be imposed consists of a set of weights, $\{W\} = \text{col}\,(W_1, W_2, ...W_n)$. This set of weights can be imposed gradually by letting

$$\{f\} = c\{W\} \qquad 0 \leq c \leq 1$$

where c is simply a variable scalar multiplier. At full load the deflections are $\{Y\}$, where

$$\{W\} = [K]\{Y\}$$

For something less than the full load, with $c < 1$, it is true that

$$\begin{aligned} \{f\} &= c\{W\} \\ \{y\} &= c\{Y\} \end{aligned}$$

The differential work done in loading the structure is $d\,(Work)$

$$\begin{aligned} d\,(Work) &= \{f\}^T \{dy\} \\ &= \{Y\}^T \{W\}\, c\, dc \end{aligned}$$

The total work is found by integration on c from zero to one,

$$Work = V_{Max} = \frac{1}{2}\left(W_1 Y_1 + W_2 Y_2 + \cdots + W_n Y_n\right) \tag{C}$$

For the kinetic energy of the beam, remembering that $\lceil M \rfloor$ is diagonal, the total kinetic energy is

$$T = \frac{1}{2g}\omega^2 \cos^2 \omega t \left(W_1 y_1^2 + W_2 y_2^2 + \cdots + W_n y_n^2\right)$$

When the maximum value is taken and the ratio formed, the result is

$$\omega^2 = \frac{g\left(W_1 Y_1 + W_2 Y_2 + \cdots + W_n Y_n\right)}{\left(W_1 Y_1^2 + W_2 Y_2^2 + \cdots + W_n Y_n^2\right)} \tag{D}$$

Equation (D) is the equation (B) mentioned in the previous section.

When using a estimate for the deformation shape $\{Y\}$ (the first mode vector), it is vitally important that realistic estimates be used for the Y_i values. **They cannot be scaled arbitrarily**, but must be the result of an accurate estimate. This is usually done by using a static deflection calculations.

A9.3.2 A Second Alternative Form

The development above also suggests another alternative form. Return to the differential work expression just before equation (C),

$$\begin{aligned} d\,(Work) &= \{f\}^T \{dy\} \\ &= \{Y\}^T [K] \{Y\}\, c\, dc \end{aligned}$$

Again integrating, the result is

$$Work = \frac{1}{2}\{Y\}^T [K] \{Y\}$$

This leads to the second alternative form for Rayleigh's natural frequency approximation

$$\omega^2 = \frac{\{Y\}^T [K] \{Y\}}{\{Y\}^T \lceil M \rfloor \{Y\}} \tag{E}$$

This is a form often seen in matrix formulations of the vibration problem. Assume for a moment that the $\{Y\}$ are true eigenvectors. In this case, the triple matrix product in the numerator is the modal stiffness, $\mathbb{K}$, (which is equal to $\omega^2\mathbb{M}$). Also, for this case, the denominator triple product is $\mathbb{M}$, the modal mass for the fundamental mode. Thus, with true eigenvectors, the ratio reduces to an identity. With true eigenvectors employed, scaling is unimportant. This is a distinct difference between equations (D) and (E). The only problem here is that, if the true eigensolutions are already known, there is no need to estimate the first eigenvalue.

References

[1] Lord Rayleigh, *Theory of Sound*, vol. 1, Dover, 1945, p. 257.

[2] Mischke, C.R., *Elements of Mechanical Analysis*, Addison-Wesley, 1963, pp. 277-278.

[3] Carter, W.J., *Theory of Machine Design*, Hemphill's Bookstore, Austin, TX, 1962, pp. 294-295.

[4] Timoshenko, S. and Young, D.H., *Advanced Dynamics*, McGraw-Hill, 1948, p. 296.

[5] Timoshenko, S., *Vibration Problems in Engineering*, 1st ed., 1928, p. 62.

Index

(This page deliberately left blank)

(This page deliberately left blank)